Evaluating recovery post COVID-19: from the clinical to the epithelial

Dr Bavithra Vijayakumar

Thesis submitted for the degree of Doctor of Philosophy (PhD)

April 2023

National Heart and Lung Institute

Imperial College London

Supervisors:

Professor Pallav L Shah

Professor Clare M Lloyd

Dr James A Harker

Declaration of originality

I declare that the work presented in this thesis is work that I have performed myself, directly supervised or is appropriately referenced. Results from collaborations have been clearly stated. Specific contributions are as follows: The PHENOTYPE study was designed, and study documents written by me with input from Dr James Tonkin, Dr Christopher Orton and Professor Pallav Shah. Dr James Tonkin assisted with recruitment early on during the first wave. Acquisition of healthy control endobronchial samples was performed by Dr Richard J Hewitt, Dr David JF Smith and Professor Philip Molyneaux, with ethics approval sought by Professor Philip Molyneaux and Professor Toby Maher. Acquisition of endobronchial samples for post COVID-19 donors was performed by members of the interventional bronchoscopy team, but mainly Dr Justin L Garner and Dr Christopher M Orton.

Dr Keir EJ Philip assisted with development of the topic ideas for the qualitative component of quality-of-life assessment and assisted with the derivation of themes presented in Chapter 3. Professor Sujal Desai and Professor Anand Devaraj scored the CT scans from the first wave (Chapter 4) and I continued to score the scans from the second wave independently having learnt the techniques from them. Lung function tests reported in Chapters 4, 5 and 6 were performed by Chief Physiologists Leeh Faustino and Isaac Mwita at Chelsea and Westminster Hospital. Flow cytometry data for healthy controls reported in Chapter 7 was generated by Dr Patricia Ogger. Analysis of flow cytometry data reported for post COVID-19 donors in Chapter 7 was performed by Dr Patricia Ogger and Dr Karim Boustani. Sample processing and staining was performed either by them or by myself under their supervision as part of my training in wet lab skills. Haematoxylin and eosin (H+E) stains shown in Chapter 8 was performed by Lorraine Lawrence, NHLI. RNA extraction and assessment of purity in Chapter 8 was performed by me but library preparation, RNA sequencing and data analysis was performed by Genewiz (Azenta Life Sciences). The heatmaps presented in Chapter 8 were created by me based on normalised gene counts provided by Genewiz. Analysis of the bronchoalveolar lavage fluid proteomic data which resulted in the finding that DPP4 and AREG were differentially upregulated in individuals post COVID-19 compared to healthy control donors was performed by Dr Artemis Papadakis and Dr James E Peters in a collaboration. Finally, Safia Ismael and Karen Ramzy Yakoub (BSc students) assisted me with imaging and analysis of cellular proliferation in response to sitagliptin treatment and manual cell counting of Ki67+ cells presented in Chapter 9.

Copyright Statement

The copyright of this thesis rests with the author. Unless otherwise indicated, its contents are licensed under a Creative Commons Attribution-Non Commercial 4.0 International Licence (CC BY-NC).

Under this licence, you may copy and redistribute the material in any medium or format. You may also create and distribute modified versions of the work. This is on the condition that: you credit the author and do not use it, or any derivative works, for a commercial purpose.

When reusing or sharing this work, ensure you make the licence terms clear to others by naming the licence and linking to the licence text. Where a work has been adapted, you should indicate that the work has been changed and describe those changes.

Please seek permission from the copyright holder for uses of this work that are not included in this licence or permitted under UK Copyright Law.

Acknowledgements

First and foremost, I would like to thank my supervisors Professor Pallav Shah, Professor Clare Lloyd and Dr James Harker for their support, guidance, mentorship and the opportunities they have given me throughout the last 3 years which enabled this project to be created, developed and completed within the PhD timeframe.

Pallav's been a fantastic supervisor and mentor and his response, "you'll never know unless you try" when I first approached him about the Clinical Fellow job advert, was what prompted me to apply for the post and brought me from Oxford to London to embark on this PhD. These words have been hugely motivational and provided me with the encouragement and confidence to apply for multiple fellowships and grants during my PhD time. Pallav's constant emphasis on undertaking research with potential patient benefit and reminders that we are clinicians before we are researchers has been extremely valuable and stabilising on this journey. I cannot thank Clare and James enough for the patience they've shown throughout my time in the lab: It has been a steep learning curve, having started off not knowing the difference between the different pipettes to then producing the results described in the latter part of this thesis. I had been apprehensive about a lab-based PhD, but thanks to the supervision and colleagues I've met along the way, my time in the lab has ended up being productive and enjoyable, and an important part of my research training.

I'd like to offer my sincere thanks to Professor Wisia Wedzicha, my mentor, for developing my interest in small airways pathology and providing me with the tools for Chapter 6 as well as teaching me that publishing data is not just about research impact, but also a way to express gratitude for the time and effort patients have put into the research visits. Thank you also to Professor Ian Adcock and Professor Jane Davies for undertaking the Early and Late-stage reviews with me, which were extremely useful and helped me focus my time appropriately.

I have had the pleasure of working with so many people who have made the last 3 years a fun, enjoyable and fulfilling experience. Namely: Muscle laboratory and Biomedical Research Unit – Dr James Tonkin, Dr Francesca Conway, Dr Christopher Orton, Dr Justin Garner, Cielito Caneja, Dr Keir Philip, Rebecca Wawman, Dr Anand Tana, Dr Ley Chan, Dr Arafa Aboelhassan, Sarah Buttery, Parris Williams, Zander Williams, Laura Avanzi, Ines Meireles, Paul Ryan. Chelsea and Westminster Hospital – Leeh Faustino, Isaac Mwita, Jaime Carungcong, Kribashnie Nundlall, Alexander Schoolmeesters, Patricia Correia da Costa, Rhian Bull, Gina Bowd, Tori Keeble, Leke Vincent, Dhruv Sharma, Jhanet

Castillo, Gina Fernandes, Andre Haye Radiology – Professor Sujal Desai, Professor Anand Devaraj. Inflammation, Repair and Development section (NHLI) – Dr Katie Bonner, Dr Lola Loewenthal, Dr David Smith, Dr Elizabeth Scotney, Dr Lydia Finney, Dr Richard Hewitt, Dr Aran Singanayagam, Dr Patricia Ogger, Dr Karim Boustani, Dr Skye Quinn, Raphaela Konstantinidi, Emily Calamita, Ciara Campbell, Kornelija Suveizdyte, Dr Helen Stolting, Dr Gesa Albers, Minerva Garcia Martin, Leia Griffin, Poonam Ghai, Christina Michalaki, Dr Sean Giblin, Dr Shwetha Raghunathan, Safia Ismael, Karen Ramzy-Yakoub, Lucie Prior, Lorraine Lawrence, Dr Laura Yates, Simone Walker, Dr Franz Puttur, Dr Regis Joulia, Dr Mindy Gore, Gill Martin. Airways disease section (NHLI) - Dr Mairi Macleod, Dr Andrew Ritchie, Dr Dexter Wiseman

This project would not have been possible without the commitment and engagement of the patients recruited to the PHENOTYPE study, whose desire to help others through research, despite their own ill-health, was inspiring. Supporting these individuals through such a challenging time, filled with so many uncertainties, has been one of the most rewarding experiences of my clinical career so far. The trust and faith patients had in me and the medical profession during this time was truly humbling.

Finally, I would like to thank my training programme director (HETV), Dr John Wrightson and my past and present educational supervisors, Dr William Flight and Professor Najib Rahman for their advice and guidance when deciding to embark on a PhD, supporting me with the approval process and for all the career advice they have provided throughout my Specialist Registrar training.

Dedication

My parents have provided me a lifetime of support and encouragement and have taught me the importance of discipline, perseverance and hard work, which has been pivotal to my academic and professional achievements to-date. I am eternally grateful for their unwavering support and to them, I dedicate this thesis.

Funding

For the work presented in this thesis, I was part funded by the Joint Research Committee on behalf of CW+ and Westminster Medical School Research Trust, both for salary and consumables.

First author publications and presentations during PhD

Publications

Vijayakumar, B., Boustani, K., Ogger, P., Papadakis, A. et al. Immuno-proteomic profiling reveals abundant airway CD8 T cells and ongoing epithelial injury in prolonged post COVID-19 respiratory disease. *Immunity*. 2022. 55(3):542-556.e5

Vijayakumar, B., Tonkin, J., Devaraj, A., et al. CT lung abnormalities after COVID-19 at 3 months and 1 year after hospital discharge. *Radiology*. 2022. 303 (2). 444-454

Vijayakumar, B., Shah, PL. Is fibrosis, really fibrosis? [Correspondence letter]. *American Journal of Respiratory and Critical Care Medicine*. 2021. 203 (11)

Vijayakumar, B., Shah, P. Not all parenchymal changes on CT are ILD. [Correspondence letter] *Annals of the American Thoracic Society*. 2021. 18 (9)

Poster/Oral presentations arising from this PhD

Vijayakumar, B., Ritchie, A., Tonkin, J., Orton, C.M., Wedzicha, J., Shah, PL. Small airways disease post COVID-19: 1 year follow up. - *European Respiratory Society Congress, Barcelona, September 2022* [Oral]

Vijayakumar, B., Tonkin, J., Orton, CM., Faustino, L., Mwita, I., Wedzicha, J., Shah, PL. Abnormal FENO post COVID-19. *European Respiratory Society Congress, Barcelona, September 2022* [Poster]

Vijayakumar, B., Tonkin, J., Devaraj, A., Philips, KEJ., Orton, CM., Desai, SR., Shah, PL. Persistent lung abnormalities versus established fibrosis: a prospective study of COVID-19 follow up. *European Respiratory Society Congress, September 2021* [Poster]

Vijayakumar, B., Tonkin, J., Pallav L Shah 2021. Persistent abnormalities on echocardiography post hospitalization for COVID-19. *European Respiratory Society Congress, September 2021* [Oral]

Submitted abstracts to ERS 2023

Vijayakumar, B., Philips, KEJ., Tonkin, J., Conway, FM, Tana, A., Chan, L., Orton, CM., Shah, PL. Trajectory of HR-QOL post COVID-19: A mixed methods study

Vijayakumar, B., Tonkin, J., Orton, CM., Garner, JL., Smith, DJS., Hewitt, RJ., Molyneaux, PL., Harker, JA., Shah, PL., Lloyd, CM. Epithelial recovery post COVID-19

Successful grant applications

Joint Research Committee PhD Studentship - £72 300 - Phenotyping patiENts admitted to hospital with cOvid-19 infection and idenTifYing Prognostic markErs (PHENOTYPE). Awarded by the Joint Research Committee on behalf of a joint collaboration between CW+ and Westminster Medical School Research Trust (CW+), February 2021

Investigating the clinical and in-vitro effects of epithelial damage post COVID-19 - £30 000 - Awarded by the Joint Research Committee on behalf of a joint collaboration between CW+ and Westminster Medical School Research Trust (CW+), September 2021.

Evaluating the respiratory microbiome post COVID-19 - £3100 - Awarded by the Joint Research Committee on behalf of a joint collaboration between CW+ and Westminster Medical School Research Trust (CW+), March 2022.

COVID-19 impact statement

The COVID-19 pandemic necessitated a significant change in the topic of my PhD, having previously planned to undertake a project evaluating the effect of epithelial ablation in COPD. However, the change in project has given me the opportunity to be involved in and contribute to a rapidly evolving field, with immediate clinical benefit, and gain experience in a diverse range of research methodologies and skills, for which I am grateful.

Abstract

COVID-19 has resulted in significant morbidity and mortality across the globe. The aim of this thesis is to better understand recovery post COVID-19.

COVID-19 resulted in persistent clinical, psychological and quality of life impairment even 3 months post hospital discharge, necessitating a variety of patient-driven coping strategies to mitigate impact. In particular, a positive mindset, external support from family and friends, and religious faith were important factors positively impacting individuals' quality of life.

Radiological and physiological sequelae were common, but usually regressed with time, with only the minority having radiologically-evident fibrosis. Abnormal fractional exhaled nitric oxide levels were not associated with airway or peripheral eosinophilia or markers of epithelial damage and although small airways disease was detectable in some individuals, expiratory flow limitation was not seen.

Upregulation of immune cell subsets and epithelial damage markers was seen in the airways 3-6 months post COVID-19 and differential cell count analysis showed marked lymphocytosis and neutrophilia in some, even in the absence of a culture-positive micro-organism. A trend towards increased airway lymphocytes and faster radiological recovery was seen.

A defect in epithelial wound closure was seen post COVID-19, but in contrast, immunological responses to Influenza A virus were preserved compared to healthy controls. Dipeptidyl peptidase 4 and amphiregulin were both differentially upregulated in the post COVID-19 airway in vivo and show a possible counter-regulatory relationship in vitro. Additionally, inhibition of DPP4 may have immunomodulatory effects.

In summary, despite significant abnormalities post COVID-19, improvement with time is seen in the majority. Further mechanistic evaluation of some of the clinical and in vitro findings is required, to determine the clinical and translational impact of these results.

Table of contents

Declaration of originality ***2***

Copyright Statement ***3***

Acknowledgements ***4***

Dedication ***6***

Funding ***7***

First author publications and presentations during PhD ***8***

COVID-19 impact statement ***10***

Abstract ***11***

Table of contents ***12***

List of Tables ***18***

List of Figures ***19***

Abbreviations ***23***

Chapter 1 – Introduction ***26***

1.1 Severe acute respiratory syndrome coronavirus 2 (SARS-COV2) **26**

1.1.1 Background 26

1.1.2 Structure of the virus 26

1.1.3 Variants 27

1.2 Acute SARS-COV2 infection – a clinical overview **27**

1.2.1 Clinical symptoms 27

1.2.2 Radiological abnormalities 27

1.2.3 Peripheral biomarkers of disease severity 28

1.2.4 Drug treatments 29

1.3 Pathogenesis **29**

1.3.1 Target cells 29

1.3.2 Epithelial responses to SARS-COV2 infection 29

1.3.3 Local immune responses to SARS COV2 infection 31

1.3.4 Histological evidence post SARS-COV2 infection 32

1.4 Long-term consequences post COVID-19 ..... **32**

1.4.1 Clinical symptoms 33

1.4.2 Radiological abnormalities 34

1.4.3 Virus induced airway dysfunction 37

1.5 Role of the epithelium **39**

1.5.1 Role of the epithelium in viral disease 39

1.5.2 Wound healing post epithelial injury 40

1.5.3 Epithelial-mesenchymal transition 43

1.6 Summary **46**

Chapter 2 - Methods ***48***

2.1 Clinical **48**
2.1.1 Patient recruitment: Post COVID-19 donors 48
2.1.2 Patient Recruitment: Healthy control donors 63
2.1.3 Demographics of donors for in-vitro assays 63
2.2 Radiology **65**
2.3 Physiology **65**
2.3.1 Routine lung function 65
2.3.2 Small airways testing 67
2.4 Flow cytometry **69**
2.5 Airway epithelial cell culture **72**
2.5.1 Submerged culture 73
2.5.2 Air liquid interface 74
2.5.3 Media used for cell culture 75
2.6 Fibroblast cell culture **76**
2.7 Influenza Stocks **76**
2.8 General techniques **76**
2.8.1 TEER measurements 76
2.8.2 Imaging 77
2.9 Gene expression **80**
2.9.1 RNA extraction 80
2.9.2 Complementary DNA (cDNA) synthesis 80
2.9.3 RNA sequencing 81
2.9.4 Quantitative polymerase chain reaction (qPCR) 82
2.10 Protein quantification **84**
2.10.1 O-link proteomic assay 84
2.10.2 Enzyme-linked immunosorbent assay (ELISA) 85
2.11 Statistical analysis **86**
2.11.1 Proteomics 86
2.11.2 Transcriptomics 86
2.11.3 Other analyses 86
Chapter 3 - Evaluating clinical trajectory post COVID-19 ..... ***87***
3.1 Introduction **87**
3.2 Background **87**
3.3 Hypothesis and Aims **87**
3.4 Methods **88**
3.5 Results **88**
3.5.1 Consort diagram 88
3.5.2 Baseline demographics and persistent symptomatology 91
3.5.3 Blood parameters 93
3.5.4 Psychological assessment 95
3.5.5 Quality of life assessment 97
3.5.6 Semi-structured interviews 102
3.6 Discussion **120**
3.6.1 Summary of findings 120
3.6.2 Findings in context of current literature 120
3.6.3 Clinical relevance of findings 122

3.6.4 Limitations 123
3.7 Conclusion 125
Chapter 4 - Evaluating radiological trajectory post COVID-19 126
4.1 Introduction 126
4.2 Background 126
4.3 Hypothesis and Aims 127
4.4 Methods 127
4.4.1 Patient cohort 127
4.4.2 CT imaging 127
4.4.3 Initiation of outpatient steroid therapy 128
4.4.4 Radiological scoring 128
4.5 Results 130
4.5.1 Consort diagram 130
4.5.2 Baseline characteristics 132
4.5.3 Non-fibrotic radiological abnormalities at 3 months 133
4.5.4 Fibrotic changes at 3 months 143
4.5.5 Radiological abnormalities and respiratory symptoms 145
4.5.6 Radiological abnormalities and lung function parameters 146
4.5.8 Radiological abnormalities and time from acute illness 148
4.5.9 Trajectory of radiological findings 149
4.5.10 Impact of outpatient steroid therapy on radiological abnormalities 151
4.6 Discussion 154
4.6.1 Summary of findings 154
4.6.2 Findings in context of current literature 155
4.6.3 Clinical relevance of findings 159
4.6.4 Limitations 159
4.7 Conclusion 159
Chapter 5 – Evaluating physiological recovery post COVID-19: Lung function and fractional exhaled nitric oxide 160
5.1 Introduction 160
5.2 Background 160
5.3 Hypothesis and Aims 160
5.4 Methods 161
5.5 Results 162
5.5.1 Consort diagram 162
5.5.2 Baseline characteristics 162
5.5.3 Lung function testing 164
5.5.4 FENO 172
5.5.4.2 Relationship with breathlessness 172
5.5.4.5 FENO results and admission neutrophil and lymphocyte counts 175
5.6 Discussion 180
5.6.1 Summary of findings 180
5.6.2 Findings in the context of current literature 181
5.6.3 Clinical relevance of findings 183
5.6.4 Limitations 183
5.7 Conclusion 183

Chapter 6 - Evaluating physiological recovery post COVID-19: Small airways disease 185

6.1 Introduction 185

6.2 Background 185

6.2.1 Small airways disease post COVID-19 185

6.2.2 Forced oscillometry technique 186

6.3 Hypothesis and Aims 187

6.4 Methods 187

6.5 Results 190

6.5.1 Consort diagram 190

6.5.2 Baseline demographics 190

6.5.3 Prevalence of small airways disease 192

6.5.4 Validating the cut-off used for selecting patients with SAD 192

6.5.5 SAD and lung function tests 195

6.5.6 SAD and FENO 197

6.5.7 SAD and patient-reported symptoms 198

6.5.8 Expiratory flow limitation 202

6.5.9 SAD and CT findings 204

6.6 Discussion 204

6.6.1 Summary of findings 204

6.6.2 Validation of cut-off 205

6.6.3 Findings in context of current literature 205

6.6.4 Clinical relevance of findings 207

6.6.5 Limitations 207

6.7 Conclusion 207

Chapter 7 - Understanding the airway microenvironment post COVID-19 209

7.1 Introduction 209

7.1.1 The function of immune cell subsets during acute infection 209

7.1.2 Detection of immune cell subsets 210

7.1.3 Airway immune cell subsets in healthy individuals 211

7.1.4 BALF findings in acute COVID-19 211

7.2 Background 212

7.3 Hypothesis and Aims 213

7.4 Methods 213

7.4.1 Patient recruitment 213

7.4.2 Endobronchial sampling 213

7.4.3 Definitions 214

7.4.4 Flow cytometry 214

7.4.5 Differential cell count analysis 215

7.4.6 Microbial, viral and fungal assessment 215

7.5 Results 215

7.5.1 Sample flow 215

7.5.2 Baseline characteristics 216

7.5.4 Immune populations using differential cell count analysis 218

7.5.4 Microbial analysis 220

7.5.5 BALF immune populations using flow cytometry 223

7.6 Discussion 238

7.6.1 Summary of findings 238

7.6.2 Findings in context of current literature 239

7.6.3 Clinical relevance of findings 245
7.6.4 Limitations 245

7.7 Conclusion 246

Chapter 8 - Evaluating epithelial function post COVID-19 247

8.1 Introduction 247
8.1.1 Studying epithelial cell biology 247
8.1.2 Studying epithelial responses to injury 248
8.1.3 Epithelial-mesenchymal crosstalk 249

8.2 Background 249

8.3 Hypothesis and Aims 250

8.4 Methods 250
8.4.1 Baseline characteristics at ALI 250
8.4.2 Response to injury 251
8.4.3 Fibroblast scratch assay 252

8.5 Results 253
8.5.1 Epithelial cell scratch assay 253
8.5.2 Epithelial cell proliferation 255
8.5.3 Baseline characteristics at ALI 261
8.5.4 Flu challenge Model 264

8.6 Discussion 277
8.6.1 Summary of findings 277
8.6.2 Findings in context of current literature 277
8.6.3 Clinical relevance of findings 283
8.6.4 Limitations 283

8.7 Conclusion 285

Chapter 9 - Assessing the role of DPP4 in the airways 286

9.1 Introduction 286
9.1.1. DPP4 286
9.1.2 AREG 287
9.1.3 Relationship between DPP4 and AREG 288

9.2 Background 288

9.3 Hypothesis and Aims 288

9.4 Methods 289
9.4.1 Epithelial cells: Submerged culture 289
9.4.2 Epithelial cells: Air-liquid interface 290
9.4.3 Fibroblast culture 291

9.5 Results 292
9.5.1 DPP4 and AREG protein in BALF 292
9.5.2 Gene expression of AREG and DPP4 in differentiated PBECs at air-liquid interface 294
9.5.3 Baseline DPP4 and AREG levels and epithelial cell wound closure 299
9.5.4 Effect of IAV infection on DPP4 301
9.5.5 Effect of DPP4 stimulation or inhibition on PBECs cultured to air-liquid interface 302
9.5.6 Effect of DPP4 stimulation or inhibition on basal cells 314
9.5.7 Effect of DPP4 stimulation or inhibition on AREG production 319
9.5.8 Effect of DPP4 stimulation or inhibition on fibroblast activity 324

9.6 Discussion 326
9.6.1 Summary of findings 326

9.6.2 Findings in context of current literature 327
9.6.3 Clinical relevance of findings 332
9.6.4 Limitations 332
9.7 Conclusion 332
Chapter 10 - Discussion and Future work 333
10.1 Summary of thesis aims 333
10.2 Summary of findings 333
10.3 Summary of limitations 335
10.4 Implications of findings 335
10.4.1 Clinical impact 335
10.4.2 Translational impact 336
10.5 Future research 336
10.6 Conclusion 337
Chapter 11 – References 338
Chapter 12 - Appendix 374
Appendix 1: Study protocol for PHENOTYPE (V1.2 7th Feb 2021) 374
Appendix 2: Patient information sheet and informed consent form for PHENOTYPE 375
Appendix 3 Topic guide for semi-structured interviews 385

List of Tables

Table 2. 1 Modified Medical Research Council Score 50
Table 2. 2 How to convert SF36 scores to a scale of 0 - 100. 59
Table 2. 3 Calculating average scores for each domain 60
Table 2. 4 US population means and weighting coefficients for PCS and MCS scores 61
Table 2. 5 Donor characteristics for epithelial cells utilised in thesis 64
Table 2. 6 Antibodies for flow cytometry staining 71
Table 2. 7 Antibody dilutions for flow cytometry staining 71
Table 2. 8 Primary antibodies for staining of ALI sections 79
Table 2. 9 Human Taqman primers for qPCR 84
Table 2. 10 O-link assays performed on BALF samples 84
Table 2. 11 ELISA kits used 85

Table 3. 1 Demographics and hospital admission data for patients recruited to PHENOTYPE 92
Table 3. 2 Participant and interview data for semi-structured interviews 103

Table 4. 1 Baseline characteristics of patients undergoing CT imaging 132
Table 4. 2 Demographic and admission data according to CT findings (W1 and W2) 139
Table 4. 3 Demographics of patients not admitted to hospital 141
Table 4. 4 Clinical data of patients with fibrosis on 3-month CT 144

Table 5. 1 Clinical characteristics of patients undergoing PFTs (W1 and W2) 163
Table 5. 2 Clinical characteristics of patients undergoing FENO testing 164
Table 5. 3 Abnormalities in PFTs 165
Table 5. 4 Associations between % predicted TLCO at 3 months post discharge and markers of acute disease severity 167
Table 5. 5 Admission bloods and FENO results at 3- and 12-months post discharge 174
Table 5. 6 BALF differential cell count analysis in patients with abnormal FENO 177

Table 6. 1 Demographics and admission data of patients undergoing FOT 191
Table 6. 2 Resistance and reactance values of the full cohort 195
Table 6. 3 Differences in PFTs in those with SAD vs no SAD (Full cohort) 197

Table 7. 1 Clinical, radiological and physiological data of individuals undergoing endobronchial sampling 217
Table 7. 2 Clinical differential cell counts in BALF 219
Table 7. 3 Abnormal differential cell count analysis stratified according to respiratory support 220
Table 7. 4 BALF microscopy and culture results 222

List of Figures

Figure 1. 1 Illustration of ultrastructural morphology of coronaviruses 26
Figure 1. 2 CT images from two individuals hospitalized for acute SARS-COV2 infection 28
Figure 1.3 Epithelial response to viral infection 39
Figure 1. 4 Epithelial cells and wound repair 42
Figure 1. 5 EMT in wound healing 43
Figure 1. 6 Summary of PhD aims 47

Figure 2. 1 Study procedures for PHENOTYPE. 49
Figure 2. 2 Hospital Anxiety and Depression Scale (HADS) 52
Figure 2. 3 SF36 questionnaire 54
Figure 2. 4 Summary of lung volumes 67
Figure 2. 5 Tracheo-bronchial divisions 68
Figure 2. 6 Gating strategy for flow cytometry 72

Figure 3. 1 CONSORT diagram of patients recruited to the PHENOTYPE study 90
Figure 3. 2 Violin plots of admission and follow up bloods (W1) 94
Figure 3. 3 Violin plots of admission and follow up bloods (W2) 95
Figure 3. 4 HADS questionnaire results (W1) 96
Figure 3. 5 HADS questionnaire results (W2) 97
Figure 3. 6 Trajectory of SF36 scores (W1) 99
Figure 3. 7 Trajectory of SF36 scores (W2) 100
Figure 3. 8 Violin plots of SF36 component scores (W1) 101
Figure 3. 9 Violin plots of SF36 component scores (W2) 102
Figure 3. 10 Trajectory of SF36 scores in patients undergoing interviews 104
Figure 3. 11 Themes derived through qualitative analysis 105

Figure 4. 1 Comparing Radiologists' and my CT scores 129
Figure 4. 2 Consort diagram of patients undergoing CT imaging (W1) 130
Figure 4. 3 Consort diagram of patients undergoing CT imaging (W2) 131
Figure 4. 4 Patterns of radiological abnormalities at 3-month follow-up 134
Figure 4. 5 CT scores at 3-month follow-up during (W1 and W2) 135
Figure 4. 6 Classification of extent of CT abnormalities (W1 and W2) 136
Figure 4. 7 Admission blood results according to CT findings (W1) 139
Figure 4. 8 Admission blood results according to CT findings (W2) 140
Figure 4. 9 Three-month blood results according to CT findings (W1) 142
Figure 4. 10 Three-month blood results according to CT findings (W2) 143
Figure 4. 11 Fibrosis on CT imaging at 3-month follow up 145
Figure 4. 12 Patient-reported breathlessness and CT abnormality 145
Figure 4. 13 Relationship between CT score and lung function parameters at 3 months (W1) 146
Figure 4. 14 Relationship between CT score and lung function parameters at 3 months (W2) 147
Figure 4. 15 Relationship between CT score at 3 months and acute admission parameters 148
Figure 4. 16 Flow diagram of patients undergoing CT imaging at 1 year (W1) 149
Figure 4. 17 Flow diagram of patients undergoing CT imaging at 1 year (W2) 150
Figure 4. 18 Changes in CT scores over 12 months 151
Figure 4. 19 Absolute change in CT scores according to outpatient steroid therapy 151
Figure 4. 20 Radiological trajectory without steroid therapy 152
Figure 4. 21 Radiological trajectory with inpatient steroid therapy only 153
Figure 4. 22 Radiological trajectory with inpatient and outpatient steroid therapy 154

Figure 5. 1 Flow diagram of patients undergoing lung function testing 162
Figure 5. 2 Venn diagram showing overlap of PFT abnormalities at 3 months post discharge..... 165
Figure 5. 3 Patient-reported breathlessness stratified according 3-month PFTs (W1) 168
Figure 5. 4 Patient-reported breathlessness stratified according to 3-month PFTs (W2)..... 169
Figure 5. 5 Trajectory of PFTs over 1 year period (W1)..... 170
Figure 5. 6 Trajectory of PFTs over 1 year period (W2)..... 171
Figure 5. 7 FENO results at 3 and 12 months post discharge..... 172
Figure 5. 8 FENO results and degree of respiratory support during admission 173
Figure 5. 9 FENO results according to admission peripheral neutrophil and lymphocyte count..... 175
Figure 5. 10 Relationship between admission neutrophil and lymphocyte counts and FENO results 176
Figure 5. 11 Serum eosinophil count and FENO results 178
Figure 5. 12 BALF cellularity and damage markers in individuals with abnormal FENO 179
Figure 5. 13 Trajectory of FENO results over 12-month period 180

Figure 6. 1 Consort diagram of patients undergoing FOT assessment..... 190
Figure 6. 2 Resistance and reactance values of amended cohort 194
Figure 6. 3 Differences in PFTs in those with SAD vs no SAD (Amended cohort)..... 196
Figure 6. 4 Differences in FENO in those with SAD vs no SAD..... 198
Figure 6. 5 Resistance and reactance values according to patient-reported breathlessness (Amended cohort)..... 199
Figure 6. 6 Resistance and reactance values according to patient-reported breathlessness (Full cohort)..... 200
Figure 6. 7 Resistance and reactance values according to patient-reported cough (Amended cohort) 201
Figure 6. 8 Resistance and reactance values according to patient-reported cough (Full cohort)..... 202
Figure 6. 9 Expiratory flow limitation in those with SAD vs no SAD..... 203
Figure 6. 10 HRCT images of the 6 individuals diagnosed with SAD 204

Figure 7. 1: Sample flow after endobronchial sampling..... 215
Figure 7. 2 Radiological trajectory of individual with BALF lymphocytosis of 35.3% 220
Figure 7. 3 BALF immune cells detected by flow cytometry 224
Figure 7. 4 BALF immune cells according to acute disease severity 226
Figure 7. 5 Relationship between BALF cell counts and 3-month CT score 227
Figure 7. 6 Relationship between BALF immune cell proportions and 3-month CT score..... 228
Figure 7. 7 Relationship between BALF immune cells and PFTs 230
Figure 7. 8 BALF immune cells according to % predicted TLCO at 3 months 232
Figure 7. 9 Relationship between BALF immune cells and 1 CT score 234
Figure 7. 10 Relationship BALF immune cells and change in CT scores between 3 and 12 months .. 235
Figure 7. 11 BALF immune cells according to % predicted TLCO at 1 year. 236
Figure 7. 12 Relationship between immune cells detected using flow cytometry and differential cell count 238

Figure 8. 1 Overview of IAV challenge..... 252
Figure 8. 2 Wound healing assay..... 254
Figure 8. 3 Proliferation assay..... 256
Figure 8. 4 Heterogeneity in wound closure in post COVID-19 donor PBECs 257
Figure 8. 5 Relationship between wound closure and clinical and radiological parameters 258
Figure 8. 6 Relationship between wound closure and age, time from hospital admission and discharge 259

Figure 8. 7 Relationship between wound closure and peripheral blood results during acute admission 260
Figure 8. 8 AREG measured in basal supernatants during wound healing assay 261
Figure 8. 9 Transepithelial electrical resistance at 3 weeks post air exposure 262
Figure 8. 10 Gene expression of differentiation markers at 3 weeks post air exposure 262
Figure 8. 11 Visualising the epithelium 3 weeks post air exposure 263
Figure 8. 12 Changes in TEER post IAV challenge 265
Figure 8. 13 H+E stains of PBECs at ALI after IAV infection 266
Figure 8. 14 Gene expression of ISGs post IAV infection (Transcriptomics) 267
Figure 8. 15 Gene expression of EGFR ligands post IAV infection (Transcriptomics) 267
Figure 8. 16 Gene expression of matrix metalloproteinases post IAV infection (Transcriptomics) 267
Figure 8. 17 Most differentially expressed genes at 48 hours and 72 hours post IAV infection. 268
Figure 8. 18 Gene expression of ISGs and Flu M1 post IAV infection (qPCR) 270
Figure 8. 19 Inflammatory and interferon levels in basal supernatant post IAV infection (ELISA) 272
Figure 8. 20 Gene expression of EGFR ligands after IAV infection (qPCR) 273
Figure 8. 21 AREG and HBEGF in basal supernatant 72 hours post IAV infection (ELISA) 274
Figure 8. 22 Fibroblast scratch assay with conditioned media 276

Figure 9. 1 DPP4 and AREG detected by O-link in the BALF supernatants 293
Figure 9. 2 Relationship between DPP4 and AREG in BALF supernatant 294
Figure 9. 3 DPP4 and AREG gene expression at 3 weeks post air exposure 294
Figure 9. 4 DPP4 and AREG measured in the supernatants of PBECs at ALI (3 weeks post air exposure) 295
Figure 9. 5 AREG and DPP4 in supernatants of PBECs at ALI (5-7 weeks post air exposure) 296
Figure 9. 6 Relationship between DPP4 and AREG in the supernatants at 3 weeks post air exposure 297
Figure 9. 7 Relationship between DPP4 and AREG in supernatants at 5-7 weeks post air exposure. 298
Figure 9. 8 Changes in DPP4 and AREG levels at 3 and 6 weeks* post air exposure 299
Figure 9. 9 Relationship between % wound closure at 24 hours and AREG, DPP4 300
Figure 9. 10 Gene expression of DPP4 post IAV challenge 301
Figure 9. 11 DPP4 in basal supernatants of PBECs cultured at ALI post IAV challenge 302
Figure 9. 12 Cell differentiation markers after basal stimulation with DPP4 or sitagliptin for 3 weeks 303
Figure 9. 13 Cell differentiation markers after 72-hour basal stimulation with sitagliptin 304
Figure 9. 14 Differentiation and EMT markers after 72-hour basal stimulation with DPP4 or sitagliptin 305
Figure 9. 15 Immune and wound healing response to IAV challenge +/- basal sitagliptin treatment 307
Figure 9. 16 IL6 level in basal supernatants 307
Figure 9. 17 IL6 and IL8 after IAV challenge with concurrent apical or basal treatment with DPP4 or sitagliptin 309
Figure 9. 18 IL 6 and 8 after apical or basal treatment with DPP4 or sitagliptin 310
Figure 9. 19 ISG, interferon and AREG response post IAV challenge with concurrent basal treatment with DPP4 or sitagliptin 313
Figure 9. 20 IL6, IL8 and IFN beta in basal supernatant after IAV challenge and basal treatment with DPP4 or sitagliptin 314
Figure 9. 21 Basal cell proliferation in response to DPP4 stimulation 315
Figure 9. 22 Basal cell proliferation in response to sitagliptin. 316
Figure 9. 23 Wound closure in response to DPP4 treatment 317
Figure 9. 24 Wound closure in response to sitagliptin treatment 318
Figure 9. 25 AREG in supernatants after continuous basal stimulation with DPP4 or sitagliptin for 3 weeks. 319

Figure 9. 26 AREG in basal supernatant after 72-hour stimulation of differentiated epithelial cells with DPP4 or sitagliptin 320
Figure 9. 27 AREG in basal supernatant after IAV challenge and basal treatment with DPP4 or sitagliptin 321
Figure 9. 28 AREG in basal supernatant of submerged PBECs treated with DPP4 or sitagliptin for 48 hours. 322
Figure 9. 29 AREG in basal supernatant 24 hours after scratch assay and treatment with DPP4 or sitagliptin 323
Figure 9. 30 Fibroblast proliferation in response to DPP4 treatment 324
Figure 9. 31 Fibroblast proliferation in response to sitagliptin treatment 325
Figure 9. 32 Fibroblast wound closure after treatment with DPP4 or sitagliptin 326

Abbreviations

ACE 2	Angiotensin converting enzyme 2
ACTA2	Actin Alpha 2, smooth muscle
AF	Atrial fibrillation
AFB	Acid fast bacilli
ALI	Air-liquid interface
Alpha SMA	Alpha smooth muscle actin
ARDS	Acute respiratory distress syndrome
AREG	Amphiregulin
AT2	Alveolar type 2 cells
Ax	Area of reactance
BALF	Bronchoalveolar lavage fluid
MERS	Middle east respiratory syndrome
BMI	Body mass index
CD	Cluster of differentiation
CDH1	Cadherin 1
COPD	Chronic obstructive pulmonary disease
COVID-19	Coronavirus disease - 19
CPAP	Continuous positive airway pressure
CXR	Chest X-ray
CT	Computed tomography
CTPA	Computed tomography pulmonary angiography
CXCL10	C-X-C motif chemokine 10
DAD	Diffuse alveolar damage
DAPI	4’,6-diamidino-2-phenylindole
DCC	Differential cell count
DMEM	Dulbecco's Modified Eagle Medium
DPP4	Dipeptidyl peptidase 4
ECM	Extracellular matrix
EDTA	Ethylenediaminetetraacetic acid
EGF	Epidermal growth factor
ELISA	Enzyme-linked immunosorbent assay
EMT	Epithelial-mesenchymal transition
EREG	Epiregulin
FBS	Fetal bovine serum
FENO	Fractional exhaled nitric oxide
FEV1	Forced expiratory volume in 1 second
FITC	Fluorescein isothiocyanate
FN1	Fibronectin 1
FOT	Forced oscillometry testing
FOXJ1	Forkhead Box J1
Fres	Resonant frequency
FVC	Forced vital capacity
GGO	Ground glass opacification
H&E	Haematoxylin and eosin
HADS	Hospital anxiety and depression scale
HBEGF	Heparin binding EGF like growth factor
HC	Healthy control

(C)HP	(Chronic) hypersensitivity pneumonitis
HPI	Hours post infection
HR QOL	Health-related quality of life
HRCT	High resolution CT
HTN	Hypertension
IAV	Influenza A virus
IFN	Interferon
IHD	Ischaemic heart disease
IL6	Interleukin 6
IL8	Interleukin 8
ILD	Interstitial lung disease
IPF	Idiopathic pulmonary fibrosis
ISG	Interferon stimulated gene
KCO	Carbon monoxide transfer coefficient
KRT5	Cytokeratin 5
LDH	Lactate dehydrogenase
LOS	Length of stay
M C+S	Microscopy, culture and sensitivity
MCS	Mental component score
MEF 25-75	Mid expiratory flow (25 – 75% FVC)
MET	Mesenchymal epithelial transition
mg	Milligrams
µl (mcl)	Microlitre
µg (mcg)	Microgram
µmol	Micromole
ml	Millilitres
MMP	Matrix metalloproteinases
mmRC	Modified medical research council
mRNA	Messenger RNA
MUC5AC	Mucin 5AC
MV	Mechanical ventilation
NIV	Non-invasive ventilation
ng	Nanograms
NK	Natural killer
O2	Oxygen
OAD	Obstructive airways disease
OAS2	2'-5'-oligoadenylate synthetase 2
OSA	Obstructive sleep apnoea
PAS	Periodic acid Schiff
PBEC	Primary bronchial epithelial cell
pCOVID	Post COVID-19
PCS	Physical component score
PFA	Paraformaldehyde
PFT	Pulmonary function test
pg	Picograms
pH	Potential of hydrogen
PPV	Positive pressure ventilation
qPCR	Quantitative polymerase chain reaction
R20	Resistance at 20Hz
R5	Resistance at 5 Hz

R5ex	Expiratory resistance at 5Hz
R5in	Inspiratory resistance at 5Hz
RIN	RNA integrity number
rpm	Revolutions per minute
RQN	RNA quality number
RSAD2	Radical S-Adenosyl Methionine Domain Containing 2
RNA	Ribonucleic acid
rRNA	Ribosomal RNA
RV	Residual volume
SAD	Small airways disease
SARS-COV1	Severe acute respiratory syndrome coronavirus 1
SARS-COV2	Severe acute respiratory syndrome coronavirus 2
SF36	Short-form 36
sGawtot	Total specific airway conductance
SNLR	Serum neutrophil:lymphocyte ratio
sRAWtot	Total specific airway resistance
T2DM	Type 2 diabetes mellitus
TEER	Trans-epithelial electrical resistance
TGF	Transforming growth factor
TJP1	Tight junction protein 1
TLC	Total lung capacity
TLCO	Transfer capacity of the lungs for carbon monoxide
TMPRSS2	Transmembrane serine protease 2
tRNA	Transfer RNA
TNF	Tumour necrosis factor
UV	Ultraviolet
W1	Wave 1
W2	Wave 2
X5	Reactance at 5Hz
X5ex	Expiratory reactance at 5Hz
X5in	Inspiratory reactance at 5Hz

Chapter 1 – Introduction

1.1 Severe acute respiratory syndrome coronavirus 2 (SARS-COV2)

1.1.1 Background

SARS-COV2 is a pathogenic and highly transmissible coronavirus which was first discovered in Wuhan, China in December 2019. It soon spread globally and the first case was identified in the UK on 29th January 2020.[1] Soon after its virulence and pathogenicity had been realised, a pandemic was declared by the World Health Organisation (WHO) on 26th March 2020.[2] Previously, two other coronaviruses, Severe Acute Respiratory Syndrome Coronavirus 1 (SARS-COV1) and Middle East Respiratory Syndrome Coronavirus (MERS) caused fatal respiratory pneumonia, resulting in global pandemics in 2002 and 2012, and since then, emerging coronaviruses have been a public health concern.[3] To-date, SAR-COV2 has caused over 6.9 million deaths worldwide.[4]

1.1.2 Structure of the virus

SARS-COV2 is a betacoronavirus 2B lineage with 79.5% homology to the genome of SARS-COV1 and 50% homology to MERS.[5] Structurally, it consists of 4 main glycoproteins: spike (S), envelope (E), membrane (M) and nucleocapsid (N). The S protein consists of 2 subunits, S1 and S2, with S1 containing the receptor-binding domain (RBD) which binds to the host cell angiotensin converting enzyme (ACE2) receptor.[6,7] Figure 1.1 shows an illustration of the ultrastructural morphology of coronaviruses.

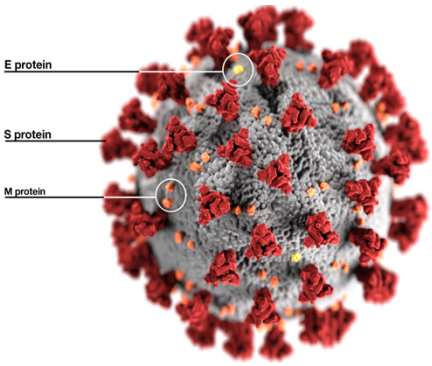


Figure 1. 1 Illustration of ultrastructural morphology of coronaviruses
Produced by the Centres for Disease Control and Prevention (CDC)

1.1.3 Variants

Four main variants have been described, in order of emergence: Alpha, Beta, Gamma, Delta and Omicron.

In the UK, the most publicised first variant was alpha B1.1.7, which was first detected in the UK in November 2020; The beta variant (B.1.351) was first detected in South Africa in May 2020; Gamma P.1. was first detected in Brazil in November 2020; Delta B.1.617.2 was detected in India in October 2020. Omicron B.1.1.529 has been circulating since November 2021 and is currently the variant of concern.[8,9]

1.2 Acute SARS-COV2 infection – a clinical overview

1.2.1 Clinical symptoms

COVID-19 causes a wide range of symptoms of varying severity in individuals, with the commonest symptoms being fever, cough, anosmia, taste disturbances, breathlessness, fatigue and diarrhoea. In some individuals, it causes only mild respiratory symptoms, which can be managed in the community, and in others, fatal pneumonia.[10,11] It is estimated that in up to 45% of COVID-19 cases, patients are asymptomatic.[12,13]

Older age, male gender, obesity, certain comorbidities (including diabetes, respiratory disease, kidney disease and cardiac disease), social deprivation and being from a black, asian or minority ethnic background are risk factors for increased mortality associated with COVID-19.[14,15]

The severity and nature of symptoms has varied between the different variants, likely a consequence of a combination of factors: reduced virulence in successive variants, immunity due to previous infection and/or vaccination and the introduction of new medical treatments to reduce the risk of disease progression.

1.2.2 Radiological abnormalities

A variety of radiological changes have been noted in the literature, with the commonest abnormalities during acute SARS-COV2 infection being ground-glass opacities (GGO), seen in >50% of individuals, and a combination of ground-glass opacities (GGO) and consolidation seen in up to 44% of

patients.[16,17] (Figure 1.2) Sometimes, ancillary findings such as crazy-paving, reversed halo sign and septal thickening are also seen.[16,18]

Moreover, a predilection for bilateral, multi-focal and peripheral radiological changes has been described in the literature.[16] Whilst the commonest finding early on is GGO, there is often a temporal change with a combination of GGO and consolidation or consolidation alone by the second to third week of disease with regression to pure GGO later on in the disease course. The peak of radiological abnormalities is often between six and eleven days after symptom onset and during the early stages of infection, computed tomography (CT) imaging findings may be unremarkable.[19,20] In fact, Bernheim et al (2020) found that 20/36 (56%) of individuals imaged within 2 days of symptom onset, had normal CT images. Furthermore, the rate of false negatives decreased to 9% 3-5 days after symptom onset and even further to 4% at 6-12 days.[21]

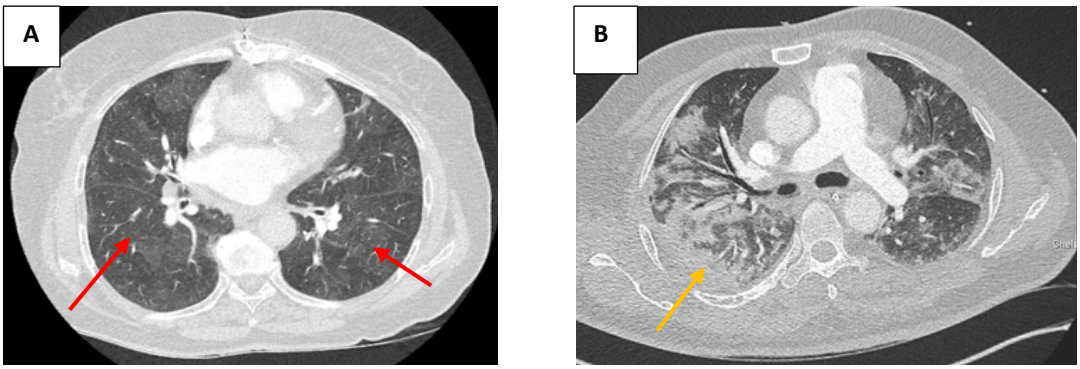


Figure 1. 2 CT images from two individuals hospitalized for acute SARS-COV2 infection
A) Bilateral ground-glass opacification (Red arrows) B) Consolidation (Yellow arrows)

Whilst the CT findings are not unique or specific to SARS-COV2 infection and can be seen in other viral pneumonias, the extent and evolution of CT findings is important to note as timing of imaging is therefore important when using CT imaging to diagnose COVID-19, and when assessing resolution. The CT findings likely represent diffuse alveolar damage and as such, more extensive radiological involvement during the acute disease has been associated with increased risk for mechanical ventilation and higher mortality risk.[22–24]

1.2.3 Peripheral biomarkers of disease severity

Peripheral blood sampling has shown that higher white cell count, C-reactive protein, D-dimer, fibrinogen and neutrophil-lymphocyte ratios, thus reflecting higher levels of systemic inflammation,

are associated with a higher risk of acute respiratory distress syndrome (ARDS) and death.[25–27] Furthermore, peripheral lymphopenia, although sometimes seen in other viral illnesses, is often more prolonged and protracted in SARS-COV2 infection and associated with more severe disease with reduction in both CD4 and CD8 T cell subsets.[28,29]

1.2.4 Drug treatments

A number of drug treatments with mortality benefits or benefits in reducing the risk of disease progression have now been approved for the acute management of COVID-19 in the UK. These include oral steroids in those requiring hospital admission and respiratory support,[30] antivirals,[31–33] monoclonal antibodies[34–37] and janus kinase inhibitors[38,39] and have been incorporated in the National Institute of Clinical Excellence (NICE) guidelines.[40] In addition, inhaled budesonide has been shown to be efficacious in reducing hospitalizations for COVID-19 if administered early[41] and more recently, favipiravir has been shown to improve clinical outcomes in certain groups of hospitalised patients.[42]

1.3 Pathogenesis

1.3.1 Target cells

The initial site of SARS-COV2 infection is the sino-nasal epithelium.[43] However, failure of the host innate immune response to contain the infection can result in rapid and progressive involvement of the epithelial cells lining the conducting airways and alveoli.[44] The SARS-COV2 spike (S) protein has a high affinity for the cell surface ACE 2 receptor and the transmembrane protease TMPRSS2 facilitates viral entry into the host cell by cleaving the S protein. Therefore, cells expressing these surface markers, such as secretory goblet cells, multi-ciliated epithelial cells and alveolar type 2 (AT2) epithelial cells, are the primary targets for SARS-COV2 infection.[45] Alveolar Type 1 (AT1) epithelial are more resistant to direct infection from SARS-COV2 and damage to these cells is likely due to the significant inflammatory response triggered by the acute infection.[46]

1.3.2 Epithelial responses to SARS-COV2 infection

One of the first cellular responses to viral infection is the production of type 1 (IFN I) and type III (IFN III) interferons, followed by upregulation of interferon-stimulated genes (ISGs).[47] The type I interferons are predominantly IFN alpha and beta and type III interferons are IFN lambda (1-4). These interferons are crucial in controlling viral replication and facilitating viral clearance from infected cells.

In primary cell cultures, an attenuated type I and III response to SARS-COV2 has been shown, which may contribute to the pathogenicity of the virus. To support this, in this study, treatment with interferon beta resulted in reduced viral replication in alveolar cells.[48] This is line with what was observed in mouse models, where infection with SARS-COV1 resulted in delayed IFN I signalling promoting the accumulation of inflammatory macrophages and significant cytokine release as well as T cell apoptosis.[49] The authors concluded that early, but cautious introduction of IFN beta may alleviate the damage from an exuberant immune system.

Similarly, the utility of interferon lambda needs to be carefully considered. In a mouse model of SARS-COV2, IFN lambda administration, both prophylactically (18 hours pre infection) or therapeutically (12 hours post infection) to primary human airway epithelial cells resulted in reduced SARS-COV2 viral replication.[50] However, delayed IFN lambda administration, as performed by Major et al. in a mouse model of influenza infection, impaired lung repair by reducing epithelial cell proliferation and differentiation.[51] Therefore, whilst IFN lambda may be efficacious in controlling viral replication, it can impair tissue repair mechanisms if administered late. Moreover, chronic exposure to IFN lambda may result in further damage to the lung epithelium and increased susceptibility to bacterial infections as seen in the study by Broggi et al., where repeated activation of toll-like receptor 3 (TLR3) resulted in increased production of IFN lambda by dendritic cells, further perpetuating tissue damage. The authors conclude that TLR3 stimulation can also be from viral remnants in dying cells, rather than infected dendritic cells which could be one of the driving factors for the immunopathology seen in SARS-COV2 (and also seen in SARS-COV1)[52,53] where immune activation persists, even beyond peak viral loads.[54,55]

Furthermore, epithelial cell damage during SARS COV2 ARDS is likely due to cellular necrosis, rather than apoptosis, with the former thought to be much more immunogenic, through the release of damage associated molecular patterns (DAMP) from dying cells. This in turn may drive the ARDS seen in COVID-19. Furthermore, in a COVID-19 animal model, administration of an inhibitor of high mobility group box 1 protein (HMGB1), which is a DAMP, reduced alveolar tissue injury, again suggesting that DAMP-driven epithelial cell necrosis could be contributing to the exaggerated immune cascade seen in COVID-19.[56]

Despite the promising effects of IFN beta in open label and phase 2 trials,[57,58] subcutaneous delivery of IFN beta 1a in combination with remdesivir in a phase 3 randomised controlled trial showed no superiority to remdesivir alone, and instead, in patients requiring higher respiratory support at

baseline, administration of IFNbeta 1a, resulted in deterioration of clinical outcomes compared to placebo alone, especially in respiratory status.[59] On the contrary, treatment with pegylated interferon lambda resulted in an accelerated decline in viral clearance in outpatients, in a phase 2 trial, again emphasising that timing of treatment is key to response.[60]

1.3.3 Local immune responses to SARS COV2 infection

Endobronchial sampling in individuals with SARS-COV2 ARDS requiring mechanical ventilation has revealed increased cellularity of the bronchoalveolar lavage fluid (BALF), with significant neutrophilia and increased lymphocytosis. In addition, the lymphocytosis consisted mainly of activated lymphocytes if endobronchial sampling was performed earlier on after intubation.[61] Adding to this, single-cell RNA sequencing data has shown an increase in monocyte-derived macrophages relative to tissue-resident macrophages in patients with severe COVID-19. In severe disease, mononuclear phagocytes comprised 80% of total BALF cells, as compared to 60% in mild cases, with healthy controls only having 40%.[62] Furthermore, chemokines associated with monocyte recruitment to the airways (for instance, CCL2 and CCL7) were upregulated in the BALF,[63] again, suggesting that recruitment of monocytes to the airways is important during acute disease. The reason for this is not clear, but the observation that monocyte infiltration was low where BALF resident T cells was elevated, may suggest that monocyte recruitment was to facilitate viral clearance.[64] Additionally, paired T cell receptor tracking has shown evidence of migration of T cells from the peripheries to the airways, providing a possible explanation for the peripheral lymphopenia reported in severe, acute COVID-19.[65] An alternative theory proposed for peripheral lymphopenia is lymphocyte apoptosis. Xiong et al (2020) showed using transcriptomics on peripheral blood, that genes associated with p53 signalling are upregulated post COVID-19, thus suggesting that apoptosis may be the mechanism by which peripheral lymphopenia occurs in severe COVID-19.[66] It is also possible, that even without apoptosis, T cell exhaustion, as evidenced by reduced activated T cells, in both the peripheries and BALF in individuals with longer duration of disease, might be contributing to pathogenesis in COVID-19.[67] In this latter study, a negative relationship between peripheral T Cells and BALF T cells was not found, contradicting the theory of T cell migration to the site of infection. Regardless, there is evidence of an altered immune signature, both in the BALF and peripheries in COVID-19.

The reason for an overactive immune system is not clear. However, persistent viral antigen driving immune activity to facilitate viral clearance is one possibility. Indeed, studies have shown long durations of viral shedding, from several weeks to even months after onset of symptoms so persistent viral antigen is a plausible explanation.[68,69] Furthermore, in the context of T cell exhaustion and a low

Type 1 interferon response to SARS-COV2,[49,70] effective anti-viral killing may not be possible, resulting in further recruitment of neutrophils and monocytes to the airways, thus perpetuating the inflammatory cascade.[49] In addition, as previously discussed, necrotic death of the alveolar cells in response to severe infection could also be triggering the inflammatory cascade.[56]

1.3.4 Histological evidence post SARS-COV2 infection

The main source of histological evidence in COVID-19 is from autopsy findings. Severe injury of the infected bronchial epithelium has been shown, with resultant inflammatory infiltrate, predominantly T lymphocyte in origin, as well as detectable SARS-COV2 virus in ciliated cells.[71]

Examination of the alveolar cells has shown similar changes, with evidence of diffuse alveolar damage (DAD), desquamation of pneumocytes, formation of hyaline membranes and alveolar oedema.[71,72] Furthermore, SARS-COV2 viral particles could be detected in the AT2 cells as well.[71,73] Reassuringly, proliferating cells were seen in the alveoli, larger airways and smaller airways suggesting initiation of epithelial repair mechanisms in the respiratory and alveolar epithelium.[74] Importantly, histological appearances seen in SARS-COV2-induced DAD were similar to that from other causes.[75,76] They were also similar to that seen in SARS-COV1 and MERS.[77,78]

AT2 cells have many functions, but two main functions worth highlighting are a) production of surfactant and b) epithelial cell regeneration after acute lung injury.[79] Alveolar regeneration post COVID-19 has been described in vitro[80] but the timescale for this recovery in vivo is not known. In the instance of delayed recovery, increased alveolar collapse on expiration due to insufficient surfactant production may contribute to the persistent airway disease, and in particular small airways disease.

1.4 Long-term consequences post COVID-19

At the time of commencing this PhD, the long-term effects of SARS-COV2 infection were not known. The Severe Acute Respiratory Syndrome coronavirus 1 (SARS-COV1) and Middle East Respiratory Virus (MERS) pandemics had resulted in persistent respiratory morbidity including physiological and radiological abnormalities lasting up to 1 year post hospital discharge. It is therefore possible that patients' recovery post COVID-19 can also be complicated.

1.4.1 Clinical symptoms

After SARS-COV1, clinical symptoms, physiological and quality of life impairment were present even 6 months post hospital discharge. Persistent symptoms included breathlessness, cough and fatigue.[81,82]

However, persistent symptoms post a viral illness are not uncommon. A post-viral cough can linger for more than 3 weeks and if lasting more than 8 weeks, is deemed to be "chronic" in nature and requiring further investigations.[83] During the acute phase, a variety of factors induced by viral injury can precipitate a cough: epithelial inflammation, increased tachykinins, reduced neutral endopeptides and increased mucous production.[84] A persistent cough can occur in some individuals after a viral infection due to cough hypersensitivity with airway inflammation causing changes in airway mucosal innervation[85]and even if the aetiology is benign, can have a significantly negative impact on quality of life.[86,87]

Additionally, about 50% of individuals who develop chronic fatigue syndrome (CFS) do so after an acute viral illness.[88] The precise mechanism for this is not known, but, an immunological basis is possible.[89] Furthermore, low mood and anxiety, which are likely to be experienced by patients post COVID-19, given the significant impact of COVID-19 on social factors, is associated with chronic fatigue.[90]

Breathlessness is a complex symptom and often multifactorial, caused by many factors including respiratory or cardiac disease, raised body mass index and mood disturbances.[91] Sometimes, there is a discordance between true breathlessness and the perception of breathlessness[92,93] with a variety of coping mechanisms employed to reduce impact on quality of life. Better understanding the underlying aetiology of breathlessness, beyond physiological and radiological impairment, is crucial to enable effective management of symptoms.[94]

It is important to note that psychological stressors during COVID-19, including bereavement, job loss and social isolation could all contribute to altered or heightened perception of residual symptoms, so a holistic approach needs to be taken when evaluating and managing these individuals.

1.4.2 Radiological abnormalities

1.4.2.1 Radiological abnormalities post viral pneumonia

Radiological abnormalities during the recovery phase after the SARS-COV1 and MERS pandemics were common, with GGO being the most frequently seen abnormality.[95,96]Antonio et al. (2003) showed during the SARS pandemic that abnormalities on CT were present in 96% (n=23/24) at an average of 36.5 days post hospital discharge.[97] Even at 6 month follow up, the prevalence of abnormalities remained high at 75% in Ng et al's study of 43 individuals.[98]

In addition, lung fibrosis was frequently seen in patients during the SARS and MERS pandemics.[97,99,100] For instance, in one study of 311 SARS-COV1 survivors, fibrosis was identified in 67 (21.5%) individuals within 65 days of discharge when fibrosis was defined as the presence of parenchymal bands, traction bronchiectasis, a thickened interstitium or irregular interfaces. There was a selection bias in this study with only individuals with an impaired TLCO <80% predicted undergoing CT imaging, suggesting that the true prevalence of fibrosis in this cohort may have been higher. However, reassuringly, improvement of fibrotic changes was seen at 12 month follow up. This is concert with findings by Zhang et al in a 15-year follow up study post SARS COV-1, where further regression of radiological abnormalities was seen.[99]

Importantly, data from SARS COV-1 also suggests that the severity of acute illness may indeed be associated with the presence of parenchymal abnormalities at follow up, including the presence of fibrosis, therefore this may be an important factor to consider when selecting individuals for further imaging during the follow up phase.[97,101]

Despite extant literature describing the radiological sequelae post the aforementioned coronavirus pandemics, these studies are limited by small numbers, selection bias and a variety of descriptors being used to denote fibrosis, thus posing challenges in drawing conclusions and reliably estimating the prevalence of fibrosis during the pandemics.

Regardless, it remains plausible that individuals recovering post COVID-19 may too be at risk of persistent radiological abnormalities.

1.4.2.2 Aetiology of radiological abnormalities

The aetiology of the underlying radiological abnormality is important to understand to allow effective management strategies to be utilised.

1.4.2.2.1 Ground-glass opacities (GGO)

As aforementioned, the commonest abnormalities seen were GGO. GGO represent an increased area of density of the lung, without any obscurement of the underlying bronchial or vascular structures.[102] Pathologically, this represents accumulation of fluid or cellular infiltrate in the alveolar sacs and/or thickening of the alveolar walls or interstitium.[103,104] It can therefore be caused by a variety of pulmonary pathologies. In fact, GGO can be seen as a consequence of viral pneumonias, interstitial lung disease, pulmonary oedema, pulmonary haemorrhage and drug toxicity.[105,106] Distinguishing between the pathologies can be challenging and may require additional investigations, such as endobronchial sampling, and interpretation of the radiology within the clinical context to determine future clinical management, both acute and chronic. However, where GGO represent inflammatory cellular infiltrate,[107] this may be a promising finding suggesting potential response to immunosuppressive therapy.

1.4.2.2.2 Fibrosis

In the diagnosis of idiopathic pulmonary fibrosis, honeycombing, with or without the presence of traction bronchiectasis on CT is the hallmark of fibrosis, with this correctly identifying an usual interstitial pneumonia (UIP) pattern on histopathological assessment. Reticulation, on the other hand, refers to a linear opacity which is suggestive of interlobular septal thickening and should not be used interchangeably with honeycombing.[102] Traction bronchiectasis is a consequence of irreversible bronchial and bronchiolar dilatation due to fibrosis and distortion of the adjacent lung parenchyma.[102] In the literature post SARS-COV1, a variety of radiological descriptors were used to define and describe fibrosis, making it difficult to elucidate the true prevalence of fibrosis post SARS-COV1, where there is volume loss +/- traction bronchiectasis. As SARS-COV2 has been shown to activate fibrosis-related genes, fibrosis post COVID-19 is a distinct possibility.[108]

Additionally, one of the defining features of the late stages of ARDS is interstitial and intra-alveolar fibrosis, with increased collagen deposition. Histologically, the appearances are similar to that seen in fibrotic interstitial lung diseases.[109,110] It is not clear which collagens predominate during this process

and at which stage, but the composition of the matrix proteins and the degree to which they are cross-linked may have an impact on whether the fibrosis is reversible.[111,112] Moreover, barotrauma due to high sheer forces during mechanical ventilation can exacerbate acute lung injury by directly simulating the synthesis of matrix proteins[113] or by exposing a damaged basement membrane, and subsequent recruitment of inflammatory and mesenchymal cells.[114] Therefore, even in the absence of SARS-COV2 being fibrogenic, fibrosis associated with ARDS or barotrauma could occur in individuals with severe disease presentations of COVID-19. Importantly, the trajectory of fibrotic changes is likely to depend on the underlying aetiology of fibrosis.[102,115]

1.4.2.3 Viral pneumonia and interstitial lung disease (ILD)

Viruses have been implicated in the pathogenesis and progression of both fibrotic and non-fibrotic interstitial lung disease. Three of the main ILDs associated with viruses are hypersensitivity pneumonitis, organising pneumonia and idiopathic pulmonary fibrosis.

In hypersensitivity pneumonitis, an interstitial lung disease which is immunologically-mediated, a viral infection can provide the inciting antigenic stimulus to precipitate a host immunological response.[116] In addition, viruses can increase the antigen-presenting capacity of the host immune system in genetically susceptible individuals, therefore making the host more sensitive to other environmental antigens, which may in turn precipitate the onset of hypersensitivity pneumonitis.[117]

Organizing pneumonia is a highly steroid-responsive interstitial lung disease, histologically characterised by the filling of alveolar sacs with fibroblasts and myofibroblasts.[118] Viral infection can induce a secondary organizing pneumonia which can be indistinguishable radiologically and clinically to cryptogenic forms.[119] Organizing pneumonia has been reported after the MERS and SARS-COV1 pandemics[120,121] and the radiological and histological features of acute COVID-19 have been likened to organizing pneumonia.[122–124] In addition, the significant mortality benefits derived from inpatient steroid therapy during COVID-19[30] would be compatible with reversal of a disease process that is highly steroid-responsive, like organising pneumonia.

Furthermore, viruses have been associated with the pathogenesis of idiopathic pulmonary fibrosis, in particular, Epstein Barr Virus (EBV), hepatitis C Virus (HCV) and human herpes viruses (HHV 7 and 8). It has been postulated that repeated epithelial cell injury, followed by aberrant epithelial repair in susceptible individuals, results in pulmonary fibrosis.[125,126] Viruses can cause pulmonary fibrosis through two main mechanisms: Firstly, direct damage to the lung followed by aberrant wound healing

mechanisms as aforementioned or secondly, immune-mediated injury, whereby immune cell infiltration in an attempt at viral clearance results in the accumulation of pro-inflammatory and pro-fibrotic cytokines which in turn cause significant lung damage and promote fibrosis.[127]

To complicate matters further, between 2 and 9% of the population have interstitial lung abnormalities (ILA), defined as non-dependent abnormalities in the lung affecting >5% of the lung parenchyma in an individual not known to have ILD.[128,129] In a proportion of these individuals, the ILA is associated with fibrosis and fibrotic progression can occur over time.[128] Therefore, fibrosis seen post COVID-19 may represent or reveal underlying pre-existing parenchymal pathology not directly linked to SARS-COV2. However, viruses can also precipitate an acute exacerbation of ILD, including fibrosing ILD, resulting in further morbidity.[130]

1.4.3 Virus induced airway dysfunction

Viral infections have been implicated in the pathogenesis of obstructive airway disease. For instance, childhood infection with respiratory syncytial virus (RSV) may increase allergen sensitization and increase the risk of developing asthma.[131,132] A variety of mechanisms have been proposed for the development of obstructive airway disease post infection: a) increased airway hyperresponsiveness b) changes in neural control of the airways c) changes in the airway calibre and d) Increased airway inflammation.[133]

An important factor to note is that the nature and distribution of airway involvement may be specific to the virus. For instance, only certain strains of rhinovirus have been shown to affect the lower airways.[134,135] Furthermore, it is not clear if direct infection of lower airway epithelial cells is required to induce viral airway hyperresponsiveness or whether infection of the upper airways will suffice. Interpretation of studies involving BALF sampling are further complicated by the bronchoscope needing to pass through the upper airways before reaching the lower airways, therefore making it difficult to distinguish whether upper airway or lower airway infection is driving airway pathology.

Aside from the type of virus, host responses may have an impact on the effect the virus has on the airways. For instance, in some studies, hyperresponsiveness to a viral trigger was predominantly seen in individuals displaying atopic tendencies.[136]

Overactivation of the parasympathetic nervous system and subsequent reflex bronchoconstriction is another proposed mechanism. Furthermore, activation of airway sensory C fibres can cause bronchoconstriction either via the brainstem, or via release of neuropeptides, which in turn can cause airway oedema and smooth muscle contraction.[133,136] Another proposed mechanism for airway hyperresponsiveness is a reduction in airway neutral endopeptidase, which usually inactivates neuropeptides such as tachykinin,[137,138] accumulation of which would otherwise result in smooth muscle contraction and subsequent bronchospasm.[139]

Despite viruses such as rhinoviruses causing airway hyperresponsiveness, the degree of cytopathology induced by these viruses is minimal.[140,141] In contrast, RSV and influenza result in significant cytopathic effects[142,143] and SARS-COV2[144] has been shown to have this effect also. Epithelial damage can render the nerves more exposed and therefore more susceptible to stimulation from other environmental allergens. Furthermore, epithelial-derived nitric oxide (NO) is important for the relaxation of smooth muscles and airway tone, therefore depletion of NO in the context of epithelial injury and insufficient epithelial repair may result in prolonged or increased susceptibility to bronchospasm.[145,146]

During acute SARS-COV2 infection, significant immune cell infiltrate, especially lymphocytes, have been noted. CD8 T cells are pivotal to antiviral killing,[147] but a CD4 T helper 2 (Th2) cell-driven response can hinder anti-viral activity.[148] A Th2 response has been seen in in the nasal mucosa during SARS-COV2 infection and has been associated with an increased risk of clinical deterioration in COVID-19.[149] An exaggerated Th2 response is seen in asthma[150] and is associated with hyperresponsiveness, so again, this may act as a driving mechanism for airway disease.

Notably, the airway compartment predominantly affected by SARS-COV2 infection, for instance bronchial compartment versus alveolar compartment, may affect the severity of airway disease, if present. As aforementioned in section 1.3.4, alveolar epithelial cells are an important source of surfactant. Pulmonary surfactant plays an important role not only in pathogen clearance, but also in dampening inflammatory responses and maintaining the patency of distal airways, thereby reducing airway collapse during expiration.[151] In the context of ineffectual AT2 cell repair and resultant impairment in surfactant production, small airways disease may occur.

The small airways are often the first or earliest signs of pathogenesis of obstructive airway disease[152] and as significant disease burden is often required prior to changes in lung function parameters, routine spirometry may not be sufficient in detecting changes in the small airways in this cohort.

Therefore, to summarise, a multitude of pathophysiological processes could contribute to the inception or deterioration of airway disease post COVID-19 and airway disease should be considered in individuals presenting with persistent respiratory morbidity.

1.5 Role of the epithelium

1.5.1 Role of the epithelium in viral disease

The airway epithelium plays an important role in the response against pathogens and acts an interface between the external environment and the lungs. Covering the airway mucosa, it forms a physical barrier to pathogens. Epithelial cells are joined to adjacent epithelial cells by cell-cell junctions, the most important of which is the tight junction, which is present on the apical surface of the epithelial cell and is integral to maintaining epithelial integrity.[153]

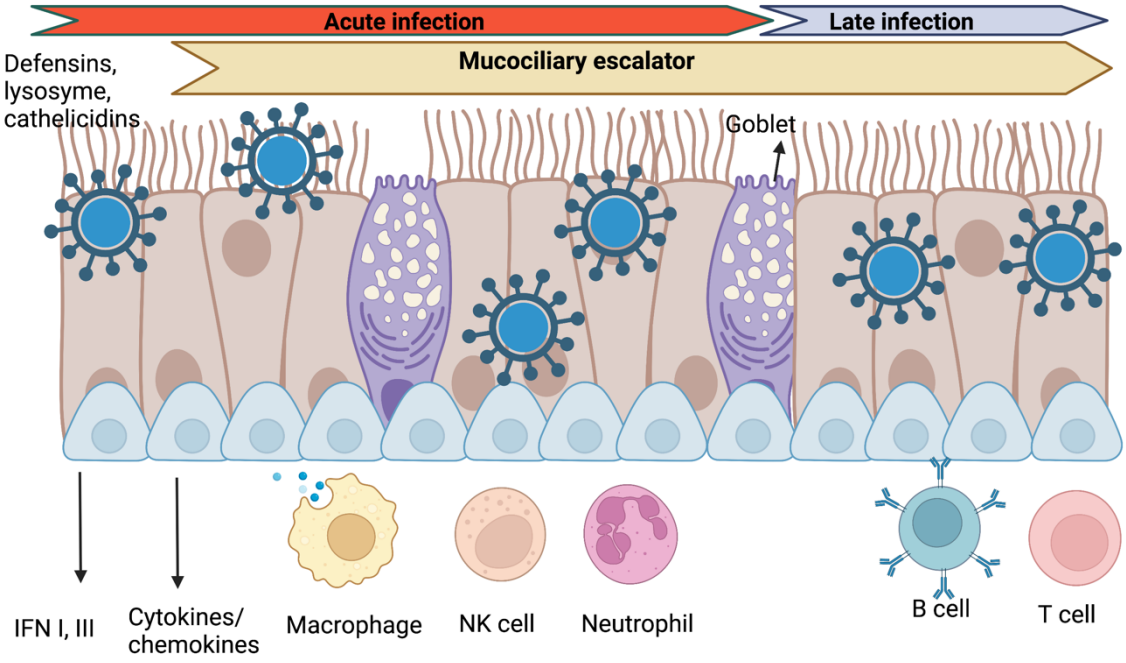


Figure 1.3 Epithelial response to viral infection

Adapted from Yan, H & Yang, J. Mucosal epithelial cells: the initial sentinels and responders controlling and regulating immune responses to viral infections. *Cell Mol Immunol* 18, 1628–1630 (2021)

Mucous is secreted by intraepithelial goblet cells and submucosal glands towards the apical side of respiratory epithelium. This forms another membrane, impermeable to respiratory pathogens. Along with this, the muco-ciliary escalator, created by the beating actions of cilia, drives pathogens and unwanted environmental particles from the distal airways to the trachea.[154] During a respiratory infection, mucous production is increased to facilitate viral and bacterial clearance,[155,156] but overproduction of mucous can result in mechanical obstruction of small and larger airways, resulting in partial or total airway collapse, thereby inducing and exacerbating respiratory symptoms of breathlessness and cough, in an attempt to clear secretions.

In addition to the physical barrier it provides, the role of the epithelium in initiating immune responses is crucial to minimising viral replication and invasion. Pathogens are recognised by toll-like receptors on the surface of the epithelial cell, resulting in initiation of the Type I and Type III IFN response.[157] The TLR3 receptor is especially important as it recognises a variety of viruses including influenza virus and rhinovirus.[158,159] In addition, intracellular viral sensors are also important, of which retinoic acid-inducible gene-I (RIG-1)[160] and nucleotide oligomerization domain (NOD)- like receptors have been shown to be important in anti-viral immunity.[161,162]

After recognition, a range of immune responses are initiated by the epithelium, including secretion of interferons. Type I and III interferons are important in stimulating downstream ISGs and nitric oxide,[163] which has a role in reducing viral replication[164]. Additionally, the respiratory epithelium is important in the recruitment of immune cells, ranging from cells of the innate immune system (neutrophils, monocytes, macrophages and NK cells) to the cells of adaptive immunity (T cells and B cells) in order to provide an anti-viral response (Figure 1.3).[165]

1.5.2 Wound healing post epithelial injury

1.5.2.1 Damage to the epithelium post viral infection

Widespread damage to the respiratory epithelium can occur in response to viral infection, as seen in SARS-COV2 infection. Respiratory viruses can directly cause apoptosis or necrosis[56] of infected epithelial cells or result in increased production of mediators that can upregulate this process. Morphological changes in cells, such as loss of cilia, can reduce the efficacy of the muco-ciliary escalator as previously described, and can also interfere with airway homeostasis.[166,167]

Moreover, disruption of the epithelial barrier can be a direct effect of the virus and associated cytopathic effects[56], or through the immune-mediated inflammatory cascade[168]. Accordingly, suboptimal repair of the disrupted epithelium can disturb this physical barrier against pathogens and impede future immune responses to viral or bacterial triggers.

1.5.2.2 The process of epithelial repair post injury

Wound healing after epithelial injury requires epithelial cell proliferation and migration in a process called epithelial restitution.[169] Epithelial cell migration requires careful co-ordination of the cell-cell adhesions and cell-matrix adhesions. For smaller wounds, epithelial cell migration alone may suffice to close the wound, but for larger injuries, epithelial cell proliferation is also required.[170] Epithelial derived proteins such epidermal growth factor (EGF) and transforming growth factor beta 1 (TGF beta 1) are important in co-ordinating and promoting this repair process.[171] Furthermore, plasmin and matrix metalloproteinases (MMPs) are important in cleaving the matrix, thus allowing cell migration.[172] Fibroblasts, which are recruited to the site of the wound, produce collagens, in order to replace the old, now degraded matrix, with newer formed matrix. This process is regulated by proteins such as TGF beta and vascular endothelial growth factor (VEGF). Finally, myofibroblasts produce contractile forces to close the wound and form a scar.[170,173] Figure 1.4 summarises the epithelial response to injury.

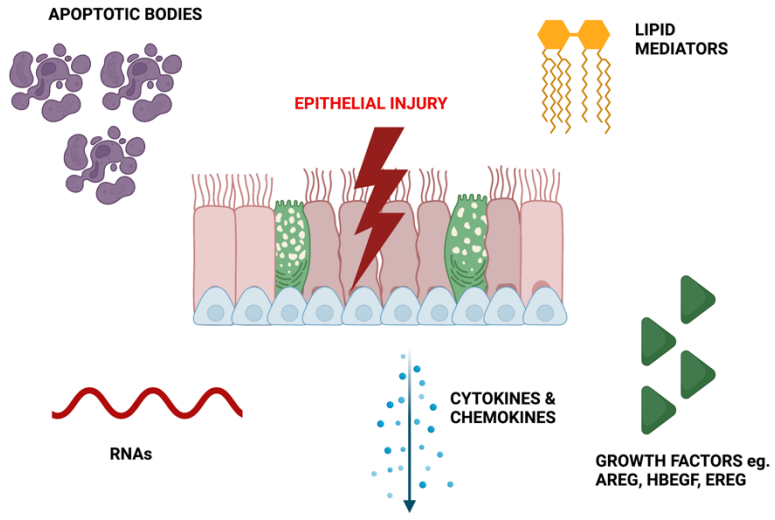


Figure 1. 4 Epithelial cells and wound repair

Amended from Lucchini et al. (2021). Epithelial Cells and Inflammation in Pulmonary Wound Repair *Cells.* 10(2): 339

Additionally, immune cells recruited to the mucosa play a role, not only in anti-microbial defence against pathogens, but also restoration of the damaged epithelium. For instance, neutrophils are important in activating the beta catenin signalling pathway,[174] which facilitates epithelial cell proliferation, and are an important source of nitric oxide and TGF beta, which both have roles in wound healing.[170,175,176] Furthermore, macrophages, and in particular tissue-resident macrophages

play a pivotal anti-inflammatory role and promote wound healing. There is some plasticity between monocyte-driven macrophages (which are pro-inflammatory and recruited early to the site of disease) and tissue-resident macrophages, so an attempt to repair the injured epithelium can occur, even during acute infection.[177,178]

1.5.3 Epithelial-mesenchymal transition

1.5.3.1 Overview of epithelial-mesenchymal transition

Epithelial-mesenchymal transition (EMT) is a process whereby cells lose their epithelial phenotype (loss of cell-cell adhesion and apico-basal polarity) and gain a mesenchymal phenotype (with migratory capacity). EMT is an important part of re-epithelialisation and response to epithelial injury, but the persistence of myofibroblasts, instead of undergoing change back to an epithelial phenotype or apoptosis, gives rise to fibrosis.[179–181] Figure 1.5 shows this greater detail.

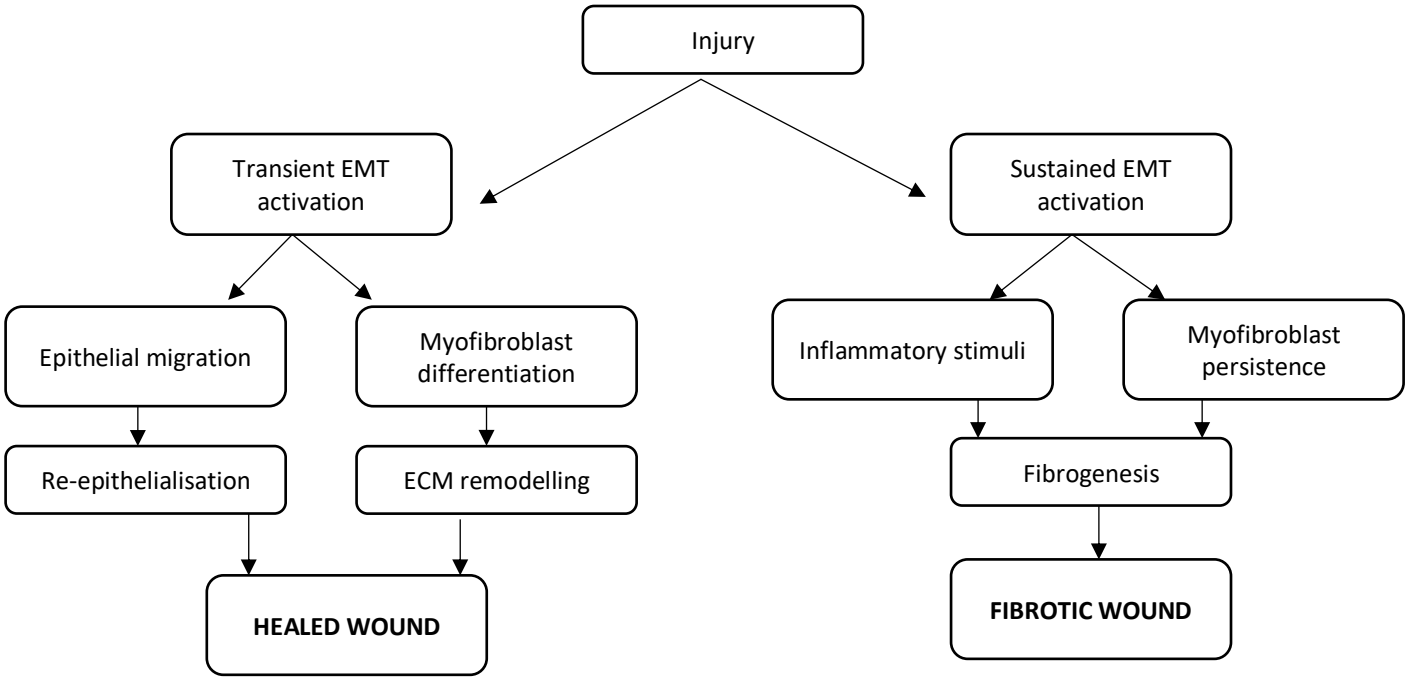


Figure 1. 5 EMT in wound healing

Adapted from figure in Stone RC et al (2016) Epithelial-mesenchymal transition in tissue repair and fibrosis. *Cell Tissue Research* 365(3):495-506.

Firstly, the epithelial cell undergoes loss of epithelial markers, of which, E-cadherin is one of the first to be lost. E-cadherin is important in cell-cell contact via adherens junctions and prevents cell mobility. With downregulation of E-cadherin, there is concomitant upregulation of vimentin, a mesenchymal

marker. There is also upregulation of other mesenchymal markers such as fibronectin and alpha smooth muscle actin.[179,181] Additionally, the loss of apical-basal cell polarity helps increase cell motility.

A variety of cell-signalling pathways have been implicated in EMT. Firstly, the fibroblast growth-factors, and in particular fibroblast growth factor 2 (FGF2)[182] is associated with EMT, with downregulation of E-cadherin and upregulation of MMPs to degrade the extracellular matrix (ECM). Secondly, epidermal growth factor receptor (EGFR) ligands such as epiregulin (EREG), heparin-binding epidermal like growth factor (HB-EGF), amphiregulin (AREG) and transforming growth factor (TGF) alpha are important in wound healing and have similar effects on EMT as FGF2. Thirdly, TGF beta, which, through the TGF beta-SMAD complex has a potent role in angiogenesis, re-epithelialisation and can also induce the EMT pathway.[182–184]

After scar formation due to contractile forces from myofibroblasts, the myofibroblasts undergo apoptosis or MET (mesenchymal-epithelial transition). Persistence of myofibroblasts is pathological and results in fibrogenesis.

1.5.3.2 Disease states associated with epithelial injury

1.5.3.2.1 COPD

Epithelial injury, DAMP release and subsequent activation of the immune response is thought to play a role in COPD and in particular, it is necrosis related to smoke, rather than apoptosis that triggers a vigorous immune cell response.[185,186] In support of this, dysregulation of DAMPs and pathogen recognition receptors have been seen in COPD[187]. Necroptosis, a form of necrosis, has been shown to result in inefficacious clearance of damaged cells by the innate immune system, thus perpetuating the immune cascade and potentially resulting in further damage. Furthermore, aberrancy in epithelial repair mechanisms has been implicated in the chronic bronchitis phenotype of COPD, whereby increased goblet cell hyperplasia contributes to persistent symptom burden and recurrent exacerbations, which is associated with accelerated disease progression and higher mortality.[188–190] In COPD, there is also evidence of increased EMT.[191,192] EMT is upregulated in COPD through increased WNT/beta catenin signalling, TGF beta signalling and pro-inflammatory cytokines such as IL1beta and TNF alpha.[11,193–195] Furthermore MMP 9, which is increased in the airways of patients with COPD,[196] may result in persistent activation of EMT.[197]

1.5.3.2.2 Idiopathic pulmonary fibrosis (IPF)

Idiopathic pulmonary fibrosis is thought to be a consequence of repetitive alveolar injury and ineffectual repair mechanisms with chronic TGF beta and WNT signalling.[126,198] Increased alveolar epithelial cell apoptosis has been shown to play a role in IPF[199] and abnormal epithelial cell proliferation has also been described.[200] Increased cell death is particularly evident around sites of myofibroblasts[201] which are resistant to apoptosis.[202] Persistent EMT[181] and WNT signalling, as seen in IPF, can also occur when the epithelium is unable to regenerate completely, which in turn results in activation of fibroblasts.[203] Therefore, fibrosis could result in individuals post COVID-19 if normal epithelial repair mechanisms fail.

1.6 Summary

Literature from acute SARS-COV2 infection highlights the range of disease presentations, the diverse radiological patterns and varying extents of parenchymal involvement in individuals admitted to hospital with COVID-19 and the significant luminal, epithelial and interstitial immune cell infiltrate, diffuse alveolar damage and epithelial cell necrosis that this virus promotes.

With the degree of immune and epithelial damage induced by SARS-COV2, epithelial recovery mechanisms are important to understand as incomplete or dysregulated repair mechanisms may increase susceptibility to development of chronic lung disease, including fibrotic lung disease or chronic airway pathology.

After SARS-COV1 and MERS, persistent radiological abnormalities and clinical and quality of life impairments were common and noted several months after the acute infection. Despite this, assessment of the airway microenvironment was not performed during the convalescent phase to further assess and evaluate persistent morbidity.

Therefore, not only is there a critical gap in the literature in understanding the clinical and radiological trajectory of patients recovering post COVID-19, but there is a critical gap in the literature in understanding the local airway microenvironment and epithelial recovery mechanisms post viral-induced epithelial injury.

Hypothesis: Sustained inflammation and aberrant immune-epithelial cell interactions result in persistent pulmonary pathology post SARS-COV2 infection.

Aims:

1. To characterise the clinical trajectory of patients recovering post COVID-19
2. To characterise the radiological trajectory of patients recovering post COVID-19
3. To examine how local immunity in patients post COVID-19 relates to clinical and radiological features of residual lung disease
4. To examine epithelial function in the post-COVID airway

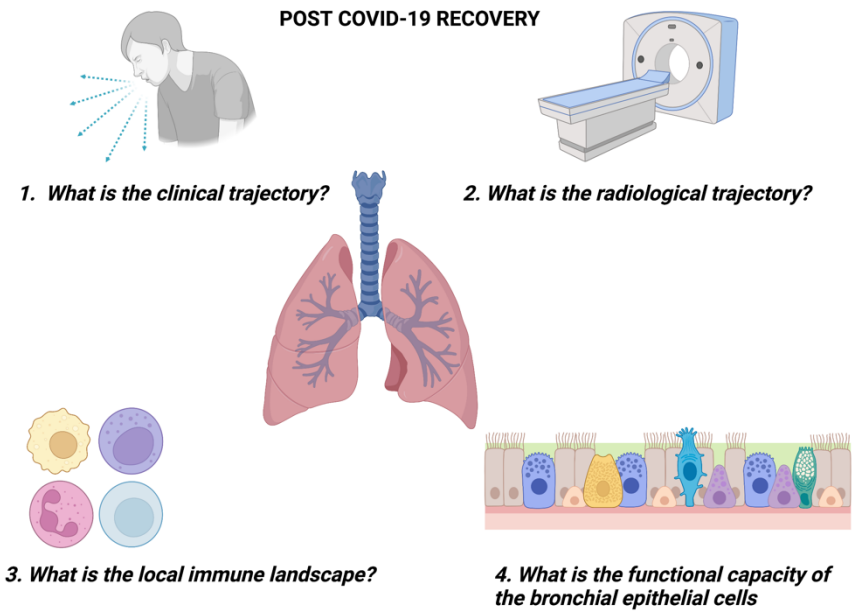


Figure 1. 6 Summary of PhD aims

Chapter 2 - Methods

The chapter outlines the study procedures and clinical and scientific measurements undertaken to derive the results presented in this thesis. This chapter aims to provide an overview of the techniques with additional methodological considerations described in the relevant results chapters.

2.1 Clinical

2.1.1 Patient recruitment: Post COVID-19 donors

The clinical data shown was collected as part of the PHENOTYPE study (PHenotyping patiENts admitted to hospital with cOvid-19 infection and idenTifYing Prognostic markErs), registered on Clinical Trials.gov (NCT 04459351). The study protocol was written by myself with input from Dr James Tonkin, Dr Christopher Orton and Professor Pallav Shah. Dr Samuel Kemp and Dr Gary Davies internally reviewed the documents prior to submission for ethical review. A favourable ethical outcome was issued by the Yorkshire & The Humber Sheffield Research Ethics Committee (reference 20/YH/0186) on 16th June 2020. Subsequent to this, two substantial amendments were submitted by me to the Health Research Authority (HRA). The first amendment was to allow research nurses to obtain consent for the study and to allow patients with ongoing symptoms post COVID-19 in the community to be recruited to the study. This received ethical approval on 16th September 2020. The second amendment was submitted to allow patients to undergo follow up for up to 2 years post hospital discharge and to permit usage of the data in my PhD thesis. This was approved by the ethics committee on 8th March 2021. The most recent protocol for PHENOTYPE (V1.2), the patient information sheet (PIS, V1.5) and informed consent form (ICF, V1.5) can be found in the Appendices 1 and 2 (Chapter 12).

2.1.1.1 Clinical data

As outlined in the study protocol, the protocol is based on structured, holistic follow-up of patients for clinical purposes, with acquisition of additional research samples, both blood and endobronchial (BALF and epithelial brushings). The protocol also permits usage of data collected prior to enrolment, such as details about the COVID-19 admission, using electronic health care records kept at Chelsea and Westminster Hospital, London.

Figure 2.1 shows a study schema for the study. Whilst this schema was followed during the second wave, delay in setting up the clinical service resulted in the first visit being performed at approximately 3 months post discharge for the first wave.

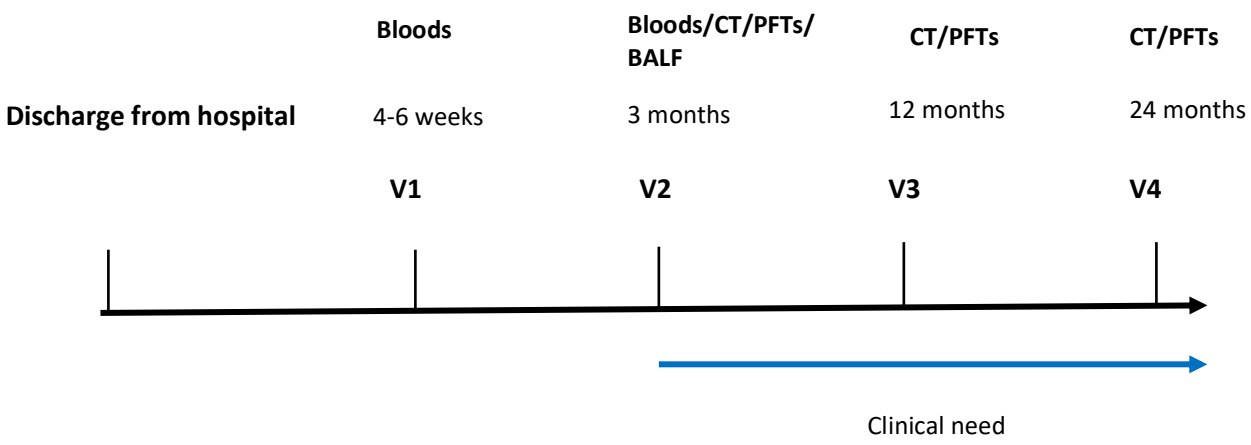


Figure 2. 1 Study procedures for PHENOTYPE.

Visits beyond 3 months were based on clinical need. Abbreviations: V – visit, CT – computed tomography, PFTs – pulmonary function tests, BALF – bronchoalveolar lavage

2.1.1.2 Questionnaires

Patients were asked to complete a set of questionnaires at sequential timepoints post discharge to facilitate a holistic review of the patient's recovery. Namely, these were the Modified Medical Research Council score, Hospital Anxiety and Depression Scale and the Short-Form 36 Survey.

a) Modified Medical Research Council score

The modified Medical Research Council (mMRC) score is a validated score for assessing the impact of breathlessness on functional disability and correlates well with other scores assessing the degree of breathlessness experienced by a patient.[204,205] Table 2.1 shows the components of this scoring system in greater detail. Patients completed the questionnaire independently, but clarification of scores discordant with the rest of the patient's clinical history was done by myself. Heterogeneity in the scores chosen by patients has been described[206] thus emphasising the importance of reviewing scores with patients.

Description	Score
I only get breathless with strenuous exercise	0
I get short of breath when hurrying on level ground or walking up a slight hill	1
On level ground, I walk slower than people of my age because of breathlessness, or I have to stop for breath when walking at my own pace on the level	2
I stop for breath after walking about 100 yards or after a few minutes on level ground	3
I am too breathless to leave the house or I am breathless when dressing/undressing	4

Table 2. 1 Modified Medical Research Council Score

b) Hospital Anxiety and Depression Scale (HADS)

The HADS scale is routinely available and used to screen for depression and anxiety in the community. It is a well-validated score that is relatively easy to use[207–209] and assesses a range of physical and psychological symptoms that patients may experience prior to a formal diagnosis of anxiety or depression, for instance restlessness and anhedonia. The anxiety and depression sections have to be scored separately and a cut off score of 8 has been shown to have a specificity of 0.78 and sensitivity of 0.9 for detecting anxiety. Additionally, a cut-off of 8 has been shown to have a specificity of 0.79 and sensitivity of 0.83 for depression[207], although using a lower cut-off of 7 can increase the sensitivity

further.[208] For the results presented in Chapter 3, the standard cut-off of 8 was utilised for detecting abnormalities.

Figure 2.2 shows the HADS questionnaire utilised for data collection for this thesis.

Hospital Anxiety and Depression Scale (HADS)

Tick the box beside the reply that is closest to how you have been feeling in the past week.
Don't take too long over you replies: your immediate is best.

D	A		D	A	
		I feel tense or 'wound up':			**I feel as if I am slowed down:**
	3	Most of the time	3		Nearly all the time
	2	A lot of the time	2		Very often
	1	From time to time, occasionally	1		Sometimes
	0	Not at all	0		Not at all
		I still enjoy the things I used to enjoy:			**I get a sort of frightened feeling like 'butterflies' in the stomach:**
0		Definitely as much		0	Not at all
1		Not quite so much		1	Occasionally
2		Only a little		2	Quite Often
3		Hardly at all		3	Very Often
		I get a sort of frightened feeling as if something awful is about to happen:			**I have lost interest in my appearance:**
	3	Very definitely and quite badly	3		Definitely
	2	Yes, but not too badly	2		I don't take as much care as I should
	1	A little, but it doesn't worry me	1		I may not take quite as much care
	0	Not at all	0		I take just as much care as ever
		I can laugh and see the funny side of things:			**I feel restless as I have to be on the move:**
0		As much as I always could		3	Very much indeed
1		Not quite so much now		2	Quite a lot
2		Definitely not so much now		1	Not very much
3		Not at all		0	Not at all
		Worrying thoughts go through my mind:			**I look forward with enjoyment to things:**
	3	A great deal of the time	0		As much as I ever did
	2	A lot of the time	1		Rather less than I used to
	1	From time to time, but not too often	2		Definitely less than I used to
	0	Only occasionally	3		Hardly at all
		I feel cheerful:			**I get sudden feelings of panic:**
3		Not at all		3	Very often indeed
2		Not often		2	Quite often
1		Sometimes		1	Not very often
0		Most of the time		0	Not at all
		I can sit at ease and feel relaxed:			**I can enjoy a good book or radio or TV program:**
	0	Definitely	0		Often
	1	Usually	1		Sometimes
	2	Not Often	2		Not often
	3	Not at all	3		Very seldom

Please check you have answered all the questions

Scoring:
Total score: Depression (D) _____ Anxiety (A) _____
0-7 = Normal
8-10 = Borderline abnormal (borderline case)
11-21 = Abnormal (case)

Figure 2. 2 Hospital Anxiety and Depression Scale (HADS)

c) Short-form 36 (SF 36) survey

The SF-36 survey is a validated, 36-item survey used in the assessment of health-related quality of life and has been shown to be reliable over a number of clinical settings.[210–213] It consists of 8 domains: PF (physical functioning), RP (role limitation due to physical health), BP (bodily pain), SF (social functioning), VT (vitality), ME (role limitation due to emotional problems), GH (general health) and MH (mental health). The questionnaire is shown in Figure 2.3. Scoring of the SF-36 survey was done in accordance with guidelines provided by the RAND coporation.[214,215]

SF-36 QUESTIONNAIRE

Name:_____ **Ref. Dr:**_____ **Date:** _____

ID#: _____ **Age:** _____ **Gender: M / F**

Please answer the 36 questions of the **Health Survey** completely, honestly, and without interruptions.

GENERAL HEALTH:
In general, would you say your health is:

○ Excellent ○ Very Good ○ Good ○ Fair ○ Poor

Compared to one year ago, how would you rate your health in general now?

○ Much better now than one year ago
○ Somewhat better now than one year ago
○ About the same
○ Somewhat worse now than one year ago
○ Much worse than one year ago

LIMITATIONS OF ACTIVITIES:
The following items are about activities you might do during a typical day. Does your health now limit you in these activities? If so, how much?

Vigorous activities, such as running, lifting heavy objects, participating in strenuous sports.
○ Yes, Limited a lot ○ Yes, Limited a Little ○ No, Not Limited at all

Moderate activities, such as moving a table, pushing a vacuum cleaner, bowling, or playing golf
○ Yes, Limited a Lot ○ Yes, Limited a Little ○ No, Not Limited at all

Lifting or carrying groceries
○ Yes, Limited a Lot ○ Yes, Limited a Little ○ No, Not Limited at all

Climbing several flights of stairs
○ Yes, Limited a Lot ○ Yes, Limited a Little ○ No, Not Limited at all

Climbing one flight of stairs
○ Yes, Limited a Lot ○ Yes, Limited a Little ○ No, Not Limited at all

Bending, kneeling, or stooping
○ Yes, Limited a Lot ○ Yes, Limited a Little ○ No, Not Limited at all

Walking more than a mile
○ Yes, Limited a Lot ○ Yes, Limited a Little ○ No, Not Limited at all

Walking several blocks
○ Yes, Limited a Lot ○ Yes, Limited a Little ○ No, Not Limited at all

Walking one block
○ Yes, Limited a Lot ○ Yes, Limited a Little ○ No, Not Limited at all

Figure 2. 3 SF36 questionnaire

Bathing or dressing yourself

Yes, Limited a Lot Yes, Limited a Little No, Not Limited at all

PHYSICAL HEALTH PROBLEMS:

During the past 4 weeks, have you had any of the following problems with your work or other regular daily activities as a result of your physical health?

Cut down the amount of time you spent on work or other activities

Yes No

Accomplished less than you would like

Yes No

Were limited in the kind of work or other activities

Yes No

Had difficulty performing the work or other activities (for example, it took extra effort)

Yes No

EMOTIONAL HEALTH PROBLEMS:

During the past 4 weeks, have you had any of the following problems with your work or other regular daily activities as a result of any emotional problems (such as feeling depressed or anxious)?

Cut down the amount of time you spent on work or other activities

Yes No

Accomplished less than you would like

Yes No

Didn't do work or other activities as carefully as usual

Yes No

SOCIAL ACTIVITIES:

Emotional problems interfered with your normal social activities with family, friends, neighbors, or groups?

Not at all Slightly Moderately Severe Very Severe

PAIN:

How much bodily pain have you had during the past 4 weeks?

None Very Mild Mild Moderate Severe Very Severe

During the past 4 weeks, how much did pain interfere with your normal work (including both work outside the home and housework)?

Not at all A little bit Moderately Quite a bit Extremely

ENERGY AND EMOTIONS:
These questions are about how you feel and how things have been with you during the last 4 weeks. For each question, please give the answer that comes closest to the way you have been feeling.

Did you feel full of pep?
- ○ All of the time
- ○ Most of the time
- ○ A good Bit of the Time
- ○ Some of the time
- ○ A little bit of the time
- ○ None of the Time

Have you been a very nervous person?
- ○ All of the time
- ○ Most of the time
- ○ A good Bit of the Time
- ○ Some of the time
- ○ A little bit of the time
- ○ None of the Time

Have you felt so down in the dumps that nothing could cheer you up?
- ○ All of the time
- ○ Most of the time
- ○ A good Bit of the Time
- ○ Some of the time
- ○ A little bit of the time
- ○ None of the Time

Have you felt calm and peaceful?
- ○ All of the time
- ○ Most of the time
- ○ A good Bit of the Time
- ○ Some of the time
- ○ A little bit of the time
- ○ None of the Time

Did you have a lot of energy?
- ○ All of the time
- ○ Most of the time
- ○ A good Bit of the Time
- ○ Some of the time
- ○ A little bit of the time
- ○ None of the Time

Have you felt downhearted and blue?

- All of the time
- Most of the time
- A good Bit of the Time
- Some of the time
- A little bit of the time
- None of the Time

Did you feel worn out?

- All of the time
- Most of the time
- A good Bit of the Time
- Some of the time
- A little bit of the time
- None of the Time

Have you been a happy person?

- All of the time
- Most of the time
- A good Bit of the Time
- Some of the time
- A little bit of the time
- None of the Time

Did you feel tired?

- All of the time
- Most of the time
- A good Bit of the Time
- Some of the time
- A little bit of the time
- None of the Time

SOCIAL ACTIVITIES:
During the past 4 weeks, how much of the time has your physical health or emotional problems interfered with your social activities (like visiting with friends, relatives, etc.)?

- All of the time
- Most of the time
- Some of the time
- A little bit of the time
- None of the Time

GENERAL HEALTH:
How true or false is each of the following statements for you?

I seem to get sick a little easier than other people
Definitely true | Mostly true | Don't know | Mostly false | Definitely false

I am as healthy as anybody I know
Definitely true | Mostly true | Don't know | Mostly false | Definitely false

I expect my health to get worse
Definitely true | Mostly true | Don't know | Mostly false | Definitely false

My health is excellent
Definitely true | Mostly true | Don't know | Mostly false | Definitely false

A series of steps need to undertaken in order to calculate the two main derivatives from the SF36 questionnaire: Mental component score (MCS) and physical component score (PCS).

Firstly, each of the scores (1-6) for each question (1-36) is converted to a score on a scale of 0-100, with higher scores representing better function (Table 2.2).

SF-36 questions	Score of S36 questionnaire					
	1	2	3	4	5	6
1, 2, 20, 22, 34, 36	100	75	50	25	0	-
3, 4, 5, 6, 7, 8, 9, 10, 11, 12	0	50	100	-		
13, 14, 15, 16, 17, 18, 19	0	100	-			
21, 23, 26, 27, 30	100	80	60	40	20	0
24, 25, 28, 29, 31	0	20	40	60	80	100
32, 33, 35	0	25	50	75	100	-

Table 2. 2 How to convert SF36 scores to a scale of 0 - 100.

Adapted from 36-Item Short Form Survey (SF-36) Scoring Instructions, RAND corporation

The scores are then converted to a domain score by averaging the scores for the questions relevant to each domain (Table 2.3).

Domain	SF-36 items	Average
Physical functioning	3, 4, 5, 6, 7, 8, 9, 10, 11, 12	Total sum / 10
Role limitations due to physical health	13, 14, 15, 16	Total sum / 4
Role limitations due to emotional problems	17, 18, 19	Total sum / 3
Energy/fatigue	23, 27, 29, 31	Total sum / 4
Emotional well-being	24, 25, 26, 28, 30	Total sum / 5
Social functioning	20, 32	Total sum / 2
Pain	21, 22	Total sum / 2
General health	1, 33, 34, 35 36	Sum of recoding points / 5

Table 2. 3 Calculating average scores for each domain

Adapted from 36-Item Short Form Survey (SF-36) Scoring Instructions, RAND corporation

To calculate the physical and mental component scores, the United States (US) population means and weightings from Table 2.4 were used.

Weightings and Population Norms	1998 US Population Norms		Weights					
	Mean	STD	Orthogonal PCS	Orthogonal MCS	Oblique PCS	Oblique MCS	RAND-36 PHC	RAND-36 MHC
SF-36 Physical Functioning: (PF)	83	23.8	0.42402	-0.22999	0.2	-0.02	0.2712	0
SF-36 Role limitations due to physical health: (RP)	77.9	35.3	0.35119	-0.12329	0.31	0.03	0.3487	0
SF-36 Pain: (BP)	70.2	23.4	0.31754	-0.09731	0.23	0.04	0.2755	0
SF-36 General Health: (GH)	70.1	21.4	0.24954	-0.01571	0.2	0.1	0.2931	0
SF-36 Energy/fatigue: (VIT)	57	21.1	0.02877	0.23534	0.13	0.29	0	0.3136
SF-36 Social Functioning: (SF)	83.6	23	-0.00753	0.26876	0.11	0.14	0	0.3112
SF-36 Role limitations due to emotion problems: (RE)	83.1	31.6	-0.19206	0.43407	0.03	0.2	0	0.1623
SF-36 Emotional well-being: (MH)	75.2	17.6	-0.22069	0.48581	-0.03	0.35	0	0.4333

Table 2. 4 US population means and weighting coefficients for PCS and MCS scores

The oblique PCS and MCS scores were utilised for results shown in Chapter 3.

A z-score is then calculated for each domain, using this formula:

$$\frac{\text{(Mean domain score) - (mean score for sample of US general population)}}{\text{Standard deviation from the US general population}}$$

To calculate the physical component score, the following formula is used:

10 x (Sum of (z score for each component x corresponding factor scoring coefficient)) + 50

A similar calculation is performed to generate the mental component score (MCS), but this time, using the corresponding MCS coefficient. Of note, a higher PCS or MCS score signifies better function.

The choice of scoring coefficient (orthagonal vs oblique) has been discussed in the literature.[216–218] The orthagonal approach assumes that neither physical nor mental health are linked. This means that SF, RE and MH negatively affect the PCS, with lower scores in these domains resulting in a higher PCS.

Similarly, PF, RP and BP have a negative effect on the MCS, with lower scores in these domains resulting in a higher MCS.[216] In a study of patients with multiple sclerosis, where significant physical disability was seen, the MCS scores were inflated using the orthagonal method.[219] Alternative methods of scoring have also been described, including the RAND-36 Health Status Inventory (HSI)[218] or the oblique methodology[217], which allow the components to be correlated. Using the latter approach has been shown to minimise the issues described with the orthagonal method. This is especially relevant and important when assessing patients recovering post COVID-19, some of whom will have been discharged from intensive care and are likely to have ongoing physical rehabilitation needs secondary to a long-ICU stay.[220,221]

2.1.1.3 Semi-structured interviews

A subset of individuals who were being followed up from the first wave were invited to take part in a semi-structured interview to further assess the factors affecting their quality of life and in particular, understand the impact of residual syptoms. Interviews per performed between December 2021 and January 2022 by myself. All interviews were performed either over the phone or microsoft teams as per the patient's wishes. The topic guide used for the interviews can be found in Appendix 3. I then transcribed the interviews verbatin and performed thematic analysis of the transcripts using methods outlined by Braune and Clarke (2006) and Terry et al (2017). [222,223]

The transcripts were reviewed several times, and the interviews played back as necessary to ensure accurate coding. Codes were subsequently collated into subthemes and themes. All recordings were deleted as soon as soon as the interviews had been transcribed, in accordance with the research ethics for the PHENOTYPE study.

2.1.1.4 Venous blood sampling

Blood samples were taken either myself or by nurses in the clinic. The following clinical blood tests were acquired: full blood count (FBC), C reactive protein (CRP), liver function tests (LFTS), including serum albumin, urea and electrolytes (U+Es), fibrinogen, D dimer and pro-calcitonin. Upper and lower limits were determined according to hospital laboratory cut-offs. For peripheral lymphopenia, a cut-off of $<1.0x10^9$/L was used to signify a low level in accordance with the hospital laboratory. In addition to prospective blood collection, venous blood results collected pre-COVID-19 (for instance, blood eosinophil count, as discussed in Chapter 5), were retrospectively acquired from electronic health records.

2.1.1.5 Endobronchial sampling

Endobronchial sampling was performed by members of the Interventional Bronchoscopy team: Dr Justin Garner, Dr Christopher Orton, Dr James Tonkin, Dr Francesca Conway, Professor Pallav Shah and myself. The majority were performed by Dr Justin Garner and Dr Christopher Orton. Bronchoscopies were performed under conscious sedation with topical lidocaine and intravenous midazolam. 150 mls of sterile 0.9% saline were infiltrated into the airways in 50ml aliquots. 10mls of the return was sent for differential cell count analysis at the Royal Brompton Hospital (Cellular Department), 10mls for microbiological analysis at Chelsea and Westminster Hospital and 10ml for flow cytometry work described in Chapter 7.

Participants signed a consent form to be enrolled into the study, and also signed a clinical bronchoscopy consent form on the day of the procedure.

2.1.2 Patient Recruitment: Healthy control donors

Endobronchial samples (BALF and endobronchial brushings) were acquired by Dr Richard J Hewitt or Dr David JF Smith under the supervision of Dr Philip L Molyneaux (Chief Investigator) or Dr Samuel Kemp. Healthy control subjects, as defined as those with no prior diagnosis of lung disease, were recruited in line with the research ethics committee approvals (NRES reference:15/LO/1399 and 15/SC/0101). All patients had provided informed, written consent.

2.1.3 Demographics of donors for in-vitro assays

Demographic data for donors whose primary bronchial epithelial cells (PBECs) were utilised in the epithelial work described in Chapters 8 and 9 are shown in Table 2.5.

		Age	Gender	Proliferation	Scratch	IAV challenge	DPP4/Sita + IAV	DPP4/ Sita proliferation	DPP4 /Sita
1017	Healthy	36	M			X			
1018	Healthy	65	M	X	X	X			
1028	Healthy	63	M	X	X	X			
1037	Healthy	55	F	X	X	X			
1061	Healthy	NK	NK		X	X			
1062	Healthy	58	M			X			
1063	Healthy	69	M	X		X			
1064	Healthy	35	M			X			
1074	Healthy	55	F	X	X		X	X	X
1072	Healthy	60	F	X	X		X	X	X
1069	Healthy	50	M	X	X		X	X	X
1060	pCOVID-19	60	M			X	X		
1073	pCOVID-19	65	M			X			
1083	pCOVID-19	58	M			X			X
1052	pCOVID-19	52	M			X		X	X
1064	pCOVID-19	49	M			X		X	X
1082	pCOVID-19	52	F			X			
1039	pCOVID-19	83	F			X			
1006	pCOVID-19	46	F			X			
1037	pCOVID-19	74	F			X			
1051	pCOVID-19	65	M			X		X	x
1046	pCOVID-19	56	M			X			
1024	pCOVID-19	74	F			X			x
1010	pCOVID-19	54	M			X			
1153	pCOVID-19	63	M			X			
1106	pCOVID-19	73	M			X			
1095	pCOVID-19	31	M			X			
1034	pCOVID-19	70	M				X		
1115	pCOVID-19	48	M				X		

Table 2. 5 Donor characteristics for epithelial cells utilised in thesis

Abbreviations: M (male), F (female), pCOVID-19 (post-COVID-19), NK (not known), IAV (influenza A virus), DPP4 (Dipeptidyl peptidase-4 inhibitor), Sita (sitagliptin)

2.2 Radiology

Unenhanced CT scans were performed by clinical radiographers at Chelsea and Westminster Hospital, using a 128-section multi–detector row CT machines (Siemens Edge or Edge plus; Siemens Healthcare) at 1.0 – 1.5 mm thicknesses. Median CT dose index was 4.2 mGy. Where contrast was required to rule out potential embolic disease, the contrast Iohexol (350 mg iodine/ml) was used.

Scoring of CTs during the first wave was performed by Professor Sujal Desai and Professor Anand Devaraj, both Thoracic Radiologists at the Royal Brompton Hospital, London. I scored CTs from the second wave. Further details on scoring can be found in Chapter 4.

2.3 Physiology

2.3.1 Routine lung function

Pulmonary function testing was performed by Leeh Faustino and Isaac Mwita, two experienced lung physiologists at Chelsea and Westminster Hospital, London, using the Love Medical Geratherm Respiratory system and BLUE CHERRY® software interface.

Spirometry, body plethysmography and gas transfer were measured in accordance with the American Thoracic Society guidelines. The following anthropometric measurements were made to allow comparison to the reference values provided by European Community for Coal and Steel (ECCS): Age, gender, height, weight, ethnicity.

2.3.1.1 Spirometry

Forced expiratory volume in 1 s (FEV1), Forced vital capacity (FVC), FEV1/FVC ratio and maximal mid-expiratory flow at 25 – 75% FVC (MMEF 25-75) were recorded. Flow volume loops were reviewed to look for a restrictive/obstructive defect. Patients were asked to breathe at tidal volume, and then deeply to total lung capacity (TLC) followed by a rapid exhalation to residual volume (RV), in order to measured FEV1 and FVC. Importantly, MMEF25-75 is considered a measure of small airways function.[224,225]

2.3.1.2 Body plethysmography

Body plethysmography allows measurement of airway resistance and lung volumes. A volume-constant chamber (the whole-body plethysmograph) was used. During the measurement, the box is sealed, and pressure transducers measure a) pressure in the box compared to ambient pressure and b) pressure at the mouth. Respiratory flow rate is also measured. Volume changes are calculated using Boyle's law. That is, at a constant temperature, in closed system, changes in volume in a gas will be affect the pressure exerted by it. In brief, P1V1 = P2V2, where P1 is the initial pressure of the gas, V1 initial volume occupied, P2, final pressure of the gas, V2, final volume occupied.

The patient is asked to sit upright to allow full expansion of the lungs. The seat height is adjusted so that the patient's feet are firmly placed on the floor and the stand height adjusted to ensure the patient can reach the mouthpiece. A noseclip is then applied and the patient is asked to make a tight seal with his/her lips around the mouthpiece. The chamber door is then closed, which the software detects. The patient is asked to breathe through the flow sensor and both the respiratory flow and changes in lung volumes are measured by assessing changes in the box pressure. The airway resistance is assessed using a ratio of volume change to airflow.

To measure intrathoracic gas volume, the mouthpiece is closed after the patient completes exhalation. This forces the patient to breathe against a known resistance, causing air in the lungs to be compressed and decompressed, resulting in measurable changes in pressure in the body plethysmograph. These pressure changes and pressure changes detected at the mouth are used to calculate intrathoracic gas volume (ITGV), from which the RV and TLC can be derived.

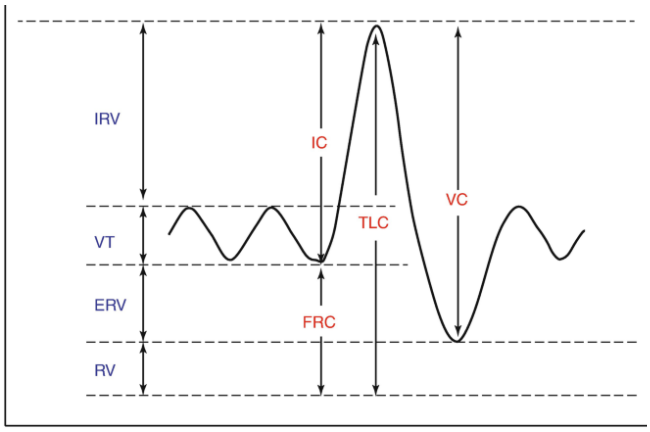


Figure 2. 4 Summary of lung volumes

Abbreviations: IRV – inspiratory reserve volume, VT – tidal volume, ERV – expiratory reserve volume, RV - residual volume, IC – inspiratory capacity, FRC – functional residual capacity, TLC – total lung capacity, VC – vital capacity

2.3.1.3 Gas transfer

Efficiency of gaseous exchange is measured using the single breath-holding technique. The patient is asked to breathe at tidal volume, then deeply to TLC, followed by full expiration to RV. The shutter then opens and the patient is asked to take a quick sharp breath to TLC, inspiring the gas mixture with a composition as follows: 0.3% carbon monoxide, 0.3% methane and 21.0% oxygen. The patient is then asked to hold their breath for 8 seconds, after which, the valve opens automatically. The first volume of gas expired is excluded from the calculations. Subsequent volumes are used to calculate total gas transfer (TLCO), alveolar volume (VA) and corrected gas transfer (KCO). Absolute and % predicted measurements are recorded after comparison with reference values.

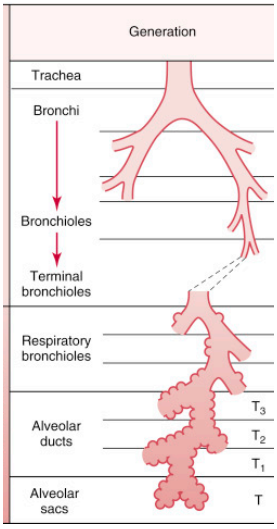
2.3.1.4 Specific airway resistance and conductance

This is measured using the panting method. After breathing at tidal volume, patients are asked to pant against an open shutter for 5 -10 seconds whist supporting their cheeks to prevent air escape through the mouth. Airway resistance (Raw) and its reciprocal, airway conductance (Gaw) were measured in this way, in kPA/L/s.

2.3.2 Small airways testing

Forced oscillometry testing is a non-invasive technique that uses sound waves of different frequencies superimposed on normal tidal breathing to evaluate respiratory mechanics. It measures respiratory impedance, which is made up of airway resistance and airway reactance.[226]

The small airways refer to airways <2mm in diameter (Figure 2.5) and usually contribute very little to airway resistance in health. Lower frequencies can reach the smaller, more distal airways, whereas higher frequencies are absorbed by the larger airways prior to reaching the distal divisions. Airway resistance is usually not frequency-dependent, but in small airways disease, airway resistance at lower frequencies rises, but at higher frequencies remains unchanged.[227]



Large airways (>2 mm diameter)	Conducting zones	**Airway**	**Airway generation**
		Trachea	0
		Bronchi	1 – 5
		Bronchioles	5 – 15
		Terminal bronchioles	16
Small airways (< 2mm diameter)	Transitional and respiratory zones	Respiratory bronchioles	17 – 19
		Alveolar ducts	20 – 22
		Alveolar sacs	23

Figure 2. 5 Tracheo-bronchial divisions

Adapted from McNulty, W & Usmani, O. (2014) European Clinical Respiratory Journal[227]

Reactance is made up of inertance (the movement of the air column in the conducting airways) and capacitance (elastic recoil/stiffness of the lung). In health, the maximal capacitance is at the lung peripheries, so at lower frequencies, the contribution of capacitance to total reactance is greater, making the reactance value negative. At higher frequencies, however, the inertance forces dominate, making the total reactance more positive.[228] In both small airways disease and fibrosis, the total reactance at low frequencies becomes more negative. Resonant frequency (Fres) is the frequency at which inertance = capacitance, i.e., total reactance is zero.[228] The resonant frequency at which this usually happens in health is between 8-12 Hz.[226] In both obstructive and restrictive disease, the resonant frequency rises (as the capacitance is more negative). Area under the reactance curve (Ax) (i.e. the area under the reactance curve between Fres and lowest frequency)[228] also increases in both obstructive and restrictive lung disease affecting the peripheries. To summarise, in obstructive lung disease, one would expect a higher airway resistance, a higher resonant frequency, a higher Ax, and more negative reactance, all at lower frequencies.

Reactance is closely correlated with lung function parameters in COPD[229] and abnormal resistance and reactance values have been noted, even in the context of normal spirometry.[230] Even in healthy individuals who are smokers, abnormal oscillometry findings have been noted, suggesting that oscillometry is a good tool to pick up early abnormalities.[231]

For the results shown in Chapter 6, forced oscillometry using Thorasys Tremoflo® C-100 Airwave Oscillometry System was used. The specific procedures related to usage of this device have been described in Chapter 6. An alternative technique would have been to use impulse oscillometry, but the device needed for this is expensive, not portable and patients have commented on FOT being more comfortable.[232] I was keen to assess small airways disease using a validated, but easily accessible and quick technique so that it can be easily integrated into clinical practice as necessary. Since there are differences between measurements using the forced and impulse oscillometry methods, all readings were taken using the same equipment.[233]

2.4 Flow cytometry

BALF was passed through a 70-micron strainer and centrifuged at 1800 rpm for 5 minutes. The cell pellet was resuspended in 2mls of phosphate buffered saline (PBS, pH 7.4, Gibco) and the number of live cells were counted using a haemocytometer. Cell viability was assessed using Trypan blue (Sigma) with a 1 in 10 dilution of cell suspension:Trypan blue. 10μl of the solution was transferred onto the grid and the number of cells in 3-4 major squares (1mm x 1mm) were counted.

The total cell count was calculated as follows:

Average cells across 3-4 squares x 10^4 x dilution factor (10) x 2 (volume of PBS in which the cells were resuspended). For instance, if an average of 10 cells were counted, the total number of cells in 2mls of PBS would be: 10 x 10^4 x 10 x2 = 2 x 10^6

Between 0.1-1 x 10^6 cells, depending on cell availability, were used for the stained sample, and 0.1 x 10^6 cells utilised for the unstained control. The antibody cocktail used to stain the sample was prepared in flow cytometry staining (FACS) buffer using the optimised, pre-determined dilutions of antibodies (Tables 2.6 & 2.7). Fcblock was added to the antibody cocktail to reduce non-specific binding.

The cell suspensions were added to a V bottom 96 well plate (Corning). A control for the live/dead stain was also plated: 1.25 x 10^5 cells which have been heat-inactivated at 60°C for 10 mins. The plate was then centrifuged 1800 rpm for 2 minutes. The cells were washed with PBS (100µl to each well) and then centrifuged at 2000 rpm, at 4°C for 2 minutes. 25µl of Live/dead Blue stain (Thermofisher) was added to all cells, except the unstained well, to which 25µl of PBS was added and the cells were resuspended. The plate was placed at 4°C for 20 minutes (in the dark). The plate was then washed with PBS and centrifuged at the aforementioned settings. 25µl of the antibody cocktail was added to the cells to be stained, cells resuspended, and then placed in the dark at 4° for 30 minutes. The plate was washed twice with 100µl of FACS buffer and spun at 1800rpm for 2 minutes. 50µl of 1% paraformaldehyde (Electron microscopy Sciences) was then added to the wells and cells resuspended. The plate was placed in the dark at room temperature for 10 minutes. The plate was washed twice again with FACS buffer and spun at 1800 rpm for 2 minutes. Finally, 200µl of FACS buffer was added to each well and resuspended and the plate kept at 4°C overnight until collection using the flow cytometer, BD LSR Fortessa III cell analyser.

Of note, the following buffers and solutions were used:
FACS buffer: 500mls of sterile PBS (pH 7.4, Gibco), 2% Fetal bovine serum (Gibco) and 2mM Ethylenediaminetetraacetic acid (EDTA). The FBS reduces antibodies binding non-specifically and EDTA reduces cell clumping.

1% paraformaldehyde (PFA) was made by adding 150mls of sterile PBS to 10 mls of 16% methanol-free PFA. PFA was stored at -80°C and thawed on the day of staining.

Live/dead Blue solution (Thermofisher) was diluted from the working stock to 1 in 1000 in PBS and made up on the day of staining.

Antibody	Manufacturer	Catalogue number
Anti-Human CD56 BUV737	BD Biosciences	Cat#612767
Anti-Human CD206, BV785	Biolegend	Cat#321142
Anti-Human CD3, BUV805	BD Biosciences	Cat#612896
Anti-Human CD45, PerCP Cy5.5	Thermofisher	Cat#45-0459-42
Anti-Human Siglec8, AF488	R & R systems	Cat#FAB7975G
Anti-Human CD19, BV421	Biolegend	Cat#302234
Anti-Human CD14, BV711	Biolegend	Cat#301838
Anti-Human CD16, BV785	Biolegend	Cat#302046
Anti-Human CD177, FITC	Biolegend	Cat#315804
Anti-Human CD56, PEdz594	Biolegend	Cat#318348
Anti-Human CD3, PE Cy7	Biolegend	Cat#300420
Anti-Human FcE, AF700	Biolegend	Cat#334630
LIVE/DEAD Fixable NIR Cell Stain	Thermofisher	Cat#L34976

Table 2. 6 Antibodies for flow cytometry staining

The antibody dilutions used for staining of post COVID-19 cells:

Marker	Dilution
CD19	1 in 100
CD4	1 in 100
CD117	1 in 25
CD14	1 in 100
CD16	1 in 100
CD177	1 in 50
CD45	1 in 50
Siglec 8	1 in 100
CD56	1 in 100
CD3	1 in 100
CD206	1 in 100
FcE	1 in 50

Table 2. 7 Antibody dilutions for flow cytometry staining

The major immune populations were gated using FlowJo (FlowJo Inc., USA).

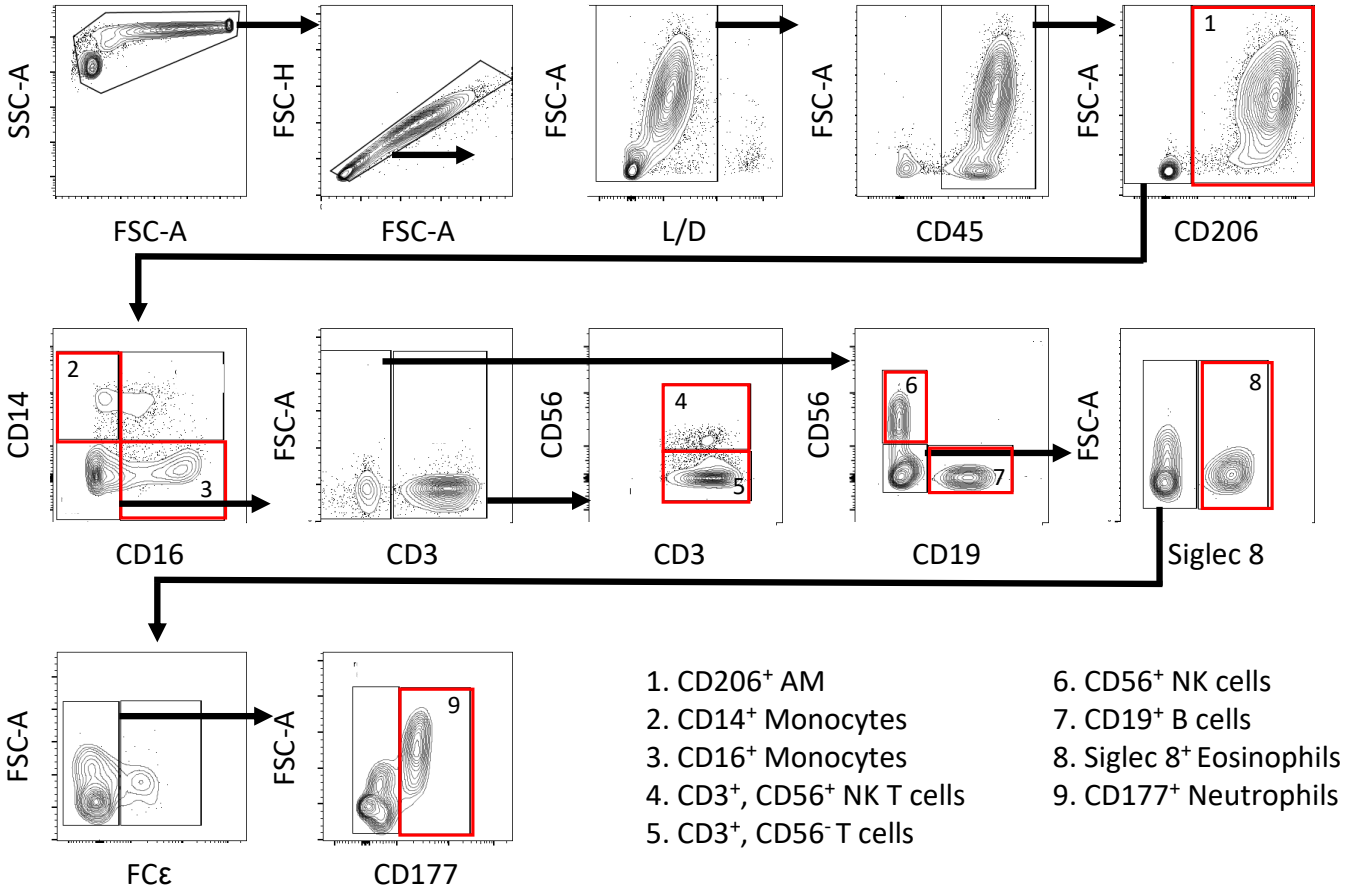


Figure 2. 6 Gating strategy for flow cytometry

2.5 Airway epithelial cell culture

All cells, whether in submerged culture or at air-liquid interface were cultured in an incubator at 37°C with a humidified atmosphere of 5% CO2.

Brushings

Cells were cryopreserved at passage 2 in freezing media consisting of 80% Airway epithelial cell growth medium (Promocell), 10% dimethyl sulphur oxide (DMSO, Sigma) and 10% Fetal bovine serum (FBS, Gibco). Ideally, cells were cryopreserved at 1x 10^6/cryovial. Cryovials were stored in at -80°C overnight

in a freezing vessel (Mr Frosty, Thermoscientific) and then transferred to liquid nitrogen for long-term storage.

Expansion from cryopreservation

Primary bronchial epithelial cells which were cryopreserved were expanded into a T75 flask, coated with Type 1 collagen (Advanced Biomatrix) and cultured in Airway Epithelial Cell Growth medium (Promocell). This involved thawing the cells rapidly in a waterbath at 35°C, then resuspending the cells in 10mls of Airway epithelial cell growth medium in a 15ml Falcon (Corning). The cell suspension was centrifuged at 1800rpm for 5 mins. The supernatant was discarded, and the cell pellet resuspended in 2 ml of Airway Epithelial Growth Medium and then added to the T75 flask, containing 10mls of Airway Epithelial Cell Growth Medium.

Once the flask was 80-90% confluent (usually 5-7 days post seeding), the cells were passaged using 10mls of TrypleTM Express (without Phenol red, Gibco). The reaction was stopped using 10mls of PBS (Gibco). The cell suspension was collected in a 50ml falcon (Corning) and centrifuged at 1800rpm for 5 minutes. The supernatant was discarded and the cell pellet resuspended in 2 ml of Airway Epithelial Cell Growth Medium (Promocell). The cells were counted as described before but this time using a 1 in 2 dilution with Trypan Blue (Thermofisher). Cells were seeded for submerged culture, air-liquid interface or both as described below depending on the number of viable cells.

2.5.1 Submerged culture

2.5.1.1 Proliferation assay

Primary human bronchial epithelial cells from post COVID-19 donors and healthy control donors at passage 3 were seeded at a density of 3 x 10^4 cells/ well in a Type 1 collagen-coated 24-well plate (Corning). Cells were cultured in 500µl of Airway epithelial cell growth medium (Promocell). Media was refreshed every 48 hours. Capture time-lapse Brightfield images were taken using JuLi Stage real-time cell-history recorder (NanoEnTek, Seoul, Korea) for 48 – 120 hours. Experimental triplicates or quadruplicates were run for each donor and an average of the wells taken. Analysis of confluence was performed by the Juli Stage Software. Log2fold change from baseline confluence was calculated for each donor.

For DPP4 and sitagliptin experiments (Chapter 9), a Type 1 collagen-coated (Advanced Biomatrix) 48-well plate (Corning) was used, and cells were seeded at a density of 1.5 x 10^4 per well. Cells were cultured in 250µl of Airway epithelial cell growth media (Promocell) for the control wells, and different dilutions of DPP4 (Abcam) or Sitagliptin (Selleckhem) in Airway epithelial cell grown medium, as described in Chapter 9. Log2fold change from baseline was calculated.

2.5.1.2 Scratch assay

Primary human bronchial epithelial cells at passage 3 were seeded at a density of 3 x 10^4 cells/ well in a Type-1 collagen-coated (Advanced BioMatrix) 24-well plate (Corning) as above. Cells were cultured in Airway epithelial cell growth media (Promocell) until full confluence was reached (500µl of media per well). The media was refreshed and a single, linear wound was made in each well using a yellow pipette tip (P200). Brightfield, time-lapse images were taken of the wound by JuLi Stage real-time cell-history recorder (NanoEnTek, Seoul, Korea) every 2 hours for 24 hours. Multiple focus points were applied per well with at least experimental duplicates (usually quadruplicates) used. Percentage wound closure was calculated using Juli Stage Software. Percentage wound closure at time 0 was 0% and 100% if complete wound closure was achieved.

For DPP4 (Abcam) and Sitagliptin (Selleckhem) experiments in Chapter 9, a 48-well plate was used, and cells seeded at a density of 3 x 10^4 cells per well. Once confluent, a linear wound was made using a P200 yellow pipette tip. Brightfield, time-lapse images were captured as above. 250µl of Airway epithelial cell growth media (Promocell) was added to the control wells and different dilutions of DPP4 (Abcam) or Sitagliptin (Selleckhem) in Airway epithelial cell grown medium added to the other wells, as outlined in Chapter 9.

2.5.2 Air liquid interface

Airway epithelial cells at passage 3 were seeded at a density of 3 x 10^4 cells onto Transwell polyester membrane inserts (Corning, 6.5mm diameter; 0.4µm pore size). Transwell inserts were coated with purified Collagen 1 (Advanced Biomatrix) for 30 mins prior to cell seeding. DMEM-ALI mix (constituents discussed below) was used until a confluent monolayer was formed. The cells were seeded in 200µl of DMEM-ALI mix apically and 500µl basally. The media (apical and basal) were refreshed every 2-3 days until the cells were confluent. Once confluent (which was usually 4-7 days post seeding), the cells were air-exposed to allow cells to differentiate. The basal media was changed to PneumaCult™-ALI

Medium with hydrocortisone (0.48μg/ml). The basal medium was refreshed every 48-72 hours until cells had fully differentiated and were ready for experimentation (5-8 weeks post air exposure). If significant mucus build up was seen, this was removed weekly by washing the cells with 100μl of PBS for 5 minutes. Regardless, the apical compartment was washed with 100μl of PBS 48 hours prior to the experiment, and then again on the day of the experiment to ensure mucus build-up did not interfere with cell stimulation.

48 hours prior to the experiment, the basal media was changed to PneumaCult™-ALI Medium without supplemental hydrocortisone. This steroid-free medium was utilised throughout the experiment.

2.5.3 Media used for cell culture

2.5.3.1 Media for submerged culture:

<u>Medium for submerged culture from bronchial brush to P1</u>

Airway epithelial cell growth medium (Promocell) with addition of 100μg/ml Primocin, 4μl/ml of bovine pituitary extract (BPE), 10ng/ml of rhEGF, 0.5μg/ml of rhInsulin, 0.5μg/ml of hydrocortisone, 0.5μg/ml of epinephrine, 6.7ng/ml of triiodo-L-thyronine, 10microgram/ml of rhTransferrin and 0.1ng/ml of retinoic acid.

<u>Media for submerged culture P2 onwards</u>

Airway epithelial cell growth medium (Promocell) with addition of 100U/ml Penicillin-streptomycin, 4μl/ml of bovine pituitary extract (BPE), 10ng/ml of rhEGF, 0.5μg/ml of rhInsulin, 0.5μg/ml of hydrocortisone, 0.5μg/ml of epinephrine, 6.7ng/ml of triiodo-L-thyronine, 10microgram/ml of rhTransferrin and 0.1ng/ml of retinoic acid.

2.5.3.2 Media for ALI culture

DMEM-Ali mix - 1:1 mix of Airway epithelial cell growth medium (Promocell) and DMEM (high glucose, GlutaMAX™ Supplement, pyruvate, Gibco) with the following supplements added: pencillin-streptomycin (100U/ml), 25mM HEPES, 1.5μg/ml Bovine serum albumin, 4μl/ml bovine pituitary extract, 10ng/ml rhEGF (epidermal growth factor), 5μg/ml rhInsulin, 0.5μg/ml hydrocortisone, 0.5μg/ml epinephrine, 10μg/ml of rhTransferrin and 0.1ng/ml retinoic acid.

PneumaCultTM -ALI medium (Stemcell) supplemented with 100U/ml penicillin-streptomycin, 0.0004% heparin, 0.48μg/ml hydrocortisone, PneumaCult™-ALI 10X Supplement and 5mls PneumaCult™-ALI Maintenance Supplement (100x).

2.6 Fibroblast cell culture

Human lung fibroblasts (Lonzo) were expanded from cryopreservation as described in Section 2.5 but using Dulbecco's Modified Eagle Medium (DMEM) supplemented with penicillin-streptomycin and 10% Fetal bovine serum (FBS). Prior to experimentation, the cells were serum-starved for 24 hours. Further details of the specific experimental plans for fibroblast work are given in Chapters 8 and 9.

2.7 Influenza Stocks

Influenza A virus (A/England/195/2009) stocks were obtained from Dr James Harker (Supervisor) and was made up into stocks of 1.0 multiplicity of index (MOI) based on the assumption that $3x10^4$ cells were seeded onto each transwell insert. This was then further diluted to a MOI of 0.01 in serum-free DMEM (Gibco). As a control, some aliquots were ultraviolet (UV)-inactivated using the Stratalinker UV 1800 Crosslinker (Stratagene).

2.8 General techniques

2.8.1 TEER measurements

TEER is a well-established method for detecting barrier function and is a measure of the ionic conductance of the epithelial monolayer.[234,235] 100μl of warmed phosphate-buffered saline (PBS, Gibco) was added to the apical monolayer for 10 minutes. The EVOM2 Epithelial Voltohmmeter (World Precision Instruments) was checked using the manufacturer-provided calibration probe which has a known resistance of 1000 Ohms. The STX2 electrode was sterilized in 70% ethanol for 5 minutes and then thoroughly rinsed in PBS. TEER is temperature-sensitive as conductance increases with temperature, thereby reducing TEER values. Therefore, a special effort was made to only take plates out of the incubator once ready to perform measurements. The plate was placed flat in the tissue culture hood and the probe was held perpendicular, ensuring the basolateral probe was touching the well bottom and the apical electrode in the apical compartment in the PBS. The TEER values were allowed to stabilize prior to a value being recorded. The probe was held at the same angle for all TEER measurements and all TEER measurements reported in this thesis were performed by myself to avoid

user variability. To avoid cross-contamination, the probe was decontaminated with 70% ethanol between different experimental conditions, which was especially important when dealing with UV and IAV-infected epithelial cells described in Chapter 8.

The TEER value of the blank insert (usually between 125 – 150 Ohms), was subtracted from the resistance of the well, and then multiplied by the area of the insert, to obtain a value for Ohms/cm^2. For instance, if the resistance of a well was 1000 and blank insert 150, with an insert area of 0.33cm^2, the final TEER value for the well is:

(1000 – 150) * 0.33 = 281 Ohms/cm^2

Multiple TEER readings were taken for each experimental condition to increase the reliability of the results. Absolute TEER values and % drop in TEER from a pre-defined time point, were calculated.

2.8.2 Imaging

2.8.2.1 Fixation

16% paraformaldehyde (PFA, Electron microscopy sciences) was diluted to 4% in PBS for use in fixing cells.

Images from ALI cultures were fixed in 4% PFA. 200µl 4% PFA was added to the apical surface for 20 mins at room temperature. The apical surface was then washed 2-3 times with PBS. The inserts were stored in PBS (500µl in the apical compartment and 1ml in the basal compartment) at 4°C until they were ready for agarose embedding.

Cells in submerged culture were fixed in PFA as described above and stored in 250µl of PBS in the well until staining.

2.8.2.2 Agarose embedding

Low melting point agarose (Thermofisher R0801) was diluted to 4% in PBS and heated in a microwave until fully dissolved. Agarose was kept in a water bath at 35°C whilst embedding was performed. The ALI membrane was cut using a scalpel and lowered into a well in a 24-well plate (cell-side up) into which 1 – 1.5 mls of agarose had already been pipetted. It was important to ensure that the agarose

hadn't solidified before lowering the membrane to avoid cell shearing. Once the agarose had solidified, the agarose block was removed using forceps. The blocks were cut to allow them to fit into the histology cassettes. The cassettes were dehydrated in increasing concentrations of Industrial methylated (IMS) spirit diluted in water to concentrations of 30%, 50%, 70%, each for 15 mins and left submerged in 70% IMS at 4°C until wax embedding and sectioning were performed by Lorraine Lawrence, NHLI. Sections were cut to 4 micron thickness. Haematoxylin and eosin (H&E) and Periodic acid Schiff (PAS) staining were also performed by Lorraine Lawrence.

2.8.2.3 Staining

2.8.2.3.1 Staining ALI sections

The cells were dewaxed in Gentaclear (Genta Medical, UK and then rehydrated through 100%, 90% and 70% alcohol for 1 minute each, and then placed in distilled water. The antigen retrieval buffer (1mM Ethylenediaminetetraacetic acid [EDTA], pH 8.0) was heated to 90°C and the slides were submerged in this buffer for 30 minutes at room temperature. The area on the slide to be stained was demarcated using a PAP pen (Sigma) and the cells were permeabilised for 1 hour at room temperature by adding approximately 100µl of buffer: 10% donkey serum, 0.5% Tween. The slide was washed twice in PBS, allowing the slides to soak for 5 minutes each time. The primary antibody (Ab) (see Table 2.8) was diluted in 1% Bovine serum albumin (BSA, Sigma), diluted in PBS and approximately 60µl was added per section and incubated overnight at 4°C in a humidified chamber. The slides were washed again in PBS, 5 minutes per wash at room temperature. The secondary Ab was diluted in 1% BSA/PBS and 60µl added to the areas to be stained. The cells were further incubated for 1 hour at room temperature in a humidified staining chamber. The cells were washed once again in PBS and then stained with DAPI (4',6-diamidino-2-phenylindole) at a dilution of 1 in 20 000 in PBS for 5-10 minutes at room temperature. The cells were mounted using ProLong™ Diamond Antifade Mountant (Thermofisher) and left for 24 hours in the dark room temperature to cure. The stained slides were stored at 4°C until acquisition using Aperio VERSA slide scanner (Leica). Images were acquired at 5x, 10x and 20 x magnification.

Antigen	Host	Clone	Fluorochrome	Supplier	Dilution
Cytokeratin 5	Rabbit	EP1601Y	AF647	Abcam # 193895	1 in 200
MUC5AC	Rabbit	EPR16904	AF555	Abcam 218714	1 in 100
ZO-1	Mouse	ZO1-1A12	AF 488	Invitrogen #339188	1 in 200
FOXJ1	Goat		Unconjugated	R&D biosystems #AF3619	1 in 200
DAPI				Sigma Aldrich# D9542	1 in 20 000

Table 2. 8 Primary antibodies for staining of ALI sections

2.8.2.3.2 Staining basal cells: Ki67 staining

Ki67 staining was performed on submerged cells to further assess if the cells were in the proliferative phase (Chapter 9). The cells had already been fixed in 4% PFA as previously described. Cells were washed with 400µl of PBS and then permeabilised with 200 µl of permeabilization buffer (PBS + 1% BSA + 10% normal goat serum + 0.3% Triton-X (Sigma) for 30 minutes at room temperature. The cells were then washed twice with 400µl PBS and blocked with 200 µl of Block buffer (PBS + 1% BSA + 10% normal goat serum) at room temperature for 1 hour. Ki67 monoclonal Ab (SolA15, Invitrogen) was prepared at a 1 in 250 dilution in antibody diluent (PBS + 1% BSA + 0.05% Triton-X (Sigma). The cells were washed again, twice in 400µl of PBS and 200µl of Ki67 Ab was added to each well and left to incubate overnight at 4°C. The cells were then washed twice in 400µl of Wash buffer (PBS + 1% BSA + 0.05% Triton-X). 200µl of secondary antibody (Cy3 Goat Anti-Rat Antibody, Jackson Immuno) diluted to 1 in 250 in the aforementioned antibody diluent was added to each well and allowed to incubate for 1 hour at room temperature. Special care was taken to avoid exposure to light. Cells were washed again in PBS and DAPI (Invitrogen) diluted to a concentration of 1 in 1000 in PBS was added (200µl) to each well and allowed to incubate for 10 minutes at room temperature. Cells were washed three times in PBS. The plate was stored at 4°C until fluorescence imaging using JuLi Stage real-time cell-history recorder (NanoEnTek, Seoul, Korea). The DAPI stain was viewed using the DAPI channel (Excitation 390/40, Emission 452/45) and Ki67 under the RFP channel (Excitation 525/50, Emission 580LP). Images were taken at 10x and 20x magnification. Where appropriate, cell counting was performed by JuliStage, and elsewhere, manual counting was performed. A ratio between Ki67+ and DAPI+ cells was calculated to ascertain the proportion of cells that were in the proliferative stage.

2.9 Gene expression

RNA was harvested during experiments at pre-defined timepoints. Cells were lysed by adding 350µl Buffer RLT (Qiagen) containing 1% beta-mercaptoethanol (ß-ME). The guanidinium isothiocyanate (GITC) in buffer RLT temporarily denatures RNAses. This, in addition to the reducing effects of ß-ME which irreversibly denatures RNAses, facilitates preservation of the harvested RNA.

2.9.1 RNA extraction

RNA was extracted using the RNeasy plus MiniKit (Qiagen) as per the manufacturer's instructions. Quantification of RNA was performed using Nanodrop ND1000 spectrophotometer (Thermoscientific), after loading 1µl of RNA into the system. The spectrophotometer gives absorbance readings at 230nm, 260nm and 280nm. RNA has a maximal absorption at 260nm and therefore this value reflects the quantity of RNA present in the sample. The Beer Lambert Law is then used to calculate the quantity of RNA. The law states an inverse relationship between the transmission of light through a substance (which in turn is the inverse of absorbance), and the molar concentration and thickness of the substance.[236] A high absorbance at 280nm, is suggestive of protein contamination and RNA without contamination usually has a 260/280 ratio of about 2.0. Absorbance at 230nm is often due to contamination with guanidine salts or phenol, which are found in reagents utilised as part of the RNA extraction process.[237] The Nanodrop is a very useful spectrophotometer as it only requires a small volume of RNA (1µl) to give a reading. RNAse-free water (Qiagen) was used as the blank control as this is the RNA elution solution used as per the protocol. Therefore, using the Nanodrop, the RNA quantity and purity can be assessed. Purified RNA was stored at -80°C until cDNA synthesis or transported on dry ice for standard RNA sequencing.

2.9.2 Complementary DNA (cDNA) synthesis

cDNA was synthesised using High-capacity cDNA reverse transcription kit (Applied biosystems). 10µl of Real-time (RT) qPCR master mix was calculated at the following ratios: 10xRT buffer:25x deoxyribonucleotide triphosphate (dNTP) mix: 10x RT random primers: Multiscribe reverse transcriptase: Nuclease-free water. – 2: 0.8: 2.0:1.0: 4.2. The quantity of RNA to convert was determined by the maximum capacity of the conversion kit (2µg per reaction). 10µl of total sample was prepared, with supplementation with RNAse-free water (Qiagen) as necessary. A set reaction volume of 20µl was used (10µl sample and 10µl reaction mix). The sample was loaded into the Thermocycler and passed through 4 temperature settings, optimised for use with the High capacity

CDNA kit: 25°C for 10 min, 37 °C for 120 min, 85°C for 5 min and 4°C thereafter. cDNA was diluted 1 in 10 with RNAse-free water. The dilutions depended on the quantity of RNA that was converted, with lower quantities requiring lower dilutions. cDNA was stored at -20°C until ready for assessment with quantitative PCR.

2.9.3 RNA sequencing

2.9.3.1 Sample selection

RNA from the IAV challenge at ALI described in Chapter 8 was sent for RNA sequencing. RNA was extracted as described in section 2.9.1

RNA from 2 healthy control donor PBECs and 3 post COVID-19 donor PBECs were pooled into 2 groups (healthy control vs post COVID-19) at different timepoints post IAV infection. 1μg of RNA was sent for each group, at each time point (4, 24, 48, 72 hours post infection). Therefore, in total, 8 samples were sent for RNA sequencing. Samples were transported on dry ice.

2.9.3.2 Quality control

RNA sequencing was performed by Genewiz (Azenta Life Sciences, Germany). To ensure adequate and reliable transcriptomic results, the RNA has to be of good quality. The RNA integrity number (RIN) and RNA quality number (RQN) is a number assigned to rate the quality of the RNA. The scale runs from 1 – 10, with 1 representing degraded RNA and 10 representing perfect RNA.[238] For RNA sequencing, a RIN>=6.0 was requested. RNAses are ubiquitous and can result in degradation of the RNA, which emphasises the importance of RNA integrity assessment prior to transcriptomic analysis. RNA integrity can be measured using electrophoresis where RNA is placed on denaturing agarose which has been stained with ethidium bromide. Two ribosomal RNA bands should be seen, one at 28S and the other at 16S. The band at 28S should be more prominent than the band at 16S if the RNA is intact, usually with a ratio of 2:1.[239] RNA integrity was not assessed prior to sending samples to Genewiz, but RQN was assessed by the sequencing team as part of the quality control (QC) process using the Agilent 5200 Fragment Analyser system, which is an automated capillary electrophoresis-based technology. In addition, the concentration of the RNA sent was calculated as part of the QC process using a Qubit-assay, a fluorescence assay which uses specific dyes that bind to pre-defined targets and emit a fluorescent signal.

2.9.3.2 Library preparation

There are three main types of RNA that are involved in protein synthesis (ribosomal RNA [rRNA], messenger RNA [mRNA] and transfer RNA [tRNA]).[240] Ribosomal RNA forms about 80% of the total RNA, but for RNA sequencing, the rRNA needs to be removed to allow more in depth and accurate assessment of mRNA. The target RNA for the RNA sequencing was mRNA. Both positive PolyA selection and negative rRNA depletion can be performed to select mRNA. However, the former is thought to be superior and was performed in my samples.[241] Illumina Novseq with 2x150 bp configuration was used for sequencing. During each sequencing run, the Illumina software assigns a quality score to each base call, based on quality predictor variables (such as intensity of signal, and signal:noise ratio) and a quality model. A quality score of 30, suggests a 1 in 1000 error rate of the wrong base being identified. The higher the quality score, the more reliable the results.[242]

2.9.3.3 Data analysis

Bioinformatic analysis was performed by the Bioinformatic scientists at Genewiz. The sequences were then trimmed to remove adapter sequences and poor-quality nucleotides. Trimmomatic V.0.36 was utilised for this. STAR aligner V2.5.2b was used to map the trimmed reads onto the human genome. This software can detect splice junctions, therefore allowing differentiation between the coding exons and non-coding introns. Subread package V1.5.2 was then utilised to calculate unique gene hit counts, ensuring that only reads within the exon regions are made. The normalised counts rather than the raw counts were used to assess differential gene expression to enable correction for differences in read depths between the samples. DeSeq2 was used to compare gene expression between the groups i.e., healthy control vs post COVID-19 at the different timepoints. The Wald test was used to generate p values and the variance was set at zero as there were no replicates. The p value was set as 0.1 to identify differentially expressed genes.

2.9.4 Quantitative polymerase chain reaction (qPCR)

Samples were prepared as per volumes required for a 384 well plate (Applied biosystems MicroAmp optical 384 well reaction plate). Total volume per well was 6µl (3.6µl reaction mix and 2.4µl cDNA). Reaction mix was made with 0.3µl Taqman primer assay, 0.3µl nuclease-free water (Qiagen) and 3µl Taqman Fast Advance Mastermix (Applied Biosystems). 2.4µl of cDNA was pipetted into each well (in

duplicates) in addition to 3.6µl of reaction mix. The plate was centrifuged for 5 minutes at 1800rpm after covering with an adhesive cover, and then placed at 4°C until analysis. The PCR was performed using ViiA 7 Real-time PCR system (Applied Biosystems). The following run method was programmed: Step 1 at 95°C for 20 minutes (Hold stage); Step 2: 95°C for 1 minute and 60°C for 20 minutes (PCR stage). The instrument was set to capture 40 cycles.

The cycle threshold (Ct) values were exported into an excel sheet. An average Ct value was calculated for the housekeeping gene (HKG) and for the gene of interest. The Ct value for the HKG was then subtracted from the Ct value for the gene of interest (delta CT). Relative expression was calculated using the following calculation: 2^(- delta CT). The primers used are shown in Table 2.9. A custom-designed primer (Taqman) from Thermofisher was used for Flu A M1: Forward (CAAGACCAATCTTGTCACCTCTGAC), Reverse (GCATTTTGGACAAAGCGTCTACG), Probe (TGCAGTCCTCGCTCACTGGGCACG), Chemistry (FAM-MGB).

Gene	Assay ID	Gene	Assay ID
IFITM3	Hs03057129_s1	**KRT5**	Hs00361185_m1
IFIT1	Hs00356631_g1	**FOXJ1**	Hs00230964_m1
RSAD2	Hs00369813_m1	**MUC5AC**	Hs01365616_m1
OAS2	Hs00942643_m1	**MUC5AB**	Hs00861595_m1
AREG	Hs00950669_m1	**TJP1**	Hs01551861_m1
HBEGF	Hs00181813_m1	**CDH1**	Hs01023895_m1
DPP4	Hs00897386_m1	**YWAHZ (housekeeping)**	Hs01122445_g1
CXCL10	Hs01124252_g1	**CXCL8**	Hs00174103_m1
TNF	Hs00174128_m1	**ACTA2**	Hs00426835_g1
FN1	Hs01549976_m1	**VIM**	Hs00958111_m1

Table 2. 9 Human Taqman primers for qPCR

2.10 Protein quantification

2.10.1 O-link proteomic assay

Cryopreserved BAL from donors post COVID-19 and healthy control donors were sent for protein measurement using the O-link proximity extension immunoassay platform. Five panels were used: "Inflammation", "Cardiometabolic", "Cardiovascular 2", "Cardiovascular 3" and "Immune response". In total, 435 different proteins were measured per sample. Details of the specific assays are shown in Table 2.10.

Target 96 Cardiometabolic Assay	Olink	Cat#91802
Target 96 CVD II Assay	Olink	Cat#91202
Target 96 CVD III Assay	Olink	Cat#91203
Target 96 Immune Response Assay	Olink	Cat#91701
Target 96 Inflammation Assay	Olink	Cat#91301

Table 2. 10 O-link assays performed on BALF samples

2.10.2 Enzyme-linked immunosorbent assay (ELISA)

Protein-evaluation was performed using ELISAs as they are a very sensitive, highly specific and a relatively quick assay to perform. In fact, apart from the albumin ELISA, all other ELISAs listed have a minimal detectable threshold in pg/ml (ng/ml for albumin).

ELISAs were performed using 96 well (Corning) plates. Sandwich ELISAs were used, due to their sensitivity and specificity. The process involved firstly, immobilizing the antigen using a capture antibody specific to the antigen. The plate was incubated with the capture antibody overnight. The plate was washed with wash buffer and Block buffer was then added to prevent non-specific binding. After this and further washing of the plates, the sample and standard were added in duplicates to the plate. The plate was washed again and then detection antibody, specific to a different antigen was added. After incubation for the pre-defined time according to the protocol, Streptavidin conjugated with horseradish peroxidase (HRP) enzyme was added to the plate. After appropriate incubation, the plate was washed again and substrate (Enhanced K BlueR TMB substrate, Neogen) was added and the plate kept in the dark. The streptaviridin binds to the biotin in the detection antibody and the HRP allows enzyme activity once the substrate has been added. In order to stop the reaction, stop solution (2 N H2SO4 [R&D Systems, Catalog # DY994]) was added. The optical density (OD) of each well was measured using a SpectraMax® i3x plate reader (Molecular Devices, San Jose, USA) at one wavelength (450nm) for albumin or two wavelengths (450 and 540nm) as per the protocol. Quantification was performed by the Spectramax software and an average of the duplicates was recorded. Table 2.11 shows the ELISAs used in this thesis.

Elisa	**Manufacturer**	**Catalogue number**
DPP4 ELISA	R&D Biosystems	#DY1180
Albumin ELISA	Bethyl Laboratories	#E80-129
Human AREG duoset ELISA	R&D Biosystems	#DY262
Human IFN beta Duoset Elisa	R&D Biosystems	#DY814-05
Human IL-29/IL-28B (IFN-lambda 1/3) DuoSet ELISA	R&D Biosystems	#DY1598B
Human IL6 Duoset Elisa	R&D Biosystems	#DY206
Human IL8/CXCL8 Duoset ELISA	R&D Biosystems	#DY208

Table 2. 11 ELISA kits used

2.11 Statistical analysis

2.11.1 Proteomics

The data analysis for the proteomic dataset was analysed by Dr Artemis Papadaki and Dr James E Peters in a collaboration (Chapter 9).

2.11.2 Transcriptomics

The bioinformatics statistical analysis pathway has been described in Section 2.9.3.3.

2.11.3 Other analyses

Graphpad Prism version 9.0 [86] for Mac, GraphPad Software [*www.graphpad.com*]) was used for all other analyses. Normality testing was performed where possible and where a Gaussian distribution was shown, parametric analyses were performed. Data has been shown as n (%n), median (interquartile range) or mean (+/- standard error of mean) throughout. Inter group comparisons were made using unpaired non-parametric Mann Whitney U test or parametric student's T test. Paired analyses were used performed using non-parametric Wilcoxon paired signed rank test or paired student T test. A p value <0.05 was considered statistically significant. The p value significance has been documented in the figure legends: *<0.05, ** <0.01, ***<0.001, ***<0.0001.

Whilst a hypothesis has been stated in each Chapter, the data presented in this thesis was largely observational which little or no pre-existing data from which to derive a hypothesis. This, coupled with the fact that all clinical recruitment was performed during the pandemic, means that statistical powering was not performed and clinical recruitment and endobronchial samples were based on what could feasibly be acquired by myself during my PhD years.

Chapter 3 - Evaluating clinical trajectory post COVID-19

3.1 Introduction

Chronic symptoms such as cough and fatigue are common post a viral illness, but are usually self-limiting and require no additional treatment.[83,84,88] After the SARS COV1 and MERS pandemics, a significant number of patients had persistent symptoms, even several months after discharge.[81,82] It was not known if individuals post COVID-19 would suffer similar morbidity.

An individual's quality of life (QOL) can be impacted on by a number of factors, but QOL impairment due to physical symptoms, has been well-described.[243,244] Indeed, the relationship between physical and psychological symptoms is important to consider when dealing with patients with chronic disease, as psychological morbidity, for instance, depression or anxiety, can have a profound impact on the individual's perception of physical symptoms.[245,246]

3.2 Background

At the commencement of my PhD, it was not known whether individuals post COVID-19 will have persistent symptoms at follow up, and what the nature of these symptoms might be. Furthermore, it was not known if the severity of the acute disease presentation would impact the likelihood of persistent morbidity.

3.3 Hypothesis and Aims

Hypothesis

Persistent physical and psychological symptoms are common post COVID-19 and negatively impact quality of life during recovery

Aims

a) To explore residual symptoms post COVID-19
b) To describe the psychological impact of COVID-19
c) To assess the effect of COVID-19 on health-related quality of life (HR-QOL)

3.4 Methods

Patients recruited to the PHENOTYPE study, as described in Chapter 2, were reviewed at sequential time points post hospital discharge. Patients were recruited during the first wave (admitted to hospital between March – April 2020) and the second wave (admitted to hospital between September 2020 and February 2021).

The first follow-up visit for patients recruited during the first wave was performed at a median of 99 (IQR 86 – 124) days post discharge. The first visit was therefore around 3 months post discharge, rather than 4-6 weeks as intended by the study protocol. This was due to delays in setting up a follow-up service at a time when services were already overwhelmed. In contrast, during the second wave, the first follow up visit was performed approximately 42 (IQR 37 – 44) days post discharge.

At each clinical visit, patients underwent a thorough clinical assessment, with assessment of persistent symptomatology and acquisition of venous blood samples. Patients were asked to report if they were experiencing new or worsening symptoms (for instance, breathlessness or cough), as compared to their pre-COVID-19 baseline. This was especially important as some individuals in this cohort had pre-existing respiratory conditions and may therefore have experienced a degree of breathlessness even prior to their admission with COVID-19.

Questionnaires were administered, as described in Chapter 2, to assess respiratory morbidity (mMRC), psychological morbidity (HADS) and HR-QOL (SF-36). A subset of individuals recruited during the first wave (n=17), underwent semi-structured interviews to elucidate the factors affecting their quality of life. These interviews were conducted and transcribed verbatim by myself and analysed to identify themes and sub-themes using Braun and Clarke (2006) methodology.[222]

3.5 Results

3.5.1 Consort diagram

Figure 3.1 shows the patients recruited to the study and patients attending follow up. 205 patients in total were recruited to PHENOTYPE between June 2020 and March 2021. Individuals who had not been admitted for COVID-19-related illness were subsequently excluded from data analysis. In brief, 89 patients were recruited from the first wave and 9 patients were excluded as a positive SARS-COV2

swab was an incidental finding. This high number requiring exclusion was in part due to difficulties recruiting during the first wave, requiring retrospective review of the notes documented on electronic health records. 116 patients were recruited during the second wave.

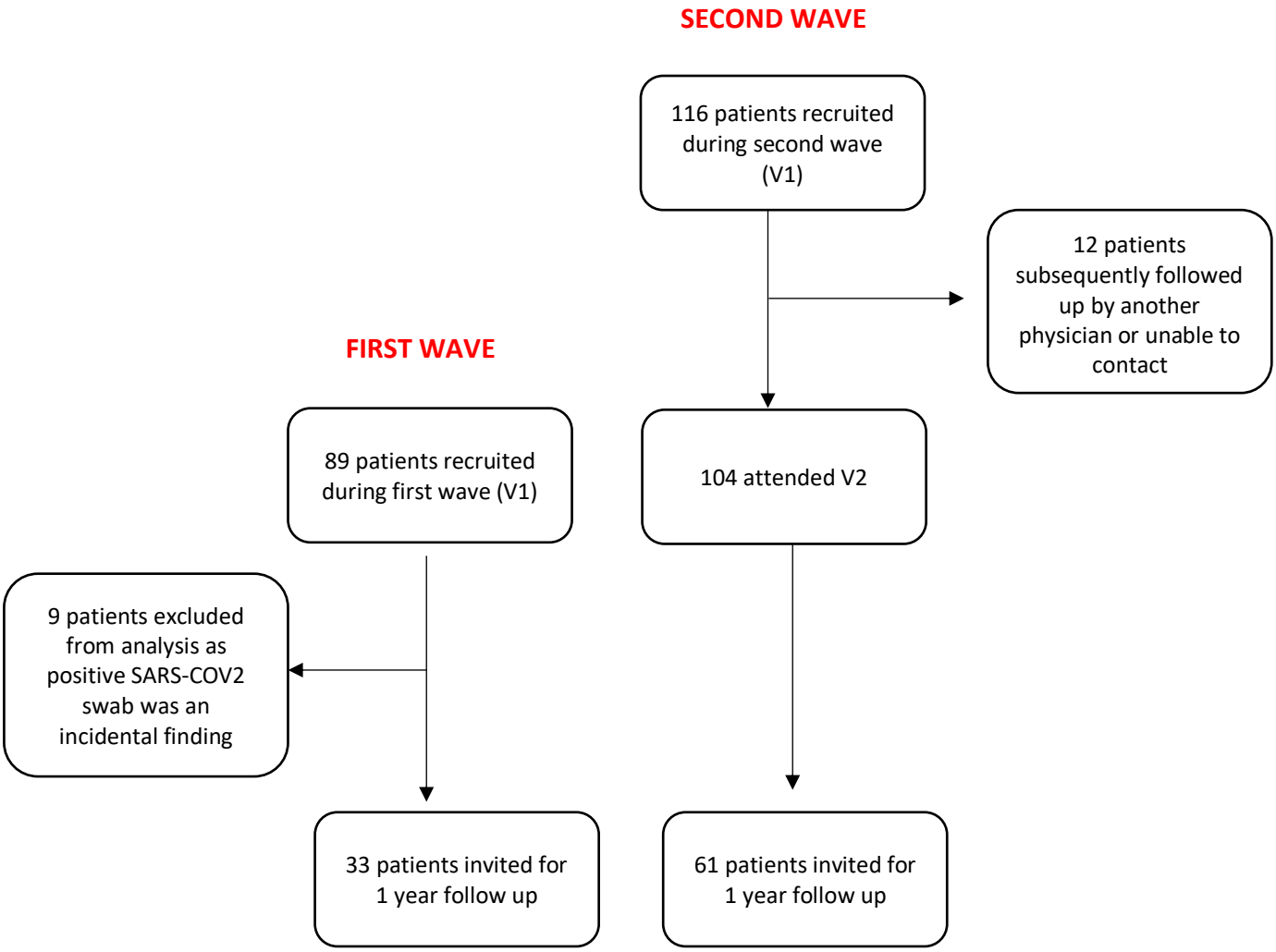


Figure 3. 1 CONSORT diagram of patients recruited to the PHENOTYPE study

V1 (Visit 1) - performed approximately 3 months post discharge during the first wave, and 6 weeks post discharge during the second wave. V2 (Visit 2) - performed approximately 3 months post discharge during the second wave.

3.5.2 Baseline demographics and persistent symptomatology

Table 3.1 shows the demographics of individuals recruited to the PHENOTYPE study between June 2020 and March 2021. The symptoms shown are those reported by the patients at approximately 3 months post discharge (Visit 1 for Wave 1, Visit 2 for Wave 2).

The commonest reported abnormality was fatigue, with more than 50% of individuals complaining of this across both waves. Secondly, patient-reported breathlessness was common and reported in about 41% of individuals, and cough in 31%. Whilst not assessed in Wave 1, memory disturbances were also common in about 16% of individuals being followed up during Wave 2.

During the first wave, 30/80 (37.5%) of individuals had a deterioration in their mMRC score of at least 1 score from their pre-morbid baseline. This was in comparison to 37/80 (46.3%) of individuals who reported breathlessness. During the second wave, this scoring system was not utilised, and the prevalence of breathlessness was assessed based on patient-reported symptoms only.

		Wave 1 (n=80)	Wave 2 (n=116)	Combined Wave 1 + Wave 2 (n=196)
Gender, M		53 (66)	81 (69.8)	134 (68.4)
Age		58.6 (+/-1.4)	55.5 (+/-1.3)	56.8 (+/- 0.98)
Respiratory comorbidities	Asthma	10 (13)	10 (8.6)	20 (17.2)
	COPD	6 (7.5)	6 (5.2)	12 (6.1)
	OSA	2 (2.5)	5 (4.3)	7 (3.6)
Cardiovascular comorbidities	IHD	6 (7.5)	11 (9.5)	17 (8.7)
	HTN	23 (29)	25 (22)	48 (24.5)
	T2DM	18 (23)	16 (14)	34 (17.3)
Smoking status:				
	Current smoker	3 (26)	2 (1.7)	5 (2.6)
	Ex-smoker>=10 pack year	19 (24)	17 (14.7)	36 (18.4)
	Non-smoker or ex-smoker <10 packyear	58 (73)	97 (83.6)	155 (79.1)
Admitted to hospital		80 (100)	107 (92.2)	187 (95.4)
	MV	17 (21)	3 (2.6)	20 (10.2)
	NIV	15 (19)	27 (23.2)	42 (21.4)
	O2	43 (54)	72 (62.1)	115 (58.7)
Length of hospital stay (days)		8 (3-15)	7 (4-10)	7 (4 -11)
mMRC % change of at least 1 point between pre-covid and follow up		30 (37.5)	N/A	
Patient-reported breathlessness		37 (46.3)	38 (36.5)*	75 (40.8)
Cough		15 (18.8)	17 (16.4)*	32 (30.8)
Fatigue		19 (23.8)	38 (36.5)*	57 (54.8)
Palpitations		N/A	5 (4.8)*	N/A
Memory disturbances		N/A	17 (16.3)*	N/A
Anosmia/taste disturbances		N/A	7 (6.7)*	N/A
Chest pain		N/A	1 (9.6)*	N/A

*N = 104

Table 3. 1 Demographics and hospital admission data for patients recruited to PHENOTYPE

Data shown as n (%n), mean (+/- SEM) or median (IQR). Abbreviations: M (male), COPD (chronic obstructive pulmonary disease), OSA (obstructive sleep apnoea), IHD (ischaemic heart disease), HTN (hypertension), T2DM (type 2 diabetes mellitus), MV (mechanical ventilation), NIV (non-invasive ventilation), O2 (oxygen).

3.5.3 Blood parameters

Significant abnormalities were seen in blood parameters during the acute admission, with normalisation of the majority of parameters by 3 month follow up (Figure 3.2) During Wave 2, when blood tests were performed earlier post discharge, significant improvements in the blood counts were seen as early as 6 weeks, with further improvement in some biomarkers such as ferritin, fibrinogen, D dimer and albumin between 6 weeks and 3 months (Figure 3.3).

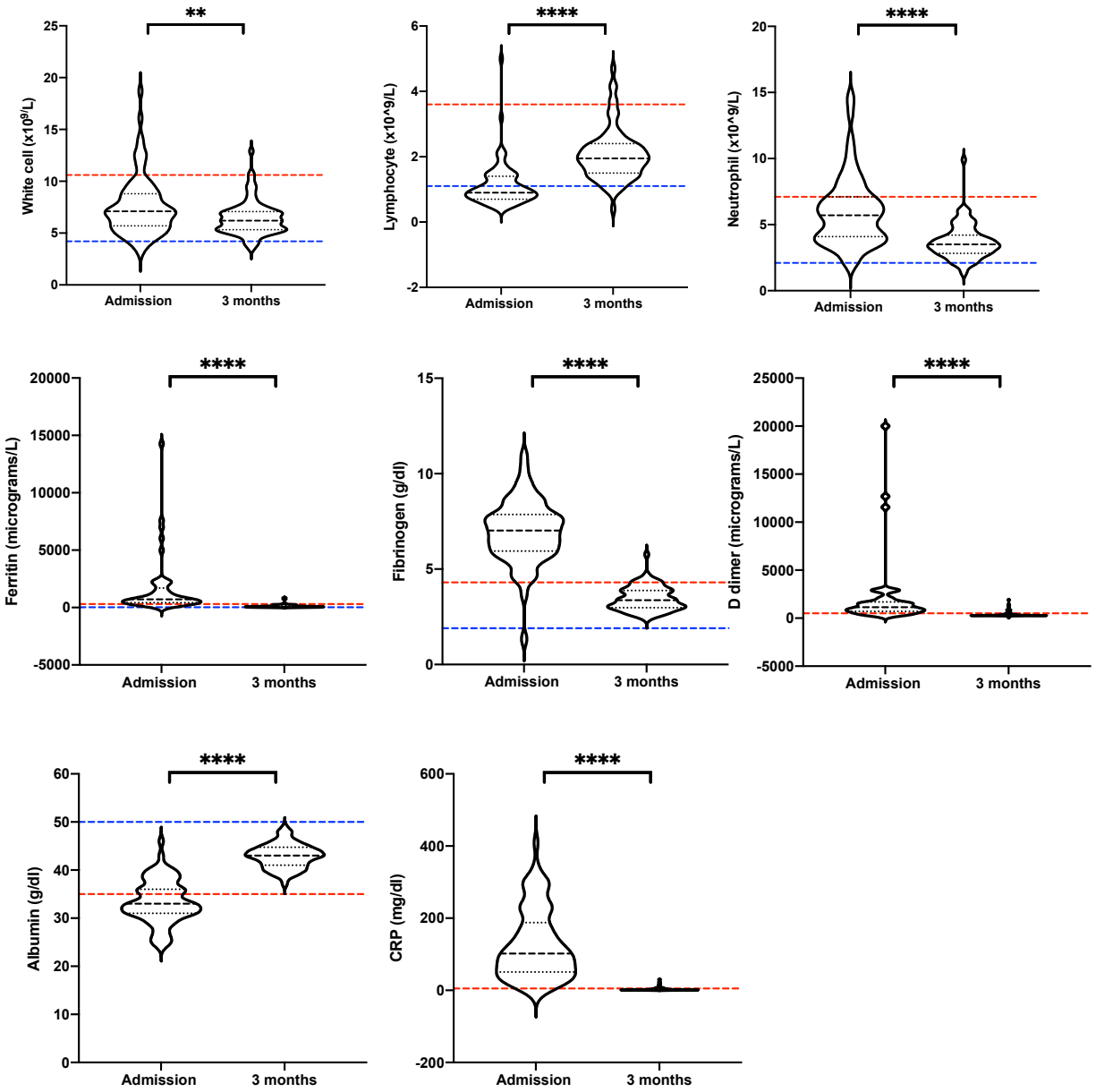


Figure 3. 2 Violin plots of admission and follow up bloods (W1)

Blood test results during admission and 3-month follow up for the first wave shown. Area between red and blue lines show normal ranges as per laboratory cut-offs. CRP <5mg/dL and D dimer<270 micrograms/L considered normal. Intergroup comparisons made using non-parametric Mann Whitney U test. P values <0.05 considered statistically significant. * p <0.05, ** p<0.01, *** p<0.001, **** p<0.0001

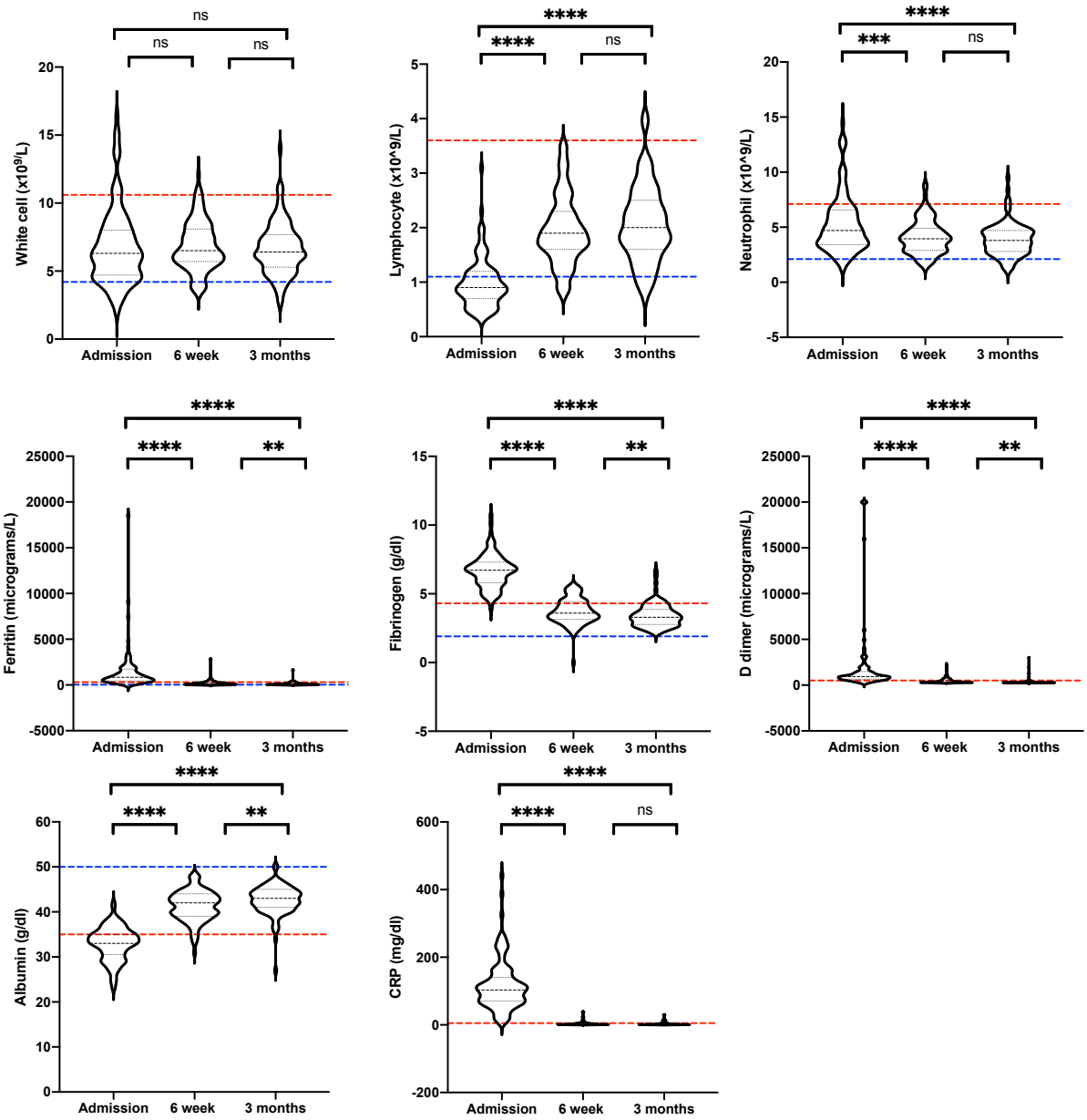


Figure 3. 3 Violin plots of admission and follow up bloods (W2)

Blood tests during admission and follow up (6 week and 3 month) for the second wave, displayed. Area between red and blue lines show normal ranges as per laboratory cut-offs. CRP <5mg/dL and D dimer<270 micrograms/L considered normal. Intergroup comparisons made using non-parametric Mann Whitney U test. P values <0.05 considered statistically significant. * p <0.05, ** p<0.01, *** p<0.001, **** p<0.0001

3.5.4 Psychological assessment

Figure 3.4 shows the anxiety and depression scores of individuals from the first wave.

There was a wide range of scores reported at the first and second visit. A non-significant difference was noted between the two visits. A slightly higher median of anxiety and depression scores was noted

at 12 months, although not statistically significant. Similarly, despite no statistically significant differences on paired testing, the majority of individuals showed stability or improvement of their anxiety and depression scores over time.

Figure 3.5 shows the anxiety and depression scores of individuals during the second wave, with results at 6 weeks, 3 months and 12 months. A statistically significant improvement was seen between 6 weeks and 3 months in both the depression and anxiety scores, with no further significant improvement thereafter.

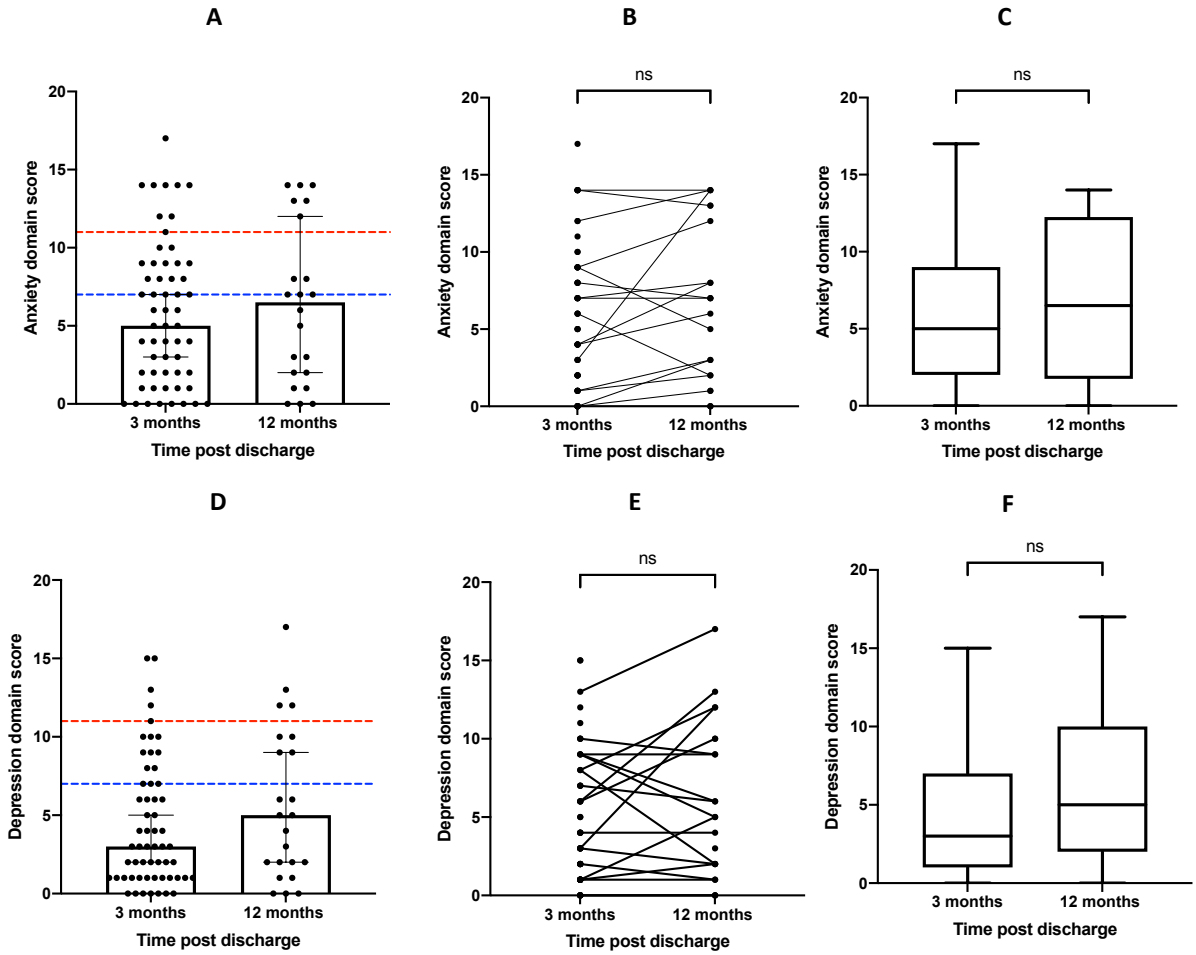


Figure 3. 4 HADS questionnaire results (W1)

Anxiety (A-C) and depression (D-F) scores during the first wave. Red line drawn at a score of 11: scores >=11 considered "abnormal"; Values below blue line (score <7) are considered "normal"; Values in between the red and blue lines (score of 8 - 10) are "borderline abnormal". Figures A and D show scatter plots with median and interquartile range. Figures C and F show box and whisker plots showing median and IQR (box), and minimum and maximum range (whiskers). Paired Wilcoxon matched pairs signed rank test used for statistical analysis in Figures B, E (n=19 pairs); Non-parametric Mann Whitney U test used for comparisons in Figures C and F. P value <0.05 considered statistically significant: * p <0.05, ** p<0.01, *** p<0.001, **** p<0.0001

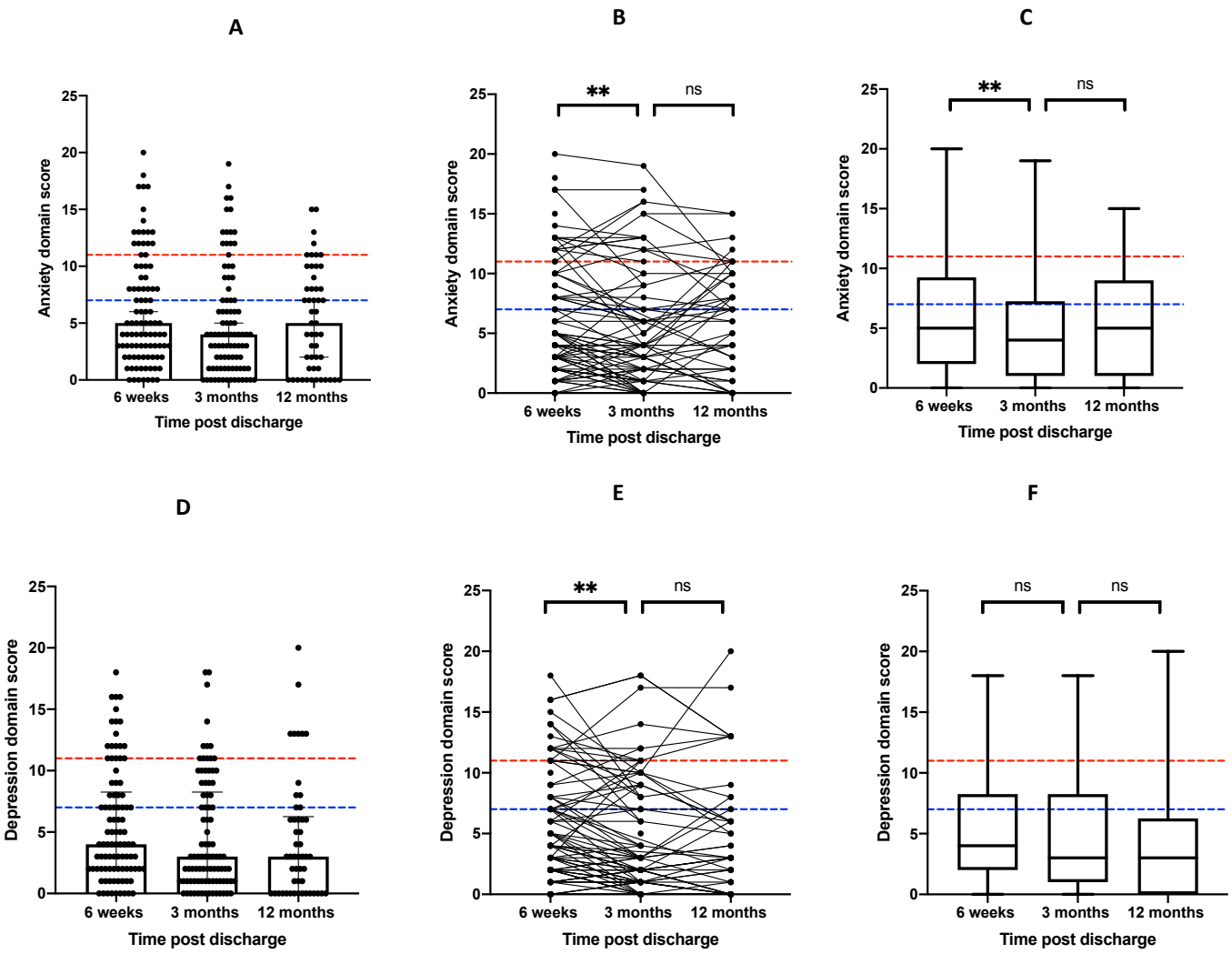


Figure 3. 5 HADS questionnaire results (W2)

Anxiety (A-C) and depression (D-F) scores during the second wave. Red line shows scores of 11: scores >=11 are considered "abnormal"; Values below blue line (score <7) are considered "normal"; Values in between red and blue lines (score of 8 - 10) are "borderline abnormal". Figures A and D show scatter plots with median and interquartile range. Figures C and F are box and whisker plots showing median and IQR (boxes), and minimum and maximum range (whiskers). Paired Wilcoxon matched pairs signed rank test used for statistical analysis in Figures B, E (n=81 pairs between 6 weeks and 3 months, and 47 pairs between 3 and 12 months); Non-parametric Mann Whitney U test used for comparisons in Figures C and F. A p value <0.05 was considered statistically significant. * p <0.05, ** p<0.01, *** p<0.001, **** p<0.0001

3.5.5 Quality of life assessment

Figure 3.6 shows the change in quality-of-life scores between 3 and 12 months in patients from the first wave. There was a non-significant difference in mental component (MCS) scores. However, non-parametric paired testing shown marginal improvement in the physical component scores (PCS).

During the second wave (Figure 3.7), there were statistically significant differences in both the PCS and MCS scores between the first and second visits, i.e. 6 weeks and 3 months post discharge, but again no significant difference between 3 months and 12 months.

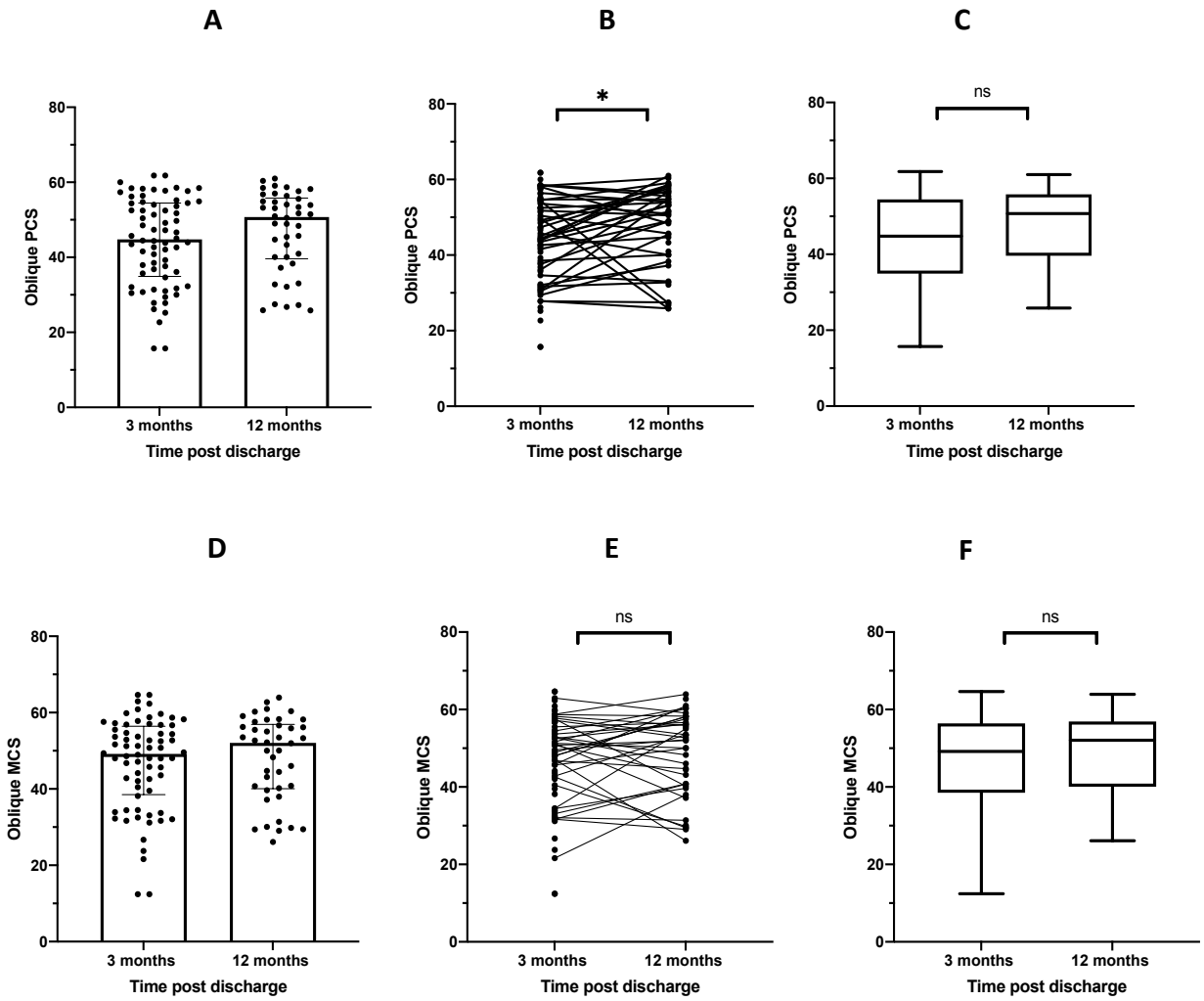


Figure 3. 6 Trajectory of SF36 scores (W1)

Oblique PCS values at 3 months and 12 months (A), Change between visits (B) and summary of values (C); Oblique MCS values at 3 months and 12 months (D), Change between visits (E) and summary of values (F). Figures A and D are scatterplots showing median and IQR, Figures C and F are box and whisker plots showing median and IQR (box) and minimum and maximum values (whiskers). Wilcoxon matched paired signed rank test used for B and E (36 pairs), Non-parametric Mann Whitney U testing performed for C and F. P value = <0.05 considered statistically significant. * p <0.05, ** p<0.01, *** p<0.001, **** p<0.0001. Abbreviations: PCS (physical component score), MCS (mental component score)

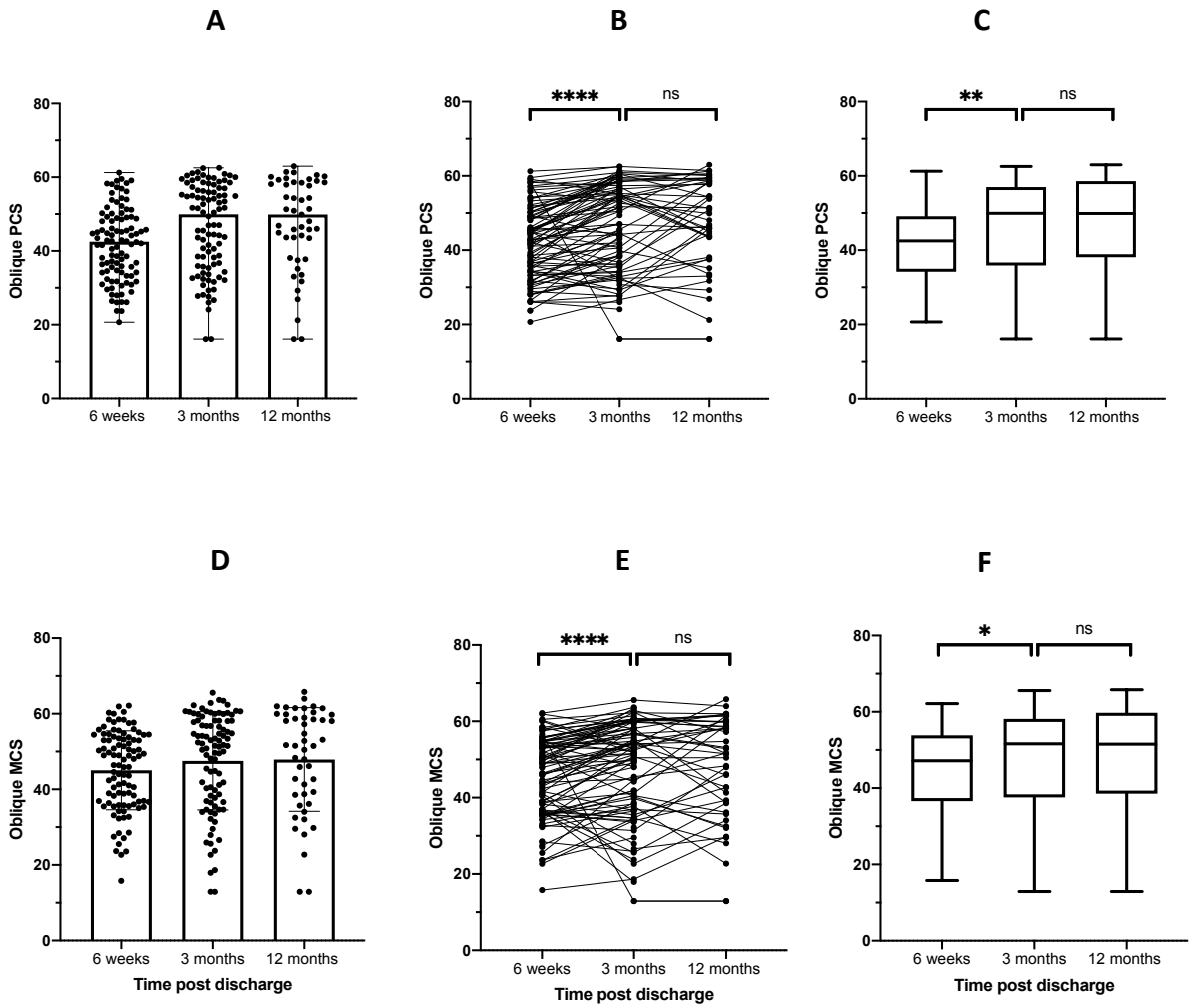


Figure 3. 7 Trajectory of SF36 scores (W2)

Oblique PCS values at 6 weeks, 3 months and 12 months (A), Change between visits (B) and summary of values (C); Oblique MCS values at 6 weeks, 3 months and 12 months (D), Change between visits (E) and summary of values (F). Figure A and D show median and interquartile range, Figures C and F shown median, IQR (box) and minimum and maximum values (whiskers). Wilcoxon matched paired signed rank test used for B and E (88 pairs between 6 weeks and 3 months, 47 pairs between 3 months and 12 months), Non-parametric Mann Whitney U testing performed for C and F. P value <0.05 considered significant. * p <0.05, ** p <0.01, *** p<0.001, **** p <0.0001 Abbreviations: PCS (physical component score), MCS (mental component score)

When assessing the specific components of the SF36 score, the main change during the first wave was an improvement in the role limitations due to physical health (RP) domain (Figure 3.8). During the second wave, statistically significant improvements were seen in physical functioning, role limitations to physical health and bodily pain, between the 6 week and 3 month visit but with no further statistically significant changes after 3 months (Figure 3.9). Importantly, in neither wave was there statistically significant differences in social functioning or components related to mental health after 3 months.

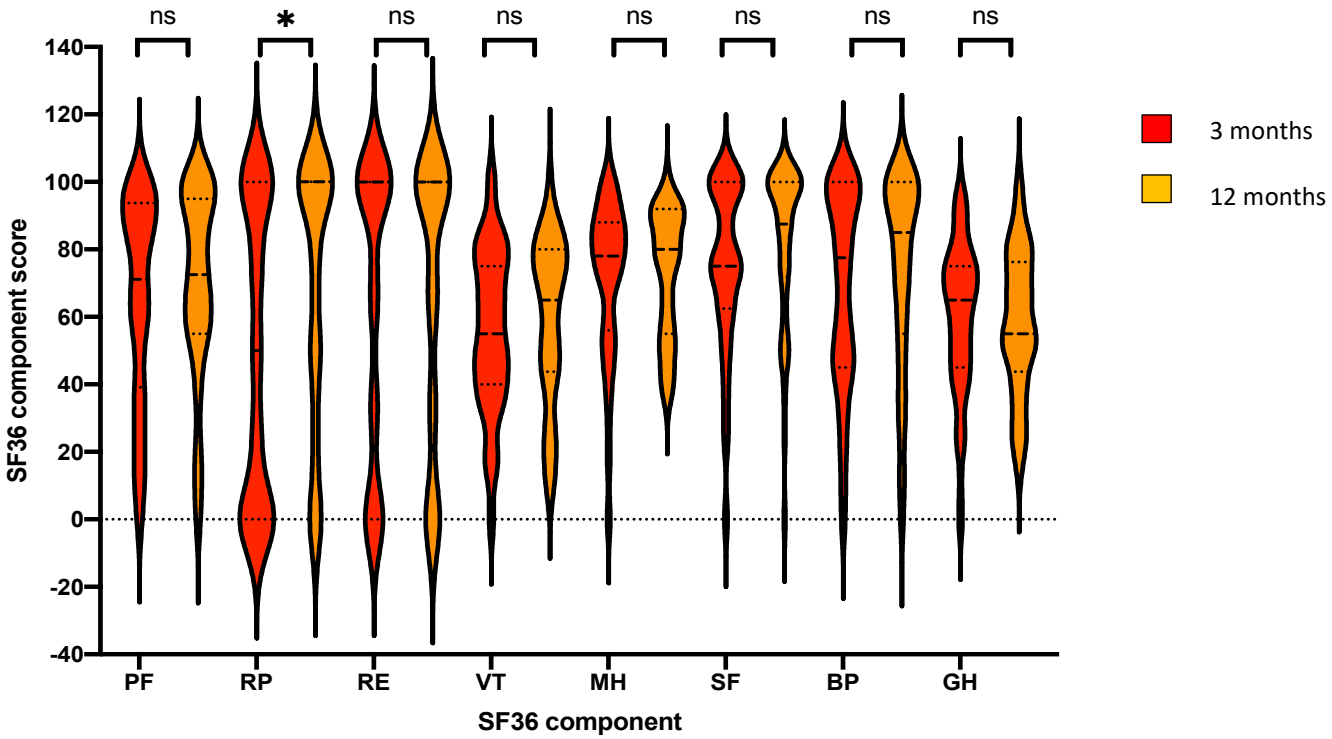


Figure 3. 8 Violin plots of SF36 component scores (W1)

Comparisons between 3 and 12 months made using non-parametric Mann Whitney U test. P value <0.05 considered statistically significant. * p <0.05, ** p <0.01, *** p<0.001, **** p <0.0001

Abbrevations: PF (physical functioning), RP (role physical), RE (role emotional), BP (bodily pain), GH (general health), VT (vitality), SF (social functioning), MH (mental health)

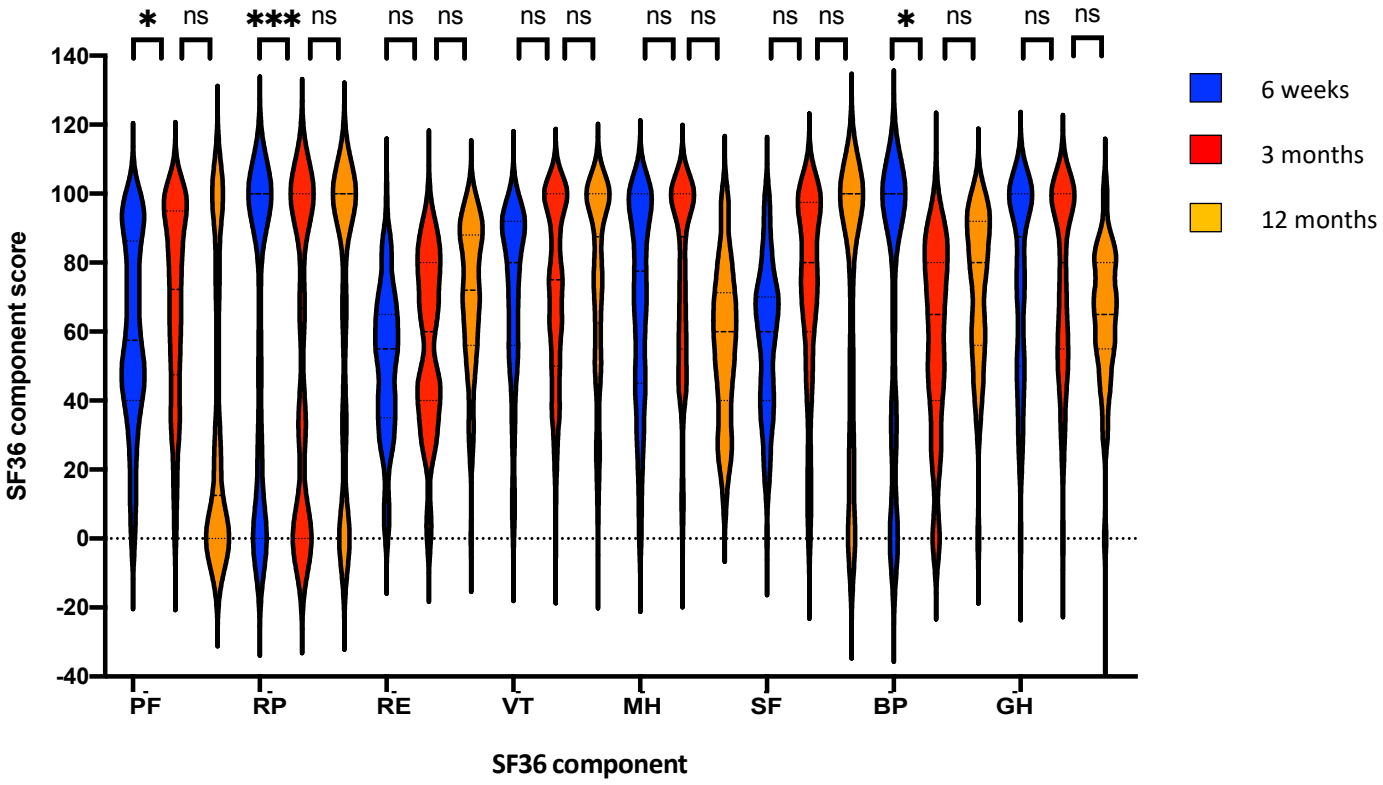


Figure 3. 9 Violin plots of SF36 component scores (W2)

Comparisons between the different timepoints were made using non-parametric Mann Whitney U test. P value <0.05 considered statistically significant. * p <0.05, ** p <0.01, *** p<=0.001, **** p <0.0001

Abbrevations: PF (physical functioning), RP (role physical), RE (role emotional), BP (bodily pain), GH (general health), VT (vitality), SF (social functioning), MH (mental health)

3.5.6 Semi-structured interviews

17 patients underwent semi-structured interviews at a median of 620 days (approximately 20 months) post hospital discharge. Table 3.2 shows the demographics, comorbidities and interview timings for these individuals. All patients had been admitted to hospital, and there was a male preponderance (65%, n=11). Convenience sampling was used to identify individuals who subjectively reported to be a) stable b) deteriorated c) improved on clinical assessment at 1 year post discharge, as compared to at 3 months.

Gender	Male	11 (65)
	Female	6 (35)
Age (years)		56 (52 – 71)
Admitted to hospital		17 (100)
Maximal ventilation status	Intubation and ventilation	5 (29)
	Non-invasive ventilation	4 (24)
	Oxygen only	8 (47)
Length of stay in hospital, days		8 (5 – 12)
Ethnicity*	White	8 (47)
	Black, African, Caribbean or Black British	6 (35)
	Asian or Asian British	3 (18)
Comorbidities	Asthma	1 (6)
	Chronic obstructive pulmonary disease	1 (6)
	Obstructive sleep apnoea	1 (6)
	Hypertension	4 (24)
	Ischaemic heart disease	2 (12)
	Atrial fibrillation	1 (6)
	Type 2 diabetes mellitus	3 (18)
	Anxiety	1 (6)
Timing of first SF36 survey from discharge (days)		86 (85 – 110)
Timing of second (1 year) SF36 survey from discharge (days)		365 (361 – 377)
Timing of third (2 year) SF36 survey from discharge (days)		719 (713-724)
Timing of interview from hospital discharge (days)		620 (613-628)
Duration of interview (minutes)		51 (40-63)

Table 3. 2 Participant and interview data for semi-structured interviews

Demographics, clinical characteristics and interview details for participants undertaking semi-structured interviews *Ethnicity classifications as per 2021 Census (https://www.ethnicity-facts-figures.service.gov.uk/style-guide/ethnic-groups#2021-census) All values expressed as n (%n) or median (IQR)

These 17 individuals also had an assessment of their SF36 scores at 2 years post discharge. The overall trend was an improvement in PCS over time, but this was not mirrored in the MCS scores (Figure 3.10).

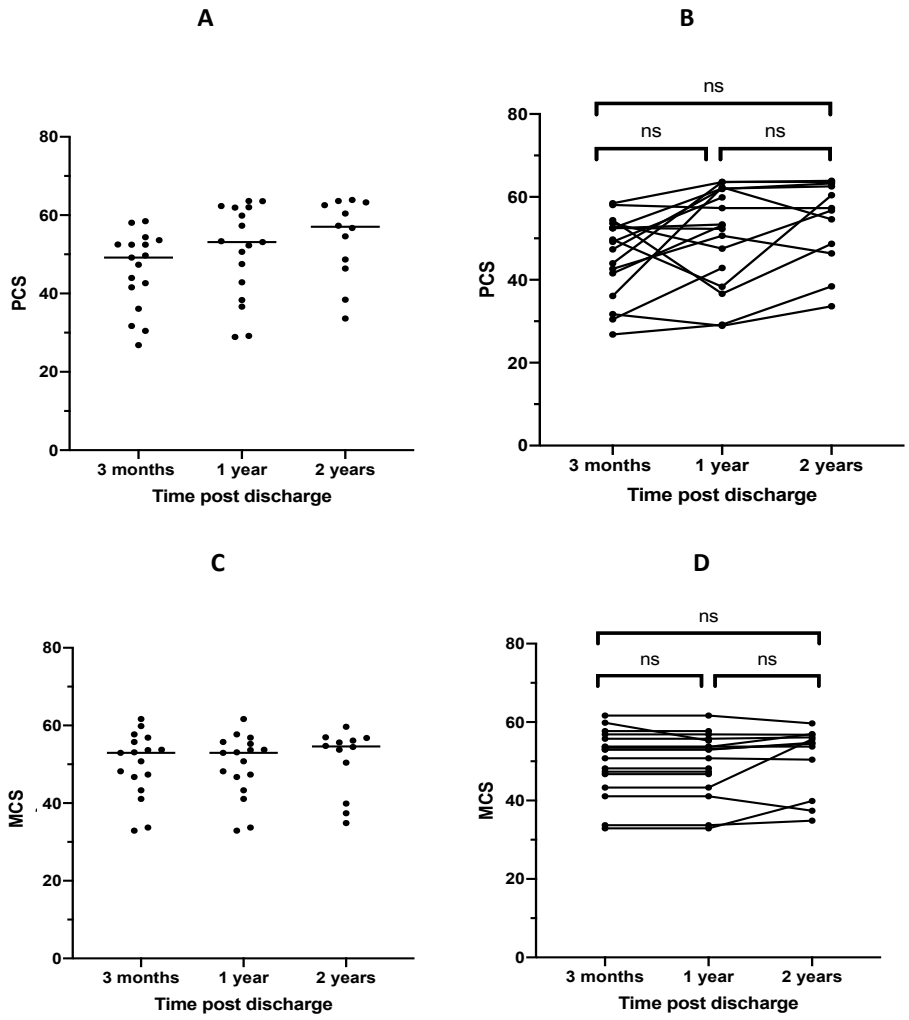


Figure 3. 10 Trajectory of SF36 scores in patients undergoing interviews

A, C: Scatterplots showing distribution of scores at 3 time points post discharge. Horizontal line shows median score. B, D: Line graphs showing change in individuals' scores over time. Comparisons were made using non-parametric paired Wilcoxon matched pairs signed rank test. P value <0.05 considered statistically significant. * p <0.05, ** p <0.01, *** p<0.001, **** p <0.0001

Thematic analysis of interview transcripts identified 4 main themes which were associated with the impact of symptoms on quality of life: 1. Impact of symptoms on self, 2. Patient-driven coping strategies, 3. External support and 4. External factors (Figure 3.11).

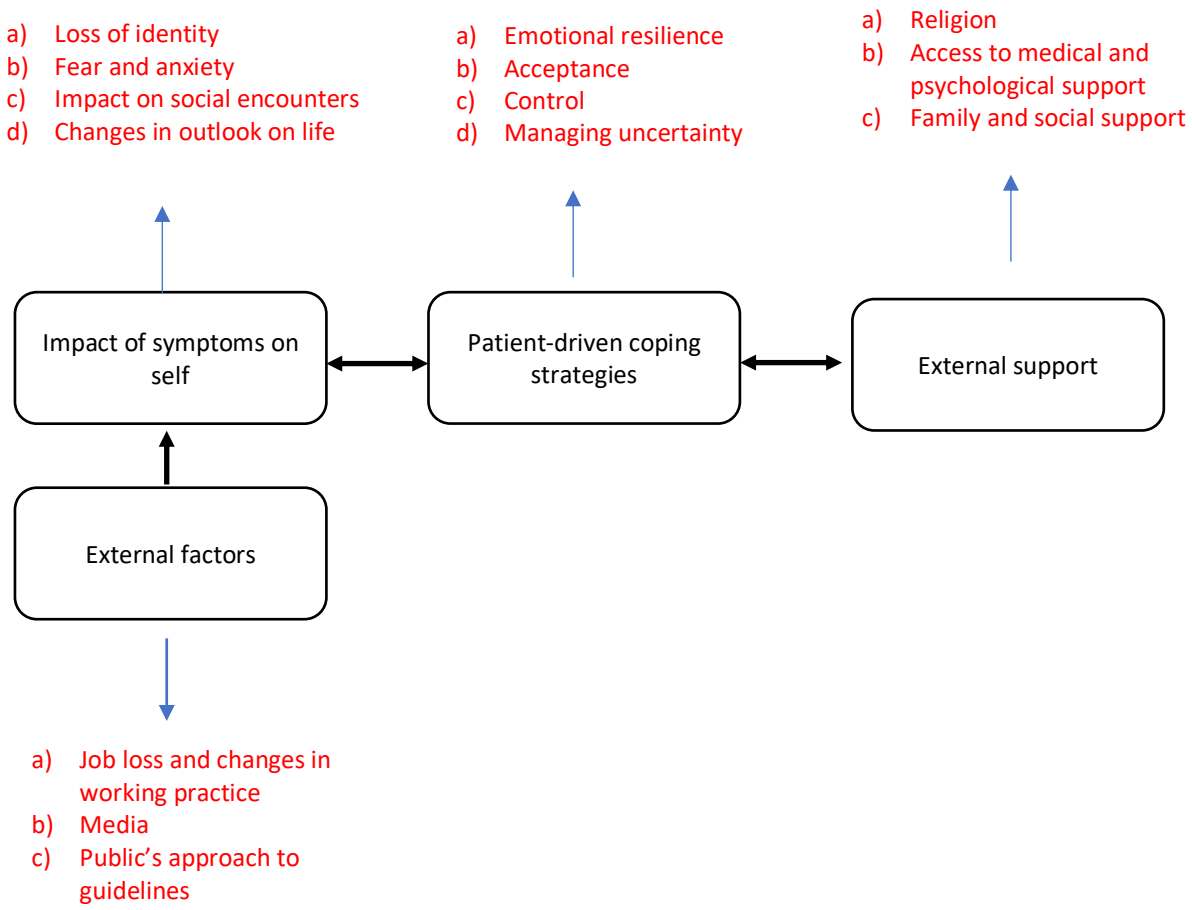


Figure 3. 11 Themes derived through qualitative analysis

Main themes (in boxes) and associated subthemes (in red) are shown. Black arrows show relationships between themes

Supporting quotes for the themes and subthemes described in Figure 3.11 are shown below. The gender and age (years) of the individual making the statement is shown in brackets.

Theme 1: Impact of symptoms on self

Patients were suffering from both physical and psychological symptoms post COVID-19, both having significant impacts on their quality of life, leaving them with a range of emotions.

Subtheme 1.1. Loss of identity

Persistent symptoms resulted in some individuals losing their sense of identity and not feeling like their "old self" *(Male, 49)*

The symptoms also resulted in some individuals feeling like they had aged significantly during the pandemic,

> *"There are days I feel that I went into the pandemic as a 51-year-old and I've come out as an 80-year-old" (Male, 51)*

> *"Some days I feel 90" (Male, 53)*

Furthermore, it even made one individual question the legitimacy of his symptoms,

> *"I do question myself right then, you know, has this become a bit of a rut? Has this become… Is this some psychosomatic type thing?" (Male, 51)*

The stark difference between tiredness from a hectic life and COVID-19 fatigue was made by one individual,

> *"I had babies. I worked. I flew around the world for work. This is not tired. It's different. It's like just physically not being able to open your eyes" (Female, 54)*

The desperate desire to return to their baseline way of living was described,

"I want to be like my old self you know, like I used to go out .. shopping, swimming. I enjoy swimming. That's the thing. And cooking" (Female, 46)

Subtheme 1.2 Fear and anxiety

The psychological impact of the admission was profound, with significant impacts on social behaviour. One individual said,

"I couldn't go out. I couldn't go out my front door. There was a period where I was home for about 6 weeks without stepping out of my front door." (Female, 54)

Furthermore, fear of becoming ill again resulted in a hypervigilant state in one individual:

"I had a fear of ermm..started paying more attention to what was happening to my body. Any little twinge here and I will go into panic overdrive" (Female, 54)

The stay in hospital had resulted in significant psychological morbidity in some individuals, who had developed claustrophobia during their acute admission,

"just seemed like I'm in a the box and they just closed the door from the outside" (Female, 46)

The claustrophobia had an impact on one individual's behaviour when he returned home also,

"The claustrophobia, I remember the first couple of days when I came out, I was jumping out the house and sitting in the backyard" (Male, 53)

Furthermore, memories of the hospital stay resulted in sleep disturbances in one individual,

"I have lots of snapshots of the people still in my face of in hospital, you know. And and it's it's something I can't, I can't remove because they are the stark memories of, you know, people in pain that I can't get rid of. And so they used to keep me awake at night." (Male, 53)

Subtheme 1.3 Impact on social encounters

The negative impact on social activities was quite significant. One individual said,

> *"..the fatigue is the most major thing. For example, I used to dance a lot professionally in my life, so I love dancing. Last week when I was cooking, there was a tune I love and I wanted to dance and just once. I was literally breathless and I had to stop everything, sit down so that my heartbeat can come back to normal and the tiredness in my legs, as if I'd run 20 kilometres and it was just maybe 10 seconds, 15 seconds." (Female, 42)*

Avoidance of social activities was mentioned by one individual,

> *"Nowadays I just avoid them (relatives). I just don't want to because they're talking and I just get tired, talking too much". (Female, 46)*

The fatigue was often a contributing factor:

> *"Lack of energy, it means not being able to think clearly. So, you kind of become less social in a way, less outgoing, less effective. Getting less done in your day" (Male, 51)*

One individual who had suffered job loss, commented on feeling "discriminated" and the negative impact his symptoms had on securing a new job,

> *"I'm looking for jobs but every time I get to a job, if I go for interview, I have to climb stairs to see them, they're always up on the first floor in the lounge. When I get there, I have no voice. I've got... I've just got this…Breathing fast, heavy, heavy breathing and they say what's wrong and then you have to tell them and then they kind of go off." (Male, 52)*

Subtheme 1.4 Change in outlook on life

Despite residual symptoms, the experience had changed many individuals' outlook on life and individuals expressed a great sense of gratitude for surviving.

"Now, I'm grateful each morning I get out of my bed, I can get up out of my bed and walk around and do things. So yeah, I appreciate life much more now than I used to". (Female, 54)

"I'm always looking on the plus side of life, but I think more now and I think that it's more pronounced now because, you know, I sit here, I look around in terms of what I have, where I am, what I'm doing, etc. And I'm blessed and I'm lucky." (Male, 53)

In some individuals, it gave them a real sense of purpose,

"I've got more to do in this life than just existing this time. Because it wasn't my time" (Male, 62)

"It was a bad year, but I am always looking at the flip side and say look I'm here. Every day is valuable. Every day means something and and if I can do anything for anybody, it means I, you know, I'm here for reason. So, I think it's put that in perspective". (Male, 53)

It also heightened one individuals' awareness of her own mortality:

"You will have never seen me sitting down to think about what it is like dying, but, since I got COVID, I think about dying every day" (Female, 54)

Furthermore, the disbelief that this could happen to him made one individual feel vulnerable,

"Life, where I am. I never thought I'd be in this position, ever. Uhm.. all because of COVID, you know? Unbelievable" (Male, 53)

Theme 2: Patient-driven coping strategies

A variety of coping strategies were employed by the participants to deal with the residual symptoms.

Subtheme 2.1 Emotional resilience

Some participants alluded to previous life experiences and cultural background contributing to emotional resilience which allowed them to cope with the stresses experienced during the COVID-19 pandemic and residual symptoms. One individual said,

> *"When you're in the Caribbean, you're taught to be very independent from a very early age……. And yeah, I think I think it's my mindset that got me to in this place where I am right now that even COVID, I don't, I don't see it as a hindrance, it's just one of those things" (Male, 62)*

Another said,

> *"You know, resilience and that strength of you know, my father died really young and I had to look after the family from the age of 16. That kind of stuff. And where we had no money that you have to do things, you have to react and you have to balance. And that's kind of stayed with me and I think that's kind of helped me through this as well because no matter what you throw at me, I'll find a way through and deal with it." (Male, 53)*

The importance of a positive mental attitude was mentioned by one individual,

> *"Well, I believe I can do anything and everything and that's ..I've always taken life from that approach, that mentally there is nothing impossible to do. If you say you can do something, your mind works in a way that will open the door for you to do it. If you say you can't, the same thing will happen. So, I've always been of a positive mindset." (Male, 62)*

Subtheme 2.2 - Acceptance

Some participants emphasised the importance of "acceptance" of residual symptoms and "not comparing yourself to others" (with respect to the trajectory of symptoms) [Female, 54]. Furthermore, acceptance of symptoms was felt to be important to minimise fear provoked by the symptom burden,

> *"As you can see, I'm not scared. I'm not scared. I'm in this acceptance because that grief, long grief happened. Accepting what is finished and something happened to me". (Female, 42)*

Additionally, comparing their situation to worst-case scenarios, helped process their symptom burden,

> *"So, I definitely went through a phase of like why me? What have I ever done wrong in my life to be sorted out? But then you know, that's you just…You quickly realize that so many people are so much worse off, so it's fine. But you definitely go through that cycle. You know it's first like just trying to survive and then when you feel like yeah, I've survived this, then it's anger. Then the why me? And then the frustration that it doesn't go quicker. (Female, 54)*

Acceptance was not restricted to symptoms alone, but unpredictability of life in general,

> *"I think it it, it showed them that life can be very fickle. You know you can be here one minute and gone the next day." (Male, 61)*

Subtheme 2.3 Control

Taking control of the narrative and symptoms was an important subtheme. Making a conscious choice not to let the environment affect you was mentioned by one ICU survivor,

> *"We either act out of fear or we act out of love. Well, the world right now is living in fear. Our governments motivate us by fear, the news, but I don't want to live out of the fear space. I want to live out of the love space, so I make a conscious choice to do that, but doesn't mean I don't get afraid of something." (Male, 58)*

The importance of focussing on what can be controlled was highlighted by one individual:

> *"And then when you want to pack a lot into your life, you know there are things that you can, you can control and things that you can't control, and there's no point. Kind of worrying, sleepless nights about stuff that you can't control and you know, but let's just focus on the things that we can." (Male, 55)*

Moreover, the importance of being able to compartmentalise an experience to minimise potential impact was noted by one participant,

"I think I'm reasonably good at, you know, putting things into a box and saying, well, OK, that was an experience that happened and it you know you you have to learn from it and and what not, but it's not going to dominate my life" (Male, 55)

However, the relapsing-remitting nature of symptoms often contributed to lack of control over one's symptoms,

"I'm I'm really good. I felt really good and all of a sudden it will come back" (Male, 49)

"I mean, it's some days that I could walk forever and other days I could walk to the end of the road and come back and sleep. You know, just different days ..it's strange." (Male, 52)

However, one individual emphasised the importance of remaining physically active to enhance recovery,

"And you can make yourself a lot better if you went out, even if you just went out for walks." (Male, 74)

Subtheme 2.4: Managing uncertainty

The uncertainty of recovery and timescale for recovery was mentioned by individuals. One individual said,

"Am I still in recovery. I mean, how long is it gonna take, if the lungs are ever going to get back to normal, which I don't think they will, not now, that's over a year and a half now so. I can't see them getting any better from what they are. I don't feel it anyway. You know, I'm trying everything" (Male, 52)

Furthermore, one individual acknowledged that uncertainty was often a key factor contributing to psychological stress.

"I think that what is what what what can be worrying is actually uncertainty, and so, uh, of all nature and the, the, the difficulty at the moment is that I think there is more uncertainty all around us and and and uncertainty creates concerns because your your brain basically tries to

compute what outcome is likely, uh, under various scenarios, and so on. And and sometimes I think I sort of overcomplicate stuff" (Male, 50)

Theme 3: External support

Access to external support was very important in coping with persistent symptomatology.

Subtheme 3.1 Religion

Religion and belief in a higher being or "Creator" was mentioned by several participants as being important in their approach to recovery post COVID-19, in particular the feeling of support they derived from it,

"I think I think faith…is is the starting point of not being alone……., we can go into the discussion as to whether it meets reality, philosophy, but .. when you believe in it, that belief is in itself helpful." (Male, 50)

However, in one individual it also stirred up feelings of anger,

"I think I'm really angry with God because they always say God doesn't give you more than you can accept or that you can handle and I'm like, well, you're wrong in this one guy..or woman, depending who or what he is." (Female, 54)

Faith allowed one participant to not be dominated by his symptoms,

"*My faith is what helped me from not being a victim" (Male, 61)*

The strength derived from religion was described by one participant,

"I'm not saying that I was healed by the spirit of God. I wouldn't believe that, but I believe God gave me the strength to fight it." (Female, 54)

Finally, some participants talked about destiny and the final outcome not being under human control as well as the positive impact of relinquishing control,

"Well, as a Christian you believe in God. And you always put your trust in God. So, if he's ready for you to die, you will die. If he's not ready for you to die, he will save you from dying. We will all have to die someday" (Male, 65)

"I believe it wasn't my time. 'cause we we we trust in God to set our path for us. I believe God has set my path to reflect that it wasn't my time yet. And he intervened on my behalf in the spirit world to stop me from dying in any way possible." (Female, 54)

Subtheme 3.2 – Access to medical and psychological support

The impact of access to medical and psychological care was thought to be important.

One participant said:

"Well, actually for me it was like I have a very good GP and to be able to send him a text and say, look I have this new symptom" (Female, 54)

In addition to dealing with the physical symptoms, one participant suffering from anxiety commented on the importance of face-to-face rather than telephone appointments in managing her symptoms:

"They're not seeing people as much as they used to see and people like me, we like, we need to see their GP face to face because telephone appointments are not good enough for us because you know, some people like me when they see the doctor, they feel better." (Female, 46)

Patients have also used alternative approaches to seek medical care, but have struggled in some instances:

"I have doctor IQ which has been good. So, like any medications, like my inhaler, that's been pretty quick so I I guess I could try to go on, I'm going to try to go on probably this week and now the holiday is almost over and try to make an appointment maybe through Doctor IQ but a lot of times they're just saying we're not taking appointments right now unless it's an emergency." (Male, 66)

Aside from medical advice, psychology input was sought by some of the participants to help alleviate symptoms of anxiety and low mood. One participant said,

> *"So I think it's reassurance because when you have that ..when you used to be so active and so outgoing and involved in society and then instantly can't do anything, it's the reassurance that it will come back because there is no progress day by day." (Female, 54)*

Furthermore, receiving medical follow up post hospital discharge made one participant feel valued,

> *"It was beautiful because somebody was concerned about my being well or not. They don't know me, but they're still concerned that makes you feel you're wanted still, you know, and it's very difficult to explain and you want to thank them saying thank you for phoning" (Male, 73)*

Subtheme 3.3 Family and social support

The impact of family support was considered crucial in individuals' approach to their illness and symptoms:

> *"I think that, knowing that you are useful to to people outside is is is something that that is actually quite quite important. So the the the relationship and the love is is is quite central to this. And I I think I think feeling feeling that uh, and people want you to be around. Uhm, and and having those connections is is critical" (Male, 53)*

In addition to support from family, the effect the individual's illness and symptoms were having on family members was important and brought families together,

> *"I could see what they've been through and it was harder for them and I felt what happened to me was hard for them and I think it was quite important for me to see that they were getting better. And I it's brought us all very, very much closer together, so it's been a bit of a real kind of journey." (Male, 53)*

It also increased awareness of one's role within their family. One individual said,

"And I know that if anything happens to me, I'm not saying that my family will be completely lost, but I know if anything happens to me and I'm not there, it will create a huge hole in my family base, if I'm not there because they they rely on me for a lot of things, being the oldest in my family." (Female, 54)

COVID-support groups were also a source of support as it allowed individuals to normalise their symptoms. One individual said,

"Support groups were mentioned as helpful, to help validate symptoms: The long covid support Group is good. Uh, just to know…Uh, like that your symptoms are not made up" (Female, 54)

One individual even felt the need to apologise to her family members for what they'd been put through as a consequence of the illness,

….. "she just she said she she was just sitting there the whole night in her overcoat waiting for someone to call and say this is it, that I'm not there anymore, so and I had to apologize to everyone, my whole family for putting them through that 'cause I realized, even though I was going through, I was going through physically, they were going through as well in one way or the other, so I felt I needed to make them feel better and get them to and it was all down to me. You know whether it was, my fault or not, it was all down to me that they went through that trauma with me as well. So I felt the need to apologize to them as well and to my friends who you know, helped me. I had to apologize to everyone. Just say sorry and some of them were saying it wasn't your fault and I said yeah but I still feel the need to apologize." (Female, 54)

Whilst social interaction was very important in maintaining general well-being, the "fear of going out" as one individual (*Male, 73*) said, often limited social interaction. Another said,

"I'm very cautious in things that I do, places where I go. If I was to go to the shops, supermarkets, I making sure I sanitise, wear my mask and just keep my distance" (Male, 65)

Furthermore, the attitudes of other individuals towards COVID-19 fuelled frustrations in those who had survived COVID-19,

"I get very frustrated for like you know, people not wearing mask or standing next to me, like come on. Or saying that you know there is no COVID it and it's like,
it's fine to have your own opinion, but don't put others in danger because this this has not been fun". (Female, 54)

Finally, a generational split in attitudes to socializing was noted,

"I'm seeing younger people and friends of every age, so I I see younger people in Soho going out Thursday night, Friday night, woohoo, we're invincible. Everybody thought they were invincible in their 20s, right? And then I'm seeing people over the age of 50 who are all afraid of dying and they're not doing anything or going anywhere, and they're recoiling in in horror." (Male, 58)

Theme 4: External factors

There were other factors, not specifically related to the management of physical symptoms that were also contributing to general well-being and psychological morbidity.

Subtheme 4.1: Job loss and changes in work practice

A number of individuals had lost their job during the course of the pandemic. One individual commented on having extra time being a factor exacerbating his problems,

"I've always worked in my life. I've never been doing nothing… sitting in the house. You know, my day is always filled with work. You know, to do nothing, it's like everything goes through your head." (Male, 52)

Another individual said,

"He (partner) says probably the thing is because I'm not working, I have too much time on my hands to think, which is true, which is true." (Male, 66)

One individual mentioned the effect of job loss on his "self-worth,"

"Your kind of sense of self-worth is dropped because you are the provider in the house, right? You've got to make sure that things are ticking over." (Males 53)

One participant described his job loss as resulting in a loss of "*sense of direction because you hang yourself around work" (Male, 55)* and the loss of routine. Furthermore, changes in work practice and working from home had variable consequences on individuals:

"….obviously with the lock down, I'm working from home which is quite convenient …… but obviously being locked in is a bit psychologically difficult." (Male, 54)

It also perpetuated procrastination:

I would probably say the negative part is not having more or less that daily routine. So you know it's OK. Yeah now I…I can be a bit of a procrastinator, but now it's gotten worse. Like, yeah, I can do that later. I'll get it done. I did something yesterday that you know, I've been looking at for like 2 weeks to do. (Male, 66)

However, positives of job loss were also described, with time being freed up to explore other interests:

"I think what's driving me today is actually the fact that I still have projects as to what I want to do with my life. And I think that, uh having a lot to read and being in interested in reading and wanting to learn, continue to learn on topics which were of interest but probably left unattended during my professional career is also helping" (Male, 50)

Subtheme 4.2 Media

The impact of the media was commented on by one individual as motivating individuals through fear. This individual speaks further on the effect of media,

"I think we're at a point in time where we have more access to more information and that can be overwhelming for people who don't know how to think. And sometimes I think a lot of people aren't, remember, I was taught to question my own religious upbringing. You know,

thinking is part of my upbringing, a lot of people were taught to just follow what you're told." (Male, 58)

The influence of personality traits was described by one individual,

"The percentage of people with COVID that probably had their confidence taken away because of the doom and gloom with the deaths, which is fair enough. But you know, I mean, if I think if you have a slightly weaker disposition than me, you,. I don't know whether you don't fight so hard or whether you you you have a different …whether the the condition sort of brings you down mentally more" (Female, 74)

Subtheme 4.3 Public's approach to guidelines

The attitudes towards government guidelines and social isolation have been a source of frustration for many individuals,

"Even now, people don't wear a mask and they don't seem to realize it affects other people very badly. They don't care. It's not the point. They should care about other people" (Male, 73)

One individual commented on making mask-wearing compulsory:

"I've always taken, you know from the time it started and I got it, I've always worn a mask. You know, I mean, you go on buses and trains or supermarkets, there's half a dozen people without masks on. It should be compulsory. And there should be like a 200 pound fine" (Male, 74)

When asked whether enforcement of guidelines would affect his behaviour, one individual said,

"Yes it will it will. It will help me help me feel safe when I go for a walk or when I go anywhere or do anything" (Male, 73)

The importance of feeling a sense of duty towards others' well-being was emphasised,

"You see the attitude of, I'm alright Jack, doesn't work with everything in life. If you are alright you must see that other people are alright now." (Male, 73)

3.6 Discussion

3.6.1 Summary of findings

Persistent symptoms post COVID-19 are common, with the commonest symptoms being fatigue, breathlessness, cough and memory disturbances. Abnormalities in blood tests during admission, have often normalised or shown significant improvements as early as 6 weeks post hospital discharge. Abnormal scores on metrics evaluating psychological morbidity are not uncommon, with improvement between 6 weeks and 3 months, but not thereafter. Similarly, abnormalities in HR-QOL show measurable improvement between 6 weeks and 3 months, with little further improvement at the 12-month visit. A multitude of factors affect a patient's quality of life during the recovery phase post COVID-19, including patient-derived coping strategies and external support.

3.6.2 Findings in context of current literature

3.6.2.1 Persistent symptoms

Persistent respiratory symptoms and non-respiratory symptoms were common in both waves. This is in concert with literature since published. [11,247–250] Similarly, quality of life impairments and increased reporting of mood-related symptoms was common, as seen in my cohort.[251–254] Additionally, it has been noted that improvement in mood disorders occurs within a couple of months, which is consistent with my findings during the second wave, when significant improvements occurred between the 6 week and 3 month follow up visit.[255]

The results of psychological and quality of life scores need to be interpreted in context. There were a number of differences between the waves in terms of knowledge and access to services, and this is likely to have contributed to varied experiences in individuals admitted and followed up during the different waves. For instance, during the first wave, it was difficult for me to provide reassurance about the trajectory of symptomatology, lung function or CT abnormalities as this was a new disease. Notably, Visit 1 for the first wave (3 months post discharge), was in June 2020, only 3-4 months after the first case of COVID-19 was identified in the UK on 28th February 2020.[1] By the time of the second wave, a general trajectory towards improvement in the majority has been established, more services

were available including psychological input, which would have positively contributed to patients' health and well-being considerably.

3.6.2.2 Trajectory of blood tests

The improvement in blood tests from admission to follow up has again been shown in subsequent studies.[256,257]

3.6.2.3 Theories surrounding qualitative data

The themes derived from the semi-structured interviews are consistent with those gleaned from other qualitative studies, which also corroborate that loss of control, loss of identity, coping mechanisms and access to medical support are important factors affecting patient experience after COVID-19.[258–260]

The factors highlighted in the qualitative data are consistent with theories described in the literature. Integration of illness or residual symptoms into one's identity is an important component of coping with chronic illness.[261] In my interviews, patients adopted different states: engulfment in patients who could no longer identify with themselves and reported not being their usual self; rejection in those who didn't see themselves as being ill, regardless of symptom burden; acceptance in those who tried to learn to live with the symptoms; and enrichment in those who used the experience to change their lifestyle, by for instance undertaking more exercise. Those who had residual symptoms expressed a sense of loss or grief towards their current state and even described going through the cycles of grief, as per Kubler-Ross (1969).[262,263]

A particularly relevant and troublesome aspect of recovery post COVID-19 is dealing with uncertainty: uncertainty regarding the aetiology of residual symptoms and prognosis.[264] Illness uncertainty can result in increased perception of symptoms.[265,266] The unpredictability and relapsing-remitting nature of symptoms as described by patients, coupled with the relative deficiency in knowledge pertaining to long-term outcomes will have contributed to illness uncertainty in this cohort.[267] Furthermore, this led to a perceived loss of control in some individuals, which is known to be an additional psychological stressor.[268,269] One way to cope with uncertainty in chronic disease is through acceptance and tolerance of uncertainty,[270]and some participants allude to this in their interviews, by not allowing symptoms and symptom trajectory dominate their life, and rather focussing on variables that can be controlled only.

Mental fortitude and emotional resilience are important factors in dealing with chronic illness. [271,272]Participants mentioned the impact of personality traits, cultural background and previous personal experiences on developing mental resilience. Additionally, cognitive reframing of events was also a technique some patients employed as a coping mechanism.[273,274] For instance, comparing their situation to worst-case scenarios and consciously avoiding being a victim of cognitive distortions such as catastrophising or mental filters.

Self-efficacy can determine the degree of impact an illness or symptoms have on your life.[275,276] In my cohort, residual symptoms sometimes affected hobbies and even impacted ability to socialise due to fatigue from simply talking. Some patients undertook self-management techniques to improve their cognitive self-efficacy by seeking medical and psychological help where necessary, as well as joining support groups to further their understanding of residual symptoms and trajectory. In others, the lack of self-efficacy resulted in them giving up hobbies and adopting a nihilistic view of the world and a state of learned helplessness, as is sometimes the consequence of failed self-efficacy.[277,278]

Calman's theory states that quality of life is the difference between expectations and experience.[279] In my cohort, there was an expectation that the symptoms would wane with time at a more rapid rate than they did, but also that individuals could exercise more control over their recovery, and the absence of this, resulted in mental frustration. However, where expectations were appropriately managed, for instance through reassurance, overall mental state in some individuals improved.

The impact of support on mental fortitude and psychological wellbeing was clear. For instance, a sense of love and belonging, offered through family and community support and their perceived role in the family, for instance financial or caring responsibilities, was a motivational tool for recovery. This is in concert with Maslow's hierarchy of needs, where in addition to basic needs such physiological and safety (e.g. a job), love and belonging and self-esteem (for instance through confidence and respect of others) are important for motivation.[280]

3.6.3 Clinical relevance of findings

The results highlight the importance of adopting a holistic approach to the follow up of patients post COVID-19. Whilst the questionnaires allowed in depth assessment of individuals' experiences, questions were often incorrectly completed and needed to be reviewed, which may be a result of questionnaire fatigue. However, whilst quantitative assessment in a clinical setting is not required,

early identification of psychological needs is important to facilitate onward referrals and ensure the patient is adequately supported during their recovery.

3.6.4 Limitations

3.6.4.1 Instruments utilised

The SF-36 survey, although a well-validated tool for evaluating health-related quality of life, has a few limitations. Firstly, it does not allow calculation of a composite score and instead generates separate scores for physical and mental function, which can be inter-related, especially in chronic illness. Secondly, the SF36 survey is a lengthy questionnaire, which in combination with the other questionnaires may result in questionnaire fatigue, thus reducing the reliability of the answers. Thirdly, participants found some questions difficult to comprehend due to the terminology used. One question that was often left out and required further explanation is “Did you feel full of pep.” A significant proportion of individuals being reviewed required further explanation of the meaning of “pep”. Moreover, the definition of “emotional” problems is rather vague and individuals may not classify anxiety, which in some cases limited social contact, as an emotional problem. Finally, questions pertaining to social activities being limited due to physical or emotional health had to be answered speculatively, due to the enforcement of national lockdown and other social distancing measures which limited social contact. Similarly, some individuals had suffered job loss during the pandemic, which meant the impact of physical symptoms on work activities was consequentially reduced.

For the HADS score, it is important to note that being categorised as “abnormal” using the tool does not equate to a positive diagnosis, which requires more in-depth psychological assessment.

The mMRC score was utilised during the first wave to provide a quantitative assessment of breathlessness. However, this was abandoned during the second wave, and although this may be considered a limitation given the resultant absence of quantitative assessment of breathlessness in the second wave, this decision was based on feedback from patients who said that the scoring system did not capture the subtleties of their breathlessness, and whilst they felt breathless, functionally they were not limited. Whilst it would have been interesting to compare the differences between functional limitation due to breathlessness and perception of breathlessness, the number of questionnaires being filled out simultaneously was resulting in inaccuracies in completion and interpretation. For instance, patients recording a mMRC grade of 3 or 4 despite having walked to the hospital appointment.

There was limited quantification of disease symptoms with the questionnaires I used. Assessment of fatigue using the Functional Assessment of Chronic Illness Therapy—Fatigue (FACIT-Fatigue questionnaire), and new disability post COVID-19 using the Washington Disability Group (WG) Short Form as used by the ISARIC 4C and PHOSP-COVID investigators would have been useful.[248] Furthermore, a focussed assessment of post-traumatic stress disorder (PTSD), for instance, using the PTSD checklist would have provided further insights into the residual psychological morbidity experienced by these individuals.

3.6.4.2 Other methodological considerations

There are other limitations which are also important to note. The majority of the data was from hospitalized patients, and therefore these findings do not encapsulate the experiences or symptom burden of patients who were managed in the community. There was a lot of missing data in the first wave but less so in the second wave. This was a consequence of the challenges of data collection during the first wave of the pandemic. With long-term follow up, recall bias is likely to play a role in the reporting of symptoms. Additionally, the questionnaires were only given at three time points (or 2 time points during the first wave) and given the relapsing and remitting nature of the condition, it is possible that the symptom burden and QOL changes documented are not representative of their overall recovery.

To further characterise the cohort, I could have assessed acute disease severity using the ISARIC 4C mortality score, rather than solely stratifying according to the level of respiratory support required during the acute admission. Data collection on use and duration of steroid therapy during the inpatient stay was challenging and therefore has not been presented in this Chapter. However, steroid therapy was not routinely used during the first wave in the local hospital from which the patient cohort is derived and in the second wave, all inpatients requiring oxygen therapy will have received steroid therapy in accordance with local and national guidelines after the mortality benefits shown by the RECOVERY collaborative group.[30]

The qualitative interviews were only performed in patients who were diagnosed during the first wave of the pandemic. The level of understanding of the disease process and trajectory, availability of psychological support and government support had augmented significantly between the first and second waves, therefore, we cannot generalise the experiences of individuals during the first wave, when uncertainty was a dominating issue, with the experiences of individuals during the second wave.

3.7 Conclusion

In conclusion, significant clinical, psychological and HR-QOL impairments are present during recovery after acute COVID-19. Reassuringly, there is a trend towards improvement in some of these symptoms with time, especially, early post discharge. A multitude of patient-driven and external factors can affect the impact of residual symptoms on a patient's quality of life, therefore, a holistic approach to management should be adopted to support individuals in their recovery post COVID-19.

Chapter 4 - Evaluating radiological trajectory post COVID-19

Some of the results in this Chapter have already been published:

Vijayakumar B, Tonkin J, Devaraj A, Philip KEJ, Orton CM, Desai SR, Shah PL. CT Lung Abnormalities after COVID-19 at 3 Months and 1 Year after Hospital Discharge. Radiology. 2022 May;303(2):444-454. doi: 10.1148/radiol.2021211746

4.1 Introduction

As highlighted in Chapter 3, a vast number of patients post COVID-19 reported persistent breathlessness even 3 months post discharge from hospital. One possible reason for this is parenchymal inflammation or scarring, causing persistent physiological impairment, and thus persistent symptoms. In SARS-COV1 and MERS, radiological abnormalities were common in the recovery phase.[82,95,100] Whilst chest radiographs are a good screening tool, given the uncertainty of the virus impact, potential long-term complications and the burden of respiratory symptoms, I was interested to understand the radiological findings on computed tomography (CT) assessment of these individuals at 3 months post discharge. CT imaging is a very sensitive way of assessing the parenchyma[281,282] and therefore more likely to identify subtle changes. However, it's therefore also important to ensure that scanning is optimised to allow adequate time for natural parenchymal recovery, and also to prevent unnecessary irradiation from repeated follow-up scans.

4.2 Background

At the time of commencement of data collection, very little was known on the radiological outcomes post COVID-19. Evidence showed persistent chest X-ray (CXR) findings but there was limited data on CT-based findings.[283] During the first wave, the RECOVERY study showed that inpatient treatment with dexamethasone for those requiring oxygen or other respiratory support lowered 28-day mortality rates.[30] As a result of this, hospital guidelines were changed to include treatment with dexamethasone as part of routine standard care. The impact of steroid therapy on parenchymal abnormalities had not been assessed in the context of a clinical trial, but there was emerging evidence that steroid therapy after discharge might hasten the recovery of parenchymal abnormalities, the nature of which were still undetermined.[284] However, the aforementioned study was limited by the absence of a control arm and could therefore not assess if parenchymal recovery could occur with time and no additional treatment.[285] Regardless, clinicians around the globe had started utilizing steroid therapy in patients

with persistent ground-glass abnormalities, on a case-by-case basis, in the outpatient setting. If the lesions are steroid-responsive, it is possible that inpatient steroid therapy during the second wave may reduce the prevalence or extent of radiological abnormalities at follow up after the second wave. Indeed, after SARS and MERS, the prevalence of radiological abnormalities during follow up was less than that reported in COVID-19, and this was potentially attributed to steroids being more widely used during the SARS and MERS pandemics.[286,287]

In this Chapter, I will discuss the radiological findings and evolution of radiological abnormalities over a 1-year period in my cohort. Given I have mainly studied inpatients, who, during the second wave all received steroid therapy, improved timeliness of follow up during the second wave, and differences in circulating variants between the first and second waves, I have reported my findings for the first and second waves separately.

4.3 Hypothesis and Aims

Hypothesis

Persistent radiological abnormalities are common 3 months post hospital discharge with improvement over time, even without additional medical therapy.

Aims

1. To assess the prevalence of radiological abnormalities post COVID-19
2. To assess the trajectory of radiological abnormalities up to 2 years post discharge.
3. To assess risk factors for persistent radiological abnormalities

4.4 Methods

4.4.1 Patient cohort

All patients had been recruited to the PHENOTYPE study as described in Chapter 2.

4.4.2 CT imaging

Most patients underwent high-resolution CT imaging of their lung at approximately 3 months post hospital discharge. In individuals who had a raised D dimer at follow up, a computed tomography pulmonary angiogram (CTPA) was performed, ideally with high resolution CT cuts prior to injection of intravenous contrast. The rationale for a CTPA, is that whilst thrombotic events were common during the acute phase of COVID-19,[288] it wasn't clear whether patients were pro-thrombotic during the convalescence stage. During the first wave, the majority of patients had not undergone CT imaging during their inpatient stay, therefore imaging of the pulmonary arteries would not have been performed in the majority. In the second wave, CT imaging, including imaging of the pulmonary arteries, was performed routinely during the acute admission.

All CT scans were performed by Radiographers at Chelsea and Westminster Hospital. Participants were scanned with one of two 128-section multi–detector row CT machines (Siemens Edge or Edge plus; Siemens Healthcare) at 1.0 mm thicknesses. Patients who had abnormal imaging at 3 months had repeat imaging at 12 months post hospital discharge. In a subset of individuals from the first wave, repeat imaging was performed up to 2 years post discharge.

4.4.3 Initiation of outpatient steroid therapy

All clinical follow up was performed by me so any patients who received steroid therapy during the outpatient setting received prednisolone 30mg once daily (OD) for 4 weeks, followed by a wean of 5mg every 2-3 days to stop. The decision to commence a trial of steroid therapy was based on a) the extent of radiological abnormalities b) differential cell count analysis c) risk factors for adverse effects d) patient preference. As the efficacy and/or need for steroid therapy in the management of these individuals was not known, an honest conversation with the patient, emphasising the lack of evidence-base for the approach was essential. The rationale explained was to hasten recovery of the radiological findings, with prevention of irreversible scarring if the abnormalities noted on the CT findings were representative of a poorly controlled inflammatory process (either residual or new since the initial viral insult), as seen in the inflammatory interstitial lung diseases.

4.4.4 Radiological scoring

The scans performed during the first wave were visually scored by Professor Sujal Desai and Professor Anand Devaraj (Consultant Thoracic Radiologists at the Royal Brompton Hospital, London). The following scores were derived: a) Overall parenchymal abnormality of any nature b) Ground glass opacification c) Radiological bands d) Fibrosis. Scoring was performed independently by the

Radiologists, and the final score was derived by consensus and rounded to the nearest 5%. Fibrosis was defined as the presence of volume loss +/- traction bronchiectasis.

I was present during the sessions when the Radiologist scored the scans and was also taught how to score scans myself. I then used this knowledge and experience to score the CT scans from the second wave. Initially, I scored 20 scans that the radiologists had already scored (10 from each wave), blindly, to assess correlation between their scores and mine (Figure 4.1). All scoring of subsequent CTs was performed by myself across two sessions. At the beginning of each session, I re-tested my scoring against the Radiologists' scores from the first wave to ensure accuracy.

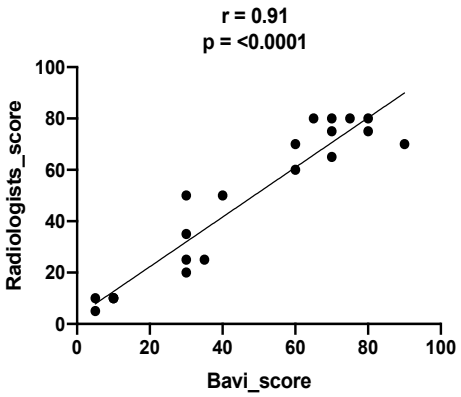


Figure 4. 1 Comparing Radiologists' and my CT scores

Spearman rank correlation analysis comparing Radiologists' and my scores of CTs performed during the first wave. P value <0.05 considered statistically significant

4.5 Results

4.5.1 Consort diagram

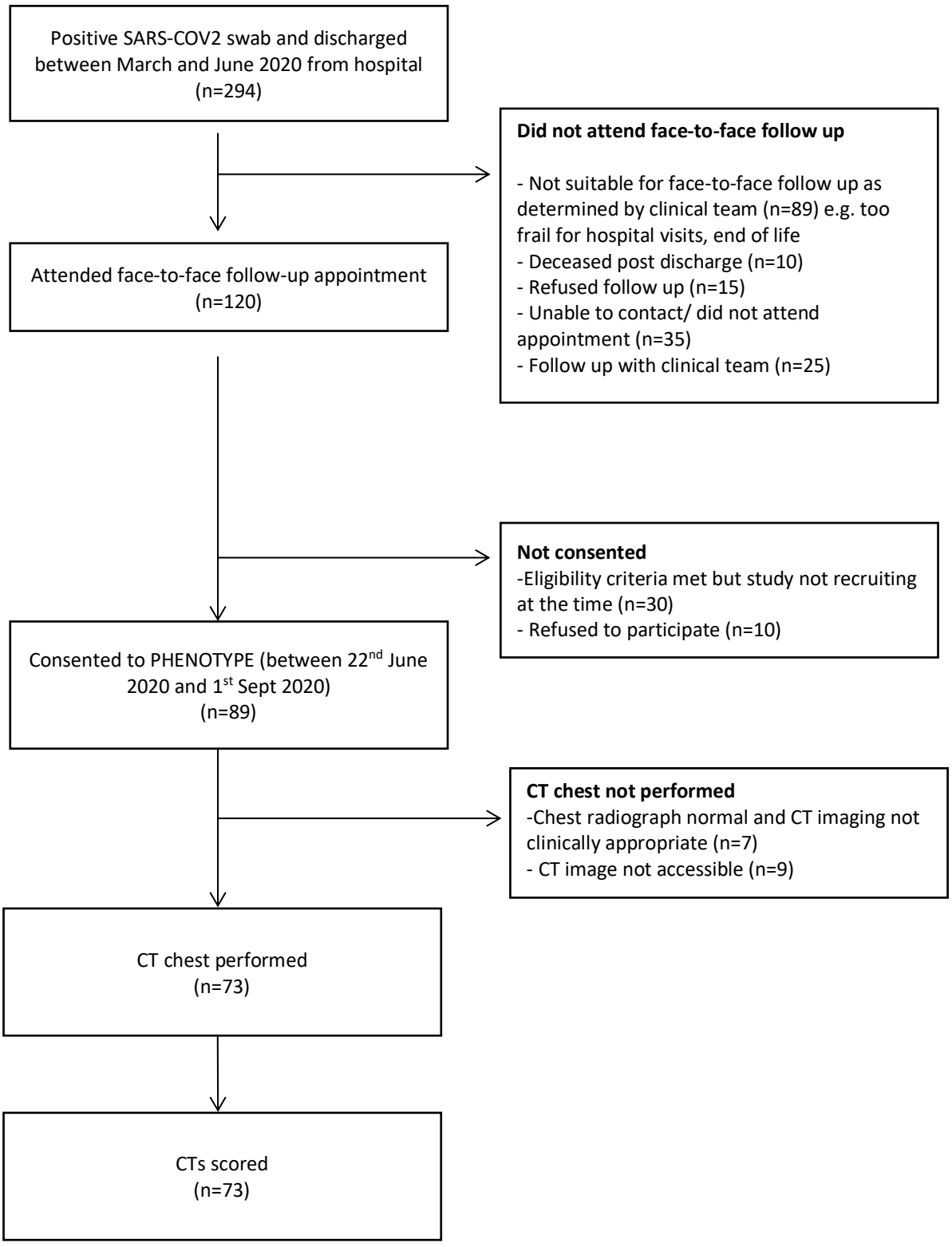


Figure 4. 2 Consort diagram of patients undergoing CT imaging (W1)

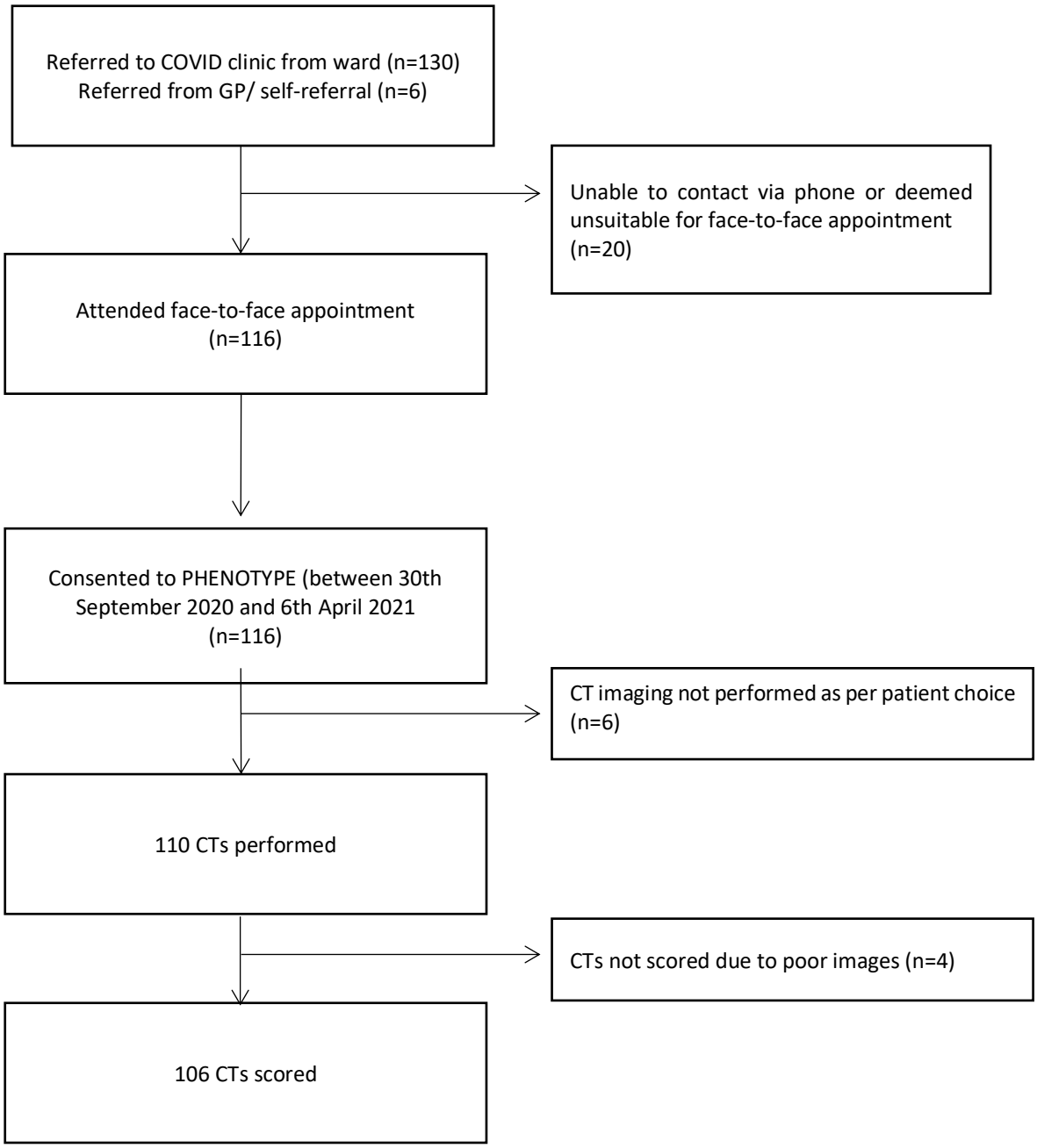


Figure 4. 3 Consort diagram of patients undergoing CT imaging (W2)

4.5.2 Baseline characteristics

		First wave	Second wave
Gender, M		48 (65.8)	79 (71.8)
Age, years		59.6 (+/- 1.4)	55.8 (+/- 1.3)
Smoking history	Current smoker	2 (2.7)	4 (3.6)
	Ex-smoker (>=10 pack year)	13 (17.8)	16 (14.5)
	Non- smoker	58 (79.5)	90 (81.8)
Admitted to hospital		73 (100)	102 (92.7)
Maximal respiratory support	MV	16 (21.9)	3 (2.9)
	NIV/PPV	29 (39.7)	26 (25.4)
	O2 only	23 (31.5)	73 (71.6)
	No respiratory support	5 (6.8)	8 (7.2)
Length of stay (days)		7.5 (3 – 14.5)	6 (4-10)
Respiratory comorbidities	Asthma	10 (13.7)	10 (9.1)
	COPD	6 (8.2)	5 (4.5)
	OSA on CPAP	1 (1.4)	4 (3.6)
	Nil	51 (69.9)	86 (78.2)
Cardiovascular	HTN	22 (30.1)	25 (22.7)
	IHD	6 (8.2)	10 (9.1)
	Valvular disease	3 (4.1)	5 (4.5)
	Nil	44 (60.3)	71 (64.5)
T2DM		16 (21.9)	15 (13.6)

Table 4. 1 Baseline characteristics of patients undergoing CT imaging

Data shown as n (%n), mean (+/- SEM) or median (IQR). Abbreviations: M- male, MV – mechanical ventilation, NIV – non-invasive ventilation, PPV – positive pressure ventilation, O2 – oxygen, COPD – chronic obstructive pulmonary disease, OSA – obstructive sleep apnoea, CPAP – continuous positive airway pressure, HTN – hypertension, IHD – ischaemic heart disease, T2DM – type 2 diabetes mellitus

4.5.3 Non-fibrotic radiological abnormalities at 3 months

41/73 (56.1%) of patients from the first wave and 70/106 (66%) from the second wave had abnormalities on their CT performed approximately 3-6 months post hospital discharge. The commonest abnormalities found were ground glass opacification (Figure 4.4a), radiological bands (Figure 4.4b) and associated consolidation (Figure 4.4c).

35/41 (85.4%) of those with abnormalities had predominantly ground-glass opacities in Wave 1, with the corresponding proportion in wave 2 being 63/70 (90%). Therefore, the majority of the changes contributing to persistent abnormalities in both waves were ground-glass opacities.

The median overall score was 25% (IQR 10-60) in the first wave, compared to 27.5 (5-50) in the second wave in those with abnormal CTs. The median proportional ground-glass changes in the first wave was 22.5 (6-57) compared to 20 (5-50) with no statistically significant differences between the two waves (Figure 4.5).

The degree of CT abnormality was divided using arbitrary cut-offs of <30% (mild), 30-60% (moderate), >60% (extensive). With these classifications, 22/41 (54%), 10/41 (24%) and 9/41 (22%) of CTs performed during the first wave showed mild, moderate and extensive changes, respectively. A similar assessment was performed during the second wave data with 35/70 (50%), 21/70 (30%) and 14/70 (20%) classified as mild, moderate and extensive. Therefore, the extent of residual abnormality was similar between both waves, despite inpatient steroid therapy being used during the second wave (Figure 4.6).

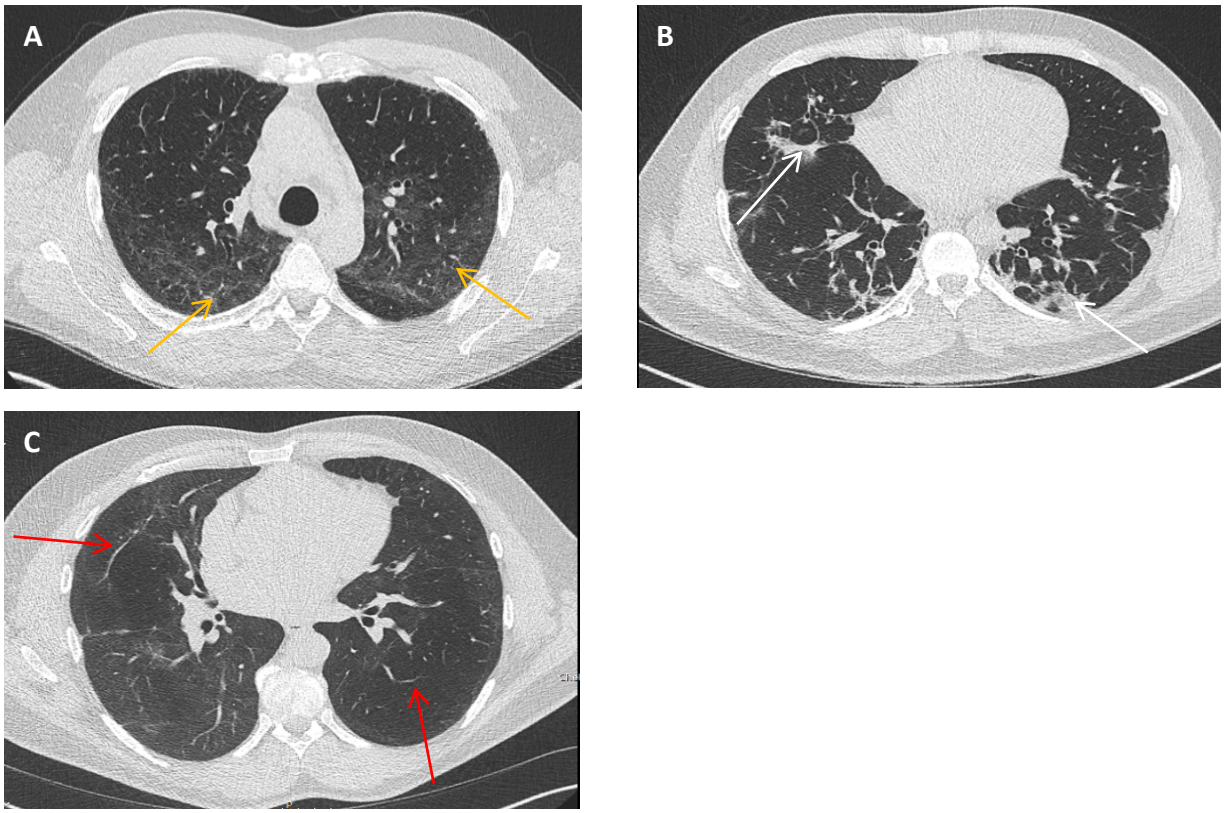


Figure 4. 4 Patterns of radiological abnormalities at 3-month follow-up

A) Ground glass changes (yellow arrows), B) Bands and consolidation (white arrows), C) Bands (red arrows)

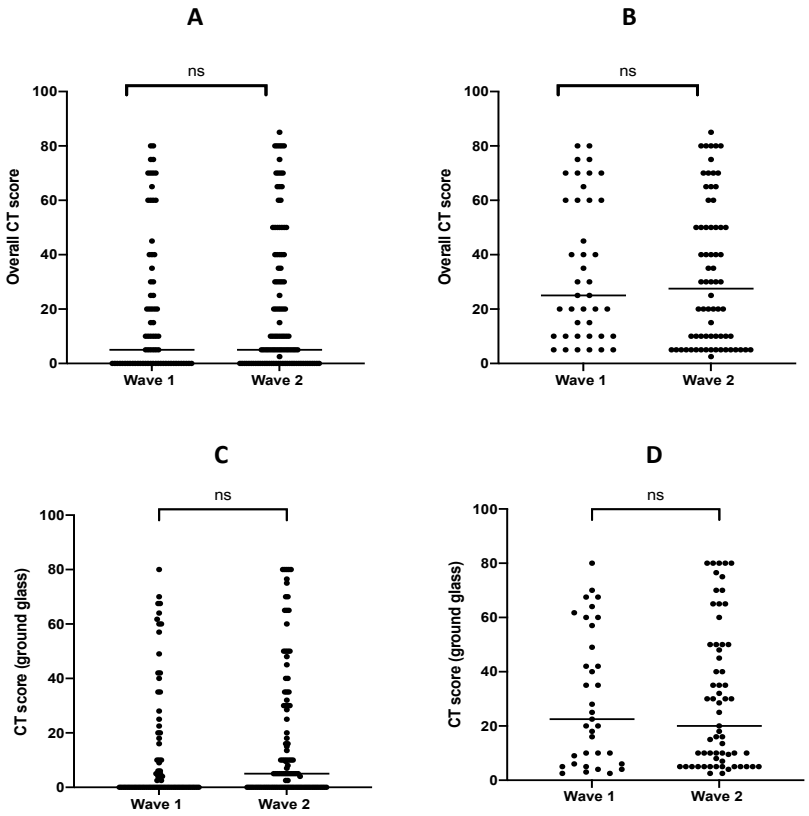


Figure 4. 5 CT scores at 3-month follow-up during (W1 and W2)

Overall percentage abnormality (A-B), percentage ground-glass abnormality (C-D), including whole cohort (A, C) and those with CT abnormalities only (B, D). Line drawn at median value. Comparisons made using non-parametric Mann Whitney U test. P<0.05 considered to be statistically significant.

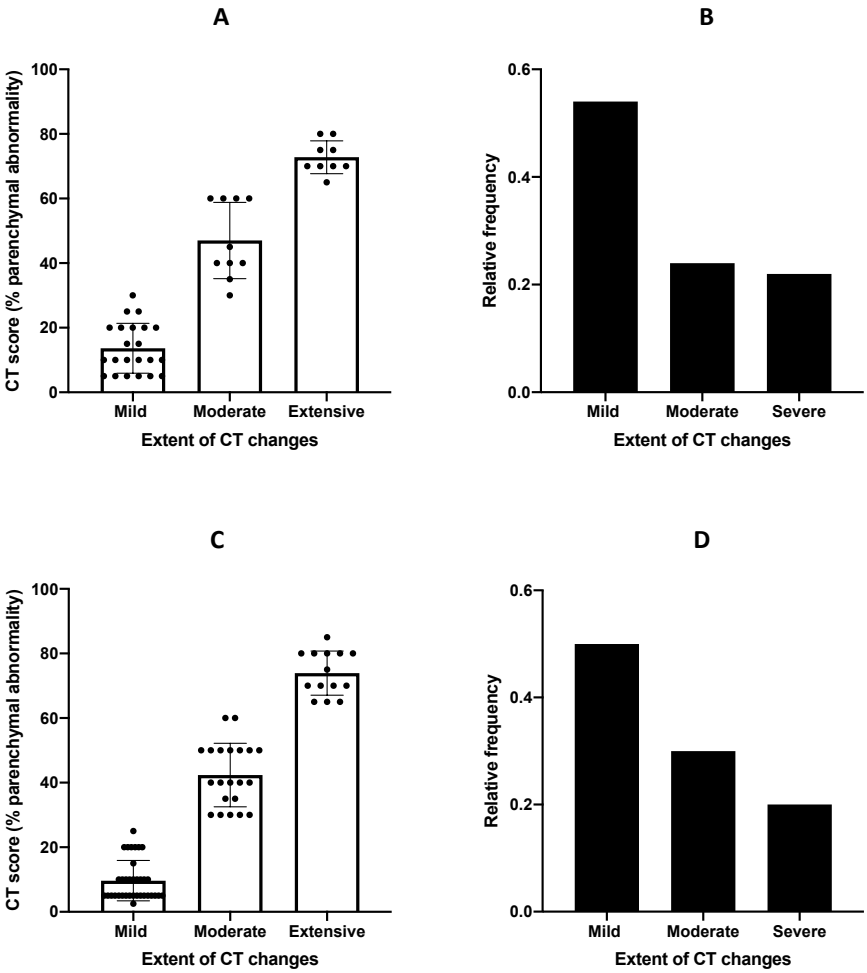


Figure 4. 6 Classification of extent of CT abnormalities (W1 and W2)

CT abnormalities during first wave (A, B) and second wave (C, D). Scatterplot shows percentage of parenchyma involved (A, B) with median and inter-quartile range shown. Relative frequency of those with abnormal CTs displaying varying extents of parenchymal involvement shown in B and D. Extent of abnormality classified as follows: mild <30%, moderate 30-60%, extensive >60%.

4.5.3.1 Non-fibrotic radiological abnormalities and disease severity

There are different ways in which acute disease severity can be defined. However, for the purposes of this Chapter, I have used two main approaches: a) Degree of respiratory support required during the inpatient stay b) Blood markers associated with acute severity: White cell count, neutrophil count, lymphocyte count, serum neutrophil:lymphocyte ratio, fibrinogen, ferritin, albumin and C-reactive protein. I wanted to assess whether the severity of the acute illness was associated with persistent radiological abnormalities at follow up.

Patients hospitalised for COVID-19

In both waves, those with persistent abnormalities were older ($p<0.05$). The degree of respiratory support and length of hospital stay was associated with abnormalities on CT chest during the first wave, but this was not mirrored during the second wave (Table 4.2).

In the first wave, individuals with an abnormal CT scan at follow up had a statistically significant higher fibrinogen (7.5 [6.44 – 8.55] vs 6.49 [5.17 – 7.65], p = 0.013), higher CRP (122.1 [60.1 – 231] vs 77.1 [29.4 – 114], p = 0.006) and lower albumin (34.0 [31.8 – 39.0] vs 32 [31 – 36], p = 0.050) during the acute admission. There was no statistically significant difference between the groups in terms of white cell count, neutrophils, lymphocytes, neutrophil: lymphocyte ratio, D dimer or ferritin (Figure 4.7). In the second wave, individuals with an abnormal CT had a higher SNLR (5.54 [3.97 – 8.96] vs 4.34 [3.08 – 6.24], p = 0.03) and lower albumin (33 [29.3 – 35.0] vs 35 [32 – 37], p = 0.023). There were no differences in the other parameters, however (Figure 4.8).

First wave					
Characteristic	Abnormal CT N=41	Normal CT N=32	Odds ratio	P value	95% CI
Age (years)	62 +/- 1.6	56 +/-2.4		**0.04**	
Gender, M	28 (68)	20 (63)	1.3	0.61	0.5-3.5
BAME	23 (56)	16 (50)	1.3	0.60	0.5 - 3.2
Ethnicity: White	18 (43.9)	16 (50)			
Ethnicity: Black, African, Caribbean or Black British	7 (17.1)	4 (12.5)			
Ethnicity: Asian or Asian British	16 (39.0)	12 (37.5)			
Smoker/ex-smoker	23 (56)	12 (38)	2.1	0.11	0.9-5.7
OAD	8 20)	8 (25)	0.7	0.57	0.3-2.1
Cardiac history	14 (34)	7 (22)	1.8	0.25	0.6-4.9
T2DM	11 (27)	6 (19)	1.6	0.42	0.5-5.2
MV	14 (34)	2 (6.3)	**7.8**	**0.004**	1.7-36
PPV	22 (54)	7 (22)	**4.1**	**0.006**	1.5-11
LOS (days)	10 (5.3-27)	6.0 (3.0-8.8)		**0.008**	
Second wave					
	Abnormal (n=70)	Normal (n=28)			
Age (years)	59.3 (+/-1.5)	49.9 (+/- 2.3)		**0.003**	
Gender, M	52 (74)	21 (75)	0.96	0.94	0.37 – 2.56
BAME	46 (66)	16 (57)	1.44	0.43	0.60 – 3.44
Ethnicity: White	24 (34.3)	12 (42.9)			
Ethnicity: Black, African, Caribbean or Black British	7 (10)	3 (10.7)			
Ethnicity: Asian or Asian British	39 (55.7)	13 (46.4)			
Smoker/ex-smoker	24 (34)	14 (50)	0.52	0.15	0.23 – 1.25
OAD	11 (16)	4 (14)	1.12	0.86	0.33 – 3.45
Cardiac history	26 (37)	7 (25)	1.77	0.25	0.64 – 4.48
T2DM	9 (13)	4 (14)	0.89	0.85	0.27 – 2.80
MV	2 (3)	1 (4)	0.79	0.85	0.09 – 11.9
PPV	19 (27)	6 (21)	1.30	0.62	0.47 – 3.78
LOS (days)	7 (4 – 11)	6 (4 – 8)		0.10	

Table 4. 2 Demographic and admission data according to CT findings (W1 and W2)

Baseline characteristics and admission details for patients with normal and abnormal CT findings during the first and second wave. Results are presented as number (%n), mean (+/-SEM) or median (IQR). Statistical analysis performed using Chi-squared testing or non-parametric Mann Whitney U test. P value <0.05 considered statistically significant. Odds ratio and 95% confidence interval (CI) displayed. Abbreviations: M (male), BAME (black, Asian and minority ethnic), OAD (obstructive airways disease), T2DM (type 2 diabetes mellitus), LOS (length of stay), MV (mechanical ventilation), PPV (positive pressure ventilation)

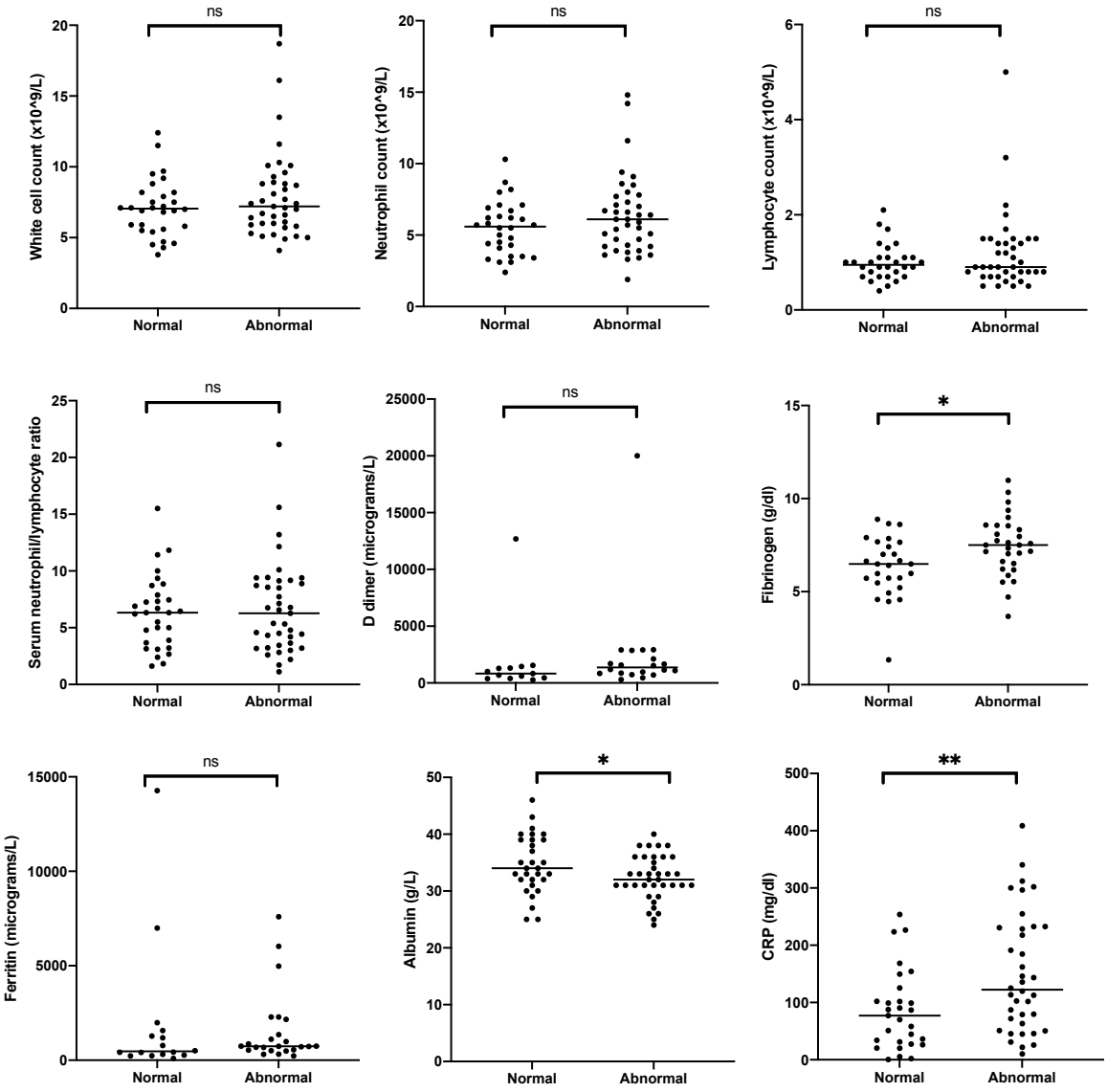


Figure 4. 7 Admission blood results according to CT findings (W1)

Admission bloods and CT findings at 3 month follow up, classified as normal (score of 0) or abnormal during Wave 1. Scatter plots with line drawn at median. Inter-group comparisons performed using Mann Whitney U test. P value <0.05 considered statistically significant *p<0.05, **p<0.01, ***p<0.001

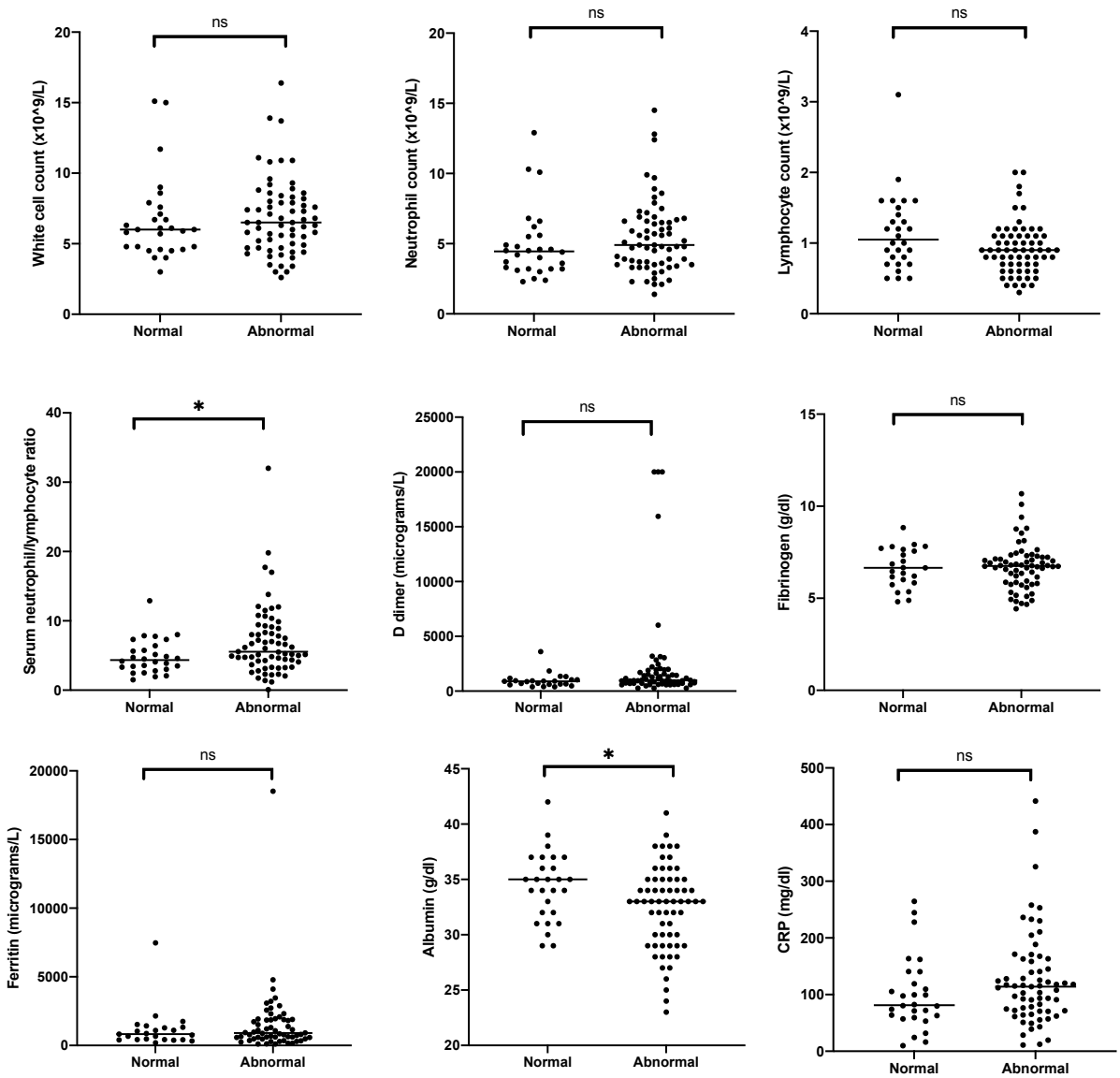


Figure 4. 8 Admission blood results according to CT findings (W2)

Admission bloods and CT findings at 3 month follow up, classified as normal (score of 0) or abnormal during Wave 2. Scatter plots with line drawn at median. Inter-group comparisons performed using Mann Whitney U test. P value <0.05 considered statistically significant. *p<0.05, **p<0.01, ***p<0.001

Patients not hospitalised for COVID-19

8 patients recruited during the second wave not been admitted to hospital. All had CT scores of 0 and none had any pre-existing comorbidities (Table 4.3)

Gender, M	4 (50)
Age	41.2 (+/- 3.6)
OAD	0 (0)
Cardiac *	0 (0)
T2DM	0 (0)
Smoker/ex-smoker	0 (0)

Table 4. 3 Demographics of patients not admitted to hospital

Data shown as n (% n) or mean (+/- SEM). *One patient had pericarditis post viral infection, which resolved
Abbreviations: M (male), OAD (obstructive airways disease), T2DM (type 2 diabetes mellitus).

4.5.3.2 Non-fibrotic radiological abnormalities and blood parameters at 3 month follow-up

Despite some differences in blood parameters during acute admission in those with normal or abnormal CTs, no differences were seen between the groups in blood parameters at follow up, neither in the first wave (Figure 4.9), nor second wave (Figure 4.10).

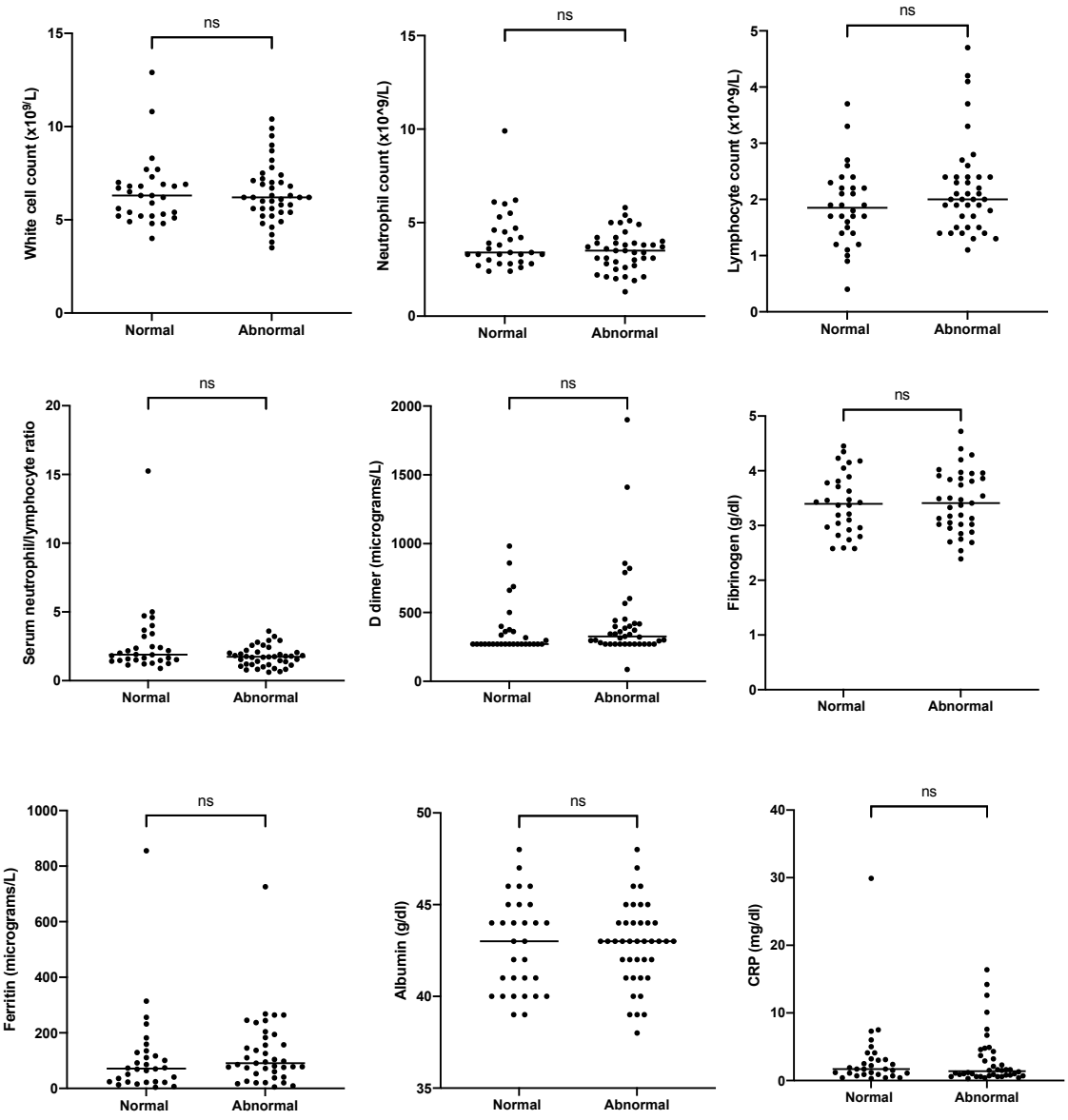


Figure 4. 9 Three-month blood results according to CT findings (W1)

Differences in blood parameters at 3-month follow-up visit in patients with normal and abnormal CT scans during the first wave. Scatter plots with line drawn at median value. Inter-group comparisons performed using Mann Whitney U test. P value <0.05 considered statistically significant. * p<0.05, ** p<0.01, *** p<0.001

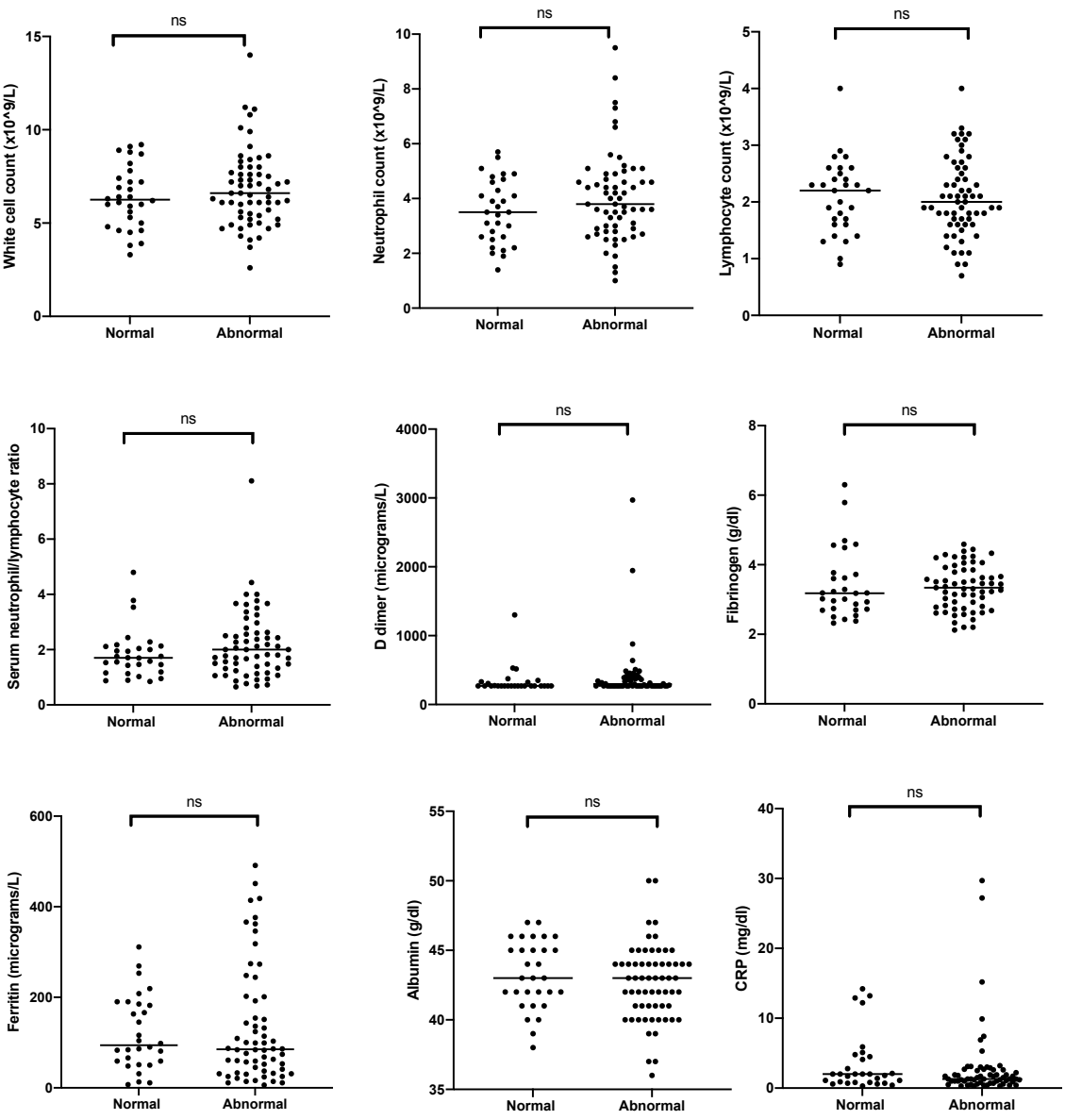


Figure 4. 10 Three-month blood results according to CT findings (W2)

Differences in blood parameters at 3-month follow-up visit in patients with normal and abnormal CT scans during the second wave. Scatter plots with line drawn at median value. Inter-group comparisons performed using Mann Whitney U test. P value <0.05 considered statistically significant. * p<0.05, ** p<0.01, *** p<0.001

4.5.4 Fibrotic changes at 3 months

During the first wave, 9 individuals had features of fibrosis (volume loss +/- traction bronchiectasis). In the second wave, 3 individuals had features of fibrosis, however the imaging features were different

to that seen in the first wave (Figure 4.11). Notably 8/9 individuals with fibrosis in the first wave had required mechanical and/or positive pressure ventilation (Table 4.4).

	% Overall parenchymal abnormality	Volume loss	Wave	Age (years)	Gender	Ethnicity	Comorbidities	LOS (days)	Maximum respiratory support
Participant 1	60	Yes	1	73	Male	Asian	IHD, HTN, T2DM	12	Positive pressure
Participant 2	5	Yes	1	68	Male	White	IHD, HTN, T2DM	6	Oxygen
Participant 3	25	No	1	56	Male	Black	DVT 2018	5	Positive pressure
Participant 4	70	Yes	1	55	Male	Asian	Asthma, HTN, T2DM	32	Mechanical ventilation
Participant 5	75	Yes	1	65	Male	Black	HTN, T2DM	8	Positive pressure
Participant 6	70	No	1	52	Male	White	Nil	50	Mechanical ventilation
Participant 7	80	No	1	66	Female	Black	T2DM, high cholesterol	22	Mechanical ventilation
Participant 8	30	Yes	1	59	Male	Black	Nil	37	Mechanical ventilation
Participant 9	40	Yes	1	58	Male	Asian	HTN, T2DM	49	Mechanical ventilation
Participant 10	50	No	2	73	Male	White	Nil	13	Positive pressure
Participant 11	70	No	2	74	Male	Asian	OSA [on CPAP], HTN	6	Oxygen
Participant 12	50	No	2	86	Male	Black	HTN, T2DM	7	Oxygen

Table 4. 4 Clinical data of patients with fibrosis on 3-month CT

Abbreviations: IHD (ischaemic heart disease), HTN (hypertension), T2DM (type 2 diabetes mellitus), LOS (length of stay, CPAP (continuous positive airway pressure), OSA (obstructive sleep apnoea)

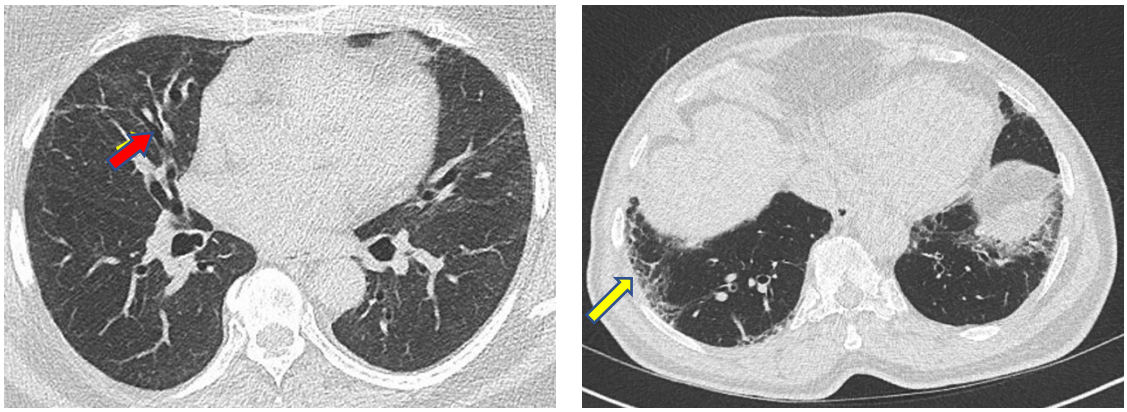


Figure 4. 11 Fibrosis on CT imaging at 3-month follow up

CT changes in 2 individuals with fibrosis at follow up: A: 59-year-old gentleman requiring mechanical ventilation during the first wave. Red arrows point to non-tapering airways suggestive of traction bronchiectasis. B: 86-year-old gentleman requiring oxygen therapy during admission in the second wave. Yellow arrow points to area of honeycombing.

4.5.5 Radiological abnormalities and respiratory symptoms

21/41 (51.2%) compared to 26/67 (28.9%) of those with an abnormal CT at follow-up reported breathlessness during the first and second waves respectively. Similarly, 15/32 (46.8%) compared to 7/28 (25%) of those with normal CTs reported breathlessness. Chi squared analysis revealed no significant difference between those with breathlessness and abnormal CT vs normal CT in the first wave (OR 1.2 [0.5 – 2.9], p=0.71 or second wave (OR 1.9 [0.73 – 4.81], p=0.20) (Figure 4.12).

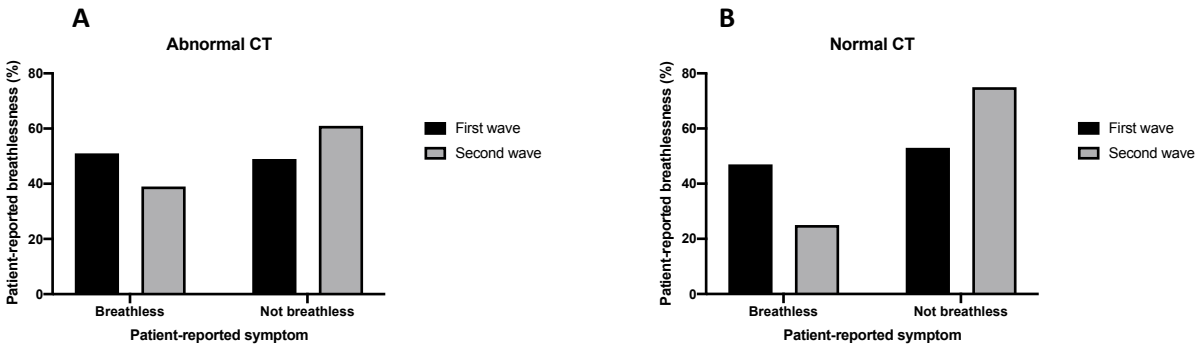


Figure 4. 12 Patient-reported breathlessness and CT abnormality

Abnormal CT (A) or normal CT (B) during the first and second wave

4.5.6 Radiological abnormalities and lung function parameters

Spirometry and body plethysmography were performed at approximately 3 months post hospital discharge. There was no correlation between absolute lung function parameters and overall % CT abnormality at 3 months for individuals in the first wave (Figure 4.13) but weak, negative, but statistically significant correlations were present in the second wave. The strongest correlation was with gas transfer (TLCO) where r was – 0.49 (p <0.0001) (Figure 4.14).

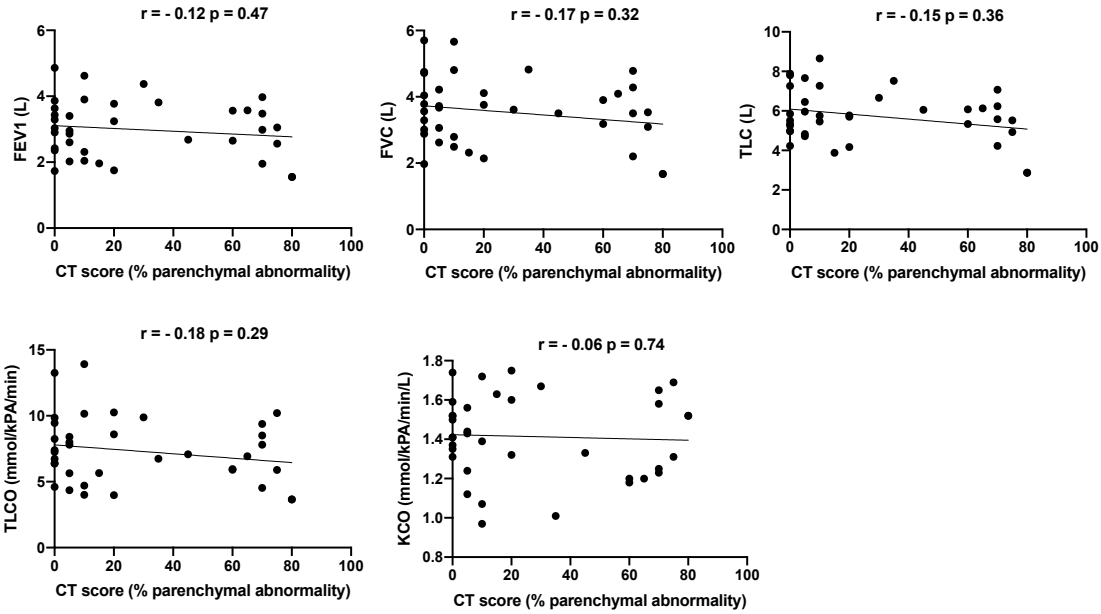


Figure 4. 13 Relationship between CT score and lung function parameters at 3 months (W1)

Correlation analysis performed using Spearman rank correlation analysis. P value <0.05 considered statistically significant. Abbreviations: FEV1 – forced expiratory volume in 1 second; FVC – forced vital capacity; TLC – total lung capacity; TLCO – transfer capacity of the lung for the uptake of carbon monoxide; KCO – carbon monoxide transfer coefficient; L (litres); kPA (kilopascals), mmol (millimoles)

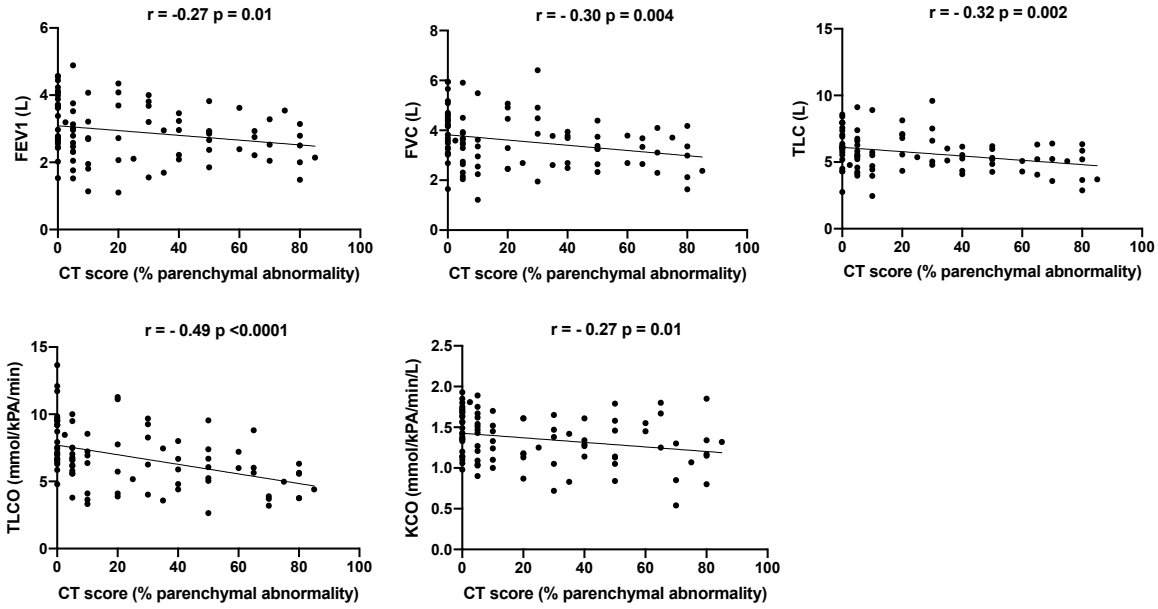


Figure 4. 14 Relationship between CT score and lung function parameters at 3 months (W2)

Correlation analysis performed using Spearman rank correlation analysis. P value <0.05 considered statistically significant. Abbreviations: FEV1 – forced expiratory volume in 1 second; FVC – forced vital capacity; TLC – total lung capacity; TLCO – transfer capacity of the lung for the uptake of carbon monoxide; KCO – carbon monoxide transfer coefficient; L (litres); kPA (kilopascals), mmol (millimoles)

4.5.8 Radiological abnormalities and time from acute illness

There was no convincing relationship between the degree of CT abnormality at 3 months and time from the acute admission or discharge (Figure 4.15).

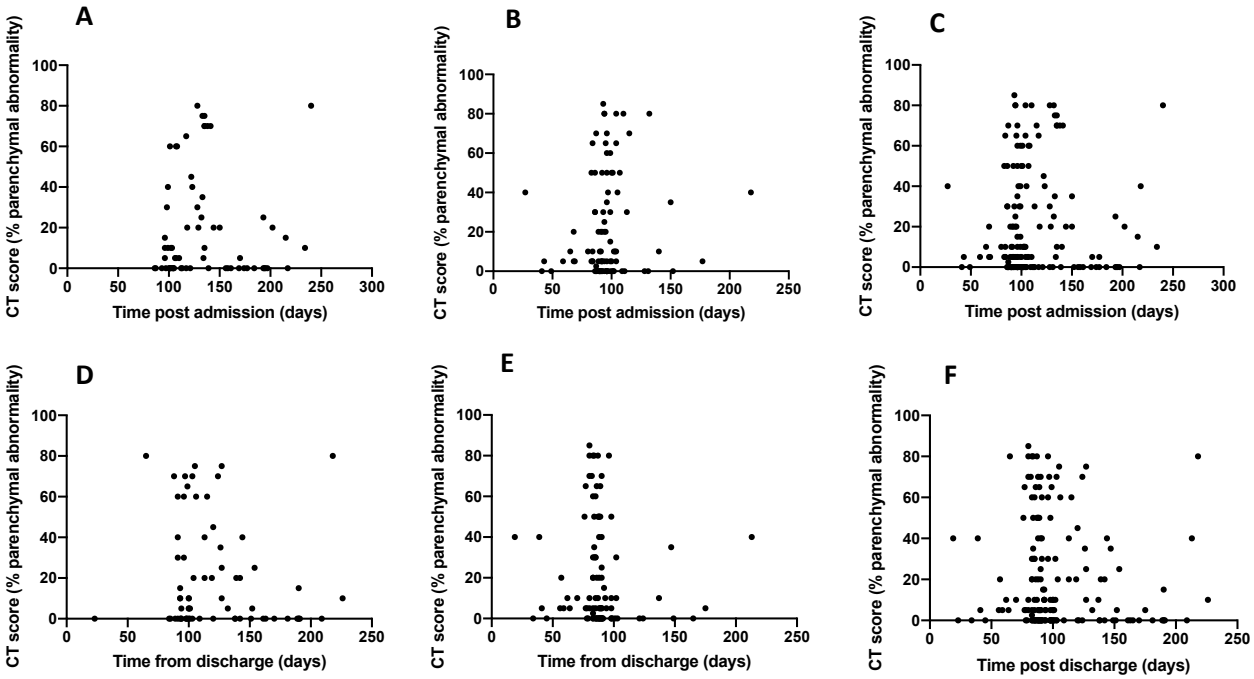


Figure 4. 15 Relationship between CT score at 3 months and acute admission parameters

Relationship between CT score and time from admission (A-C) and discharge (D-F) during the first wave (A, D), second wave (B, E) and both waves combined (C, F).

4.5.9 Trajectory of radiological findings

Patients with an abnormal CT chest at 3 months underwent repeat imaging at 1 year. Figures 4.16 and 4.17 show the individuals undergoing repeat imaging.

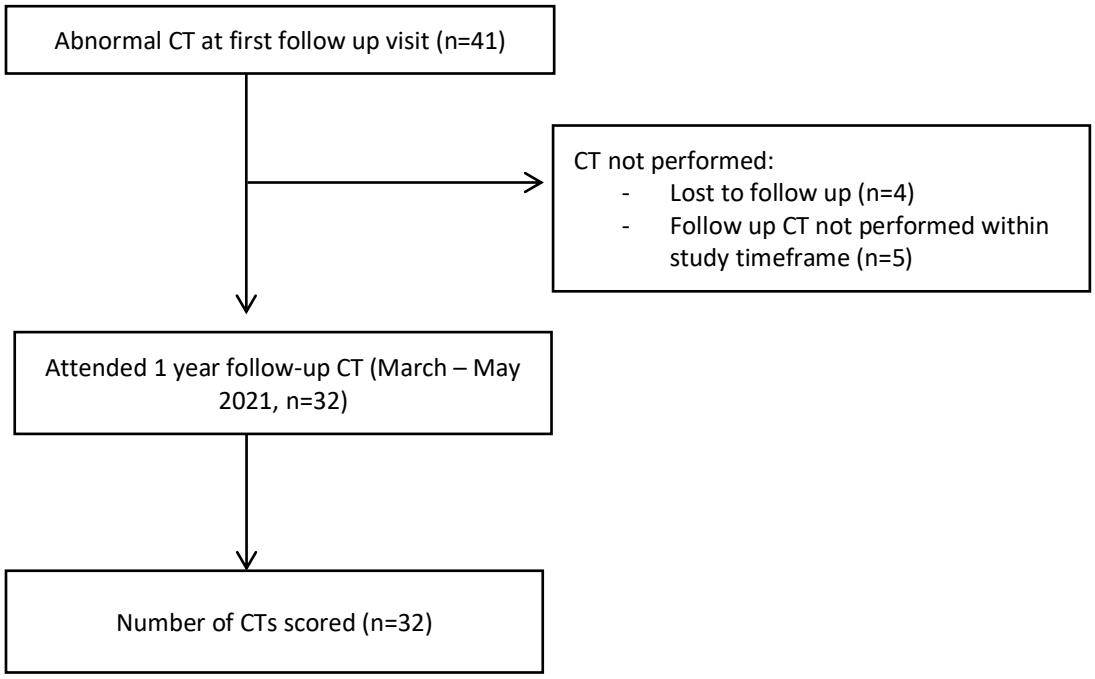


Figure 4. 16 Flow diagram of patients undergoing CT imaging at 1 year (W1)

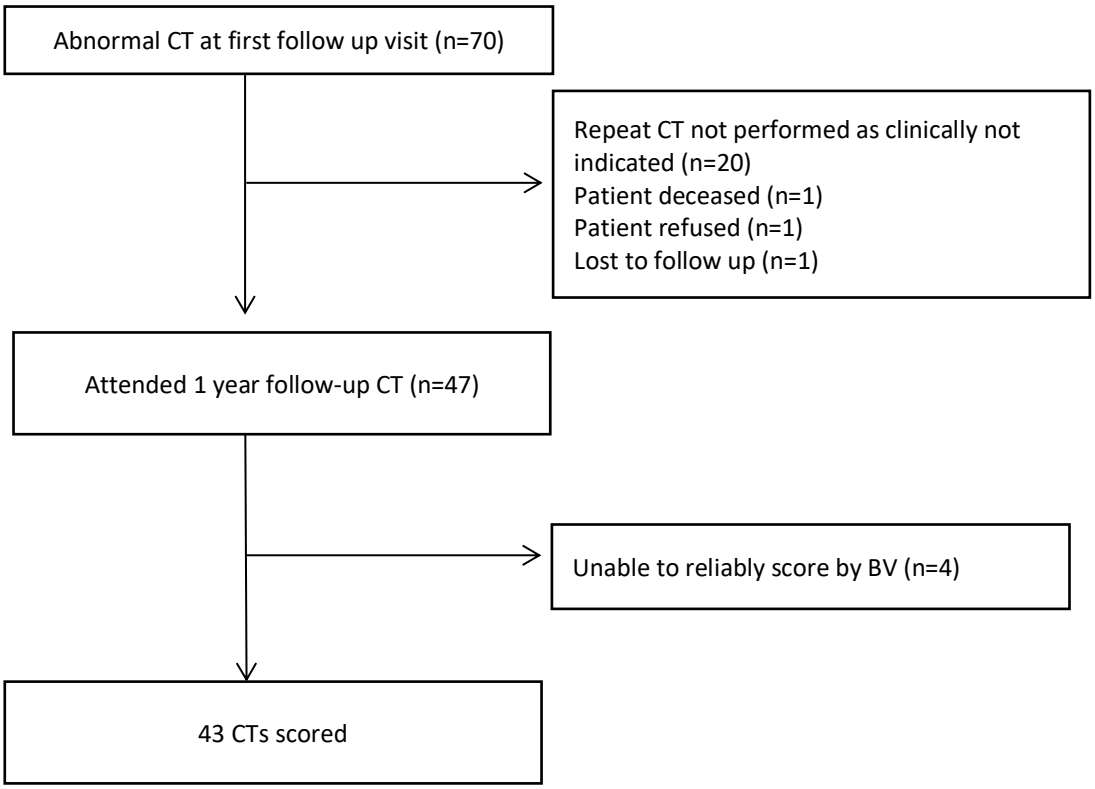


Figure 4. 17 Flow diagram of patients undergoing CT imaging at 1 year (W2)

Statistically significant improvements were seen in CT scores over a 1-year period, both in the first and second waves (Figure 4.18).

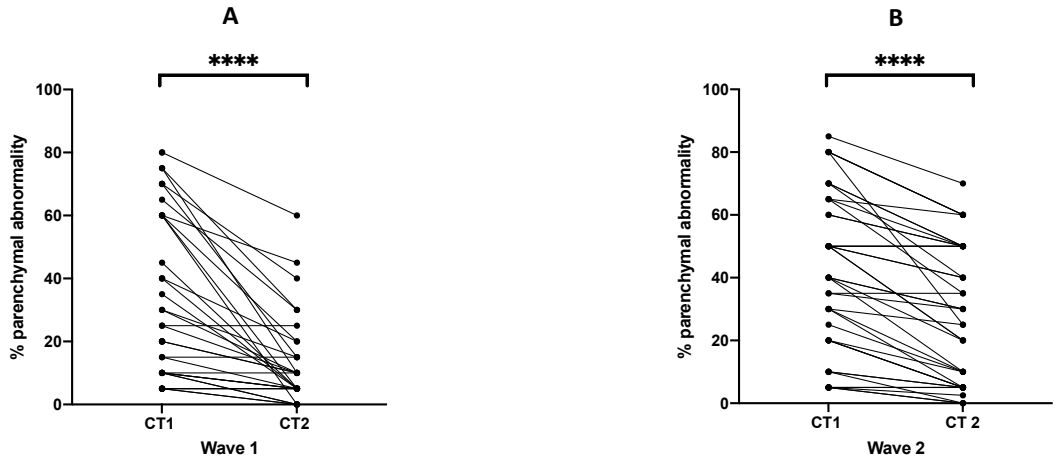


Figure 4. 18 Changes in CT scores over 12 months

Changes in CT scores between first and second CT in Wave 1 (A) and Wave 2 (B). First CT was performed approximately 3 months post discharge; Second CT approximately 1 year post discharge. Paired Wilcoxon signed rank test used to compare change in scores. A p value <0.05 considered statistically significant. *p<0.05, ** p<0.01, ***p<0.001, ****p<0.0001

4.5.10 Impact of outpatient steroid therapy on radiological abnormalities

The degree of improvement of CT scores was similar, regardless of whether outpatient steroid therapy had been administered (Figure 4.19).

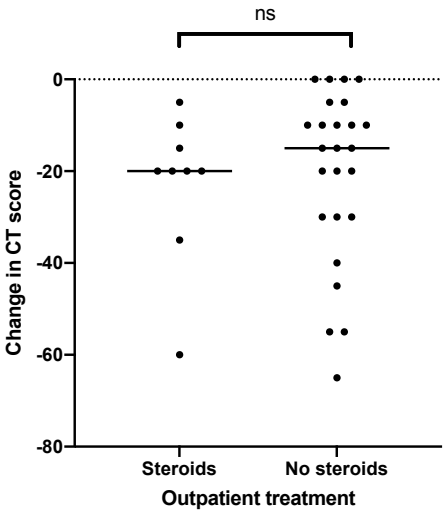


Figure 4. 19 Absolute change in CT scores according to outpatient steroid therapy

Absolute change in CT scores between 3- and 12-months post discharge, according to whether the patient received outpatient steroid therapy. Inter-group comparisons performed using non-parametric Mann Whitney U test. P value <0.05 considered statistically significant

As evident from figures 4.20 - 4.22, there was improvement in CT findings over time, irrespective of whether they were from the first wave (4.20) or second wave (4.21), whether they received no steroid therapy (4.20), inpatient steroid therapy alone (4.21) or received both inpatient and outpatient steroid therapy (4.22).

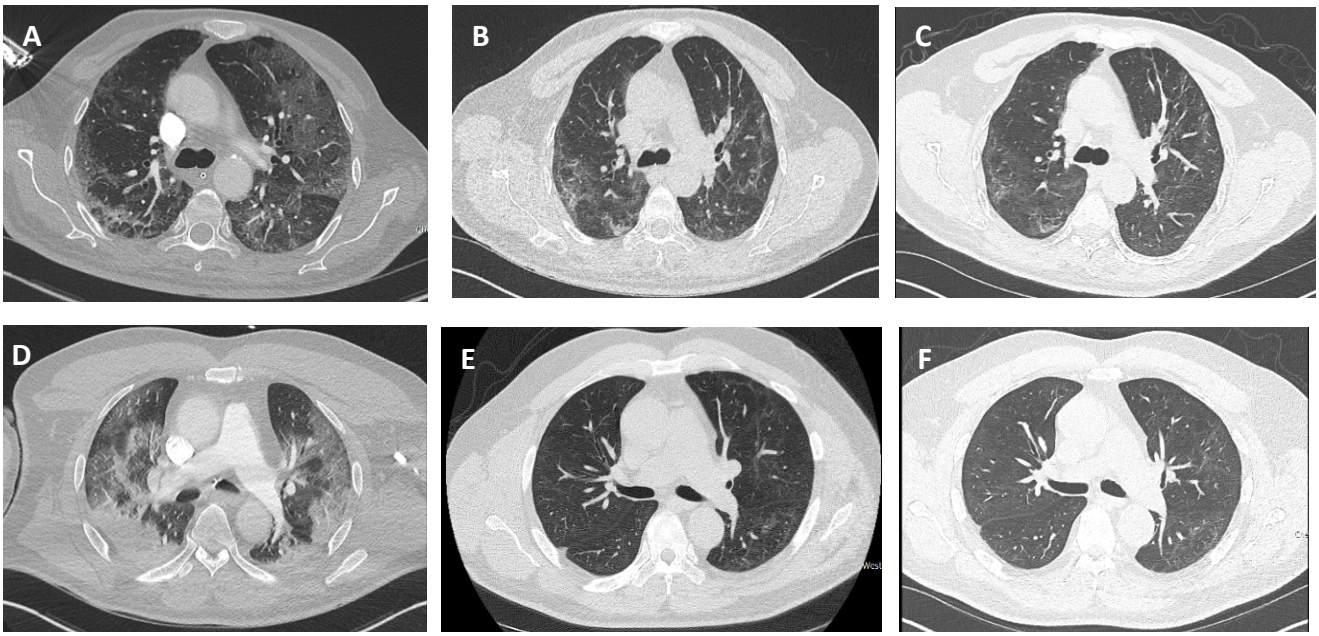


Figure 4. 20 Radiological trajectory without steroid therapy

HRCT images taken during admission (A, D), 1 year post discharge (B, E) and 2 years post discharge (C, F) of 58-year-old gentleman (top panel) and 61-year-old gentleman (bottom panel), both requiring intubation and ventilation for COVID-19 ARDS during the first wave. Note, improvement in ground-glass changes over time, with replacement of consolidation in D with ground glass in E and F, and persistent architectural distortion in top panel. Patients did not receive inpatient or outpatient steroid therapy. Improvements seen despite no steroid treatment.

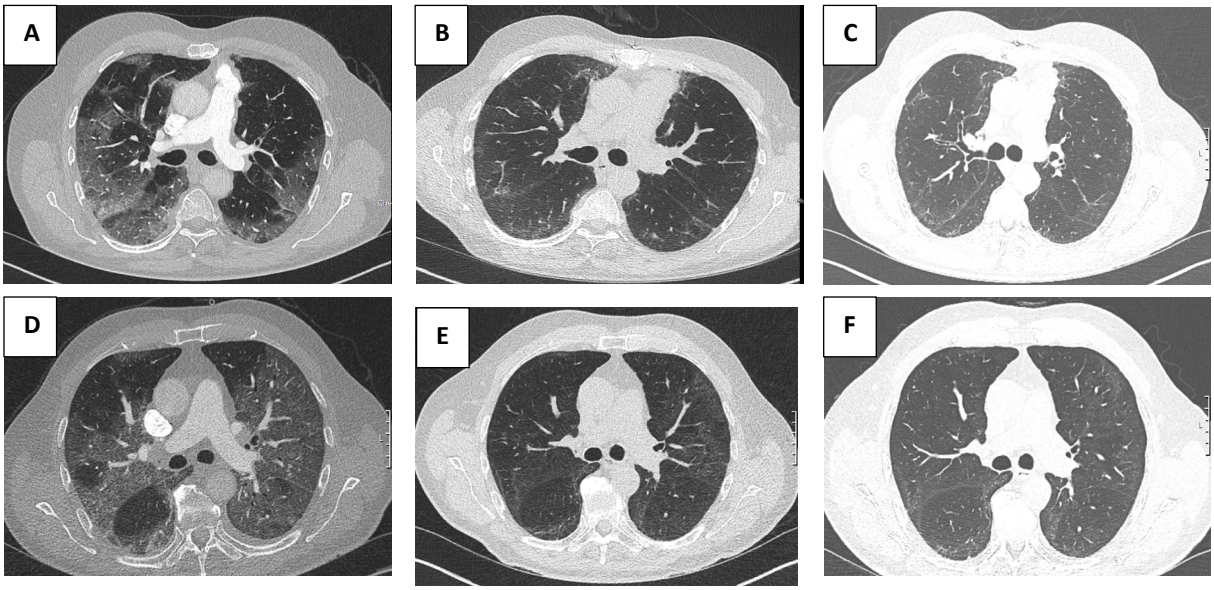


Figure 4. 21 Radiological trajectory with inpatient steroid therapy only

HRCT images of patients admitted with COVID-19 ARDS during the second wave who had received inpatient steroid therapy, but no outpatient steroid treatment. Images taken during admission (A, D), 3 months post discharge (B, E) and 1 year post discharge (C, F). 64-year-old gentleman (top panel) and 76-year-old gentleman (bottom panel), both requiring oxygen therapy only. Note improvement in parenchymal features over time in both individuals.

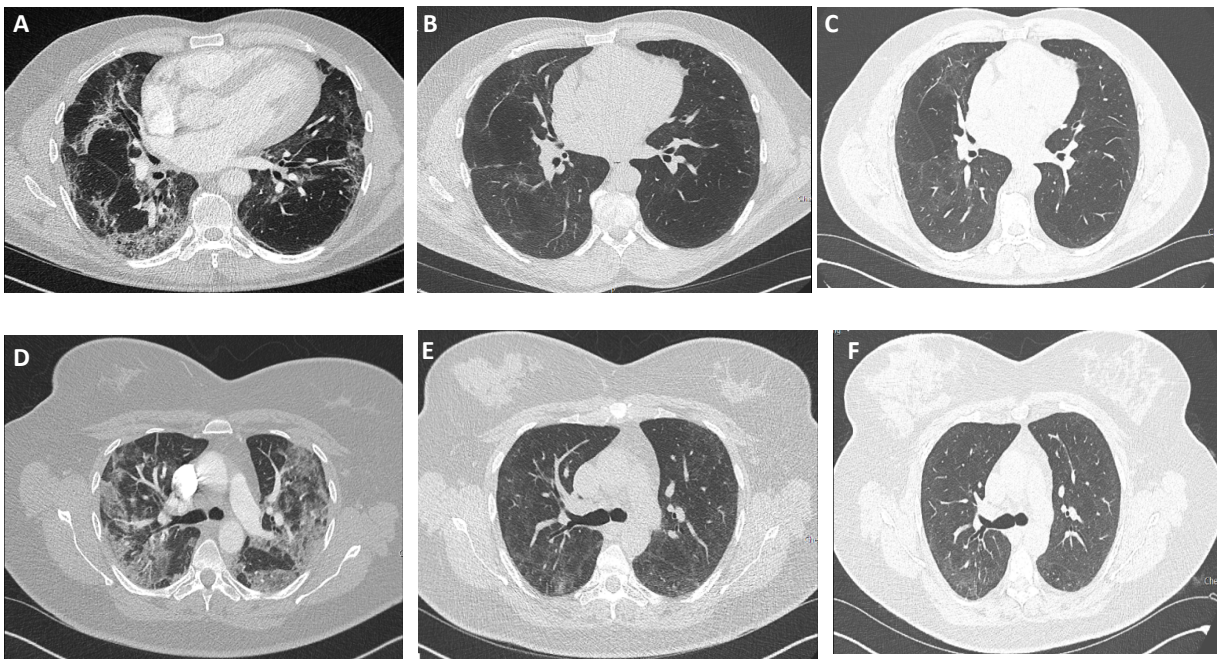


Figure 4. 22 Radiological trajectory with inpatient and outpatient steroid therapy

HRCT images of 55-year-old gentleman (top panel) and 49-year-old female, admitted during second wave with COVID-19 ARDS. Images taken during admission (A, D), at 3 months post discharge (B, E) and 1 year post discharge (C, F). Both patients received inpatient steroid therapy and were commenced on steroid therapy after the 3-month scan. Note improvement seen over time in both individuals.

4.6 Discussion

4.6.1 Summary of findings

My results show that persistent abnormalities post COVID-19 are common, even beyond 3 months post hospital discharge, with the commonest abnormalities being ground-glass opacification or radiological bands. Fibrosis was uncommon, with 12.3% affecting the first wave and 2.9 % of those admitted to hospital and 2.7% overall, in the second wave. Residual parenchymal abnormalities were associated with markers of acute disease severity (inflammatory markers and degree of respiratory support) in the first wave, but not the second. There was no association between patient-reported respiratory symptoms and the presence of radiological abnormalities. Lung function testing showed weak correlations with CT score in the second wave, reflecting a restrictive pattern, with the strongest correlation with TLCO. No significant relationship was found in the first wave. There were no significant differences in the prevalence of CT abnormalities between the two waves, despite the widespread use of inpatient steroid therapy during the second wave. In a small subset of individuals who had outpatient steroid therapy, there was no significant improvement in the extent of

radiological abnormalities over a 1-year period when compared to those for whom steroid therapy was not prescribed.

4.6.2 Findings in context of current literature

4.6.2.1 Persistent non-fibrotic radiological abnormalities

Persistent radiological abnormalities post COVID-19 have since been widely reported and my results are in accordance with published literature in which ground-glass abnormalities and radiological bands have been noted to be the commonest findings post COVID-19.[17,289–293] The underlying processes potentially contributing to these radiological features are important to understand, especially in the absence of histopathological evidence. Ground-glass opacities represent an area of air-space opacification and can occur in viral infections (acutely), be a feature of resolving lung injury or represent ongoing inflammation, such as in certain interstitial lung diseases.[105] Whilst an alarming percentage of patients recovering post COVID-19 have persistent abnormalities, in the absence of traction bronchiectasis and volume loss, this is likely to represent a process that is reversible.

Radiological bands were the second most common finding. In some studies, these findings have been thought to denote fibrosis,[289] although they could also represent parenchymal healing and recovery.[294,295] Regression with time, as observed in my results and published may suggest the latter.[296]

There is a paucity of literature evaluating histopathological evidence during the recovery period post COVID-19, but Ravaglia et al (2021) have shown, using transbronchial cryobiopsies in patients with persistent symptoms and radiological abnormalities affecting >5% of the parenchyma, that different patterns of lung injury can be seen three months post discharge, including fibrotic NSIP, organizing pneumonia, an overlap or OP/NSIP and diffuse alveolar damage.[297]

Histopathological evidence during the acute disease has shown features of diffuse alveolar damage and organizing pneumonia, with predominantly lymphocytic infiltration of parenchymal tissue.[294,298]

One could therefore postulate that if the radiological abnormalities noted during admission are inflammatory or in fact represent organizing pneumonia, a highly steroid-responsive condition,[299] inpatient steroid therapy may have reduced the prevalence of ground glass abnormalities in the second wave, by accelerating parenchymal recovery. This was not the case, however. One possibility

is that the treatment duration was inadequate, as the suggested duration from the RECOVERY trial was ten days, in contrast to the traditional, initial dosing regime of 3 months for treatment of organising pneumonia. [30,300]

4.6.2.2 Severity of disease

My findings of severity of acute disease being associated with radiological sequelae has been reported in other studies also. In particular, associations with duration of oxygen therapy, older age, and need for non-invasive or mechanical ventilation, longer length of stay, peripheral lymphopenia, higher CRP and D dimer during admission, extent of radiological involvement at admission and peak inflammatory response were associated with CT changes, including fibrotic changes at follow up.[247,293,301,302]

Older age was associated with abnormal radiology in my results, both during the first and second waves. Abnormal radiological findings were also associated with requirement for non-invasive/ mechanical ventilation and longer length of stay in the first wave, but this association was absent in the second wave. This disparity could be due to two reasons: Firstly, 62% of those undergoing CT imaging had required MV/PPV versus 29% in the second wave, so there might have been under-representation of those with more severe disease in the second wave. During the first wave, due to uncertainties about progression, there was a push towards early intubation and commencement of positive pressure ventilation to provide respiratory support. With the second wave, improvement in clinician confidence and experience might have resulted in changes in management approaches, especially after the mortality benefits shown with steroid treatment in the RECOVERY trial.[303] Furthermore, early initiation of steroid therapy during the second wave might have obviated need for PPV/MV and subsequent length of stay. Similarly, association with higher blood inflammatory markers (CRP, fibrinogen) and lower albumin (an acute phase reactant) and residual CT abnormalities was seen in the first wave. In the second wave, there was a trend towards a higher CRP, lower albumin and higher serum neutrophil-lymphocyte ratio at admission in those with abnormal CTs. The relevance of the differences in serum neutrophil:lymphocyte ratio, in the second wave, but not first, might be in part due to the effect of steroid therapy administered during the second wave, suppressing peripheral lymphocyte counts.[304]

4.6.2.3 Fibrosis

Fibrosis was relatively uncommon in my study compared to other reported literature. For instance, it was found in 12.3% of the first wave cohort and 2.7% of the second wave cohort. The reason for the disparity may be two-fold. Firstly, a variety of descriptors have been used to denote fibrosis. In my results from the first wave, the Thoracic radiologists defined fibrosis as volume loss +/- traction bronchiectasis, and with this definition nine individuals were identified. When using this criterion, no individuals were identified in the second wave. Other definitions that have been utilised in the literature include "fibrous bands," "reticulations" and "cord-like lesions". For instance, Van Gassel et al (2021) reported that 91% of patients in their study had fibrosis when reticulations were used to define fibrosis. Using a variety of descriptors is therefore likely to over-estimate the prevalence of fibrosis.[305]

However, in some individuals, fibrosis is a feature, as early as 3 months post hospital discharge. This cannot be assumed to be a direct consequence of the virus itself. Acute respiratory syndrome (ARDS) results in diffuse alveolar damage and a fibroproliferative phase is well-described in the healing process after ARDS.[110,111,306] In addition, mechanical ventilation can result in barotrauma-induced fibrosis. In fact, 8/9 of the individuals in with fibrosis in the first wave had required positive pressure ventilation during their admission stay. However, whilst an association exists, it is unlikely to be the sole reason as lung-protective ventilation strategies are widely used.

It is important, also, to distinguish between the different patterns of fibrosis. For instance, subpleural reticulations with honey-combing (a usual interstitial pneumonia [UIP]) pattern is characteristic of idiopathic pulmonary fibrosis.[115] The majority of the cohorts in both waves are middle-aged men, and therefore share risk factors for idiopathic pulmonary fibrosis.[307–309] In the second wave, the patients who had fibrosis had features of UIP or reticulations alone and in the absence of baseline images, it is possible that these patients had IPF or age-related reticular changes prior to their COVID-19 illness. However, viruses have also been in implicated in the pathogenesis of IPF.[310] Furthermore, SARS-COV2 affects alveolar epithelial cells, the primary site of pathogenesis in IPF, and increased transcription of genes associated with fibrosis has been seen in lung epithelial cells after SARS-COV2 infection. [108] However, SARS COV2 infection alone might not be sufficient to promote fibrosis.[311] Furthermore, hyperinflammation can result in fibrosis[312] and extant literature and my results suggest a more inflammatory phenotype during the acute phase may be associated with a higher prevalence of CT abnormalities at follow-up. Whilst the risk factors for developing fibrosis post SARS-COV2 may be

poorly understood, and likely to be multifactorial, the existence of fibrotic changes post COVID-19 has been confirmed histologically on lung cryobiopsies taken 3 months post COVID-19.[297]

4.6.2.4 Breathlessness

The lack of association with breathlessness and CT findings has been mirrored in other studies with severity of the acute illness not contributing to persistent symptomatology either.[247,303,313] Breathlessness post COVID-19 is a complicated issue, with multiple contributing factors, such as weight gain, deconditioning and dysfunctional breathing pattern disorder, all of which were seen in this cohort. The modified medical research council score was utilised in the first wave, but not in the second wave based on patient feedback that the scoring system did not capture the subtleties of their perceived symptoms.

4.6.2.5 Lung function abnormalities

A restrictive lung function, associated with CT scores was noted in my results, with the strongest correlation with TLCO. This is as expected given the degree of parenchymal involvement (which will affect the gas transfer for carbon monoxide) in these individuals at follow up and the likely nature of the underlying pathology. The lack of correlation of CT scores with lung function parameters in the first wave but might be an effect of a small sample size. Access to lung function testing was limited during the first wave, therefore only 38/73 individuals underwent lung function assessment. Restrictive lung function abnormalities have been shown in other studies also. For instance, Shah et al (2020) reported reduced gas transfer in 52% of their cohort, with abnormalities in total lung capacity (TLC) in nearly half of those with an abnormal gas transfer.[247] Furthermore, as with my results, CT scores were shown to be associated with a restrictive pattern of lung disease by Axelsson et al (2022), with a negative correlation with FVC and TLCO.[314]

4.6.2.6 Radiological trajectory with time

My findings showed regression of CT abnormalities at 1 year and no progression in fibrotic changes, in the small subset who had fibrosis. This is concert with other studies, which, again showed further improvement with time and up to 75% showing resolution[302] as well as a change in the pattern of parenchymal involvement at 1 year.[293,315–317] However, the extent of CT abnormalities was not related to time of imaging from discharge or admission suggesting that time isn't the only determinant of the rate of radiographic improvement.

4.6.3 Clinical relevance of findings

The clinical implications of these results are important to note. Firstly, CT abnormalities at follow up are common but regress with time, in the majority. Appropriate timing of imaging is therefore important to avoid exposing patients to unnecessary radiation. Patient-reported breathlessness is unlikely to be helpful in identifying patients who would benefit from CT imaging, but imaging patients with severe presentations during the acute illness might be useful, as acute disease severity is associated with radiological sequelae.

4.6.4 Limitations

There are limitations to note. Firstly, the absence of baseline imaging poses challenges in determining whether the abnormalities at follow up, in particular, fibrosis, is as a consequence of COVID-19. Secondly, there is a selection bias of those undergoing CT imaging at 1 year, as repeat imaging was performed based on clinical need. Thirdly, my cohort is limited by sample size and a larger cohort would be useful to corroborate these findings.

4.7 Conclusion

In this Chapter I have shown that radiological abnormalities post COVID-19 are common, with ground-glass opacification and radiological bands being the commonest findings at follow-up. Radiological abnormalities tend to regress with time and steroid therapy during admission does not affect the prevalence of CT abnormalities at follow up. Importantly, radiologically-evident fibrosis was only found in the minority.

Chapter 5 – Evaluating physiological recovery post COVID-19: Lung function and fractional exhaled nitric oxide

5.1 Introduction

As highlighted in Chapter 4, despite the high prevalence of CT abnormalities, there was no association between an abnormal CT and persistent breathlessness. A restrictive pattern of lung function abnormality was seen, especially in the second wave, presumably related to the parenchymal pathology. Literature after the SARS-COV1 pandemic describes significant abnormalities on lung function testing, which persisted up to 1 year post discharge.[81,82,318] It is therefore possible that similar problems may arise post COVID-19.

5.2 Background

At the time of commencement of my PhD, little was known about the physiological outcomes post COVID-19. Emerging evidence reported abnormalities in lung function at early follow-up,[247] but neither the trajectory of these findings nor clinical relevance were known. Lung function testing was difficult during the first wave due to hospitals being overwhelmed, therefore, lung function testing had to be reserved for patients will clear clinical indications. I noticed that some patients post COVID-19 during the first wave presented with features of airway hyper-responsiveness, for instance nocturnal cough and chest tightness, even 3-6 months post discharge, and in the absence of pre-existing airway disease. In some of these individuals, fractional exhaled nitric oxide (FENO) results were measured, which were often in the intermediate range (25-50 parts per billion). In a small number of individuals, a short trial of inhaled corticosteroids was beneficial, suggestive of possible steroid-responsive airway pathology. Viruses can cause airway hyperresponsiveness and obstructive airway disease, but whether this was likely to be a problem post COVID-19 was not known. I therefore sought to investigate this in greater detail.

5.3 Hypothesis and Aims

Hypothesis

Lung function abnormalities are present post COVID-19 and improve with time.

Aims

1. To assess the impact of COVID-19 on lung function parameters (spirometry, body plethysmography and gas transfer)
2. To assess the trajectory of lung function parameters over a 1-year period
3. To assess the prevalence and relevance of abnormal FENO post COVID-19

5.4 Methods

Patients recruited from both the first and second wave of the pandemic underwent formal lung function testing (spirometry, body plethysmography and gas transfer). As aforementioned, due to reduced service availability, lung function testing was reserved for those with a clear clinical need during the first wave. To systematically assess whether an airway phenotype may exist post COVID-19, all patients being followed up during the second wave of the pandemic underwent FENO testing in addition to the standard lung function.

Lung function and FENO testing were performed by Leeh Faustino and Isaac Mwita (experienced respiratory physiologists at Chelsea and Westminster Hospital, London). Lung function testing was performed and interpreted in accordance with the American Thoracic Society Guidelines.[319,320] FENO was measured using Niox Vero (Circassia, USA). Readings were taken at a standardized rate of 50ml/second and a constant exhalation rate was ensured using visual feedback provided by the device. Two readings were taken and an average calculated. The following categories were used to interpret the FENO results, as suggested by the American Thoracic Society guidelines: <25: normal; 25-50: Intermediate; >50 – high.[321]

All patient clinical visits and assessment of symptomology were performed by me. The clinical bronchoalveolar lavage fluid differential cell count analysis reported was calculated from cytospins by the Cellular pathology laboratory at Royal Brompton Hospital, London.

Data pertaining to the individual's admission (for instance, blood tests and maximal respiratory support) was obtained from electronic health records.

5.5 Results

5.5.1 Consort diagram

Figure 5.1 shows the number of individuals undergoing lung function testing during the first and second waves of the pandemic.

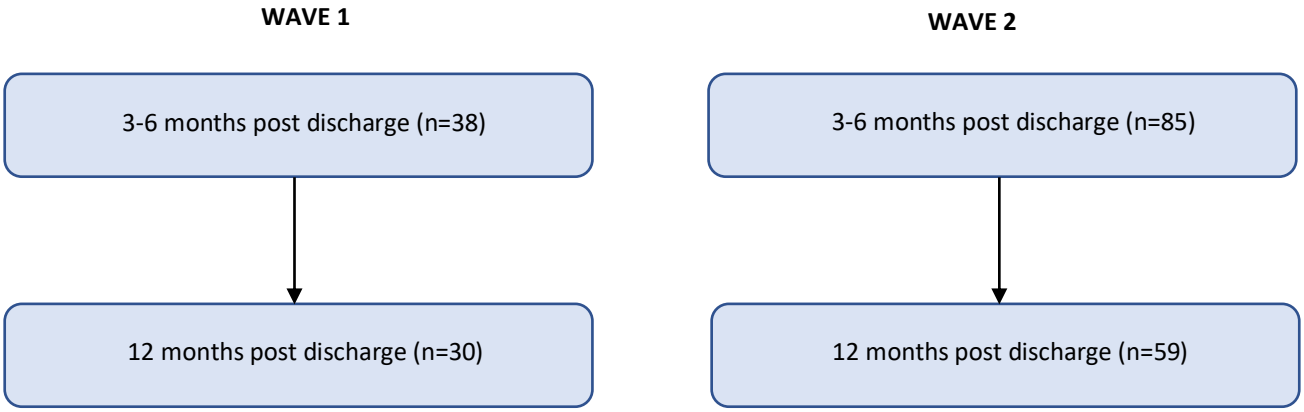


Figure 5. 1 Flow diagram of patients undergoing lung function testing

5.5.2 Baseline characteristics

The baseline characteristics of those undergoing physiological testing is shown in Table 5.1 and Table 5.2. In both waves, there was a male preponderance. The first wave had a much higher representation of individuals with severe disease presentations (i.e. those requiring mechanical ventilation or positive pressure ventilation), as compared to the second wave. Routine FENO testing was only performed in the second wave, with the majority of individuals tested having required oxygen therapy as the maximum degree of respiratory support during their admission.

Wave 1			
		3-6 months (n=38)	**12 months (n=30)**
Gender, M		28 (74)	22 (73)
Age, years		60 (+/-1.7)	60 (+/- 2.1)
Admitted		38 (100)	30 (100)
Length of hospital stay, days		8 (3.5 – 20)	9 (2.8 – 29)
Maximal Respiratory support	Mechanical ventilation	11 (29)	10 (33)
	Positive pressure ventilation	7 (47)	5 (17)
	Oxygen therapy only	20 (53)	15 (50)
	No Oxygen	0 (0)	0 (0)
Smoking status	Non-smokers*	26 (68)	20 (67)
	Ex-smoker**	12 (32)	10 (33)
	Current smoker	0 (0)	0 (0)
Respiratory co-morbidities	Asthma	4 (11)	4 (13)
	COPD	1 (2.6)	2 (6.7)
	Obstructive Sleep apnoea	1 (2.6)	0 (0)
	Nil	32 (84)	25 (83)
Cardiac comorbidities	Ischaemic heart disease	4 (11)	3 (10)
	Hypertension	13 (34)	10 (33)
	Nil	28 (74)	18 (60)
Type 2 diabetes mellitus		8 (21)	5 (17)
Wave 2			
		3 months (n=85)	**12 months (n=59)**
Gender, M		62 (73)	44 (75)
Age, years		56.4 (+/- 1.5)	59.6 +/- 1.5
Admitted		85 (100)	59 (100)
Length of hospital stay, days		6 (4 – 10)	7 (5 – 11)
Maximal Respiratory support	Mechanical ventilation	3 (3.5)	1 (1.7)
	Positive pressure ventilation	18 (21)	16 (27)
	Oxygen therapy only	61 (72)	41 (69)
	No Oxygen	3 (3.8)	1 (1.7)
Smoking status	Non-smokers*	68 (80)	45 (76)
	Ex-smoker**	14 (16)	13 (22)
	Current smoker	3 (3.5)	1 (1.7)
Respiratory co-morbidities	Asthma	7 (8.2)	5 (8.5)
	COPD	3 (3.8)	3 (5.1)
	Obstructive Sleep apnoea	3 (3.8)	2 (3.4)
	Nil	67 (79)	46 (78)
Cardiac comorbidities	Ischaemic heart disease	7 (8.2)	6 (10)
	Hypertension	19 (22)	14 (24)
	Nil	57 (67)	37 (63)
Type 2 diabetes mellitus		12 (14)	7 (12)

Table 5. 1 Clinical characteristics of patients undergoing PFTs (W1 and W2)

Data displayed as n (%n), mean (+/-SEM) or median (IQR). Abbreviations: M – male, COPD – chronic obstructive pulmonary disease, PFTs – pulmonary function tests. *Lifelong non-smoker or pack year <10 **Ex-smoker with pack year >=10

		3-months (n=79)	12 months (n=58)
Gender, M		58 (73)	44 (75.9)
Age, years		55.9 (+/-1.4)	59.3 (+/-1.5)
Admitted		79 (100)	58 (100)
Length of hospital stay, days		6.4 (4 – 10)	7 (4.8 – 11)
Maximal Respiratory support	Mechanical ventilation	3 (3.8)	0 (0)
	Positive pressure ventilation	18 (23)	16 (27.6)
	Oxygen therapy only	55 (69)	40 (69.0)
	No Oxygen	3 (3.8)	1 (1.7)
Smoking status	Non-smokers*	63 (81)	45 (77.6)
	Ex-smoker**	12 (15)	11 (19.0)
	Current smoker	3 (3.8)	2 (3.4)
Respiratory co-morbidities	Asthma	8 (10)	6 (10.3)
	COPD	2 (2.6)	2 (3.4)
	Obstructive Sleep apnoea	3 (3.8)	2 (3.4)
	Previous pneumothorax	1 (1.2)	1 (1.7)
	Previous tuberculosis	1 (1.2)	1 (1.7)
	Previous pulmonary embolism	1 (1.2)	0 (0)
Cardiac comorbidities	Ischaemic heart disease	7 (9.0)	6 (10.3)
	Hypertension	18 (23)	14 (24.1)
Type 2 diabetes mellitus		11 (14)	7 (12.1)

Table 5. 2 Clinical characteristics of patients undergoing FENO testing

All participants were recruited during the second wave. Data displayed as n (%n), mean (+/-SEM) or median (IQR). Abbreviations, M – male, COPD – chronic obstructive pulmonary disease. *Lifelong non-smoker or pack year <10 **Ex-smoker with pack year >=10

5.5.3 Lung function testing

5.5.3.1 – Detectable abnormalities on lung function testing

The commonest abnormalities found in both waves were in TLCO, FVC and TLC, as defined as a value <80% predicted. Overall, there was a lower prevalence of abnormalities at 1 year, compared to 3 months post discharge, suggesting resolving pathology (Table 5.3).

	Wave 1				Wave 2			
	3 months (n=38)		12 months (n=30)		3 months (n=85)		12 months (n=59)	
Lung function parameter	<80% predicted	<70% predicted	<80% predicted	<70% predicted	<80% predicted	<70% predicted	<80% predicted	<70% predicted
FEV1	3 (7.9)	2 (5.3)	1 (3.3)	1 (3.3)	17 (20)	5 (5.9)	7 (12)	4 (6.8)
FVC	7 (18)	1 (2.6)	2 (6.7)	0 (0)	22 (26)	8 (9.4)	9 (15)	3 (5.1)
TLC	5 (13)	1 (2.6)	0 (0)	0 (0)	10 (12)	4 (4.7)	8 (14)	3 (5.1)
TLCO	13 (34)	6 (16)	8 (27)	5 (17)	37 (44)	25 (29)	21 (36)	12 (20)
KCO	4 (11)	0 (0)	3 (10)	2 (6.7)	16 (19)	9 (11)	13 (22)	6 (10)

Table 5. 3 Abnormalities in PFTs

Percentage predicted values shown. Data displayed as n (%n)

Abbreviations: FEV1 – forced expiratory volume in 1 second, FVC – forced vital capacity, TLC – total lung capacity, TLCO - transfer factor of the lung for carbon monoxide, KCO – carbon monoxide transfer coefficient).

When evaluating measures of restrictive lung function, that is, low FVC, TLC and TLCO, 4/9 (44%) of individuals with abnormalities in these parameters in the first wave, had abnormalities in all three parameters. In the second wave, 8/42 (19%) had an overlap of abnormalities in all these parameters, 9/42 (21%) had abnormalities in both FVC and TLCO, and 20/52 (48%) had abnormalities in TLCO alone (Figure 5.2).

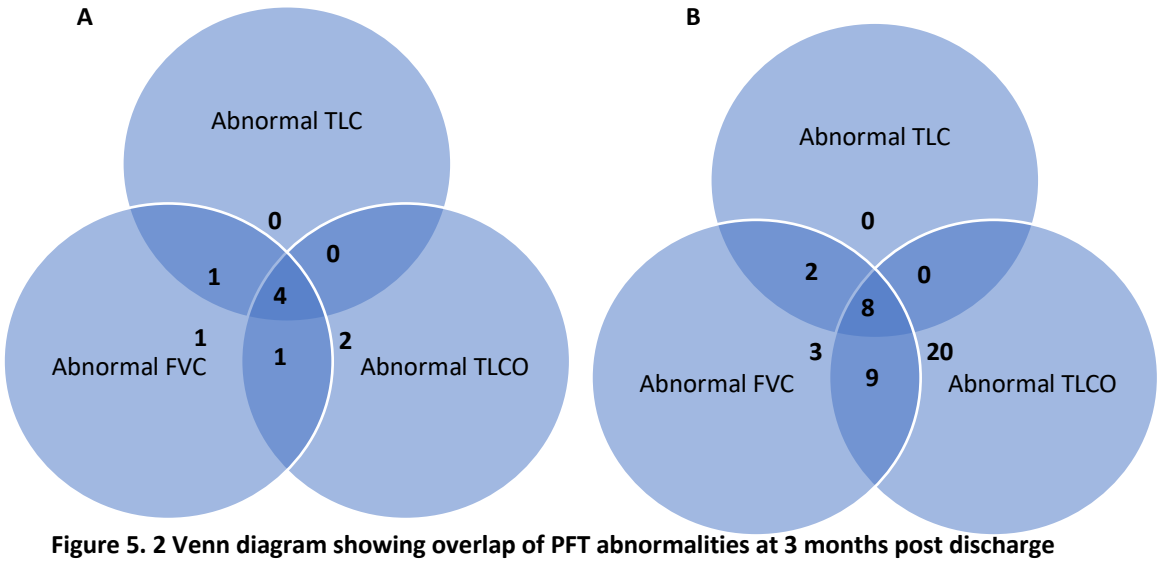


Figure 5. 2 Venn diagram showing overlap of PFT abnormalities at 3 months post discharge

Number of individuals with abnormalities (<80% predicted) in the listed lung function parameters (TLC, TLCO, FVC) in the first wave (A) and second wave (B).

Abnormal TLCO and markers of severity

I wanted to assess whether an abnormal TLCO at follow-up was associated with a more severe acute disease presentation, as defined by the need for ventilatory support or high inflammatory markers. However, there was no obvious association between need for higher levels of respiratory support during the inpatient stay (mechanical ventilation or positive pressure ventilation) and an abnormal TLCO. Similarly, there was no association between admission inflammatory markers and an abnormal TLCO at 3 months post discharge, in either wave. (Table 5.4)

	Wave 1			**Wave 2**		
	TLCO <80% predicted (n=13)	TLCO>=80% predicted (n=25)		TLCO <80% predicted (n=37)	TLCO>=80% predicted (n=47)	
Mechanical ventilation or NIV	9 (69)	9 (36)	OR 4.0 (CI 0.93 – 13.9), p=0.05	12 (32)	8 (17)	OR 2.3 (CI 0.80 – 6.8), p=0.10
Oxygen or less	4 (31)	16 (64)		25 (68)	39 (83)	
White cell count (x10^9/L) (4.2 – 10.6))	8.2 (6.5 – 12.7)	7.2 (5.9 – 8.5)	0.23	6.2 (4.8 – 8.3)	6.3 (4.7 – 7.7)	0.93
Neutrophils (x109/L) (2.1-7.1)	6.3 (4.9 – 10.7)	6.1 (4.2 – 6.7)	0.28	4.7 (3.4 – 6.5)	4.8 (3.3 – 6.6)	0.74
Lymphocytes (x10^9/L (1.1 – 3.6)	0.95 (0.53 – 1.4)	0.9 (0.7 – 1.4)	0.68	0.9 (0.6 – 1.1)	0.9 (0.8 – 1.2)	0.49
SNLR	7.3 (4.5 – 14.0)	7.1 (3.3 – 8.8)	0.36	5.3 (3.2 – 9.3)	5.2 (3.4 – 6.9)	0.47
Fibrinogen (g/L) (1.9-4.3)	7.3 (6.7 – 8.0)	7.6 (6.4 – 8.7) (n=18)	0.60	6.7 (5.8 – 7.3)	6.7 (5.8 – 7.3)	0.80
Ferritin (micrograms/L) (20 – 300)	2266 (513 – 5988) (n=9)	1115 (647 – 2138) (n=13)	0.79	854 (413 - 2005)	887 (622 - 1728)	0.67
D dimer (microgram/L) (<500)	2096 (818 – 7189) n=6	1251 (900 – 1671) (n=10)	0.37	942 (626 – 1912)	960 (714 – 1578)	0.97
Albumin (g/dL) (35 – 50)	32 (27 – 33)	33 (31 – 36)	0.34	33 (30 – 35)	34 (31 – 36)	0.27
C reactive protein (mg/L) (0 – 5)	162 (50.5 – 302)	113 (71 – 226)	0.59	99 (72 – 162)	111 (64 – 163)	0.81

Table 5. 4 Associations between % predicted TLCO at 3 months post discharge and markers of acute disease severity

Data displayed as n (%n), median (IQR). Inter-group comparisons made using Mann Whitney U testing or Chi-squared as appropriate. A p value <0.05 considered to be statistically significant. Abbreviations: SNLR – serum neutrophil:lymphocyte ratio, NIV – non-invasive ventilation. Units and reference ranges (in brackets) given for blood parameters.

5.5.3.2 – Relationship to breathlessness

I also wanted to assess what proportion of individuals with abnormal lung function parameters at follow-up, as defined by % predicted lung function parameters <80%, reported new breathlessness compared to their pre-COVID-19 baseline. In fact, a similar proportion were symptomatic irrespective of lung function abnormality in both waves. (Figures 5.3 – 5.4).

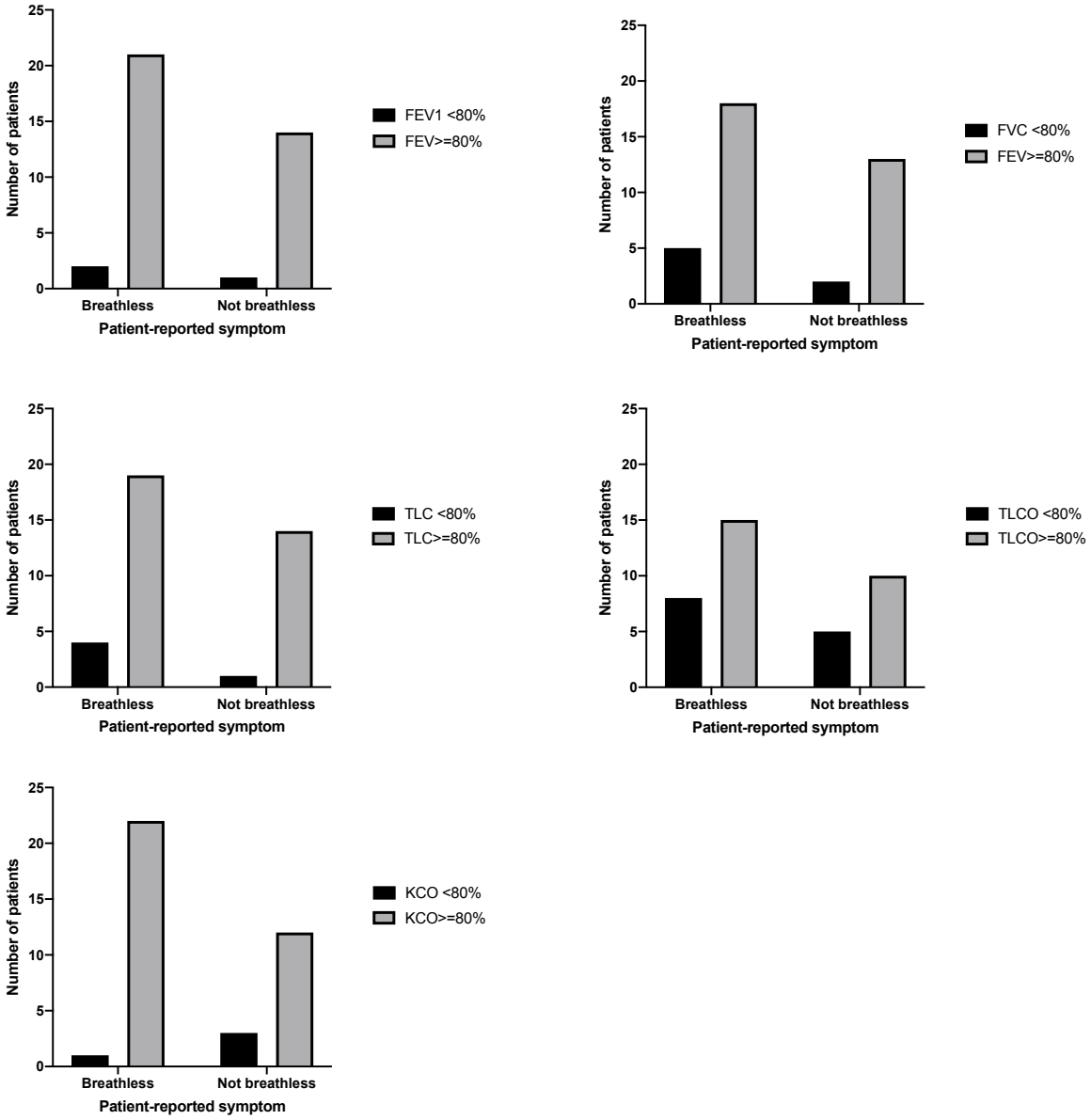


Figure 5. 3 Patient-reported breathlessness stratified according 3-month PFTs (W1)

Bar charts showing number of participants with abnormalities in lung function parameters (<80% predicted) reporting breathlessness at 3 months post hospital discharge

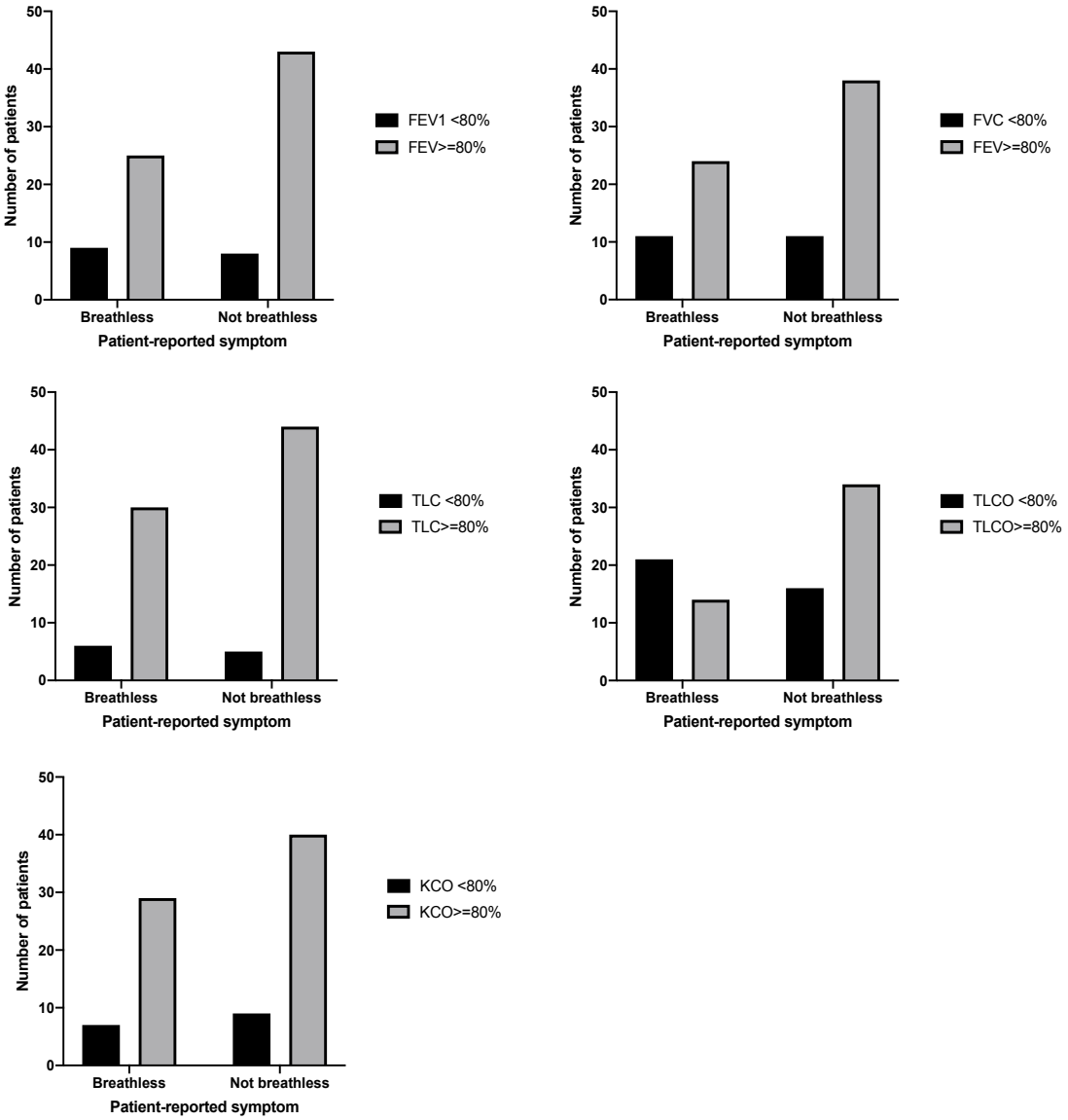


Figure 5. 4 Patient-reported breathlessness stratified according to 3-month PFTs (W2)

Bar charts showing number of participants with abnormalities in lung function parameters (<80% predicted) reporting breathlessness at 3 months post hospital discharge

5.5.3.3 – Long-term outcomes

I then wanted to assess whether, as seen with CT scores in Chapter 4, lung function abnormalities too improved with time. A non-significant change in lung function parameters (both absolute values and percentage predicted values) was seen between 3 months and 1 year during the first wave. In the second wave, however, there was a statistically significant improvement in all parameters except absolute value of FEV1, over the 1-year period (Figures 5.5 – 5.6).

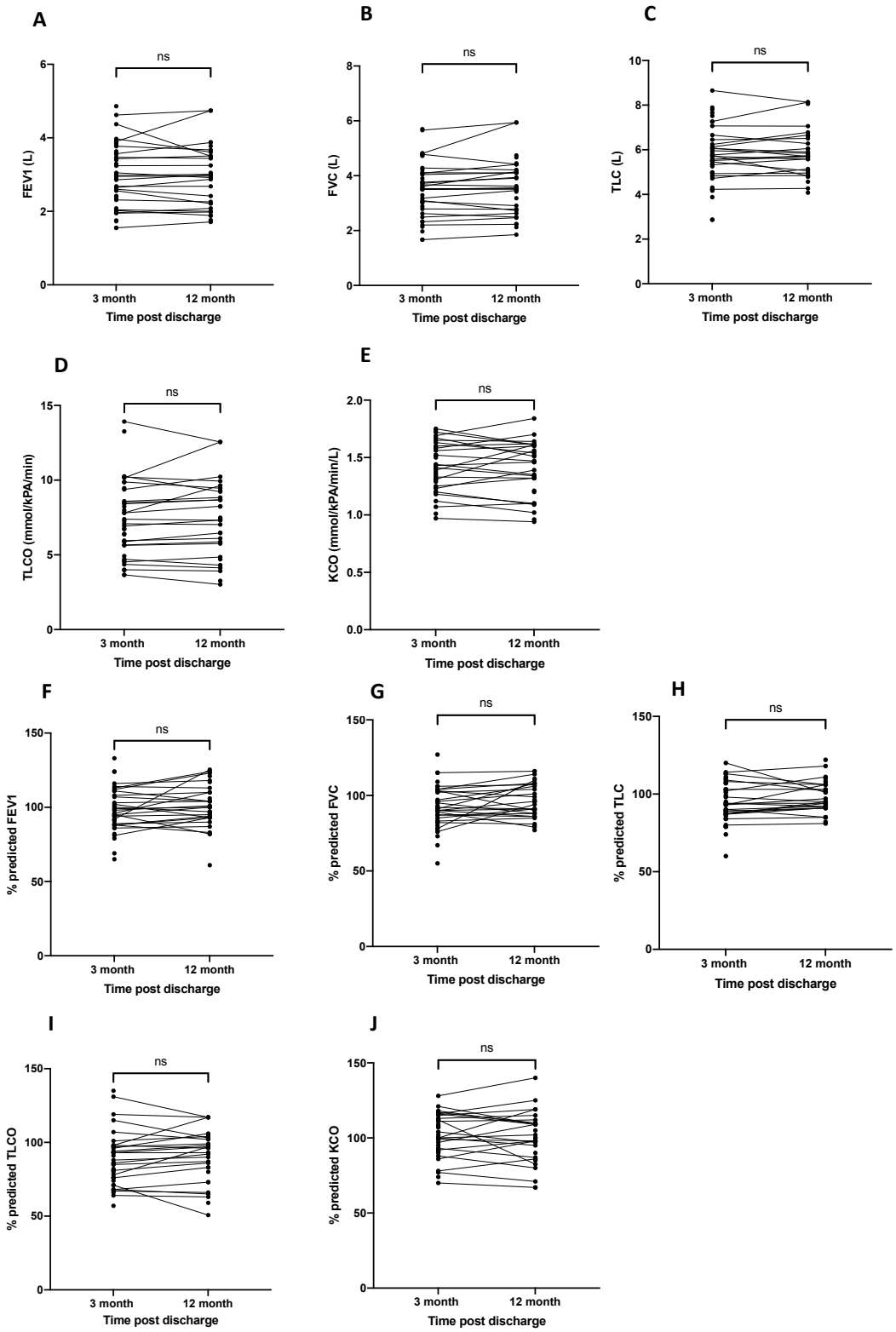


Figure 5. 5 Trajectory of PFTs over 1 year period (W1)

Absolute values (A-E) and % predicted values (F-J). Comparisons made using Wilcoxon-matched pairs signed rank test. P value < 0.05 considered statistically significant * p <0.05, ** p<0.01, *** p<0.001, **** p<0.0001

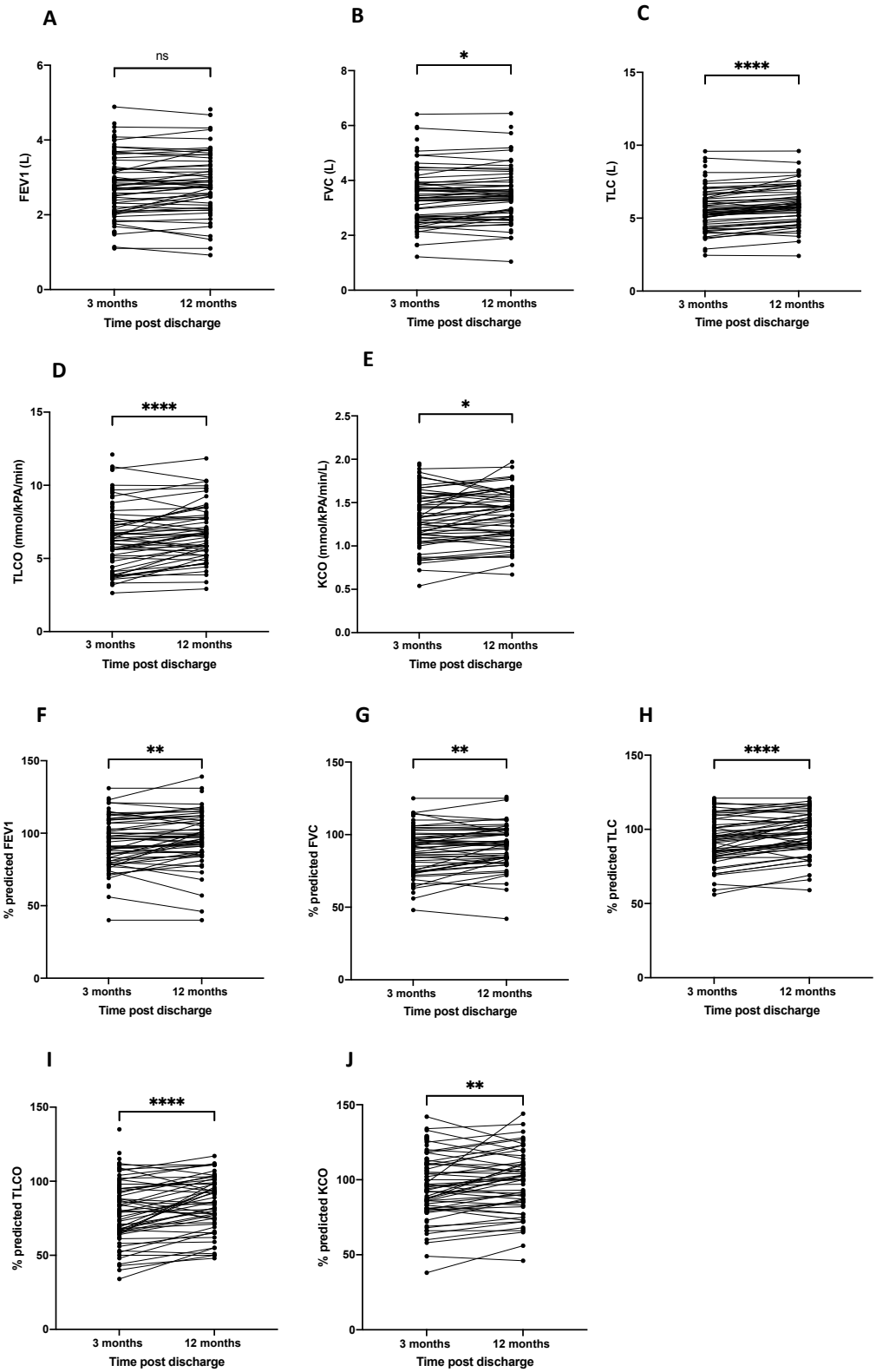


Figure 5. 6 Trajectory of PFTs over 1 year period (W2)

Absolute values (A-E) and % predicted values (F-J). Comparisons made using Wilcoxon-matched pairs signed rank test. P value < 0.05 considered statistically significant * p <0.05, ** p<0.01, *** p<0.001, **** p<0.0001

5.5.4 FENO

5.5.4.1 Distribution of FENO results

FENO results were evaluated in patients recruited during the second wave in order to assess whether abnormalities in this parameter was common post COVID-19 and what the trajectory of readings was over a 1-year period. Median FENO was 21 (IQR 16-29) at 3 months, compared to a median of 24.3 (IQR 18.4-35.1) 12 months post discharge. Only 2 of the participants with abnormal FENO had a diagnosis of asthma. 29/79 were abnormal (24/78 intermediate [30.4%] and 5/78 [6.3%] high) at 3 months post discharge. 28/58 (48.3%) at 1 year were abnormal: 24/58 (41.3%) within the intermediate range and 4/58 (6.9%) within the high categories. Figure 5.7 shows this in greater detail.

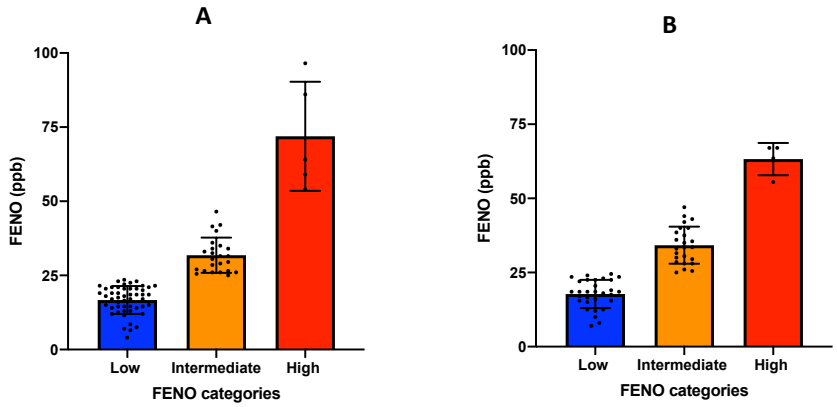


Figure 5. 7 FENO results at 3 and 12 months post discharge

Spread of FENO results at 3 months (A) and 12 months (B) post discharge. Individual values and median and IQR shown. Low FENO <25 parts per billion (ppb), Intermediate (25-50), High >50

5.5.4.2 Relationship with breathlessness

The majority of patients reporting breathlessness both at 3 months and 12 months, had a normal FENO result. Of those who were breathless at 3 months, only 10/32 (31%) had a FENO >=25; Meanwhile, 18/46 (39%) of those who were not breathless, also had a FENO>=25 (OR 0.71 [0.29 to 1.77, p=0.48]). Similarly, in individuals reporting breathlessness at 1 year, 10/22 (45%) had a FENO>=25, and 17/32 (53%) of individuals who were not breathless had a FENO >=25, OR 0.74 CI 0.24 to 2.2, p=0.58.

5.5.4.3 Relationship between FENO results and ventilation status

One postulate is that individuals with more severe acute disease presentations are more likely to have persistent small airways inflammation. 9/29 (31%) of those with FENO >=25 compared to 12/50 (24%) of those with a FENO <25 had required intubation or positive pressure ventilation. Chi-squared analysis revealed no significant difference between need for MV/PPV during the inpatient stay and FENO>=25 (OR 0.7 [0.27 – 1.92], p=0.50). Figure 5.8 shows the relatively frequency of individuals requiring varying levels of respiratory support divided according to FENO results.

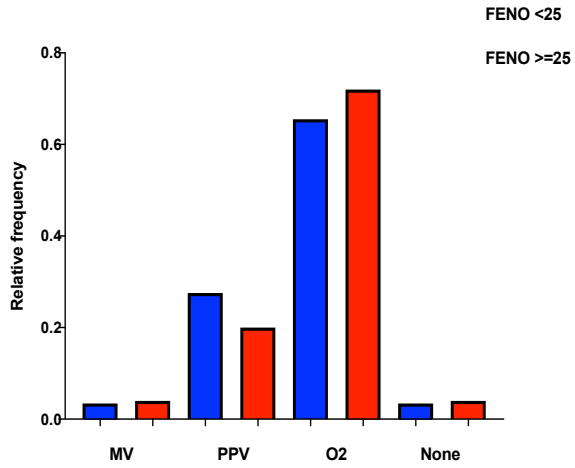


Figure 5. 8 FENO results and degree of respiratory support during admission

Bar chart showing relative frequency of abnormalities in FENO readings according to level of respiratory support required during the inpatient stay. Relative frequency calculated as per total cohort and represents the proportional representation of the cohort. Abbreviations: MV (mechanical ventilation), PPV (positive pressure ventilation), O2 (oxygen therapy)

5.5.4.4 Relationship between FENO and admission bloods

Tables 5.5 show the differences between admission bloods as stratified according to normal and abnormal FENO results. Statistically significant higher admission neutrophil counts (4.2 [IQR 3.3 – 5.4] vs 5.6 [IQR 3.4 – 6.9], p = 0.048) and fibrinogen (6.6 [5.8- 7.0] vs 6.96 [6.2-7.96], p =0.044) were found in patients with higher FENO results (>=25) at 3 months. This was not reflected in other inflammatory parameters, including white cell count, D dimer, lymphocyte count, ferritin or C-reactive protein. There were also no differences between admission inflammatory profile and 12-month FENO results.

	3 months			12 months		
	FENO <25	**FENO >=25**	**Intergroup difference (p value)**	**FENO <25**	**FENO>=25**	**Intergroup difference (P value)**
White cell count (x109/L) (4.2 – 10.6)	6.0 (4.7 – 7.1)	7.0 (4.9 – 8.5)	0.095	6.5 (4.85 – 8.5)	7.1 (4.4 – 8.2)	0.92
Haemaglobin (g/L) (130 – 160)	138 (134 – 147)	141 (131 – 151)	0.47	138 (131 – 146)	142 (133 – 152)	0.30
Platelets ($x10^9$/L) (130 – 370)	214 (168 – 261)	221 (181.3 – 256)	0.65	215 (177 – 274)	211 (145 – 261)	0.39
Neutrophils ($x10^9$/L) (2.1-7.1)	4.1 (3.3 – 5.4)	5.6 (3.4 – 6.9)	**0.048**	4.9 (3.6 – 6.9)	5.6 (3.3 – 6.8)	0.98
Lymphocytes ($x10^9$/L (1.1 – 3.6)	0.9 (0.8 – 1.2)	0.85 (0.6 – 1.1)	0.29	1.0 (0.7 – 1.1)	0.8 (0.6 – 1.0)	0.30
D dimer (microgram/L) (<500)	924 (687 – 1527)	1117 (710 – 1653)	0.55	930 (747 – 1621)	1117 (698 – 1617)	0.88
Fibrinogen (g/L) (1.9-4.3)	6.6 (5.8 – 7.0)	6.96 (6.2 – 7.96)	**0.044**	6.75 (6.04 – 7.20)	6.96 (6.15 – 7.38)	0.50
Ferritin (micrograms/L) (20 – 300)	670 (478 – 1530)	1255 (668 – 1873)	0.13	706 (477 – 1893)	1728 (833 – 2312)	0.06
Albumin (g/dL) (35 – 50)	34 (31.8 – 35.3)	33 (29 – 34)	0.068	33 (29 – 34.5)	33 (29.8 – 35)	0.68
C reactive protein (mg/L) (0 – 5)	98.3 (62 – 162)	115.6 (72.8 – 166.4)	0.298	115.4 (67.9 – 166.9)	117 (72.2 – 167.5)	0.68

Table 5. 5 Admission bloods and FENO results at 3- and 12-months post discharge

Differences between admission blood tests stratified according to FENO results at 3 months and 12 months. Median (IQR) shown. Intergroup comparisons performed using Mann Whitney U testing. A p value <0.05 considered statistically significant.

5.5.4.5 FENO results and admission neutrophil and lymphocyte counts

A high neutrophil and low lymphocyte count during the admission has been associated with more severe acute COVID-19.[26] I therefore wanted to assess whether a high neutrophil or low lymphocyte count on admission was associated with abnormalities in FENO.

Higher FENO results were found in patients with a serum neutrophil count of >7.1 x10^9/L (laboratory cut-off for abnormality) at 3 months, but not at 12 months. A serum lymphocyte count <1.0 x10^9/L on admission was associated with a higher FENO at 12 months, but not 3 months. A statistically significant, positive, but weak relationship between admission serum neutrophil count and FENO at 3 months post discharge was seen (r=0.29, p=0.01) but no similar relationships were found with 12-month FENO or admission lymphocyte counts. Figures 5.9 and 5.10 show this in greater detail.

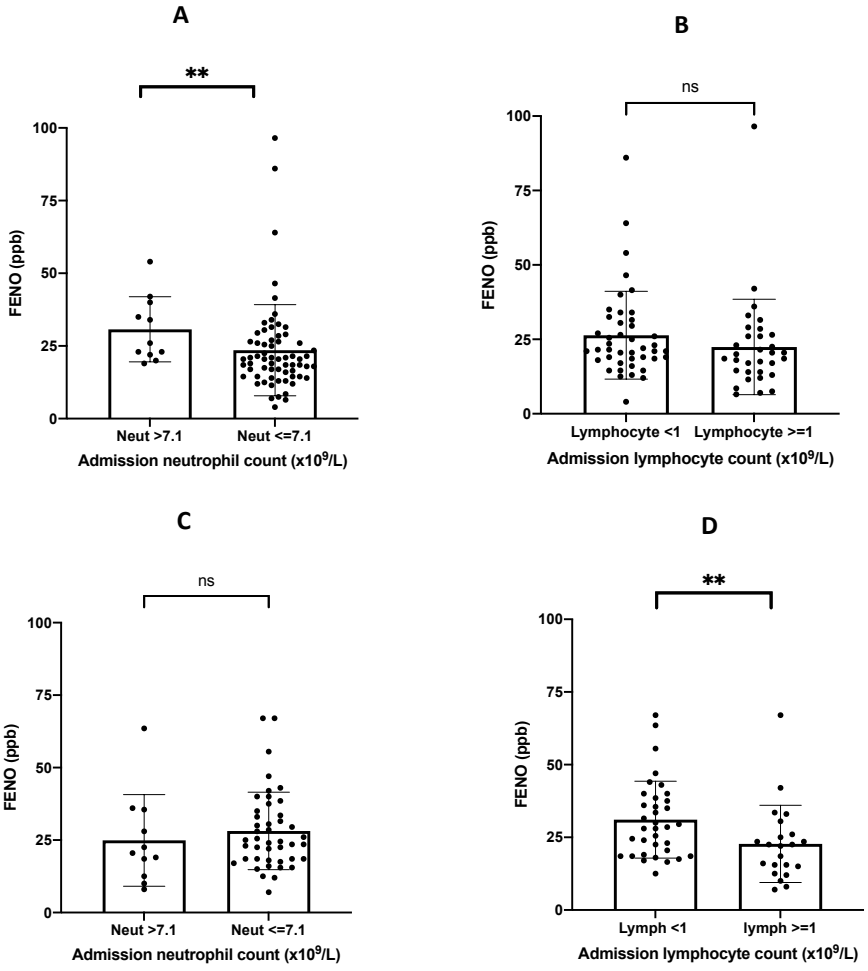


Figure 5. 9 FENO results according to admission peripheral neutrophil and lymphocyte count

Differences in FENO results at 3 months (A-B) and 1 year (C-D) as stratified according to admission neutrophil and lymphocyte counts. Median and IQR displayed. Inter-group comparisons performed using Mann Whitney U testing. P value <0.05 considered statistically significant. *p<0.05 **<0.01 ***<0.001

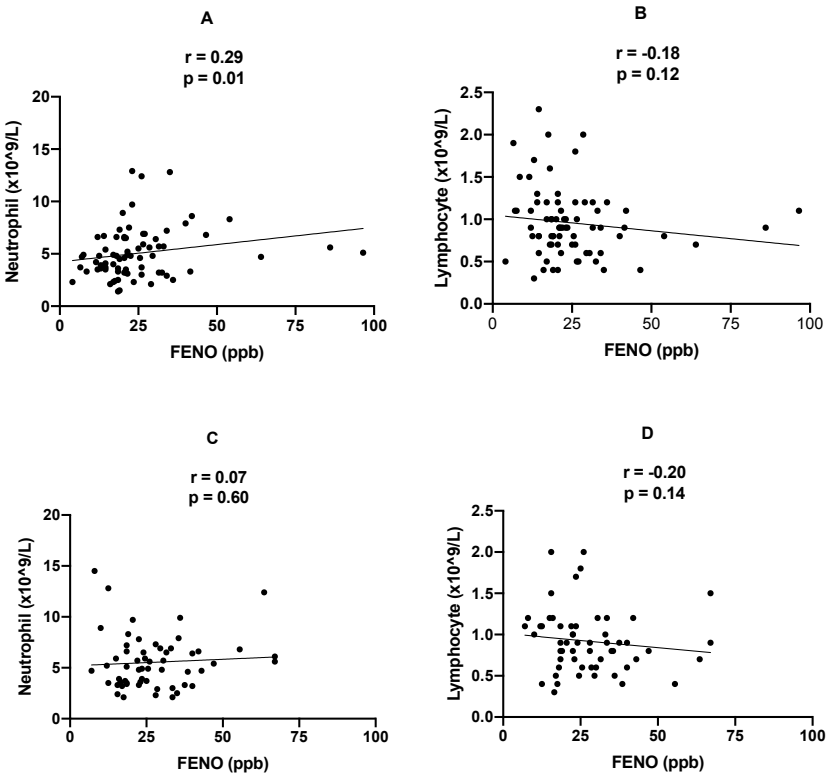


Figure 5. 10 Relationship between admission neutrophil and lymphocyte counts and FENO results

Spearman rank correlations between admission blood neutrophil and lymphocyte counts and FENO at 3 months (A-B) and FENO at 12 months (C-D) post discharge. P value <0.05 considered statistically significant

5.5.4.6 FENO and eosinophilic inflammation

FENO is a well-recognised marker of eosinophilic inflammation in asthma.[322] I therefore wanted to assess if individuals with an abnormal FENO had evidence of eosinophilia in their BALF. Only one individual (Case 2) had eosinophilia on differential cell count analysis of BALF (Table 5.6). Additionally, this was in the context of lymphocytosis and neutrophilia. Clinically, this individual was an ex-smoker, with a significant smoking pack year history and emphysema on CT imaging. There were no signs of atopy and no prior diagnosis of asthma. This individual had a persistently abnormal FENO, within the intermediate range, even at 1 year post discharge. Other abnormalities seen on differential cell count analysis, were lymphocytosis and neutrophilia. There was one individual with a high (>50ppb) FENO at 3 months post discharge, and 2 such individuals at 12 months post discharge. None of these individuals had eosinophilia on differential cell count analysis, and instead 2/3 had lymphocytosis (albeit mild, 15.7 and 14.7%).

		3 months						**12 months**			
Case	**FENO (ppb)**	**Mac (%)**	**Lymph (%)**	**Neut (%)**	**Eos (%)**	**Case**	**FENO (ppb)**	**Mac (%)**	**Lymph (%)**	**Neut (%)**	**Eos (%)**
1	35.0	97.3	2.7	0	0	2	33.5	67	23	5.7	4
2	29.0	67	23	5.7	4	3	63.5	92.7	7	0.3	0
3	26.0	92.7	7	0.3	0	4	44	82.7	15.7	0.33	1.33
4	58.5	82.7	15.7	0.33	1.33	5	40	78.1	8.3	11	2.7
5	31.5	78.1	8.3	11	2.7	6	33	94.7	3	0.67	1.67
6	26.5	94.7	3	0.67	1.67	8	36	91	3.7	2.3	3
7	26.5	90.3	9.3	0.3	0	9	67	83.7	14.7	1.3	0.3
						10	40	NP	NP	NP	NP
						11	42	93.3	4.67	2	0

Table 5. 6 BALF differential cell count analysis in patients with abnormal FENO

BALF differential cell count analysis in individuals with an abnormal FENO at 3 months and 12 months. FENO>25 deemed abnormal. Differential cell count analysis was performed on BALF obtained approximately 3 months post hospital discharge from the second wave. Abbreviations: Mac (macrophages), Lymph (lymphocytes), Neut (neutrophils), Eos (Eosinophils), NP (not performed). Abnormal values as per laboratory cut-offs highlighted in red

As FENO has been associated with peripheral eosinophilia,[323] I wanted to assess whether there was any association between peripheral eosinophilia (>=0.3 x10^9/L) in the past year and an abnormal FENO. However, such an association was not present, neither at 3 months, nor 12 months. However, at 3 months, a FENO>50 was associated with a raised peripheral eosinophil count (Figure 5.11), although it is important to note that this was a very small subgroup (n=5 at 3 months, n=4 at 12 months).

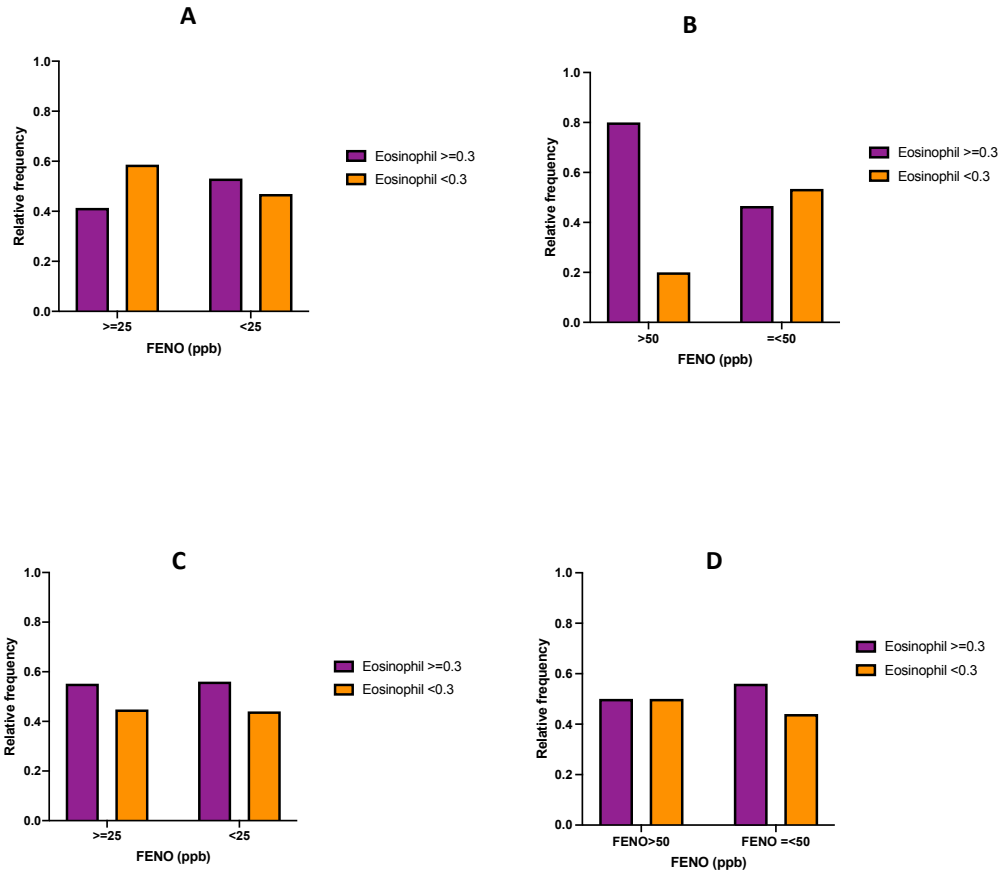


Figure 5. 11 Serum eosinophil count and FENO results

Bar charts showing relative frequency of individuals with abnormal FENO at 3 months (A-B) and 12 months (C-D) stratified according to eosinophil count (x 10^9/L)

5.5.4.7 FENO results and epithelial damage markers

Since FENO levels were not associated with BALF or peripheral eosinophilia, I wanted to assess if the nitric oxide was being released by the airway epithelium. In a small subset of individuals, BALF albumin

and LDH (markers of epithelial damage) were measured. Again, there was no association between an abnormal FENO and these epithelial damage markers or total cellularity of the lavage fluid (Figure 5.12).

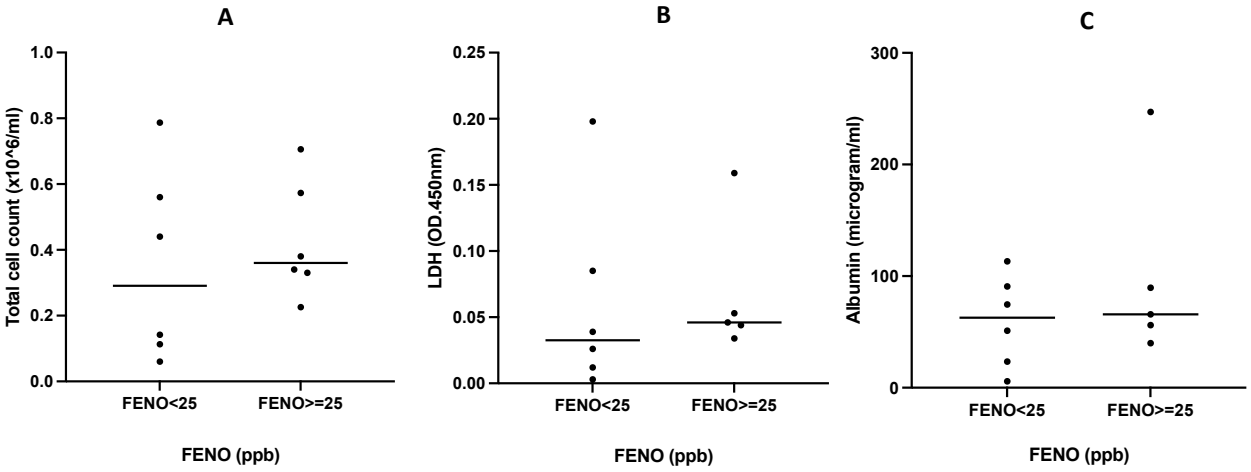


Figure 5. 12 BALF cellularity and damage markers in individuals with abnormal FENO

Scatter plots showing total BALF cell count (A) and markers of epithelial damage (B, C), displayed according to FENO levels at 3 months. Line drawn at median value displayed. LDH and albumin levels obtained through collaboration with Harker and Lloyd labs.

5.5.4.8 – Long term trajectory of FENO

As with CT and other lung function parameters, I assessed the trajectory of FENO results, without any intervention. In 33/52 (63%), FENO results did not change categories: 1/52 (1.9%) and 12/52 (23%) stayed in the high and intermediate categories, respectively. 7/52 (13.5%) showed improvement in their FENO results and 10/52 (19.2%) showed a deterioration, both defined as a change in category. 5 patients had normalization of their FENO results, despite one individual starting off with a FENO of >50. Figure 5.13 shows this in greater detail. Notably, these changes were in the absence of inhaled corticosteroid therapy.

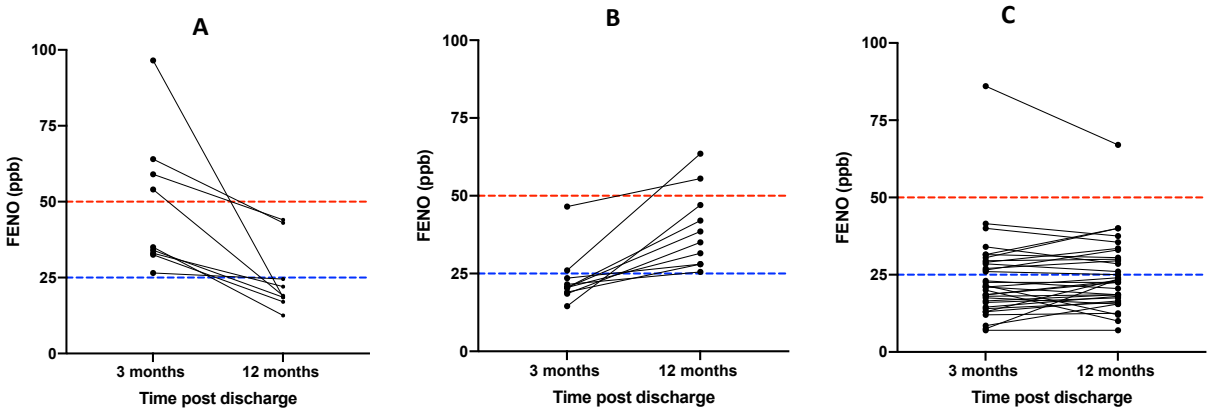


Figure 5. 13 Trajectory of FENO results over 12-month period

Improvement (A), deterioration (B) and stability (C) of FENO seen in patients. Blue and red lines show FENO category cut-offs: > 50 high, 25-50 intermediate, <25 low/normal

5.6 Discussion

5.6.1 Summary of findings

Lung function abnormalities post COVID-19 are common, with the commonest abnormality being a low % predicted TLCO. In the majority, lung function abnormalities improve with time, although persistent lung function abnormalities are present in some even at 1 year post discharge. There was no association between markers of disease severity during the acute admission and the presence of an abnormal TLCO at follow up.

Abnormalities in FENO are also common post COVID-19, the underlying aetiology for which is unclear. A higher serum neutrophil count at admission may be associated with higher FENO at 3 month follow

up. Importantly, there was no evidence of eosinophilic airway inflammation in the small subset who underwent endobronchial sampling. In this cohort, markers of epithelial damage (LDH and albumin) were not elevated. Peripheral eosinophilia was also not associated with an abnormal FENO (>=25 ppb) but might be associated with a FENO >50. The trajectory of FENO was variable, with some returning to normal levels and others deteriorating, both in the context of no additional medical management. There was no reliable association between patient-reported breathlessness and abnormal FENO levels at 3 or 12 months post hospital discharge.

5.6.2 Findings in the context of current literature

5.6.2.1 Lung function

The prevalence of lung function abnormalities and trajectory of improvement over a 1-year period is in concert with other published literature.[247,291,324,325] However, whilst my results did not show an association between the severity of the acute disease presentation and abnormalities in lung function, other studies have shown this to be the case. [291,326–328] The reason for this, may in part be due to small sample size or the arbitrary cut-off of 80% predicted I used.

5.6.2.2 FENO

FENO post COVID-19 was found not to be a useful biomarker by Maniscalco et al (2022), who reported similar FENO readings in post COVID-19 individuals as in healthy controls when evaluated within 2 months of the acute illness, with mean values within the normal range in both cohorts.[329] 19/68 (27.9%) in their cohort had a FENO >25, comparable to that found in my study of 29/79 (36.7%) when a cut-off of >=25 was used. Cameli et al (2021) found that although FENO measured at an exhalation rate of 50ml/s was similar in post COVID-19 patients compared to healthy controls, when measured at higher flow rates, FENO results were significantly higher post COVID-19, thus suggesting ongoing alveolar pathology, as at higher flow rates, the readings correspond to alveolar nitric oxide levels.[330] Additionally, Lindahl et al (2021) showed that 7/20 (35%) of patients post COVID-19 evaluated approximately 3-6 months post discharge had FENO levels within the intermediate range,[331] which is similar to my findings. Whilst I did not have healthy controls to compare my dataset with, the significant number of individuals in my cohort who had FENO abnormalities, in the absence any patient-reported atopic tendencies suggests that recent SARS-COV2 infection may be driving this.

Traditionally, FENO is associated with eosinophilic inflammation and correlates with sputum and BALF eosinophilia in both asthma and COPD.[322,323,332,333] It is therefore of interest, that in the small subset of patients with abnormal FENO who underwent endobronchial sampling, BALF eosinophilia was not seen in the majority. Differential cell count analysis can be prone to inaccuracies if not processed appropriately and in a timely manner.[334] Therefore, one possible explanation is that the differential cell count results were inaccurate and underreported eosinophilia. However, an alternative, plausible explanation is the underlying pathophysiological processes driving nitric oxide synthesis is different to that seen in asthma and not related to Type 2 inflammation.

The majority of nitric oxide produced in cells is through the conversion of L-arginine to citrulline by inducible nitric oxide synthase gene II (iNOS).[335,336] Expression of this gene can be upregulated directly by specific viruses, for instance, rhinovirus[337] or respiratory syncytial virus[338,339] and by pro-inflammatory cytokines produced during viral infection (for instance, tumour necrosis factor [TNF] alpha and interleukin-1 [IL-1]).[340] Nitric oxide can also be produced by immune cells attracted to the site of viral infection as part of the body's innate immunity, or directly by the injured epithelium.[145,336] It is possible that it is an immune-mediated process that is driving the nitric oxide synthesis. Whilst this is possible at 3 months post discharge, it is unlikely to be the cause at 12 months. To add validity to this, immune cell upregulation was seen post COVID-19 using flow cytometry (discussed in Chapter 7), and again, eosinophilia was not a feature.[341] The one individual who did have eosinophilia using a laboratory-based cut-off of >3% had concurrent lymphocytosis and neutrophilia, suggesting that the underlying process is unlikely to be solely Type 2 inflammation-driven, if at all.

An alternative theory is that the nitric oxide is originating from the damaged epithelium. However, there was no significant differences between BALF LDH and albumin when stratified according to FENO results. It is important to note, though, that the sample size is small and this result therefore needs to be interpreted with caution. Regardless, epithelial-derived NO as a source of NO would be a plausible reason for the elevated FENO results seen at 12 months.

At different exhalation flow rates, it is possible to differentiate between bronchial-derived and alveolar-derived nitric oxide.[342] FENO is closely correlated with bronchial-derived nitric oxide, therefore potentiating its use in the diagnosis and management of asthma. In contrast, alveolar nitric oxide has been associated with interstitial lung disease, with a role in monitoring disease progression.[343,344] SARS-COV2 causes significant diffuse alveolar injury and measurement of alveolar-derived nitric oxide would therefore have been useful.

5.6.3 Clinical relevance of findings

The general trend towards improvement in lung function findings over time is reassuring. However, the lack of association between patient-reported breathlessness and lung function abnormality makes it difficult to use patient-reported symptoms to assess need for lung function testing. This is also the case for FENO assessment. A restrictive pattern of lung function abnormality was most commonly seen which is likely being driven by parenchymal abnormalities (as suggested in Chapter 4).

The absence of eosinophilic inflammation needs further study. It does suggest, however, that clinicians should not assume that a raised FENO warrants treatment with inhaled corticosteroid therapy and a case-by-case approach should be adopted. Despite the absence of eosinophilic inflammation in the majority, there was evidence of lymphocytic or neutrophilic inflammation in some of these individuals, suggesting immune cell activity even 3-6 months post discharge. FENO is a marker of airway inflammation and it is possible that persistent, untreated airway inflammation could result in small airways disease. This will be further discussed in Chapter 6.

5.6.4 Limitations

There are some limitations to note. Firstly, due to COVID-19 restrictions, only a small number of individuals underwent lung function testing during the first wave. Secondly, follow up was based on clinical need and the majority of individuals undergoing repeat lung function testing, was in the context of CT abnormalities which were being followed up, resulting in a selection bias. Thirdly, FENO testing was performed at standard exhalation rates of 50ml/s. Evaluation at higher flow rates would have been useful to differentiate between nitric oxide produced from the alveolar and bronchial compartments. Fourthly, formal allergy testing was not performed, therefore it is not possible to ascertain if those with abnormal FENO were those with increased susceptibility to develop persistent airway inflammation post viral disease. Finally, the FENO results were all obtained from the second wave, so the findings cannot be generalised to other variants as variant and degree of local immunity provided by vaccination may result in less alveolar injury and more airway-centric disease.

5.7 Conclusion

In this Chapter, I have shown that lung function abnormalities can persist post COVID-19, with the commonest being an abnormal TLCO. Similar, to radiological changes described in Chapter 4, there is

a trend towards improvement with time. Abnormal FENO results are also seen, the underlying aetiology of which is not clear, but may not be associated with eosinophilic inflammation or epithelial damage.

Chapter 6 - Evaluating physiological recovery post COVID-19: Small airways disease

6.1 Introduction

The small airways refer to airways <2mm in diameter and are an important site of pathogenesis in obstructive lung disease.[227,345,346] In health, they contribute very little to airflow resistance but increased resistance in the small airways is a feature of obstructive airway disease. Viruses are a known trigger for the initiation and progression of small airways pathology.[133,347–349] Often, the small airways are the first site of pathogenesis in obstructive airway disease and significant disease burden is required prior to measurable changes in lung function. A variety of methods have been proposed to evaluate small airways pathology, including measurement of FENO, body plethysmography and impulse oscillometry.[227]

SARS-COV2 primarily affects the AT2 cells which are responsible for producing surfactant, a component important in reducing the collapsibility of airways during expiration.[350,351] Whilst there is evidence that AT2 cells do recover after SARS-COV2 infection, the timescale for recovery in vivo is not known.[80] It is therefore possible that some patients post COVID-19 will develop small airways disease, which may contribute to persistent respiratory symptomatology.

6.2 Background

6.2.1 Small airways disease post COVID-19

A small Finnish study evaluating small airways pathology post COVID-19 concluded that small airways disease was not detectable, when evaluated using impulse oscillometry at 3-6 months post hospital discharge.[331] On the contrary, CT-based evaluation of air trapping, a surrogate measure of small airways disease, has shown a higher proportion of the lung parenchyma to be involved in patients recovering post COVID-19 compared to healthy controls, irrespective of the severity of the acute illness. However, in the absence of baseline imaging, it is not possible to assign causality between SARS-COV2 infection and air-trapping.

From Chapters 4 and 5, it is clear that patient-reported breathlessness was not associated with CT findings, lung function abnormalities or FENO performed at 3-6 months post hospital discharge.

Furthermore, an abnormal FENO was seen in a large proportion of individuals, and if this represents ongoing airway inflammation, these individuals may be at higher risk of developing small airways disease in the long-term. Given the number of individuals potentially at risk of small airways disease, especially if severity of acute disease is not a risk factor for the development of small airways pathology, as suggested in the literature, we require a method of detecting and monitoring small airways disease that is simple, quick and cost-effective, so that it can be integrated easily into clinical practice.

A number of different devices for measuring small airways parameters exist, which differ in size and cost.[352] A challenge for interpretation of oscillometry data is that clear cut-offs for the detection of abnormalities are not stated in the literature. Furthermore, studies don't always specify if impulse oscillometry or forced oscillometry techniques were used. However, since there are significant differences in the values generated depending on the technique used, this is an important distinction to make and means results cannot be compared between devices.[233]

Small airways pathology had not been evaluated 1 year post hospital discharge at the time of data collection for this Chapter.

6.2.2 Forced oscillometry technique

The forced oscillation technique (FOT) is a non-invasive method to assess respiratory impedance by sending oscillatory signals into airways during tidal breathing and then assessing the pressure-flow relationship. The device utilised to collect measurements presented in this Chapter, Tremoflo C100 (Thorasys), has a vibrating mesh oscillator which generates frequencies between 5 – 37 Hz.[352]

Respiratory impedance consists of two components: Resistance (R) and Reactance (X). Resistance assesses the calibre of the respiratory tract, from the oropharynx and larynx down to the chest wall. The Tremoflo device assesses the resistance to different frequencies. Lower frequencies (5Hz) penetrate throughout the entire respiratory tract, down to the small airways, whereas higher frequencies (for instance, 20Hz) are absorbed proximally and therefore represent the resistance of the conducting airways. Therefore, by subtracting the resistance at 20 Hz (resistance of the conducting airways) from the resistance at 5 Hz (resistance of the entire respiratory tract), the resistance of the peripheral airways can be determined.[353] Reactance (X) is a composite of respiratory inertia and elastance (elastic recoil/ stiffness of the lung tissue). At low frequencies (for instance 5Hz), reactance is related to peripheral airway obstruction.[353]

Forced oscillometry is widely used in the research setting for the evaluation of small airways pathology. As such, it has been extensively utilized not only in asthma and COPD research, but also, in the evaluation of interstitial lung disease, where reactance values have been shown to correlate well with the degree of parenchymal abnormality. [231,353–355] FOT is also used in the clinical setting in some centres to evaluate patients with severe asthma.

Given that FENO, a measure of airway inflammation, was raised in my cohort (as reported in Chapter 5), I wanted to assess the prevalence of small airways disease (SAD) post COVID-19.

6.3 Hypothesis and Aims

Hypothesis

Patients post COVID-19 can develop small airways disease as detected using forced oscillometry technique.

Aims

1. To assess the prevalence of SAD at 1 year post discharge in patients with COVID-19 respiratory failure
2. To assess the association between SAD and patient-reported symptoms (breathlessness and cough)
3. To assess the association between SAD using FOT and lung function parameters

6.4 Methods

Patients who had been recruited to the PHENOTYPE study and already undergoing follow up at 1 year post discharge were identified and a subset recruited (n=44) to undergo further assessment with forced oscillometry testing between November 2021 and February 2022. Patients had been recruited to the PHENOTYPE study during the second wave of the pandemic, between October 2020 and February 2021. Patient underwent clinical assessment of symptomatology, lung function testing (spirometry, body plethysmography and FENO) and forced oscillometry testing. Lung function testing was performed by Chief Physiologists, Leeh Faustino and Isaac Mwati at Chelsea and Westminster

Hospital using the Love Medical Geratherm Respiratory system. FENO assessments were performed as outlined in Chapters 2 and 5. All FOT measurements and clinical assessments were performed by me.

Patients withheld their long-acting bronchodilator inhaled therapy (as appropriate), the night before the assessment was performed.

Age, height and weight of the patient were recorded on the day of FOT assessment.

The FOT device was calibrated using the manufacturer's calibration kit prior to the patient assessments being recorded. Patients were asked to sit upright in a chair, wore a noseclip and supported their cheeks to minimise air leak. Patients were then asked to make a firm seal with their lips around the mouthpiece and breathe at tidal volume. Patients were given adequate time to adjust to this process prior to recording the resistance and reactance values.

Quality control was performed using measures inbuilt into the Tremoflo software (artefact detection and measurement validation). Once 3 measurements that had passed measurement validation and with a coefficient of variance <=15% had been obtained, no further readings were taken. Patients usually performed the test approximately 3 -6 times to capture 3 valid measurements. An average of these 3 values was taken.

The following measurements were calculated by the Tremoflo software:

- Resistance at 5 Hz (R5), inspiratory resistance at 5 Hz (R5in), expiratory resistance at 5Hz (R5ex)
- Resistance at 20Hz (R20)
- Reactance at 5 Hz (X5), inspiratory reactance at 5Hz (X5in), expiratory reactance at 5Hz (X5ex)
- Area under the reactance curve (AX)
- Resonant frequency (Fres)

All readings were given in cmH20/s. These values were converted to kPA/L/s by dividing by 10.172. Resonant frequency values were generated in Hz and required no further adjustments.

A R5-R20 cut-off of >0.07 kPA/L/s was used to denote the presence of small airways disease.[152]

Patient cohort

44 patients were prospectively, consecutively enrolled to undergo small airways testing. Small airways testing was performed at a median of 371 days (IQR 359 – 382) post hospital discharge. Lung function and FENO assessment was performed within 9 days (IQR 4-15) of small airways testing. Clinical assessment of symptoms and general wellbeing was performed at 368 days (IQR 360 – 373) days after hospital discharge.

Subsequent analysis was performed on the full cohort (n=44) and after exclusion of patients with other possible risk factors for small airways disease, the amended cohort (n=34, n=10 excluded). Throughout this Chapter, I will refer to these as the "full cohort" and "amended cohort."

6.5 Results

6.5.1 Consort diagram

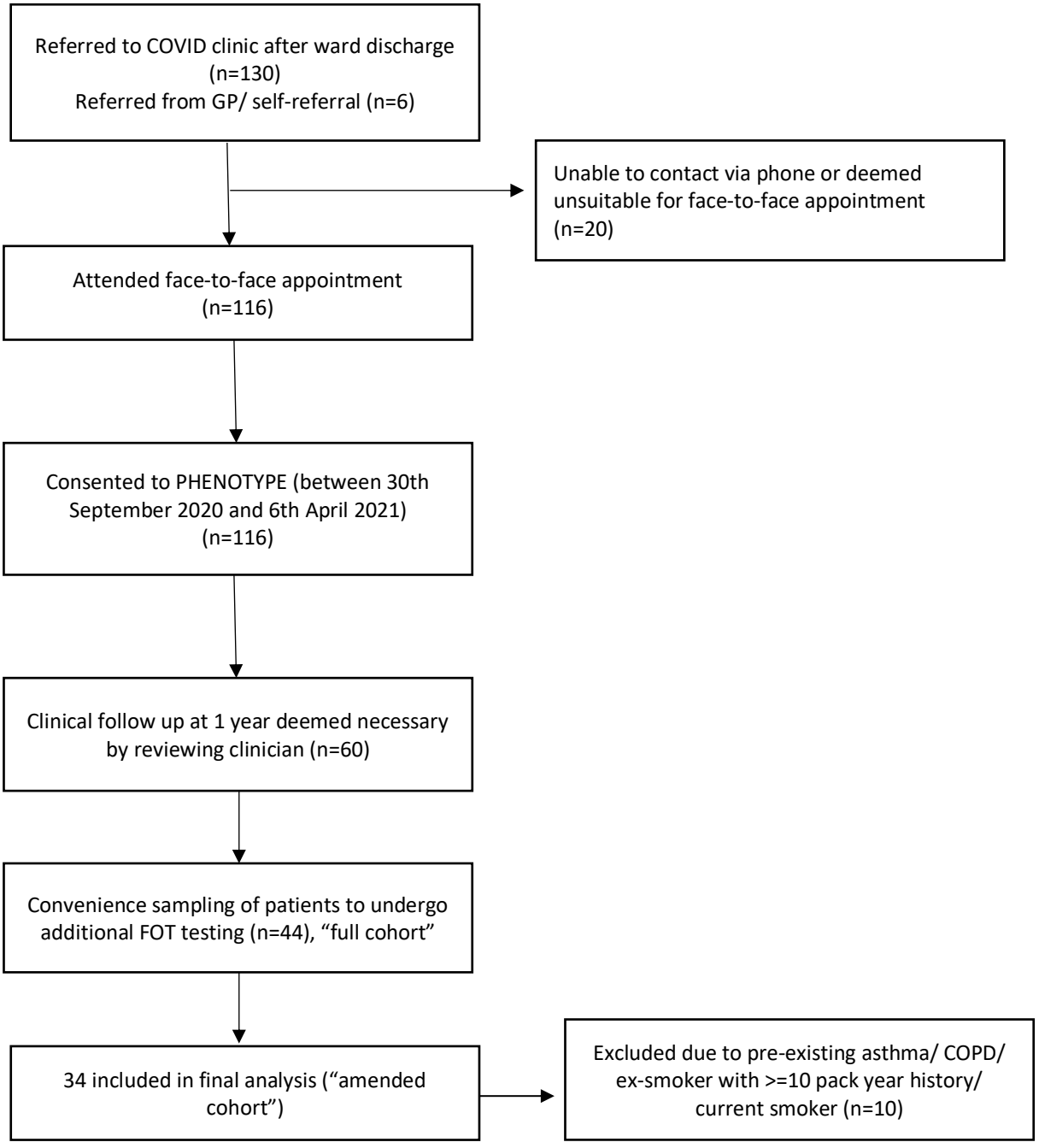


Figure 6. 1 Consort diagram of patients undergoing FOT assessment

6.5.2 Baseline demographics

Amended cohort			
	SAD (n=6)	**No SAD (n=28)**	**P value**
Age, years (IQR)	57.2 (+/- 6.0)	60.2 (+/- 2.0)	0.65
Gender, M (%)	4 (67)	21 (75)	0.67 OR 0.67 (CI 0.12 – 4.15)
BMI, kg/m2 (IQR)	28.7 (25.5 – 32.7)	29.5 (26.8 – 33.5)	0.64
Admitted to hospital, n (%)	6 (100)	28 (100)	
Oxygen as maximal supportive therapy during admission	4 (67)	19 (68)	
NIV or CPAP as maximal supportive therapy during admission	2 (33)	9 (32)	
Mechanical ventilation as maximal supportive therapy during admission	0 (0)	0 (0)	
LOS in hospital, days (IQR)	5 (2.8-12.5)	9 (6-11.8)	0.32
Full cohort			
	SAD (n=11)	**No SAD (n=33)**	**P value**
Age	62 (51-72)	59.0 (50.5-69.5)	0.67
Gender	7 (64)	25 (76)	0.43 [OR 0.56 CI 0.15-2.1]
BMI (kg/m2)	29.2 (27.5-31.9)	28.7 (26.8 – 33.4)	0.87
Pre-existing asthma*	2 (27)	1 (3)	0.08 [OR 7.1 CI 0.72-105]
COPD	0 (0)	1 (3)	0.56 [OR 0 CI 0.0 - 27.0]
Current smoker or ex-smoker (>=10 pack year)	4 (36.3)	4 (12.1)	0.07 [OR 4.14 CI 0.97-16.1]
Oxygen as maximal	9 (82)	23 (70)	0.43 (OR 2.0 CI 0.42 – 10.2)
NIV or CPAP during admission	2 (27)	10 (30)	0.43 [OR 0.51 CI 0.10-2.38]
Mechanical ventilation during admission	0 (0)	0 (0)	
LOS in hospital (days)	5 (3-12)	7 (5-11.5)	0.27

Table 6. 1 Demographics and admission data of patients undergoing FOT

All numbers displayed as n (%n). Median and interquartile ranges given where appropriate. Inter-group comparisons performed using Mann Whitney U test or Chi squared as appropriate. OR (odds ratio) and 95% confidence interval stated. Statistical significance denotes a $p<0.05$.

*2 patients were on inhaled corticosteroids for presumed asthma: One had a 25-pack year smoking history (ex-smoker). Abbreviations: BMI (body mass index), LOS (length of stay), FEV1 (forced expiratory volume in 1 second), FVC (forced vital capacity), TLC (total lung capacity), TLCO (transfer factor of the lung for carbon monoxide), KCO (Carbon monoxide transfer coefficient), FENO (fractional exhaled nitric oxide), ppb (parts per billion), RV (residual volume), MEF (maximal expiratory flow). R5 or R20 = resistance at 5 or 20 Hz; R5ex = resistance at 5 Hz during expiration; R5in = resistance at 5 Hz during inspiration; R5-R20, fall in resistance from 5Hz to 20Hz

X5 = reactance at 5 Hz; X5ex = reactance at 5 Hz during expiration; X5in = reactance at 5 Hz during inspiration. Ax, area of low-frequency reactance, Fres, resonant frequency

6.5.3 Prevalence of small airways disease

11/44 (25%) of the full cohort and 6/34 (17.6%) of the amended cohort, had SAD using the aforementioned cut-off. The groups (SAD vs no SAD) were otherwise similar, in terms of age, gender (with a male preponderance in both groups), BMI and length of hospital stay. From Table 6.1, it is clear that patients with asthma and those who are current smokers or have an extensive smoking packyear history contributed to a higher proportion of individuals with SAD. On the contrary, there was an equal number of patients with COPD who had SAD vs no SAD. All patients had had COVID-19 respiratory failure as evidenced by the need for respiratory support during the admission, but none had required mechanical ventilation. A similar proportion had required oxygen therapy or non-invasive ventilation in each group.

Based on the above results, the decision was made to do two sets of analyses (full and amended cohort). I analysed the full cohort as well as the amended cohort as a) the n number drops by nearly 25% after exclusion b) not all patients with pre-existing airway disease have small airways involvement according to the FOT data.

6.5.4 Validating the cut-off used for selecting patients with SAD

As aforementioned, I used the cut-off of R5-R20>0.07 kPa/L/s to identify the presence of small airways disease. This is the cut-off used by Crissauli et al in-COPD research.[152] Figure 6.2 (amended cohort) and Table 6.2 (full cohort), show the difference in resistance and reactance values between those

identified as having SAD and those without this. The results are as would be expected and help validate the cut-off utilised.

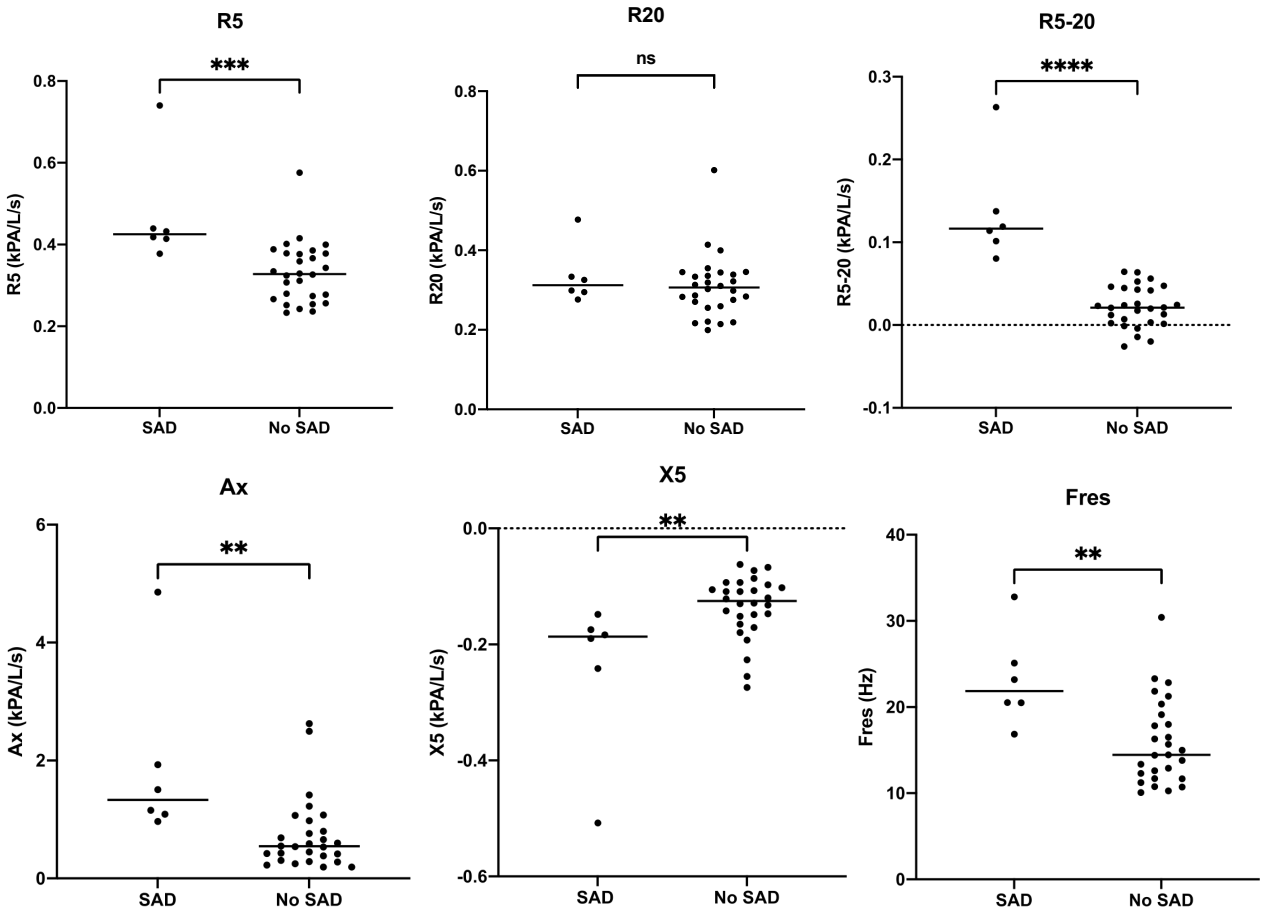


Figure 6. 2 Resistance and reactance values of amended cohort

Line drawn at median value. Abbreviations: R5 – resistance at 5Hz, R20 – resistance at 20 Hz, R5-20 – fall in resistance between 5 and 20 Hz, Ax – area under the reactance curve, X5 - reactance at 5Hz, Fres – resonant frequency. Inter-group comparisons made using Mann Whitney U test. P value <0.05 deemed statistically significant. *= <0.05, ** = p<0.01, ***= p<0.001, *** = p<0.0001

	SAD (n=11)	No SAD (n=33)	P value
R5 (kPA/L/s)	0.43 (0.38-0.57)	0.33 (0.27-0.38)	<0.0001
R20 (kPA/L/s)	0.33 (0.29-0.45)	0.30 (0.26-0.34)	0.16
R5-20 (kPA/L/s)	0.11 (0.08-0.19)	0.02 (0.003-0.04)	<0.0001
X5 (kPA/L/s)	-0.19 (-0.32- -0.15)	-0.13 (-0.16 - -0.10)	0.0006
Ax (kPA/L/s)	1.51 (1.0 – 2.43)	0.54 (0.34-0.88)	<0.0001
*F*Res (Hz)	23.2 (20.5 – 25.1)	14.4 (11.7-18.8)	0.0001

Table 6. 2 Resistance and reactance values of the full cohort

Small airways parameters in the full cohort, divided according to the presence or absence of SAD. Median and interquartile ranges shown. Abbreviations: R5 – resistance at 5Hz, R20 – resistance at 20 Hz, R5-20 – fall in resistance between 5 and 20 Hz, Ax – area under the reactance curve, X5 - reactance at 5Hz, Fres – resonant frequency. Comparisons made using Mann Whitney U testing. P<0.05 deemed statistically significant.

6.5.5 SAD and lung function tests

As not all clinical centres will have access to FOT, I wanted to assess whether abnormalities were present on lung function testing in those with small airways disease. There were no significant differences between lung function parameters in those identified as having SAD versus those without, in the amended cohort (Figure 6.3) or full cohort (Table 6.3).

In particular, there were no differences in the spirometric indices (FEV1 or FVC) or body plethysmography data associated with small airways disease (RV, TLC, RV/TLC) between the groups. However, when assessing lung function parameters associated with small airways function (MEF25-75 or sRawtot/sGawtot), these were significantly higher in the small airways disease group, as expected.

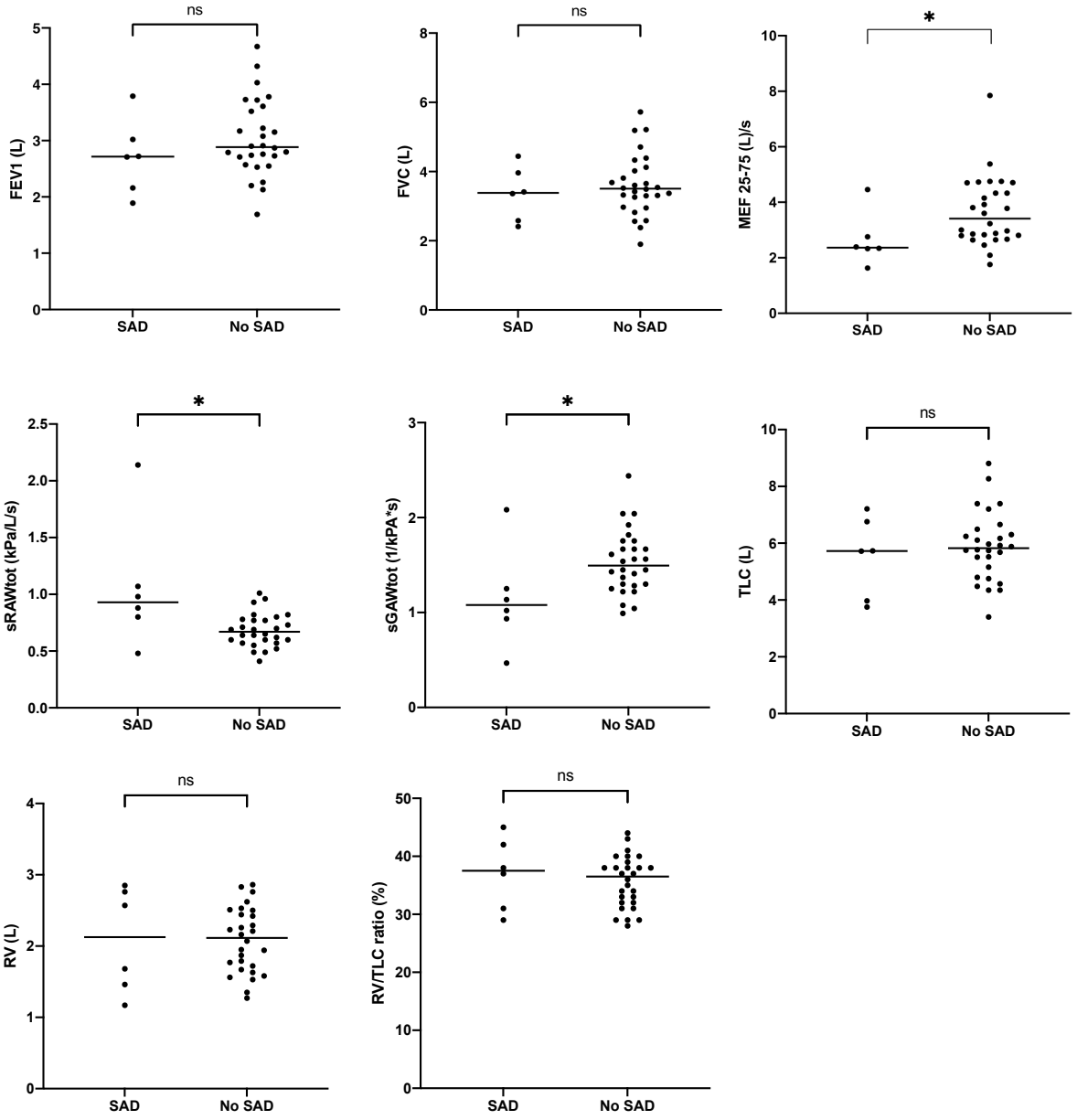


Figure 6. 3 Differences in PFTs in those with SAD vs no SAD (Amended cohort)

Line drawn at median. Comparisons made using Mann Whitney U testing. P value <0.05 deemed statistically significant: * <0.05, ** p<0.01, ***p<0.001, *** p<0.0001

Abbreviations: FEV1 – forced expiratory flow in 1 second, FVC – forced vital capacity, MEF 25 – 75 – mid-expiratory flow at 25-75% of FVC, sRawtot – specific total airway resistance, sGawtot – specific total airway conductance, TLC – total lung capacity, RV – residual volume

	SAD (n=11)	No SAD (n=33)	P value
FEV1(L)	2.7 (2.2-3.8)	2.9 (2.6-3.6)	0.38
% predicted FEV1	95 (87-112)	97 (88-105)	0.82
FVC (L)	3.4 (2.6-4.4)	3.5 (2.9-4.2)	0.69
% predicted FVC	98 (84-106)	92 (84-98)	0.27
TLC (L)	5.7 (4.6-7.3)	5.8 (5.0-6.6)	0.97
% predicted TLC	100 (91-113)	93 (89-105)	0.27
TLCO (mmol/kPa/min)	6.9 (5.9-8.2)	6.7 (5.4-8.4)	0.70
% predicted TLCO	93 (80-102)	92 (74-99)	0.43
KCO (mmol/kPa/min/L)	1.4 (1.1-1.6)	1.5 (1.2-1.6)	0.61
% predicted KCO	103 (85-116)	100 (88-113)	0.94
RV (L)	2.6 (1.6-2.9)	2.2 (1.7-2.5)	0.39
% predicted RV	126 (90-138)	106 (98-126)	0.43
RV/TLC	37 (34-45)	37 (33-40)	0.48
MEF 25-75	2.4 (1.8-3.8)	3.0 (2.6-4.3)	0.10
% predicted MEF 25-75	108 (87-144)	126 (99-165)	0.34
sRAWtot (kPA/L/s)	0.93 (0.75-1.03) [n=10]	0.69 (0.60-0.82)	**0.03**
sGAWtot (1/ kPa*sec)	1.08 (1.0 – 1.35) [n=10]	1.45 (1.22– 1.67)	**0.03**

Table 6. 3 Differences in PFTs in those with SAD vs no SAD (Full cohort)

Inter-group comparisons made using Mann Whitney U test. Abbreviations: FEV1 – forced expiratory flow in 1 second, FVC – forced vital capacity, MEF 25 – 75 – mid-expiratory flow at 25-75% of FVC, TLCO – transfer capacity of the lung for the uptake of carbon monoxide, KCO – carbon monoxide transfer coefficient, sRAWtot – specific total airway resistance, sGawtot – specific total airway conductance, TLC – total lung capacity, RV – residual volume., SAD – small airways disease. P<0.05 deemed statistically significant.

6.5.6 SAD and FENO

There was no association between FENO results, neither at 3 months post discharge, nor 12 months post discharge, and the presence of small airways disease (Figure 6.4).

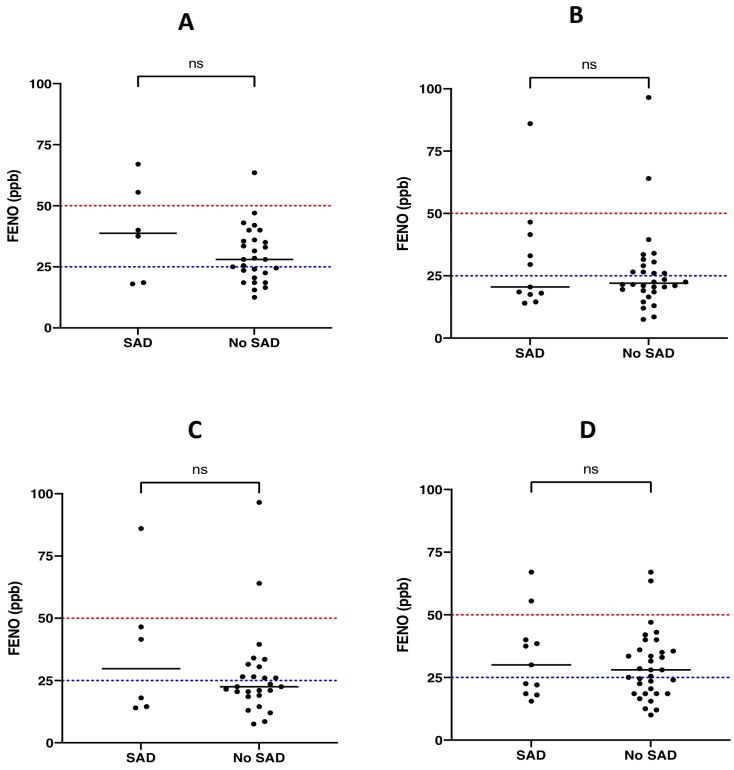


Figure 6. 4 Differences in FENO in those with SAD vs no SAD

A-B show FENO results at 3 months, C-D FENO results at 12 months. Full cohort shown in B, D and amended cohort in A, C. Comparisons made using Mann Whitney U testing. P<0.05 deemed statistically significant Abbreviations: FENO – fractional exhaled nitric oxide, ppb – parts per billion, SAD – small airways disease.

6.5.7 SAD and patient-reported symptoms

6.5.7.1 Patient-reported breathlessness

There were no significant differences between patient-reported breathlessness and small airways parameters, neither in the amended (Figure 6.5) nor full cohort (Figure 6.6). However, there was a trend towards a higher R5, Fres and Ax in individuals reporting breathlessness.

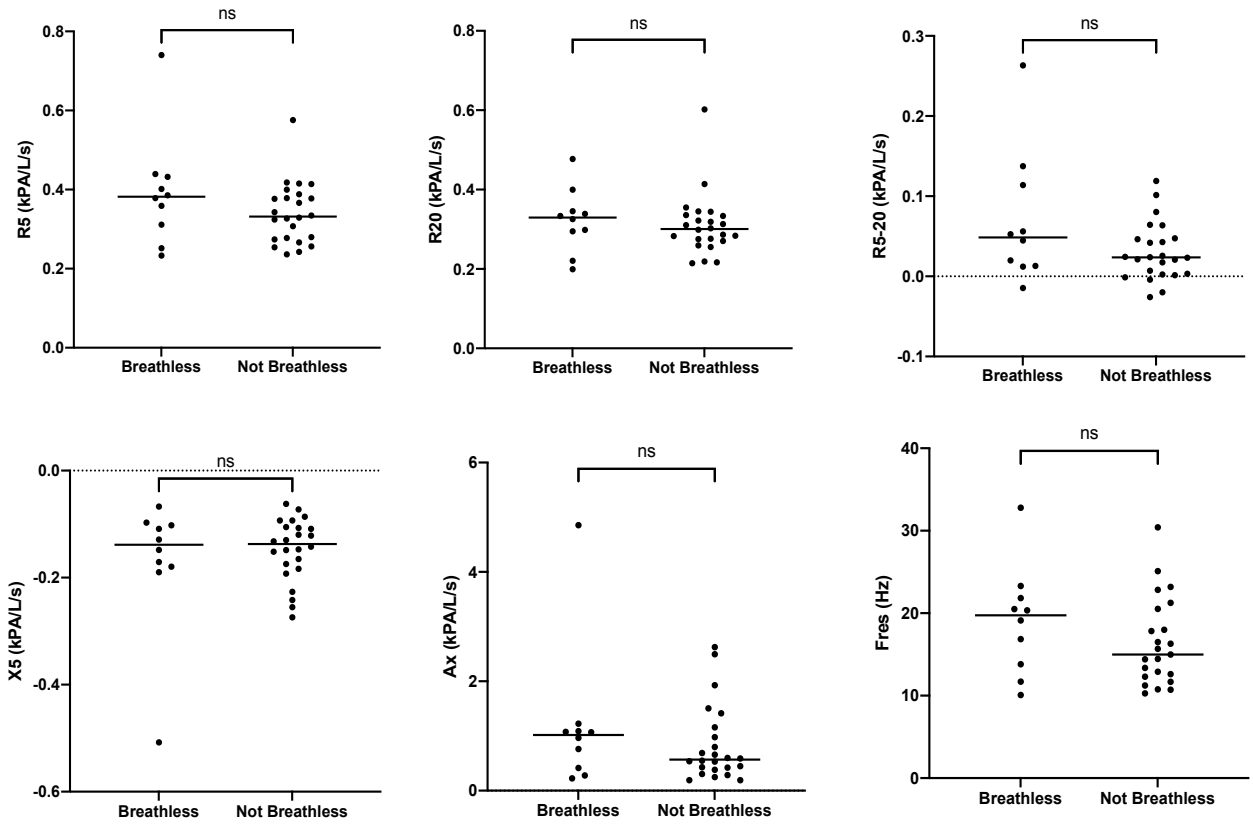


Figure 6. 5 Resistance and reactance values according to patient-reported breathlessness (Amended cohort)

Inter-group comparisons made using Mann Whitney U testing. p value <0.05 considered statistically significant. Abbreviations: R5 – resistance at 5Hz, R20 – resistance at 20 Hz, R5-20 – fall in resistance between 5 and 20 Hz, Ax – area under the reactance curve, X5 - reactance at 5Hz, Fres – resonant frequency.

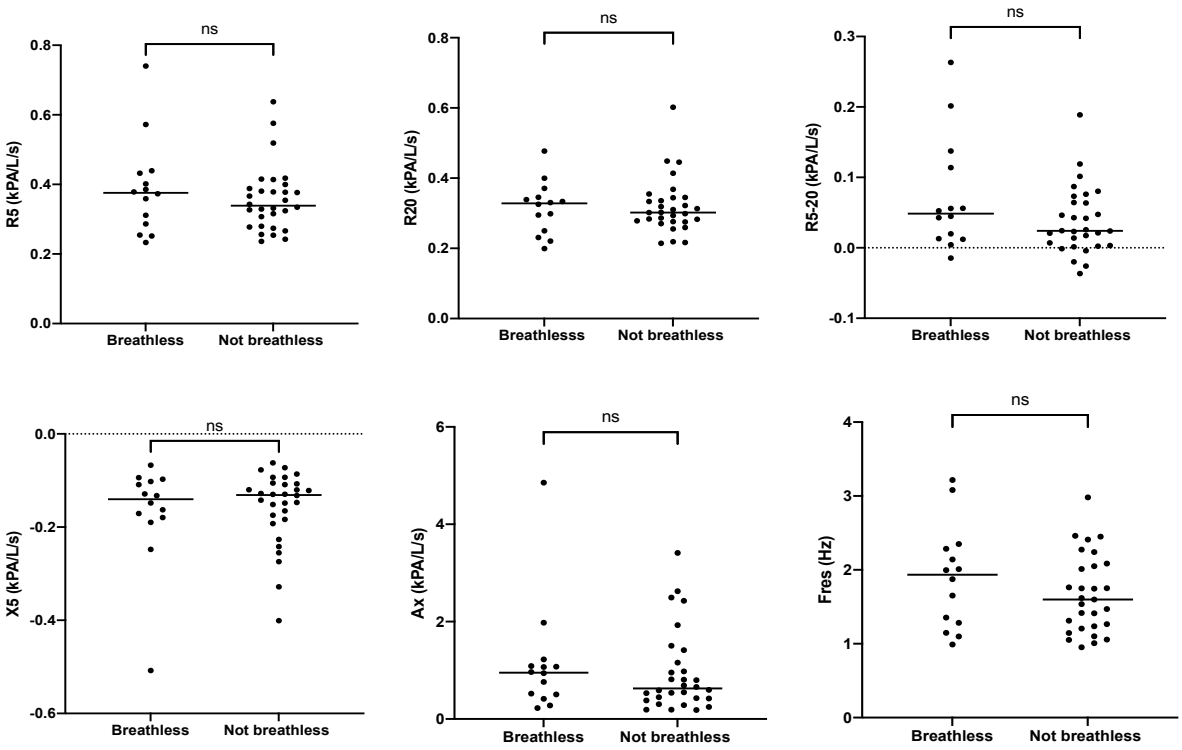


Figure 6. 6 Resistance and reactance values according to patient-reported breathlessness (Full cohort)

Inter-group comparisons made using Mann Whitney U testing. p value <0.05 considered statistically significant. Abbreviations: R5 – resistance at 5Hz, R20 – resistance at 20 Hz, R5-20 – fall in resistance between 5 and 20 Hz, Ax – area under the reactance curve, X5 - reactance at 5Hz, Fres – resonant frequency.

6.5.5.7 Patient-reported cough

There was no statistically significant difference in resistance or reactance values in patients reporting cough at 1 year, neither in the amended cohort nor full cohort. There was, however, a trend towards a greater fall in resistance between 5 and 20 Hz (R5-R20), a more negative reactance (X5), a higher area under the reactance curve and resonant frequency in those reporting cough at 1 year (Figures 6.7 and 6.8).

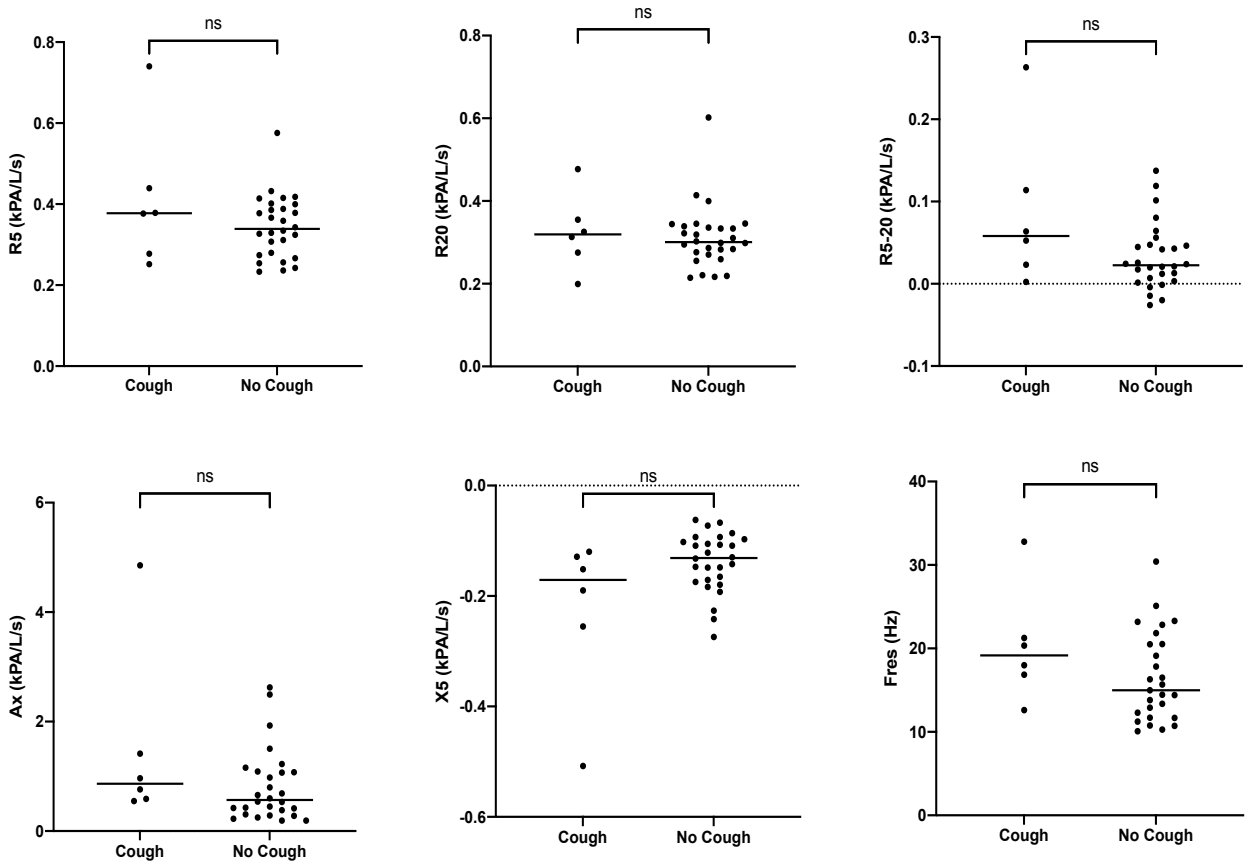


Figure 6. 7 Resistance and reactance values according to patient-reported cough (Amended cohort)

Inter-group comparisons made using Mann Whitney U testing. p value <0.05 considered statistically significant. Abbreviations: R5 – resistance at 5Hz, R20 – resistance at 20 Hz, R5-20 – fall in resistance between 5 and 20 Hz, Ax – area under the reactance curve, X5 - reactance at 5Hz, Fres – resonant frequency.

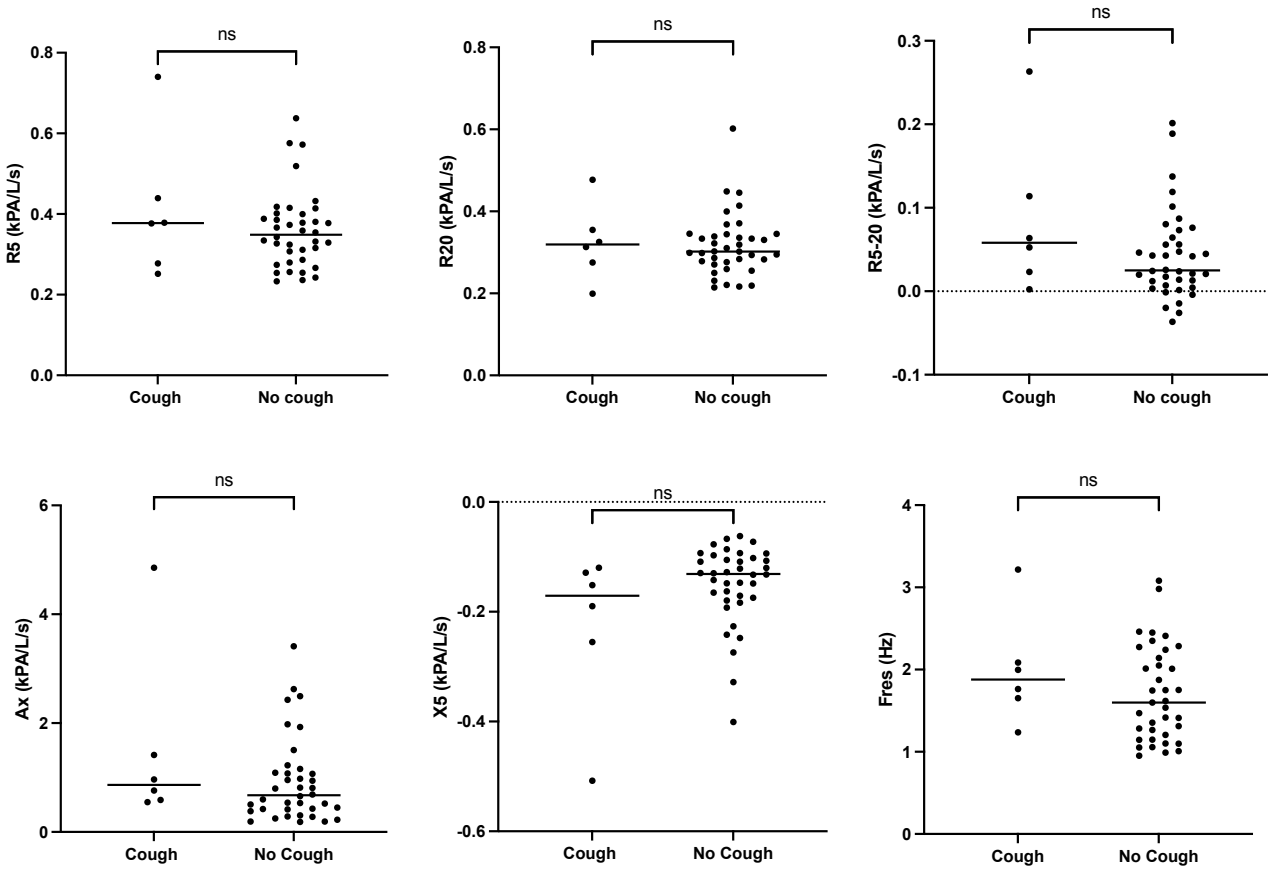


Figure 6. 8 Resistance and reactance values according to patient-reported cough (Full cohort)

Inter-group comparisons made using Mann Whitney U testing. p value <0.05 considered statistically significant. Abbreviations: R5 – resistance at 5Hz, R20 – resistance at 20 Hz, R5-20 – fall in resistance between 5 and 20 Hz, Ax – area under the reactance curve, X5 - reactance at 5Hz, Fres – resonant frequency.

6.5.8 Expiratory flow limitation

No individuals had expiratory flow limitation in the amended cohort. However, in the full cohort, two individuals had a change in X5>0.28kPA/L/s. One patient was a known asthmatic, on inhaled corticosteroids, with a 25-pack year smoking history (Case 1) and the other, was an ex – smoker with a 40-pack year history (Case 2). Both individuals had abnormal RV/TLC ratios: 50% and 54%, respectively.

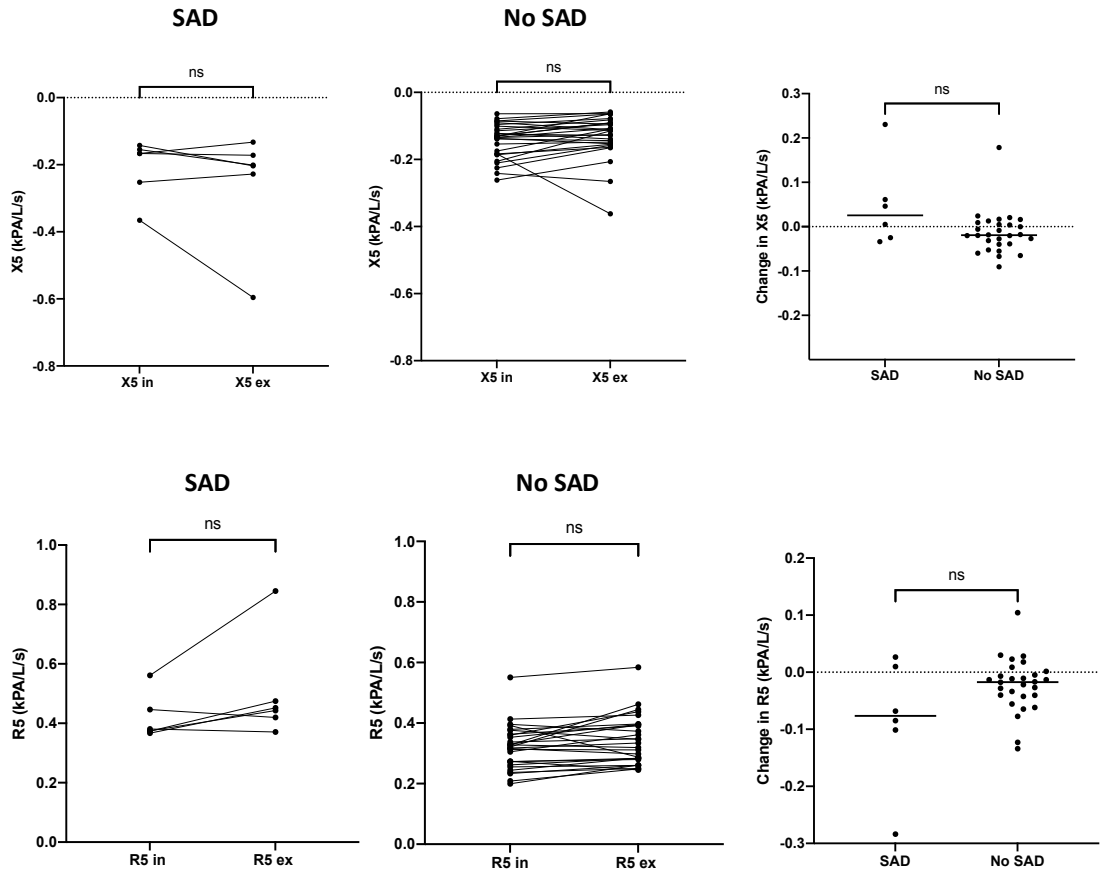


Figure 6. 9 Expiratory flow limitation in those with SAD vs no SAD

Inter-group comparisons made using Mann Whitney U testing. p value <0.05 considered statistically significant. Abbreviations: R5 – resistance at 5Hz, R5 in – inspiratory resistance at 5Hz, R5ex – expiratory resistance at 5Hz, X5 - reactance at 5Hz, X5in – inspiratory reactance at 5Hz, X5ex – expiratory reactance at 5Hz.

6.5.9 SAD and CT findings

Whilst some radiological abnormalities were detectable on CT imaging in patients with SAD, these findings were subtle and regressed with time. No individuals had features of fibrosis or interstitial lung disease on their CT scans (Figure 6.10).

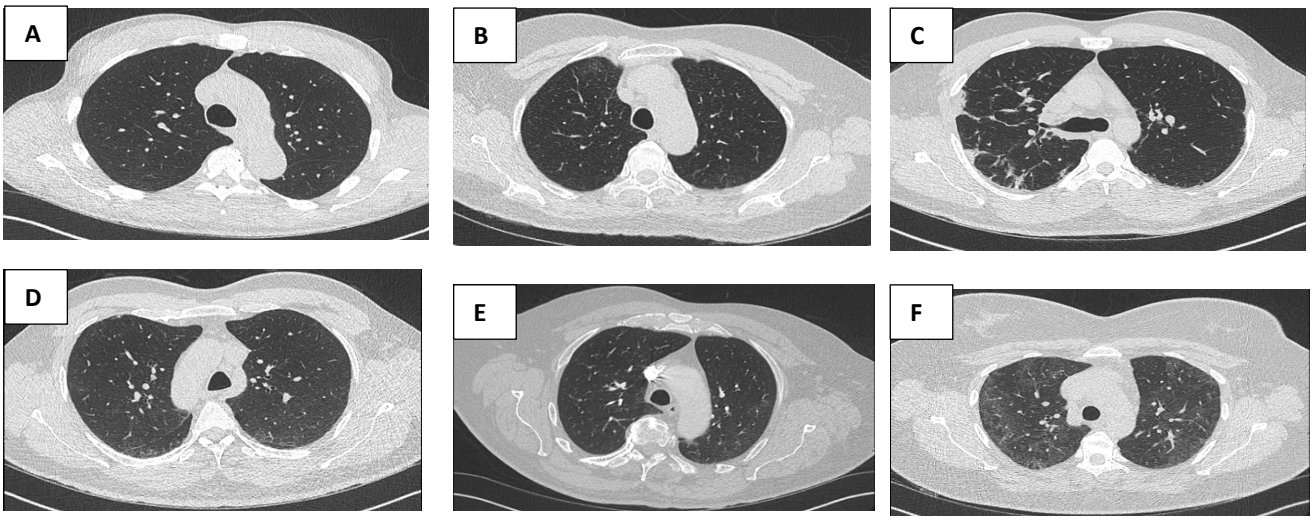


Figure 6. 10 HRCT images of the 6 individuals diagnosed with SAD

Each image is from a separate individual. Images A, B, D, E show largely unremarkable CT slices with minimal ground-glass in D. Image C shows radiological bands with consolidation. Image F shows evidence of ground glass opacification. Notably, fibrosis is not seen in any of the scans.

6.6 Discussion

6.6.1 Summary of findings

My results shows that small airways pathology is present in 17.6% of patients hospitalized for COVID-19. There is no association between patient-reported symptoms, routine lung function parameters or FENO results. None of the individuals with small airways disease had expiratory flow limitation or radiological evidence of interstitial lung disease, or more specifically, fibrosis.

6.6.2 Validation of cut-off

I utilized a cut-off of R5-20>0.07k PA/L/s to denote the presence of small airways disease, a cut-off widely used in COPD research.[152] Further splitting the group according to the presence or absence of small airways pathology showed statistically significant differences between the groups in terms of the small airways parameters, as expected, thus validating the cut-off used. For instance, one would expect a higher resistance at R5 (total resistance of the airways), normal resistance at R20 (resistance of conducting airways) and higher resonant frequency in those with small airways disease, and this was shown in my results. The differences in the reactance values between the groups can be due to two reasons. Firstly, higher reactance values are seen in restrictive lung pathologies, where loss of elastic recoil results in larger pressure swings when a fixed volume of air is applied at the mouthpiece. Fibrosis and interstitial abnormalities post COVID-19 have been widely reported in the post COVID-19 cohort. However, no one with SAD in my cohort had radiological evidence of fibrosis. Secondly, changes in reactance values are often seen in peripheral airways disease, where heterogenous airway closure during expiration, results in patchy ventilation of the lungs and pressure swings similar to that seen in restrictive lung pathologies. [353] In my cohort, the latter is the most likely reason for the differences in reactance values between the group with SAD and the group without.

6.6.3 Findings in context of current literature

6.6.3.1 Prevalence of small airways disease

In my cohort, small airways disease was present in 17.6% of individuals, which is higher than the prevalence reported in the literature (5%) in healthy controls.[355] Post COVID-19, Lindahl et al (2021) reported the absence of small airways disease when 20 patients were assessed approximately 3-6 months post discharge.[331] The disparity between my work and the aforementioned study may be the timepoint at which the measurements were made, thus possibly suggesting that small airways disease presents as late-stage complication after SARS-COV2 infection.

6.6.3.2 Small airways disease and lung function parameters

There were no differences in lung function parameters between those with small airways disease and those without. This is as expected as it is well known that oscillometry is more sensitive than lung function tests in identifying small airways pathology and a significant burden of disease is required prior to abnormalities in spirometric parameters being detected.[227] The differences between the

groups in lung function parameters corresponding to the small airways, MEF 25-75 and sRawtot/ sGawtot, is again in keeping with the cut-offs we used accurately selecting those with small airways pathology. However, determining clinical cut-offs using the spirometric and body plethysmographic parameters to identify patients with small airways disease is difficult as these parameters are thought not to be completely reproducible, with variability between different lung function departments.

6.6.3.3 Small airways disease and FENO

The lack of association with FENO, is interesting. FENO is a marker of eosinophilic airway inflammation in asthma, [322,356,357] and a reasonable hypothesis is that those with higher FENO levels, or elevated FENO levels are more likely to develop small airways pathology due to persistent airway inflammation, especially in the absence of inhaled corticosteroid treatment. However, this was not the case in my cohort. This lack of association may be due to limitations posed by the small sample size, or as alluded to in Chapter 5, a different pathophysiological process resulting in the elevation of nitric oxide levels in these individuals.

6.6.3.4 Small airways disease and patient-reported symptoms

The lack of association between small airways parameters and patient-reported symptoms is not surprising, due to the multi-factorial nature of respiratory symptomatology post COVID-19. However, a trend towards values consistent with small airways disease was seen in patients reporting cough, therefore it is possible that small airways pathology may contribute to ongoing symptomatology in these individuals, and as aforementioned, a larger sample size might have helped strengthen this relationship.

6.6.3.5 Expiratory flow limitation

Expiratory flow limitation (EFL) is a feature of chronic obstructive pulmonary disease.[358–361] Different thresholds have been proposed in the literature to identify EFL, with a change in X5 of >0.28 kPA/L/s,[362] thought to be the most sensitive and specific cut-off, although a cut-off of 0.1 kPA/L/s[359] has also been suggested. No patients in our cohort had a change in X5>0.28 but one met the cut-off of 0.1. However, one individual without SAD also met this latter cut-off, so the relevance of this is unclear. In the full cohort (n=11 SAD), 2 individuals met the cut-off of 0.28, with both individuals having a RV/TLC >=50%, suggesting hyperinflation, and consistent with published literature that that EFL is

associated with hyperinflation.[363] EFL is rarely seen in asthma[364,365] but is a common feature in COPD[359,362]. The absence of EFL in our cohort, despite SAD, may imply that the process is dissimilar to COPD and may even have a reversible component. The absence of EFL may have treatment implications as EFL has been associated with response to inhaled bronchodilator therapy in COPD.[231,366]

6.6.4 Clinical relevance of findings

Small airways disease exists post COVID-19 and can be detected using FOT. Neither lung function testing (including spirometry, body plethysmography or FENO) or patient-reported symptoms are helpful in differentiating between those with small airways disease and those without. This, therefore, poses challenges in selecting individuals who need further assessment for small airways pathology. Longer term studies with accurate phenotyping of allergy status are required to better understand the clinical relevance of these findings and trajectory of small airways pathology.

6.6.5 Limitations

There are a few limitations to discuss. Firstly, FOT measurements were not taken at baseline, therefore causality between SARS-COV2 infection and small airways disease cannot be assumed. Secondly, there was no data from healthy controls (negative controls) or individuals with pre-existing airway disease (positive controls), both of which would have helped me make comparisons. Thirdly, this study does not include any patients who had received mechanical ventilation during their admission. Hypothetically, it is possible that those with more severe acute illness, and therefore a more significant epithelial cell insult, carry a higher risk for small airways pathology, especially if epithelial cell regeneration occurs in an aberrant manner. Therefore, it is possible that the prevalence of small airways disease has in fact been underestimated in my study. Fourthly, the trajectory of small airways pathology is important to understand, but this has not been addressed in my results. Finally, this study is small, but it does offer preliminary data: A much larger cohort is required to robustly elicit the true prevalence of small airways disease post COVID-19.

6.7 Conclusion

In this chapter, I have shown that small airways disease can be detected using FOT in some individuals at 1 year post discharge for COVID-19 respiratory failure. The presence of small airways disease is

associated with abnormalities in small airways parameters in the PFTs but not routine spirometry or body plethysmography. In those with SAD, expiratory flow limitation was not seen raising the possibility that the pathophysiological process may be dissimilar to that seen in COPD.

Chapter 7 - Understanding the airway microenvironment post COVID-19

Some of the results in this Chapter have already been published:

Vijayakumar B, Boustani K, Ogger PP, Papadaki A, Tonkin J, Orton CM, Ghai P, Suveizdyte K, Hewitt RJ, Desai SR, Devaraj A, Snelgrove RJ, Molyneaux PL, Garner JL, Peters JE, Shah PL, Lloyd CM, Harker JA. Immuno-proteomic profiling reveals aberrant immune cell regulation in the airways of individuals with ongoing post-COVID-19 respiratory disease. *Immunity*. 2022 Mar 8;55(3):542-556.e5. doi: 10.1016/j.immuni.2022.01.017. 2022

7.1 Introduction

7.1.1 The function of immune cell subsets during acute infection

The innate and adaptive immune system are crucial in protection against pathogenic invasion.[367] Innate immune cells such as monocytes, macrophages, neutrophils, dendritic cells and natural killer cells have a range of pattern recognition receptors (PRRs) to detect pathogen associated molecular patterns (PAMPs) and can result in a rapid immune response to invading pathogens.[368,369]

Macrophages originate independently, or from precursors, circulating monocytes, and migrate to various tissues where they undergo differentiation into macrophages.[370] Macrophages have a range of functions, which depends somewhat on their phenotype.[371] In brief, they can be classified into M1 macrophages, which produce pro-inflammatory cytokines such as IL-1, IL-6 and TNF alpha, or M2 macrophages which exert anti-inflammatory effects, producing cytokines such as IL-10 and TGF beta.[372,373] To complicate matters further, macrophages display plasticity and can switch from a M1 phenotype to an anti-inflammatory M2 phenotype during tissue repair, for instance.[374] This is especially important as the cell surface markers expressed may also vary, depending on the macrophage phenotype.[375]

Human monocytes can be subdivided into three main subsets: Classical (CD14+CD16-), non-classical (CD14-CD16+) or intermediate (CD14+CD16+).[376] Tissue-resident macrophages are eventually replaced by monocytes after migration to the lungs[377] and monocyte recruitment is crucial to defend against pathogens.[378] In addition to their role in defence against infection, classical monocytes have been implicated in the pathogenesis of idiopathic pulmonary fibrosis and associated with poorer outcomes.[379,380]

Neutrophils are also an important early responder to infection and kill pathogens through phagocytosis, degranulation, oxidative burst and extracellular traps.[381,382] Natural killer (NK) cells provide early immunity against viral pathogens and depletion of NK cells has been associated with recurrent infections.[383,384] However, NK cells can also contribute to lung immunopathology by causing excessive inflammation.[385]

In contrast to the innate immune system which provides an immune response that is non-specific in nature, the adaptive immune system produces antigen-specific responses, creates immunological memory in case the same pathogen is encountered again, and differentiates between "non-self" and "self" antigens. [386] Broadly speaking, this consists of B and T lymphocytes and NK-T cells.

Lymphocytes (T cells, B cells, NKT cells and NK cells) are an important mediator of immunity. T cells can be further subdivided into cells with a cytotoxic function (CD8+ cells) or T helper function (CD4+ cells). Furthermore, subsets of CD4+ cells can be seen. For example, Th1, Th2, Th17 and Treg, which display different functions.[386] B cells exercise their effector function through antibody secretion and enable memory cell formation to facilitate a more rapid host immune response if the pathogen were to be encountered again.[387,388]

Finally, NKT cells, another lymphocyte group, harbour both the T cell and NK receptor and therefore serve as part of both the innate and adaptive immune system.[389] In contrast to T cells that require antigen presentation by MHC class II (CD4+T cells) or MHC class I (CD8+ T cells) molecules, NKT cells can recognise antigens presented by CD1 antigens.[386,389,390]

7.1.2 Detection of immune cell subsets

Flow cytometry is a well-established method of single cell analysis and is commonly used in immunophenotyping of cells.[391] Flow cytometry can measure cell characteristics using visible light scatter: Forward scatter (FSC) measures the size of the cell and side scatter (SSC) measures the granularity of the cell. Forward scatter can therefore help distinguish immune populations based on size. For instance, monocytes are large in contrast to lymphocytes, which are smaller and exhibit a less intense forward scatter. Similarly, granulocytes, such as neutrophils, can be distinguished by higher intensity side scatter due to their granularity. Emitted light is channelled through filters which detect light of varying wavelengths, to a photomultiplying detector, which subsequently converts the

fluorescent signal into a digital signal. The use of flow cytometry has significantly enhanced our understanding of airway immunology during acute infection[392] and interstitial pneumonias.[393]

Differential cell count analysis is a well-established and widely used method for assessing immune cell subpopulations in patients with suspected interstitial lung disease. Cytocentrifuging of bronchoalveolar lavage fluid, followed by staining and enumeration of at least 300 cells is usually the process by which differential cell count assessment is performed. An increase in specific immune cell populations can point towards a particular diagnosis, although often, there is an overlap of phenotypes.[334]

7.1.3 Airway immune cell subsets in healthy individuals

In healthy non-smokers, alveolar macrophages comprise the most predominant immune cells (about 85%), followed by lymphocytes (10%), neutrophils (about 5%), eosinophils and basophils (<1%). In smokers, cellularity can be increased.[334,394]

7.1.4 BALF findings in acute COVID-19

Endobronchial sampling has been performed during acute COVID-19 in critically ill individuals. Consistently, studies have reported increased neutrophilia in the BALF of individuals with severe COVID-19. Furthermore, Voiriot et al (2022) showed in 76 critically individuals that BALF neutrophil and a raised BALF neutrophil: lymphocyte ratio was associated with a worse prognosis, and that IL8, a potent chemoattract for neutrophils, was significantly elevated in the BALF compared to in the peripheral circulation.[395] This mirrored data published by Pandolfi et al (2020)[396] and Zhou et al (2020) who showed that in addition to neutrophil chemoattractants, cytokines such as CCL2 and CCL7 which facilitate monocyte recruitment, were part of the chemokine bundle that were upregulated in the SARS-COV2 airway, compared to that seen in community acquired pneumonia.[63] Moreover, single-cell sequencing showed increased proportions of pro-inflammatory macrophages in BALF in acute COVID-19.[62] Whilst the reason for this is not clear, one postulate is that ineffective viral clearance increases monocyte recruitment to the lung, as evidenced by individuals in whom resident T cells were elevated in BALF fluid, infiltration of monocytes was lower.[64]

Another feature of acute COVID-19 is profound peripheral lymphopenia, which is associated with poorer disease outcomes.[397,398] Peripheral lymphopenia is also seen in other viral infections but is often short-lived and less severe than that seen in COVID-19. [399] The precise reason for peripheral

lymphopenia is not clear, but selective recruitment of lymphocytes from the peripheries to the airways is one possibility and paired T cell receptor tracking confirmed migration of T cells from the peripheries to the airways in severe disease presentations of COVID-19.[400,401] Furthermore, post-mortem analysis of pulmonary tissue post SARS-COV2 infection has shown significant macrophage and lymphocyte infiltration, thus reinforcing the theory that sequestration of lymphocytes to the lungs is a plausible explanation for peripheral lymphopenia.[402]

Whilst neutrophil recruitment is a normal response of the innate immune system to infection, BALF neutrophilia has been associated with a greater risk of mortality in acute respiratory distress syndrome,[403] with abundant synthesis of neutrophil-derived mediators such as neutrophil elastase and oxidase being associated with clinical disease progression.[404] By contrast, BALF lymphocytosis >20% in ARDS is associated with a better prognosis suggesting that lymphocyte recruitment to the airways may be beneficial perhaps through its anti-viral effect.[405]

Zhou et al (2020) showed that interferon-stimulated gene (ISG) response in the airways, especially IFITs and IFITMs, which have a broad range of anti-viral activity were significantly elevated during SARS-COV2 infection.[63] However, impaired Type 1 immunity has been seen in individuals who have life-threatening presentations of COVID-19,[406,407] therefore a suboptimal immune response to SARS-COV2 infection may contribute to acute disease severity.

To summarise, significant recruitment of immune cells to the airways is seen during the acute disease but whether this resolves with time, the timeframe for resolution and the clinical implications of persistent immune activation, if this occurs, is not known.

7.2 Background

In Chapter 4, I showed that persistent parenchymal abnormalities were common post COVID-19, with the commonest abnormality being ground-glass opacities. Ground-glass opacities are the predominant finding in certain interstitial lung diseases, including chronic hypersensitivity pneumonitis, an interstitial lung disease associated with significant BALF lymphocytosis.[334] It is therefore possible that assessment of airway immune subsets at follow up may assist with the diagnosis and treatment of persistent parenchymal abnormalities seen during the recovery phase.

Despite the emerging body of evidence evaluating the airway microenvironment during acute disease, at the time of starting my PhD, the airway microenvironment had not been evaluated during the convalescent phase, neither post SARS-COV2 infection, nor any other severe viral pneumonia.

7.3 Hypothesis and Aims

Hypothesis

Persistent immune activation in the airways is seen in patients with abnormal radiology at follow up

Aims

1. To assess immune populations in the airway microenvironment post COVID-19
2. To relate the findings from 1 to radiological and physiological recovery at 1 year post hospital discharge
3. To understand the utility of endobronchial sampling in evaluating post COVID-19 radiological abnormalities

7.4 Methods

7.4.1 Patient recruitment

A subset of individuals recruited to the PHENOTYPE study underwent clinically-justified endobronchial sampling approximately 3-6 months post hospital discharge. All patients consented to the acquisition of additional lavage samples and epithelial brushings for research purposes. Further consent to the bronchoscopy procedure was taken on the day of the procedure after explaining the risks and benefits of endobronchial sampling.

7.4.2 Endobronchial sampling

Acquisition of endobronchial samples was performed by members of the interventional bronchoscopy team (myself, Dr James Tonkin, Dr Christopher Orton, Dr Justin Garner and Professor Pallav Shah). The majority of individuals underwent sampling under conscious sedation (with administration of midazolam +/- alfentanil), with a few bronchoscopies performed under deep sedation. 150mls of 0.9% saline was infiltrated into the airways in 50 ml aliquots. 10mls of the return was sent for clinical

differential cell count analysis at the Royal Brompton Hospital, London, 10mls was sent for clinical microbial analysis at Chelsea and Westminster Hospital, London, and 10mls utilised for flow cytometry. The lavage was taken from the most affected lung segment as identified on CT imaging. Epithelial brushings (which will be further discussed in Chapters 8 and 9) were taken from the left upper lobe bronchus.

7.4.3 Definitions

Disease severity classifications were made based on the maximal degree of respiratory support required during the inpatient admission: Moderate (oxygen therapy), Severe (non-invasive ventilation), Very severe (intubation and ventilation)

Proportional change in CT = (CT score at 1 year – CT score at 3 months)/ CT score at 3 months. Therefore, a more negative proportional change, means a greater degree of improvement from baseline. Absolute changes in CT scores (i.e. CT score at 1 year minus CT score at 3 months) were not calculated due to the varying extents of CT abnormalities.

Total lymphocyte count (or proportion) = T cells + B cells + NK T cells + NK cells as derived from flow cytometry data. The flow cytometry methodology and gating strategy utilised have been described in Chapter 2.

7.4.4 Flow cytometry

BALF supernatant was processed as described in Chapter 2. I was involved in the processing, staining and running of flow cytometry for the post-COVID-19 cohort, under the direct supervision of postdoctoral assistant, Dr Patricia Ogger (PO) and then PhD student, Karim Boustani (KB) who were training me in wet lab skills at the time. I learnt how to analyse flow cytometry data using FlowJo7 [https://www.flowjo.com/solutions/flowjo/downloads] from PO. The data presented in this Chapter is what was used for publication in a collaboration with Lloyd and Harker labs for which, the flow cytometry data was analysed by PO and KB. Healthy control donors were recruited by Richard J Hewitt (RJH) and flow cytometry run by PO prior to the commencement of my PhD and therefore, prior to the pandemic.

7.4.5 Differential cell count analysis

This was performed by the cellular pathology lab at the Royal Brompton Hospital, London as routine clinical samples.

7.4.6 Microbial, viral and fungal assessment

This was performed by the microbiology department at Chelsea and Westminster Hospital, London, as routine clinical samples.

7.5 Results

7.5.1 Sample flow

Endobronchial sampling was performed in 42 individuals between August 2020 and May 2021 (Figure 7.1).

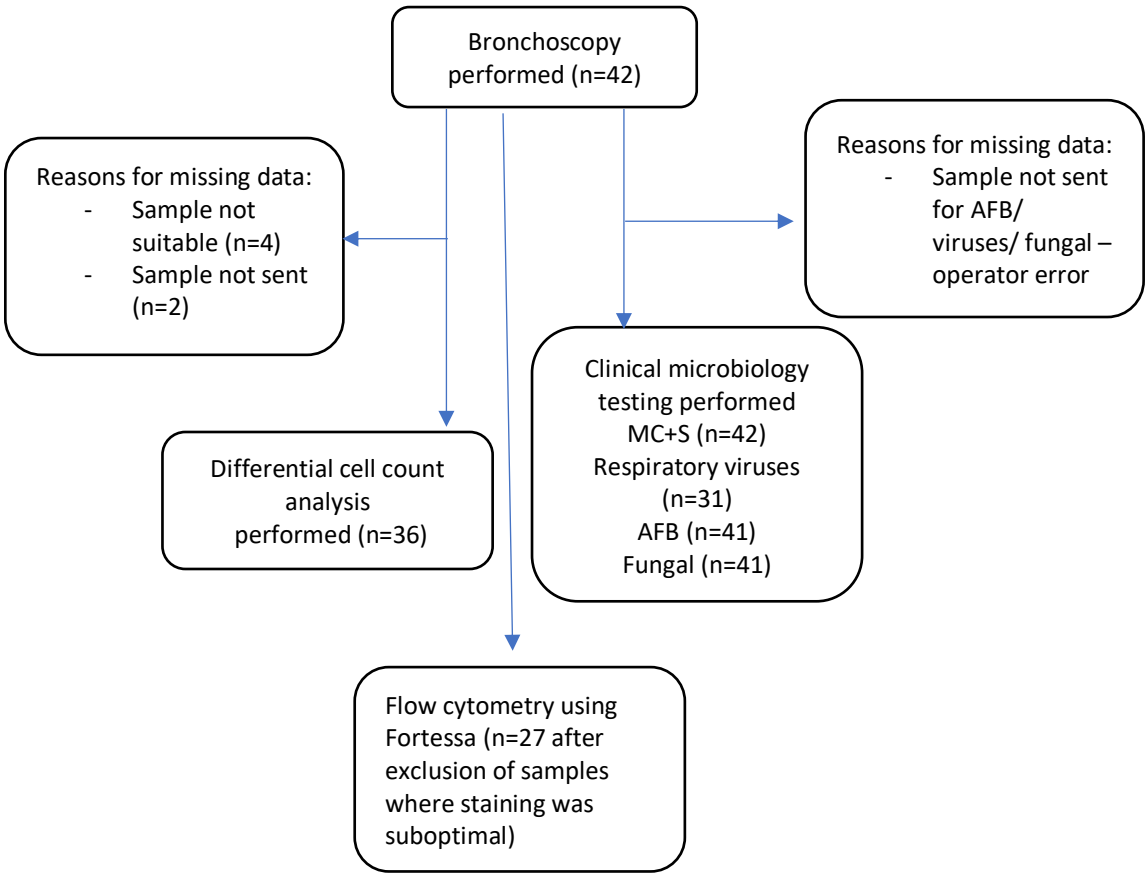


Figure 7. 1: Sample flow after endobronchial sampling

Abbreviations: AFB (acid fast bacilli), MC+S (microscopy, culture and sensitivity)

7.5.2 Baseline characteristics

The median age of the post COVID-19 individuals undergoing endobronchial sampling was 58 years. There was a male preponderance of 78.6%, reflecting the nature of the patients recruited to the PHENOTYPE study. The healthy control donors were slightly younger, with a median age of 49 years. The majority of individuals in both groups were lifelong non-smokers (Table 7.1).

Endobronchial sampling post COVID-19 was performed at a median of 124 (100-174) days post discharge, with longer intervals from discharge in patients recruited during the first wave, where arranging clinical follow-up and bronchoscopy was more challenging as the procedure is aerosol-generating, thus necessitating additional precautions to be taken.

	pCOVID (n=42)	HC (n=28)		pCOVID (n=42)	HC (n=28)
Age (years)	58 (52 - 68)	49 (40 – 55)	**CT imaging**	**n=42**	N/A
Gender, M (%n)	33 (78.6)	17 (58.6)	Days from admission to follow up CT [n=37]	117 (93.5-139.5)	
BAME (%n)	25 (59.5)	N/A	Days from discharge to follow up CT [n=39]	90 (84-127)	
Comorbidities (%n)			CT score (% abnormality)	45 (20 – 70)	
Asthma	5 (11.9)	N/A			
COPD	1 (2.4)	N/A	**Bronchoalveolar lavage fluid sampling**	**n=42**	
Previous pneumothorax	1 (2.4)	N/A	Days between admission and sampling [n=37]	153 (108-190)	N/A
Hypertension	11 (26.2)	N/A	Days between discharge and sampling [n=39]	124 (100-174)	N/A
Ischaemic heart disease	4 (9.5)	N/A	**Lung function tests**	**n=40**	N/A
Type 2 diabetes mellitus	7 (16.7)	N/A	Days between admission and lung function tests [n=35]	147 (105-183)	N/A
Smoking history			Days between discharge and lung function tests [n=37]	116 (91.5-169)	N/A
Current smoker	1 (2.4)	2 (6.8)	FEV1 (L)	2.95 (2.34 – 3.57)	N/A
Ex-smoker (>=10 pack year)	5 (11.9)	4 (13.7)	% predicted FEV1	95.5 (86.3-106)	N/A
Non-smoker or ex-smoker <10 pack year)	36 (85.7)	17 (58.6)	FVC (L)	3.70 (2.83 – 4.11)	N/A
Severity of acute illness			% predicted FVC	91.5 (81.5 – 99.3)	N/A
Hospitalized	40 (95.2)	N/A	TLC (L)	5.55 (5.07 – 6.31)	N/A
- Oxygen therapy only	17 (40.4)	N/A	% predicted TLC	87.5 (82.3 – 99.3)	N/A
- CPAP/ NIV	12 (28.6)	N/A	TLCO mmol/kPA/min	6.29 (5.03 – 8.48)	N/A
- MV	11 (26.2)	N/A	% predicted TLCO	76.0 (65.3 – 96.0)	N/A
Not hospitalized	2 (4.8)	N/A	KCO mmol/kPA/min/l	1.32 (1.18-1.60)	N/A
			% predicted KCO	97.5 (87.3-112.8)	N/A
Length of hospital stay (days) [n=37]	10.0 (5.0-24.5)	N/A			

Table 7. 1 Clinical, radiological and physiological data of individuals undergoing endobronchial sampling

Abbreviations: Gender, M (male), BAME (Black, Asian and Minority ethnic), COPD (chronic obstructive pulmonary disease), CPAP (continuous positive airway pressure), NIV (Non-invasive ventilation), MV (mechanical ventilation), CT (computed tomography), FEV1 (forced expiratory volume in 1 second), FVC (forced vital capacity), TLC (total lung capacity), TLCO (transfer factor of the lung for carbon monoxide), KCO (carbon monoxide transfer coefficient). Data presented as n (%n), median (IQR)

7.5.4 Immune populations using differential cell count analysis

10/18 (55.6%) of differential cell count analyses were abnormal from the first wave, the majority of the abnormalities being neutrophilia (70%). In the second wave, 8/18 (44%) samples had abnormalities with 4/18 (22.2%) having lymphocytosis alone, 2/18 (11.1%) neutrophilia alone, 1/18 (5.5%) eosinophilia alone and one individual with a raised lymphocyte, eosinophil and neutrophil count (Table 7.2). Percentages were calculated based on enumeration of 300 cells.

The radiological findings and trajectory of one individual who had a lymphocytosis of 35.3% (normal range <14%) is shown in Figure 7.2. Even without any additional medical management at follow up, such as initiation of oral corticosteroid therapy, there was near total resolution of the ground-glass opacities by 1 year post hospital discharge.

Additionally, the proportion of individuals with specific abnormalities in their differential cell count results who had required different levels of respiratory support during the acute admission, was similar (Table 7.3).

First wave					Second wave				
Participant number	**Mac (%)**	**Lymph (%)**	**Neut (%)**	**Eos (%)**	**Participant number**	**Mac (%)**	**Lymph (%)**	**Neut (%)**	**Eos (%)**
1	78	20.7	1	0	1	86	2	11	1
2	84	10	5.3	0.7	2	67	23	5.7	4
3	83	12	5	0	3	83.7	14.7	1.3	0.3
4	62	35.3	2.3	0	4	97.3	2.7	0	0
5	91	5	3.3	0.3	5	95.3	2.3	1.7	0.7
6	83.4	10	5.6	0	6	91	9	0	0
7	82.7	16	0	1	7	88	10	2	0
8	90.7	7	2	0	8	84	11	0.7	4.3
9	85.7	12.6	1.3	0.3	9	80	16.7	1	2.3
10	94.7	3	2	0.3	10	94.7	3	0.67	1.67
11	92	2	5	1	11	82.7	15.7	0.33	1.33
12	92	6	1	0	12	93.3	4.67	2	0
13	74	10	14	1	13	92.7	7	0.3	0
14	95.6	3.3	0.7	0.3	14	73.7	24	1.7	0.7
15	92	3.7	4.3	0	15	90.3	9.3	0.3	0
16	85	4	5.7		16	89.7	9	0.3	1
17	89.7	10	0	0.3	17	91	3.7	2.3	3
18	95	4.5	0.5	0	18	78.1	8.3	11	2.7

Table 7. 2 Clinical differential cell counts in BALF

Abnormal readings are highlighted in red, based on laboratory cut-offs at the Royal Brompton Hospital, London: lymphocyte>14%, neutrophil>4%, eosinophil >4%.

Abbreviations: Mac (macrophages), Lymph (lymphocytes), Neut (neutrophils), Eos (eosinophils)

Differential cell count (BALF) [n=36]	Total cohort	O2 only (n=16)	CPAP/ NIV (n=10)	MV (n=10)
Lymphocytosis (>14%)	8 (22.2)	2 (25)	3 (37.5)	3 (37.5)
Neutrophilia (>4%)	10 (27.7)	5 (50)	3 (30.0)	2 (20.0)
Eosinophilia (>3%)	2 (5.6)	1 (50)	1 (50)	0 (0.0)

Table 7. 3 Abnormal differential cell count analysis stratified according to respiratory support

Abnormal differential cell counts as defined by laboratory cut-offs, stratified according to degree of respiratory support needed during the acute admission. Results displayed as n (%n) Abbreviations: BALF (bronchoalveolar lavage fluid), O2 (oxygen), CPAP (continuous positive airway pressure), NIV (non-invasive ventilation), MV (mechanical ventilation).

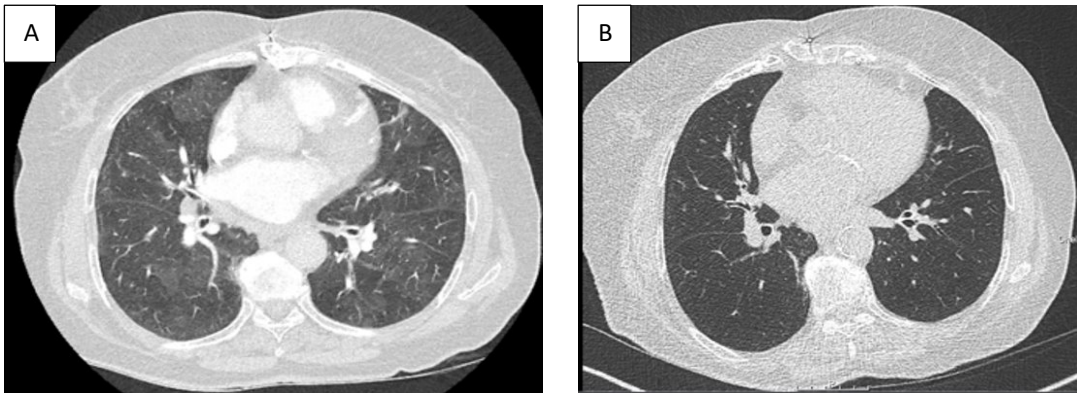


Figure 7. 2 Radiological trajectory of individual with BALF lymphocytosis of 35.3%

Individual had BALF lymphocytosis of 35.3% at 3-month follow up. CT performed at 3 months (A) and 12 months (B) post discharge from hospital. Note near total resolution of ground-glass opacities from A to B. No additional treatment was given between the two visits.

7.5.4 Microbial analysis

The lower airways were thought to be sterile, but the use of non-culture methods has suggested otherwise, with Proteobacteria, Actinobacteria and Firmicutes being the most prevalent phyla in healthy individuals.[408–410] Colonisation of the lower airways with bacteria and fungi have however been reported in patients requiring mechanical ventilation, identified using microscopy, culture and sensitivity. [411–413]

In individuals recovering post COVID-19, a variety of pathogens were detected in the lavage fluid. Two individuals were given a course of antibiotics, despite the absence of clinical symptoms. It is not possible to retrospectively determine if antibiotics were required in these instances. Positive cytomegalovirus (CMV), and fungal species were discussed with the Clinical Microbiology team and additional investigations such as beta D glucan and galactomannan (for instances where pneumocystis jirovecii or aspergillus were grown), were performed, which were subsequently negative. There was no evidence of clinical deterioration due to infection in the individuals who were not given any specific antimicrobial therapy. Interestingly, neutrophilia was not associated with the presence of clinically significant microorganisms (Table 7.4).

Positive microbiology in BALF				
Bacterial (n=42)	Klebsiella species	4 (9.5)		
	Serratia marcescens	1 (2.4)		
	Staphylococcus aureus	4 (9.5)		
	Enterobacter cloacae	1 (2.4)		
Viruses (n= 41)	Rhinovirus	2 (4.9)		
	Enterovirus	2 (4.9)		
	Parainfluenza	1 (2.4)		
	CMV	1 (2.4)		
Fungal (n= 41)	Yeast	6 (14.6)		
	Aspergillus niger	1 (2.4)		
	PCP	3 (7.3)		
	Candida albicans	1 (2.4)		
	Penicillium species	1 (2.4)		
	Filamentous fungi	1 (2.4)		
BALF microbiology in patients with BALF neutrophilia				
	Microscopy, culture and sensitivity	**Respiratory viral screen**	**Acid fast bacilli**	**Fungal culture**
Case 1	10-100 000 URT flora	Negative	Negative	Yeasts
Case 2	Negative	Negative	Negative	Negative
Case 3	Negative	Negative	Negative	Yeasts
Case 4	Negative	Negative	Negative	Penicillium sp
Case 5	10 – 100 000 Staphylococcus aureus >100 000 URT	Negative	Negative	Negative
Case 6	<10 000 Staphylococcus aureus < 10 000 URT	Negative	Negative	Negative
Case 7	<10 000 URT	Negative	Negative	Negative
Case 8	Negative	Negative	Negative	Yeasts
Case 9	Negative	Negative	Negative	Yeasts
Case 10	Klebsiella oxytoca	Negative	Negative	Yeasts

Table 7. 4 BALF microscopy and culture results

Abbreviations: URT (upper respiratory tract flora), CMV (Cytomegalovirus), PCP (pneumocystis jirovecii)

Results shown as colony forming unit/ millilitre (cfu/ml)

7.5.5 BALF immune populations using flow cytometry

Evaluation of immune populations using flow cytometry showed an upregulation of total cell count (Figure 7.3A), with the increased cellularity due an increase in airway macrophages (7.3C), T cells (7.3 D) and B cells (7.3 F) in the airways of post COVID-19 individuals compared to healthy controls. NK cells (CD56+CD3-, 7.3H), and NKT cells (CD56+CD3+, 7.3G) were in similar abundance in post-COVID-19 individuals compared to healthy controls. In contrast, the number of neutrophils was reduced, both in absolute number and relative proportion (7.3E). Classical monocytes (CD14+CD16-) were in similar abundance in healthy control and post-COVID-19 airways but significantly reduced in proportion in the post COVID-19 airways compared to healthy controls (7.3B).

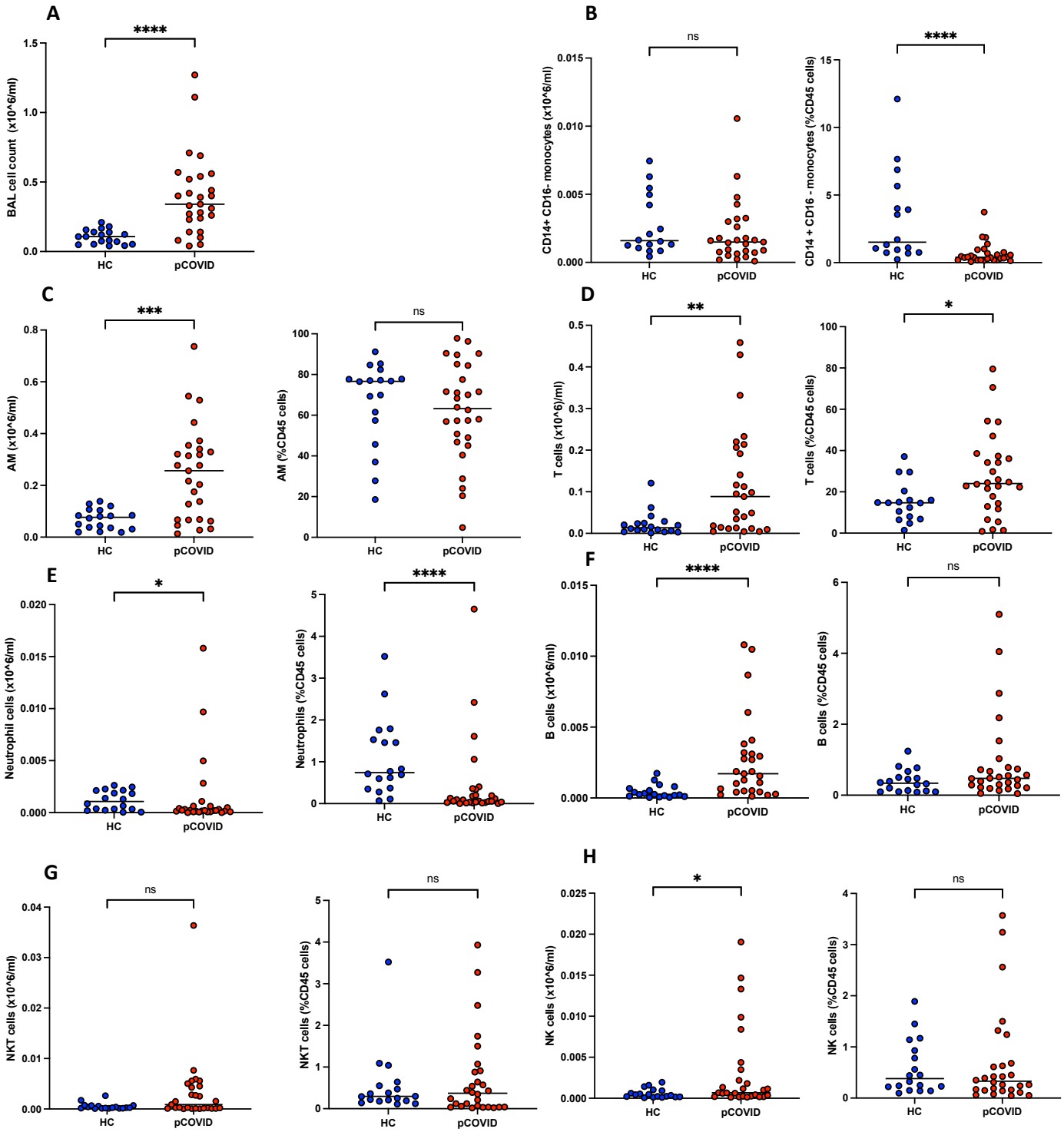


Figure 7. 3 BALF immune cells detected by flow cytometry

Immune cell populations in BALF of post-COVID-19 and HC donors. Results show absolute cell number (x10^6/ml) or percentage of total white cells (CD45+ cells). Inter-group comparisons performed using Mann Whitney U testing with p value <0.05 considered to be statistically significant: * p<0.05, ** <0.01, *** <0.001, **** <0.0001. Each dot signifies a biological donor. Blue – Healthy controls, Red – post COVID-19. Line drawn at median value

7.5.5.1. Immune populations according to severity of acute presentation

There was no significant association between the total number of white blood cells (total or specific subsets) or proportion of CD45+ cells in the post COVID-19 airway when stratified according to acute disease severity (Figure 7.4).

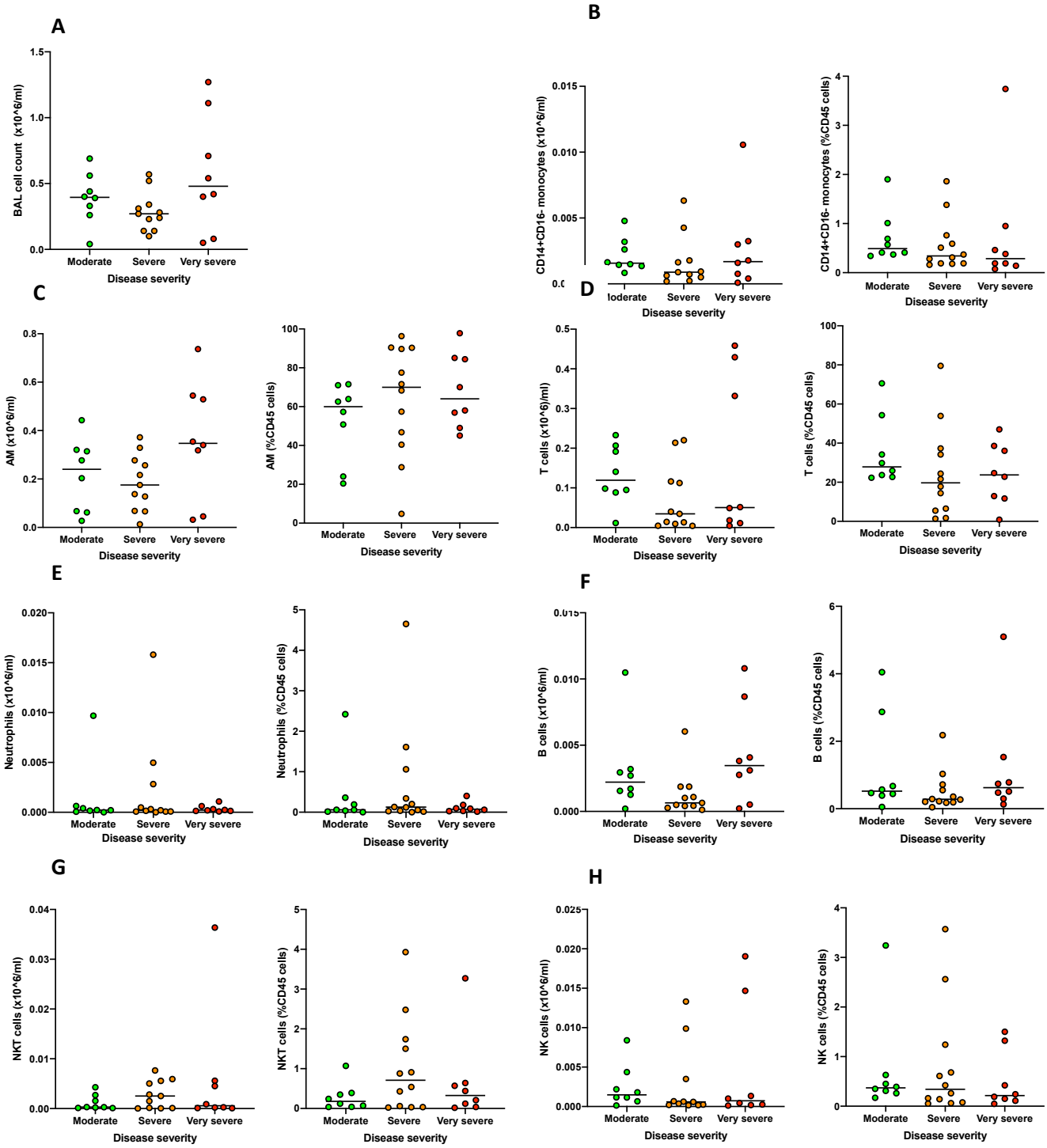


Figure 7. 4 BALF immune cells according to acute disease severity

Total BALF cellular count and % CD45+cells, stratified according to disease severity during acute admission. Results show absolute cell number (x10^6/ml) or percentage of total white cells (CD45+ cells). Line draw at median. Each dot signifies an individual biological donor.

7.5.5.2 Relationship between flow cytometry data and CT abnormalities at 3 months

A positive correlation was seen between the CT score at 3 months and total cell count in BALF (Figure 7.5A), as well as the absolute number of alveolar macrophages (7.5B) and total lymphocytes (7.5C). However, the proportion of subsets as a percentage of the total white cells (CD45+), showed no obvious relationship with the CT score (Figure 7.6). Whilst causality between the CT changes and immune cell upregulation cannot be established, these results suggest that in those with a greater extent of CT abnormalities at 3 months, a higher number of white cells, and more specifically, alveolar macrophages and lymphocytes may be seen.

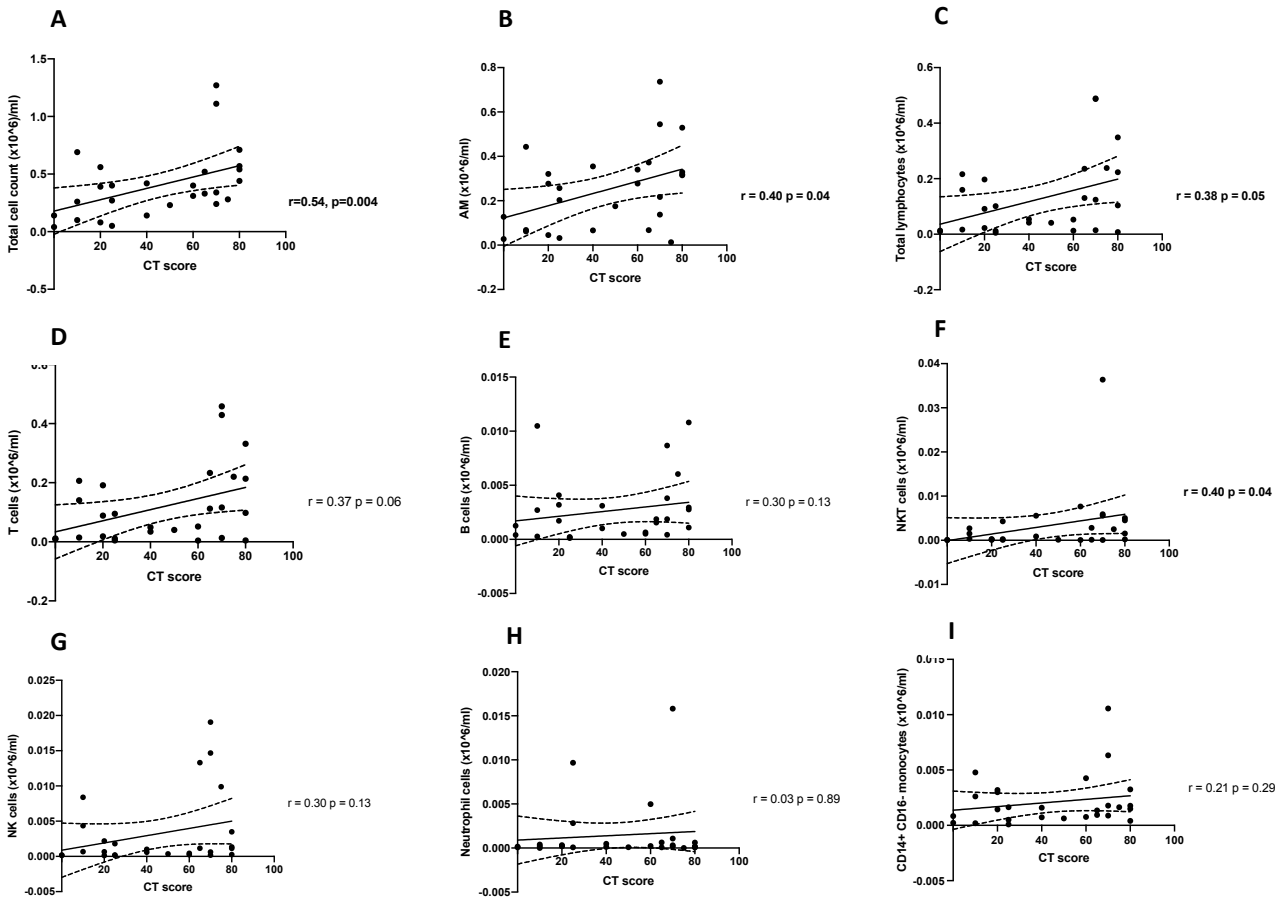


Figure 7. 5 Relationship between BALF cell counts and 3-month CT score

Absolute cell counts plotted. Spearman rank correlation analysis performed with a p value <0.05 considered statistically significant. 95% confidence interval shown by dotted lines.

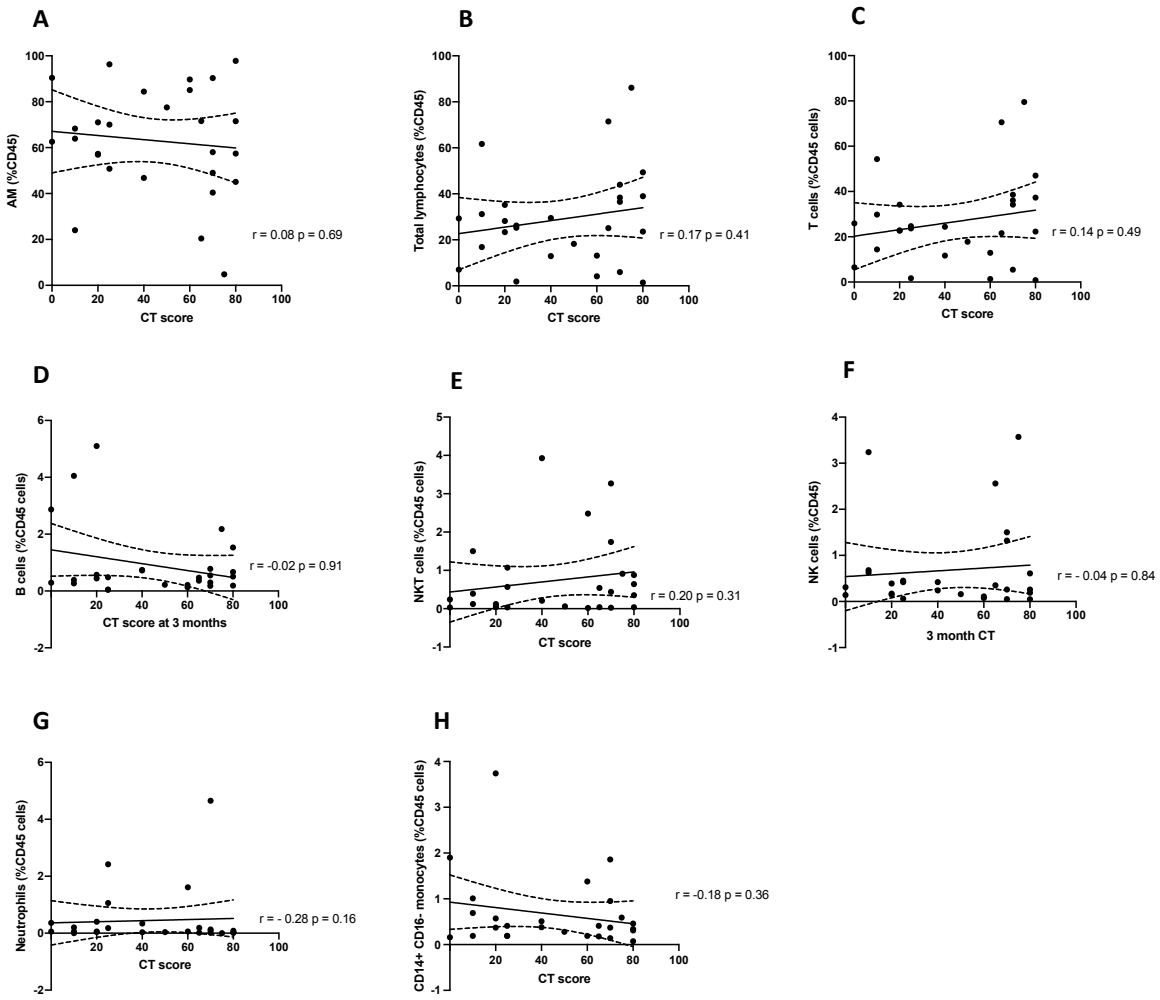


Figure 7. 6 Relationship between BALF immune cell proportions and 3-month CT score

Immune cell subsets (% of total CD45+ cells) and 3-month CT score plotted. Spearman rank analysis performed, with a p value <0.05 considered statistically significant. 95% confidence intervals shown by dotted lines.

7.5.5.3 Lung function abnormalities and immune cells

As shown in Chapter 5, lung function abnormalities were common post COVID-19. In particular, a restrictive lung function with abnormalities in gas transfer (TLCO), forced vital capacity (FVC) and total lung capacity (TLC) were seen. I therefore wanted to assess whether there was a relationship between these parameters at 3 months post discharge and immune cells in the post-COVID-19 airway (Figure 7.7). There was a trend towards higher total cell count (7.7A), airway macrophages (7.7B) and total lymphocytes (7.7C) in those with lower values of TLC, TLCO, and FVC, suggesting ongoing immune cell filtration may contribute to physiological impairment, or may be a consequence of attempted tissue

repair pathways in individuals whose disease burden has resulted in physiological impairment. Absolute values for lung function parameters were used rather than % predicted values to minimise any inaccuracies arising from usage of incorrect height or weight values when calculating percentage predicted values.

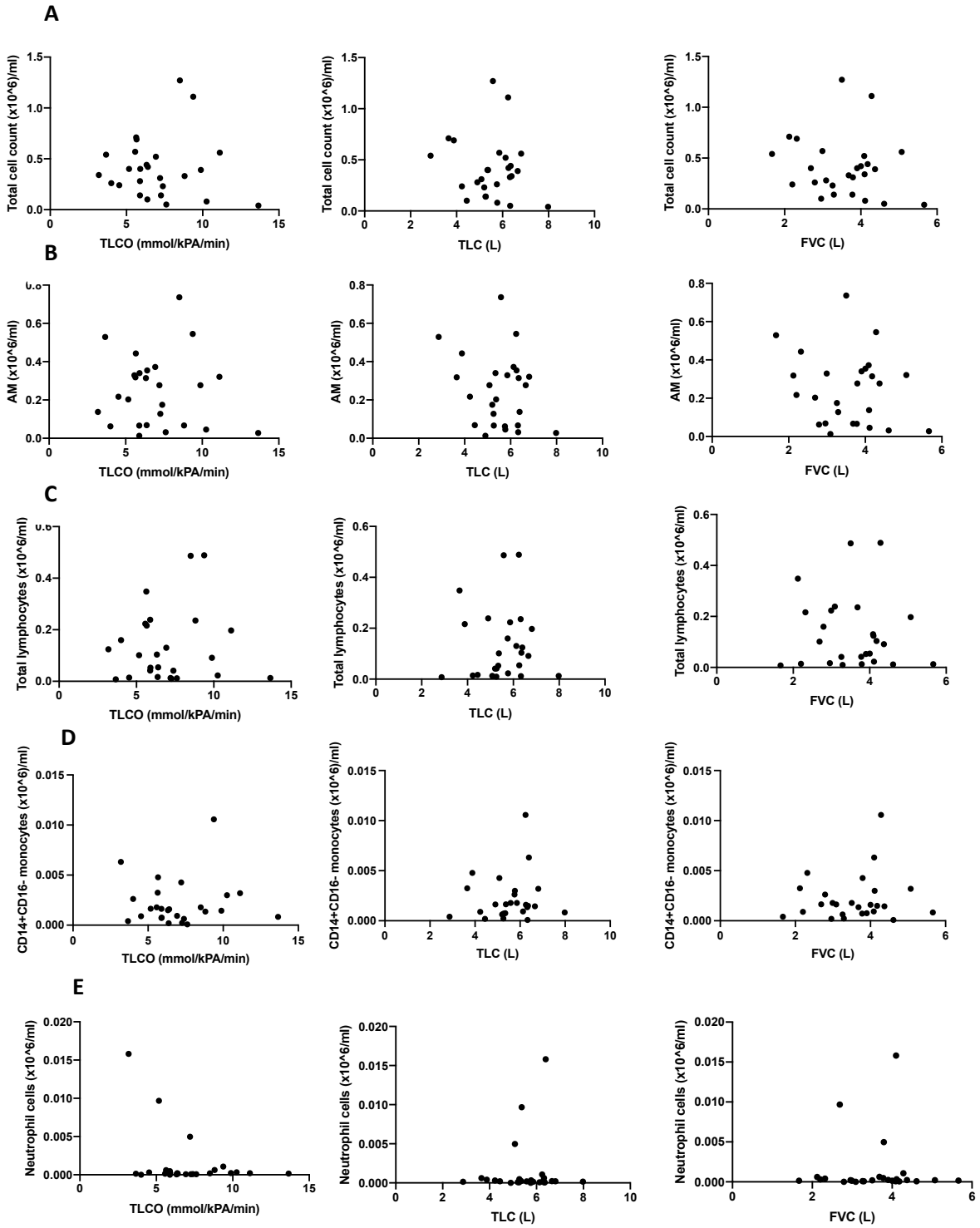


Figure 7. 7 Relationship between BALF immune cells and PFTs

Abbreviations: FVC (forced vital capacity), TLC (total lung capacity), TLCO (transfer capacity of the lung for the uptake of carbon monoxide), L (litres), AM (alveolar macrophages), PFTs (pulmonary function tests).

In Chapter 5, TLCO was shown to be the most common abnormality found on lung function testing. I therefore assessed if an abnormal TLCO, defined as <80% predicted, was associated with any trends in the immune populations. A non-significant difference in the total and absolute number of immune cell subsets was seen (Figure 7.8), with a trend towards a higher number of alveolar macrophages (7.8B) in individuals with an abnormal TLCO.

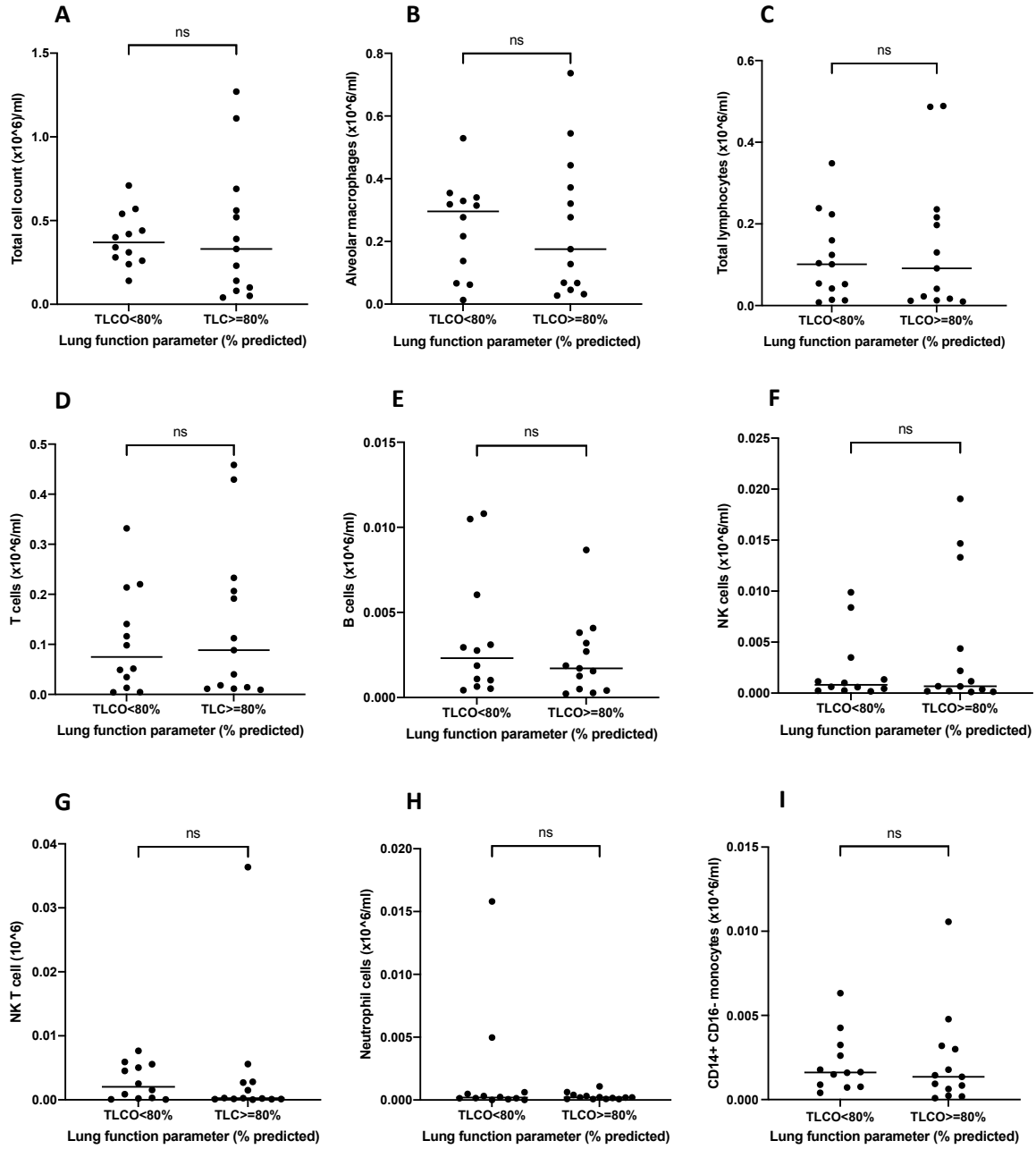


Figure 7. 8 BALF immune cells according to % predicted TLCO at 3 months

TLCO <80% predicted represents abnormal TLCO. Inter-group comparisons performed used Mann Whitney U testing and a p value <0.05 was considered statistically significant. Line drawn at median. Abbreviations: NK (natural killer), NKT (natural killer T) cell, TLCO (transfer capacity of the lung for the uptake of carbon monoxide)

7.5.5.4 Immune populations and change in CT scores over 1 year

If upregulation of immune cells in the post-COVID-19 is non-pathological, but instead due to epithelial repair mechanisms, and the radiological changes reflect resolving parenchymal inflammation (as discussed in Chapter 4), then a relationship may exist between the immune subsets and changes in the extent of CT abnormalities at 1 year. To investigate this further, I looked at the relationship between the immune subsets and CT score at 1 year (Figure 7.9) and the proportional change in CT scores between the first CT (performed 3-6 months post discharge) and second CT (performed approximately 1 year post discharge, Figure 7.10).

Whilst not statistically significant, there were trends towards a higher proportion of alveolar macrophages and lower total lymphocyte and T cell proportion associated with more severe disease extent at 1 year (Figure 7.9). Furthermore, those who had a higher proportion of lymphocytes (and T lymphocytes) in the airway at 3 months, seemed to have a greater improvement of their CT findings by 1 year (Figure 7.10).

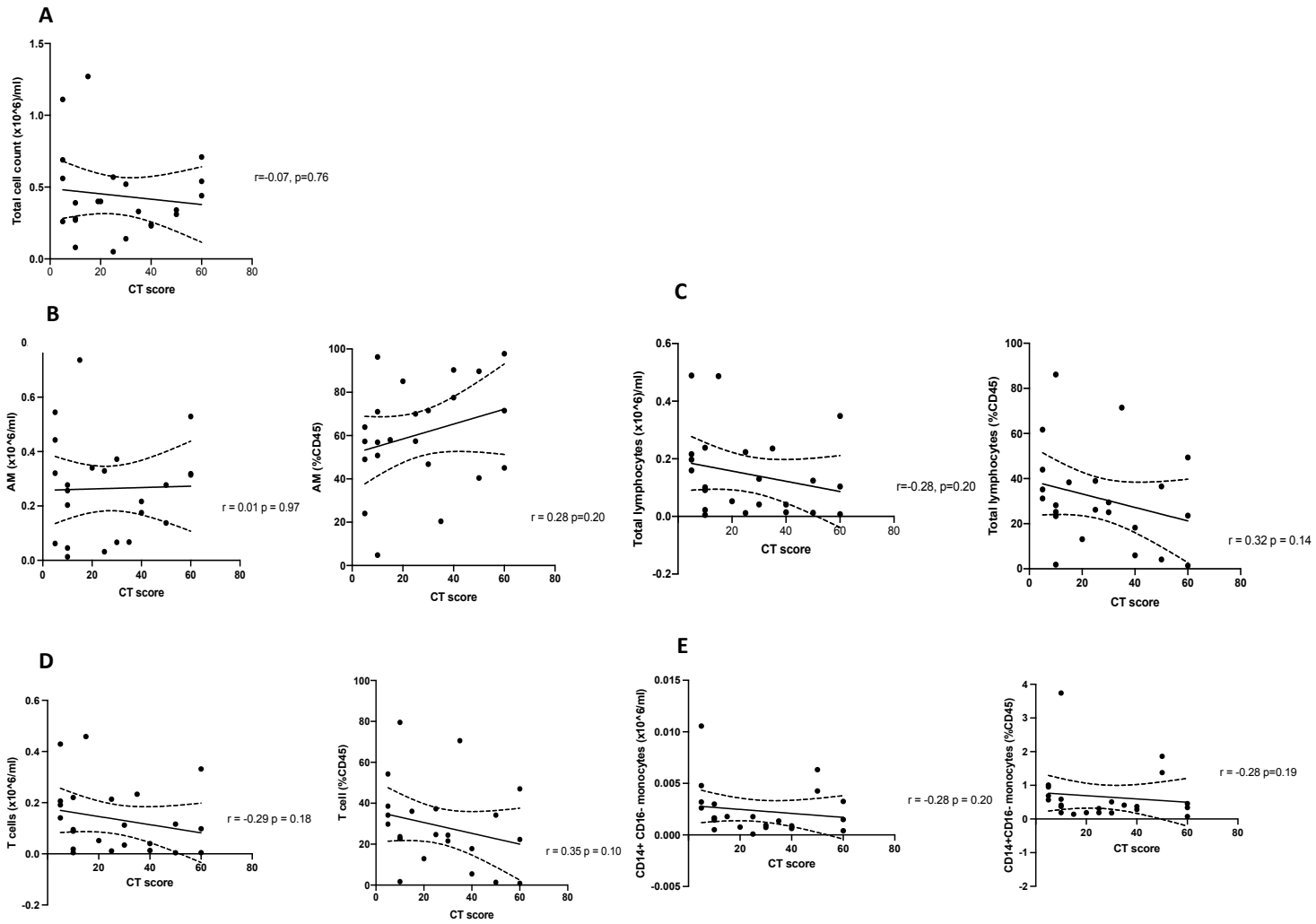


Figure 7. 9 Relationship between BALF immune cells and 1 CT score

Correlation between total white cell count (A), and absolute and % CD45+ cells of alveolar macrophages (B), total lymphocytes (C), T cells (D) and classical monocytes (E) and CT score at 1 year post discharge. Spearman rank correlation analysis performed and a p value <0.05 considered to be statistically significant. Dotted lines show 95% confidence intervals

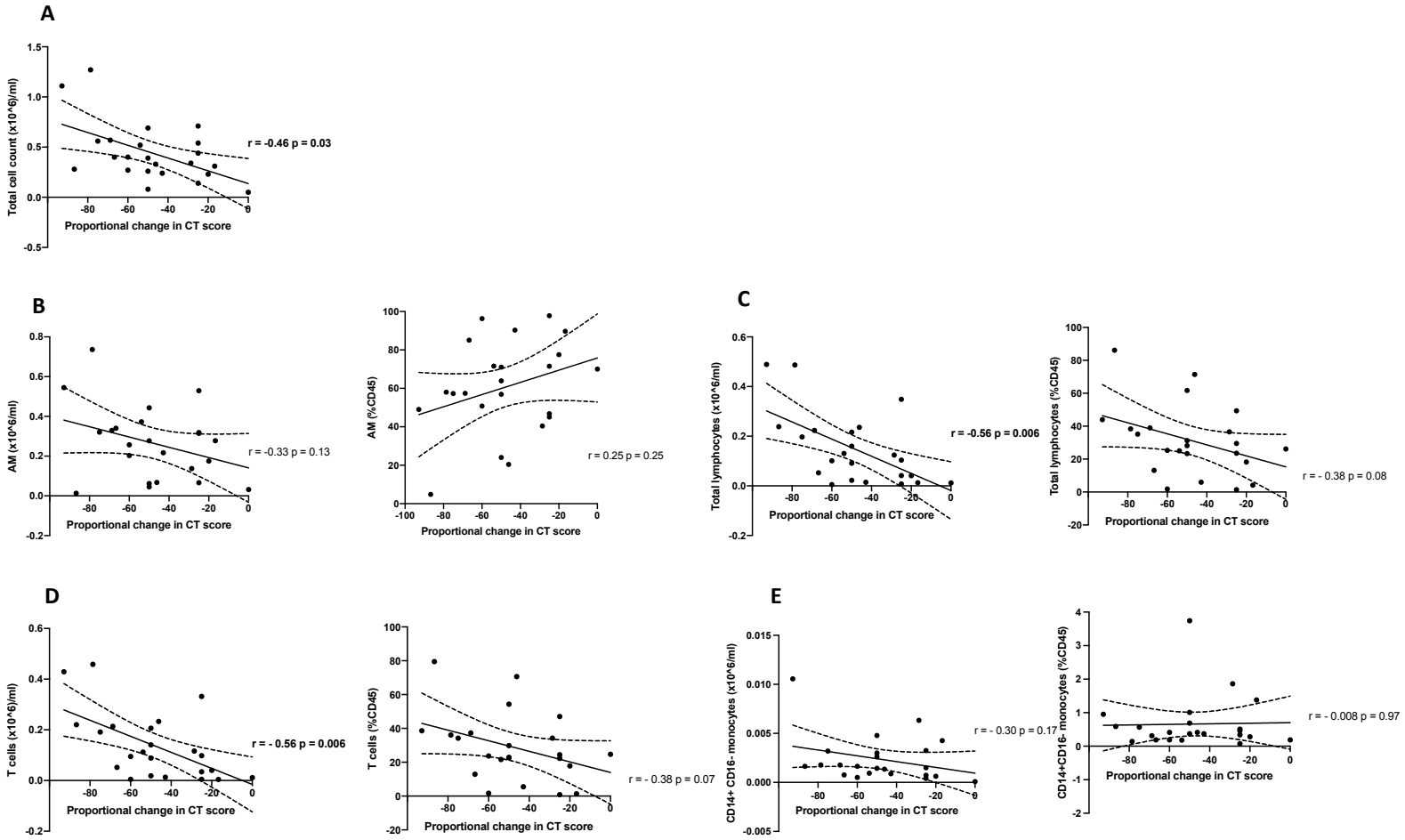


Figure 7. 10 Relationship BALF immune cells and change in CT scores between 3 and 12 months

Spearman rank correlation between total white cell count (A), absolute and %CD45+ cells of alveolar macrophages (B), total lymphocytes (C), T cells (D) and classical monocytes (E) and proportional change in CT score between first and second CT. P value <0.05 considered statistically significant

7.5.5.5 Association between immune populations and residual physiological abnormality at 1 year

To assess whether the immune subsets were associated with residual physiological abnormality at 1 year, I looked at the differences in immune subsets in individuals with normal (>=80%) and abnormal (<80%) predicted TLCO. There were no significant differences in total cell count or absolute counts of alveolar macrophages, total lymphocyte count or T cell count (Figure 7.11).

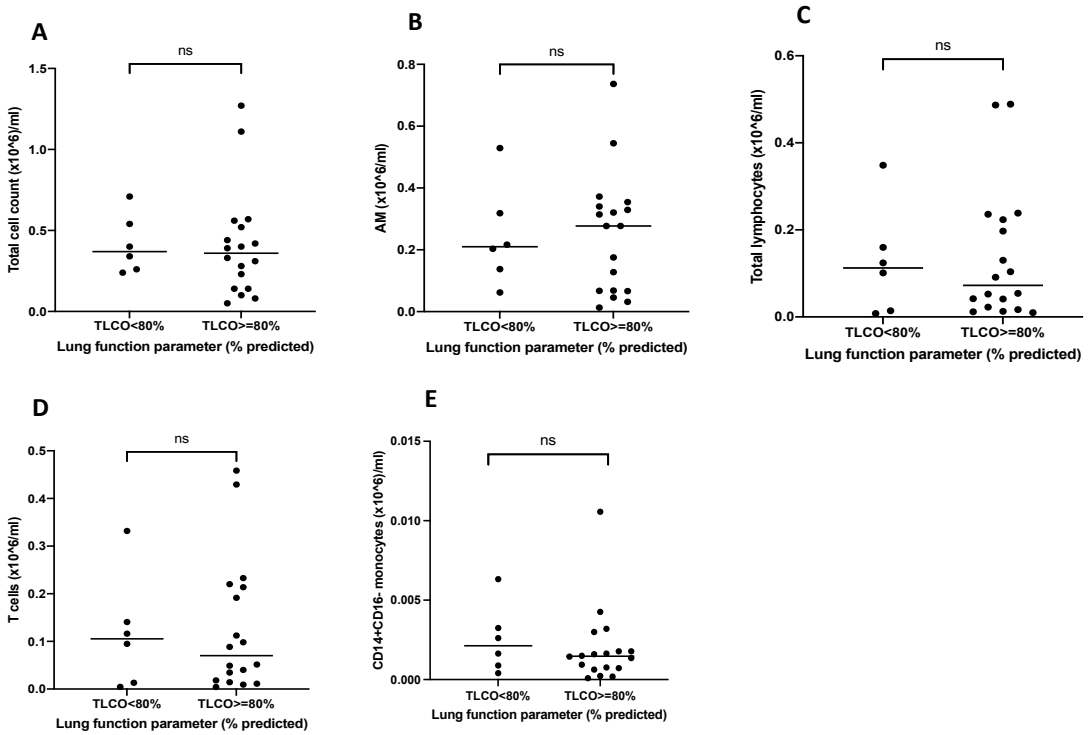


Figure 7. 11 BALF immune cells according to % predicted TLCO at 1 year.

Abbreviations: TLCO (transfer capacity of the lung for carbon monoxide), AM (alveolar macrophages). Inter-group comparisons performed used Mann Whitney U testing and a p value <0.05 was considered statistically significant. Line drawn at median.

7.5.5.6 Relationship between differential cell count analysis and flow cytometry

As described, both BALF differential cell count analysis and flow cytometry showed upregulation of immune cells in the post-COVID 19 airway 3-6 months post discharge.

Flow cytometric assessment of BALF is predominantly a research technique and is not used in the diagnostic work-up of interstitial lung diseases. However, differential cell count analysis is a well-accepted method for investigating ILD.[334]

I was therefore keen to establish whether there was any relationship between the relative abundance of alveolar macrophages, lymphocytes, eosinophils and neutrophils in the differential cell count analysis and flow cytometry data.

A positive correlation was noted between % lymphocyte on DCC and total lymphocytes detected by flow cytometry, as well as specifically with T and B cells. However, the correlation between total lymphocytes on flow cytometry and % lymphocytes on DCC was modest with a r value of 0.56 (p=0.005). Of note, even in individuals with significantly raised total lymphocytes as calculated as a percentage of CD45 cells, normal differential cell count results were seen. In addition, the proportions of lymphocytes detected by flow cytometry were higher than that seen by differential cell count analysis. In contrast, the proportion of alveolar macrophages and neutrophils were lower using flow cytometry compared to differential cell count analysis. A positive correlation was also seen between alveolar macrophages detected using flow cytometry and %macrophages on DCC (r=0.46, p=0.02).

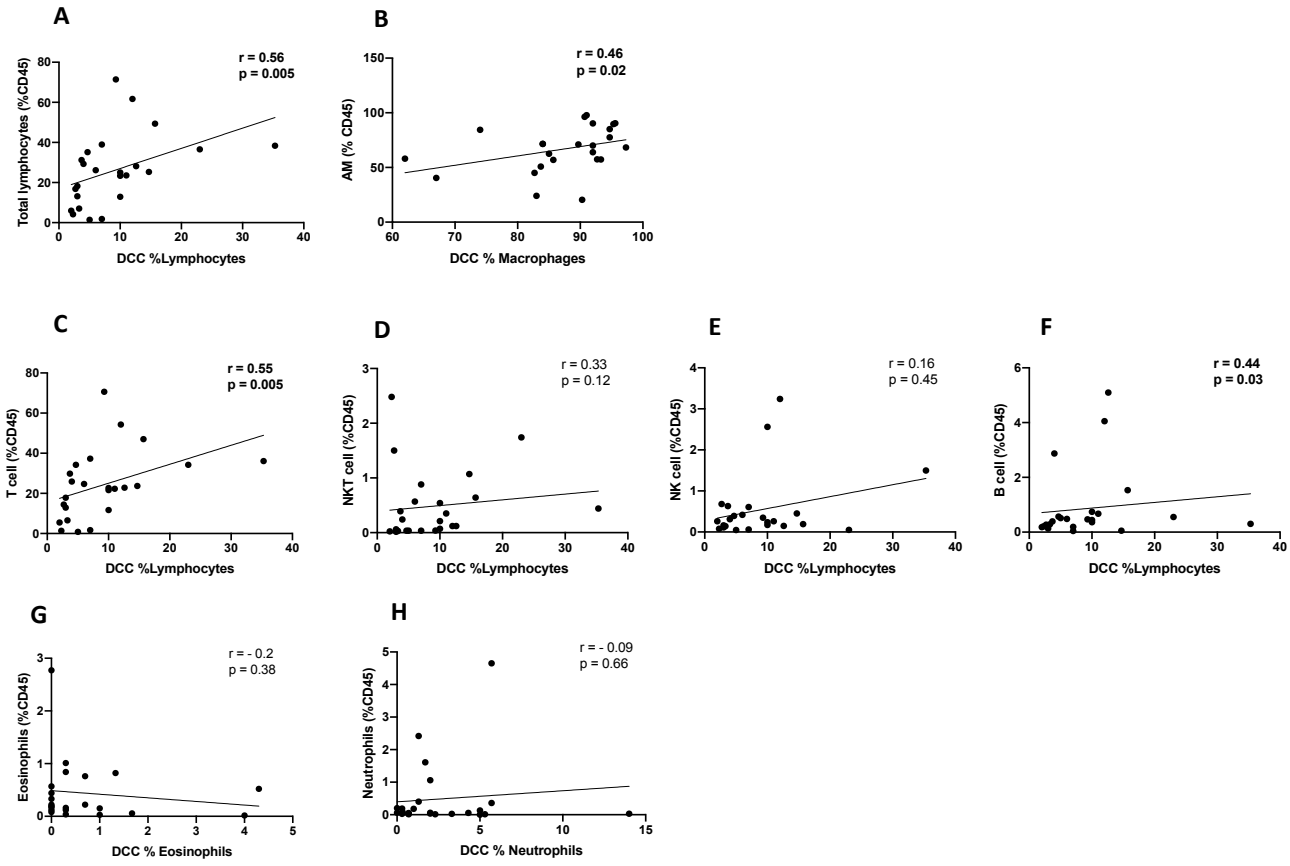


Figure 7. 12 Relationship between immune cells detected using flow cytometry and differential cell count

Different cell count (x axis), Flow cytometry counts (y axis.) Spearman rank correlation analysis performed, with a p value <0.05 demonstrating statistical significance. Correlations performed for Lymphocytes (total [A] and lymphocyte subsets [C-F]), Alveolar macrophages (B), Eosinophils (G) and Neutrophils (H). Abbreviations: DCC (differential cell count)

7.6 Discussion

7.6.1 Summary of findings

Upregulation of immune cells 3-6 months post hospital discharge for COVID-19 was noted, as identified using flow cytometry and differential cell count analysis. A higher immune cell burden was seen in those with more severe lung function abnormalities and more extensive CT involvement at 3 months. In addition, there was a trend suggesting that a higher lymphocyte proportion in the airways at 3 months may be associated with increased rate of recovery of CT abnormalities at 1 year.

Flow cytometry data only showed a modest correlation with clinical differential cell count results in terms of lymphocytosis and macrophage proportions, and no correlation with neutrophil or eosinophil proportions. Higher lymphocyte and lower macrophage and neutrophil proportions were seen using flow cytometry compared to differential cell count analysis. Significant lymphocytosis and neutrophilia were the commonest abnormalities on differential cell count analysis, and in the absence of clinically significant, detectable microbial trigger.

7.6.2 Findings in context of current literature

7.6.2.1 Upregulation of airway immune cells post COVID-19

In addition to the flow cytometry data described in this chapter, samples from this cohort were assessed using deeper immunophenotyping methods (Cytek Aurora, Cytek Bio) and sent for protein analysis using O-link. The results from this collaboration have not been covered in this Chapter but have been published.[341] The relationship between markers of respiratory disease, namely lung function parameters and CT abnormalities and flow cytometry data obtained using BD LSRFortessa (BD biosciences, USA) was corroborated by the results from the Aurora panel. Interestingly, a higher neutrophil count, higher NK cell count and higher intermediate monocyte count (CD14+CD16+) were associated with a CT abnormality >45% and a higher neutrophil count and higher B cell count associated with a FVC <90% using Aurora. These are arbitrary cut-offs, with little clinical significance, and a similar association was not seen using the data derived by Fortessa.

Similarly, with lung function tests performed at 3 months, there was a trend towards higher alveolar macrophages and lymphocytes, in individuals with lower values of FVC, TLCO and TLC (a restrictive lung function pattern) based on Fortessa data. Finally, stratifying the data according to abnormal (<80%) or normal (>=80% predicted) TLCO, there was no difference when using Fortessa, but a significantly higher neutrophil burden was seen in those with lower TLCO using the Aurora panel.

The Aurora panel allowed us to differentiate between CD4 and CD8 T cells; the raised lymphocytes in the post-COVID-19 airways were predominantly CD8+ T cells as suggested by strong correlations between T cell populations and CD8a protein but not CD4.

The decrease in CD14+CD16- (classical monocyte) proportions seen in the post COVID-19 airways using the Fortessa data was discordant with another study evaluating the post-COVID-19 airway microenvironment at follow up, where an increase in monocytes was seen.[414] However, CD8+ T cells,

as in our results, were also found to be the commonest abnormality in the airways in individuals with persistent CT abnormalities post COVID-19. Peripheral immune subsets, however, were comparable to that found in healthy controls.[415]

7.6.2.2 Potentials reasons for immune cell upregulation

7.6.2.2.1 Epithelial repair

The reason for persistent upregulation of immune cells is not clear but the significantly raised lactate dehydrogenase (LDH) in the post-COVID-19 cohort compared to healthy controls might offer an explanation. The presence of LDH, an intracellular enzyme, in the extracellular space is suggestive of loss of epithelial cell integrity, thus suggesting persistent epithelial damage and by inference, incomplete repair mechanisms.[416] Furthermore, a raised LDH in the peripheral circulation has prognostic significance in many respiratory conditions, including interstitial lung disease[417] and has similarly been shown to be a good predictor of respiratory failure in COVID-19.[418]

One could postulate from this, that it is epithelial damage that is causing persistent activation of the immune system. Conversely, it is also possible that an overactive immune system is in fact the culprit perpetuating epithelial damage, which may explain why the BALF LDH continued to rise in 2 of the 3 individuals who underwent repeat endobronchial sampling at 1 year post discharge. To add to this, CD8a protein was strongly correlated with CASP3 and EPCAM in the proteomics, which are markers of ongoing epithelial damage. In particular, CASP3 is produced by expanding CD8+ T cells in response to an antigen, even in the absence of cellular death.[419] However, caspases are well recognised mediators of cell death[420] and as proteomic assessment of BALF at 1 year post-COVID 19 was not performed, it is not possible to decipher whether upregulation of CASP3 at 3 months was a transient effect or represents the initiation of programmed cell death. However, continual improvement in CT changes and lung function parameters (as described in Chapters 4 and 5) might infer that it is the former.

Neutrophilic infiltration was seen in both the differential cell count analysis and Aurora data, but not Fortessa data. Neutrophils play a prominent role in tissue repair through activation of matrix metalloproteinase 9 (MMP 9).[404,421] The persistence of neutrophilia in the post-COVID-19 airway may therefore be a result of ongoing repair processes in the lung. They also have a role in inducing angiogenesis which is necessary for wound healing.[422–424] However, as one of the early responders of the innate immune system to infection, primarily killing pathogens through oxidative burst and phagocytosis, neutrophils also release neutrophil extracellular traps (NETS) to counter pathogens,

which can be deleterious to the surrounding tissue.[425,426] The role of NETosis in acute-COVID-19 has been well established,[427] and more recently, NETosis has been implicated in persistent respiratory morbidity at follow-up.[311] Furthermore, in patients with established idiopathic pulmonary fibrosis, BALF neutrophilia is associated with worse disease outcomes, namely higher mortality and increased disease progression.[428] Therefore, persistent neutrophilia may cause ongoing immune injury to the epithelium and lung parenchyma contributing to the persistent morbidity seen post COVID-19.[429,430]

7.6.2.2.2 Persistent antigenic stimulation

It remains possible that local immune activation is in response to a persistent microbial trigger, which hasn't been identified on routine clinical tests.

Viral antigen

A study in Spain showed the persistence of viral RNA in the peripheries of patients with persistent clinical symptoms, 4 weeks post-acute illness and in another study,[256] persistent viral RNA in the BALF was detectable up to 46 days after the onset of symptoms.[431]

In the collaborative work, published in Immunity, there was a strong relationship between SARS-COV2 specific antibodies and activated CD4 and CD8 T cells, in the absence of immunization at time of bronchoscopy. This again suggests ongoing adaptive immune responses to a viral antigen, with persistence of antigen being a plausible reason. Measuring viral RNA in the BALF pellets may add clarity to this hypothesis.

Microbial antigen

In addition, a dysregulated microbial signature has been seen in acute COVID-19, with a predisposition for opportunistic pathogens,[432] of which more than 50% were viruses. However, whilst these organisms were potentially pathogenic, whether they were causing true infection in these individuals is not known. Furthermore, evaluation of the respiratory microbiome during severe illness shows reduced alpha diversity, patient-specific microbial findings and dynamic changes, with Staphylococcus being a common finding.[433] In addition to this, autopsy samples have suggested dominance of taxa capable of causing secondary infections, such as Staphylococcus aureus, Klebsiella pneumonia and Enterococcus faecium in individuals post COVID-19.[434] It is important to note, however, that the lung

microbiome can also be altered in mechanically ventilated individuals who did not have COVID-19.[435,436]

Fungal antigen

A fungal signature has also been shown, for instance, candida species, in intubated individuals compared to non-intubated patients.[437]

Autoantigen

Hypersensitivity pneumonitis (HP), with which the CT findings may be compatible, is thought to be due to immune hyperactivation in response to an inhaled antigenic stimulus.[438] Whilst sometimes, this stimulus can be identified, for instance, exposure to avian antigens, in >50%, the stimulus is unknown.[439] The inciting antigen could be microbial in origin and additionally, viruses have been shown to increase susceptibility to hypersensitivity pneumonitis by augmenting the antigenic-presenting capacity of macrophages and also delaying antigen clearance, thus perpetuating an inflammatory cascade.[117] In this manner, another possibility worth considering is that infection with SARS COV2 may have increased susceptibility to environmental antigens, not related to the acute infection, in genetically-prone individuals.

Summary

In our cohort, a variety of fungi and viruses were detected, and the dominant bacteria were Klebsiella and Staphylococcal species. It is likely, however, that these were merely commensals, rather than causing true infection as determined by the patients' clinical status and trajectory. Whilst speculative at this stage, in the absence of evaluation of the microbiome in the post COVID-19 cohort, it is possible that host-immune interactions due to an altered microbial signature may be contributing to the upregulation of immune cells seen. However, dysregulated repair mechanisms, unrelated to a pathogenic trigger is also possible.

7.6.2.3 Immune subsets and severity of acute disease

In neither the flow cytometry, nor the differential cell count data was there any association between severity of acute disease and immune subsets. This may be due to host factors, independent of the degree of epithelial damage, playing a role in recovery.

7.6.2.4 Better resolution of CT abnormalities in individuals with higher T Cell populations

In the data described, a higher T proportion was associated with a greater rate of radiological resolution at 12 months and individuals with lower T cells at 3 months had more significant CT findings at 1 year. As described, the likelihood is that the T cell population is being driven by CD8+ T cells, so it is possible that enhanced antigenic clearance by the CD8+ T cells may be related to accelerated radiological resolution. In contrast, those who have not mounted an appropriate T cell response, may not be able to clear the antigen as swiftly.

7.6.2.5 Reasons for differences between the immunophenotyping methods

The differences between Fortessa data and differential cell count analysis are important to note. Firstly, a lower macrophage percentage was noted using flow cytometry. The CD206 cell surface marker was utilised to identify macrophages, a cell-surface marker associated with tissue-resident macrophages. As aforementioned, macrophages display plasticity and the cell surface markers may vary accordingly.[374] Furthermore, the decrease in classical monocyte proportions seen in the post COVID-19 airways in conjunction with an increase in alveolar macrophages, could suggest an increase in M1 (pro-inflammatory) macrophages, and a more specific marker for M1 macrophages, for instance CD80 might have identified higher macrophage numbers. A lower neutrophil proportion was seen in the post COVID-19 cohort as compared to healthy controls in the flow cytometry data. Red lysis buffer can result in neutrophil death, although whilst a plausible theory, the same protocol was utilised for both healthy controls and post-COVID-19 donors. The CD177 cell surface marker was used to identify neutrophils, a marker associated with neutrophil activation and shown to be associated with disease severity in COVID-19.[440] It is possible, that whilst neutrophils are present in the post COVID-19 airways, they are not activated. By using other neutrophil markers, such as CD15, a marker for immature neutrophils or CD16, for mature neutrophils, the results might have shown a different trend and been more in line with the Aurora and differential cell count data.[441] Finally, the differences in lymphocyte proportions might be due to lymphocytes in the post COVID-19 airway being predominantly activated CD8+ T cells (as confirmed using the Aurora panel), which are typically larger, morphologically, and may be misidentified as macrophages, especially as no distinction was made between monocytes and macrophages in the differential cell count analysis.

7.6.2.5 Clinical Utility of BALF in investigation radiological changes post COVID-19

The clinical utility of BALF differential cell count analysis has for long been questioned, even in non-COVID-19 illnesses. These results are often affected by multiple variables, including sampling site, operator experience, transport and handling of the samples and timeliness of analysis.[334] Furthermore, moderate increases in immune subset proportions may not be associated with clinical pathology. In my cohort, no consistent immunological change was seen, thus potentially pointing towards multiple overlapping phenotypes.

BALF lymphocytosis >25% is often seen in granulomatous infiltration, such as sarcoidosis or chronic hypersensitivity pneumonitis (CHP), but lymphocytosis can also be seen in other interstitial lung diseases such as non-specific interstitial pneumonia or organizing pneumonia.[442,443] Typically, BALF lymphocytosis is higher in CHP than in other interstitial lung diseases, such as IPF or sarcoidosis, but a sensitive and specific cut-off is difficult to define.[444] Although the CT changes seen post COVID-19 are similar to that seen in chronic hypersensitivity pneumonitis, the degree of BALF lymphocytosis was only modest. One individual had a significantly raised BALF lymphocyte proportion of 35%. The medical treatment of HP is dependent on multiple factors, but steroid therapy is often initiated in those who have significant lung function impairment, radiological changes and/or symptom burden.[445] In this aforementioned individual, despite the significant lymphocytosis and lack of steroid therapy, there was significant improvement in both radiological and clinical features at 1 year, with further improvement at 2 years. This may suggest that a) if antigenic stimulation was the causative factor, then antigen clearance is likely to have been achieved by 1 year b) the antigenic stimulation is less likely to be due to increased and maintained susceptibility to environmental antigens as the patient's environmental exposures had not changed. Furthermore, from a clinical standpoint, subjecting a patient to an invasive procedure may not in fact alter the clinical management as no additional medical management was initiated in this case.

Next to lymphocytosis, neutrophilia was the commonest finding on differential cell count analysis. Again, as discussed earlier, clinically significant microbial triggers were not identified, again questioning the utility of sampling in these individuals.

Whilst eosinophilia was seen in our cohort, eosinophil counts were not raised to levels seen in acute eosinophilic pneumonia[446] and did not influence clinical management. Again, eosinophils are important in response to tissue repair which may have been the reason for the elevation seen.[447]

Finally, in my cohort, mixed cellularity was seen in one individual, which can be found in organizing pneumonia[448] a phenomenon sometimes seen post viral infection or ARDS [120,295] and one of the histological findings in SARS-COV2 infection.[294,449]

So, to summarise, the clinical differential cell count analysis results, whilst informative, have not shown much utility in pin-pointing a diagnosis or guiding clinical treatment. It is possible that the abnormalities seen reflect ongoing repair mechanisms in the lung, or represent a self-limiting, immune-mediated interstitial lung disease.

7.6.2.6 Temporal improvement

In a small subset of individuals who underwent repeat endobronchial sampling 1 year post discharge, there was a decrease in the number of T cells, B cells, NK T cells, NK cells, neutrophils and alveolar macrophages, nearly to the levels of healthy individuals. The proportion of CD8+ T cells decreased with time, although the degree of activated T cells remained constant.[341] Again, one potential reason for this is ongoing attempt at pathogen clearance. Of note, only three individuals had repeat endobronchial sampling, with all having had severe or very severe acute disease presentations. Therefore, it is not possible to comment on whether these findings can be extrapolated to other disease severities and the possibility of donor-specific findings is important to consider.

7.6.3 Clinical relevance of findings

So far, this work suggests that endobronchial sampling to investigate CT abnormalities is of unclear benefit. Abnormalities found don't point towards any specific ILD. Ongoing activation of immune cells 3-6 months post COVID-19 in the absence of a microbial trigger is potentially an alarming finding, but in the context of an overall improvement in CT findings in the majority, it is possible that these immune findings represent ongoing repair mechanisms and may not be pathological in nature.

7.6.4 Limitations

Firstly, the small sample size is a limitation, but this is the largest sample size published on to-date. Secondly, timing from sampling to differential cell count analysis is not known, with longer time delay resulting is less reliable results. However, this is the same process by which clinical differential cell counts are calculated in clinical practice so reflects the challenges in interpretation of differential cell count analysis in clinical work. Thirdly, the lack of BALF collected during the acute infection is also a limitation, as it prevents interpretation of the trajectory of the immune populations from acute disease presentations to follow up. Fourthly, the healthy control data utilised was using endobronchial samples collected before the COVID-19 pandemic. A better control group would have been individuals who had been treated for COVID-19 and had normal CT scans at follow-up. Finally, it is important to note that the majority of the individuals sampled had been admitted to hospital for COVID-19, and we therefore sampled the severe end of disease presentations. Sampling those requiring community management only would have enabled further understanding of whether the severity of the acute presentation affects the immune signature at follow up. This latter two suggestions would necessitate an amendment to the protocol and ethics in order to enable endobronchial sampling in the absence of clinical need, i.e. for research purposes.

7.7 Conclusion

In this Chapter, I have shown that there is persistent immune cell upregulation post COVID-19, even 3-6 months post hospital discharge. The underlying mechanism driving this is not clear, but the possibility of a microbial trigger should be considered and would be compatible with the additional observation of accelerated CT recovery in individuals with higher airway lymphocytes.

Chapter 8 - Evaluating epithelial function post COVID-19

8.1 Introduction

8.1.1 Studying epithelial cell biology

The airway epithelium is the first line of defence against pathogens and not only forms a mechanical barrier, but also initiates part of the first immune response against invading pathogens.[450] The differentiated airway epithelium, consisting of ciliated cells, goblet cells and club cells, which together form the muco-ciliary escalator, facilitates the movement of pathogens from the airways to the back of the throat. In addition to this, tight junctions and the apico-basal polarity of the epithelial cells further enhance the mechanical barrier function thus protecting the airway epithelium and underlying lung parenchyma from microbial injury.[450] After SARS-COV2 infection, extensive damage to the airway epithelium and alveolar cells has been reported and although there is evidence of epithelial regeneration in vitro, the timescale for this in vivo is not known.[76,124,451]

Through RNA sequencing, different cell types lining the respiratory epithelium have been identified. These specific cell types can be identified according to the cell surface markers they express. For instance, basal cells harbour the surface markers keratin 5 (KRT5) and transcription factor tumour protein p63 (TP63); Goblet cells express MUC5AC; Ciliated epithelial cells express FOXJ1.[452,453] In addition, differences in cellular distribution have been shown, with basal cells being found in greater abundance in the lower airways compared to the upper airways and in different cell states, depending on their maturity: For instance, less mature basal cells express greater amounts of TP63. Similarly, two different states for goblet cells and ciliated cells have been described, with the lower airways consisting of goblet 2 cells, which highly express genes associated with immune cell recruitment, such as CXCL10, and ciliated 1 cells, which express genes associated with cytoprotection, such as PROS1:[453,454] a gene encoding Protein S, which has been shown to be protective in idiopathic pulmonary fibrosis.

Basal cells are the stem cells of the respiratory epithelium and are the precursors to secretory and ciliated cells.[455] The airway epithelium is continuously replaced by basal cells and this process is especially important after epithelial injury.[456] Basal cells can transition from a quiescent stage to enter the cell cycle in the context of inflammation, and one proposed trigger for this is through the detection of apoptotic cells.[457] Furthermore, it has been suggested that epithelial basal cells may retain memory of their disease state, thus resulting in persistence of a disease phenotype.[458] Studying the behaviour

of basal cells is therefore extremely important in furthering our understanding of the regenerative capacity of the airway epithelium after SARS-COV2 infection.

Epithelial cells can be studied in submerged culture, but in this model, cells do not undergo differentiation or form tight junctions. In contrast, using the air-liquid interface (ALI) model, where the cells are in contact with media basally and in contact with air, apically, basal cells undergo differentiation to mimic the pseudostratified epithelium seen in the airways.[452,459,460] Using the latter approach is therefore more representative of the human airway epithelium. Differentiated epithelial cells grown at ALI may also retain age[461] and disease characteristics of the donor[462], thus making them a useful model to study human epithelial behaviour. In fact, our understanding of many diseases has been enhanced by the use of ALI cultures.[462–466]

In vitro studies have shown that the alveolar epithelium does regenerate after SARS-COV2 infection, but neither the timescale for this in vivo, nor the regeneration potential of bronchial epithelial cells, is known.[80] In the event of aberrant or ineffectual repair mechanisms, the damaged epithelium may result in an ineffective response to further injury, thus potentially further perpetuating epithelial damage. In a clinical context, this may result in increased susceptibility to recurrent respiratory tract infections, or result in chronic airway or parenchymal abnormalities, such as those seen in COPD and IPF.

8.1.2 Studying epithelial responses to injury

Epithelial response to injury can be assessed by inducing a mechanical wound or by introducing an infective agent.

8.1.2.1 Mechanical injury

A scratch assay is a relatively cheap and easy method for assessing wound healing and cell migration in vitro.[467] Repair of an epithelial layer defect is dependent on cell migration and in larger wounds, cell proliferation,[170] therefore defects in wound closure may indicate problems in either of these mechanisms.

8.1.2.2 Virus-induced epithelial injury

Influenza A and B viruses cause seasonal epidemics and account for between 12 and 52 000 deaths per year.[468] In vitro studies have shown that infection with influenza can result in altered immunity for 1 month after infection, conferring additional protection against bacterial infection.[469] Influenza A virus (IAV) infects epithelial cells lining both the upper and lower respiratory tract through binding of haemagglutinin to α2,6-linked sialic acid (α2,6-SA) on the host cell.[470] Viral replication and release of viral particles can occur as early as 24 hours post infection, with resultant cellular apoptosis in an attempt to control the infection and subsequent desquamation of the airway epithelium.[471–473] Epithelial cell regeneration then occurs with proliferation of uninfected cells, differentiation of progenitor basal cells and mucous metaplasia.[474] Since influenza causes significant morbidity and mortality, epithelial responses to IAV in PBECs post COVID-19 would offer new insights into additional precautions that might be important for individuals post COVID-19 during the influenza season.

8.1.3 Epithelial-mesenchymal crosstalk

Fibroblasts play an important role in repair[475] and produce a range of extracellular matrix proteins and growth factors which facilitate wound healing.[476] After acute lung injury, fibroblast proliferate and differentiate into myofibroblasts, expressing alpha SMA, with myofibroblasts being the predominant source of type 1 collagen, across which, epithelial cells can migrate.[477] Fibroblasts attend the site of injury within 24-48 hours of the injury[478] and break down the fibrin clot by secreting metalloproteinases (MMPs) and also deposit extracellular matrix components such as collagens, laminin and proteoglycans.[479] Fibroblasts are summoned to the site of injury by molecules such as platelet-derived growth factor (PDGF) and other epithelial-derived mediators, which subsequently regulate fibroblast proliferation.[480] Therefore, epithelial-mesenchymal crosstalk is essential to ensure timely and effective wound healing.[170] Abnormalities in epithelial-mesenchymal communication have been associated with the development of chronic disease.[481,482]

8.2 Background

In Chapter 7, I showed that there is upregulation of immune cells in the post COVID-19 airway, even several months after initial infection with SARS-COV2. Coupled with the sustained upregulation of markers associated with epithelial cell damage, these findings suggest that epithelial repair mechanisms may still be impaired at this timepoint.

8.3 Hypothesis and Aims

Hypothesis:

PBECs from patients post COVID-19 display aberrant wound healing and mount an exaggerated immune response to infection with influenza A in comparison to PBECs from healthy individuals.

Aims:

1. To assess the baseline characteristics of post-COVID-19 airway epithelial cells at air-liquid interface
2. To assess epithelial response to both mechanical injury and viral injury (IAV)
3. To assess the effect of conditioned media from IAV-infected PBECs on fibroblast migration.

8.4 Methods

Epithelial cells were expanded from cryopreservation and grown in submerged culture or to air-liquid-interface as described in Chapter 2.

8.4.1 Baseline characteristics at ALI

Epithelial cells were cultured at air-liquid interface and either harvested for RNA or fixed in 4% PFA for imaging at 3 weeks post air-exposure. Barrier integrity was assessed by measuring trans-epithelial electrical resistance (TEER). TEER measurements were taken from 12 inserts per donor using EVOM2 Epithelial Volt/Ohm Meter (World Precision Instruments) and an average calculated.

Epithelial cell differentiation was assessed by evaluating genes associated with specific cell types, as discussed earlier, using qPCR, visualisation of cilia and immunofluorescence staining.

8.4.2 Response to injury

8.4.2.1 Mechanical injury: Submerged culture

Epithelial cells were seeded at a density of 3 x10^4 cells in a 24-well plate (Corning), pre-coated with Type 1 collagen (PureCol, Advanced BioMatrix) and allowed to proliferate in airway epithelial cell growth media (Promocell) until a confluent monolayer was formed. A linear wound was then made to the surface with a P200 (yellow) pipette tip and the rate of wound closure assessed over a 24-hour period using JuliTM Stage Real-Time Cell History Recorder (NanoEnTek,Seoul, Korea) which captured time-lapse Brightfield images. Adequate response to injury was defined as achieving wound closure in a similar timeframe to healthy control PBECs (i.e., individuals who had no prior diagnosis of lung disease). Percentage wound closure from baseline was calculated over time using JuliStat (JuliStage software). 2-4 experimental replicates were used for each donor, with 3-4 images taken of each well, where possible.

8.4.2.2 Influenza challenge at air-liquid interface

Fully differentiated airway epithelial cells were infected with either live influenza A Virus/England/195/09 or UV-inactivated influenza A virus (mock) at a multiplicity of infection of 0.01. Barrier integrity was measured using TEER, and apical and basal supernatant collected 24-hourly for measurement of interferons, inflammatory and wound healing proteins using ELISA. RNA was harvested every 24 hours to allow assessment of gene expression using qPCR. Finally, cells were fixed in 4% PFA for Haematoxylin and Eosin (H+E), Periodic acid Schiff (PAS) and immunofluorescence staining. To summarise, the timepoints for collection were a) Baseline (pre-infection) b) 24hpi c) 48hpi d) 72hpi and d) 96hpi.

Influenza A virus was constituted in serum-free DMEM (Gibco) and 100 mcl of live IAV or UV-inactivated IAV was added to the apical compartment for one hour, and then subsequently removed. UV inactivation was performed using Stratalinker UV 1800 Crosslinker (Stratagene). Figure 8.1 outlines the measurements taken for the IAV challenge.

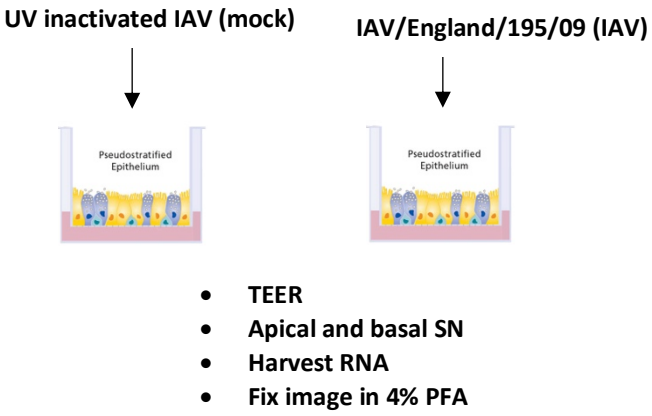


Figure 8. 1 Overview of IAV challenge

8.4.3 Fibroblast scratch assay

Human lung fibroblasts from healthy donors (Lonza, P5) were expanded from cryopreservation in a T75 uncoated flask and allowed to proliferate in DMEM (Gibco) supplemented with 10% FBS (Gibco). When 80-90% confluent, the cells were split and seeded at a density of 1.5 x 10^4 cells in an uncoated 48-well plate (Corning). When a confluent monolayer had formed, the cells were serum-starved for 24 hours before experimentation. A linear wound was made to the surface of the monolayer with a P200 (yellow pipette). 200µl of conditioned media from the IAV-infected ALI cells was added in a 1:2 dilution with DMEM/FBS. Time-lapse brightfield images were taken every 2 hours for 24 hours using JuliTM Stage Real-Time Cell History Recorder. Percentage wound closure was calculated using the JuliStat (JuliStage software).

8.5 Results

8.5.1 Epithelial cell scratch assay

Figure 8.2A shows how wound closure was calculated: Epithelial cells are detected by the JuliSTAT software after careful adjustment of the exposure and sensitivity settings on the Juli. Wound closure is set at 0% at time zero (i.e. a fully open wound) and as the epithelial cells migrate closer, the percentage of the wound closed is calculated. Therefore, when there is no break in the epithelial barrier, 100% wound closure has been achieved. The top panel shows the wound in PBECs from HC donor 1037, with the bottom panel showing images from the post COVID-19 donor 1082.

At 24 hours after scratch, post COVID-19 donor PBECs had achieved a mean of 72.3% +/- 5.8 wound closure compared to 98.3% +/- 1.0 achieved by healthy control (HC) PBECs (p=0.01) [Figure 8.2B]. The healthy control donors from whom PBECs were obtained for Figure 8.2B were collected before the COVID-19 pandemic and therefore these individuals would not have had exposure to SARS-COV2. After adding further HC donors for comparison, the mean % wound closure achieved by HC PBECs was lowered to 88.2 +/- 4 (8.2 C) and no statistically significant difference was present between post COVID-19 and HC PBECs at 24 hours (p=0.25). Whilst this may be due to biological variance in HC donors, with a larger sample size therefore being more representative of the variance seen, the possibility of aberrant behaviour of epithelial cells from HC donors collected during the pandemic needs to be considered. In fact, there was a difference in wound closure between HC PBECs collected pre- and post-pandemic, with the latter only achieving 75.8% (+/-9.1) wound closure compared to 98.3% (+/-1.3) pre-pandemic (8.2D) at 24 hours.

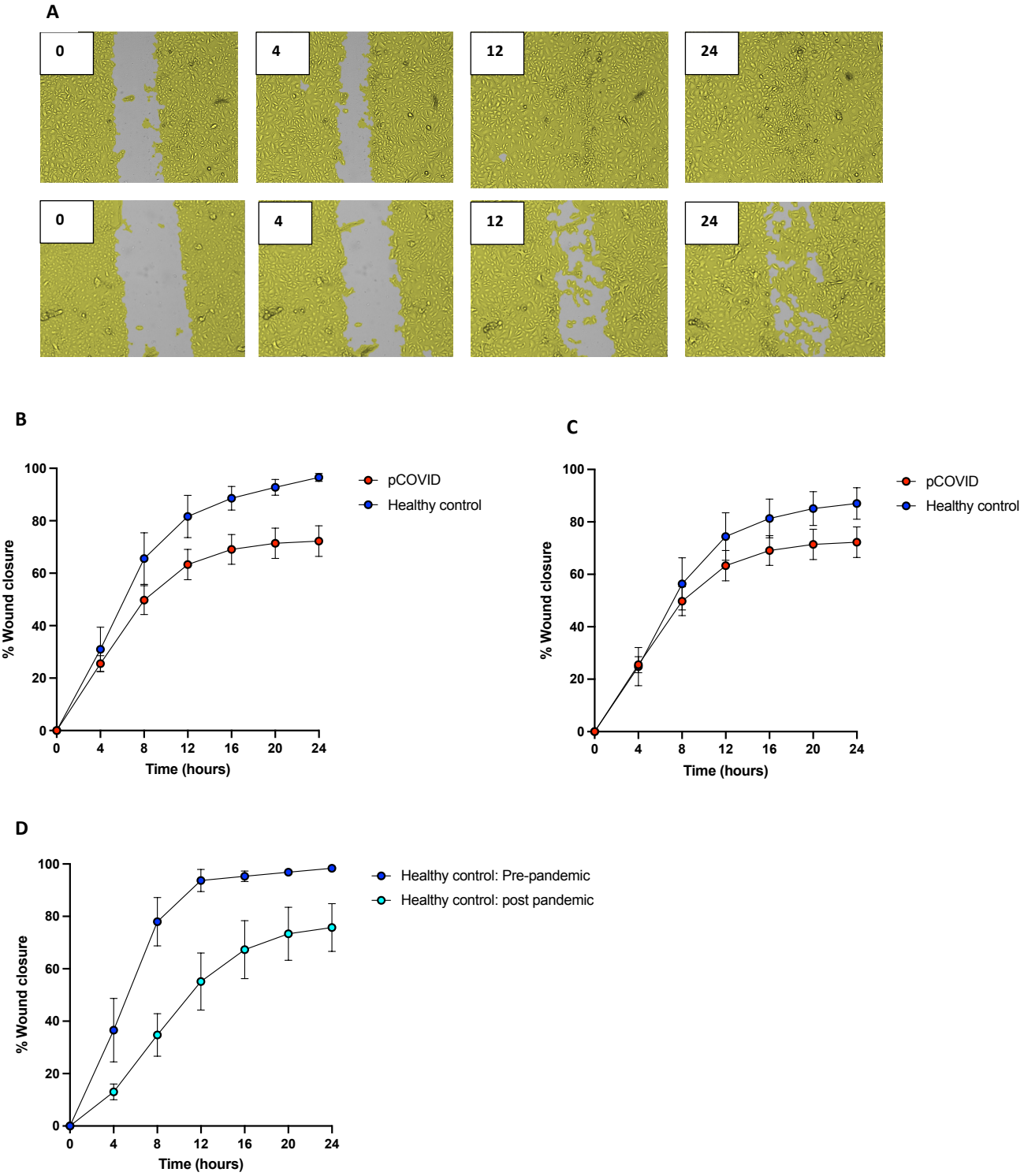


Figure 8. 2 Wound healing assay.

Wound closure in PBECs from post COVID-19 donors (n=16) and healthy controls (n=8). Results for post COVID-19 and healthy control donor PBECs collected pre-pandemic only (n=4) (B) and all healthy control donors (n=8) (C) shown. Differences between wound closure in healthy control PBECs pre- and post-pandemic shown in D. Representative images shown in A in healthy control (top panel) and post COVID-19 donor (bottom panel), at time points 0, 4, 12 and 24 hours post injury. Data displayed as mean (+/-SEM).

8.5.2 Epithelial cell proliferation

The defect in wound closure may be due to a defect in cellular migration, or due to ineffectual cellular proliferation. In small wounds, epithelial cell migration alone might be sufficient to close the gap. However, in larger wounds, cell proliferation is also required.[170] To investigate this, PBECs from post COVID-19 and HC donors were seeded on a 24-well plate (Corning) at a seeding density of 3×10^4 cells/ well and allowed to grow in airway epithelial growth media (Promocell), which was refreshed every 48 hours. Figure 8.3A shows examples of how epithelial cells were identified by JuliStat and the change in confluence over time in a HC donor (1037) and post COVID-19 donor (1052). Initially, the proliferation assay was run for 7 days, which revealed that full confluence is achieved in approximately 4-5 days (96 – 120 hours) post seeding, at which point the proliferation rate plateaus (8.3B). There were no obvious differences between HC and post COVID-19 PBECs. Due to limited availability of the JuliTM Stage Real-Time Cell History Recorder, subsequent proliferation assays (n=3 HC) were run for 48 hours, and Figure 8.3C shows the similarity in proliferation indices when measured up to 48 hours in HC and post COVID-19 PBECs. Log2fold change from baseline was calculated, rather than % confluence alone, as the % confluence varied slightly between wells, although was usually between 30-40% at time zero. Therefore, a change relative to the baseline was elicited. As wound closure was different between healthy controls pre- and post-pandemic in Figure 8.2D, I wanted to assess if this was due to a difference in cellular proliferation, which was subsequently shown to not be the case (8.3D). Overall, proliferation rates were comparable between HC and post COVID-19 donor PBECs.

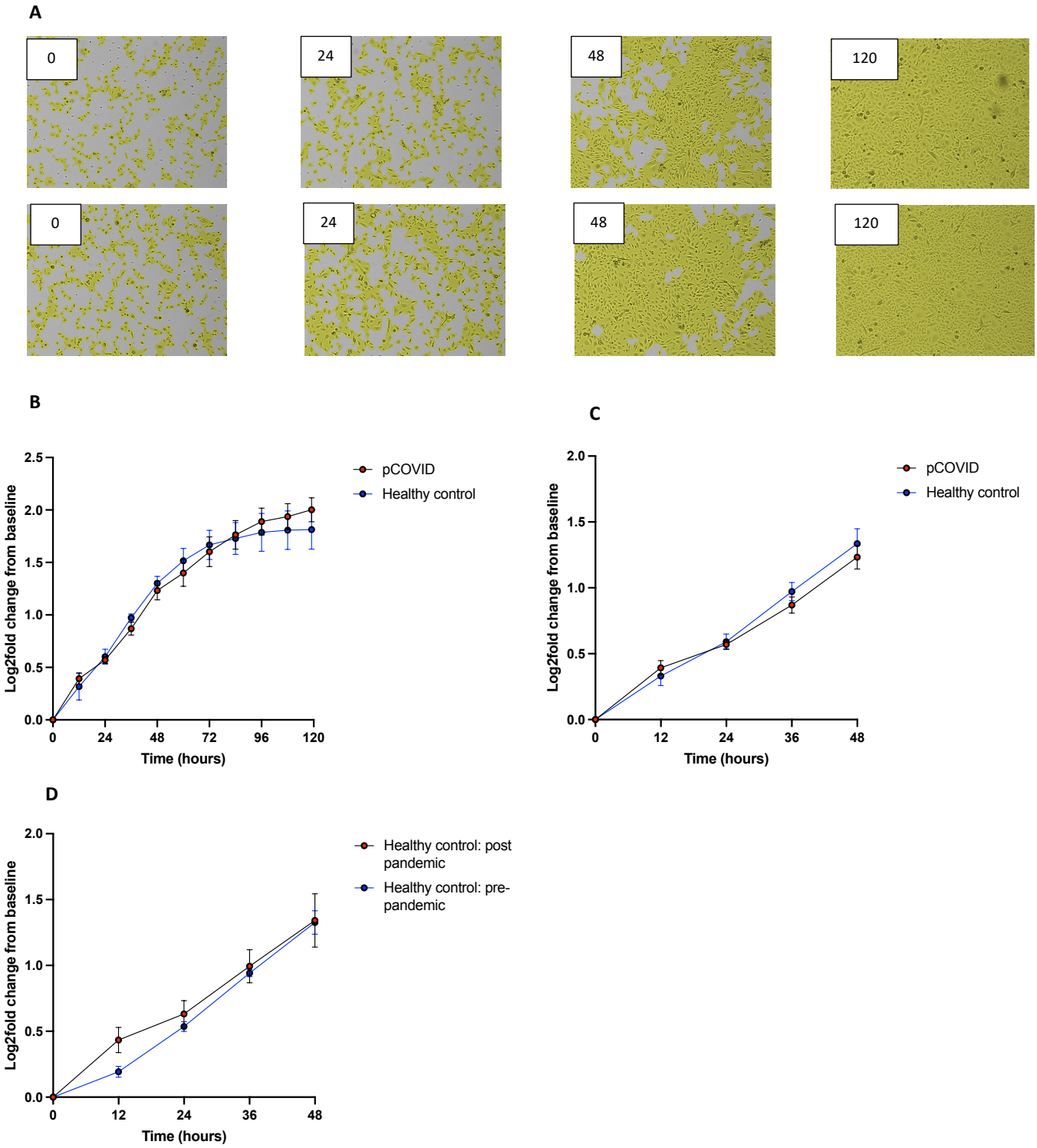


Figure 8. 3 Proliferation assay

Proliferation assay run for 120 hours in n=4 HC and n=15 pCOVID donors (B) shows similar proliferation rates from baseline with proliferation rates plateauing between 96 and 120 hours. Representative images shown in A, in HC donor (top panel) and post COVID-19 donor (bottom panel). Proliferation rates over 48 hours shown in n=7 HC and n=15 pCOVID (C). Proliferation rates in healthy control PBECs pre COVID-19 (n=3) and post COVID-19 (n=4) shown in D. Data displayed as mean (+/-SEM).

There was significant heterogeneity in wound closure in post COVID-19 PBECs (Figure 8.4). To assess this further, I integrated the % wound closure at 24 hours of hospitalised individuals (n=15) with clinical parameters to look for any associations or relationships. Figures 8.5A and B show wound closure stratified according to acute disease severity during the hospital stay as defined by the maximal level of respiratory support required: Moderate (oxygen therapy), severe (positive pressure ventilation), very severe (intubation and ventilation). There was possibly a trend towards those with lower severity acute disease achieving more rapid wound closure, but statistical significance was not reached. There was also no relationship between length of hospital stay (with a longer hospital stay often associated with more severe disease) and wound closure (8.5C). A range of CT abnormalities were seen post COVID-19 as described in Chapter 4. The overall extent of CT abnormality was not linked with wound closure (8.5D). Additionally, it is possible that as with radiological and clinical features which often improve with time, epithelial abnormalities too may regress with time. Therefore, I assessed whether time from acute illness or recovery from the acute illness (with admission and discharge dates used as surrogates for this) was associated with wound closure (Figure 8.6 A, B), but this was not the case. Increasing age is associated with idiopathic pulmonary fibrosis, a condition where aberrancy in epithelial repair mechanisms is key to its pathogenesis. However, in my cohort, age did not correlate with wound closure (8.6C). I assessed the relationship between wound closure and blood parameters during admission, as a higher inflammatory state during admission has been associated with more severe disease (Figure 8.7). Although statistical significance was not reached, there was a trend towards a higher neutrophil count, white cell count, fibrinogen and CRP being negatively correlated with wound closure. With CRP, after exclusion of two outliers, a statistically significant relationship was seen (Figure 8.7B).

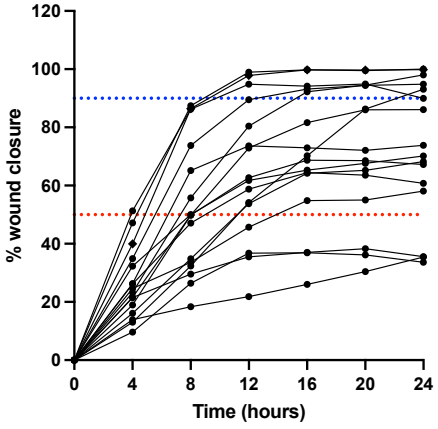


Figure 8. 4 Heterogeneity in wound closure in post COVID-19 donor PBECs

Blue line shows 90% wound closure and red line shows 50% wound closure. Note how PBECs from some donors achieved over 90% closure (n=5) whilst in others (n=3), below 40% is achieved.

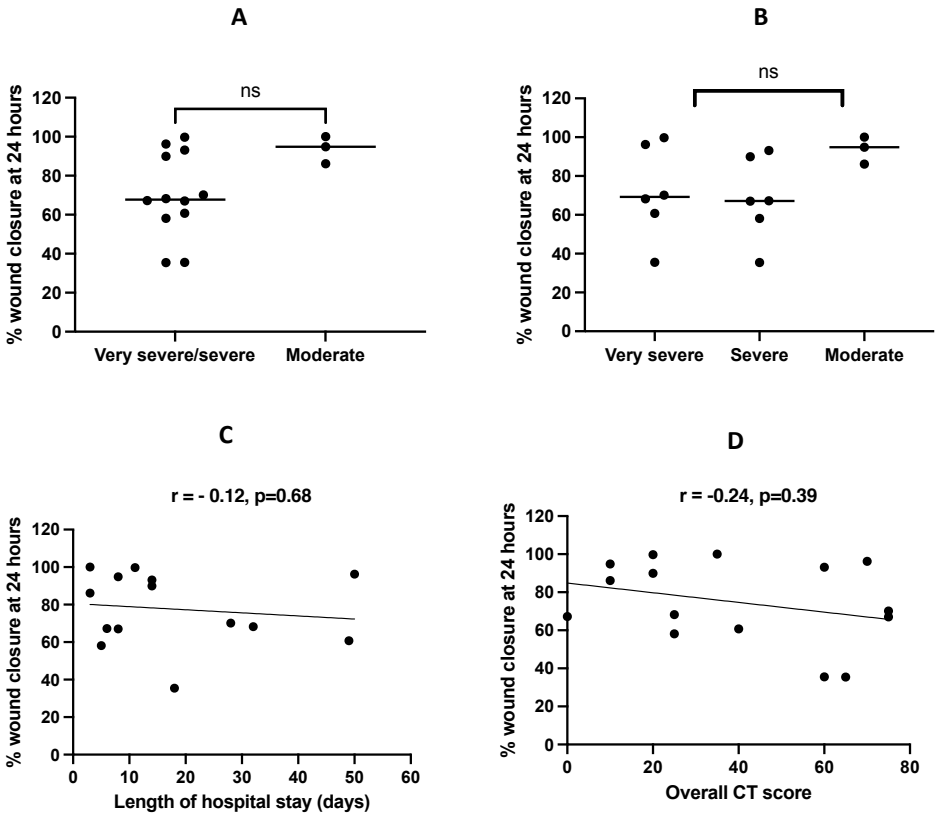


Figure 8. 5 Relationship between wound closure and clinical and radiological parameters

Wound closure at 24 hours displayed according to degree of respiratory support during acute admission (A-B), length of hospital stay (C) and overall CT score (D). Intergroup comparisons performed using Mann Whitney U test (A) or Kruksalis -Wallis (B). Spearman rank correlation analysis used for C and D. P value <0.05 considered statistically significant. Severity classified according to maximal respiratory support required during admission: moderate (oxygen therapy only), severe (positive pressure ventilation), very severe (mechanical ventilation).

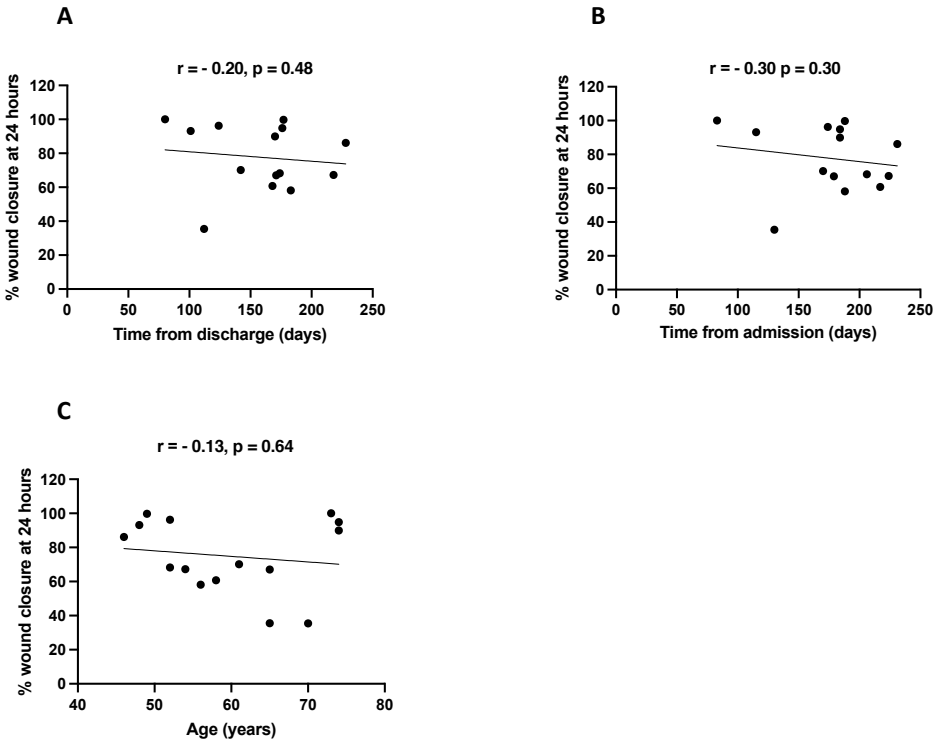


Figure 8. 6 Relationship between wound closure and age, time from hospital admission and discharge

Spearman rank correlation analysis of wound closure at 24 hours and days from discharge (A), admission (B) and age (C), with p value <0.05 considered statistically significant

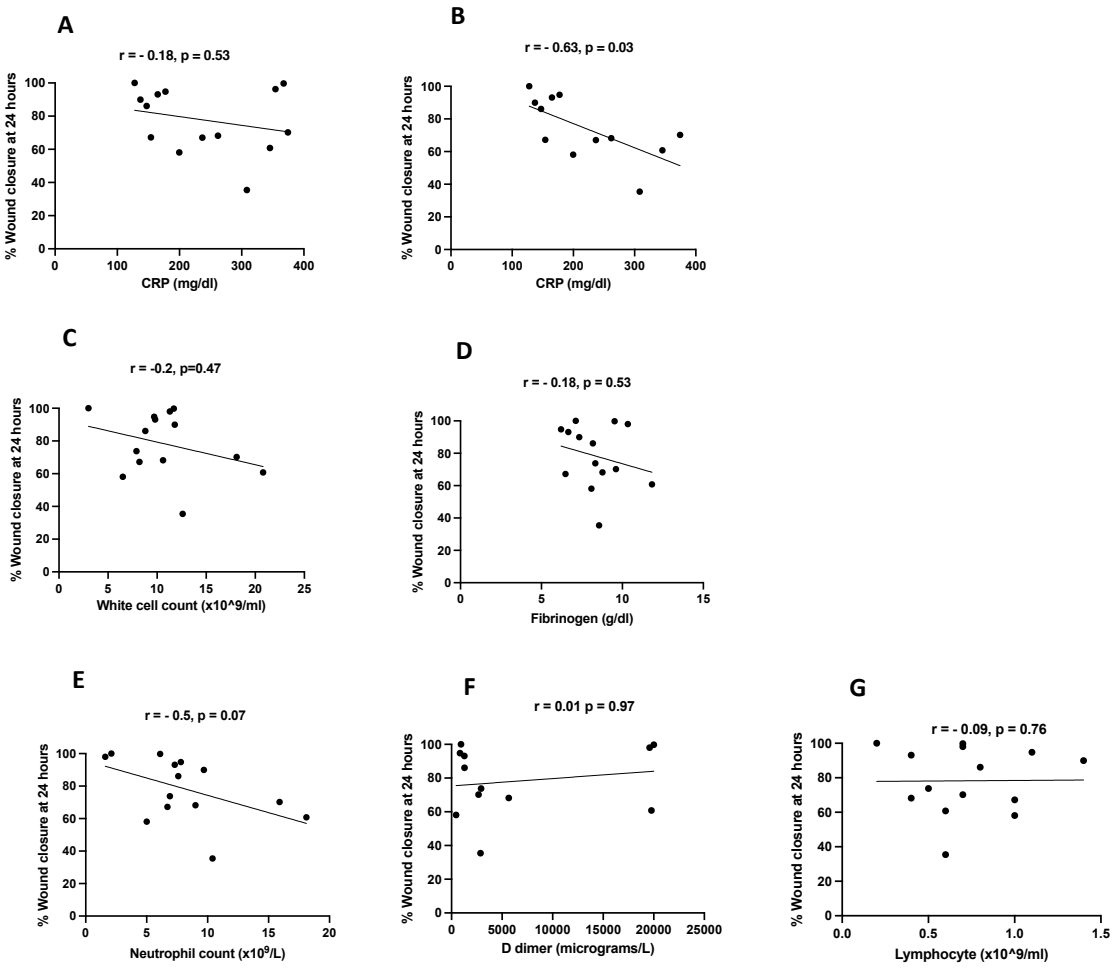


Figure 8. 7 Relationship between wound closure and peripheral blood results during acute admission

Spearman rank correlation analysis between the highest recorded value of CRP, WCC, fibrinogen, neutrophil and D dimer (A-F) and lowest lymphocyte count (G) shown. Figure 8.7A shows the CRP values for the full cohort and B shows the CRP after 2 outliers were excluded. P value <0.05 considered statistically significant

In order to understand why there might be a difference in wound closure between healthy control PBECs and post-COVID-19 PBECs, DPP4 and AREG, two proteins, which were upregulated in post-COVID-19 airway[341] and further discussed in Chapter 9, were measured in the basal supernatant of 3 post-COVID-19 and 3 healthy control PBECs, pre and post scratch assay (Figure 8.8). No significant differences were seen in AREG. DPP4 could not be detected by ELISA in the basal supernatant despite a 1 in 2 dilution (lowest limit of detection 31.25pg/ml).

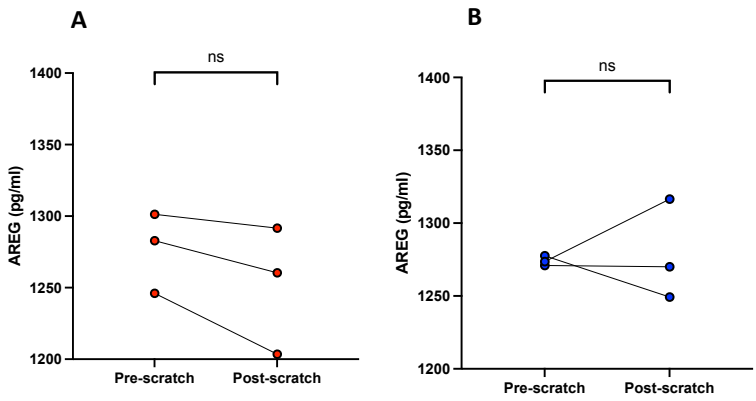


Figure 8. 8 AREG measured in basal supernatants during wound healing assay

Each biological dot represents an individual biological donor. Results shown for 3 post COVID-19 donor PBECs (A) and 3 HC PBECs (B). Inter-group comparisons made using non-parametric Mann Whitney U test. P value <0.05 considered statistically significant

8.5.3 Baseline characteristics at ALI

Having assessed basal cell function, I wanted to assess how PBECs post COVID-19 responded at air-liquid interface. As aforementioned, the ALI model allows us to mimic the respiratory epithelium in vivo, and therefore will enable me to further understand epithelial function post COVID-19. In particular, I wanted to assess the cells' ability to differentiate as well as their ability respond to viral injury.

Barrier integrity was assessed by measuring TEER. TEER values in HC PBECs (N=7) and post COVID-19 PBECs (n=8) were comparable at 3 weeks post air exposure (Figure 8.9). Median TEER in healthy controls was 309 (212- 406) Ohms/cm^2 compared to 243 (159 – 335) in post COVID-19 donors.

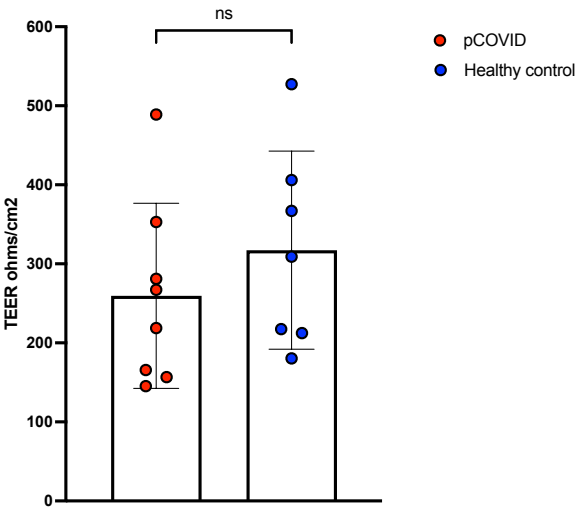


Figure 8. 9 Transepithelial electrical resistance at 3 weeks post air exposure

Median and interquartile ranges displayed. Each dot represents a biological donor. Inter-group comparisons were performed using Mann Whitney U test. P value <0.05 was considered statistically significant.

There was a reduction in gene expression of FOXJ1 in post COVID-19 PBECs compared to HC PBECs. However, expression of KRT5 (basal cells), TJP1 (ZO-1), CDH1 (E-cadherin) and MUC5AC (goblet cells) were comparable between the two groups (Figure 8.10).

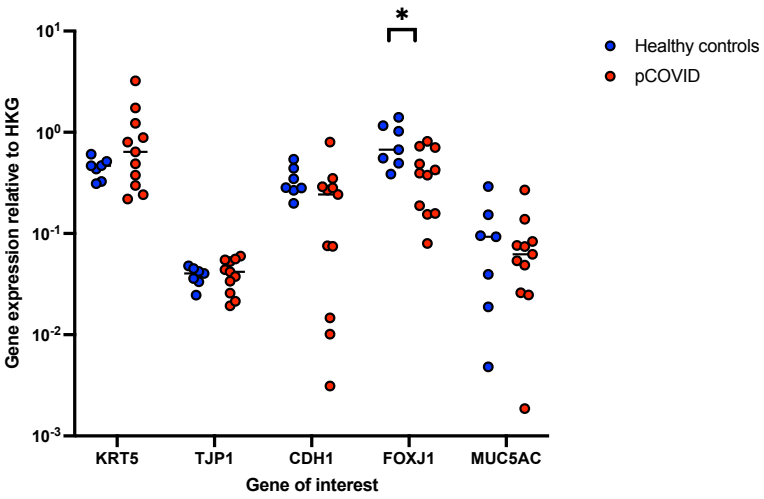


Figure 8. 10 Gene expression of differentiation markers at 3 weeks post air exposure

Gene expression measured using qPCR in cell lysate. Each dot represents an individual biological donor. Mann Whitney U testing using to compare groups. *p<0.05, ** p<0.01

Imaging was taken at 3 weeks post air exposure using an inverted Leica microscope at 5x, 10x and 20x magnification (Figure 8.11). This showed similar appearances between post COVID-19 and healthy controls. Beating cilia could be seen in all donors PBECs at ALI.

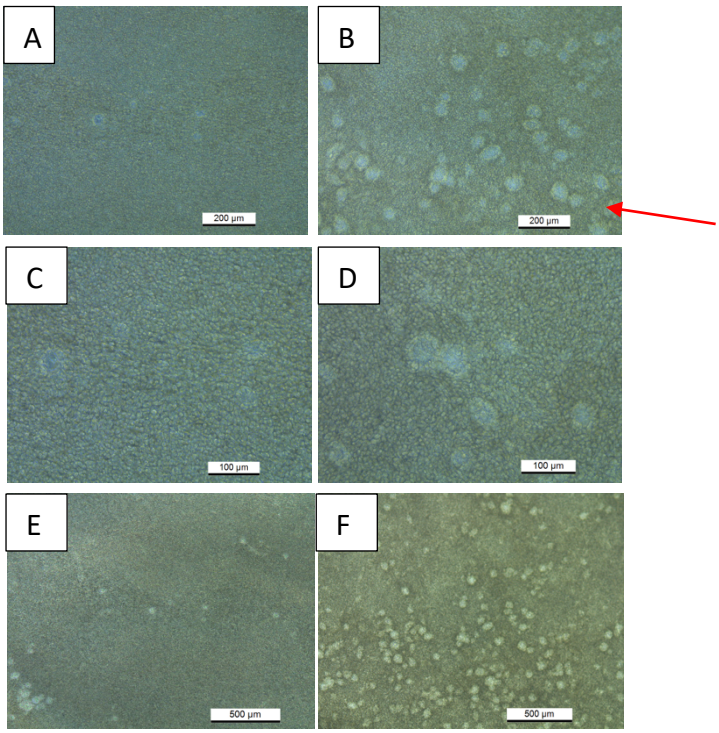


Figure 8. 11 Visualising the epithelium 3 weeks post air exposure

Microscopy images in PBECs from a healthy donor (A, C, E) and post COVID-19 donor (B, D, F) at 3 weeks post air exposure. Images taken at 20x magnification (A, B), 10x magnification (C, D) and 5x magnification (E, F). Mucous globules can be seen (red arrow).

8.5.4 Flu challenge Model

8.5.4.1 Barrier integrity

Infection with influenza virus is known to impair barrier integrity, so I was interested to ascertain whether there was a difference in the degree of impairment or recovery between post COVID-19 and healthy control PBECs. TEER measurements were taken every 24 hours from n=8 healthy controls and n=16 post COVID-19 donors. Absolute TEER values and percentage drop in TEER from baseline are shown. Baseline values were taken about 4-6 hours prior to infection with IAV. A drop in TEER of 40-50% was seen in both the cells treated with UV IAV (8.12C) as well as live IAV (8.12 D). The TEER values remained stable thereafter in the UV-IAV group (8.12 A, C). With live IAV infection, a maximal drop in TEER was seen between 48 hours and 72 hours post infection, with some recovery at 96 hours (8.12 B, D). A statistically significant difference was seen between TEER values at 24 and 48 hours in both healthy controls and post-COVID-19 donors in the IAV treated-groups, but no difference in the UV-IAV treated groups at those timepoints. Of note, there was no significant difference between TEER values at 48 hours after IAV infection in HC vs post COVID-19 PBECs (8.12 E).

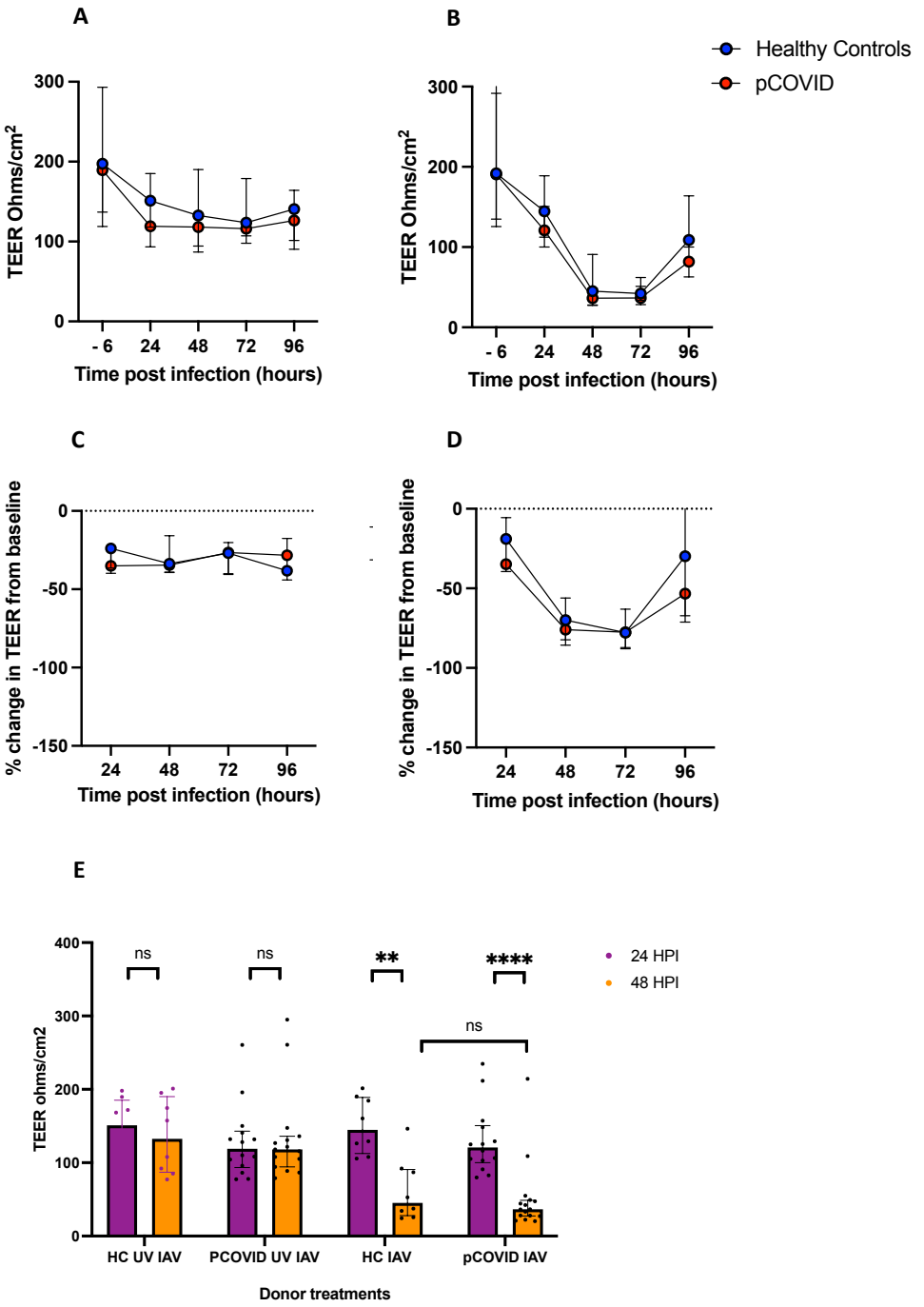


Figure 8. 12 Changes in TEER post IAV challenge

TEER values after UV-IAV (A, C) or live IAV (B, D) infection in PBECs from HC (blue) or post COVID-19 (red) donors. Absolute TEER values (A, B) and % change from baseline (C, D) at sequential time points post infection shown. Baseline readings were taken approximately 6 hours before infection. Median and interquartile ranges shown. Comparisons between TEER values at 24hpi and 48hpi in E were performed using Mann Whitney U testing. P values: * <0.05, **<0.01, ***<0.001 Abbreviations: hpi (hours post infection)

8.5.4.2 Morphological changes

Secondly, I was interested to see if the morphology of the cells changes after influenza infection. Loss of ciliated cells and epithelial height was noted at 72 hours post infection in PBECs from healthy controls and post COVID-19 donors. (Figure 8.13).

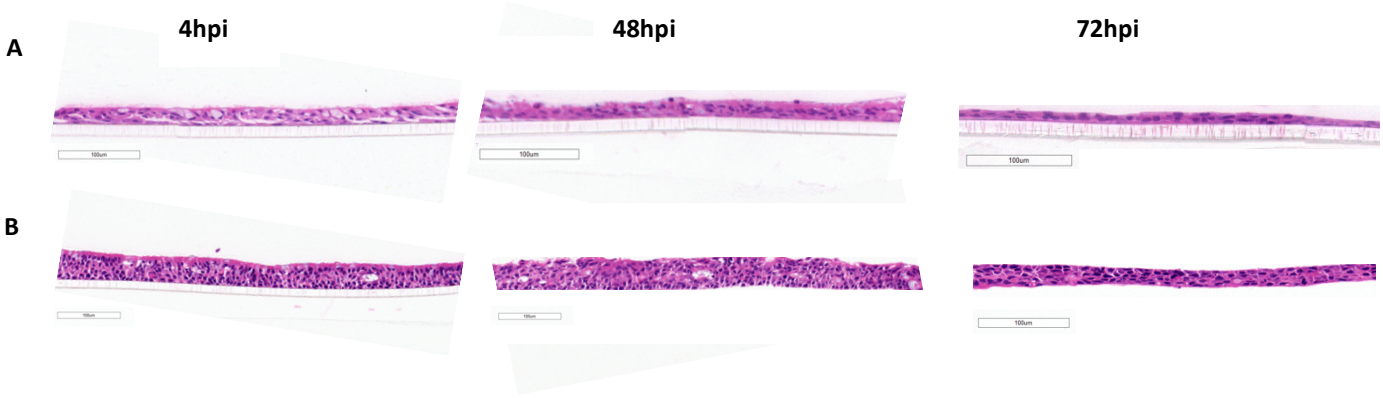


Figure 8. 13 H+E stains of PBECs at ALI after IAV infection

Morphological changes as noted on H+E staining in HC donor (A) and post COVID-19 donor (B) at sequential timepoints post IAV infection. Abbreviations: hpi - hours post infection

8.5.4.3 Transcriptomic profiling

In order to be able to refine qPCR targets and timepoints, RNA was sent for transcriptomic analysis (as described in Chapter 2).

Normalised counts, raw counts, differential gene expression analysis and gene ontology analysis were performed by the Biostatistical team at Genewiz. I was interested in assessing interferon-stimulated genes and wound healing proteins (matrix metalloproteinases and EGFR ligands), and therefore interrogated the transcriptomic data to assess gene expression for these particular groups (Figures 8.14 – 8.16).

Upregulation of ISGs was predominantly seen at 48 hours and 72 hours post infection, in both the healthy control and post-COVID-19 PBECs (Figure 8.14). Similarly, there was increased gene expression of EGFR ligands at 48 and 72 hours, but also higher expression in healthy control PBECs, with maximal expression of AREG at 4 hours post infection (Figure 8.15). In general, gene expression of the matrix metalloproteinases was reduced in donor PBECs post COVID-19 compared to healthy controls, with

the exception of MMP 9, 11 and 24, which were upregulated (Figure 8.16). This difference was especially marked with MMP-9.

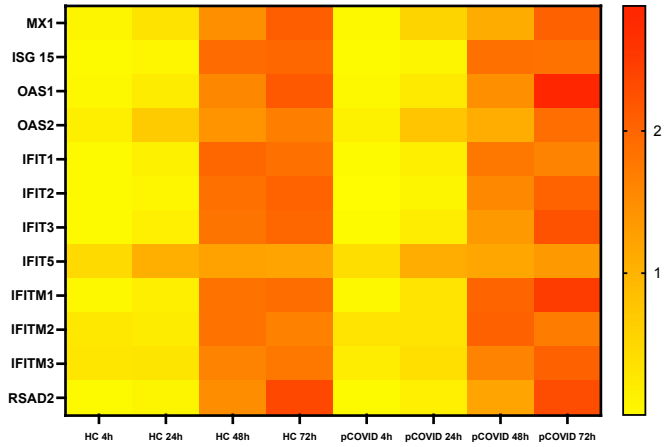


Figure 8. 15 Gene expression of ISGs post IAV infection (Transcriptomics)

Normalised counts were further normalised to the average for healthy controls across all timepoints. Upregulation of ISGs was seen predominantly at 48 hours and 72 hours post infection in both the healthy and post-COVID-19 donor PBECs.

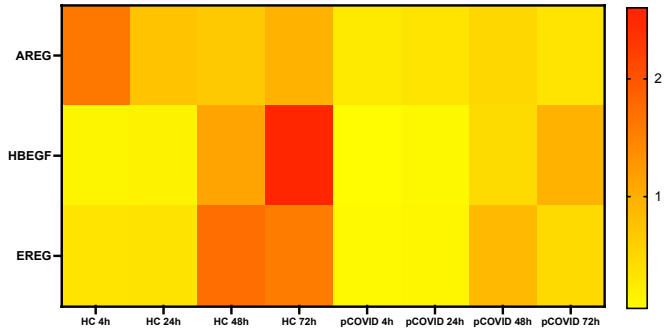


Figure 8. 15 Gene expression of EGFR ligands post IAV infection (Transcriptomics)

Normalised counts of EGFR ligands, again, normalized to the average for healthy controls at each time point. Upregulation, predominantly seen at 48-72 hours post infection.

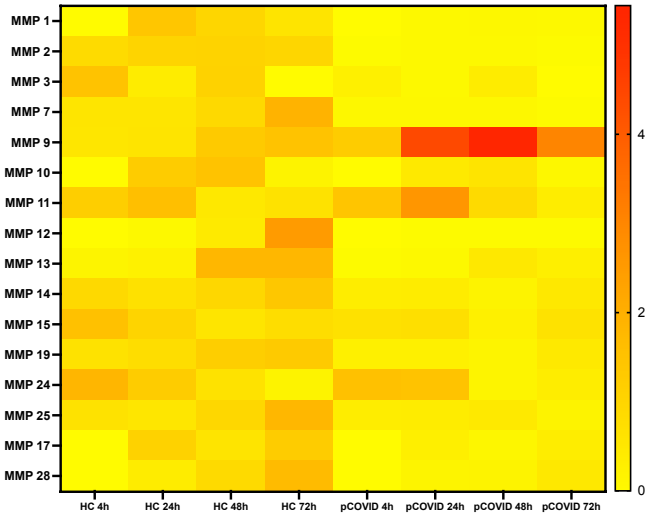
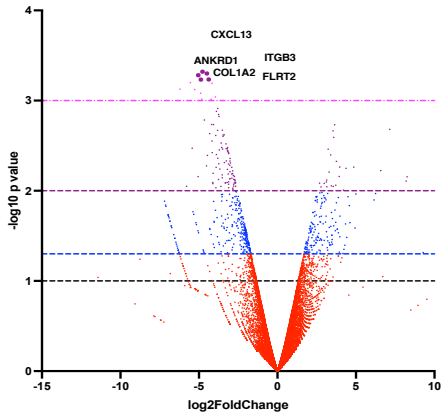


Figure 8. 15 Gene expression of matrix metalloproteinases post IAV infection (Transcriptomics)

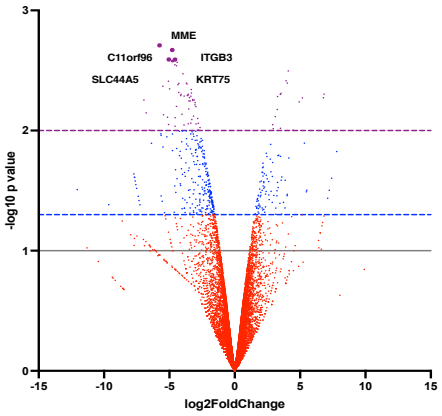
Normalised counts of MMPs, normalised to the average for healthy controls at each timepoint. Note, significant upregulation of MMP 9 at 48 hours in post COVID-19 donors.

From the transcriptomic data, it was clear that upregulation of the ISGs and EGFR ligands was predominantly seen at 48 and 72 hours post infection. I was then interested to understand which genes were maximally differentially expressed at those specific timepoints (Figure 8.17 A-C). In brief, COL1A2, CXCL13 and FLRT2 genes were the most significantly differentially expressed with lower expression in PBECs post COVID-19 compared to HC PBECs ($p<0.001$). Meanwhile, ITGB3, MME and C11orf96 were the most differentially expressed genes at 72 hours, with downregulation in post COVID-19 PBECs.

A



B



C

48 hours post infection			72 hours post infection		
Gene	Log2FC	-log10 (p value)	Gene	Log2FC	-log10 (p value)
COL1A2	-4.770616	3.320865	MME	-5.750359	2.708901
CXCL13	-4.498593	3.300553	ITGB3	-4.778798	2.670825
FLRT2	-5.042395	3.28148	C11orf96	-5.047682	2.591137
ITGB3	-4.378882	3.234297	KRT75	-4.565442	2.590312
ANKRD1	-4.874451	3.232726	SLC44A5	-4.762283	2.578666
ITGA4	-5.550011	3.199484	VGLL3	-4.392991	2.567548
GPNMB	-4.162366	3.191738	PAMR1	-4.578461	2.547729
NNMT	-6.20436	3.127216	INA	-4.459929	2.53891
CALB2	-5.274378	3.121618	CHL1	4.08932	2.496752
LGALS7	-4.891878	3.081392	GATA3	-3.958193	2.472371

Figure 8. 16 Most differentially expressed genes at 48 hours and 72 hours post IAV infection.

Volcano plot of differentially expressed genes at 48 hours (A) and 72 hours (B) post IAV infection. Black dotted line denotes p value of 0.1, blue line p = 0.05, purple line p = 0.01, magenta line p = 0.001. C shows tabulated results of 10 most differentially expressed genes, ranked according to p value. P values not corrected for multiple hypothesis testing.

8.5.4.4 Assessing ISG response according to flu

To validate the results from the transcriptomic data, some of the interferon-stimulated genes were evaluated by qPCR from 48 – 96 hours post infection (Figure 8.18). As expected, an increase in ISG response was seen in the IAV groups, compared to UV IAV, with a trend towards increasing gene expression of ISGs up to 96 hours post infection (8.18 B-D). This corresponded with a decrease in Flu-M1 gene expression from 48 hours to 96 hours (8.18 A). There were, however, no differences between the responses generated by HC vs post COVID-19 PBECs.

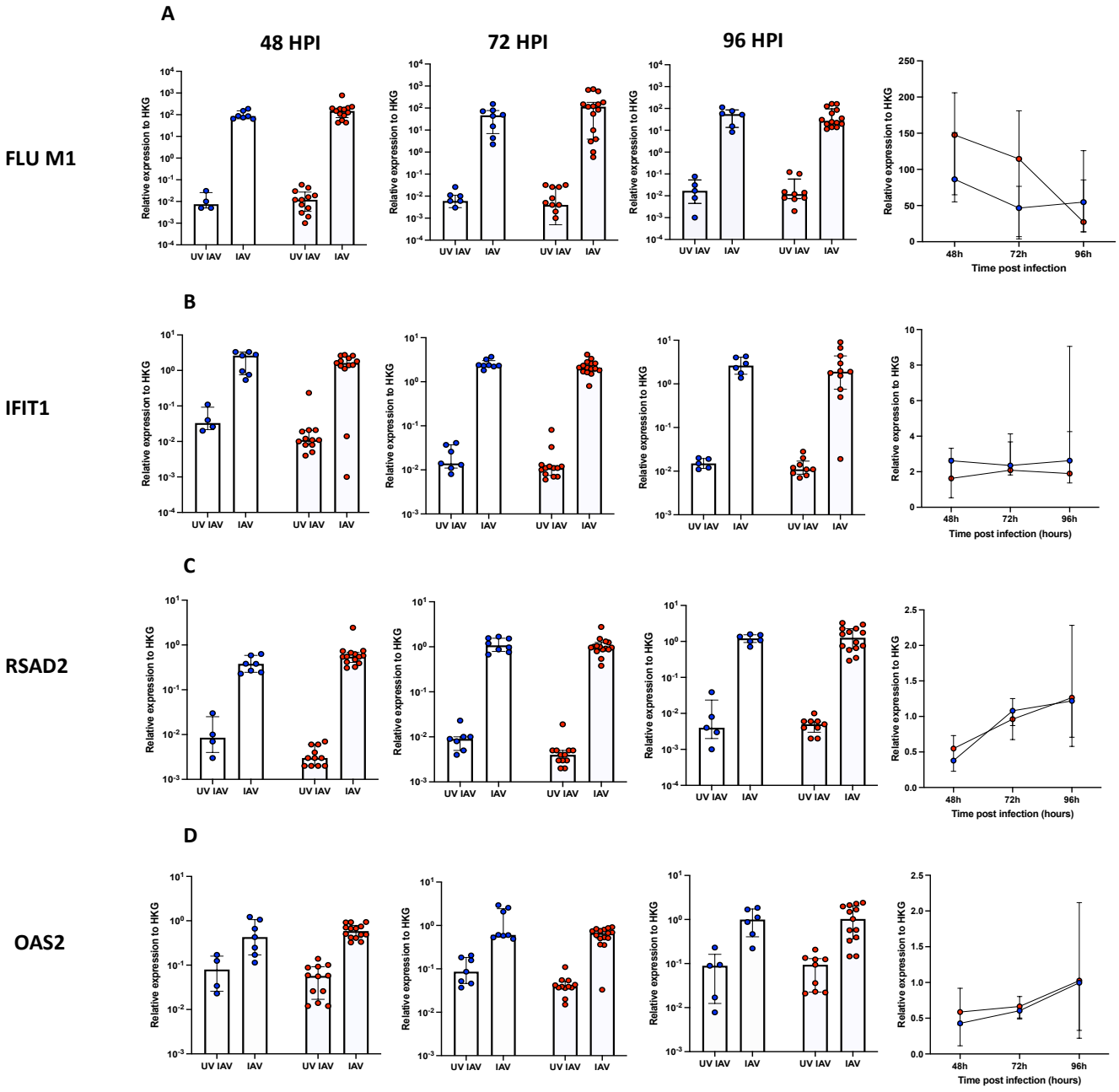


Figure 8. 17 Gene expression of ISGs and Flu M1 post IAV infection (qPCR)

Scatter plots showing gene expression of ISGs (IFIT1, RSAD2, OAS2, B-D) and Flu M1 (A). Median and interquartile ranges shown. Each dot signifies an individual biological donor. Abbreviations: hpi (hours post infection)

8.5.4.5 Interferon and inflammatory response

In addition to ISGs, I was keen to assess the inflammatory and interferon response at sequential timepoints post IAV infection. Basal media was used to assess these parameters by ELISA. Peak inflammatory and interferon response was seen at 72 hours post infection (Figure 8.19). A statistically significant difference in IL-6 was seen between the UV-IAV and IAV from 24 hours post infection onwards (8.19 A). By contrast, at 24 hours, there was no significant difference in IL-8 between UV-IAV and live-IAV treatment groups (8.19 B). A difference was seen 48 hours onwards, however. IFN beta and lambda were not detectable in the UV-IAV groups or at 24 hours post infection in the IAV group. Again, a peak was seen at 72 hours post infection (8.19 C-D).

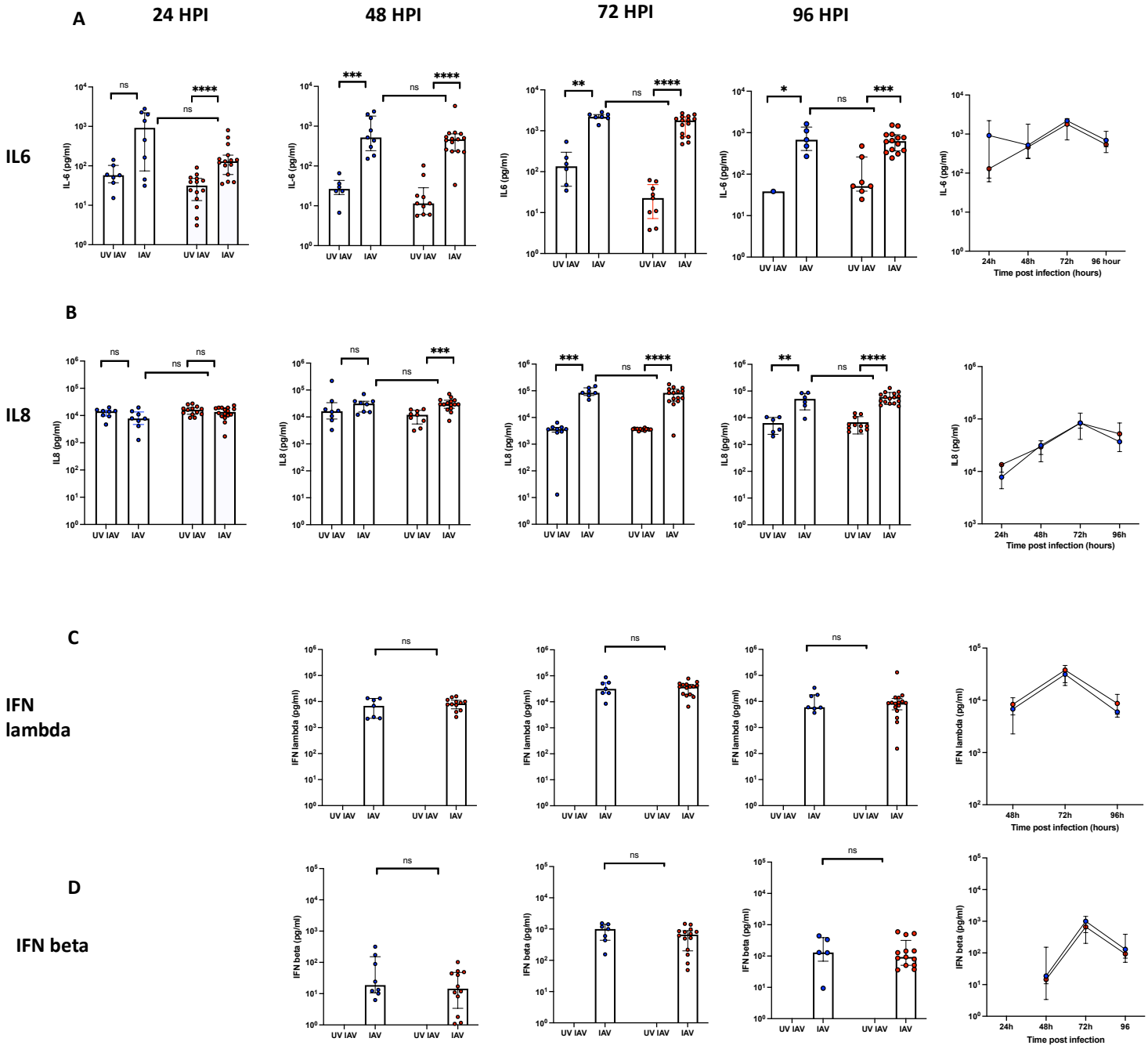


Figure 8. 18 Inflammatory and interferon levels in basal supernatant post IAV infection (ELISA)

Inflammatory (A, B) and interferon (C, D) responses post IAV infection, measured by ELISA in the basal supernatant of cells cultured at ALI. Blue dot – healthy control donor, red dot – post COVID-19. Each dot represents an individual biological donor. Inter-group comparisons performed using Mann Whitney U testing. Median and interquartile range shown. P values as follows: * <0.05, **<0.01, *** <0.001, ****<0.0001

8.5.4.6 EGFR ligands

In addition, there was an upregulation of gene expression for AREG and HBEGF, with statistically significant differences between the UV-IAV group and live IAV groups at 72 and 96 hours post infection (8.20). This difference was not seen, however, for AREG expression at 48hpi (8.20 A). A statistically significant difference was seen between UV-IAV and live IAV for HBEGF expression in PBECs post COVID-19 at 48 hours, but not in HC PBECs (8.20 B).

AREG and HBEGF protein were measured by ELISA in the basal supernatant 72 hours post infection (Figure 8.21) and as expected, there was a statistically significant upregulation in AREG in IAV-infected PBECs compared to UV-IAV. Whilst AREG could be detected even in UV-IAV infected PBECs (8.21 A), HBEGF was not detectable (8.21 B).

There were no significant differences in AREG or HBEGF between PBECs from healthy control or post-COVID-19 donors, either on gene expression at 48, 72 or 96 hours post IAV infection, or on protein level at 72 hours post infection.

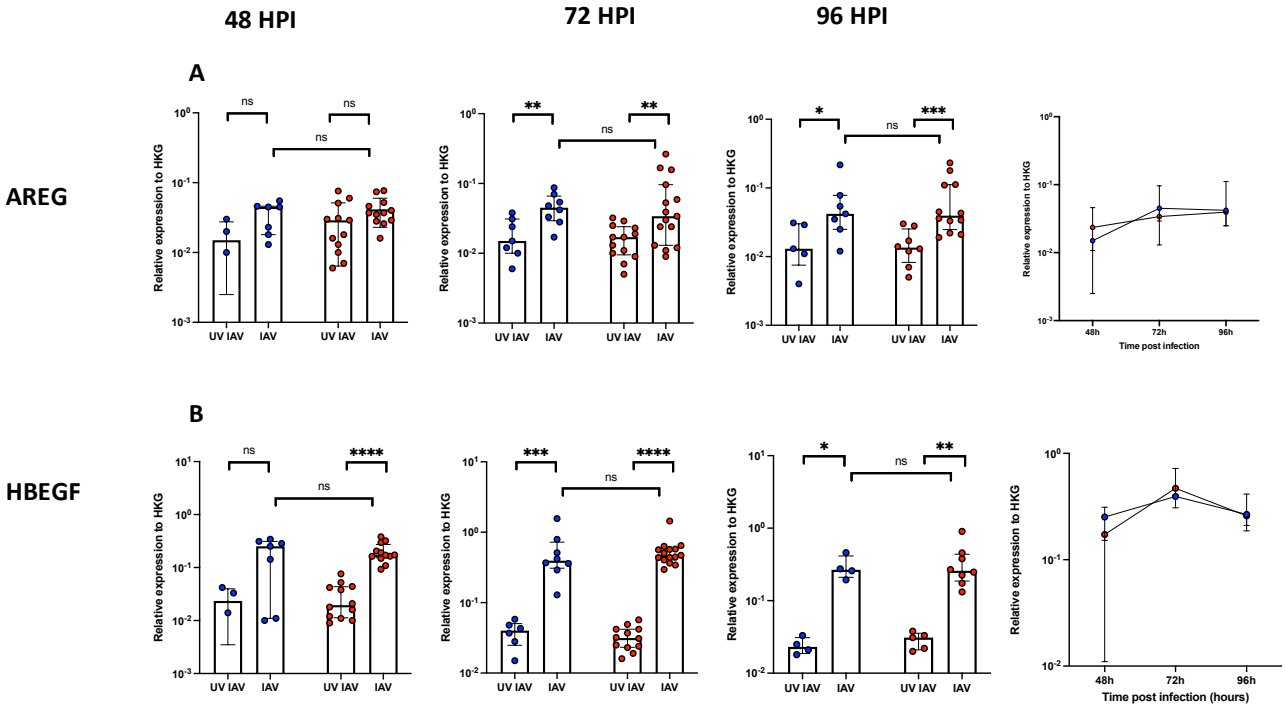


Figure 8. 19 Gene expression of EGFR ligands after IAV infection (qPCR)

Inter-group comparisons made using Mann Whitney U test. Median and interquartile range shown. Blue dot – healthy control, red dot – post COVID-19. P values as follows: * <0.05, **<0.01, *** <0.001, ****<0.0001

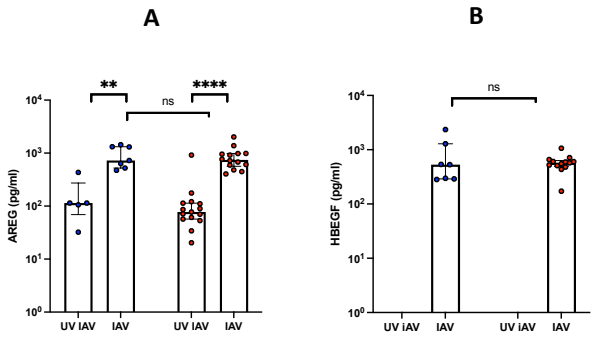


Figure 8. 20 AREG and HBEGF in basal supernatant 72 hours post IAV infection (ELISA)

AREG and HBEGF measured in basal supernatant 72 hours post IAV infection in PBECs cultured at ALI. Inter-group comparisons made using Mann Whitney U testing. Blue dot – HC donor, Red dot – post COVID-19 donor. Each dot represents an individual biological donor. Median and interquartile range shown. P values as follows: * <0.05, ** <0.01, *** <0.001, **** <0.0001

8.5.4.7 Impact of basal supernatant from IAV infected PBECs on fibroblast migration

As aforementioned, epithelial-derived mediators can affect fibroblast activity, and epithelial-mesenchymal crosstalk is important to ensure effective wound healing. I therefore wanted to assess the effect of basal supernatant from IAV-infected ALI cultures (n=5 HC, n=4 post COVID-19) on a wound healing assay of human lung fibroblasts. Wound closure was monitored using JuliTM Stage Real-Time Cell History Recorder over a 24-hour period. Mean wound closure was 59.3% (+/-2.0) when conditioned media from HC PBECs was added compared to 40.0% (+/-3.1) when media from post COVID-19 PBECs (p=0.01) was added. Basal supernatants of IAV-infected cells accelerated wound closure compared to DMEM/FBS alone, suggesting epithelial cell-derived mediators released post IAV infection can alter fibroblast function (Figure 8.22).

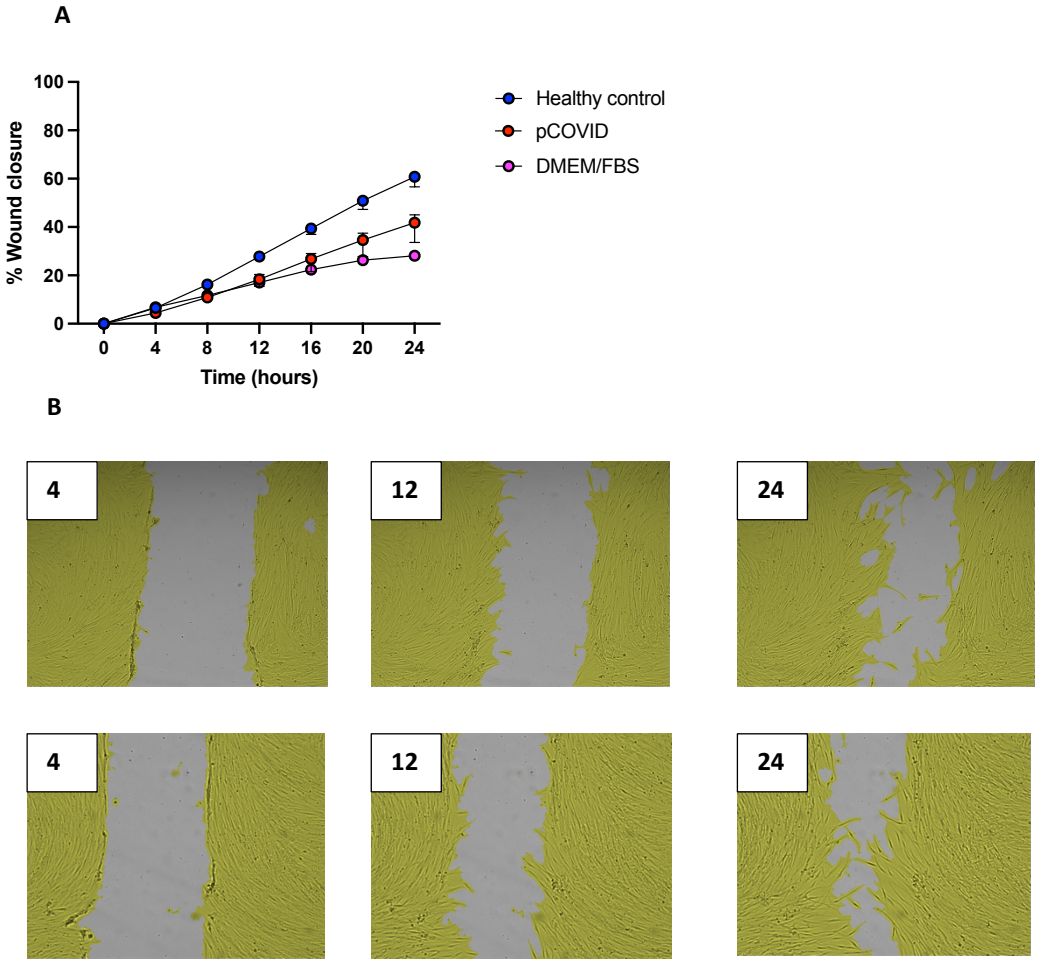


Figure 8. 21 Fibroblast scratch assay with conditioned media

Fibroblast wound closure after treatment of fibroblasts with conditioned media after IAV infection of PBECs from HC and post COVID-19 donors (A). Mean +/- SEM of experimental replicates (n=3) displayed. Representative images of fibroblast wound closure after basal supernatant from HC PBEC (top panel) and post COVID-19 PBEC (bottom panel) applied shown (B). Numbers in B denote hours post linear wound was made.

8.6 Discussion

8.6.1 Summary of findings

PBECs from post-COVID-19 donors display a defect in wound healing response to mechanical injury compared to healthy controls, but significant heterogeneity amongst donors is seen, with a trend towards greater defects in individuals with more severe acute disease presentations or a higher inflammatory state during admission. Cellular proliferation is, however, preserved.

PBECs from both post-COVID 19 and healthy control donors have fully differentiated by 3 weeks post air exposure. In response to infection with influenza A virus, both post COVID-19 and HC PBECs show a comparable ISG and interferon response. Barrier function is impaired in both PBECs from post COVID-19 and HC donors at 48-72 hours post infection. Conditioned media from IAV-infected HC PBECs enhanced fibroblast wound closure more so than media from post-COVID-19 PBECs.

8.6.2 Findings in context of current literature

6.6.2.1 Differentiation and barrier function

TEER values were comparable at 3 weeks post air exposure between post COVID-19 and healthy donor PBECs. These findings are in accordance with the similar gene expression seen between HC and post COVID-19 donor PBECS in TJP1 (ZO1) and CDH1 (E-cadherin) at this timepoint - genes which play an important role in the barrier function of the respiratory epithelium.[483] The downregulation of FOXJ1 in post-COVID-19 cells is not consistent with microscopy findings, where beating cilia were visible in both HC and post COVID-19 PBECs at 3 weeks post air exposure. Acute SARS-COV2 infection has been shown to decrease FOXJ1 expression, a potent regulator of ciliogenesis, prior to ciliary loss. However, the impact on cellular differentiation post recovery has not been assessed other than what's presented in this chapter. Further assessment and quantification of FOXJ1+ (ciliated cells) using immunofluorescence staining would have been useful. Additionally, evaluation of cilia-associated genes such as *DNAH7*, as well as assessment of ciliary function using ciliary beat frequency would have helped understand the functional consequence of this differential gene expression.[484] Impairment of ciliogenesis or ciliary function post COVID-19 is potentially a concerning feature, as this can result in impairment in muco-ciliary clearance thus increasing patients' risk of respiratory tract infections.

8.6.2.2 Impaired wound healing

No studies have been published to-date on the functional capacity of PBECs post COVID-19 during the convalescent phase. The differences in wound healing response to mechanical scratch is interesting and significant inter-donor variation suggests that not all individuals have a defect in wound healing. As mentioned earlier, wound healing responses are dependent on both cellular proliferation and migration.[170] A similar proliferative rate was seen between healthy controls and post-COVID-19 PBECs suggesting that it might be differences in migratory effect that is contributing to the impaired wound healing seen.[485]

Severe COVID-19 has been associated with significant alveolar injury.[486] There was a trend in my results showing that those with moderate disease (oxygen therapy only), might have better wound closure than those who had severe or very severe disease presentations. However, firm conclusions cannot be made with the small number of individuals who had moderate disease. In theory, it is possible that those with more severe epithelial injury are the ones with persistent abnormalities. Two issues with interpretation of the severity of acute disease are a) our cohort predominantly sampled patients who had more severe disease presentations (as evidenced by the need for hospital admission) b) the degree of maximal respiratory support required during admission was obtained retrospectively from hospital notes and may not be reflective of acute disease severity as decision to escalate therapy may depend in part on the clinician's practice. Correlating wound closure with highest (or lowest lymphocyte) blood parameters during the acute admission showed a negative trend (non-significant) with white cell count, neutrophil and CRP. These are all markers of severity during the acute disease[487–489] and again, this suggests that acute disease severity may have an impact on epithelial function at follow up. One postulate is that the epithelial recovery occurs with time. However, no relationship was seen between wound closure and number of days from hospital admission or discharge. There are two possible reasons for this: Firstly, samples were collected in a short time frame and therefore the spread wasn't significant enough to robustly answer this question. Secondly, admission and discharge are often determined by multiple factors, including patient factors such as health-seeking behaviour and clinician factors such as duration of treatment and/ or observation prior to discharge. These endpoints therefore don't fully reveal when the patient actually deteriorated to a level necessitating hospital treatment (admission) or the timepoint at which recovery was sufficient for outpatient management.

Additionally, there was a difference in wound healing response in the healthy control donor PBECs taken pre- and post-pandemic. Whilst there are many reasons for this, such as a change in the research team acquiring and handling the samples, it is also important to consider that HCs post pandemic might have had SARS-COV2 infection, unknowingly, resulting in epithelial cell defects. To complicate matters further, we are unable to assess the timing of SARS-COV2 infection in these donors, thus posing challenges in drawing conclusions when comparing with post COVID-19 PBECs collected at 6 months post hospital discharge.

Cellular proliferation was assessed by evaluating the change in percentage confluence over time. However, to validate this, I could have stained cells for Ki67, a nuclear antigen present during S, G2 and M phases of the cell cycle, but not G0, therefore a good representation of proliferating cells.[490,491] A lack of difference in Ki67+ cells using quantitative analysis between post COVID-19 and HC PBECs would have added validity to the observation that a proliferative defect does not exist between post COVID-19 and HC PBECs.

8.6.2.3 IAV challenge

During acute influenza infection, a significant drop in TEER was noticed at 48-72 hours, with some recovery at 96 hours. This impairment in barrier function has been replicated in other studies where in addition a drop in TEER, significant disruption of the ZO-1 protein has been shown.[492,493] A drop in TEER was seen in both the UV-IAV and IAV groups at 24 hours post infection and was consistent between donors and experiments. One possible explanation for this is that repeated aspirations of the apical surface has resulted in cellular stress, as evidenced by an increase in IL8, even in the UV-IAV treated groups and similar in quantity to the IAV-treated groups at 24 hours post infection, which in turn could result in increased permeability.[494]

Type I and III interferons are upregulated in response to influenza infection, and in turn, upregulate ISGs. A variety of ISGs have been reported including MX1, IFITs/IFITMs, viperin/RSAD2 and ISG15, which are all involved in controlling viral replication and promoting viral clearance.[492,495] In this Chapter, ISGs were detectable at 48 hours post infection and continued to rise up to 96 hours post-infection. The ISGs weren't assessed at an earlier timepoint, but it is possible that they could have been detected earlier also.

Flu M1 gene expression reduced from 48 hours onwards, which is consistent with other studies where maximal detection was around 36 hours post infection, with levels falling thereafter.[496] Additionally,

this decrease in Flu M1 gene expression corresponded with an increase in ISG expression. However, the peak of interferon response, both interferon lambda and beta was at 72 hours. The rise in ISG after this point might suggest that there is ongoing viral replication within the cells that have not yet undergone apoptosis or pyroptosis, resulting in further stimulation of ISG production. Assessing the interferon response at a later time point after 96 hours would have helped elucidate whether there is a further peak in interferon beta and lambda protein. Whilst both interferon beta and lambda were produced in response to IAV infection, a higher concentration of IFN lambda could be detected. This is in concert with other studies showing that IFN lambda is the predominant interferon produced in response to influenza infection.[497]

Interleukins 6 and 8 are known to be released by the epithelium in response to influenza infection and may contribute to the cytokine storm seen after severe viral infection.[498,499] The maximal secretion of IL8 and IL6 was at 72 hours post infection, when the peak of the immune response was noted. There was a statistically significant difference in IL6 and IL8 at this time point between the UV-IAV- and IAV-treated PBECs, and similar differences were seen at earlier timepoints for IL6. However, as aforementioned, a significant IL8 response was seen even in the UV-IAV-treated cells. The reason for this is not clear, but could be contributed to by the growth media, (including EGFR ligands in the media) and cellular stress from repeated cell handling through TEER measurements and apical washes.[500–502]

EGFR ligands play an important role in epithelial repair.[173,503] Post COVID-19, differential upregulation of amphiregulin (AREG), was seen in the airways compared to healthy controls.[341] In response to IAV infection, HBEGF and AREG were increased in in vitro cultured cells both at the mRNA level and protein level, with maximal response at 72 hours. AREG was also detected in baseline basal supernatants (i.e. before IAV infection) and is consistent with our knowledge that AREG can be detected at homeostasis and is involved in epithelial cell proliferation.[504,505] In contrast, HBEGF was not detected at baseline, and this may be due to the high-affinity it has to its receptor, in comparison with AREG, with has a lower affinity, suggesting the former may be in a membrane-bound state.[506] They can, however, be cleaved from the membrane and released as soluble growth factors where they have their biological activity. Furthermore, the absence of HBEGF in the basal supernatant of the UV-treated mock also suggests that activation is required for cleavage of the protein from the membrane.

The transcriptomic data allowed us to pinpoint the time point when maximal response was seen to help direct qPCR evaluation. For the ISGs, a rise was seen at 48 hours, with a peak at 72 hours post

infection. This was confirmed through quantitative PCR. The genes were also detectable at 24 hours, in the transcriptomic data, a time-point which wasn't assessed on qPCR. Similarly, the EGFR ligands were again, upregulated at 48 – 72 hours post infection. According to the transcriptomic data, however, gene expression of the EGFR ligands was, overall reduced at all timepoints in the post COVID-19 donor cells compared to healthy controls. This, however, was not replicated with gene expression assessed through quantitative PCR. It is important to note that a small sample size was sent for transcriptomic analysis and the RNA for the donors was pooled, and this might have resulted in some inaccuracies.

With respect to MMPs, all were relatively downregulated at transcription level in post COVID-19 donors compared to healthy control donors, apart from MMP 9, 11 and 24. MMP-9 is an important mediator of wound healing and in MMP-9 knockout mice, delayed wound closure has been seen.[507] Furthermore, deficiency in MMP-9 has been associated with reduced cellular proliferation.[508] Finally, MMP-9 has an important role in angiogenesis, through stimulation of vascular endothelial growth factor (VEGF), which is important for tissue regeneration and repair.[509] The careful balance of MMPs and their inhibitors is important in wound healing and if this is disturbed, can result in excess degradation of the extracellular matrix, resulting in impaired wound closure.[510,511] There is evidence of increased expression of MMP 11 in tissue repair,[512] but the precise role that 11 and 24 play in wound healing is not clear.[513] MMPs were not assessed using qPCR or ELISAs, but future work could include assessing MMP 9 in the basal supernatants by ELISA, to validate the transcriptomic findings.

Of the ten most differentially expressed genes described earlier in this Chapter, significant downregulation of genes associated with wound healing was seen at 48 and 72 hours post IAV infection. For instance, the chemokine CXCL13, a chemokine that has been shown to promote cellular migration and epithelial-mesenchymal transition,[514] both important processes in wound healing, was significantly downregulated by a log2FC >-4 in post COVID-19 PBECs compared to HC PBECs. Furthermore, CXCL13 has been implicated in promoting T Cell recruitment in mouse LPS models thus suggesting that immune cell recruitment in response to IAV infection may also be impaired post COVID-19.[515]

Collagen type 1 alpha 2 chain (Col1A2) was also downregulated in post COVID-19 PBECs compared to healthy controls. Col1A2 is necessary for the synthesis of Type 1 collagen[516,517] an important collagen for the migration of epithelial cells. Similarly, fibronectin leucine rich transmembrane protein 2 (FLRT2) and Ankyrin Repeat Domain 1 (ANKRD1) both of which play an important role in the modelling

of the extracellular matrix and regulation of MMPs were downregulated post COVID-19. [518, 519] Cell-matrix adhesions are pivotal to epithelial cell migration and integrin cell-surface receptors allow anchorage of epithelial cells to the extracellular matrix.[520] Integrin Subunit Beta (ITGB3) a protein associated with cell-matrix adhesion[521] was one of the top most differentially expressed (downregulated) genes in post-COVID-19 PBECs at both 48 hours and 72 hours post infection. To validate this finding, quantification of ITGB3 by ELISA in the basal supernatants at 48 hours and 72 hours would be helpful.

Therefore, to summarise, the transcriptomic data points towards genes associated with cell migration and cell-matrix adhesions being downregulated in post-COVID-19 compared to HC PBECs. Important to note, however, is that gene expression does not necessarily correlate with protein synthesis. Also, to note is that this differential gene expression was seen in the context of infection with IAV, a highly potent, cytopathic virus, which is very immunogenic, and may not be comparable in the context of a mechanical injury, such as with the scratch assay, or with less potent viral injury.

8.6.2.4 Fibroblast migration

Fibroblast migration was accelerated in the presence of basal supernatants from IAV-infected PBECs, compared to DMEM/FBS, which suggests that there are fibroblast-activating mediators in the supernatant. One potential epithelial-derived factor that could be contributing is vascular endothelial growth factor (VEGF), a growth factor important in activating fibroblasts and inducing extracellular matrix synthesis.[522,523] Protein quantification in the basal supernatant using ELISA might offer a clue as to the mechanism driving the differences seen and whether there is differential production of these factors by HC PBECs compared to post COVID-19 PBECs.

Important to note is that in my fibroblast experiments, migration was assessed in plates that were not coated with Type 1 collagen and whether coating the plates would have changed the results is not known. Additionally, this experiment was only performed once and has to be repeated at least twice to ensure the findings are reproducible. The conditioned media was UV-inactivated prior to the fibroblast migration assay as experiences from colleagues in the Lloyd lab is that without this, fibroblast cell death was seen, suggesting that live viral particles may be present in the basal supernatant. However, it is possible that in an attempt to preserve the assay, UV-inactivation could have resulted in denaturing of important proteins, although his would have been consistent across both sets of supernatants.

8.6.3 Clinical relevance of findings

Preserved epithelial immune responses to influenza A virus post COVID-19 is reassuring and reflects clinical practice where an increase in morbidity due to influenza has not been seen post COVID-19.

The clinical relevance of the defect in wound closure in response to a linear scratch is not known. It is possible, however, that milder injuries to the epithelium (than that seen with IAV infection) may result in less effective wound healing. Influenza A is a very potent and cytopathic virus and it would be important to assess if comparable immune responses are seen with less potent viruses.

8.6.4 Limitations

8.6.4.1 Bronchial epithelial cells

The experiments and data presented in this Chapter have been performed using bronchial epithelial cells and not alveolar epithelial cells, so inferences about epithelial function and the onset of parenchymal disorders such as idiopathic pulmonary fibrosis, where alveolar cells are assumed to be the primary site of aberrant wound repair, should be made with caution. In IPF, the bronchiolarisation of alveolar epithelial cells facilitates the use of bronchial epithelial cells to be used as a surrogate to evaluate alveolar pathology, but this is not known to be the case post COVID-19.[524]

8.6.4.2 Barrier function

TEER is a validated measure of assessing barrier function.[234] However, significant variability in the results can occur and it is influenced by the external factors such as temperature and the angle at which the probe is held. To mitigate inaccuracies related to TEER measurements, a calibrator with a known resistance of 1000 Ohms was assessed before the TEER probe was used and the same cell culture hood was used for each experiment. In addition, TEER measurements were taken from every well, which meant an average of measurements from 36 or more wells for each donor for the first time point was derived, which reduced in number with subsequent timepoints. The inherent variability of the technique means that although a significant difference was not seen between post COVID-19 and healthy control PBECs post IAV infection, this may be due to TEER assessments not being sensitive enough to detect subtle changes in barrier integrity.

An alternative method for assessing barrier function would have been to use fluorescein isothiocyanate (FITC)-Dextran assay to assess permeability of the cell layer to the dextran solution through quantification of leakage into the basal compartment using fluorescence.[525] However, a significant number of PBS washes are required as part of the protocol, which, in the context of IAV infection where cells are already friable, can result in removal of the cell monolayer with subsequent washes.

8.6.4.3 Flu challenge model

A MOI of 0.01 of IAV ENG/195/09 was utilised as there is a well-established protocol for this in our lab. There were morphological changes, maximal at 72 hours post infection, when maximal loss of ciliated cells was seen. I chose influenza A virus as I wanted to asssess the in-vitro effects of a highly virulent virus which causes significant respiratory morbidity and mortality in the UK every year. My results are specific to this virus only, and it is possible that if a different virus, such as rhinovirus, which is not as cytopathic to infected epithelial cells was utilised, the degree of immune response may have been different. After COVID-19, a dysregulated immune response resulting in exacerbation of pre-existing autoimmune pathology and new onset autoimmune disease has been reported.[526] Furthermore, in individuals with long-COVID, there is evidence of persistent immune activation even 8 months after recovery.[527] Timing of assessment of immune response to influenza may therefore be crucial, with a hyper-active immune response early post discharge. The majority of the epithelial cells utilised for this analysis were within a similar timeframe, therefore this time-dependent response is mitigated to some extent.

My initial experimental plan was for 168 hours (7 days) so that I could assess wound healing. However, it was difficult to maintain cell viability for 7 days, even in the UV-treated mocks, therefore the experiment was shorted to 96 hours in subsequent rounds. Possible reasons for this include daily TEER measurements and collection of apical supernatants resulting in cellular damage. A better approach might have been to perform 48-hour collection of apical supernatants and only taking TEER measurements from a smaller number of wells (e.g. 6) from the final timepoint. However, as aforementioned, this further reduces the reliability of the TEER results.

My current model allowed epithelial-derived immune responses to be adequately assessed. However, to assess local wound healing, a funnel approach to enable delivery of the virus to a small section of the epithelial monolayer may have been better, although it remains possible that given the potent

nature of the virus, rapid viral replication and cellular apoptosis may result in cellular damage to the entire epithelial monolayer, regardless.

8.6.4.4 Challenges with the ALI model

The ALI model is a well-established model for the study of airway epithelial cells. However, significant heterogeneity can occur even between wells from the same donor, exposed to the same experimental condition. This may be due to slight differences in seeding density or because the individual replicates have been growing independently of each other for 4-5 weeks at the point of experiments. For the purposes of this thesis, basal supernatants were pooled and an average of experimental replicates taken for protein quantification. A large number of donors have been used for these experiments, which helps increase the validity of the results presented.

8.6.4.5 Challenges with interpretation of transcriptomic data

Firstly, as aforementioned, gene expression does not necessarily correlate with protein synthesis and therefore the biological significance of the upregulation in gene expression seen needs to be interpreted with caution. Secondly, we pooled RNA from 2 healthy control and 3 post-COVID-19 donors. This is a small sample size which may reduce the reliability of the results, especially given the biological variability that exists between human donors. A better approach would have been to pool RNA from a higher number of donors (e.g. 6) or send RNA from individual donors separately. However, in order to balance costs with results, we chose to pool donor RNA and sample more timepoints and this was informative for our purposes and mostly corroborated through qPCR.

8.7 Conclusion

In this Chapter, I have shown that epithelial function has not fully recovered post COVID-19. Wound healing responses are impaired in some individuals, however, immune responses to influenza A infection are preserved when compared to healthy controls. There might also be intrinsic differences in the ciliated cells post COVID-19, but further in vitro studies are required to better understand this.

Chapter 9 - Assessing the role of DPP4 in the airways

9.1 Introduction

Dipeptidyl-peptidase 4 (DPP4) and amphiregulin (AREG) were both upregulated in the post-COVID-19 airway[341] compared to healthy controls, but the reason for this and role that DPP4 plays in epithelial biology is poorly understood.

9.1.1. DPP4

DPP4 is a serine-type peptidase which is expressed on multiple cell types. It exists in two forms: a transmembrane protein and a soluble, protein once cleaved from the membrane.[528] Its peptidase activity allows cleavage of many different substrates, including extracellular matrix proteins such as fibronectin and collagen.[529]

Elevated DPP4 expression has been noted in diabetes and obesity, and manipulation of the DPP4-incretin axis has garnered much interest as a method of regulating blood glucose, resulting in DPP4 inhibitors being approved and widely used in the management of diabetes.[530]

The role DPP4 plays in lung disease is less clear, but there is evolving evidence that DPP4 inhibitors may have a role in attenuating pulmonary fibrosis through regulation of the extracellular matrix[531] and reducing epithelial-to-mesenchymal transition (EMT).[532] Further validating this is that in 16HBEs (human bronchial epithelial cell lines), TGF beta 1-induced EMT is promoted in the presence of DPP4 and attenuated in the presence of a DPP4-inhibitor, sitagliptin.[533] Additionally, the membrane-bound form of DPP4 is the receptor for the Middle East Respiratory Virus (MERS), so it may also have a role in facilitating viral entry into epithelial cells.[534,535]

DPP4 plays a role in inflammation, with soluble DPP4 being able to increase secretion of IL6 and IL8.[536] In addition, after lipopolysaccharide (LPS)-induced lung injury, treatment with sitagliptin (DPP4 inhibitor) has been shown to reduce IL6, 8 and TNF alpha.[537] Furthermore, the soluble form of DPP4 was seen to increase in the peripheral circulation after influenza infection in mice, with a positive correlation with CD8 cells.[538]

In bronchial epithelial cells derived from asthmatics cultured to air-liquid interface, IL-13 increases DPP4 mRNA expression. In addition, in freshly isolated PBECs from the distal airways, DPP4 mRNA

expression positively correlated with exhaled nitric oxide, suggesting a role in type 2 inflammation. In addition, recombinant DPP4 stimulation has been shown to increase human lung fibroblast proliferation and fibronectin gene and protein expression from both human lung fibroblasts and bronchial smooth muscle cells in a dose-dependent manner.[539] Therefore, DPP4 has been implicated in the pathogenesis of asthma and considered to have a role as a potential biomarker.

During acute COVID-19, there was considerable interest in the effect of sitagliptin on acute severity of disease. These results were, however, conflicting, with no convincing evidence that individuals already on sitagliptin (for Type 2 diabetes mellitus) had a more benign disease course or suppression of inflammatory markers such as CRP and IL6.[540–542]

Whilst DPP4 has been associated with a variety of chronic lung diseases, there still remains a gap in the literature for understanding its role in epithelial repair. There have been no studies to-date evaluating the role of DPP4 or its inhibition on bronchial epithelial cells derived from patients recovering post COVID-19.

9.1.2 AREG

Amphiregulin (AREG) is an epidermal growth factor receptor (EGFR) ligand and plays a crucial role in tissue repair. It is expressed by multiple immune cells, and has been thought to be associated with type 2 immune-mediated tolerance.[543] A variety of mediators have been shown to upregulate AREG, including TGF beta[544] and IL33, an alarmin, which alerts the immune system to cellular damage.[545] At baseline, AREG is expressed in small quantities, but is upregulated in the context of epithelial injury to promote wound healing.[546] AREG has also been shown to be upregulated in chronic lung diseases such as COPD and asthma and is thought to play both pro-inflammatory and pro-fibrotic roles.[505] In comparison to other EGFR ligands, AREG has a low-affinity binding capacity to the epidermal growth factor receptor which may help to explain some of its diverse effects.[547]

AREG-EGFR signalling is important for the expansion of basal cells, stem cells of the respiratory epithelium, which then subsequently differentiate to provide the mucosal barrier discussed earlier in this thesis.[505] AREG is produced by basal cells but also innate lymphoid (ILCs) and T regulatory cells (Tregs).[543] Whilst important in the regulation of wound healing and repair, excess AREG can promote basal cell hyperplasia, as seen in smoking-related lung disease, and result in excess deposition of extracellular matrix (ECM) proteins, thus having a pro-fibrotic effect.[548]

9.1.3 Relationship between DPP4 and AREG

Currently, there is no literature evaluating the relationship between DPP4 and AREG, but both mediators were upregulated in the post-COVID-19 airway, as compared to healthy controls.

9.2 Background

Whilst it is likely that AREG upregulation is a response to epithelial injury, the reason for the upregulation of DPP4 in the post-COVID-19 airway is not known. In the absence of endobronchial sampling of human participants after other infections causing a severe epithelial insult, such as influenza, it is difficult to decipher if the upregulation in DPP4 is specific to SARS-COV2 infection, or indeed an epithelial response to severe viral injury. Furthermore, it is not known if the cellular source contributing to the increase in protein seen, is the epithelium or immune cells, as previously discussed.

In Chapter 8, I showed that although there is no difference between the interferon or interferon-stimulated gene response to influenza A infection in patients recovering post COVID-19 compared to healthy controls, epithelial cells from some post COVID-19 donors have aberrant responses to wound closure after a linear scratch is applied. Therefore, at 3-6 months post discharge from hospital after acute COVID-19, epithelial cells from some donors retain intrinsic abnormalities impairing their response to epithelial damage. The role that DPP4 plays in promoting this or reducing this abnormality is not known.

This Chapter aims to further our understanding of DPP4 and its role in epithelial cell structure, and function, and to elicit if a relationship between DPP4 and AREG exists at baseline, upon stimulation with recombinant DPP4 or its inhibitor (sitagliptin), and in response to epithelial injury.

9.3 Hypothesis and Aims

Hypothesis

DPP4 plays an immunomodulatory role in response to viral epithelial injury and its upregulation promotes wound healing. Increased DPP4 positively induces AREG secretion from epithelial cells.

Aims

a) To assess the effect of DPP4 and its inhibition on epithelial cell response to mechanical and viral epithelial injury
b) To assess the effect of DPP4 and its inhibition on epithelial cell proliferation and differentiation
c) To assess the effect of DPP4 and its inhibition on fibroblast activity
d) To assess the relationship between DPP4 and AREG both in vivo and in vitro

9.4 Methods

Recombinant DPP4 (Abcam) was used to stimulate cells with DPP4. Sitagliptin is one of the most potent inhibitors of DPP4 and inactivates the peptidase activity of DPP4.[549] Therefore, sitagliptin (Selleckhem) was used as the DPP4 inhibitor for the in vitro studies described.

9.4.1 Epithelial cells: Submerged culture

9.4.1.1 Proliferation

Epithelial cells were expanded from cryopreservation into a T75 flask as described in Chapter 2 and cells detached using Tryple (Gibco) once the flask was 80-90% confluent. Cells were seeded in a 48-well plate (Corning), pre-coated with 1 in 100 Type 1 collagen (Advanced Biomatrix), at a seeding density of 1.5 x 10^4 cells per well in Airway epithelial cell growth media (Promocell).

48 hours after seeding, once the cells had attached to the plate, the media was refreshed with 200µl of the following conditions: a) Airway epithelial cell growth medium (control) b) DPP4 100ng/ml b) DPP4 200ng/ml c) DPP4 400ng/ml c) Sitagliptin 20 µmol/L d) Sitagliptin 40 µmol/L e) Sitagliptin 80 µmol/L. Each experimental condition was evaluated in duplicates. All treatments were constituted in airway epithelial cell growth media.

The cells underwent constant stimulation with the aforementioned mediators for 48 hours, at which point, basal supernatant was collected, and cells fixed for imaging with 4% PFA. Ki67 staining was performed as outlined in Chapter 2. Multi-channel fluorescence imaging was performed using the DAPI and RFP channels on JuliTM Stage Real-Time Cell History Recorder (NanoEnTek, Seoul, Korea.) 2-3 images were taken per well under both channels. Automated cell counting was performed using

JuliStat (JuliStage Software) at 10x magnification, where possible. Where the cells were not being adequately recognised by the software, cells were counted manually. A ratio was derived between the number of Ki67+ and DAPI+ cells. In addition to assessment of cells in the proliferative stage, the percentage confluence of each well (2-3 positions per well) was calculated for the control and treatment groups using JuliStat (JuliStage software).

9.4.1.2 Scratch

A 48-well plate was seeded at a density of 3 x 10^4 cells per well and once confluency was achieved, the media was refreshed with 200µl of Airway epithelial cell growth media (control) or varying concentrations of DPP4 or sitagliptin as utilised for the evaluation of cellular proliferation (described above). A linear wound was made using a yellow (P200) pipette tip and brightfield, time-lapse images were taken every 2 hours for 24 hours using JuliTM Stage Real-Time Cell History Recorder (NanoEnTek, Seoul, Korea). Basal supernatant was collected, and RNA harvested 24 hours after the linear wound was applied. Each experimental condition was evaluated in duplicates.

9.4.2 Epithelial cells: Air-liquid interface

PBECs were grown to air-liquid interface as described in Chapter 2 and a series of experiments were carried out to assess cellular differentiation and function.

9.4.2.1 Differentiation

To assess the effect of DPP4 or its inhibition on differentiation, cells were cultured in Pneumacult (Stemcell) with different concentrations of DPP4 (100, 200, 400ng/ml) or sitagliptin (20, 40, 80µmol/L) from the point of air exposure. The basal media was refreshed every 72 hours and replaced with media containing DPP4 or sitagliptin so that the cells received continuous stimulation. Cells were harvested for RNA and apical and basal supernatant collected, 3 weeks post air exposure, at which point, the cells were assumed to have fully differentiated, based on experience conducting experiments in Chapter 8.

9.4.2.2 Assessing the effect of DPP4/inhibition on inflammatory and immunomodulatory pathways

Experiments were performed 3 weeks post air exposure, at which point epithelial cell differentiation had occurred. Epithelial cell differentiation was confirmed through visualization of beating cilia using the Leica SP5 inverted microscope and LAS AF platform.

DPP4 and sitagliptin were delivered either apically or basally. For basal delivery, cells were pre-treated with DPP4 (D0-5: DPP4 50, 100, 200, 400, 800 or 1600ng/ml) or sitagliptin (S1-5: 10, 20, 40, 80, 160 µmol/L) in steroid-free Pneumacult (Stemcell) media for 2 hours prior to infection with IAV apically. IAV (made to a concentration of MOI 0.01 in 100µl of serum-free DMEM, as outlined in Chapter 8) was added to the apical surface and subsequently removed after 1 hour. The cells underwent continuous stimulation with DPP4 or sitagliptin for 72 hours.

For apical delivery of DPP4 or sitagliptin, pre-treatment of the epithelial cells was performed for 2 hours and then the apical treatments were removed. The cells were then infected with IAV at a MOI of 0.01 for one hour as described above.

For the controls (UV-IAV or DMEM), either UV-inactivated IAV or serum-free DMEM was added to the apical surface instead of IAV. The basal compartment for the controls contained steroid-free Pneumacult media only. For the sitagliptin or DPP4 only groups, 100µl of serum-free DMEM was added to apical surface (instead of IAV) and removed after 1 hour.

Apical and basal supernatant and RNA were collected 72 hours after the treatment as described above. Where possible, images were fixed with 4% PFA for immunofluorescence staining.

9.4.3 Fibroblast culture

9.4.3.1 Fibroblast proliferation

Human lung fibroblasts (Lonzo) were expanded from cryopreservation in an uncoated T75 flask (Corning) and split using Tryple (Gibco) when 80-90% confluence had been reached. Cells were seeded at density of 1.5 x 10^4 cells/ well in a 48-well plate (Corning) in serum-free DMEM (Gibco). After 24 hours, once the cells had adhered to the plate surface, 200µl of DPP4 (50, 100, 200, 400, 800 ng/ml) or sitagliptin (20, 40, 80, 160 µmol/L) constituted in DMEM supplemented with 10% FBS, was added

to the fibroblasts in submerged culture. Each experimental condition was evaluated in triplicates. Brightfield, time-lapse images were taken every 2 hours for 24 hours using JuliTM Stage Real-Time Cell History Recorder (NanoEnTek, Seoul, Korea and percentage confluence in each well was calculated after averaging results from 2-3 positions per well using JuliStat (Julistage software).

9.4.3.2 Fibroblast scratch assay

Fibroblasts were seeded at a density of 3 x 10^4 cells in DMEM supplemented with 10% FBS. Once confluent, cells were serum-starved for 24 hours prior to experimentation. The media was then refreshed with media containing DPP4 (50, 100, 200, 400, 800ng/ml) or sitagliptin (10, 20, 40, 80, 160µmol/L) in DMEM containing 10% FBS. A linear wound was applied to the confluent fibroblast monolayer with a yellow (P200) pipette tip. Images of wound closure were taken using JuliTM Stage Real-Time Cell History Recorder (NanoEnTek, Seoul, Korea) and percentage wound closure over time calculated using JuliStat (Juli Stage software).

9.5 Results

9.5.1 DPP4 and AREG protein in BALF

Proteomic analysis of BALF supernatants showed a statistically significant upregulation of DPP4 and AREG in the airways of patients recovering post COVID-19 compared to healthy controls (Figure 9.1).

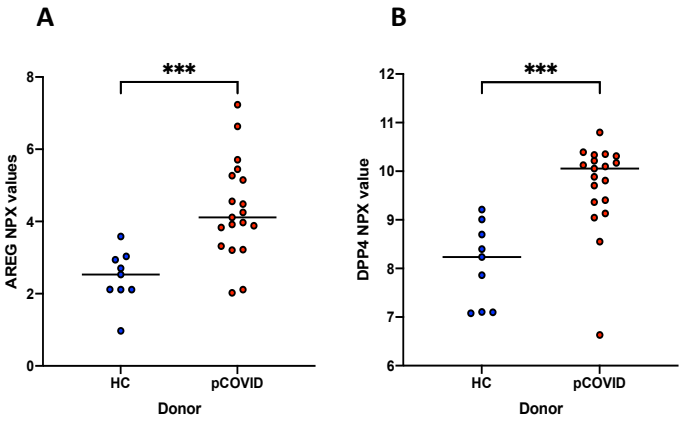


Figure 9. 1 DPP4 and AREG detected by O-link in the BALF supernatants

Abbreviation: NPX (normalised protein expression). Inter-group comparisons performed using Mann-Whitney U testing. P values: * <0.05, ** <0.01, *** <0.001

As the EGFR ligands and in particular, AREG, is associated with epithelial wound healing and repair, I wanted to assess whether a relationship existed between DPP4 and AREG, to help decipher if the elevation in airway DPP4 was related to epithelial repair mechanisms. A strong, positive correlation between DPP4 and AREG, both in the post COVID-19 donors (Figure 9.2A), healthy controls (Figure 9.2B) and combined cohort (Figure 9.2C) was seen. The presence of detectable AREG and DPP4 in the airways of healthy donors, with the assumption that these individuals had not been subject to a recent severe viral pneumonia or any other significant forms of epithelial injury, suggests that these proteins are present in the airway microenvironment, even at homeostasis. One possibility is that the upregulation of both AREG and DPP4 in the post-COVID-19 cohort, and therefore differential abundance post COVID-19 compared to healthy controls, is in response to recent epithelial injury (in this case, caused SARS-COV2 infection).

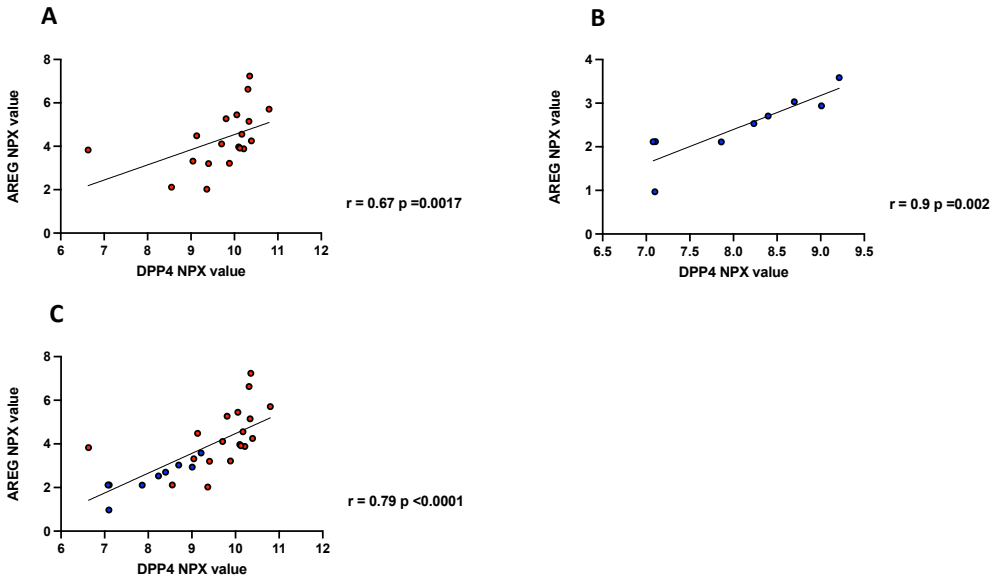


Figure 9. 2 Relationship between DPP4 and AREG in BALF supernatant

Protein measured by O-link assay in BALF supernatant. Non-parametric, Spearman rank correlation analysis performed. P value <0.05 considered statistically significant. Key: Red– post COVID-19 donors, Blue – healthy control donors. Each dot signifies an individual biological donor

9.5.2 Gene expression of AREG and DPP4 in differentiated PBECs at air-liquid interface

I wanted to assess whether the findings in vivo could be reproduced in vitro. Gene expression of DPP4 and AREG were measured by qPCR and protein concentration measured by ELISA at 3 weeks post air exposure at air-liquid interface. There was upregulation of gene expression of both DPP4 ($p < 0.05$) and AREG (not significant) in PBECs post COVID-19 compared to healthy controls (Figure 9.3). However, detection of protein in the apical (Figure 9.4 A, C) and basal supernatants (Figure 9.4 B, D) were comparable between post COVID-19 and healthy control donors.

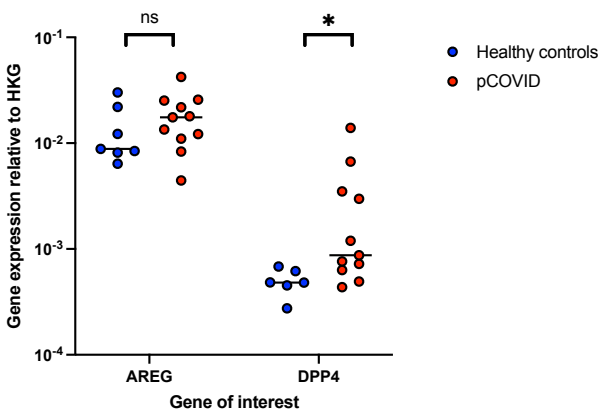


Figure 9. 3 DPP4 and AREG gene expression at 3 weeks post air exposure

Inter-group comparison performed using Mann Whitney U testing. P value <0.05 considered statistically significant. * <0.05. Each dot denotes an individual biological donor.

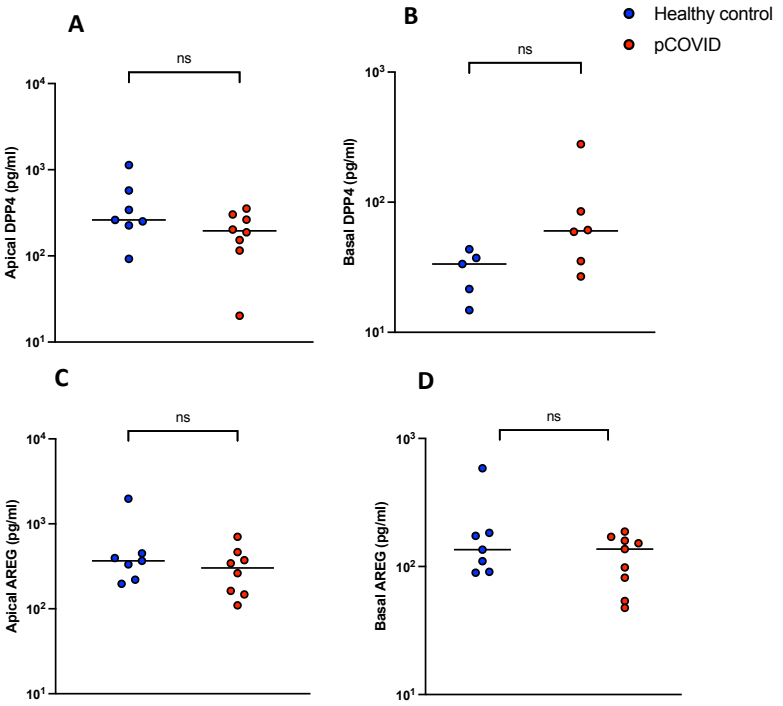


Figure 9. 4 DPP4 and AREG measured in the supernatants of PBECs at ALI (3 weeks post air exposure)

DPP4 and AREG measured in apical (A, C) and basal supernatants (B, D) of PBECs cultured at ALI, 3 weeks post air exposure. DPP4 was not detectable in the basal supernatants for 2 pCOVID-19 donors and 2 healthy control donors. Lower limit of detection for DPP4 ELISA is 31.25pg/ml. Basal supernatants were analysed neat. Each dot represents an individual biological donor

In the absence of differences in protein secretion, despite the differences in gene expression, I wanted to assess whether protein secretion would change with time post air exposure, i.e., if there is a delay between gene expression and protein secretion. I therefore, measured AREG and DPP4 in the apical and basal supernatants of cells air exposed for 5-7 weeks. There was a statistically significant lower concentration of AREG in the basal supernatant in post COVID-19 donors (Figure 9.5 C) but non-significant differences in DPP4 (B, D) or AREG in the apical compartment (A). The drop in AREG was therefore not related to a preferential shift into the apical compartment. In fact, although, not statistically significant, median levels of AREG in the apical supernatants of post COVID-19 donors at 5-7 weeks was lower at 269 (225 – 408) pg/ml compared to 302 (151 – 443) pg/ml at 3 weeks.

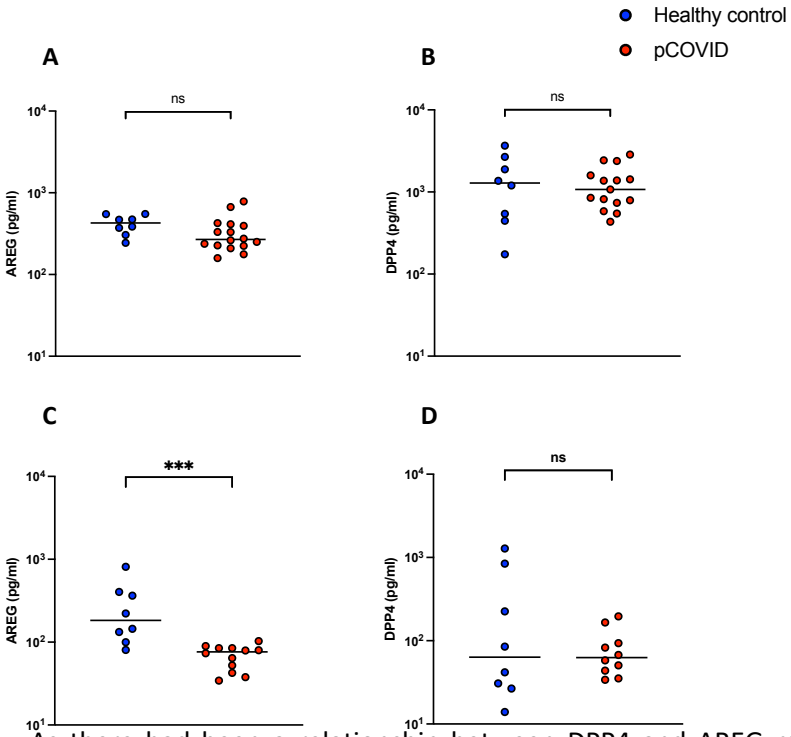


Figure 9. 5 AREG and DPP4 in supernatants of PBECs at ALI (5-7 weeks post air exposure)

Protein detected in the apical supernatant (A, B) and basal supernatant (C, D). Inter-group comparisons performed using Mann Whitney U testing. P value <0.05 considered statistically significant. * <0.05, ** <0.01, *** <0.001. Each dot represents an individual biological donor.

As there had been a relationship between DPP4 and AREG measured by proteomics in the BALF supernatants, I wanted to assess whether this was replicated in vitro when cells were grown to ALI. A strong, statistically significant positive correlation (r = 0.81, p = 0.01) was noted between DPP4 and AREG detected in the apical supernatant (Figure 9.6 A) and a negative correlation (although not statistically significant (r = -0.77, p = 0.10) in the basal supernatant (9.6 D) of PBECs from post-COVID-19 donors, but not healthy control donors. As protein concentrations of DPP4 and AREG at 3 weeks post air exposure were comparable in post COVID-19 and healthy control donors (Figure 9.4), the cohorts were combined, and again, a statistically significant positive correlation (r=0.67, p=0.01) in the apical supernatants and statistically significant negative correlation (r=-0.73, p=0.01) in the basal supernatants was seen, although the latter was driven slightly by two outliers, identified by Grubb's testing: one post COVID-19 donor with a AREG concentration of 280pg/ml and one healthy control donor with a DPP4 concentration of 585pg/ml).

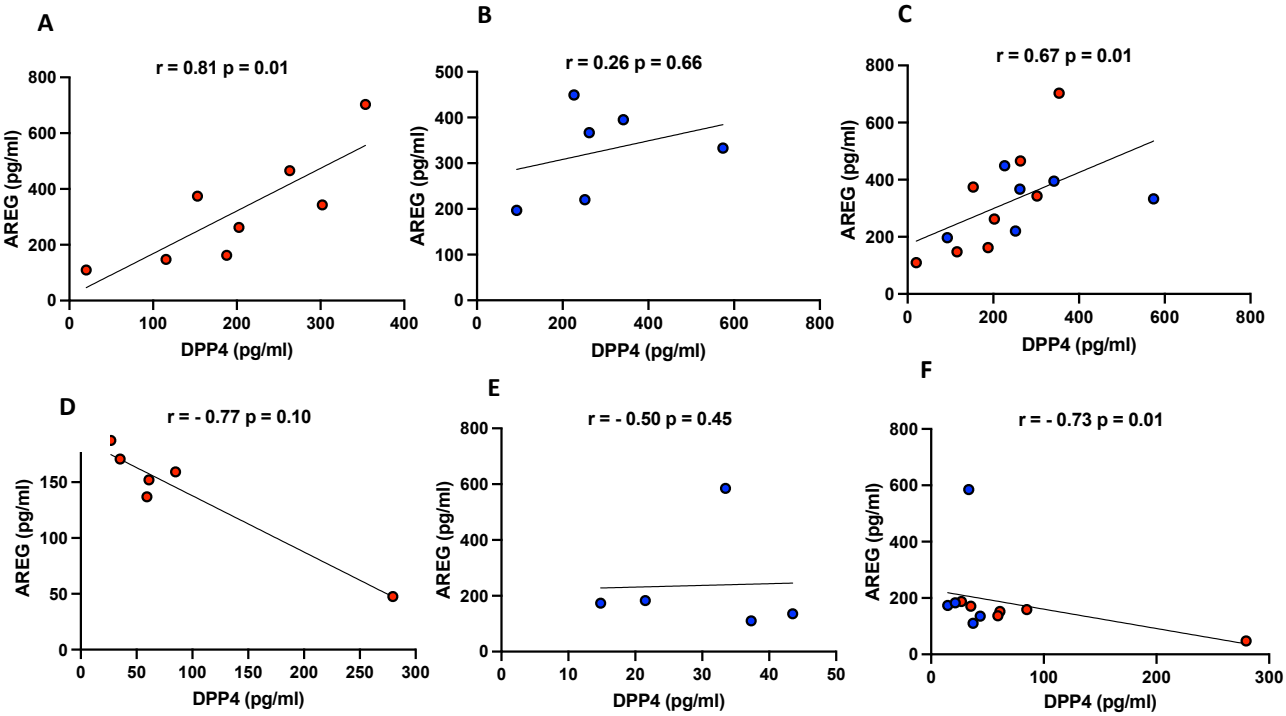


Figure 9. 6 Relationship between DPP4 and AREG in the supernatants at 3 weeks post air exposure

Protein concentration in apical supernatant (A-C) and basal supernatant (D-F) of PBECs cultured at ALI from post COVID-19 donors (A, D), healthy control donors (B, E) and combined cohort (C, F). Each dot denotes a biological donor. Non-parametric Spearman rank correlation analysis performed. P value <0.05 considered statistically significant. Exclusion of one outlier in healthy control data (identified by Grubbs) with DPP4 value of 1134 pg/ml and AREG of 1978 pg/ml in apical supernatant.

Assessment of the same relationship in PBECs at ALI air exposed for 5-7 weeks showed no significant relationship between DPP4 and AREG in neither the apical (Figure 9.7 A-C) nor basal (D-F) compartments.

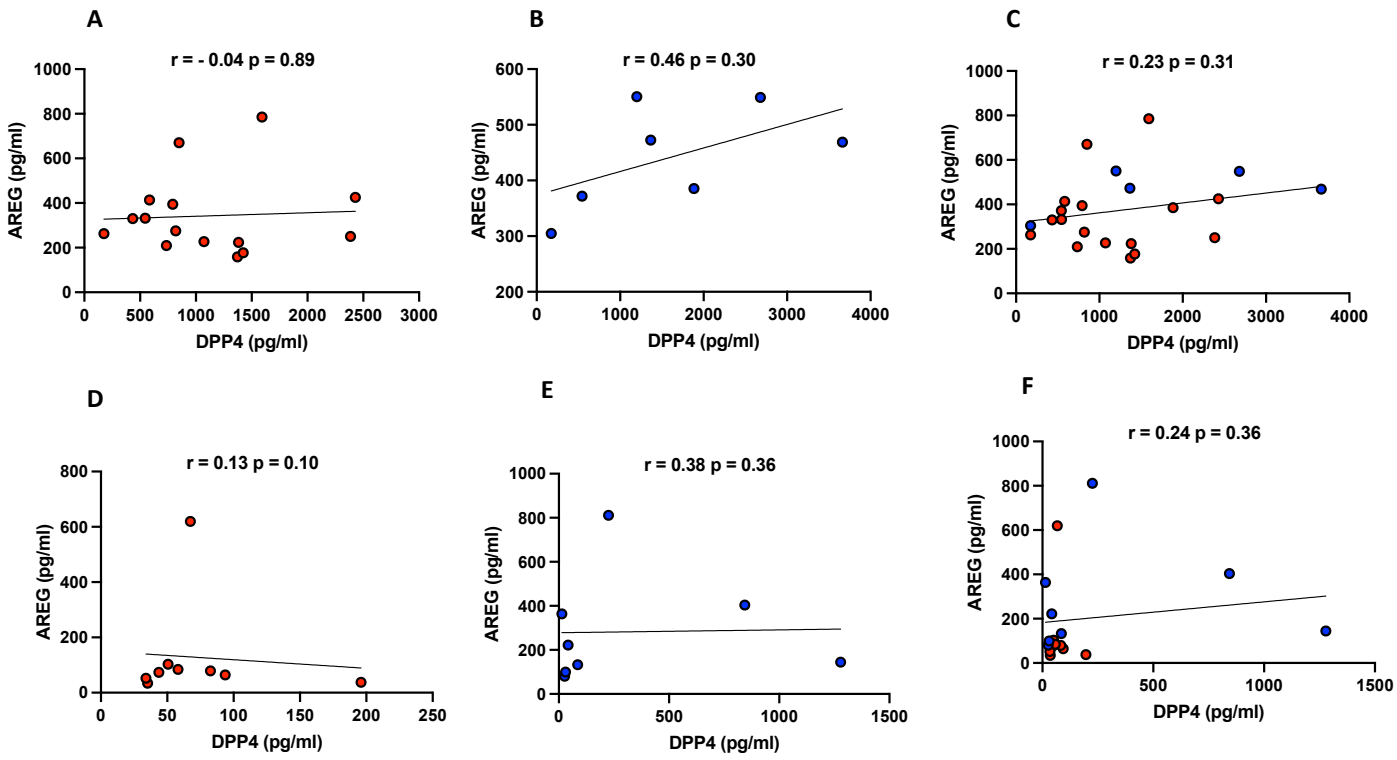


Figure 9. 7 Relationship between DPP4 and AREG in supernatants at 5-7 weeks post air exposure.

Protein concentration in apical supernatant (A-C) and basal supernatant (D-F) of PBECs from post COVID -19 donors (A, D), healthy control donors (B, E) and combined cohort (C, F). Each dot denotes a biological donor. Non-parametric Spearman rank correlation analysis performed. P value <0.05 considered statistically significant.

Furthermore, a time-related increase in DPP4 secretion into the apical compartment was seen in both PBECs from post COVID-19 donors and healthy controls between 3 and 6 weeks, with greater increases in DPP4 secretion in PBECs from post-COVID 19 donors (Figure 9.8A). By contrast, there were no significant differences in AREG secretion into the apical or basal compartment with time (9.9 B, D) or DPP4 secretion into the basal compartment (9.9 C). Whilst not statistically significant, basally detected AREG levels were lower in post COVID-19 PBECs at 6 weeks compared to at 3 weeks post air exposure (median 76 [IQR 45 – 85]pg/ml vs 137 [68 – 165] pg/ml, p=0.07). By contrast, basal AREG levels were higher at 6 weeks in HC PBECs compared to 3 weeks: 183 (108 – 393) vs 136 (91 – 183). At 3 weeks post air exposure, there was a slightly lower level of DPP4 in the apical supernatants of post COVID-19 PBECs compared to HC PBECs (195.2 (125 – 293) vs 262.0 (226 – 574) pg/ml. This was also replicated at 6 weeks post exposure (961 (622 – 1551) vs HC vs 1367 (542 – 2680) pg/ml, although not statistically significant.

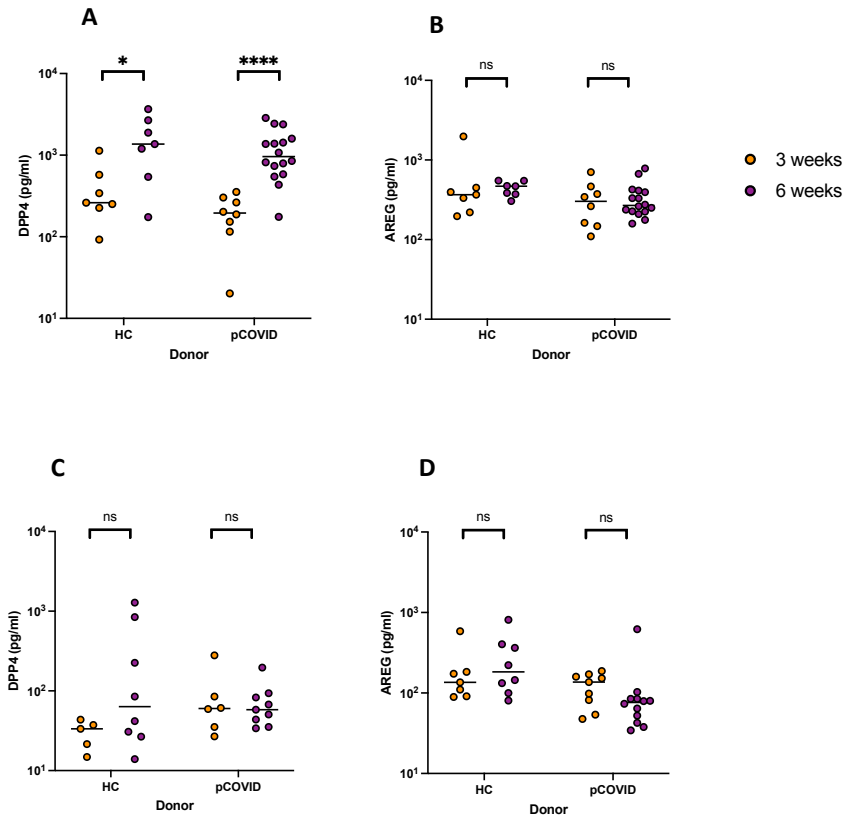


Figure 9. 8 Changes in DPP4 and AREG levels at 3 and 6 weeks* post air exposure

Protein concentration noted in apical supernatant (A, B) and basal supernatant (C, D) of PBECs cultured at ALI. *5-7 weeks post air exposure. Each dot represents a biological donor. Inter-group comparisons made using Mann Whitney U testing. P value <0.05 considered statistically significant. Abbreviation: HC (healthy controls), pCOVID (Post COVID-19)

9.5.3 Baseline DPP4 and AREG levels and epithelial cell wound closure

In Chapter 8, I showed that in PBECs from some post COVID-19 donors, there is incomplete wound closure at 24 hours in response to a mechanical linear wound. I wanted to assess if the baseline DPP4 and AREG levels, as quantified using proteomics, or in the apical supernatants at ALI bore any relationship to the % wound closure achieved at 24 hours. The 24-hour timepoint was chosen as by this timepoint, most of the healthy control donor PBECs will have achieved 100% wound closure. There was, however, no relationship between DPP4 or AREG in the BALF and wound closure at 24 hours (Figure 9.9 A, B). Gene expression of AREG and DPP4 at 3 weeks post air exposure, was again, not related to wound closure (9.9 G, H). Whilst not significant, there is a trend towards greater wound closure being present in individuals with higher DPP4 levels in the apical SN at 3 weeks ($r = 0.64$, $p = 0.14$) (Figure 9.9 D), but not in AREG (9.9 C), or at 5-7 weeks post air exposure (9.9 E, F).

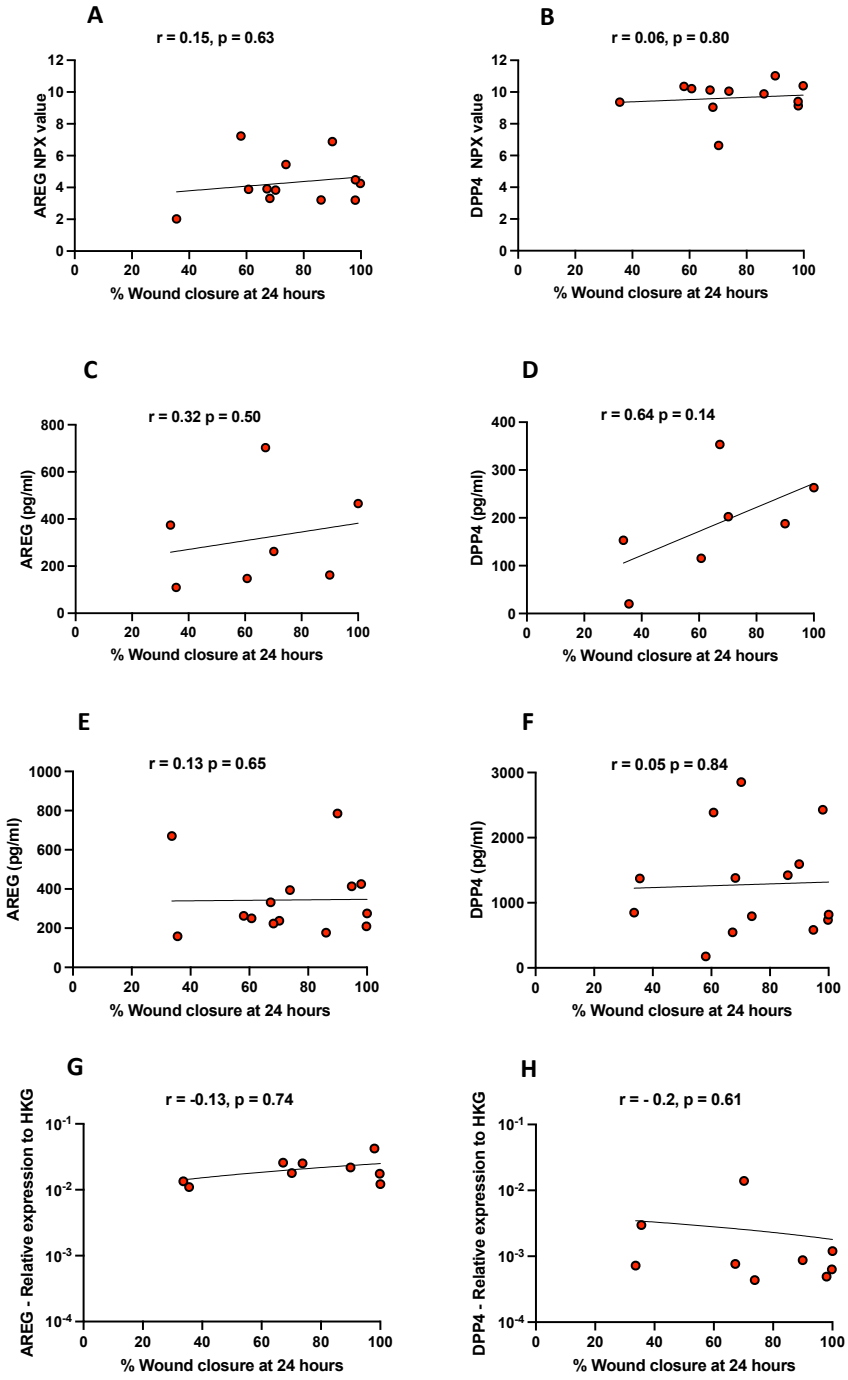


Figure 9. 9 Relationship between % wound closure at 24 hours and AREG, DPP4

Relationship between wound closure and AREG (A, C, E, G) and DPP4 (B, D, F, H) in vivo in BALF (A, B), apical supernatant at ALI at 3 weeks (C, D), gene expression in cell lysate at 3 weeks (G, H) and apical supernatant at ALI at 5-7 weeks (E, F) post air exposure. All data points show post-COVID-19 donors only. Non-parametric Spearman rank correlation analysis used. P value <0.05 considered statistically significant

9.5.4 Effect of IAV infection on DPP4

One potential theory is that DPP4 is upregulated in the airways post COVID-19 as part of the epithelial response to viral injury. I measured gene expression and protein levels of DPP4 in the IAV-infected PBEC cell lysate and basal supernatants, described in Chapter 8, at sequential timepoints. Gene expression using qPCR showed downregulation of DPP4 in IAV-infected cells compared to UV-IAV infected cells. Statistically significant differences were noted especially in the post COVID-19 donor PBECs with maximal effect at 72 hours post infection (Figure 9.10). As previously shown in Chapter 8, there is also upregulation of AREG in response to IAV infection. Evaluation of DPP4 by ELISA revealed peak response at 72 hours, in keeping with the peak responses noted of other inflammatory mediators (Figure 9.11).

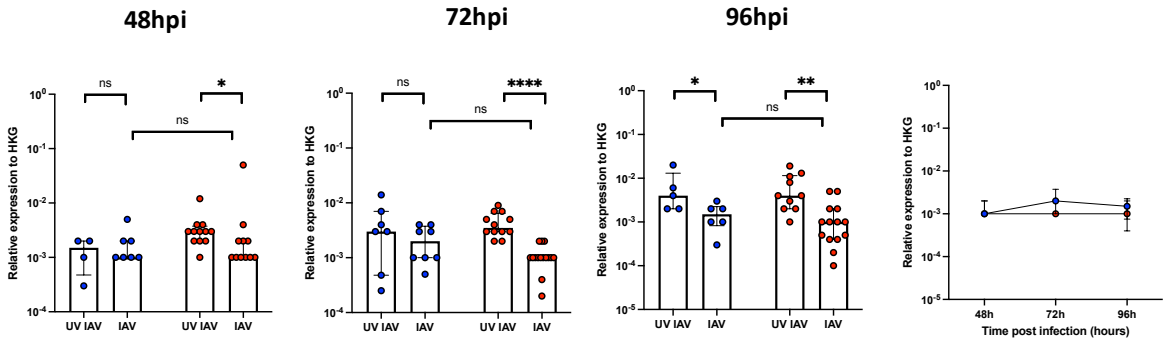


Figure 9. 10 Gene expression of DPP4 post IAV challenge

Inter-group differences assessed using Mann Whitney U testing. p values as follows – * <0.05, ** <0.01, *** <0.001, ****<0.0001. Each dot represents an individual biological donor. Median and inter-quartile ranges shown.

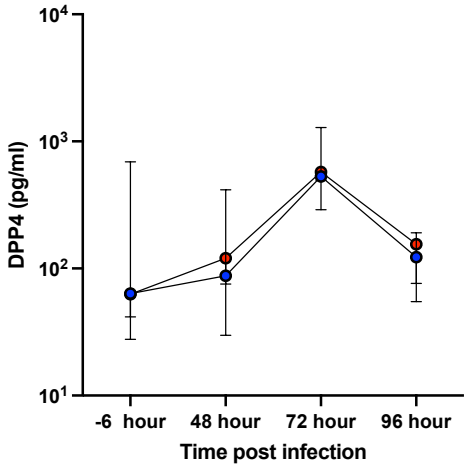


Figure 9. 11 DPP4 in basal supernatants of PBECs cultured at ALI post IAV challenge

DPP4 measured by ELISA in basal supernatant. Value at -6 hours, denotes baseline basal supernatant, collected approximately 6 hours prior to infection with IAV. Note, blue dot signifies healthy control donor and red dot, post COVID-19 donor. Median and interquartile ranges shown. Donor numbers range from 3-8 for healthy controls and 4-13 for post COVID-19 donors. The lowest donor representation was found at 96 hours where basal levels were less readily detectable at a 1 in 2 dilution.

9.5.5 Effect of DPP4 stimulation or inhibition on PBECs cultured to air-liquid interface

9.5.5.1 Epithelial cell differentiation

Next, to investigate the effect of DPP4 or its inhibition on epithelial cell differentiation, PBECs received continuous basal stimulation with DPP4 or sitagliptin during the differentiation process (i.e. when transitioning from basal cells to differentiated epithelium) for 3 weeks post air exposure. Upregulation of MUC5AC gene expression was seen in both the DPP4-stimulated group (9.12 A) as well as sitagliptin-simulated treatment group at the lower concentrations of 20 and 40µmol/L, but downregulation at the highest dose of 80µmol/L. FOXJ1 expression was downregulated at all doses of sitagliptin (9.12 B).

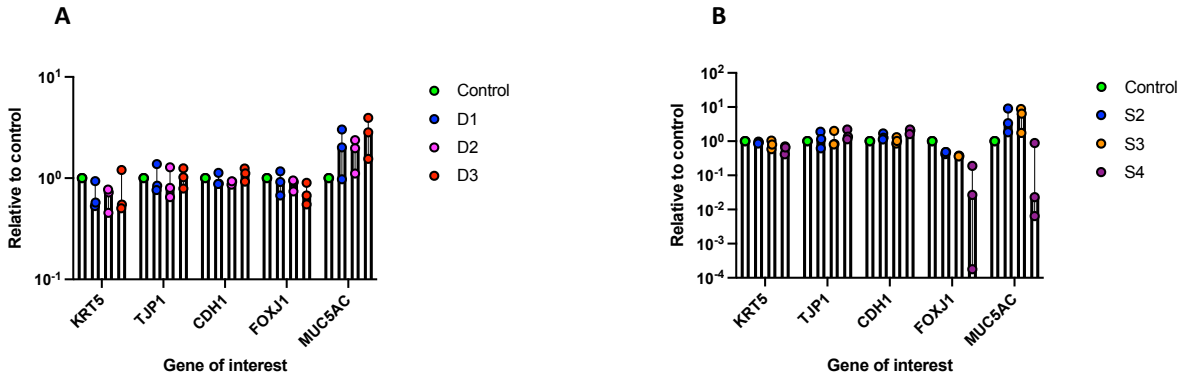


Figure 9. 12 Cell differentiation markers after basal stimulation with DPP4 or sitagliptin for 3 weeks

Gene expression using qPCR after continuous stimulation with DPP4 or sitagliptin. YWAHZ used as housekeeping gene for normalization and values relative to gene expression for the control well, shown. Each dot represents an individual biological healthy control donor. D1-3 correspond to DPP4 doses of 100, 200, 400ng/ml; S2-4 correspond to sitagliptin doses 20, 40, 80 µmol/L

Similar effects were seen after 72 hour stimulation of fully differentiated PBECs with sitagliptin at different concentrations (Figure 9.13): In healthy control PBECs (9.13 A, B), there was an upregulation of MUC5AC at the lower doses of sitagliptin (10 and 40 µmol/L) and downregulation at 80 µmol/L. A shift in gene expression of KRT5 was also seen, with a reduction in gene expression with higher doses of sitagliptin. There was also a shift towards increased expression of CDH1 at most of the sitagliptin doses. There were differences between the changes seen in PBECs from HC donors and post COVID-19 donors (9.13 C, D). For instance, MUC5AC expression was reduced at all doses of sitagliptin in post COVID-19 PBECs whereas upregulation was seen at some doses in HC PBECs.

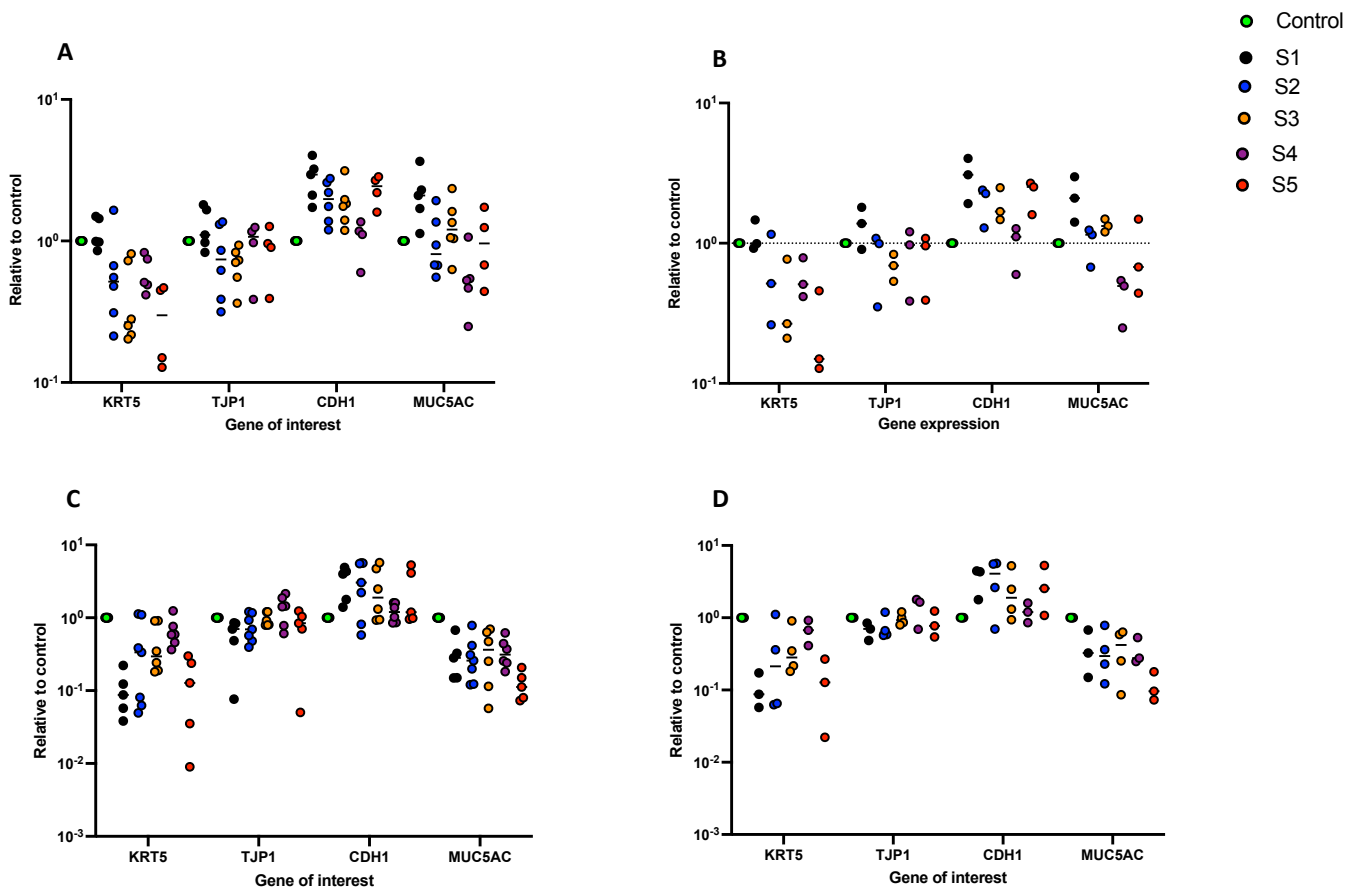


Figure 9. 13 Cell differentiation markers after 72-hour basal stimulation with sitagliptin

Differences in gene expression in PBECs cultured at ALI from healthy control donors (A, B) or post COVID-19 donors (C, D) after sitagliptin stimulation. S1-5 correspond to sitagliptin doses 10, 20, 40, 80, 160 µmol/L. Each dot represents a single well (A, B) or individual biological donor (B, D).

9.5.5.2 Epithelial-mesenchymal transition

The literature suggests that DPP4 might upregulate mesenchymal markers with the opposite effect seen with sitagliptin. I therefore assessed this further in PBECs undergoing constant stimulation with DPP4 or sitagliptin during differentiation. No significant changes were seen in genes associated with a mesenchymal phenotype (vimentin [VIM] or alpha smooth muscle actin [ACTA2]) with increasing doses of DPP4 or sitagliptin (Figure 9.14 A, B). The effect of sitagliptin at different doses was assessed after 72-hour continuous stimulation of differentiated epithelial cells, which showed contradicting findings. In healthy controls, the lowest dose (10µmol/L) showed trends towards increasing VIM and ACTA2 gene expression, but CDH1 was also upregulated (9.14 C). This was also seen with the highest dose of sitagliptin (160µmol/L). In post COVID-19 donor PBECs, however, the lowest and highest doses

resulted in downregulation of VIM and upregulation of ACTA2 (9.14 D). I then evaluated the effect of 800ng/ml DPP4 on PBECs, and again, this again did not upregulate markers associated with a mesenchymal phenotype or promote changes in cell differentiation markers (9.14 E).

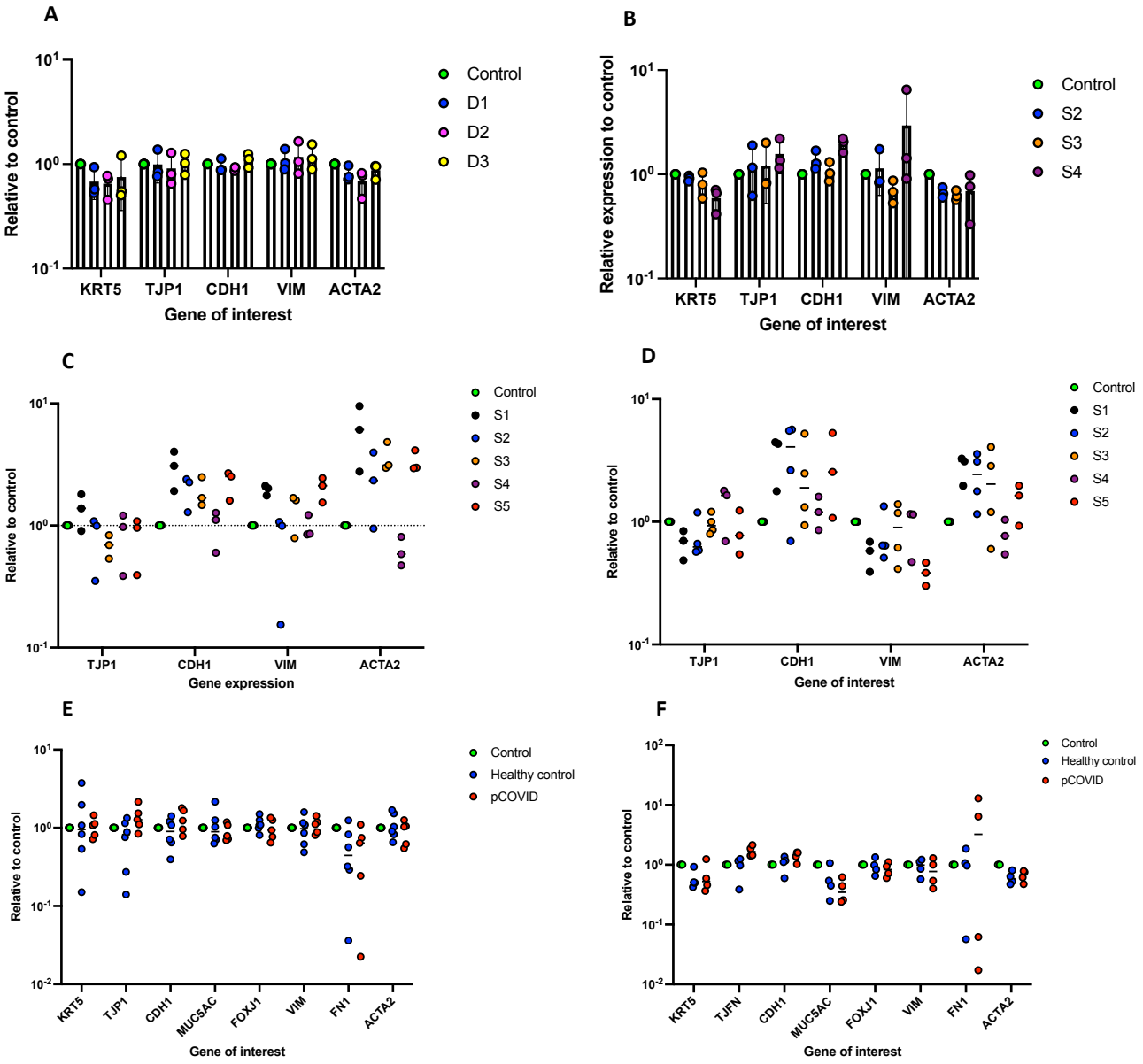


Figure 9. 14 Differentiation and EMT markers after 72-hour basal stimulation with DPP4 or sitagliptin

Continuous stimulation every 72 hours for 3 weeks from point of air exposure (A, B) or 72-hour stimulation of differentiated cells (C-D). 72-hour stimulation with DPP4 at D4 (E) or sitagliptin at S4 (F). A-C show results from HC PBECs; D post COVID-19 PBECs, E-F – both HC and post COVID-19 PBECs. Each dot represents an individual biological donor (A-D) or well (E-F). D1-4: DPP4 100, 200, 400, 800ng/ml. S1-4: sitagliptin doses 10, 20, 40, 80µmol/L). In E and F, the control is the well which received no treatment, for each donor. All values plotted in E and F are relative to the control wells.

9.5.5.3 Assessing the immunomodulatory effect of DPP4 and its inhibition on response to infection with IAV

9.5.5.3.1 Optimisation 1

To assess whether DPP4 could have any impact on the immune response or wound healing response to infection with IAV, I conducted optimisation studies based on literature in 16HBEs at ALI where a basally delivered dose of DPP4 at 50ng/ml and sitagliptin dose of 10 µmol/L was sufficient to elicit a difference in markers of epithelial-mesenchymal transition. Whilst this wasn't the endpoint decided, I utilised spare Transwell inserts when conducting experiments in Chapter 8, to assess the impact of basally delivered sitagliptin at 10µmol/L on gene expression of ISGs, inflammatory mediators and EGFR ligands on PBECs from 4 post-COVID-19 donors. Cells were pre-treated with sitagliptin (as appropriate) or steroid-free Pneumacult medium (control) for 2 hours prior to infection with IAV as described earlier and in Chapter 8. Apical and basal supernatant was collected and cells harvested for RNA at 48 hours post IAV infection. There was upregulation in gene expression of ISGs (RSAD2, OAS2, CXCL10), interferons (IFN beta and lambda), inflammatory mediators (IL8) and the EGFR ligand, AREG, in the group with IAV alone or sitagliptin plus IAV, but no obvious differences between the two IAV-infected groups (Figure 9.15). Flu M1 gene expression was similar between both IAV-infected groups.

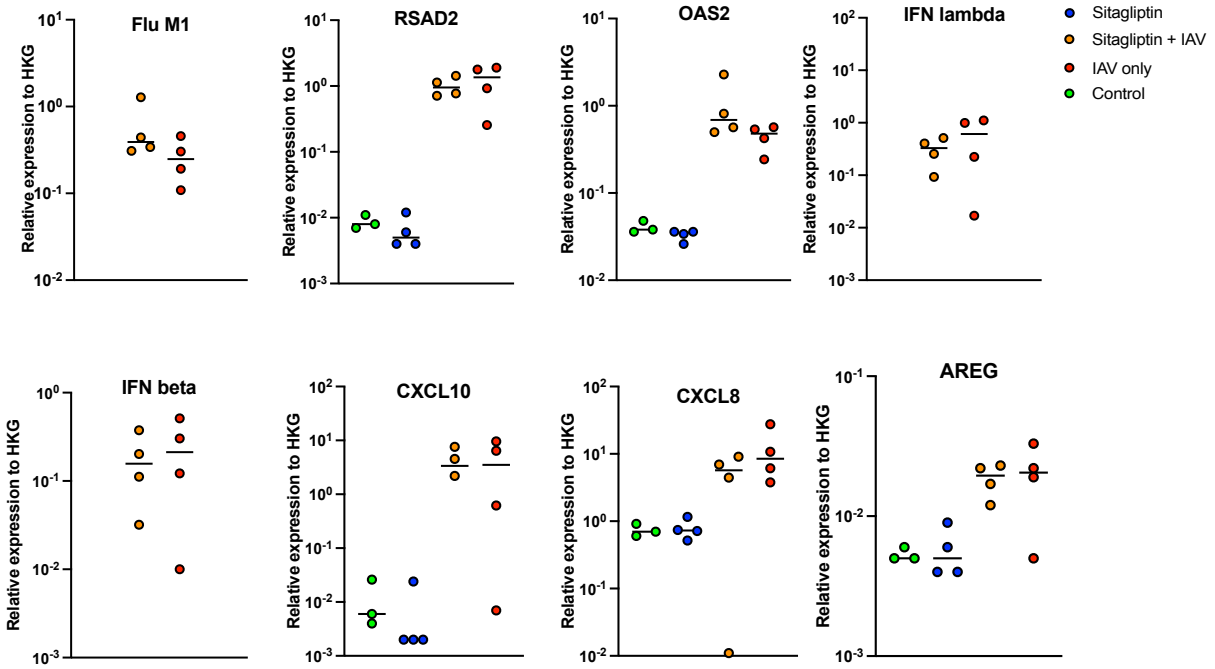


Figure 9. 15 Immune and wound healing response to IAV challenge +/- basal sitagliptin treatment

Gene expression in PBECs from n=4 post COVID-19 donors. Line drawn at median value. Each dot represents an individual biological donor.

Since, sitagliptin has been shown to reduce inflammatory mediators post LPS injury, I measured IL6 in the basal supernatant (Figure 9.16) from the above experiment. Again, there was upregulation of IL6 in the IAV groups, compared to no treatment or treatment with sitagliptin alone. A trend towards higher IL6 in patients treated with sitagliptin and IAV was seen.

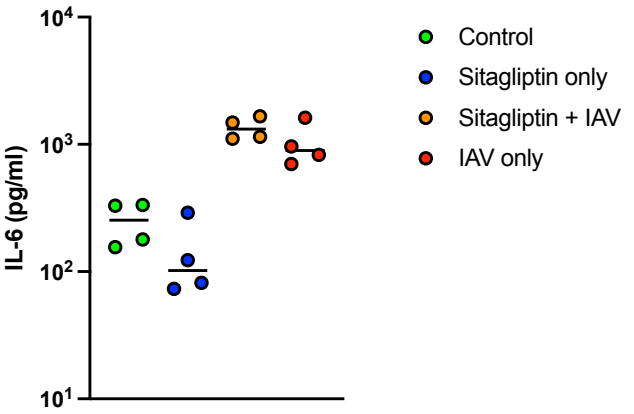


Figure 9. 16 IL6 level in basal supernatants

PBECs cultured at ALI underwent constant stimulation with sitagliptin or control (steroid-free Pneumacult) for 48 hours prior to collection of supernatants. Line drawn at median. Note slightly increased IL6 levels in response to sitagliptin and IAV compared to IAV alone

9.5.5.3.2 Optimisation 2

To further investigate whether the compartment (apical versus basal) of treatment delivery or the treatment dose might affect response, I conducted another set of optimisation experiments with dose titrations.

Firstly, I wanted to see if there was any change in IL6 or IL8 as detected by ELISA. It was evident from Chapter 8 that both IL6 and IL8 can be detected in the basal compartment at baseline and upregulated in response to IAV. I therefore measured these as my endpoints, in response to IAV alone, DPP4 + IAV, DPP4 alone, Sitagliptin alone, Sitagliptin + IAV, UV-inactivated IAV and control (no IAV and no treatment in basal media). The doses delivered were as follows:

A) DPP4 doses 1-5 (100, 200, 400, 800, 1600 ng/ml)
B) Sitagliptin doses 1-5 (10, 20, 40, 80, 160 µmol/L)

For the rest of this chapter, D1-5 and S1-5 refer to the doses stated above. Where IAV infection was performed to cells pre-treated with DPP4 or sitagliptin, the abbreviation DF1-5 and SF1-5 have been used.

As expected, there were higher levels of IL-6 in the IAV-treated PBECs compared to UV-IAV treated cells (Figure 9.17), which mirrors what was presented in Chapter 8. In contrast, IL8 was seen in IAV-treated PBECs as well as UV-IAV treated cells (9.17 E-F). Consistent with findings in Figure 9.16, basal delivery of sitagliptin in conjunction with IAV infection, resulted in an increase in IL6 relative to cells treated with IAV alone (Figure 9.17 C), especially at the higher doses. Co-administration of DPP4 did not, however, result in the opposite effect (9.17 A, B).

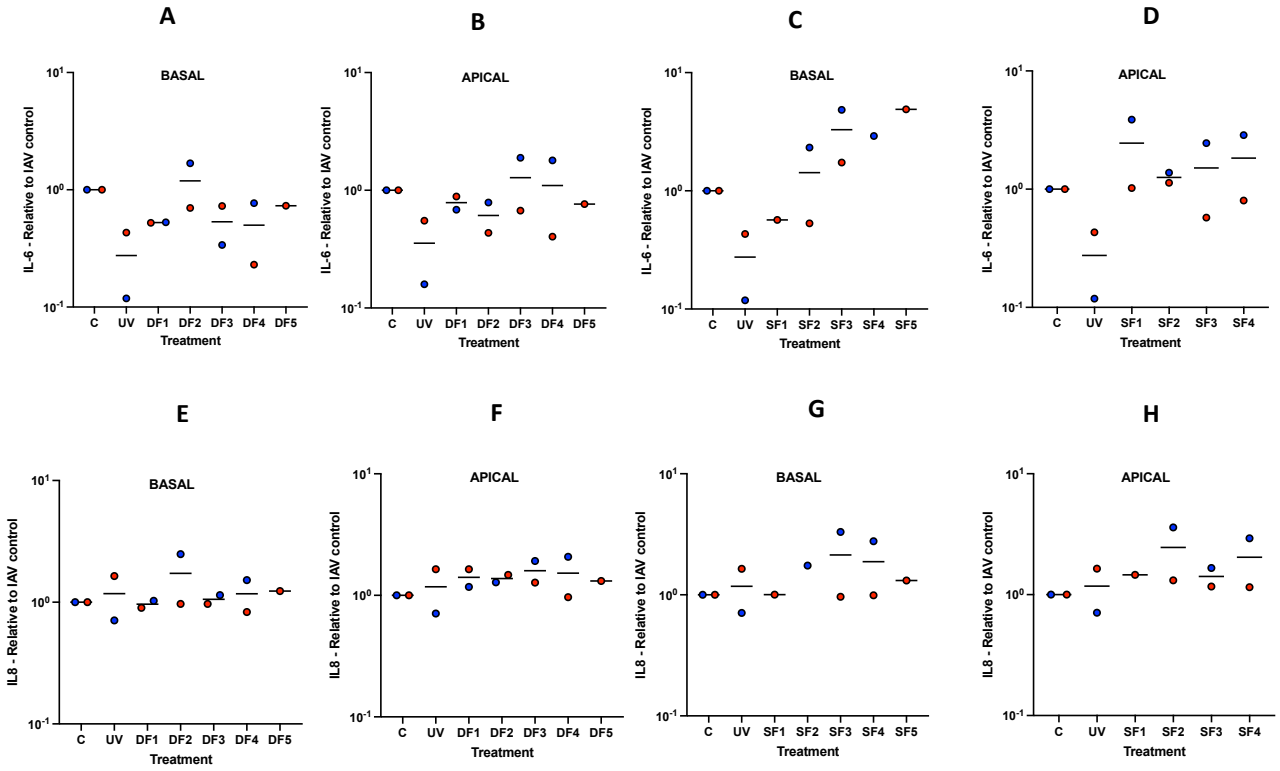


Figure 9. 17 IL6 and IL8 after IAV challenge with concurrent apical or basal treatment with DPP4 or sitagliptin

IL6 and IL8 measured in basal supernatant of 2 post COVID-19 donors' PBECs cultured at ALI after treatment with increasing doses of sitagliptin or DPP4. Cells treated apically with IAV, UV-IAV, DMEM, or combination of IAV and increasing doses of Sitagliptin (SF doses 1-5) or DPP4 (DF doses 1-5). Sitagliptin delivered basally (C, G) or apically (D, H); DPP4 delivered basally (A, E) or apically (B, F). Line drawn at median. Data presented as values relative to the control (C) which consisted of IAV-treated cells without DPP4 or sitagliptin stimulation. S1 -5: Sitagliptin 10, 20, 40, 80, 160 µmol/L, D1-5: DPP4 100, 200, 400, 800, 1600ng/ml.

In case IAV induced too strong an inflammatory response to be modified by DPP4 or sitagliptin, I assessed IL8 and IL6 in PBECs at ALI treated with sitagliptin or DPP4 alone, as compared to mock (i.e., untreated media) (Figure 9.18). There was a trend towards lower IL6 and IL8 with higher doses of sitagliptin, when basally delivered (C, G) but no significant differences in IL6 or IL8 with DPP4 treatment (A, B, E, F).

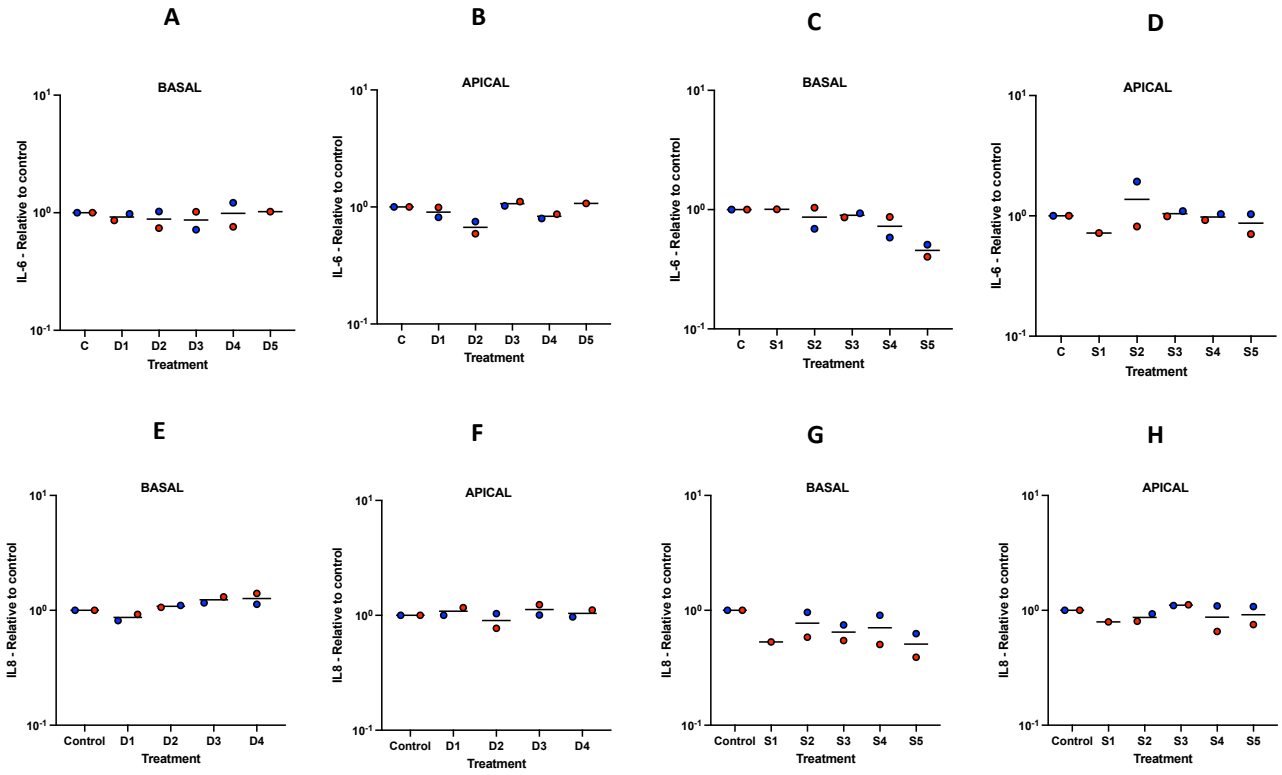


Figure 9. 18 IL 6 and 8 after apical or basal treatment with DPP4 or sitagliptin

IL6 and IL8 levels measured by ELISA in basal supernatants of PBECs at ALI from 2 post COVID-19 donors, subject to treatment with DPP4 (D1-5) or Sitagliptin (S1-5) delivered apically (B, D, F, H) or basally (A, C, E, G). The control well was treated with Pneumacult media (basally) only. Values plotted have been calculated relative to the measurements from the control well. S1 -5: Sitagliptin 10, 20, 40, 80, 160 µmol/L, D1-5: DPP4 100, 200, 400, 800, 1600ng/ml.

Based on this optimisation experiment, there was a trend towards the higher doses of sitagliptin resulting in reduction in endogenous secretion of IL6 and IL8. In the context of IAV infection, sitagliptin resulted in higher IL6 levels. Importantly, trends were seen more convincingly with basal delivery of sitagliptin. However, it is important to note that the basal and apical delivery methods cannot be directly compared due to the differences in duration of stimulation.

With basal delivery, cells were subject to 72 hours of continuous stimulation. With apical delivery, stimulation was only performed for 2 hours. This time duration was chosen as other students in the Lloyd Lab had submerged epithelial cells at ALI for 2 hours without compromising cell survival. It is also clear, that even in cells treated with DMEM alone, or UV inactivated mock, there was a significant rise in IL8 (a marker of cellular stress). In Chapter 8, I showed that despite IL8 being present at homeostasis, 72 hours post IAV infection, there is a statistically significant difference in IL8 levels between the UV-IAV treated cells and IAV treated cells. This difference was not seen, in this experiment, and whilst the experimental design is also different (for instance, basal media was changed every 24 hours for experiments in Chapter 8), I was keen to minimise cell handling through repeated aspirations of the apical surface and repeated subsequent experiments with basal delivery of DPP4 or sitagliptin only.

9.5.5.3.3 Assessing the immunomodulatory response of DPP4 and inhibition on response to IAV

I repeated the experimental design in 9.5.5.3.1 in 3 healthy control donor PBECs and 4 post COVID-19 donor PBECs, all with basal delivery of DPP4 or sitagliptin due to the aforementioned reasons.

I was keen to assess whether co-treatment with DPP4 or sitagliptin would result in modulation of the immune response to IAV. I, therefore, measured gene expression of the immune mediators known to be upregulated in response to IAV (as discussed in Chapter 8) after treatment with IAV and different concentrations of DPP4 and sitagliptin. I also measured AREG as this too was upregulated in the post-COVID-19 airway.

Flu M1 gene expression was similar in healthy control PBECs irrespective of concomitant treatment with DPP4 or sitagliptin (9.19 A, B). Gene expression of IFIT1 and IFITM3 was higher in the groups treated with higher doses of sitagliptin (SF3 and SF4) (9.19 B), though not statistically significant. There was a reduction in OAS2 expression in healthy control PBECs at SF2 ($p=0.06$) and SF4 ($p=0.13$), as well as a reduction in RSAD2 expression at SF2 ($p=0.09$). In post COVID-19 donors, there was an increase in OAS2 gene expression at SF2 ($p=0.01$) and SF4 ($p=0.003$). Additionally, a trend towards higher expression of RSAD2, IFIT1 and IFITM3 was seen with all doses of sitagliptin but was not statistically significant.

Interestingly, in healthy controls, DF1 resulted in significantly lower expression of IFIT 1 ($p=0.01$), IFITM3 ($p=0.01$), OAS2 ($p=0.01$), RSAD2 ($p=0.07$) and IFN lambda ($p=0.01$). Similar changes were seen for DF2: IFIT 1 ($p=0.004$), IFITM3 ($p=0.004$), RSAD2 ($p=0.004$), OAS2 ($p=0.004$) (Figure 9.19 A). This was despite, non-significant differences in Flu M1 gene expression in DF1 ($p=0.17$) or DF2 ($p=0.26$). Although trends towards lower expression were seen at the higher DPP4 doses, these weren't statistically significant. In post COVID-19 PBECs, such trends were not seen with co-administration of different doses of DPP4 (Figure 9.19 C).

Consistently, there was a trend towards higher AREG expression with increasing doses of sitagliptin, although only statistically significant at SF4 in post COVID-19 donors: In post COVID-19 PBECs, SF2 ($p=0.09$), SF3 $p=0.08$, SF4 $p=0.02$; in healthy control donors, SF2 ($p=0.59$), SF3 ($p=0.08$), SF4 ($p=0.13$). Given similar trends, the datasets were combined and statistically significant increases in AREG at SF3 ($p=0.04$) and SF4 ($p=0.02$) were seen, but statistical significance was not achieved for the ISGs, although a trend towards higher expression was seen in the groups co-treated with sitagliptin. DPP4 treatment did not convincingly have any impact on gene expression of AREG.

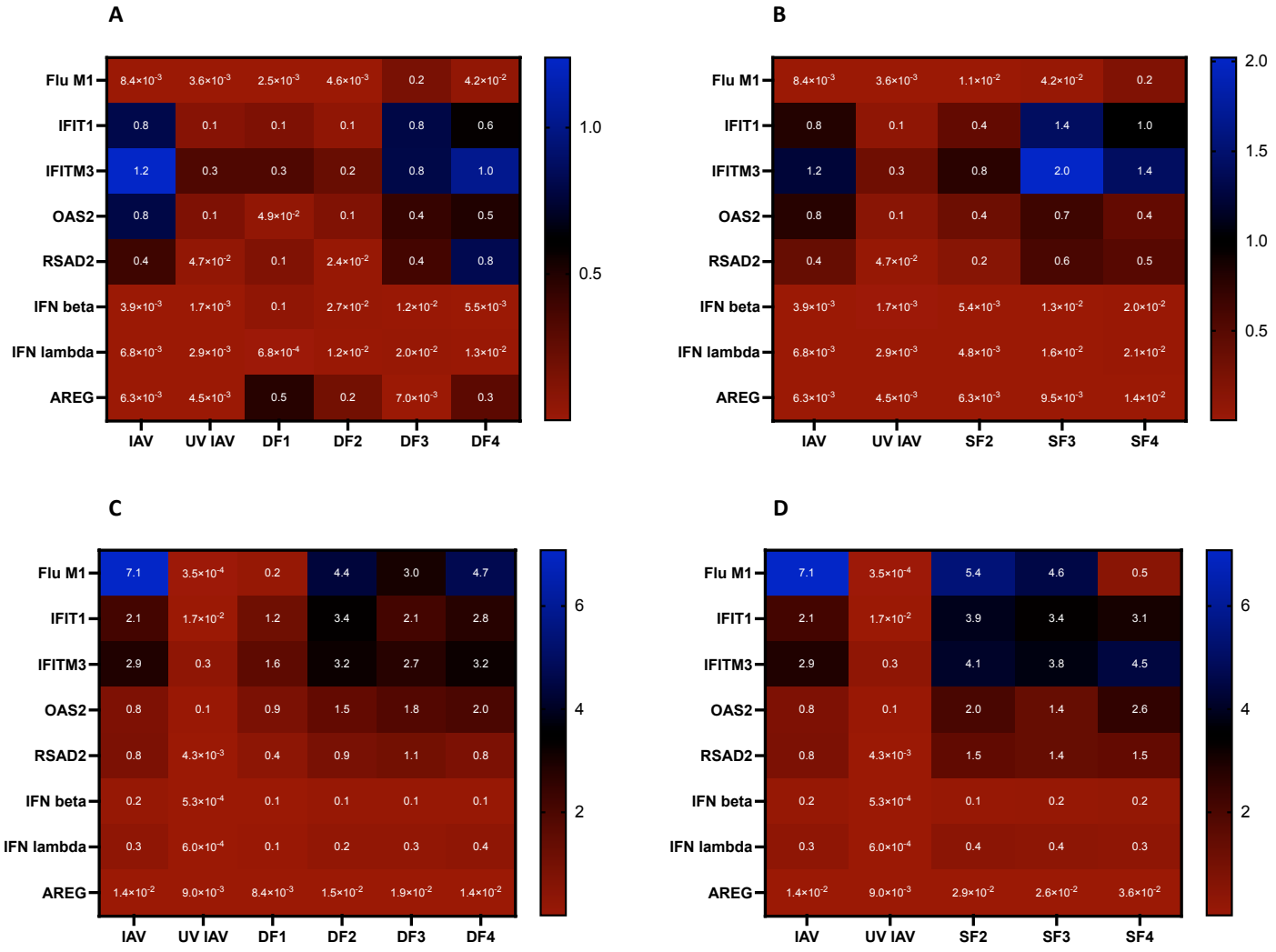


Figure 9. 19 ISG, interferon and AREG response post IAV challenge with concurrent basal treatment with DPP4 or sitagliptin

A, B show results for n=3 healthy control donors with 3-6 readings evaluated for each condition. C, D show results for n=5 post COVID-19 donors with results showing 5-10 readings for each experimental condition. Mean of values displayed in heat map.

Next, I evaluated inflammatory proteins and interferon beta in the basal supernatants of post COVID-19 PBECs treated with IAV +/- DPP4/ sitagliptin. In contrast to, previous findings, IL6 was only elevated in one sitagliptin treated groups (SF4). Additionally, IL8 was increased in response to the lowest sitagliptin dose (10 μmol/L). IFN beta levels, were however, consistently increased with sitagliptin treatment (SF1-4, Figure 9.20 C).

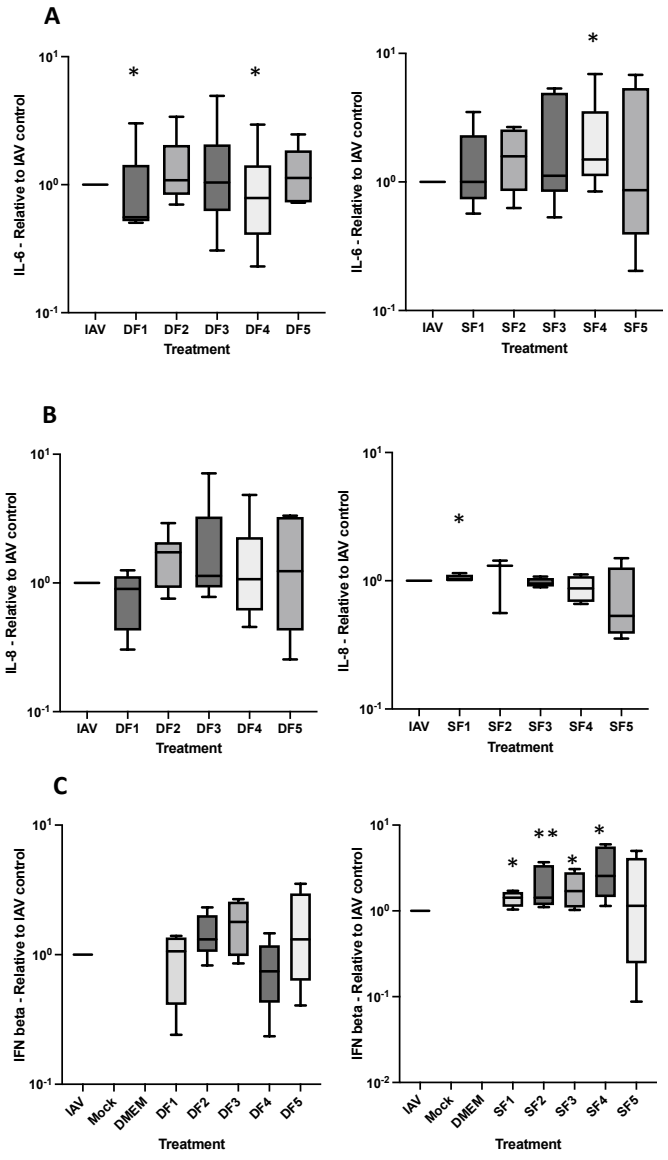


Figure 9. 20 IL6, IL8 and IFN beta in basal supernatant after IAV challenge and basal treatment with DPP4 or sitagliptin

Protein levels measured in basal supernatants after IAV infection in combination with DPP4 or sitagliptin treatment in PBECs from 5 post COVID-19 donors cultured at ALI

Comparisons performed using Mann Whitney U testing. P values as follows: * p<0.05, ** p<0.01

9.5.6 Effect of DPP4 stimulation or inhibition on basal cells

As basal cells play an integral role in regeneration of the epithelial cells, I wanted to assess if the upregulation of DPP4 in the airways had a role in stimulating basal cell proliferation or accelerating wound repair after mechanical injury.

9.5.6.1 Assessing the effect on basal cell proliferation

There was no significant impact on submerged basal cell proliferation after stimulation with recombinant DPP4 or DPP4 inhibition with sitagliptin, neither on assessment of percentage confluence (Figure 9.21 A-C, Figure 9.22 A-C) nor visualisation of Ki67+ cells (Figure 9.21 D-F and 9.22 D-F). The response to sitagliptin in post COVID-19 donors was different to healthy controls, with a reduction in percentage confluence, in the absence of visible cell death (Figure 9.22 C).

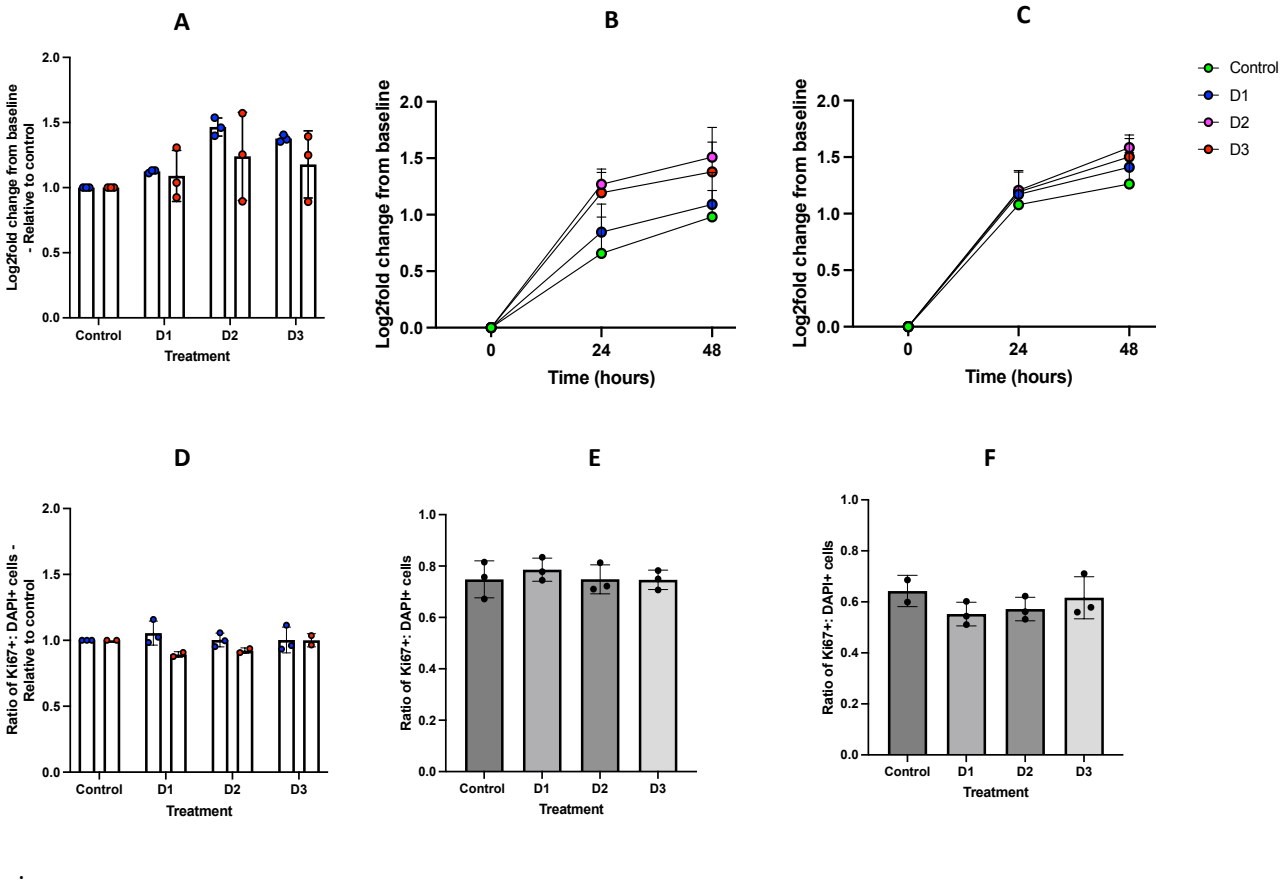


Figure 9. 21 Basal cell proliferation in response to DPP4 stimulation

Time-lapse Brightfield images captured using JuliTM Stage Real-Time Cell History Recorder and % confluence calculated using JuliStat (Juli software) (A-C). Results shown for n=3 HC (B, E) and n=3 post COVID-19 donors (C, F). A, D: Blue dots show HC donors; Red dots pCOVID-19

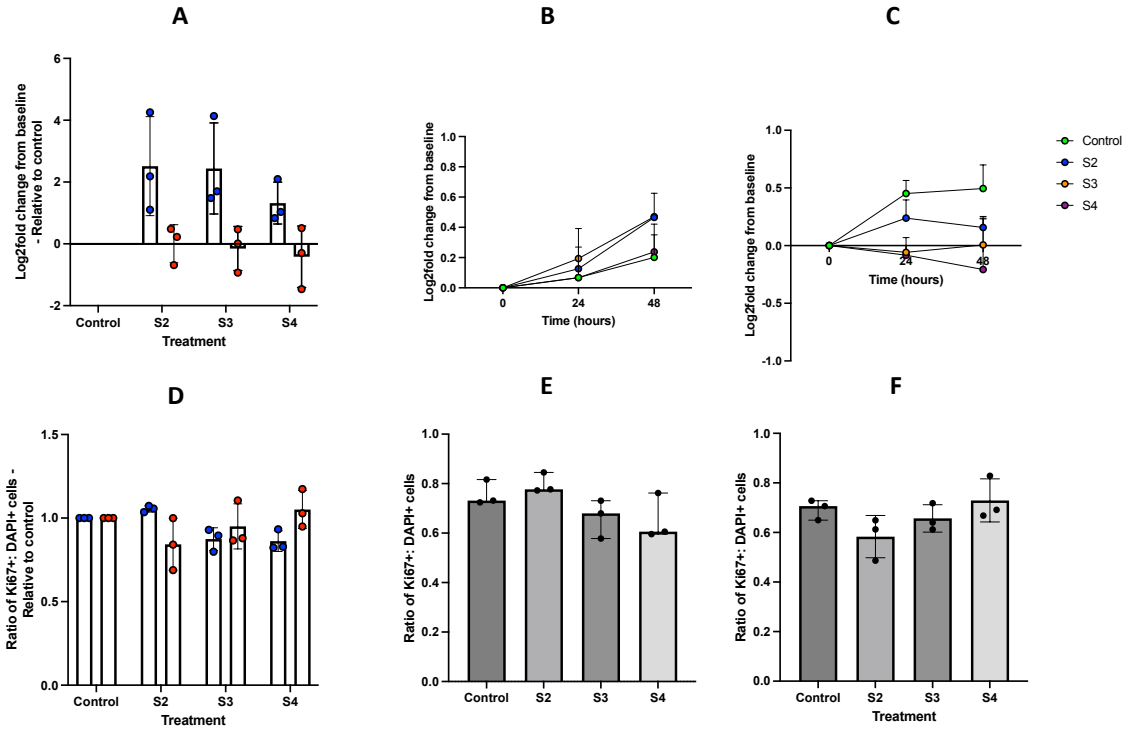


Figure 9. 22 Basal cell proliferation in response to sitagliptin.

Images for A-C taken manually using inverted Leica microscope, with one image taken per well. Analysis performed using confluency analysis Macro. Results shown for n=3 HC (B, E) and n=3 post COVID-19 donors (C, F). A, D: Blue dots show HC donors; Red dots pCOVID-19

9.5.6.2 Assessing the effect of DPP4 (and inhibition) on wound closure assay

Wound closure was also not affected by increasing doses of DPP4 (Figure 9.23) or sitagliptin (Figure 9.24). Notably, less wound closure was being achieved in the post-COVID-19 donor PBECs at 24 hours compared to healthy controls, which is keeping with what was described in Chapter 8.

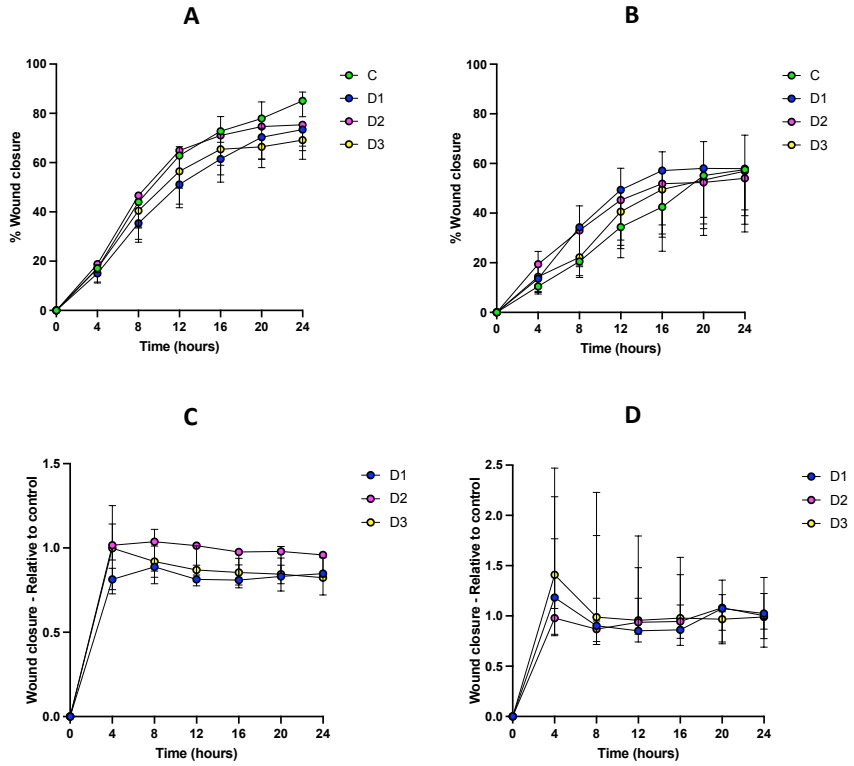


Figure 9. 23 Wound closure in response to DPP4 treatment

Wound closure in n=3 healthy control PBECs (A, C) and n=5 post COVID-19 PBECs (B, D). Results shown as % wound closure over time (A, B) and relative to an average of the control wells (C, D). Median and interquartile ranges displayed. D1-3: DPP4 100, 200, 400ng/ml

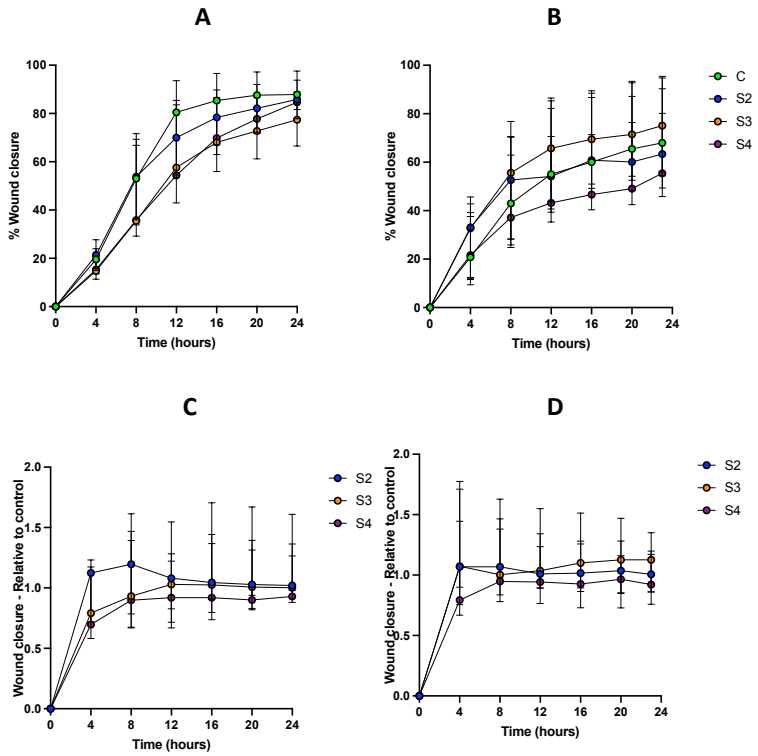


Figure 9. 24 Wound closure in response to sitagliptin treatment

Wound closure in n=3 healthy control PBECs (A, C) and n=5 post COVID-19 PBECs (B, D). Results shown as % wound closure over time (A, B) and relative to an average of the control wells (C, D). Median and interquartile ranges displayed. S2-4: Sitagliptin 20, 40, 80µmol/L

9.5.7 Effect of DPP4 stimulation or inhibition on AREG production

As there was a strong correlation between DPP4 and AREG, I next wanted to assess if DPP4 stimulation or inhibition, resulted in alteration of AREG production, both in basal cells and in cells cultured at air-liquid interface. I was also keen to understand whether any trends were only seen in the context of injury (e.g. mechanical scratch or IAV infection) or at baseline also.

9.5.7.1 PBECs at air liquid interface

9.5.7.1.1 Intact epithelium

In PBECs from healthy control donors that are undergoing differentiation, increasing doses of sitagliptin, resulted in increased AREG production, both when assessed in the basal supernatant (Figure 9.25 A) and in apical supernatant (9.25B).

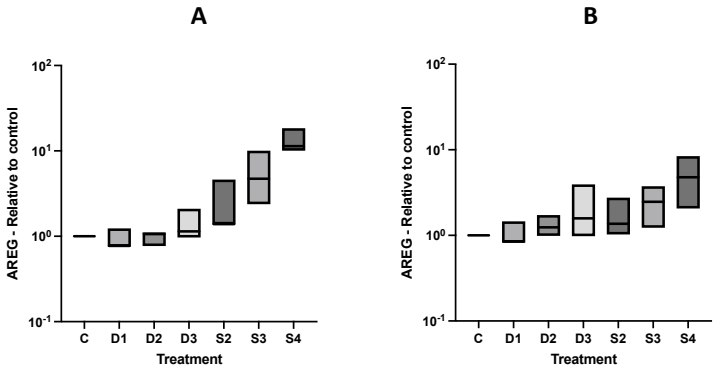


Figure 9. 25 AREG in supernatants after continuous basal stimulation with DPP4 or sitagliptin for 3 weeks.

AREG measured in the apical (A) and basal supernatants (B) of PBECs from n=3 healthy control donors cultured at ALI and treated with DPP4 or sitagliptin during the differentiation process. Floating bars show line at median and minimum and maximum values. D1-3: DPP4 100, 200, 400ng/ml S2-4: Sitagliptin 20, 40, 80µmol/L

This trend was less apparent after 72-hour stimulation of differentiated cells, although a statistically significant increase in AREG in post-COVID-19 PBECs treated with the highest doses of sitagliptin (S4 and S5) was seen (Figure 9.26). Additionally, although not significant, a higher median level of AREG was seen at S1 in healthy control PBECs. Interestingly, and not consistent with previous results, D2 and D4 treatment resulted in upregulation of AREG.

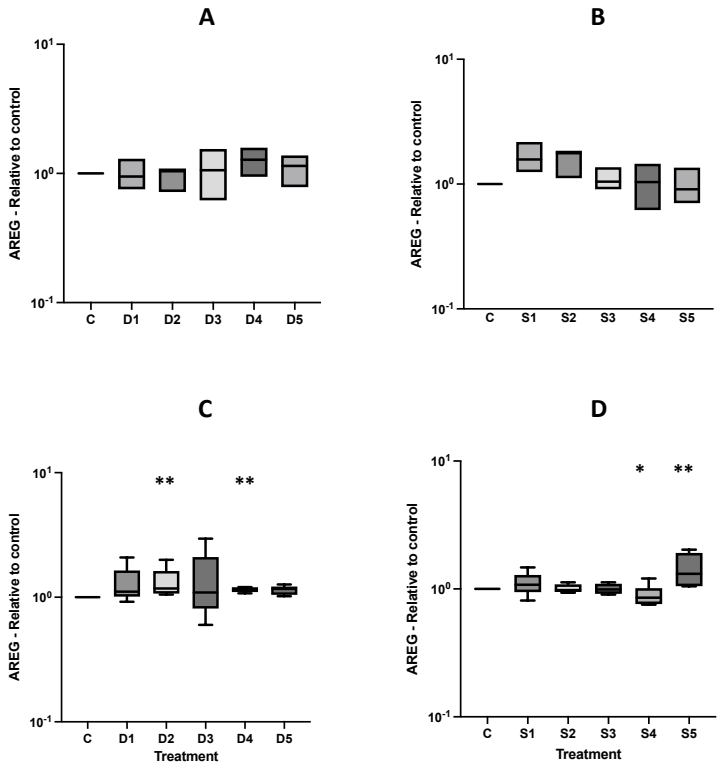


Figure 9. 26 AREG in basal supernatant after 72-hour stimulation of differentiated epithelial cells with DPP4 or sitagliptin

A and B show results in PBECs from n=3 healthy control donors, with line drawn at median and boxes displaying minimum and maximum values. C and D are box and whisker plots displaying results in PBECs from n=6 post COVID-19 donors with line drawn at median and whiskers showing minimum and maximum. Statistical analysis performed using non-parametric Mann Whitney U testing. P values as follows: * $p<0.05$, ** $p<0.01$
D1-5: DPP4 100, 200, 400, 800, 1600ng/ml S1-5: Sitagliptin 10, 20, 40, 80, 160µmol/L

9.5.7.1.2 Injured epithelium: IAV infection

In the context of epithelial injury induced by IAV infection, AREG levels increased in a dose dependent manner with sitagliptin treatment in post COVID-19 PBECs (Figure 9.27B). A trend similar trend was seen in healthy control donor PBECs also (9.27A) and for the combined cohort, the highest doses of sitagliptin resulted in statistically significant increases in AREG compared to the IAV control (9.27C). Co-treatment with DPP4 did not affect the concentration of AREG protein detected in the basal supernatant.

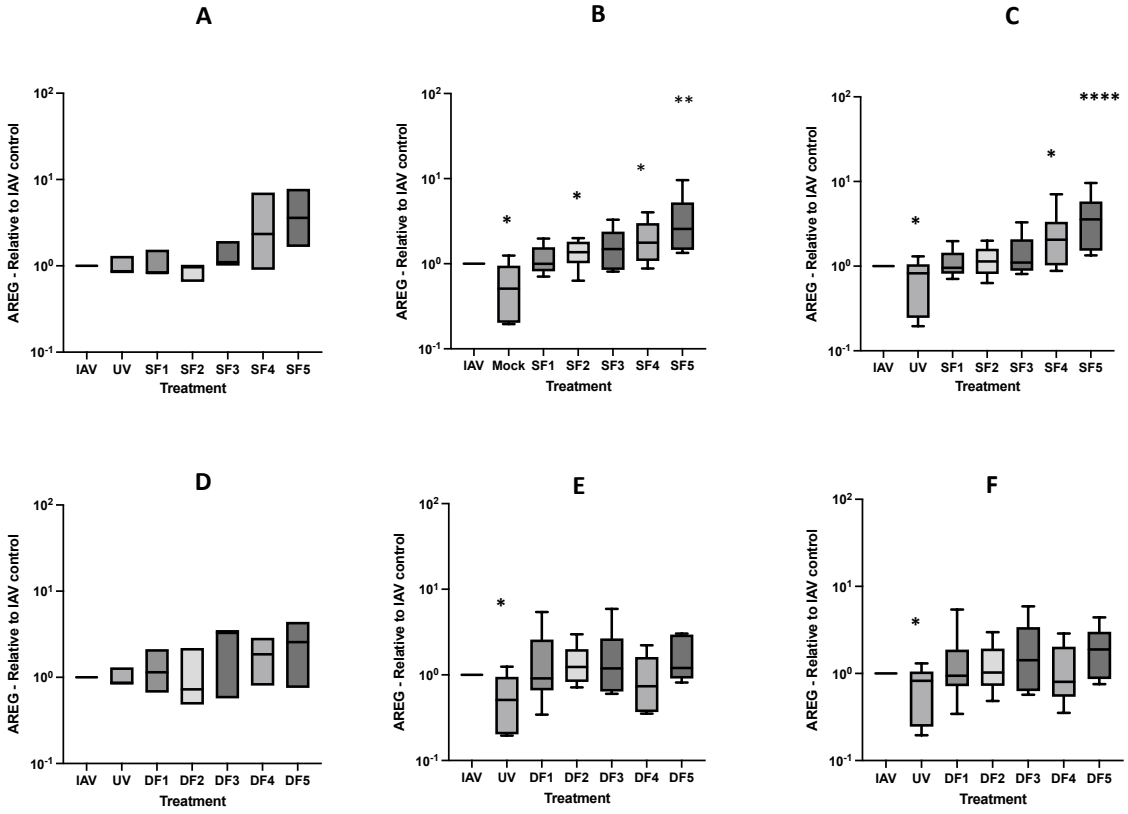


Figure 9. 27 AREG in basal supernatant after IAV challenge and basal treatment with DPP4 or sitagliptin

A and D show n=3 HC donor PBECs with line drawn at median and floating bars showing minimum and maximum levels. B and E show results from n=5 post COVID-19 donor PBECs with line drawn at median and whiskers showing minimum and maximum. C and F show the combined cohort (n=3 HC, n=5 pCOVID). Inter-group differences between control and treatment groups performed using Mann Whitney U testing. * P<0.05, **p <0.01, ***p<0.001, ****p<0.0001

9.5.7.2 PBECs in submerged culture

9.5.7.2.1 Basal cell proliferation

In proliferating basal cells, again, there was a trend towards increasing AREG levels after 48 hours of DPP4 stimulation (Figure 9.28 B,C) in both healthy control and post COVID-19 donors but no statistically significant differences from the control group (9.28A). Sitagliptin treatment, however, reduced AREG production in basal cells from healthy control donors (9.28E), but this change was not seen in post COVID-19 donors (9.28F). As a result, there was a greater difference in AREG concentration in the basal supernatants of PBECs from post COVID-19 donors compared to healthy control donors in response to sitagliptin treatment (Figure 9.28 D).

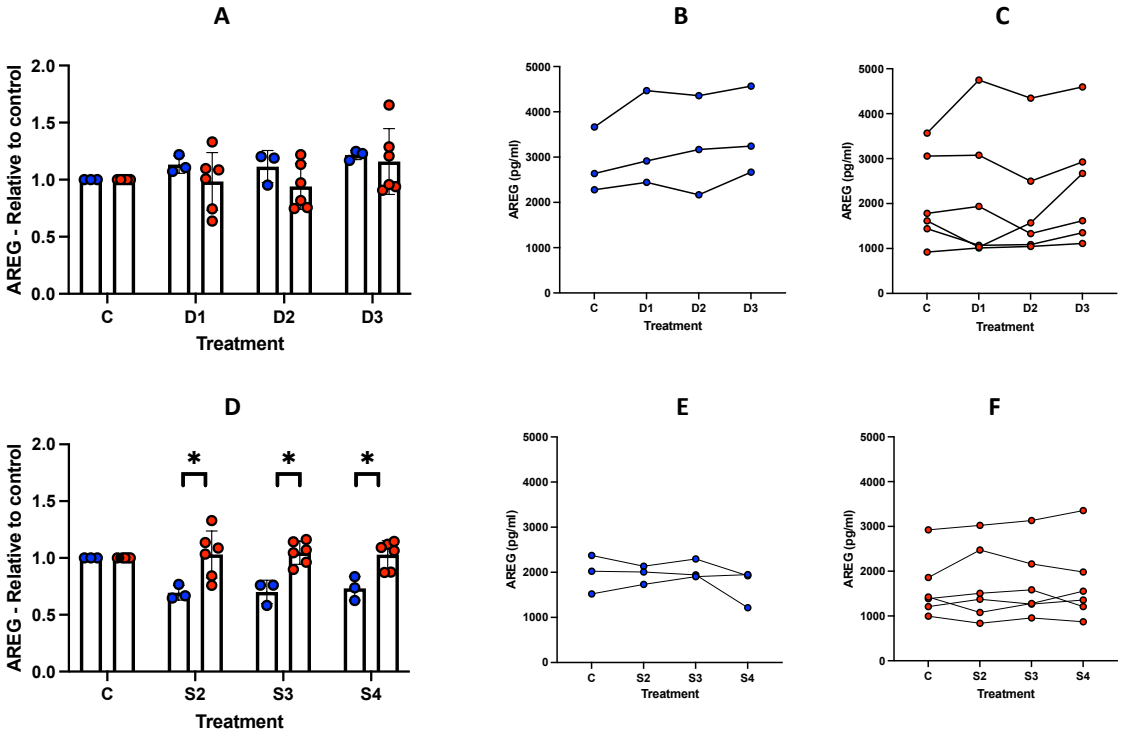


Figure 9. 28 AREG in basal supernatant of submerged PBECs treated with DPP4 or sitagliptin for 48 hours.

Results shown for n=3 healthy control PBECs (B, E) and n=5 post COVID-19 PBECs (C, F). Change in AREG levels relative to the untreated control and differences between HC and pCOVID PBECs are shown in A and D: Blue dot – healthy control, red dot – post-COVID-19. Non-parametric Mann Whitney U testing performed. * p <0.05
D1-3: DPP4 100, 200, 400ng/ml S2-4: Sitagliptin 20, 40, 80µmol/L

9.5.7.2.2 Basal cell scratch assay

There was similarly a decrease in AREG concentration with increasing doses of sitagliptin detected in the basal supernatant of healthy donor PBECs after mechanical scratch (Figure 9.29 E), but not in post COVID-19 donors (9.29F). No significant changes were noted in the DPP4 treatment groups.

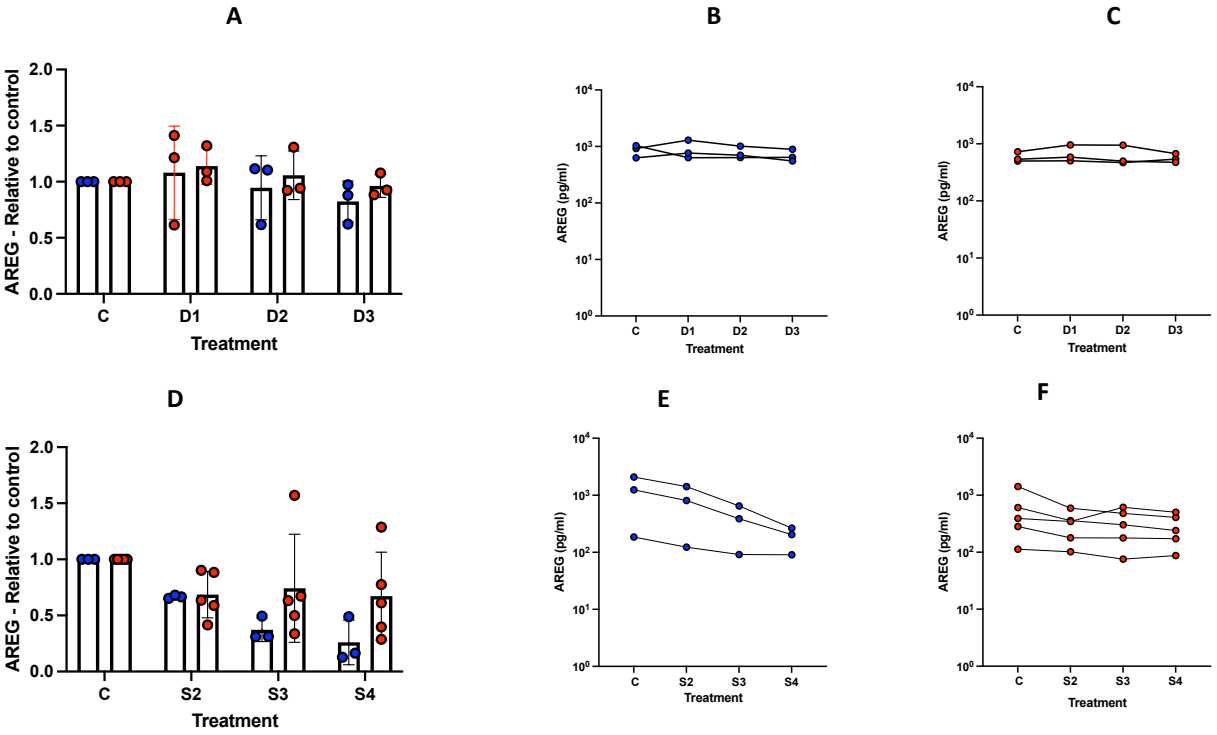


Figure 9. 29 AREG in basal supernatant 24 hours after scratch assay and treatment with DPP4 or sitagliptin

Linear wound made to confluent monolayer in the presence of DPP4 (A-C) or sitagliptin (D-F) at increasing doses. Each dot represents a different biological donor. PBECs from n=3 healthy control donors and n=5 post COVID-19 donors were evaluated. Change in AREG levels relative to the untreated control and differences between HC and post COVID-19 PBECs are shown in A and D: Blue dot – healthy control, red dot – post-COVID-19. Non-parametric Mann Whitney U testing performed. P<0.05 considered statistically significant.
D1-3: DPP4 100, 200, 400ng/ml; S2-4: Sitagliptin 20, 40, 80µmol/L

9.5.8 Effect of DPP4 stimulation or inhibition on fibroblast activity

Although the results so far suggest a potential immunomodulatory role for inhibition of DPP4, it is not clear which cell type DPP4 or its inhibition, primarily effects. As literature suggests that treatment with recombinant DPP4 can increase human lung fibroblast proliferation[539], a process integral to wound healing and repair, I wanted to assess whether DPP4 or its inhibition had an impact on fibroblast proliferation or wound healing.

9.5.8.1 Fibroblast proliferation

A trend was seen towards the highest doses of DPP4 (D3 and D4) and lowest dose D0 increasing proliferation, as suggested by greater change in confluency from baseline (Figure 9.30 B) and relative to the control (9.30 C).

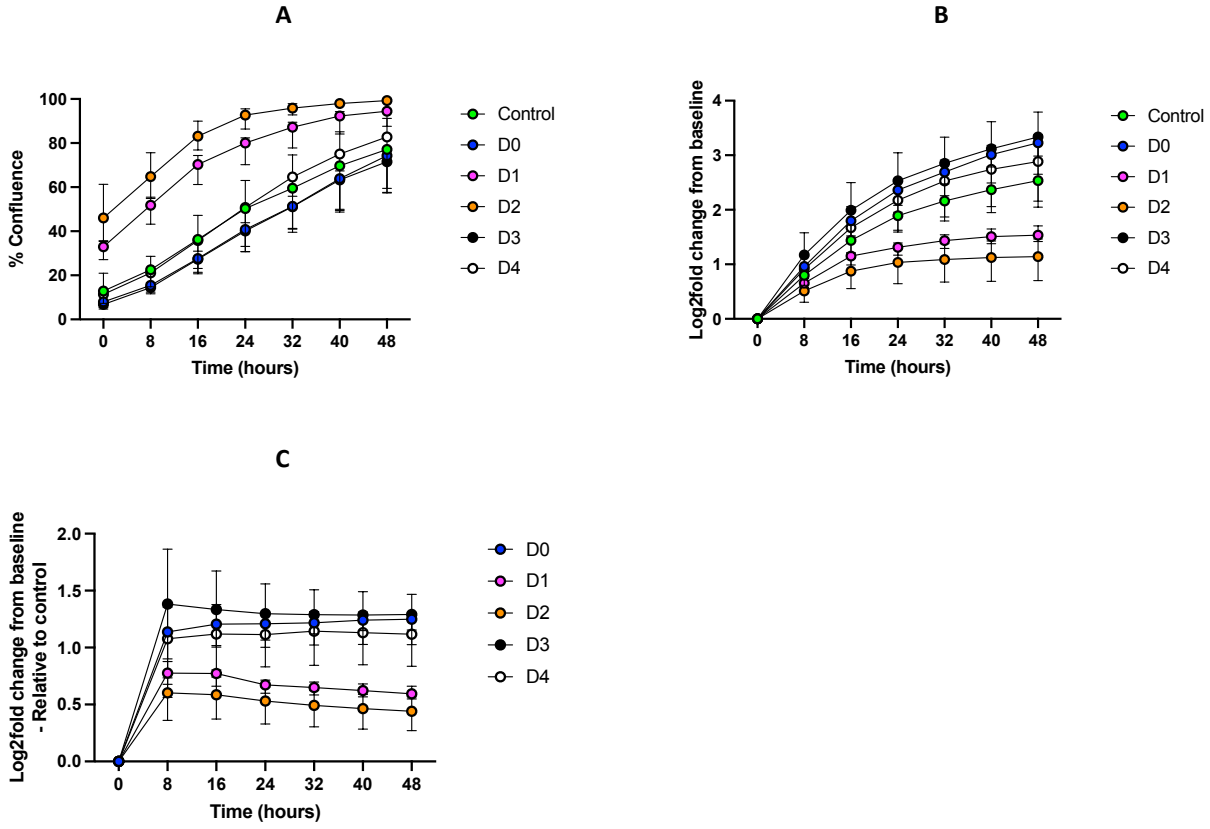


Figure 9. 30 Fibroblast proliferation in response to DPP4 treatment

Fibroblast proliferation as measured by % confluence (A), log2FC from baseline (B) and relative to control (C) in response to increasing doses of DPP4 treatment: D0-5: 50, 100, 200, 400, 800, 1600ng/ml. The control wells were treated with DMEM and 10% FBS only and all doses of DPP4 were diluted in DMEM/10% FBS after an initial period of serum starvation. Median and interquartile ranges shown.

With sitagliptin treatment, the highest dose, S5, showed trends in reducing fibroblast proliferation (Figure 9.31 B, C).

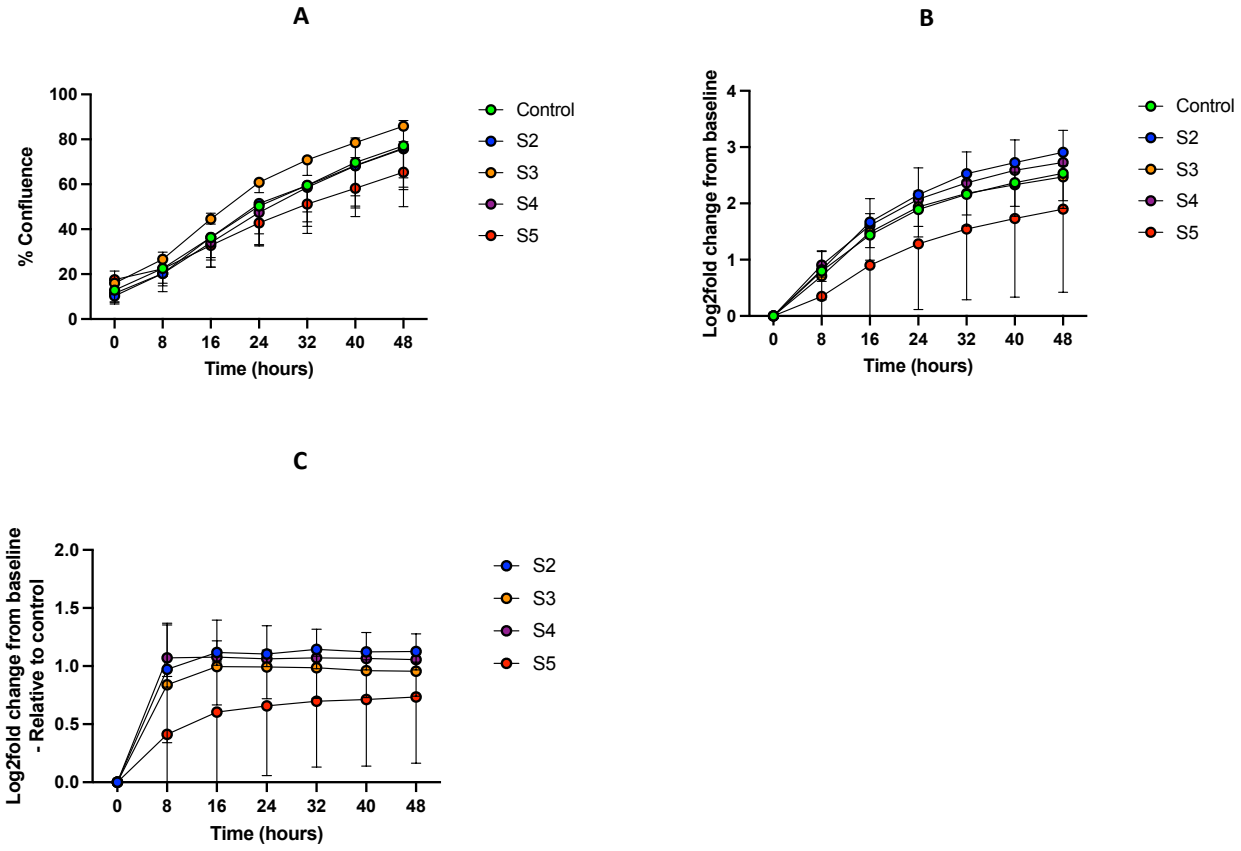


Figure 9. 31 Fibroblast proliferation in response to sitagliptin treatment

Fibroblast proliferation as measured by % confluence (A), log2FC from baseline (B) and relative to control (C) in response to increasing doses of sitagliptin treatment: S2-5: 20, 40, 80, 160µmol/L. The control wells were treated with DMEM and 10% FBS and all doses of sitagliptin were diluted in DMEM/10% FBS after an initial period of serum starvation. Median and interquartile ranges shown.

9.5.8.2 Assessing the effect of DPP4 and inhibition on fibroblast scratch assay

There was no significant difference seen after delivery of different doses of DPP4 (Figure 9.32 A) or sitagliptin (9.32B) in wound closure compared to the DMEM/FBS control, except for the highest dose of sitagliptin (S5), which resulted in delayed wound closure.

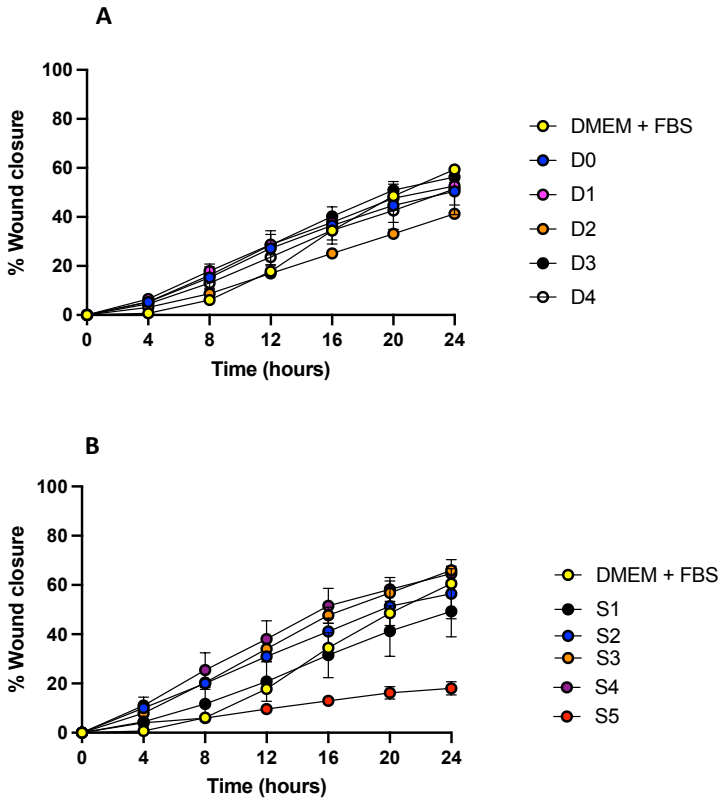


Figure 9. 32 Fibroblast wound closure after treatment with DPP4 or sitagliptin

DMEM and 10% FBS was the control. An average of two experimental replicates was taken. For the DMEM/FBS well in A, results were only obtained from one well. DPP4 doses: D0-D4: 50, 100, 200, 400, 800ng/ml. Sitagliptin doses: S1-5: 10, 20, 40, 80, 160µmol/L

9.6 Discussion

9.6.1 Summary of findings

There is upregulation of both DPP4 and AREG in the post-COVID-19 airway compared to healthy controls, with a strong positive correlation between the two. In vitro, in differentiated primary bronchial epithelial cells cultured at air-liquid interface, DPP4 gene expression is higher in PBECs from individuals post COVID-19 compared to healthy controls, although this is not reflected in DPP4 protein

levels in the apical or basal compartment. A higher quantity of DPP4 is detectable in the apical compartment 5-7 weeks post air exposure in both healthy control and post COVID-19 PBECs compared to at 3 weeks post air exposure.

DPP4 is upregulated on protein measurements post IAV infection, and this is accompanied by a reduction in DPP4 gene expression, with maximal change seen at 72 hours post infection. DPP4 inhibition with sitagliptin decreases MUC5AC and KRT5 gene expression but is associated with increased CDH1 expression. There is a trend towards increased MUC5AC gene expression with continuous recombinant DPP4 stimulation.

There was no significant effect on wound closure with sitagliptin or DPP4 treatment.

Sitagliptin therapy shows trends in increasing ISG expression in the context of concomitant IAV infection, as well as increasing IFN beta protein in the basal supernatant. A trend towards the opposite effect with ISGs was seen with DPP4 treatment in healthy controls, but in post COVID-19 donors.

Consistently, sitagliptin therapy increased AREG production, both in the context of epithelial injury (IAV infection) and also at baseline in cells cultured at ALI.

Importantly, the effect of DPP4 and sitagliptin varied, depending on whether the donor cells were from healthy individuals or post COVID-19.

Fibroblast wound closure is impeded by the highest dose of sitagliptin therapy.

9.6.2 Findings in context of current literature

9.6.2.1 Findings in vivo

The upregulation of DPP4 and AREG in the BALF supernatant of individuals post COVID-19 compared to healthy controls may be an effect of recent severe viral injury. The strong positive correlation with AREG, a protein associated with wound healing and repair and in particular, basal cell proliferation, a process integral to repair of the damaged epithelium, suggests that DPP4 and AREG may influence each other, either directly or through an intermediate agent upregulated in epithelial injury, for instance a metalloproteinase involved in epithelial repair, especially since such proteases are known to promote shedding of both DPP4 and AREG[528,543,550]

9.6.2.2 Findings in vitro

9.6.2.2.1 Epithelial cell culture at air-liquid interface

9.6.2.2.1.1 3 weeks post air exposure

The discrepancy between gene expression of DPP4 and protein production at 3 weeks post air exposure could be due two mechanisms: Firstly, although there were non-significant differences in DPP4 levels in the apical supernatant between healthy control and post COVID-19 donors, there were slightly lower levels of DPP4 in post COVID-19 donors, which was persistent at 5-7 weeks post air exposure. The increased gene expression compared to healthy controls, might therefore be to compensate for the lower protein levels. Assessment of gene expression at 5-7 weeks post air exposure would have helped corroborate this theory. An alternative theory is that DPP4 needs to be cleaved (or shed) from its transmembrane position before it is detectable in the supernatant, therefore whilst gene expression may have resulted in increased DPP4, soluble protein quantities remain unchanged in the absence of adequate protein cleavage. Important to note is that there is an increase in DPP4 protein levels between 3 weeks and 6 weeks in both post COVID-19 and healthy control donors, perhaps implying that DPP4 is preferentially produced by differentiated cells rather than basal cells. This would be consistent with the difficulty detecting DPP4 in the basal supernatant of cells in submerged culture described in Chapter 8. Additionally, important to note is that in this Chapter, I have focussed on the effects of soluble DPP4 protein, and the upregulation of gene expression in post COVID-19 PBECs may be resulting in increased membrane-bound protein, which, I haven't assessed.

Although not significant, there was a trend towards higher gene expression of AREG in the post COVID-19 donors at 3 weeks post air exposure. Again, whilst no significant differences were seen in AREG on protein levels at 3 weeks, neither in the apical nor basal supernatant, at 5-7 weeks post air exposure, there were statistically significant lower levels of AREG in the basal compartment in post COVID-19 donors, with no preferential shift to the apical compartment. There was also a drop in basal AREG between 3 and 5-7 weeks in the post COVID-19 donors (not statistically significant) but a corresponding increase in HC donors (not statistically significant) which will have contributed to the differences in levels seen at 5-7 weeks. Since preferential shift to the apical compartment was not seen, the reduction in AREG in post COVID-19 donors is likely due to reduced production overall or increased usage. Since basal cells are the primary source of AREG in the ALI model, a change in proportion of basal: differentiated cell in post COVID-19 donors compared to healthy controls is another possibility but is not supported by the similar gene expression profile for markers of

differentiation seen at 3 weeks post air exposure, described in Chapter 8. However, it is possible that there is a change in gene expression at 5-7 weeks, but as this was not measured, this theory remains speculative. An alternative theory is that the abnormality isn't related to cell numbers, but rather individual cell production of AREG is reduced post COVID-19.

A positive correlation was seen between DPP4 and AREG in the apical supernatant of post COVID-19 individuals at 3 weeks post air exposure, which mirrors the relationship seen in vivo. However, the opposite relationship was seen in the basal supernatant. The latter was not statistically significant and consisted of only a few data points, so the results need to be interpreted with caution. A positive relationship was less apparent in the apical supernatants from healthy control donors, but even in vivo, the relationship between DPP4 and AREG was weaker. The reason for the opposite relationship in the different compartments might be that DPP4 is preferentially secreted apically, and enzymes required for cleavage are located more apically, compared to AREG. AREG, also perhaps more apically produced, might however be easier to process for release than DPP4. Whilst not conclusive, this does have implications on which cells DPP4 might have an impact on, in vivo (i.e. more likely epithelial cells, rather than fibroblasts).

9.6.2.2.1.2 Effect on Differentiation

72-hour stimulation of differentiated epithelial cells with varying doses of sitagliptin resulted in a reduction in MUC5AC and KRT5 gene expression in both post COVID-19 and healthy control PBECs. By contrast, DPP4 stimulation increased MUC5AC gene expression. The latter would be consistent with what's been anecdotally observed in clinical practice, where patients with no atopic features have developed persistent bronchitis symptoms after COVID-19. Reduced KRT5 expression, and reduced MUC5AC expression suggests differentiation into a different cell type. FOXJ1 expression was not assessed for the dose-titrations, but when assessing after S4 treatment, there was downregulation of FOXJ1 as well, suggesting maybe transition is into a non-ciliated, non-goblet cell type. Interestingly, genes associated with mesenchymal features for instance, vimentin and alpha smooth muscle actin were not significantly elevated, suggesting that it isn't transition into a non-epithelial phenotype that is the underlying cause for the change in gene expression. Assessment therefore, of rarer epithelial types and assessing the maturity of the basal cells by evaluating expression of TP63, would have been valuable.[452]

The findings from stimulation of differentiated epithelial cells for 72 hours are slightly discordant with what was seen with continuous stimulation of cells since air exposure (i.e. during the differentiation process), where sitagliptin seemed to upregulate MUC5AC gene expression at lower doses. With the

latter, basal cells were stimulated through to differentiation, and one possibility is that it is the timing of treatment during the differentiation process that determines the functional phenotype of the differentiated cell.

9.6.2.2.1.3 Immunomodulation

In the IAV-treated epithelial cells described in Chapter 8, upregulation of DPP4 was seen in the basal supernatant, with a maximal response seen at 72 hours post infection, which was the timing of peak response for other immune mediators. The downregulation of gene expression for DPP4 after IAV infection is likely to signify a negative feedback mechanism, whereby there is a reduction in gene expression in response to an increase in soluble protein. The difficulty in detecting DPP4 in the UV-IAV group, again suggests that cleavage of DPP4 is necessary for protein detection. The upregulation of DPP4 post IAV is in accordance with what's described in the literature in mouse models, although the cellular source was peripheral lymphocytes in this study.[538] Ideally, I would have wanted to introduce infection with SARS-COV2 in PBECs from healthy control donors and measure protein secretion of DPP4, however, in the absence of access to BSL3 facilities, I resorted to evaluating the relevance of DPP4 in the IAV-infected cells as described.

In this Chapter, my results show upregulation of ISGs in the sitagliptin and IAV-treated groups, in comparison to IAV-only groups. IFN beta levels were also increased on protein measurement, which is consistent with the how ISGs are activated i.e. by Type 1 (such as Interferon beta) and Type 3 interferons.[551] The lack of change in IFN beta gene expression might be as increased gene expression occurs at an earlier time point to protein secretion. Interestingly, the findings were not consistent between healthy control and post COVID-19 PBECs. In addition, the opposite effect was not consistently seen with DPP4, other than for 2 doses of DPP4 in healthy control PBECs, where a reduction in ISG expression was seen.

9.6.2.2.2 Submerged epithelial cell culture

The lack of effect of DPP4 or its inhibition on wound closure suggests DPP4 may not play a role in basal cell response to mechanical injury. Similarly, no significant change was noted in basal cell proliferation. Stimulation studies on basal cells have not previously been performed to compare my results with.

9.6.2.2.3 Submerged fibroblast culture

It is difficult to draw firm conclusions from the fibroblast experiments as these were only conducted once. Whilst a trend towards more rapid achievement of confluence in fibroblasts treated with 100 and 200ng/ml (D1, D2) of DPP4 is seen, these wells started at a higher % confluence and the effect of contact-mediated proliferation signals might have played a part.[552,553] In the sitagliptin-treated groups, the highest dose (160µmol/L) seemed to reduce proliferation. The mechanism by which sitagliptin achieves this is not known.

Assessment of wound healing in lung fibroblasts when treated with the highest dose of sitagliptin, resulted in a reduction of wound closure compared to the other doses and also the control wells. As would closure is dependent on cellular proliferation and migration[170] halting proliferative capacity at the highest dose may in part explain this finding.

9.6.2.3 Comparing in vivo and in vitro findings

Whilst there was upregulation of DPP4 and AREG in the post COVID-19 airway in vivo, this was not replicated in in vitro. One possible reason is that both are predominantly produced by immune cells: T cells as the primary source for DPP4 and T regulatory cells and ILCs as the primary source for AREG in vivo. One explanation for the upregulation of both, as evidenced by increasing AREG levels with increasing doses of sitagliptin, is that a counterregulatory relationship between DPP4 and AREG exists, whereby AREG inhibits DPP4, thus inhibiting DPP4 results in upregulation of AREG.

The doses trialled in this Chapter were based on literature in 16HBEs and doses that showed increased fibroblast and bronchial smooth muscle proliferation.[533,539] As these doses did not elicit a significant effect, higher doses were trialled in my experiments. It is likely that these doses are higher than the concentrations seen in vivo.

9.6.2.4 Comparing healthy control and post COVID-19 donors

There were differences in cell responses, for instance in AREG production from basal cells, between healthy donors and post COVID-19 donors. Whilst not tested, the possibility of chronic exposure to DPP4 in post COVID-19 cells altering cellular responses to further stimulation, needs to be considered.

9.6.3 Clinical relevance of findings

Although these findings have no direct clinical relevance, if sitagliptin does indeed have immunomodulatory properties, this may have translational implications.

9.6.4 Limitations

To improve the validity of these findings, ideally, I would repeat the experiments on more healthy control PBECs aiming for at least n=6. The fibroblast experiments need to be repeated at least twice to ensure reproducibility of the results. As aforementioned, I have focussed on soluble DPP4 in this Chapter. The distribution and activity of the membrane-bound form has not been assessed and may provide clues to the differences in gene expression seen at 3 weeks post air exposure and also the differences in the epithelial cell behaviour of healthy control and post COVID-19 donor PBECs. Additionally, despite the assumption made that upregulated DPP4 levels in the post COVID-19 airway equates to increased activity, this may not be the case.[554] Therefore, in order to assess this further, DPP4 activity levels in the BALF supernatant should be measured.

9.7 Conclusion

This Chapter demonstrates the differential protein abundance of DPP4 and AREG in BALF post COVID-19 compared to healthy controls, and the effects of DPP4 and sitagliptin (DPP4 inhibitor) on bronchial epithelial cells and human lung fibroblasts. Sitagliptin treatment has an impact on cellular differentiation markers, and has a potential immunomodulatory role, as well as increasing epithelial cell AREG production. Further in vitro studies are required to understand the mechanisms through which sitagliptin has these effects and to assess if it could potentially have a translational benefit..

Chapter 10 - Discussion and Future work

10.1 Summary of thesis aims

The main aim of this thesis was to evaluate recovery post-COVID-19 in order to enhance our understanding of potential sequelae, from the clinical to the epithelial, and allow identification of potential therapeutic mechanisms that could enhance patient recovery. The thesis consisted of four main objectives. Firstly, to understand clinical recovery, including residual symptoms and health-related quality of life impairments. Secondly, to evaluate radiological sequelae and trajectory with time. Thirdly, to assess local airway immunity and relationship with clinical parameters. Fourthly, to evaluate epithelial cell function post COVID-19. Two extra objectives were subsequently added, based on incidental discoveries during data collection: a) To evaluate physiological recovery, including small airways function post COVID-19 and b) To evaluate the function of DPP4, a serine peptidase upregulated in the post-COVID-19 airway.

10.2 Summary of findings

Clinical symptom burden was common post COVID-19, even three months post discharge from hospital, with the commonest residual symptoms being breathlessness and fatigue. Psychological and HR-QOL impairments were also common, but with a trajectory towards improvement with time. Important to note was that several external factors, such as emotional resilience and mental attitude, social support and religious faith were important in influencing the impact of residual symptoms on individuals' quality of life (Chapter 3).

Radiological abnormalities detectable on CT imaging post COVID-19 were common, with the most frequently seen abnormalities being ground-glass opacification and radiological bands. However, in the majority, regression of radiological abnormalities was seen with time and only a small proportion of individuals showed radiological evidence of fibrosis. Furthermore, persistent radiological abnormalities were associated with the severity of acute disease presentation (Chapter 4).

Lung function abnormalities were also common during the recovery phase, commonly restrictive in nature, again with a trend towards improvement with time. Abnormalities in FENO were seen, with no significant association with breathlessness, peripheral eosinophilia or epithelial damage markers (Chapter 5). The aetiology of the abnormal FENO in this cohort remains unclear, thus necessitating

cautious clinical interpretation. Small airways pathology was detectable using FOT in some individuals at 1 year, but expiratory flow limitation was not seen. Additionally, neither patient-reported symptoms nor FENO results were associated with the detection of small airways pathology (Chapter 6).

Upregulation of immune cells, especially T cells and alveolar macrophages was seen in the post-COVID 19 airway along with upregulation of markers associated with epithelial damage (Chapter 7). Differential cell count analysis showed lymphocytosis and neutrophilia in some individuals, even in the absence of a microbial trigger. Increased lymphocyte count and in particular, T cell proportions, in the airways at 3 months post discharge was associated with accelerated radiological recovery at 1 year. The underlying reason for persistent immune activation at 3-6 months post hospital discharge is not clear, but a plausible theory is the persistence of an antigenic stimulus. Near-normalisation of the immune cell subsets at 1 year, in the small group who were sampled at this time point, is again in keeping with resolving pathology.[341]

In the context of persistent signs of epithelial damage at 3 – 6 months post discharge, epithelial cell function post COVID-19 was important to study (Chapter 8). As reported, differences were elicited in some differentiation markers (FOXJ1, a marker for ciliated cells), but the functional consequences of this are yet to be determined. Epithelial responses to IAV infection were preserved and comparable to healthy control donor PBECs. However, mechanical scratch assay showed reduced wound closure post COVID-19, although significant inter-donor variability was noted, which may be associated with the degree of the acute disease severity.

Finally, DPP4, a serine peptidase was upregulated in the post-COVID 19 airway with a strong, positive relationship with AREG, which too was higher in the airway microenvironment post COVID-19 (Chapter 9). AREG plays an important role in wound healing after epithelial injury, but the biological effects of DPP4 are poorly understood. The in vivo findings were not replicated in vitro, raising the possibility that DPP4 and AREG in the post-COVID-19 airway might not be epithelial in origin. Furthermore, in in vitro studies evaluating the effects of DPP4 inhibition with sitagliptin, upregulation of AREG was seen, thus suggesting a potential counter-regulatory relationship between DPP4 and AREG. In addition, a trend was seen between sitagliptin treatment and upregulation of interferon-stimulated genes in IAV infection. Sitagliptin at the highest doses reduced fibroblast proliferation and delayed wound closure, and in epithelial cells at ALI, resulted in reduced KRT5 expression (basal cells), MUC5AC (goblet cells), and FOXJ1 (ciliated cells). Whilst the precise mechanism by which sitagliptin is

causing these effects is unclear, the highest dose does seem to have a potentially inhibitory impact on cell biology.

10.3 Summary of limitations

For the clinical sections of this thesis, the main limitation is the lack of baseline assessments and that relatively small numbers were studied. The data described in this thesis are from individuals presenting during the first and second waves of the pandemic, and pre-immunisation, therefore, the assumption cannot be made that other variants will have a similar impact. Mechanistic evaluation of some of the clinical findings (for instance FENO results in Chapter 5), and longitudinal assessment of others (for instance small airways pathology in Chapter 6), is lacking.

A better control group for Chapter 7 would have been individuals who have had COVID-19 but have normal radiological findings. Immunophenotyping the local airway environment in a larger number of donors post COVID-19 at 1 year post discharge and with different acute disease severities, would have been informative. For the epithelial culture work described in Chapters 8 and 9, increasing the number of healthy donor PBECs studied would be useful in strengthening the conclusions drawn from the data presented in these chapters. Finally, although the majority of healthy control donor samples utilised in the experiments were collected before the start of this pandemic, some were collected during the pandemic, and these individuals are likely to have had COVID-19 (even if asymptomatic), and we cannot be certain, that these individuals have normal epithelial function.

10.4 Implications of findings

10.4.1 Clinical impact

The clinical chapters of this thesis highlight the significant symptom burden experienced by individuals post COVID-19 and the importance of a holistic approach to patient care to ensure both physical and psychological symptoms are appropriately addressed, thereby to minimise the interplay between psychological and physical symptoms. Timing of CT imaging is important, given radiological trajectory, and may be more useful in individuals with severe acute disease presentations. Although inpatient steroid therapy has proven mortality benefits,[30] the utility of steroid therapy in the outpatient setting to accelerate radiological recovery is not clear. Abnormal FENO readings are common and careful interpretation of these results, in the context of peripheral eosinophilia, risk factors for atopy and clinical symptoms, is required to avoid unnecessary prescription of inhaled corticosteroids, as the

aetiology of abnormal FENO in these individuals might not be related to type 2 inflammation. Small airways pathology can occur in some individuals and should be considered in patients recovering post COVID-19. Forced oscillometry testing is a quick and simple method for detecting small airways pathology and can be easily integrated into clinical practice. However, the clinical relevance and trajectory of small airways pathology in these individuals needs further assessment. The clinical utility of endobronchial sampling to further investigate radiological abnormalities is not convincing and should be reserved for individuals with deteriorating radiological or physiological findings. Also important to note it that is that patient-reported breathlessness is not useful in differentiating between individuals who might have residual radiological or physiological abnormalities.

10.4.2 Translational impact

The improvement in immune cell subsets with time[341] is in keeping with the overall improvement in clinical status over time. The normal immune responses to influenza A infection, described in Chapter 8, is consistent with what has been observed in clinical practice, whereby an increase in hospital attendance due to influenza infection in individuals post COVID-19 has not been seen. An increase in AREG in response to sitagliptin may suggest a potential role for DPP4 inhibition in promoting wound healing post epithelial injury.

10.5 Future research

Understanding the pathophysiological mechanisms driving abnormal FENO is these individuals is urgently required. A randomised, clinical trial, with baseline phenotyping of allergy status, and assessment of the effect of inhaled corticosteroid on symptom burden, FENO results and small airways pathology would be valuable. In addition, mechanistic evaluation through biopsies of the bronchial epithelium to assess inflammatory and in particular, eosinophilic infiltrate will provide more clarity on underlying mechanisms contributing to the abnormal FENO results.

Measurement of SARS-COV2 RNA in the BALF fluid, and assessment of microbial triggers using non-culture dependent methods such as through evaluation of the microbiome would provide great insights into the immune cell activation seen in Chapter 7. The reason for defects in wound healing in Chapter 8 is not known, and more in-depth assessment of cell migration might offer clues to this. Whilst immune responses to influenza, a cytopathic virus were preserved in PBECs post COVID-19, the effect of less potent viruses, such as rhinovirus, would be interesting. In addition, temporal evaluation of epithelial function would be invaluable in order the ascertain if epithelial function also improves

with time. Further work is required to understand DPP4 activity in the post-COVID-19 airway, as increased concentration may not necessarily equate to increased biological activity. Evaluation of the other peptidases and proteases upregulated in the post COVID-19 airway[341] and relationship with metalloproteinases that are known to cleave the protein is also important. In addition, whilst the focus of the DPP4 work presented in this thesis has been the soluble form, further work on the activity of the membrane-bound form would be important, especially given the relative increase in DPP4 gene expression seen in post-COVID-19 PBECs compared to HC PBECs, despite comparable levels of soluble protein. Further in vitro studies are required to understand the mechanisms by which sitagliptin increases AREG production from epithelial cells and the potential immunomodulatory effects described in Chapter 9.

Finally, it would be interesting to see if the changes described in the airway immune landscape and epithelial function are also present after other variants, as the work presented in this thesis uses endobronchial samples obtained during the first and second waves of the pandemic only. Importantly, whilst bronchial epithelial samples were utilised for this thesis, assessment of nasal brushings might be more representative of the cell types affected in patients who've had Omicron infection and predominantly upper respiratory tract symptoms.

10.6 Conclusion

COVID-19 results in significant respiratory and non-respiratory sequelae, with persistent clinical, radiological and physiological morbidity, even 3 months after hospital discharge. The airway immune landscape is abnormal at this timepoint, with differential upregulation of immune cells and proteins associated with epithelial damage. Wound healing in response to mechanical injury remains impaired in some individuals, but epithelial immune responses to IAV remain preserved. Clinical, radiological and physiological parameters show a trend towards improvement with time in the majority, but further studies are required to determine if the airway immune landscape and epithelial function also recover in this way, and the relevance of and relationship between the differentially upregulated proteins, DPP4 and AREG, in the post-COVID-19 airway.

Chapter 11 – References

1. British Foreign Policy Group. COVID-19 Timeline. April 2020 [Online] Available from: https://bfpg.co.uk/2020/04/covid-19-timeline/
2. Institute for Government. Timeline of UK government coronavirus lockdowns and restrictions. Dec 2022 [Online] Available from: https://www.instituteforgovernment.org.uk/data-visualisation/timeline-coronavirus-lockdowns
3. Cui J, Li F, Shi Z-L. Origin and evolution of pathogenic coronaviruses. *Nat Rev Microbiol* 2019; 17: 181–192.
4. WHO Coronavirus Disease (COVID-19) Dashboard. Updated 26th April 2023. [Online] Available from: https://covid19.who.int/
5. Lu R, Zhao X, Li J, et al. Genomic characterisation and epidemiology of 2019 novel coronavirus: implications for virus origins and receptor binding. *The Lancet* 2020; 395: 565–574.
6. Fehr AR, Perlman S. Coronaviruses: An Overview of Their Replication and Pathogenesis. 2015, pp. 1–23.
7. Walls AC, Park Y-J, Tortorici MA, et al. Structure, Function, and Antigenicity of the SARS-CoV-2 Spike Glycoprotein. *Cell* 2020; 181: 281-292.e6.
8. World Health Organisation. Naming SARS-CoV-2 variants. Updated 27th April 2023. [Online] Available from: https://www.who.int/activities/tracking-SARS-CoV-2-variants
9. UK Health Security Agency. COVID-19 variants identified in the UK – latest updates. Updated 21st April 2023 [Online] Available from: www.gov.uk
10. Guan W, Ni Z, Hu Y, et al. Clinical Characteristics of Coronavirus Disease 2019 in China. *New England Journal of Medicine* 2020; 382: 1708–1720.
11. Millar JE, Neyton L, Seth S, et al. Distinct clinical symptom patterns in patients hospitalised with COVID-19 in an analysis of 59,011 patients in the ISARIC-4C study. *Sci Rep* 2022; 12: 6843.
12. Oran DP, Topol EJ. Prevalence of Asymptomatic SARS-CoV-2 Infection. *Ann Intern Med* 2020; 173: 362–367.
13. Ma Q, Liu J, Liu Q, et al. Global Percentage of Asymptomatic SARS-CoV-2 Infections Among the Tested Population and Individuals With Confirmed COVID-19 Diagnosis. *JAMA Netw Open* 2021; 4: e2137257.
14. Williamson EJ, Walker AJ, Bhaskaran K, et al. Factors associated with COVID-19-related death using OpenSAFELY. *Nature* 2020; 584: 430–436.
15. Samadizadeh S, Masoudi M, Rastegar M, et al. COVID-19: Why does disease severity vary among individuals? *Respir Med* 2021; 180: 106356.

16. Ojha V, Mani A, Pandey NN, et al. CT in coronavirus disease 2019 (COVID-19): a systematic review of chest CT findings in 4410 adult patients. *Eur Radiol* 2020; 30: 6129–6138.
17. Kwee TC, Kwee RM. Chest CT in COVID-19: What the Radiologist Needs to Know. *RadioGraphics* 2020; 40: 1848–1865.
18. Chen Z, Fan H, Cai J, et al. High-resolution computed tomography manifestations of COVID-19 infections in patients of different ages. *Eur J Radiol* 2020; 126: 108972.
19. Pan F, Ye T, Sun P, et al. Time Course of Lung Changes at Chest CT during Recovery from Coronavirus Disease 2019 (COVID-19). *Radiology* 2020; 295: 715–721.
20. Wang Y, Dong C, Hu Y, et al. Temporal Changes of CT Findings in 90 Patients with COVID-19 Pneumonia: A Longitudinal Study. *Radiology* 2020; 296: E55–E64.
21. Bernheim A, Mei X, Huang M, et al. Chest CT Findings in Coronavirus Disease-19 (COVID-19): Relationship to Duration of Infection. *Radiology* 2020; 295: 200463.
22. Cozzi D, Bicci E, Bindi A, et al. Role of Chest Imaging in Viral Lung Diseases. *Int J Environ Res Public Health* 2021; 18: 6434.
23. Lanza E, Muglia R, Bolengo I, et al. Quantitative chest CT analysis in COVID-19 to predict the need for oxygenation support and intubation. *Eur Radiol* 2020; 30: 6770–6778.
24. Bayrak V, Senturk Durukan N, Demirer Aydemir F, et al. Risk factors associated with mortality in ıntensive care COVID-19 patients: the importance of chest CT score and intubation timing as risk factors. *Turk J Med Sci* 2021; 51: 1665–1674.
25. Zhou F, Yu T, Du R, et al. Clinical course and risk factors for mortality of adult inpatients with COVID-19 in Wuhan, China: a retrospective cohort study. *The Lancet* 2020; 395: 1054–1062.
26. Prozan L, Shusterman E, Ablin J, et al. Prognostic value of neutrophil-to-lymphocyte ratio in COVID-19 compared with Influenza and respiratory syncytial virus infection. *Sci Rep* 2021; 11: 21519.
27. Wu C, Chen X, Cai Y, et al. Risk Factors Associated With Acute Respiratory Distress Syndrome and Death in Patients With Coronavirus Disease 2019 Pneumonia in Wuhan, China. *JAMA Intern Med* 2020; 180: 934.
28. Liu J, Li S, Liu J, et al. Longitudinal characteristics of lymphocyte responses and cytokine profiles in the peripheral blood of SARS-CoV-2 infected patients. *EBioMedicine* 2020; 55: 102763.
29. Chen Z, John Wherry E. T cell responses in patients with COVID-19. *Nat Rev Immunol* 2020; 20: 529–536.
30. The RECOVERY Collaborative Group. Dexamethasone in Hospitalized Patients with Covid-19. *New England Journal of Medicine* 2021; 384: 693–704.
31. Beigel JH, Tomashek KM, Dodd LE, et al. Remdesivir for the Treatment of Covid-19 — Final Report. *New England Journal of Medicine* 2020; 383: 1813–1826.

32. WHO Solidarity Trial Consortium. Remdesivir and three other drugs for hospitalised patients with COVID-19: final results of the WHO Solidarity randomised trial and updated meta-analyses. *The Lancet* 2022; 399: 1941–1953.
33. Jayk Bernal A, Gomes da Silva MM, Musungaie DB, et al. Molnupiravir for Oral Treatment of Covid-19 in Nonhospitalized Patients. *New England Journal of Medicine* 2022; 386: 509–520.
34. Hermine O, Mariette X, Tharaux P-L, et al. Effect of Tocilizumab vs Usual Care in Adults Hospitalized With COVID-19 and Moderate or Severe Pneumonia. *JAMA Intern Med* 2021; 181: 32.
35. Mariette X, Hermine O, Tharaux P-L, et al. Sarilumab in adults hospitalised with moderate-to-severe COVID-19 pneumonia (CORIMUNO-SARI-1): An open-label randomised controlled trial. *Lancet Rheumatol* 2022; 4: e24–e32.
36. Lescure F-X, Honda H, Fowler RA, et al. Sarilumab in patients admitted to hospital with severe or critical COVID-19: a randomised, double-blind, placebo-controlled, phase 3 trial. *Lancet Respir Med* 2021; 9: 522–532.
37. REMAP-CAP Investigators. Interleukin-6 Receptor Antagonists in Critically Ill Patients with Covid-19. *New England Journal of Medicine* 2021; 384: 1491–1502.
38. Rubin R. Baricitinib Is First Approved COVID-19 Immunomodulatory Treatment. *JAMA* 2022; 327: 2281.
39. Selvaraj V, Finn A, Lal A, et al. Baricitinib in hospitalised patients with COVID-19: A meta-analysis of randomised controlled trials. *EClinicalMedicine* 2022; 49: 101489.
40. National Institute of Clinical Excellence. COVID-19 rapid guideline: managing COVID-19 (NG191). *23 March 2021* [Online] Available from: https://www.nice.org.uk/guidance/ng191
41. Ramakrishnan S, Nicolau D v, Langford B, et al. Inhaled budesonide in the treatment of early COVID-19 (STOIC): a phase 2, open-label, randomised controlled trial. *Lancet Respir Med* 2021; 9: 763–772.
42. Shah PL, Orton CM, Grinsztejn B, et al. Favipiravir in patients hospitalised with COVID-19 (PIONEER trial): a multicentre, open-label, phase 3, randomised controlled trial of early intervention versus standard care. *Lancet Respir Med*. 2022 [Published online]
43. Ravindra NG, Alfajaro MM, Gasque V, et al. Single-cell longitudinal analysis of SARS-CoV-2 infection in human airway epithelium identifies target cells, alterations in gene expression, and cell state changes. *PLoS Biol* 2021; 19: e3001143.
44. Bridges JP, VEszter, HHua, MRJ. Respiratory epithelial cell responses to SARS-CoV-2 in COVID-19 . *Thorax* 2022; 77: 203–209.
45. Muus C, Luecken MD, Eraslan G, et al. Single-cell meta-analysis of SARS-CoV-2 entry genes across tissues and demographics. *Nat Med* 2021; 27: 546–559.

46. Mossel EC, Wang J, Jeffers S, et al. SARS-CoV replicates in primary human alveolar type II cell cultures but not in type I-like cells. *Virology* 2008; 372: 127–135.
47. Lazear HM, Schoggins JW, Diamond MS. Shared and Distinct Functions of Type I and Type III Interferons. *Immunity* 2019; 50: 907–923.
48. Blanco-Melo D, Nilsson-Payant BE, Liu W-C, et al. Imbalanced Host Response to SARS-CoV-2 Drives Development of COVID-19. *Cell* 2020; 181: 1036-1045.e9.
49. Channappanavar R, Fehr AR, Vijay R, et al. Dysregulated Type I Interferon and Inflammatory Monocyte-Macrophage Responses Cause Lethal Pneumonia in SARS-CoV-Infected Mice. *Cell Host Microbe* 2016; 19: 181–193.
50. Dinnon KH, Leist SR, Schäfer A, et al. A mouse-adapted model of SARS-CoV-2 to test COVID-19 countermeasures. *Nature* 2020; 586: 560–566.
51. Major J, Crotta S, Llorian M, et al. Type I and III interferons disrupt lung epithelial repair during recovery from viral infection. *Science (1979)* 2020; 369: 712–717.
52. Broggi A, Ghosh S, Sposito B, et al. Type III interferons disrupt the lung epithelial barrier upon viral recognition. *Science (1979)* 2020; 369: 706–712.
53. Schulz O, Diebold SS, Chen M, et al. Toll-like receptor 3 promotes cross-priming to virus-infected cells. *Nature* 2005; 433: 887–892.
54. Munker D, Osterman A, Stubbe H, et al. Dynamics of SARS-CoV-2 shedding in the respiratory tract depends on the severity of disease in COVID-19 patients. *European Respiratory Journal* 2021; 58: 2002724.
55. Peiris J, Chu C, Cheng V, et al. Clinical progression and viral load in a community outbreak of coronavirus-associated SARS pneumonia: a prospective study. *The Lancet* 2003; 361: 1767–1772.
56. Tojo K, Yamamoto N, Tamada N, et al. Early alveolar epithelial cell necrosis is a potential driver of COVID-19-induced acute respiratory distress syndrome. *iScience* 2023; 26: 105748.
57. Hung IF-N, Lung K-C, Tso EY-K, et al. Triple combination of interferon beta-1b, lopinavir–ritonavir, and ribavirin in the treatment of patients admitted to hospital with COVID-19: an open-label, randomised, phase 2 trial. *The Lancet* 2020; 395: 1695–1704.
58. Monk PD, Marsden RJ, Tear VJ, et al. Safety and efficacy of inhaled nebulised interferon beta-1a (SNG001) for treatment of SARS-CoV-2 infection: a randomised, double-blind, placebo-controlled, phase 2 trial. *Lancet Respir Med* 2021; 9: 196–206.
59. Kalil AC, Mehta AK, Patterson TF, et al. Efficacy of interferon beta-1a plus remdesivir compared with remdesivir alone in hospitalised adults with COVID-19: a double-blind, randomised, placebo-controlled, phase 3 trial. *Lancet Respir Med* 2021; 9: 1365–1376.

60. Feld JJ, Kandel C, Biondi MJ, et al. Peginterferon lambda for the treatment of outpatients with COVID-19: a phase 2, placebo-controlled randomised trial. *Lancet Respir Med* 2021; 9: 498–510.
61. Baron A, Hachem M, Tran Van Nhieu J, et al. Bronchoalveolar Lavage in Patients with COVID-19 with Invasive Mechanical Ventilation for Acute Respiratory Distress Syndrome. *Ann Am Thorac Soc* 2021; 18: 723–726.
62. Liao M, Liu Y, Yuan J, et al. Single-cell landscape of bronchoalveolar immune cells in patients with COVID-19. *Nat Med*; 2020. 26, 842–844
63. Zhou Z, Ren L, Zhang L, et al. Heightened Innate Immune Responses in the Respiratory Tract of COVID-19 Patients. *Cell Host Microbe* 2020; 27: 883-890.e2.
64. Merad M, Martin JC. Pathological inflammation in patients with COVID-19: a key role for monocytes and macrophages. *Nat Rev Immunol* 2020; 20: 355–362.
65. Xu G, Qi F, Li H, et al. The differential immune responses to COVID-19 in peripheral and lung revealed by single-cell RNA sequencing. *Cell Discov* 2020; 6: 73.
66. Xiong Y, Liu Y, Cao L, et al. Transcriptomic characteristics of bronchoalveolar lavage fluid and peripheral blood mononuclear cells in COVID-19 patients. *Emerg Microbes Infect* 2020; 9: 761–770.
67. Saris Anno, RTD, NEJ, et al. Distinct cellular immune profiles in the airways and blood of critically ill patients with COVID-19. *Thorax* 2021; 76: 1010–1019.
68. Cevik M, Tate M, Lloyd O, et al. SARS-CoV-2, SARS-CoV, and MERS-CoV viral load dynamics, duration of viral shedding, and infectiousness: a systematic review and meta-analysis. *Lancet Microbe* 2021; 2: e13–e22.
69. Zhou B, She J, Wang Y, et al. Duration of Viral Shedding of Discharged Patients With Severe COVID-19. *Clinical Infectious Diseases* 2020; 71: 2240–2242.
70. Hadjadj J, Yatim N, Barnabei L, et al. Impaired type I interferon activity and inflammatory responses in severe COVID-19 patients. *Science (1979)* 2020; 369: 718–724.
71. Martines RB, Ritter JM, Matkovic E, et al. Pathology and Pathogenesis of SARS-CoV-2 Associated with Fatal Coronavirus Disease, United States. *Emerg Infect Dis* 2020; 26: 2005–2015.
72. Xu Z, Shi L, Wang Y, et al. Pathological findings of COVID-19 associated with acute respiratory distress syndrome. *Lancet Respir Med* 2020; 8: 420–422.
73. Li S, Jiang L, Li X, et al. Clinical and pathological investigation of patients with severe COVID-19. *JCI Insight*; 2020. 5(12):e138070
74. Fang Y, Liu H, Huang H, et al. Distinct stem/progenitor cells proliferate to regenerate the trachea, intrapulmonary airways and alveoli in COVID-19 patients. *Cell Res* 2020; 30: 705–707.
75. Bradley BT, Bryan A. Emerging respiratory infections: The infectious disease pathology of SARS, MERS, pandemic influenza, and Legionella. *Semin Diagn Pathol* 2019; 36: 152–159.

76. Konopka KE, Nguyen T, Jentzen JM, et al. Diffuse alveolar damage (DAD) resulting from coronavirus disease 2019 Infection is Morphologically Indistinguishable from Other Causes of DAD. *Histopathology* 2020; 77: 570–578.
77. Ng DL, al Hosani F, Keating MK, et al. Clinicopathologic, Immunohistochemical, and Ultrastructural Findings of a Fatal Case of Middle East Respiratory Syndrome Coronavirus Infection in the United Arab Emirates, April 2014. *Am J Pathol* 2016; 186: 652–658.
78. Ding Y, Wang H, Shen H, et al. The clinical pathology of severe acute respiratory syndrome (SARS): a report from China. *J Pathol* 2003; 200: 282–289.
79. Castranova V, Rabovsky J, Tucker JH, et al. The alveolar type II epithelial cell: A multifunctional pneumocyte. *Toxicol Appl Pharmacol* 1988; 93: 472–483.
80. Chen J, Wu H, Yu Y, et al. Pulmonary alveolar regeneration in adult COVID-19 patients. *Cell Res* 2020; 30: 708–710.
81. Hui DS. Impact of severe acute respiratory syndrome (SARS) on pulmonary function, functional capacity and quality of life in a cohort of survivors. *Thorax* 2005; 60: 401–409.
82. Chan K, Zheng J, Mok Y, et al. SARS: prognosis, outcome and sequelae. *Respirology* 2003; 8: S36–S40.
83. Morice AH. Recommendations for the management of cough in adults. *Thorax* 2006; 61: i1–i24.
84. Footitt J, Johnston SL. Cough and viruses in airways disease: Mechanisms. *Pulm Pharmacol Ther* 2009; 22: 108–113.
85. Chung KF, McGarvey L, Song W-J, et al. Cough hypersensitivity and chronic cough. *Nat Rev Dis Primers* 2022; 8: 45.
86. Kubo T, Tobe K, Okuyama K, et al. Disease burden and quality of life of patients with chronic cough in Japan: a population-based cross-sectional survey. *BMJ Open Respir Res* 2021; 8: e000764.
87. Kelsall A, Decalmer S, Webster D, et al. How to quantify coughing: correlations with quality of life in chronic cough. *European Respiratory Journal* 2008; 32: 175–179.
88. Rasa S, Nora-Krukle Z, Henning N, et al. Chronic viral infections in myalgic encephalomyelitis/chronic fatigue syndrome (ME/CFS). *J Transl Med* 2018; 16: 268.
89. Fluge Ø, Bruland O, Risa K, et al. Benefit from B-Lymphocyte Depletion Using the Anti-CD20 Antibody Rituximab in Chronic Fatigue Syndrome. A Double-Blind and Placebo-Controlled Study. *PLoS One* 2011; 6: e26358.
90. Wright A, Fisher PL, Baker N, et al. Perfectionism, depression and anxiety in chronic fatigue syndrome: A systematic review. *J Psychosom Res* 2021; 140: 110322.
91. Sandberg J, Ekström M, Börjesson M, et al. Underlying contributing conditions to breathlessness among middle-aged individuals in the general population: a cross-sectional study. *BMJ Open Respir Res* 2020; 7: e000643.

92. Guz A. Brain, breathing and breathlessness. *Respir Physiol* 1997; 109: 197–204.
93. Marlow LL, Faull OK, Finnegan SL, et al. Breathlessness and the brain: the role of expectation. *Curr Opin Support Palliat Care* 2019; 13: 200–210.
94. Annals of Thoracic Society. Dyspnea. *Am J Respir Crit Care Med* 1999; 159: 321–340.
95. Das KM, Lee EY, Enani MA, et al. CT Correlation With Outcomes in 15 Patients With Acute Middle East Respiratory Syndrome Coronavirus. *American Journal of Roentgenology* 2015; 204: 736–742.
96. Wu X, Dong D, Ma D. Thin-Section Computed Tomography Manifestations During Convalescence and Long-Term Follow-Up of Patients with Severe Acute Respiratory Syndrome (SARS). *Medical Science Monitor* 2016; 22: 2793–2799.
97. Antonio GE, Wong KT, Hui DSC, et al. Thin-Section CT in Patients with Severe Acute Respiratory Syndrome Following Hospital Discharge: Preliminary Experience. *Radiology* 2003; 228: 810–815.
98. Ng CK. Six month radiological and physiological outcomes in severe acute respiratory syndrome (SARS) survivors. *Thorax* 2004; 59: 889–891.
99. Zhang P, Li J, Liu H, et al. Long-term bone and lung consequences associated with hospital-acquired severe acute respiratory syndrome: a 15-year follow-up from a prospective cohort study. *Bone Res* 2020; 8: 8.
100. Xie L, Liu Y, Fan B, et al. Dynamic changes of serum SARS-Coronavirus IgG, pulmonary function and radiography in patients recovering from SARS after hospital discharge. *Respir Res* 2005; 6: 5.
101. Xie L, Liu Y, Xiao Y, et al. Follow-up Study on Pulmonary Function and Lung Radiographic Changes in Rehabilitating Severe Acute Respiratory Syndrome Patients After Discharge. *Chest* 2005; 127: 2119–2124.
102. Hansell DM, Bankier AA, MacMahon H, et al. Fleischner Society: Glossary of Terms for Thoracic Imaging. *Radiology* 2008; 246: 697–722.
103. Hewitt MG, Miller WT, Reilly TJ, et al. The relative frequencies of causes of widespread ground-glass opacity: A retrospective cohort. *Eur J Radiol* 2014; 83: 1970–1976.
104. Miller WT, Shah RM. Isolated Diffuse Ground-Glass Opacity in Thoracic CT: Causes and Clinical Presentations. *American Journal of Roentgenology* 2005; 184: 613–622.
105. Parekh M, Donuru A, Balasubramanya R, et al. Review of the Chest CT Differential Diagnosis of Ground-Glass Opacities in the COVID Era. *Radiology* 2020; 297: E289–E302.
106. Cozzi D, Cavigli E, Moroni C, et al. Ground-glass opacity (GGO): a review of the differential diagnosis in the era of COVID-19. *Jpn J Radiol* 2021; 39: 721–732.
107. Kim EA, Lee KS, Primack SL, et al. Viral Pneumonias in Adults: Radiologic and Pathologic Findings. *RadioGraphics* 2002; 22: S137–S149.

108. Xu J, Xu X, Jiang L, et al. SARS-CoV-2 induces transcriptional signatures in human lung epithelial cells that promote lung fibrosis. *Respir Res* 2020; 21: 182.

109. Raghu G SLHLSGE. Extracellular matrix in normal and fibrotic human lungs. *Am Rev Respir Dis* 1985; 131: 281–289.

110. Zapol W, Trelstad R, Coffey J, et al. Pulmonary fibrosis in severe acute respiratory failure. *Am Rev Respir Dis* 1979; 119: 547–54.

111. Marshall R, Bellingan G, Laurent G. The acute respiratory distress syndrome: fibrosis in the fast lane. *Thorax* 1998; 53: 815–817.

112. Marshall RP, Bellingan G, Webb S, et al. Fibroproliferation Occurs Early in the Acute Respiratory Distress Syndrome and Impacts on Outcome. *Am J Respir Crit Care Med* 2000; 162: 1783–1788.

113. Butt RP, Bishop JE. Mechanical Load Enhances the Stimulatory Effect of Serum Growth Factors on Cardiac Fibroblast Procollagen Synthesis. *J Mol Cell Cardiol* 1997; 29: 1141–1151.

114. Parker JC, Hernandez LA, Peevy KJ. Mechanisms of ventilator-induced lung injury. *Crit Care Med* 1993; 21: 131–143.

115. Raghu G, Collard HR, Egan JJ, et al. An Official ATS/ERS/JRS/ALAT Statement: Idiopathic Pulmonary Fibrosis: Evidence-based Guidelines for Diagnosis and Management. *Am J Respir Crit Care Med* 2011; 183: 788–824.

116. Bourke SJ. DJC, BG, MC, BCI, CJE. Hypersensitivity pneumonitis: current concepts. *European Respiratory Journal* 2001; 18: 81s–92s.

117. Cormier Y I-AE. The role of viruses in the pathogenesis of hypersensitivity pneumonitis. *Current Opinion Pulmonary Medicine* 2000; 6: 420–3.

118. Kligerman SJ, Franks TJ, Galvin JR. From the Radiologic Pathology Archives: Organization and Fibrosis as a Response to Lung Injury in Diffuse Alveolar Damage, Organizing Pneumonia, and Acute Fibrinous and Organizing Pneumonia. *RadioGraphics* 2013; 33: 1951–1975.

119. Drakopanagiotakis F, Paschalaki K, Abu-Hijleh M, et al. Cryptogenic and Secondary Organizing Pneumonia. *Chest* 2011; 139: 893–900.

120. Cornejo R, Llanos O, Fernandez C, et al. Organizing pneumonia in patients with severe respiratory failure due to novel A (H1N1) influenza. *Case Reports* 2010; 2010: bcr0220102708–bcr0220102708.

121. Hwang DM, Chamberlain DW, Poutanen SM, et al. Pulmonary pathology of severe acute respiratory syndrome in Toronto. *Modern Pathology* 2005; 18: 1–10.

122. Kanne JP, Little BP, Chung JH, et al. Essentials for Radiologists on COVID-19: An Update— *Radiology* Scientific Expert Panel. *Radiology* 2020; 296: E113–E114.

123. Fu F, Lou J, Xi D, et al. Chest computed tomography findings of coronavirus disease 2019 (COVID-19) pneumonia. *Eur Radiol* 2020; 30: 5489–5498.

124. Bradley BT, Maioli H, Johnston R, et al. Histopathology and ultrastructural findings of fatal COVID-19 infections in Washington State: a case series. *The Lancet* 2020; 396: 320–332.
125. Vannella KM, Moore BB. Viruses as co-factors for the initiation or exacerbation of lung fibrosis. *Fibrogenesis Tissue Repair* 2008; 1: 2.
126. Chambers RC, Mercer PF. Mechanisms of Alveolar Epithelial Injury, Repair, and Fibrosis. *Ann Am Thorac Soc* 2015; 12: S16–S20.
127. Huang WJ, Tang XX. Virus infection induced pulmonary fibrosis. *J Transl Med* 2021; 19: 496.
128. Hata A, Schiebler ML, Lynch DA, et al. Interstitial Lung Abnormalities: State of the Art. *Radiology* 2021; 301: 19–34.
129. Hatabu H, Hunninghake GM, Richeldi L, et al. Interstitial lung abnormalities detected incidentally on CT: a Position Paper from the Fleischner Society. *Lancet Respir Med* 2020; 8: 726–737.
130. Kolb M, Bondue B, Pesci A, et al. Acute exacerbations of progressive-fibrosing interstitial lung diseases. *European Respiratory Review* 2018; 27: 180071.
131. Sigurs N, Bjarnason R, Sigurbergsson F, et al. Asthma and Immunoglobulin E Antibodies After Respiratory Syncytial Virus Bronchiolitis: A Prospective Cohort Study With Matched Controls. *Pediatrics* 1995; 95: 500–505.
132. Pullan CR, Hey EN. Wheezing, asthma, and pulmonary dysfunction 10 years after infection with respiratory syncytial virus in infancy. *BMJ* 1982; 284: 1665–1669.
133. Folkerts G, Busse WW, Nijkamp FP, et al. Virus-induced Airway Hyperresponsiveness and Asthma. *Am J Respir Crit Care Med* 1998; 157: 1708–1720.
134. Skoner DP, DWJ, SJ, VDMA, FP. Lower airway responses to rhinovirus 39 in healthy allergic and nonallergic subjects. *European Respiratory Journal* 1996; 9: 1402–1406.
135. Fraenkel DJ, Bardin PG, Sanderson G, et al. Lower Airways Inflammation during Rhinovirus Colds in Normal and in Asthmatic Subjects. *Am J Respir Crit Care Med* 1995; 151: 879–886.
136. Gern JE, Calhoun W, Swenson C, et al. Rhinovirus infection preferentially increases lower airway responsiveness in allergic subjects. *Am J Respir Crit Care Med* 1997; 155: 1872–1876.
137. van der Velden, Hulsmann AR. Peptidases: structure, function and modulation of peptide-mediated effects in the human lung. *Clinical & Experimental Allergy* 1999; 29: 445–456.
138. Dusser DJ, Jacoby DB, Djokic TD, et al. Virus induces airway hyperresponsiveness to tachykinins: role of neutral endopeptidase. *J Appl Physiol* 1989; 67: 1504–1511.
139. Joos GF, Germonpre PR, Pauwels RA. Role of tachykinins in asthma. *Allergy* 2000; 55: 321–337.
140. Fraenkel DJ, Bardin PG, Sanderson G, et al. Immunohistochemical analysis of nasal biopsies during rhinovirus experimental colds. *Am J Respir Crit Care Med* 1994; 150: 1130–1136.

141. Winther B, Farr B, Turner RB, et al. Histopathologic Examination and Enumeration of Polymorphonuclear Leukocytes in the Nasal Mucosa during Experimental Rhinovirus Colds. *Acta Otolaryngol* 1984; 98: 19–24.
142. Zhang L, Collins PL, Lamb RA, et al. Comparison of differing cytopathic effects in human airway epithelium of parainfluenza virus 5 (W3A), parainfluenza virus type 3, and respiratory syncytial virus. *Virology* 2011; 421: 67–77.
143. Wang T-E, Chao T-L, Tsai H-T, et al. Differentiation of Cytopathic Effects (CPE) induced by influenza virus infection using deep Convolutional Neural Networks (CNN). *PLoS Comput Biol* 2020; 16: e1007883.
144. Zhu N, Wang W, Liu Z, et al. Morphogenesis and cytopathic effect of SARS-CoV-2 infection in human airway epithelial cells. *Nat Commun* 2020; 11: 3910.
145. Ricciardolo FLM. Multiple roles of nitric oxide in the airways. *Thorax* 2003; 58: 175–182.
146. Kesler BS, Mazzone SB, Canning BJ. Nitric Oxide–dependent Modulation of Smooth-Muscle Tone by Airway Parasympathetic Nerves. *Am J Respir Crit Care Med* 2002; 165: 481–488.
147. Swadling L, Maini MK. T cells in COVID-19 — united in diversity. *Nat Immunol* 2020; 21: 1307–1308.
148. Aleebrahim-Dehkordi E, Molavi B, Mokhtari M, et al. T helper type (Th1/Th2) responses to SARS-CoV-2 and influenza A (H1N1) virus: From cytokines produced to immune responses. *Transpl Immunol* 2022; 70: 101495.
149. Baker JR, Mahdi M, Nicolau D v, et al. Early Th2 inflammation in the upper respiratory mucosa as a predictor of severe COVID-19 and modulation by early treatment with inhaled corticosteroids: a mechanistic analysis. *Lancet Respir Med* 2022; 10: 545–556.
150. Lloyd CM, Hessel EM. Functions of T cells in asthma: more than just TH2 cells. *Nat Rev Immunol* 2010; 10: 838–848.
151. Han S, Mallampalli RK. The Role of Surfactant in Lung Disease and Host Defense against Pulmonary Infections. *Ann Am Thorac Soc* 2015; 12: 765–774.
152. Crisafulli E, Pisi R, Aiello M, et al. Prevalence of Small-Airway Dysfunction among COPD Patients with Different GOLD Stages and Its Role in the Impact of Disease. *Respiration* 2017; 93: 32–41.
153. Roche WR, Montefort S, Baker J, et al. Cell Adhesion Molecules and the Bronchial Epithelium. *American Review of Respiratory Disease* 1993; 148: S79–S82.
154. Voynow JA, Rubin BK. Mucins, Mucus, and Sputum. *Chest* 2009; 135: 505–512.
155. Voynow JA, Gendler SJ, Rose MC. Regulation of Mucin Genes in Chronic Inflammatory Airway Diseases. *Am J Respir Cell Mol Biol* 2006; 34: 661–665.
156. Tamura S KT. Defense mechanisms against influenza virus infection in the respiratory tract mucosa. *Jpn J Infect Dis* 2004; 57: 236–47.

157. Iwamura C, Nakayama T. Toll-like receptors in the respiratory system: Their roles in inflammation. *Curr Allergy Asthma Rep* 2008; 8: 7–13.

158. Guillot L, le Goffic R, Bloch S, et al. Involvement of Toll-like Receptor 3 in the Immune Response of Lung Epithelial Cells to Double-stranded RNA and Influenza A Virus. *Journal of Biological Chemistry* 2005; 280: 5571–5580.

159. Hewson CA, Jardine A, Edwards MR, et al. Toll-Like Receptor 3 Is Induced by and Mediates Antiviral Activity against Rhinovirus Infection of Human Bronchial Epithelial Cells. *J Virol* 2005; 79: 12273–12279.

160. Sasai M, Shingai M, Funami K, et al. NAK-Associated Protein 1 Participates in Both the TLR3 and the Cytoplasmic Pathways in Type I IFN Induction. *The Journal of Immunology* 2006; 177: 8676–8683.

161. Ichinohe T, Lee HK, Ogura Y, et al. Inflammasome recognition of influenza virus is essential for adaptive immune responses. *Journal of Experimental Medicine* 2009; 206: 79–87.

162. Muruve DA, Pétrilli V, Zaiss AK, et al. The inflammasome recognizes cytosolic microbial and host DNA and triggers an innate immune response. *Nature* 2008; 452: 103–107.

163. Jacobs AT, Ignarro LJ. Lipopolysaccharide-induced Expression of Interferon-β Mediates the Timing of Inducible Nitric-oxide Synthase Induction in RAW 264.7 Macrophages. *Journal of Biological Chemistry* 2001; 276: 47950–47957.

164. Sanders SP, Siekierski ES, Porter JD, et al. Nitric Oxide Inhibits Rhinovirus-Induced Cytokine Production and Viral Replication in a Human Respiratory Epithelial Cell Line. *J Virol* 1998; 72: 934–942.

165. Kopitar-Jerala N. The Role of Interferons in Inflammation and Inflammasome Activation. *Front Immunol*; 2017. 8:873.

166. Li Y, Tang XX. Abnormal Airway Mucus Secretion Induced by Virus Infection. *Front Immunol*. 12:701443

167. Zheng S, De BP, Choudhary S, et al. Impaired Innate Host Defense Causes Susceptibility to Respiratory Virus Infections in Cystic Fibrosis. *Immunity* 2003; 18: 619–630.

168. Chen I-Y, Moriyama M, Chang M-F, et al. Severe Acute Respiratory Syndrome Coronavirus Viroporin 3a Activates the NLRP3 Inflammasome. *Front Microbiol*;10:50

169. Nusrat A, Delp C, Madara JL. Intestinal epithelial restitution. Characterization of a cell culture model and mapping of cytoskeletal elements in migrating cells. *Journal of Clinical Investigation* 1992; 89: 1501–1511.

170. Leoni G, Neumann P-A, Sumagin R, et al. Wound repair: role of immune–epithelial interactions. *Mucosal Immunol* 2015; 8: 959–968.

171. ten Dijke P, Iwata KK. Growth Factors For Wound Healing. *Nat Biotechnol* 1989; 7: 793–798.

172. Cabral-Pacheco GA, Garza-Veloz I, Castruita-De la Rosa C, et al. The Roles of Matrix Metalloproteinases and Their Inhibitors in Human Diseases. *Int J Mol Sci* 2020; 21: 9739.

173. Croasdell Lucchini A, Gachanja NN, Rossi AG, et al. Epithelial Cells and Inflammation in Pulmonary Wound Repair. *Cells* 2021; 10: 339.
174. Zemans RL, Briones N, Campbell M, et al. Neutrophil transmigration triggers repair of the lung epithelium via β-catenin signaling. *Proceedings of the National Academy of Sciences* 2011; 108: 15990–15995.
175. Witte MB, Barbul A. Role of nitric oxide in wound repair. *The American Journal of Surgery* 2002; 183: 406–412.
176. Ramesh G, Jindal SK, Ganguly NK, et al. Increased nitric oxide production by neutrophils in bronchial asthma. *European Respiratory Journal* 2001; 17: 868–871.
177. Denans N, Tran NTT, Swall ME, et al. An anti-inflammatory activation sequence governs macrophage transcriptional dynamics during tissue injury in zebrafish. *Nat Commun* 2022; 13: 5356.
178. Das A, Sinha M, Datta S, et al. Monocyte and Macrophage Plasticity in Tissue Repair and Regeneration. *Am J Pathol* 2015; 185: 2596–2606.
179. Marconi GD, Fonticoli L, Rajan TS, et al. Epithelial-Mesenchymal Transition (EMT): The Type-2 EMT in Wound Healing, Tissue Regeneration and Organ Fibrosis. *Cells* 2021; 10: 1587.
180. Bartis D, Mise N, Mahida RY, et al. Epithelial–mesenchymal transition in lung development and disease: does it exist and is it important? *Thorax* 2014; 69: 760–765.
181. Kalluri R, Neilson EG. Epithelial-mesenchymal transition and its implications for fibrosis. *Journal of Clinical Investigation* 2003; 112: 1776–1784.
182. Koike Y, Yozaki M, Utani A, et al. Fibroblast growth factor 2 accelerates the epithelial–mesenchymal transition in keratinocytes during wound healing process. *Sci Rep* 2020; 10: 18545.
183. Stone RC, Pastar I, Ojeh N, et al. Epithelial-mesenchymal transition in tissue repair and fibrosis. *Cell Tissue Res* 2016; 365: 495–506.
184. Yang J, Antin P, Berx G, et al. Guidelines and definitions for research on epithelial–mesenchymal transition. *Nat Rev Mol Cell Biol* 2020; 21: 341–352.
185. Wickenden JA, Clarke MCH, Rossi AG, et al. Cigarette Smoke Prevents Apoptosis through Inhibition of Caspase Activation and Induces Necrosis. *Am J Respir Cell Mol Biol* 2003; 29: 562–570.
186. Kosmider B, Messier EM, Chu HW, et al. Human Alveolar Epithelial Cell Injury Induced by Cigarette Smoke. *PLoS One* 2011; 6: e26059.
187. Bhat TA, Panzica L, Kalathil SG, et al. Immune Dysfunction in Patients with Chronic Obstructive Pulmonary Disease. *Ann Am Thorac Soc* 2015; 12: S169–S175.
188. Puchelle E, Zahm J-M, Tournier J-M, et al. Airway Epithelial Repair, Regeneration, and Remodeling after Injury in Chronic Obstructive Pulmonary Disease. *Proc Am Thorac Soc* 2006; 3: 726–733.

189. Rehman A ur, Shah S, Abbas G, et al. Assessment of risk factors responsible for rapid deterioration of lung function over a period of one year in patients with chronic obstructive pulmonary disease. *Sci Rep* 2021; 11: 13578.

190. Whittaker HR, Pimenta JM, Jarvis D, et al. Characteristics Associated with Accelerated Lung Function Decline in a Primary Care Population with Chronic Obstructive Pulmonary Disease</p>. *Int J Chron Obstruct Pulmon Dis* 2020; Volume 15: 3079–3091.

191. Sohal SS, Reid D, Soltani A, et al. Reticular basement membrane fragmentation and potential epithelial mesenchymal transition is exaggerated in the airways of smokers with chronic obstructive pulmonary disease. *Respirology* 2010; 15: 930–938.

192. Milara J, Peiró T, Serrano A, et al. Epithelial to mesenchymal transition is increased in patients with COPD and induced by cigarette smoke. *Thorax* 2013; 68: 410–420.

193. Zou W, Zou Y, Zhao Z, et al. Nicotine-induced epithelial-mesenchymal transition via Wnt/β-catenin signaling in human airway epithelial cells. *American Journal of Physiology-Lung Cellular and Molecular Physiology* 2013; 304: L199–L209.

194. Doerner AM, Zuraw BL. TGF-β1 induced epithelial to mesenchymal transition (EMT) in human bronchial epithelial cells is enhanced by IL-1β but not abrogated by corticosteroids. *Respir Res* 2009; 10: 100.

195. Kamitani S, Yamauchi Y, Kawasaki S, et al. Simultaneous Stimulation with TGF-β1 and TNF-α Induces Epithelial Mesenchymal Transition in Bronchial Epithelial Cells. *Int Arch Allergy Immunol* 2011; 155: 119–128.

196. Atkinson JJ, Senior RM. Matrix Metalloproteinase-9 in Lung Remodeling. *Am J Respir Cell Mol Biol* 2003; 28: 12–24.

197. Liu ZZ (Ginny), Taiyab A, West-Mays JA. MMP9 Differentially Regulates Proteins Involved in Actin Polymerization and Cell Migration during TGF-β-Induced EMT in the Lens. *Int J Mol Sci* 2021; 22: 11988.

198. Chilosi M, Poletti V, Zamò A, et al. Aberrant Wnt/β-Catenin Pathway Activation in Idiopathic Pulmonary Fibrosis. *Am J Pathol* 2003; 162: 1495–1502.

199. Barbas-Filho J v. Evidence of type II pneumocyte apoptosis in the pathogenesis of idiopathic pulmonary fibrosis (IFP)/usual interstitial pneumonia (UIP). *J Clin Pathol* 2001; 54: 132–138.

200. Kasper M HG. Alterations in the alveolar epithelium after injury leading to pulmonary fibrosis. . *Histol Histopathol* 1996; 11: 463–83.

201. Uhal BD, Joshi I, Hughes WF, et al. Alveolar epithelial cell death adjacent to underlying myofibroblasts in advanced fibrotic human lung. *American Journal of Physiology-Lung Cellular and Molecular Physiology* 1998; 275: L1192–L1199.

202. Thannickal VJ. Evolving Concepts of Apoptosis in Idiopathic Pulmonary Fibrosis. *Proc Am Thorac Soc* 2006; 3: 350–356.
203. Königshoff M, Eickelberg O. WNT Signaling in Lung Disease. *Am J Respir Cell Mol Biol* 2010; 42: 21–31.
204. Bestall JC, PEA, GR, GR, JPW, WJA. Usefulness of the Medical Research Council (MRC) dyspnoea scale as a measure of disability in patients with chronic obstructive pulmonary disease. *Thorax* 1999; 54: 581–586.
205. Mahler DA, Wells CK. Evaluation of Clinical Methods for Rating Dyspnea. *Chest* 1988; 93: 580–586.
206. Sunjaya A, Poulos L, Reddel H, et al. Qualitative validation of the modified Medical Research Council (mMRC) dyspnoea scale as a patient-reported measure of breathlessness severity. *Respir Med* 2022; 203: 106984.
207. Bjelland I, Dahl AA, Haug TT, et al. The validity of the Hospital Anxiety and Depression Scale. *J Psychosom Res* 2002; 52: 69–77.
208. Wu Y, Levis B, Sun Y, et al. Accuracy of the Hospital Anxiety and Depression Scale Depression subscale (HADS-D) to screen for major depression: systematic review and individual participant data meta-analysis. *BMJ* 2021; n972.
209. Herrmann C. International experiences with the Hospital Anxiety and Depression Scale-A review of validation data and clinical results. *J Psychosom Res* 1997; 42: 17–41.
210. Brazier JE, Harper R, Jones NM, et al. Validating the SF-36 health survey questionnaire: new outcome measure for primary care. *BMJ* 1992; 305: 160–164.
211. Zhang Y, QU B, Lun S, et al. The 36-Item Short Form Health Survey: Reliability and Validity in Chinese Medical Students. *Int J Med Sci* 2012; 9: 521–526.
212. Kwan Y, Yong S, Fong W, et al. Reliability and Validity of the Short-Form 36 (SF-36) Health Survey in Patients with Spondyloarthritis. *Value in Health* 2016; 19: A854.
213. Lins L, Carvalho FM. SF-36 total score as a single measure of health-related quality of life: Scoping review. *SAGE Open Med* 2016; 4: 205031211667172.
214. Laucis NC, Hays RD, Bhattacharyya T. Scoring the SF-36 in Orthopaedics: A Brief Guide. *Journal of Bone and Joint Surgery* 2015; 97: 1628–1634.
215. RAND Corporation. 36-Item Short Form Survey (SF-36) Scoring Instructions. [Online] Available from: https://www.rand.org/health-care/surveys_tools/mos/36-item-short-form/scoring.html
216. Taft C, Karlsson J, Sullivan M. Do SF-36 summary component scores accurately summarize subscale scores? *Quality of Life Research* 2001; 10: 395–404.
217. Farivar SS, Cunningham WE, Hays RD. Correlated physical and mental health summary scores for the SF-36 and SF-12 Health Survey, V.1. *Health Qual Life Outcomes* 2007; 5: 54.

218. Hays RD, Morales LS. The RAND-36 measure of health-related quality of life. *Ann Med* 2001; 33: 350–357.
219. Nortvedt MW, Riise T, Myhr K-M, et al. Performance of the SF-36, SF-12, and RAND-36 Summary Scales in a Multiple Sclerosis Population. *Med Care* 2000; 38: 1022–1028.
220. Rawal G, Yadav S, Kumar R. Post-intensive care syndrome: An overview. *J Transl Int Med* 2017; 5: 90–92.
221. Rousseau A-F, Prescott HC, Brett SJ, et al. Long-term outcomes after critical illness: recent insights. *Crit Care* 2021; 25: 108.
222. Braun V, Clarke V. Using thematic analysis in psychology. *Qual Res Psychol* 2006; 2: 77-101.
223. Terry G, Hayfield N, Clarke V, et al. *Thematic analysis*. London: SAGE Publications.
224. Stockley JA, Ismail AM, Hughes SM, et al. Maximal mid-expiratory flow detects early lung disease in α_1-antitrypsin deficiency. *European Respiratory Journal* 2017; 49: 1602055.
225. Leuallen E, Fowler W. Maximal midexpiratory flow. *American Review of Tuberculosis and Pulmonary Diseases* 1955; 72: 783–800.
226. Oostveen E, MacLeod D, Lorino H, et al. The forced oscillation technique in clinical practice: methodology, recommendations and future developments. *European Respiratory Journal* 2003; 22: 1026–1041.
227. McNulty W, Usmani OS. Techniques of assessing small airways dysfunction. *Eur Clin Respir J* 2014; 1: 25898.
228. King GG, Bates J, Berger KI, et al. Technical standards for respiratory oscillometry. *European Respiratory Journal* 2020; 55: 1900753.
229. Gong S-G, Yang W-L, Zheng W, et al. Evaluation of respiratory impedance in patients with chronic obstructive pulmonary disease by an impulse oscillation system. *Mol Med Rep* 2014; 10: 2694–2700.
230. Frantz S, Nihlén U, Dencker M, et al. Impulse oscillometry may be of value in detecting early manifestations of COPD. *Respir Med* 2012; 106: 1116–1123.
231. Crim C, Celli B, Edwards LD, et al. Respiratory system impedance with impulse oscillometry in healthy and COPD subjects: ECLIPSE baseline results. *Respir Med* 2011; 105: 1069–1078.
232. Put W, Baars J, van der Grinten CPM. Comparing 3 forced oscillation devices in different subject groups. In: *9.1 Respiratory Function Technologists/Scientists*. European Respiratory Society, 2016, p. PA3613.
233. Soares M, Richardson M, Thorpe J, et al. Comparison of Forced and Impulse Oscillometry Measurements: A Clinical Population and Printed Airway Model Study. *Sci Rep* 2019; 9: 2130.
234. Srinivasan B, Kolli AR, Esch MB, et al. TEER Measurement Techniques for In Vitro Barrier Model Systems. *SLAS Technol* 2015; 20: 107–126.

235. Zucco F, Batto A-F, Bises G, et al. An Inter-laboratory Study to Evaluate the Effects of Medium Composition on the Differentiation and Barrier Function of Caco-2 Cell Lines. *Alternatives to Laboratory Animals* 2005; 33: 603–618.
236. Beer–Lambert law. In: *Essential Equations for Anaesthesia*. Cambridge University Press, 2014, pp. 43–44.
237. Thermo Fisher Scientific Inc. NanoDrop 1000 Spectrophotometer V3.8 User's Manual. 2010; 15. Available from: www.thermofisher.com
238. Schroeder A, Mueller O, Stocker S, et al. The RIN: an RNA integrity number for assigning integrity values to RNA measurements. *BMC Mol Biol* 2006; 7: 3.
239. Thermo Fisher Scientific Inc. Is Your RNA Intact? Methods to Check RNA Integrity. Available from: www.thermofisher.com
240. Clancy S. RNA Functions. *Nature Education* 2008; 1: 102.
241. Zhao S, Zhang Y, Gamini R, et al. Evaluation of two main RNA-seq approaches for gene quantification in clinical RNA sequencing: polyA+ selection versus rRNA depletion. *Sci Rep* 2018; 8: 4781.
242. Illumina. Understanding Illumina Quality Scores. Available from: https://emea.illumina.com/
243. Voll-Aanerud M, Eagan TM, Plana E, et al. Respiratory symptoms in adults are related to impaired quality of life, regardless of asthma and COPD: results from the European community respiratory health survey. *Health Qual Life Outcomes* 2010; 8: 107.
244. Masror-Roudsary D, Fadaee Aghdam N, Rafii F, et al. The Relationship between Experienced Respiratory Symptoms and Health-Related Quality of Life in the Elderly with Chronic Obstructive Pulmonary Disease. *Crit Care Res Pract* 2021; 2021: 1–7.
245. von Leupoldt A, Dahme B. Psychological aspects in the perception of dyspnea in obstructive pulmonary diseases. *Respir Med* 2007; 101: 411–422.
246. Leander M, Lampa E, Rask-Andersen A, et al. Impact of anxiety and depression on respiratory symptoms. *Respir Med* 2014; 108: 1594–1600.
247. Shah AS, Wong AW, Hague CJ, et al. A prospective study of 12-week respiratory outcomes in COVID-19-related hospitalisations. *Thorax* 2021; 76: 402–404.
248. Sigfrid L, Drake TM, Pauley E, et al. Long Covid in adults discharged from UK hospitals after Covid-19: A prospective, multicentre cohort study using the ISARIC WHO Clinical Characterisation Protocol. *The Lancet Regional Health - Europe* 2021; 8: 100186.
249. Drake TM, Riad AM, Fairfield CJ, et al. Characterisation of in-hospital complications associated with COVID-19 using the ISARIC WHO Clinical Characterisation Protocol UK: a prospective, multicentre cohort study. *The Lancet* 2021; 398: 223–237.

250. Groff D, Sun A, Ssentongo AE, et al. Short-term and Long-term Rates of Postacute Sequelae of SARS-CoV-2 Infection. *JAMA Netw Open* 2021; 4: e2128568.
251. Thompson EJ, Stafford J, Moltrecht B, et al. Psychological distress, depression, anxiety, and life satisfaction following COVID-19 infection: evidence from 11 UK longitudinal population studies. *Lancet Psychiatry* 2022; 9: 894–906.
252. Shah R, Ali FM, Nixon SJ, et al. Measuring the impact of COVID-19 on the quality of life of the survivors, partners and family members: a cross-sectional international online survey. *BMJ Open* 2021; 11: e047680.
253. Tarazona V, Kirouchena D, Clerc P, et al. Quality of Life in COVID-19 Outpatients: A Long-Term Follow-Up Study. *J Clin Med* 2022; 11: 6478.
254. Muñoz-Corona C, Gutiérrez-Canales LG, Ortiz-Ledesma C, et al. Quality of life and persistence of COVID-19 symptoms 90 days after hospital discharge. *Journal of International Medical Research* 2022; 50: 030006052211104.
255. Taquet M, Sillett R, Zhu L, et al. Neurological and psychiatric risk trajectories after SARS-CoV-2 infection: an analysis of 2-year retrospective cohort studies including 1 284 437 patients. *Lancet Psychiatry* 2022; 9: 815–827.
256. Tejerina F, Catalan P, Rodriguez-Grande C, et al. Post-COVID-19 syndrome. SARS-CoV-2 RNA detection in plasma, stool, and urine in patients with persistent symptoms after COVID-19. *BMC Infect Dis* 2022; 22: 211.
257. Mandal S, Barnett J, Brill SE, et al. 'Long-COVID': a cross-sectional study of persisting symptoms, biomarker and imaging abnormalities following hospitalisation for COVID-19. *Thorax* 2021;**76:**396-398.
258. Duan E, Garry K, Horwitz LI, et al. "I Am Not the Same as I Was Before": A Qualitative Analysis of COVID-19 Survivors. *Int J Behav Med*. 2022.
259. Almgren J, Löfström E, Malmborg JS, et al. Patients' Health Experiences of Post COVID-19 Condition—A Qualitative Study. *Int J Environ Res Public Health* 2022; 19: 13980.
260. Ladds E, Rushforth A, Wieringa S, et al. Persistent symptoms after Covid-19: qualitative study of 114 "long Covid" patients and draft quality principles for services. *BMC Health Serv Res* 2020; 20: 1144.
261. Michael SR. Integrating Chronic Illness into One's Life. *Journal of Holistic Nursing* 1996; 14: 251–267.
262. Ross Rothweiler B, Ross K. Fifty Years Later: Reflections on the Work of Elisabeth Kübler-Ross M.D. *The American Journal of Bioethics* 2019; 19: 3–4.
263. Bregman L. Kübler-Ross and the Re-visioning of Death as Loss: Religious Appropriation and Responses. *Journal of Pastoral Care & Counseling: Advancing theory and professional practice through scholarly and reflective publications* 2019; 73: 4–8.

264. Dong L, Chen L, Ding S. Illness uncertainty among patients with COVID-19 in the Mobile Cabin Hospital. *Nurs Open* 2022; 9: 1456–1464.
265. Etkind SN, Bristowe K, Bailey K, et al. How does uncertainty shape patient experience in advanced illness? A secondary analysis of qualitative data. *Palliat Med* 2017; 31: 171–180.
266. Shahnawaz M, Nabi W, Nabi S, et al. Relationship between intolerance of uncertainty and symptom severity in Covid-19 patients: the mediating role of illness perception and Covid-19 fear. *Current Psychology*. 2022.
267. McCormick KM. A Concept Analysis of Uncertainty in Illness. *Journal of Nursing Scholarship* 2002; 34: 127–131.
268. Williams J, Koocher GP. Addressing loss of control in chronic illness: Theory and practice. *Psychotherapy: Theory, Research, Practice, Training* 1998; 35: 325–335.
269. Gobeil-Lavoie A-P, Chouinard M-C, Danish A, et al. Characteristics of self-management among patients with complex health needs: a thematic analysis review. *BMJ Open* 2019; 9: e028344.
270. Mishel MH. Reconceptualization of the Uncertainty in Illness Theory. *Image: the Journal of Nursing Scholarship* 1990; 22: 256–262.
271. Tecson KM, Wilkinson LR, Smith B, et al. Association between psychological resilience and subjective well-being in older adults living with chronic illness. *Baylor University Medical Center Proceedings* 2019; 32: 520–524.
272. Ghanei Gheshlagh R, Sayehmiri K, Ebadi A, et al. Resilience of Patients With Chronic Physical Diseases: A Systematic Review and Meta-Analysis. *Iran Red Crescent Med J*; 2016. 18(7):e38562
273. Morey A, Loades ME. Review: How has cognitive behaviour therapy been adapted for adolescents with comorbid depression and chronic illness? A scoping review. *Child Adolesc Ment Health* 2021; 26: 252–264.
274. Clark DA. Cognitive Restructuring. In: *The Wiley Handbook of Cognitive Behavioral Therapy*. Chichester, UK: John Wiley & Sons, Ltd, 2013, pp. 1–22.
275. Bandura A. *Self-efficacy: The exercise of control*. New York: W. H. Freeman, 1997.
276. Bandura A. Self-efficacy: Toward a unifying theory of behavioral change. *Psychol Rev* 1977; 84: 191–215.
277. Hiroto DS, Seligman ME. Generality of learned helplessness in man. *J Pers Soc Psychol* 1975; 31: 311–327.
278. Seligman MEP. Learned Helplessness. *Annu Rev Med* 1972; 23: 407–412.
279. Calman KC. Quality of life in cancer patients--an hypothesis. *J Med Ethics* 1984; 10: 124–127.
280. Maslow AH. A theory of human motivation. *Psychol Rev* 1943; 50: 370–396.

281. Copley SJ, Coren M, Nicholson AG, et al. Diagnostic Accuracy of Thin-Section CT and Chest Radiography of Pediatric Interstitial Lung Disease. *American Journal of Roentgenology* 2000; 174: 549–554.
282. Walsh SLF, Devaraj A, Enghelmayer JI, et al. Role of imaging in progressive-fibrosing interstitial lung diseases. *European Respiratory Review* 2018; 27: 180073.
283. D'Cruz RF, Waller MD, Perrin F, et al. Chest radiography is a poor predictor of respiratory symptoms and functional impairment in survivors of severe COVID-19 pneumonia. *ERJ Open Res* 2021; 7: 00655–02020.
284. Myall KJ, Mukherjee B, Castanheira AM, et al. Persistent Post-COVID-19 Inflammatory Interstitial Lung Disease: An Observational Study of Corticosteroid Treatment. *Ann Am Thorac Soc* 2021; 18: 799–806.
285. Vijayakumar B, Shah PL. Not All Parenchymal Changes on Computed Tomography Are Interstitial Lung Disease. *Ann Am Thorac Soc* 2021; 18: 1597–1597.
286. Ngai JC, Ko FW, Ng SS, et al. The long-term impact of severe acute respiratory syndrome on pulmonary function, exercise capacity and health status. *Respirology* 2010; 15: 543–550.
287. Fraser E. Long term respiratory complications of covid-19. *BMJ* 2020; m3001.
288. Burn E, Duarte-Salles T, Fernandez-Bertolin S, et al. Venous or arterial thrombosis and deaths among COVID-19 cases: a European network cohort study. *Lancet Infect Dis* 2022; 22: 1142–1152.
289. Solomon JJ, Heyman B, Ko JP, et al. CT of Post-Acute Lung Complications of COVID-19. *Radiology* 2021; 301: E383–E395.
290. Frija-Masson J, Debray M-P, Boussouar S, et al. Residual ground glass opacities three months after Covid-19 pneumonia correlate to alteration of respiratory function: The post Covid M3 study. *Respir Med* 2021; 184: 106435.
291. Guler SA, Ebner L, Beigelman C, et al. Pulmonary function and radiological features four months after COVID-19: first results from the national prospective observational Swiss COVID-19 lung study. *European Respiratory Journal* 2021; 57: 2003690.
292. Huang C, Huang L, Wang Y, et al. 6-month consequences of COVID-19 in patients discharged from hospital: a cohort study. *The Lancet* 2021; 397: 220–232.
293. Han X, Fan Y, Alwalid O, et al. Six-month Follow-up Chest CT Findings after Severe COVID-19 Pneumonia. *Radiology* 2021; 299: E177–E186.
294. Copin M-C, Parmentier E, Duburcq T, et al. Time to consider histologic pattern of lung injury to treat critically ill patients with COVID-19 infection. *Intensive Care Med* 2020; 46: 1124–1126.
295. Cordier J-F. Rare diseases bullet 8: Organising pneumonia. *Thorax* 2000; 55: 318–328.
296. Vijayakumar B, Tonkin J, Devaraj A, et al. CT Lung Abnormalities after COVID-19 at 3 Months and 1 Year after Hospital Discharge. *Radiology* 2021; 303: 444–454.

297. Ravaglia C, Doglioni C, Chilosi M, et al. Clinical, radiological and pathological findings in patients with persistent lung disease following SARS-CoV-2 infection. *European Respiratory Journal* 2022; 60: 2102411.

298. Recalde-Zamacona B, García-Tobar L, Argueta A, et al. Histopathological findings in fatal COVID-19 severe acute respiratory syndrome: preliminary experience from a series of 10 Spanish patients. *Thorax* 2020; 75: 1116–1118.

299. Cottin V, Cordier J-F. Cryptogenic Organizing Pneumonia. *Semin Respir Crit Care Med* 2012; 33: 462–475.

300. Taniguchi Y, Sugimoto C, Arai T, et al. Recurrence predictive factors of cryptogenic organizing pneumonia. In: *1.5 Diffuse Parenchymal Lung Disease*. European Respiratory Society, 2015, p. PA3804.

301. McGroder CF, Zhang D, Choudhury MA, et al. Pulmonary fibrosis 4 months after COVID-19 is associated with severity of illness and blood leucocyte telomere length. *Thorax* 2021; 76: 1242–1245.

302. Pan F, Yang L, Liang B, et al. Chest CT Patterns from Diagnosis to 1 Year of Follow-up in Patients with COVID-19. *Radiology* 2022; 302: 709–719.

303. Lerum TV, Aaløkken TM, Brønstad E, et al. Dyspnoea, lung function and CT findings three months after hospital admission for COVID-19. *European Respiratory Journal* 2020; 57: 2003448.

304. Zweiman B, Atkins PC, Bedard P-M, et al. Corticosteroid effects on circulating lymphocyte subset levels in normal humans. *J Clin Immunol* 1984; 4: 151–155.

305. van Gassel RJJ, Bels JLM, Raafs A, et al. High Prevalence of Pulmonary Sequelae at 3 Months after Hospital Discharge in Mechanically Ventilated Survivors of COVID-19. *Am J Respir Crit Care Med* 2021; 203: 371–374.

306. Montgomery A, Stager M, Carrico C, et al. Causes of mortality in patients with the adult respiratory distress syndrome. *Am Rev Respir Dis* 1985; 132: 485–489.

307. Han MK, Murray S, Fell CD, et al. Sex differences in physiological progression of idiopathic pulmonary fibrosis. *European Respiratory Journal* 2008; 31: 1183–1188.

308. Sesé L, Nunes H, Cottin V, et al. Gender Differences in Idiopathic Pulmonary Fibrosis: Are Men and Women Equal? *Front Med (Lausanne)*; 8.713698

309. Zaman T, Lee JS. Risk Factors for the Development of Idiopathic Pulmonary Fibrosis: a Review. *Curr Pulmonol Rep* 2018; 7: 118–125.

310. Tang Y-W, Johnson JE, Browning PJ, et al. Herpesvirus DNA Is Consistently Detected in Lungs of Patients with Idiopathic Pulmonary Fibrosis. *J Clin Microbiol* 2003; 41: 2633–2640.

311. George PM, Reed A, Desai SR, et al. A persistent neutrophil-associated immune signature characterizes post–COVID-19 pulmonary sequelae. *Sci Transl Med*; 14 (671)

312. Meyer KC. Diagnosis and management of interstitial lung disease. *Transl Respir Med* 2014; 2: 4.

313. Arnold D, Hamilton F, Milne A, et al. Patient outcomes after hospitalisation with COVID-19 and implications for follow-up: results from a prospective UK cohort. Thorax. 2021 76(4):399-401.
314. Axelsson GT, Halldorsson AB, Jonsson HM, et al. Respiratory function and CT abnormalities among survivors of COVID-19 pneumonia: a nationwide follow-up study. *BMJ Open Respir Res* 2022; 9: e001347.
315. Liu D, Zhang W, Pan F, et al. The pulmonary sequalae in discharged patients with COVID-19: a short-term observational study. *Respir Res* 2020; 21: 125.
316. Eberst G, Claudé F, Laurent L, et al. Result of one-year, prospective follow-up of intensive care unit survivors after SARS-CoV-2 pneumonia. *Ann Intensive Care* 2022; 12: 23.
317. Wu X, Liu X, Zhou Y, et al. 3-month, 6-month, 9-month, and 12-month respiratory outcomes in patients following COVID-19-related hospitalisation: a prospective study. *Lancet Respir Med* 2021; 9: 747–754.
318. Hui DS, Wong KT, Ko FW, et al. The 1-Year Impact of Severe Acute Respiratory Syndrome on Pulmonary Function, Exercise Capacity, and Quality of Life in a Cohort of Survivors. *Chest* 2005; 128: 2247–2261.
319. Graham BL, Steenbruggen I, Miller MR, et al. Standardization of Spirometry 2019 Update. An Official American Thoracic Society and European Respiratory Society Technical Statement. *Am J Respir Crit Care Med* 2019; 200: e70–e88.
320. Stanojevic S, Kaminsky DA, Miller MR, et al. ERS/ATS technical standard on interpretive strategies for routine lung function tests. *European Respiratory Journal* 2022; 60: 2101499.
321. Khatri SB, Iaccarino JM, Barochia A, et al. Use of Fractional Exhaled Nitric Oxide to Guide the Treatment of Asthma: An Official American Thoracic Society Clinical Practice Guideline. *Am J Respir Crit Care Med* 2021; 204: e97–e109.
322. Chung KF. Increasing utility of FeNO as a biomarker of type-2 inflammation in severe asthma. *Lancet Respir Med* 2021; 9: 1083–1084.
323. Gao J, Wu F. Association between fractional exhaled nitric oxide, sputum induction and peripheral blood eosinophil in uncontrolled asthma. *Allergy, Asthma & Clinical Immunology* 2018; 14: 21.
324. Schlemmer F, Valentin S, Boyer L, et al. Respiratory recovery trajectories after severe-to-critical COVID-19: a 1-year prospective multicentre study. *European Respiratory Journal* 2023; 2201532.
325. Zhang H, Li X, Huang L, et al. Lung-function trajectories in COVID-19 survivors after discharge: A two-year longitudinal cohort study. *EClinicalMedicine* 2022; 54: 101668.
326. George PM, Barratt SL, Condliffe R, et al. Respiratory follow-up of patients with COVID-19 pneumonia. *Thorax* 2020; 75: 1009–1016.
327. Fuschillo S, Ambrosino P, Motta A, et al. COVID-19 and diffusing capacity of the lungs for carbon monoxide: a clinical biomarker in postacute care settings. *Biomark Med* 2021; 15: 537–539.

328. Zhi H, Ji X, Zhao Z, et al. Risk factors for impaired pulmonary diffusion function in convalescent COVID-19 patients: A systematic review and meta-analysis. *EClinicalMedicine* 2022; 49: 101473.
329. Maniscalco M, Ambrosino P, Poto R, et al. Can FeNO be a biomarker in the post-COVID-19 patients monitoring? *Respir Med* 2022; 193: 106745.
330. Cameli P, Bargagli E, Bergantini L, et al. Alveolar Nitric Oxide as a Biomarker of COVID-19 Lung Sequelae: A Pivotal Study. *Antioxidants* 2021; 10: 1350.
331. Lindahl A, Reijula J, Malmberg LP, et al. Small airway function in Finnish COVID-19 survivors. *Respir Res* 2021; 22: 237.
332. Gao J, Chen Z, Jie X, et al. Both fractional exhaled nitric oxide and sputum eosinophil were associated with uncontrolled asthma. *J Asthma Allergy* 2018; Volume 11: 73–79.
333. Gao J, Zhang M, Zhou L, et al. Correlation between fractional exhaled nitric oxide and sputum eosinophilia in exacerbations of COPD. *Int J Chron Obstruct Pulmon Dis* 2017; Volume 12: 1287–1293.
334. Meyer KC, Raghu G, Baughman RP, et al. An Official American Thoracic Society Clinical Practice Guideline: The Clinical Utility of Bronchoalveolar Lavage Cellular Analysis in Interstitial Lung Disease. *Am J Respir Crit Care Med* 2012; 185: 1004–1014.
335. Escamilla-Gil JM, Fernandez-Nieto M, Acevedo N. Understanding the Cellular Sources of the Fractional Exhaled Nitric Oxide (FeNO) and Its Role as a Biomarker of Type 2 Inflammation in Asthma. *Biomed Res Int* 2022; 2022: 1–9.
336. van den Berg MP, Meurs H, Gosens R. Targeting arginase and nitric oxide metabolism in chronic airway diseases and their co-morbidities. *Curr Opin Pharmacol* 2018; 40: 126–133.
337. de Gouw H, Grunberg K, Schot R, et al. Relationship between exhaled nitric oxide and airway hyperresponsiveness following experimental rhinovirus infection in asthmatic subjects. *European Respiratory Journal* 1998; 11: 126–132.
338. Gadish T, Soferman R, Merimovitch T, et al. Exhaled Nitric Oxide in Acute Respiratory Syncytial Virus Bronchiolitis. *Arch Pediatr Adolesc Med*; 2010. 164(8):727-31.
339. Mgbemena V, Segovia J, Chang T-H, et al. KLF6 and iNOS regulates apoptosis during respiratory syncytial virus infection. *Cell Immunol* 2013; 283: 1–7.
340. Karki R, Sharma BR, Tuladhar S, et al. Synergism of TNF-α and IFN-γ Triggers Inflammatory Cell Death, Tissue Damage, and Mortality in SARS-CoV-2 Infection and Cytokine Shock Syndromes. *Cell* 2021; 184: 149-168.e17.
341. Vijayakumar B, Boustani K, Ogger PP, et al. Immuno-proteomic profiling reveals aberrant immune cell regulation in the airways of individuals with ongoing post-COVID-19 respiratory disease. *Immunity* 2022; 55: 542-556.e5.

342. Paraskakis E, Brindicci C, Fleming L, et al. Measurement of Bronchial and Alveolar Nitric Oxide Production in Normal Children and Children with Asthma. *Am J Respir Crit Care Med* 2006; 174: 260–267.

343. Tiev KP, Hua-Huy T, Kettaneh A, et al. Alveolar concentration of nitric oxide predicts pulmonary function deterioration in scleroderma. *Thorax* 2012; 67: 157–163.

344. Cameli P, Bargagli E, Bergantini L, et al. Extended Exhaled Nitric Oxide Analysis in Interstitial Lung Diseases: A Systematic Review. *Int J Mol Sci* 2020; 21: 6187.

345. Wagner EM, Liu MC, Weinmann GG, et al. Peripheral Lung Resistance in Normal and Asthmatic Subjects. *American Review of Respiratory Disease* 1990; 141: 584–588.

346. Burgel P-R, de Blic J, Chanez P, et al. Update on the roles of distal airways in asthma. *European Respiratory Review* 2009; 18: 80–95.

347. Jartti T, Bønnelykke K, Elenius V, et al. Role of viruses in asthma. *Semin Immunopathol* 2020; 42: 61–74.

348. Seemungal T, Harper-Owen R, Bhowmik A, et al. Respiratory Viruses, Symptoms, and Inflammatory Markers in Acute Exacerbations and Stable Chronic Obstructive Pulmonary Disease. *Am J Respir Crit Care Med* 2001; 164: 1618–1623.

349. Singanayagam A, Joshi P v, Mallia P, et al. Viruses exacerbating chronic pulmonary disease: the role of immune modulation. *BMC Med* 2012; 10: 27.

350. Macklem PT, Proctor DF, Hogg JC. The stability of peripheral airways. *Respir Physiol* 1970; 8: 191–203.

351. Schousboe P, Wiese L, Heiring C, et al. Assessment of pulmonary surfactant in COVID-19 patients. *Crit Care* 2020; 24: 552.

352. Dandurand RJ, Lavoie J-P, Lands LC, et al. Comparison of oscillometry devices using active mechanical test loads. *ERJ Open Res* 2019; 5: 00160–02019.

353. Lundblad LKA, Siddiqui S, Bossé Y, et al. Applications of oscillometry in clinical research and practice. *Canadian Journal of Respiratory, Critical Care, and Sleep Medicine* 2021; 5: 54–68.

354. Lipworth BJ, Jabbal S. What can we learn about COPD from impulse oscillometry? *Respir Med* 2018; 139: 106–109.

355. Bonifazi M, Sverzellati N, Negri E, et al. Increased prevalence of small airways dysfunction in patients with systemic sclerosis as determined by impulse oscillometry. *Rheumatology*. 2020. 1;59(3):641-649

356. Imeri G, Ribolla F, Berti A, et al. Increase of FeNO after acute bronchodilation test in asthmatic patients: a clue for small airways disease? In: *Monitoring airway disease*. European Respiratory Society, 2019, p. PA352.

357. Schneider A, Brunn B, Hapfelmeier A, et al. Diagnostic accuracy of FeNO in asthma and predictive value for inhaled corticosteroid responsiveness: A prospective, multicentre study. *EClinicalMedicine* 2022; 50: 101533.

358. Eltayara L, Becklake MR, Volta CA, et al. Relationship between chronic dyspnea and expiratory flow limitation in patients with chronic obstructive pulmonary disease. *Am J Respir Crit Care Med* 1996; 154: 1726–1734.

359. Aarli BB, Calverley PMA, Jensen RL, et al. Variability of within-breath reactance in COPD patients and its association with dyspnoea. *European Respiratory Journal* 2015; 45: 625–634.

360. Eltayara L, Ghezzo H, Milic-Emili J. Orthopnea and Tidal Expiratory Flow Limitation in Patients With Stable COPD. *Chest* 2001; 119: 99–104.

361. Tantucci C, Duguet A, Similowski T, et al. Effect of salbutamol on dynamic hyperinflation in chronic obstructive pulmonary disease patients. *European Respiratory Journal* 1998; 12: 799–804.

362. Dellacà RL, Santus P, Aliverti A, et al. Detection of expiratory flow limitation in COPD using the forced oscillation technique. *European Respiratory Journal* 2004; 23: 232–240.

363. Dean J, Kolsum U, Hitchen P, et al. Clinical characteristics of COPD patients with tidal expiratory flow limitation. *Int J Chron Obstruct Pulmon Dis* 2017; Volume 12: 1503–1506.

364. Tantucci C, Ellaffi M, Duguet A, et al. Dynamic hyperinflation and flow limitation during methacholine-induced bronchoconstriction in asthma. *European Respiratory Journal* 1999; 14: 477–478.

365. Boczkowski J, Murciano D, Pichot M-H, et al. Expiratory Flow Limitation in Stable Asthmatic Patients During Resting Breathing. *Am J Respir Crit Care Med* 1997; 156: 752–757.

366. Dellaca RL, Pompilio PP, Walker PP, et al. Effect of bronchodilation on expiratory flow limitation and resting lung mechanics in COPD. *European Respiratory Journal* 2009; 33: 1329–1337.

367. Marshall JS, Warrington R, Watson W, et al. An introduction to immunology and immunopathology. *Allergy, Asthma & Clinical Immunology* 2018; 14: 49.

368. Diamond MS, Kanneganti T-D. Innate immunity: the first line of defense against SARS-CoV-2. *Nat Immunol* 2022; 23: 165–176.

369. Kanneganti T. Intracellular innate immune receptors: Life inside the cell. *Immunol Rev* 2020; 297: 5–12.

370. Epelman S, Lavine KJ, Randolph GJ. Origin and Functions of Tissue Macrophages. *Immunity* 2014; 41: 21–35.

371. Mills CD, Kincaid K, Alt JM, et al. M-1/M-2 Macrophages and the Th1/Th2 Paradigm. *The Journal of Immunology* 2000; 164: 6166–6173.

372. Gordon S, Martinez FO. Alternative Activation of Macrophages: Mechanism and Functions. *Immunity* 2010; 32: 593–604.

373. Chen Y, Zhang X. Pivotal regulators of tissue homeostasis and cancer: macrophages. *Exp Hematol Oncol* 2017; 6: 23.
374. Novak ML, Koh TJ. Macrophage phenotypes during tissue repair. *J Leukoc Biol* 2013; 93: 875–881.
375. Trombetta AC, Soldano S, Contini P, et al. A circulating cell population showing both M1 and M2 monocyte/macrophage surface markers characterizes systemic sclerosis patients with lung involvement. *Respir Res* 2018; 19: 186.
376. Kapellos TS, Bonaguro L, Gemünd I, et al. Human Monocyte Subsets and Phenotypes in Major Chronic Inflammatory Diseases. *Front Immunol*; 2019.10:2035
377. Liu Z, Gu Y, Chakarov S, et al. Fate Mapping via Ms4a3-Expression History Traces Monocyte-Derived Cells. *Cell* 2019; 178: 1509-1525.e19.
378. Serbina N V., Jia T, Hohl TM, et al. Monocyte-Mediated Defense Against Microbial Pathogens. *Annu Rev Immunol* 2008; 26: 421–452.
379. Ogawa T, Shichino S, Ueha S, et al. Macrophages in lung fibrosis. *Int Immunol* 2021; 33: 665–671.
380. Scott MKD, Quinn K, Li Q, et al. Increased monocyte count as a cellular biomarker for poor outcomes in fibrotic diseases: a retrospective, multicentre cohort study. *Lancet Respir Med* 2019; 7: 497–508.
381. Effah CY, Drokow EK, Agboyibor C, et al. Neutrophil-Dependent Immunity During Pulmonary Infections and Inflammations. *Front Immunol*; 2021. 12:689866.
382. Mollinedo F. Neutrophil Degranulation, Plasticity, and Cancer Metastasis. *Trends Immunol* 2019; 40: 228–242.
383. Hammer Q, Rückert T, Romagnani C. Natural killer cell specificity for viral infections. *Nat Immunol* 2018; 19: 800–808.
384. Cong J, Wei H. Natural Killer Cells in the Lungs. *Front Immunol*; 2019. 10:1416
385. Abdul-Careem MF, Mian MF, Yue G, et al. Critical Role of Natural Killer Cells in Lung Immunopathology During Influenza Infection in Mice. *J Infect Dis* 2012; 206: 167–177.
386. Bonilla FA, Oettgen HC. Adaptive immunity. *Journal of Allergy and Clinical Immunology* 2010; 125: S33–S40.
387. Allie SR, Bradley JE, Mudunuru U, et al. The establishment of resident memory B cells in the lung requires local antigen encounter. *Nat Immunol* 2019; 20: 97–108.
388. Chiu C, Openshaw PJ. Antiviral B cell and T cell immunity in the lungs. *Nat Immunol* 2015; 16: 18–26.
389. Tupin E, Kinjo Y, Kronenberg M. The unique role of natural killer T cells in the response to microorganisms. *Nat Rev Microbiol* 2007; 5: 405–417.
390. Brigl M, Brenner MB. CD1: Antigen Presentation and T Cell Function. *Annu Rev Immunol* 2004; 22: 817–890.

391. Adan A, Alizada G, Kiraz Y, et al. Flow cytometry: basic principles and applications. *Crit Rev Biotechnol* 2017; 37: 163–176.
392. Saris A, Reijnders T, Nossent E, et al. Distinct cellular immune profiles in the airways and blood of critically ill patients with COVID-19. *Thorax* 2021; 76: 1010–1019.
393. Parra ER, Noleto GS, Tinoco LJM, et al. Immunophenotyping and remodeling process in small airways of idiopathic interstitial pneumonias: functional and prognostic significance. *Clin Respir J* 2008; 2: 227–238.
394. Heron M, Grutters JC, ten Dam-Molenkamp KM, et al. Bronchoalveolar lavage cell pattern from healthy human lung. *Clin Exp Immunol* 2012; 167: 523–531.
395. Voiriot G, Dorgham K, Bachelot G, et al. Identification of bronchoalveolar and blood immune-inflammatory biomarker signature associated with poor 28-day outcome in critically ill COVID-19 patients. *Sci Rep* 2022; 12: 9502.
396. Pandolfi L, Fossali T, Frangipane V, et al. Broncho-alveolar inflammation in COVID-19 patients: a correlation with clinical outcome. *BMC Pulm Med* 2020; 20: 301.
397. Jafarzadeh A, Jafarzadeh S, Nozari P, et al. Lymphopenia an important immunological abnormality in patients with COVID-19: Possible mechanisms. *Scand J Immunol*; 2021. 93(2):e12967
398. Tan L, Wang Q, Zhang D, et al. Lymphopenia predicts disease severity of COVID-19: a descriptive and predictive study. *Signal Transduct Target Ther* 2020; 5: 33.
399. McClain MT, Park LP, Nicholson B, et al. Longitudinal analysis of leukocyte differentials in peripheral blood of patients with acute respiratory viral infections. *Journal of Clinical Virology* 2013; 58: 689–695.
400. Azkur AK, Akdis M, Azkur D, et al. Immune response to SARS-CoV-2 and mechanisms of immunopathological changes in COVID-19. *Allergy* 2020; 75: 1564–1581.
401. Wichmann D, Sperhake J-P, Lütgehetmann M, et al. Autopsy Findings and Venous Thromboembolism in Patients With COVID-19. *Ann Intern Med* 2020; 173: 268–277.
402. Carsana L, Sonzogni A, Nasr A, et al. Pulmonary post-mortem findings in a series of COVID-19 cases from northern Italy: a two-centre descriptive study. *Lancet Infect Dis* 2020; 20: 1135–1140.
403. Steinberg KP, Milberg JA, Martin TR, et al. Evolution of bronchoalveolar cell populations in the adult respiratory distress syndrome. *Am J Respir Crit Care Med* 1994; 150: 113–122.
404. Grudzinska FS, Sapey E. Friend or foe? The dual role of neutrophils in lung injury and repair. *Thorax* 2018; 73: 305–307.
405. Hirasawa Y, Nakada T, Shimazui T, et al. Prognostic value of lymphocyte counts in bronchoalveolar lavage fluid in patients with acute respiratory failure: a retrospective cohort study. *J Intensive Care* 2021; 9: 21.

406. Bastard P, Rosen LB, Zhang Q, et al. Autoantibodies against type I IFNs in patients with life-threatening COVID-19. *Science (1979)*; 370. 2020. 23;370(6515):eabd4585
407. Zhang Q, Bastard P, Liu Z, et al. Inborn errors of type I IFN immunity in patients with life-threatening COVID-19. *Science (1979)*; 2020. 370(6515):eabd4570
408. Dickson RP, Erb-Downward JR, Freeman CM, et al. Bacterial Topography of the Healthy Human Lower Respiratory Tract. *mBio*; 2017. 8 (1)
409. Erb-Downward JR, Thompson DL, Han MK, et al. Analysis of the Lung Microbiome in the "Healthy" Smoker and in COPD. *PLoS One* 2011; 6: e16384.
410. Charlson ES, Bittinger K, Haas AR, et al. Topographical Continuity of Bacterial Populations in the Healthy Human Respiratory Tract. *Am J Respir Crit Care Med* 2011; 184: 957–963.
411. EWIG S, TORRES A, EL-EBIARY M, et al. Bacterial Colonization Patterns in Mechanically Ventilated Patients with Traumatic and Medical Head Injury. *Am J Respir Crit Care Med* 1999; 159: 188–198.
412. Palabiyikoglu I, Oral M, Tulunay M. Candida colonization in mechanically ventilated patients. *Journal of Hospital Infection* 2001; 47: 239–242.
413. Jaiswal A, Chakraborti A, Verma P, et al. A prospective study of fungal colonization and invasive fungal disease in long-term mechanically ventilated patients in a respiratory intensive care unit. *Indian Journal of Critical Care Medicine* 2018; 22: 597–601.
414. Tsitoura E, Mastrodimou S, Vasarmidi E, et al. Late Breaking Abstract - Characteristics of Post-COVID-19 interstitial lung syndrome in Bronchoalveolar Lavage: Preliminary results. In: *ILD / DPLD of known origin*. European Respiratory Society, 2021, p. PA2347.
415. Cheon IS, Li C, Son YM, et al. Immune signatures underlying post-acute COVID-19 lung sequelae. *Sci Immunol*; 2021. 12;6(65):eabk1741
416. Hsu PP, Sabatini DM. Cancer Cell Metabolism: Warburg and Beyond. *Cell* 2008; 134: 703–707.
417. Fujita J, Yamadori I, Suemitsu I, et al. Clinical features of non-specific interstitial pneumonia. *Respir Med* 1999; 93: 113–118.
418. Gupta GS. The Lactate and the Lactate Dehydrogenase in Inflammatory Diseases and Major Risk Factors in COVID-19 Patients. *Inflammation* 2022; 45: 2091–2123.
419. McComb S, Mulligan R, Sad S. Caspase-3 Is Transiently Activated without Cell Death during Early Antigen Driven Expansion of CD8+ T Cells In Vivo. *PLoS One* 2010; 5: e15328.
420. Porter AG, Jänicke RU. Emerging roles of caspase-3 in apoptosis. *Cell Death Differ* 1999; 6: 99–104.
421. Bradley LM, Douglass MF, Chatterjee D, et al. Matrix Metalloprotease 9 Mediates Neutrophil Migration into the Airways in Response to Influenza Virus-Induced Toll-Like Receptor Signaling. *PLoS Pathog* 2012; 8: e1002641.
422. Phillipson M, Kubes P. The Healing Power of Neutrophils. *Trends Immunol* 2019; 40: 635–647.

423. Mantovani A, Cassatella MA, Costantini C, et al. Neutrophils in the activation and regulation of innate and adaptive immunity. *Nat Rev Immunol* 2011; 11: 519–531.
424. Bekes EM, Schweighofer B, Kupriyanova TA, et al. Tumor-Recruited Neutrophils and Neutrophil TIMP-Free MMP-9 Regulate Coordinately the Levels of Tumor Angiogenesis and Efficiency of Malignant Cell Intravasation. *Am J Pathol* 2011; 179: 1455–1470.
425. Brinkmann V, Reichard U, Goosmann C, et al. Neutrophil Extracellular Traps Kill Bacteria. *Science (1979)* 2004; 303: 1532–1535.
426. Schönrich G, Raftery MJ. Neutrophil Extracellular Traps Go Viral. *Front Immunol*; 2016. 19;7:366
427. Zhu Y, Chen X, Liu X. NETosis and Neutrophil Extracellular Traps in COVID-19: Immunothrombosis and Beyond. *Front Immunol*; 2022. 13:838011.
428. Kinder BW, Brown KK, Schwarz MI, et al. Baseline BAL Neutrophilia Predicts Early Mortality in Idiopathic Pulmonary Fibrosis. *Chest* 2008; 133: 226–232.
429. Ginzberg HH, Cherapanov V, Dong Q, et al. Neutrophil-mediated epithelial injury during transmigration: role of elastase. *American Journal of Physiology-Gastrointestinal and Liver Physiology* 2001; 281: G705–G717.
430. Boxio R, Wartelle J, Nawrocki-Raby B, et al. Neutrophil elastase cleaves epithelial cadherin in acutely injured lung epithelium. *Respir Res* 2016; 17: 129.
431. Yang Y, Yang M, Yuan J, et al. Laboratory Diagnosis and Monitoring the Viral Shedding of SARS-CoV-2 Infection. *The Innovation* 2020; 1: 100061.
432. Zhang H, Ai J-W, Yang W, et al. Metatranscriptomic Characterization of Coronavirus Disease 2019 Identified a Host Transcriptional Classifier Associated With Immune Signaling. *Clinical Infectious Diseases* 2021; 73: 376–385.
433. Merenstein C, Liang G, Whiteside SA, et al. Signatures of COVID-19 Severity and Immune Response in the Respiratory Tract Microbiome. *mBio*; 2021. 12 (4)
434. Zacharias M, Kashofer K, Wurm P, et al. Host and microbiome features of secondary infections in lethal covid-19. *iScience* 2022; 25: 104926.
435. Kelly BJ, Imai I, Bittinger K, et al. Composition and dynamics of the respiratory tract microbiome in intubated patients. *Microbiome* 2016; 4: 7.
436. Fromentin M, Ricard J-D, Roux D. Respiratory microbiome in mechanically ventilated patients: a narrative review. *Intensive Care Med* 2021; 47: 292–306.
437. Viciani E, Gaibani P, Castagnetti A, et al. Critically ill patients with COVID-19 show lung fungal dysbiosis with reduced microbial diversity in patients colonized with Candida spp. *International Journal of Infectious Diseases* 2022; 117: 233–240.

438. Hamblin M, Prosch H, Vašáková M. Diagnosis, course and management of hypersensitivity pneumonitis. *European Respiratory Review* 2022; 31: 210169.
439. Nogueira R, Melo N, Novais e Bastos H, et al. Hypersensitivity pneumonitis: Antigen diversity and disease implications. *Pulmonology* 2019; 25: 97–108.
440. Lévy Y, Wiedemann A, Hejblum BP, et al. CD177, a specific marker of neutrophil activation, is associated with coronavirus disease 2019 severity and death. *iScience* 2021; 24: 102711.
441. Estipona D. A Guide to Neutrophil Markers. *Biocompare*.
442. Adderley N, Humphreys CJ, Barnes H, et al. Bronchoalveolar lavage fluid lymphocytosis in chronic hypersensitivity pneumonitis: a systematic review and meta-analysis. *European Respiratory Journal* 2020; 56: 2000206.
443. Meyer KC, Raghu G. Bronchoalveolar lavage for the evaluation of interstitial lung disease: is it clinically useful? *European Respiratory Journal* 2011; 38: 761–769.
444. Patolia S, Tamae Kakazu M, Chami HA, et al. Bronchoalveolar Lavage Lymphocytes in the Diagnosis of Hypersensitivity Pneumonitis among Patients with Interstitial Lung Disease. *Ann Am Thorac Soc* 2020; 17: 1455–1467.
445. Raghu G, Remy-Jardin M, Ryerson CJ, et al. Diagnosis of Hypersensitivity Pneumonitis in Adults: An Official ATS/JRS/ALAT Clinical Practice Guideline. *Am J Respir Crit Care Med* 2020; 202: e36–e69.
446. Allen JN, Davis WB. Eosinophilic lung diseases. *Am J Respir Crit Care Med* 1994; 150: 1423–1438.
447. Coden ME, Berdnikovs S. Eosinophils in wound healing and epithelial remodeling: Is coagulation a missing link? *J Leukoc Biol* 2020; 108: 93–103.
448. Poletti V, Cazzato S, Minicuci N, et al. The diagnostic value of bronchoalveolar lavage and transbronchial lung biopsy in cryptogenic organizing pneumonia. *European Respiratory Journal* 1996; 9: 2513–2516.
449. Kory P, Kanne JP. SARS-CoV-2 organising pneumonia: 'Has there been a widespread failure to identify and treat this prevalent condition in COVID-19?' *BMJ Open Respir Res* 2020; 7: e000724.
450. Vareille M, Kieninger E, Edwards MR, et al. The Airway Epithelium: Soldier in the Fight against Respiratory Viruses. *Clin Microbiol Rev* 2011; 24: 210–229.
451. Deshmukh V, Motwani R, Kumar A, et al. Histopathological observations in COVID-19: a systematic review. *J Clin Pathol* 2021; 74: 76–83.
452. Hewitt RJ, Lloyd CM. Regulation of immune responses by the airway epithelial cell landscape. *Nat Rev Immunol* 2021; 21: 347–362.
453. Vieira Braga FA, Kar G, Berg M, et al. A cellular census of human lungs identifies novel cell states in health and in asthma. *Nat Med* 2019; 25: 1153–1163.

454. Urawa M, Kobayashi T, D'Alessandro-Gabazza CN, et al. Protein S is protective in pulmonary fibrosis. *Journal of Thrombosis and Haemostasis* 2016; 14: 1588–1599.
455. Rock JR, Onaitis MW, Rawlins EL, et al. Basal cells as stem cells of the mouse trachea and human airway epithelium. *Proceedings of the National Academy of Sciences* 2009; 106: 12771–12775.
456. Pardo-Saganta A, Law BM, Tata PR, et al. Injury Induces Direct Lineage Segregation of Functionally Distinct Airway Basal Stem/Progenitor Cell Subpopulations. *Cell Stem Cell* 2015; 16: 184–197.
457. Fujino N, Brand OJ, Morgan DJ, et al. Sensing of apoptotic cells through Axl causes lung basal cell proliferation in inflammatory diseases. *Journal of Experimental Medicine* 2019; 216: 2184–2201.
458. Ordovas-Montanes J, Dwyer DF, Nyquist SK, et al. Allergic inflammatory memory in human respiratory epithelial progenitor cells. *Nature* 2018; 560: 649–654.
459. BéruBé K, Prytherch Z, Job C, et al. Human primary bronchial lung cell constructs: The new respiratory models. *Toxicology* 2010; 278: 311–318.
460. Stölting H, Baillon L, Frise R, et al. Distinct airway epithelial immune responses after infection with SARS-CoV-2 compared to H1N1. *Mucosal Immunol* 2022; 15: 952–963.
461. Chason KD, Jaspers I, Parker J, et al. Age-Associated Changes in the Respiratory Epithelial Response to Influenza Infection. *The Journals of Gerontology: Series A* 2018; 73: 1643–1650.
462. Comer DM, Kidney JC, Ennis M, et al. Airway epithelial cell apoptosis and inflammation in COPD, smokers and nonsmokers. *European Respiratory Journal* 2013; 41: 1058–1067.
463. Lacroix G, Koch W, Ritter D, et al. Air–Liquid Interface *In Vitro* Models for Respiratory Toxicology Research: Consensus Workshop and Recommendations. *Appl In Vitro Toxicol* 2018; 4: 91–106.
464. Chen S, Schoen J. Air-liquid interface cell culture: From airway epithelium to the female reproductive tract. *Reproduction in Domestic Animals* 2019; 54: 38–45.
465. Mertens TCJ, Karmouty-Quintana H, Taube C, et al. Use of airway epithelial cell culture to unravel the pathogenesis and study treatment in obstructive airway diseases. *Pulm Pharmacol Ther* 2017; 45: 101–113.
466. Ostrowski LE, Stewart D, Hazucha M. Interferon γ Stimulates Accumulation of Gas Phase Nitric Oxide in Differentiated Cultures of Normal and Cystic Fibrosis Airway Epithelial Cells. *Lung* 2012; 190: 563–571.
467. Liang C-C, Park AY, Guan J-L. In vitro scratch assay: a convenient and inexpensive method for analysis of cell migration in vitro. *Nat Protoc* 2007; 2: 329–333.
468. Centers for disease control and prevention. Disease Burden of Flu. *2022*.
469. Aegerter H, Kulikauskaite J, Crotta S, et al. Influenza-induced monocyte-derived alveolar macrophages confer prolonged antibacterial protection. *Nat Immunol* 2020; 21: 145–157.

470. Couceiro JNSS, Paulson JC, Baum LG. Influenza virus strains selectively recognize sialyloligosaccharides on human respiratory epithelium; the role of the host cell in selection of hemagglutinin receptor specificity. *Virus Res* 1993; 29: 155–165.

471. Roberson EC, Tully JE, Guala AS, et al. Influenza Induces Endoplasmic Reticulum Stress, Caspase-12–Dependent Apoptosis, and c-Jun N-Terminal Kinase–Mediated Transforming Growth Factor–β Release in Lung Epithelial Cells. *Am J Respir Cell Mol Biol* 2012; 46: 573–581.

472. Roberson EC, Tully JE, Guala AS, et al. Influenza Induces Endoplasmic Reticulum Stress, Caspase-12–Dependent Apoptosis, and c-Jun N-Terminal Kinase–Mediated Transforming Growth Factor–β Release in Lung Epithelial Cells. *Am J Respir Cell Mol Biol* 2012; 46: 573–581.

473. Ludwig S, Pleschka S, Planz O, et al. Ringing the alarm bells: signalling and apoptosis in influenza virus infected cells. *Cell Microbiol* 2006; 8: 375–386.

474. Buchweitz JP, Harkema JR, Kaminski NE. Time-Dependent Airway Epithelial and Inflammatory Cell Responses Induced by Influenza Virus A/PR/8/34 in C57BL/6 Mice. *Toxicol Pathol* 2007; 35: 424–435.

475. Dos Santos CC. Advances in mechanisms of repair and remodelling in acute lung injury. *Intensive Care Med* 2008; 34: 619–630.

476. McAnulty RJ. Fibroblasts and myofibroblasts: Their source, function and role in disease. *Int J Biochem Cell Biol* 2007; 39: 666–671.

477. Phan SH. Biology of Fibroblasts and Myofibroblasts. *Proc Am Thorac Soc* 2008; 5: 334–337.

478. Forrest L. Current concepts in soft connective tissue wound healing. *British Journal of Surgery* 2005; 70: 133–140.

479. Li B, Wang JH-C. Fibroblasts and myofibroblasts in wound healing: Force generation and measurement. *J Tissue Viability* 2011; 20: 108–120.

480. Zhang S, Smartt H, Holgate S, et al. Growth factors secreted by bronchial epithelial cells control myofibroblast proliferation: an in vitro co-culture model of airway remodeling in asthma. *Lab Invest* 1999; 79: 395–405.

481. King TE, Pardo A, Selman M. Idiopathic pulmonary fibrosis. *The Lancet* 2011; 378: 1949–1961.

482. Thiery JP, Acloque H, Huang RYJ, et al. Epithelial-Mesenchymal Transitions in Development and Disease. *Cell* 2009; 139: 871–890.

483. Ghosh B, Loube J, Thapa S, et al. Loss of E-cadherin is causal to pathologic changes in chronic lung disease. *Commun Biol* 2022; 5: 1149.

484. Robinot R, Hubert M, de Melo GD, et al. SARS-CoV-2 infection induces the dedifferentiation of multiciliated cells and impairs mucociliary clearance. *Nat Commun* 2021; 12: 4354.

485. Hewitt R, Puttur F, Gaboriau D, et al. Lung extracellular matrix modulates KRT5+ basal cell activity in pulmonary fibrosis. *bioRxiv*.

486. Leisman DE, Mehta A, Thompson BT, et al. Alveolar, Endothelial, and Organ Injury Marker Dynamics in Severe COVID-19. *Am J Respir Crit Care Med* 2022; 205: 507–519.
487. Cardenas EI, Ekstedt S, Piersiala K, et al. Increased IL-26 associates with markers of hyperinflammation and tissue damage in patients with acute COVID-19. *Front Immunol*; 2022. 13:1016991
488. Malik P, Patel U, Mehta D, et al. Biomarkers and outcomes of COVID-19 hospitalisations: systematic review and meta-analysis. *BMJ Evid Based Med* 2021; 26: 107–108.
489. Xiao L-N, Ran X, Zhong Y-X, et al. Clinical value of blood markers to assess the severity of coronavirus disease 2019. *BMC Infect Dis* 2021; 21: 921.
490. Sun X, Kaufman PD. Ki-67: more than a proliferation marker. *Chromosoma* 2018; 127: 175–186.
491. Gerdes J, Lemke H, Baisch H, et al. Cell cycle analysis of a cell proliferation-associated human nuclear antigen defined by the monoclonal antibody Ki-67. *Journal of Immunology* 1984; 133: 1710–5.
492. Pharo EA, Williams SM, Boyd V, et al. Host–Pathogen Responses to Pandemic Influenza H1N1pdm09 in a Human Respiratory Airway Model. *Viruses* 2020; 12: 679.
493. Short KR, Kasper J, van der Aa S, et al. Influenza virus damages the alveolar barrier by disrupting epithelial cell tight junctions. *European Respiratory Journal* 2016; 47: 954–966.
494. Yu H, Huang X, Ma Y, et al. Interleukin-8 Regulates Endothelial Permeability by Down-regulation of Tight Junction but not Dependent on Integrins Induced Focal Adhesions. *Int J Biol Sci* 2013; 9: 966–979.
495. Schoggins JW. Interferon-stimulated genes: roles in viral pathogenesis. *Curr Opin Virol* 2014; 6: 40–46.
496. Ramos I, Smith G, Ruf-Zamojski F, et al. Innate Immune Response to Influenza Virus at Single-Cell Resolution in Human Epithelial Cells Revealed Paracrine Induction of Interferon Lambda 1. *J Virol*; 2019. 93(20):e00559-19
497. Jewell NA, Cline T, Mertz SE, et al. Lambda Interferon Is the Predominant Interferon Induced by Influenza A Virus Infection *In Vivo*. *J Virol* 2010; 84: 11515–11522.
498. Liu Q, Zhou Y, Yang Z. The cytokine storm of severe influenza and development of immunomodulatory therapy. *Cell Mol Immunol* 2016; 13: 3–10.
499. MATSUKURA S, KOKUBU F, NODA H, et al. Expression of IL-6, IL-8, and RANTES on human bronchial epithelial cells, NCI-H292, induced by influenza virus A. *Journal of Allergy and Clinical Immunology* 1996; 98: 1080–1087.
500. Qazi BS, Tang K, Qazi A. Recent Advances in Underlying Pathologies Provide Insight into Interleukin-8 Expression-Mediated Inflammation and Angiogenesis. *Int J Inflam* 2011; 2011: 1–13.
501. Richter A, O'Donnell RA, Powell RM, et al. Autocrine Ligands for the Epidermal Growth Factor Receptor Mediate Interleukin-8 Release from Bronchial Epithelial Cells in Response to Cigarette Smoke. *Am J Respir Cell Mol Biol* 2002; 27: 85–90.

502. Leung C, Wadsworth SJ, Yang SJ, et al. Structural and functional variations in human bronchial epithelial cells cultured in air-liquid interface using different growth media. *American Journal of Physiology-Lung Cellular and Molecular Physiology* 2020; 318: L1063–L1073.
503. Burgel P-R, Nadel JA. Epidermal growth factor receptor-mediated innate immune responses and their roles in airway diseases. *European Respiratory Journal* 2008; 32: 1068–1081.
504. Bolitho C, Moscova M, Baxter RC, et al. Amphiregulin increases migration and proliferation of epithelial ovarian cancer cells by inducing its own expression via PI3-kinase signaling. *Mol Cell Endocrinol* 2021; 533: 111338.
505. Berasain C, Avila MA. Amphiregulin. *Semin Cell Dev Biol* 2014; 28: 31–41.
506. Sanders JM, Wampole ME, Thakur ML, et al. Molecular Determinants of Epidermal Growth Factor Binding: A Molecular Dynamics Study. *PLoS One* 2013; 8: e54136.
507. Hattori N, Mochizuki S, Kishi K, et al. MMP-13 Plays a Role in Keratinocyte Migration, Angiogenesis, and Contraction in Mouse Skin Wound Healing. *Am J Pathol* 2009; 175: 533–546.
508. Mira E, Lacalle RA, Buesa JM, et al. Secreted MMP9 promotes angiogenesis more efficiently than constitutive active MMP9 bound to the tumor cell surface. *J Cell Sci* 2004; 117: 1847–1857.
509. Bajbouj K, Ramakrishnan RK, Hamid Q. Role of Matrix Metalloproteinases in Angiogenesis and Its Implications in Asthma. *J Immunol Res* 2021; 2021: 1–12.
510. Widgerow AD. Chronic wound fluid-thinking outside the box. *Wound Repair and Regeneration* 2011; 19: 287–291.
511. Martins VL, Caley M, O'Toole EA. Matrix metalloproteinases and epidermal wound repair. *Cell Tissue Res* 2013; 351: 255–268.
512. auf dem Keller U, Sabino F. Matrix metalloproteinases in impaired wound healing. *Metalloproteinases Med* 2015; 1.
513. Caley MP, Martins VLC, O'Toole EA. Metalloproteinases and Wound Healing. *Adv Wound Care (New Rochelle)* 2015; 4: 225–234.
514. Xie Y, Chen Z, Zhong Q, et al. M2 macrophages secrete CXCL13 to promote renal cell carcinoma migration, invasion, and EMT. *Cancer Cell Int* 2021; 21: 677.
515. Hui W, Zhao C, Bourgoin SG. LPA Promotes T Cell Recruitment through Synthesis of CXCL13. *Mediators Inflamm* 2015; 2015: 1–9.
516. Marini JC, Forlino A, Bächinger HP, et al. Osteogenesis imperfecta. *Nat Rev Dis Primers* 2017; 3: 17052.
517. Chen Y, Yang S, Lovisa S, et al. Type-I collagen produced by distinct fibroblast lineages reveals specific function during embryogenesis and Osteogenesis Imperfecta. *Nat Commun* 2021; 12: 7199.
518. Almodóvar-García K, Kwon M, Samaras SE, et al. ANKRD1 Acts as a Transcriptional Repressor of *MMP13* via the AP-1 Site. *Mol Cell Biol* 2014; 34: 1500–1511.

519. Lacy SE, Bönnemann CG, Buzney EA, et al. Identification of FLRT1, FLRT2, and FLRT3: A Novel Family of Transmembrane Leucine-Rich Repeat Proteins. *Genomics* 1999; 62: 417–426.

520. Bachmann M, Kukkurainen S, Hytönen VP, et al. Cell Adhesion by Integrins. *Physiol Rev* 2019; 99: 1655–1699.

521. Houreld N, Ayuk S, Abrahamse H. Cell Adhesion Molecules are Mediated by Photobiomodulation at 660 nm in Diabetic Wounded Fibroblast Cells. *Cells* 2018; 7: 30.

522. Kottakis F, Polytarchou C, Foltopoulou P, et al. FGF-2 Regulates Cell Proliferation, Migration, and Angiogenesis through an NDY1/KDM2B-miR-101-EZH2 Pathway. *Mol Cell* 2011; 43: 285–298.

523. Shams F, Moravvej H, Hosseinzadeh S, et al. Overexpression of VEGF in dermal fibroblast cells accelerates the angiogenesis and wound healing function: in vitro and in vivo studies. *Sci Rep* 2022; 12: 18529.

524. Adams TS, Schupp JC, Poli S, et al. Single-cell RNA-seq reveals ectopic and aberrant lung-resident cell populations in idiopathic pulmonary fibrosis. *Sci Adv*. 2020. 6(28):eaba1983

525. Natarajan R, Northrop N, Yamamoto B. Fluorescein Isothiocyanate (FITC)-Dextran Extravasation as a Measure of Blood-Brain Barrier Permeability. *Curr Protoc Neurosci*; 2017. 79. 9581–95815

526. Gracia-Ramos AE, Martin-Nares E, Hernández-Molina G. New Onset of Autoimmune Diseases Following COVID-19 Diagnosis. *Cells* 2021; 10: 3592.

527. Phetsouphanh C, Darley DR, Wilson DB, et al. Immunological dysfunction persists for 8 months following initial mild-to-moderate SARS-CoV-2 infection. *Nat Immunol* 2022; 23: 210–216.

528. Lambeir A-M, Durinx C, Scharpé S, et al. Dipeptidyl-Peptidase IV from Bench to Bedside: An Update on Structural Properties, Functions, and Clinical Aspects of the Enzyme DPP IV. *Crit Rev Clin Lab Sci* 2003; 40: 209–294.

529. Ghersi G, Zhao Q, Salamone M, et al. The Protease Complex Consisting of Dipeptidyl Peptidase IV and Seprase Plays a Role in the Migration and Invasion of Human Endothelial Cells in Collagenous Matrices. *Cancer Res* 2006; 66: 4652–4661.

530. Holst JJ, Deacon CF. Inhibition of the activity of dipeptidyl-peptidase IV as a treatment for type 2 diabetes. *Diabetes* 1998; 47: 1663–1670.

531. Liu Y, Qi Y. Vildagliptin, a CD26/DPP4 inhibitor, ameliorates bleomycin-induced pulmonary fibrosis via regulating the extracellular matrix. *Int Immunopharmacol* 2020; 87: 106774.

532. Suzuki T, Tada Y, Gladson S, et al. Vildagliptin ameliorates pulmonary fibrosis in lipopolysaccharide-induced lung injury by inhibiting endothelial-to-mesenchymal transition. *Respir Res* 2017; 18: 177.

533. Sun J, Chu S, Lu M, et al. The roles of dipeptidyl peptidase-4 and its inhibitors in the regulation of airway epithelial-mesenchymal transition. *Exp Lung Res* 2020; 46: 163–173.

534. Meyerholz DK, Lambertz AM, McCray PB. Dipeptidyl Peptidase 4 Distribution in the Human Respiratory Tract. *Am J Pathol* 2016; 186: 78–86.

535. Raj VS, Mou H, Smits SL, et al. Dipeptidyl peptidase 4 is a functional receptor for the emerging human coronavirus-EMC. *Nature* 2013; 495: 251–254.

536. Wronkowitz N, Görgens SW, Romacho T, et al. Soluble DPP4 induces inflammation and proliferation of human smooth muscle cells via protease-activated receptor 2. *Biochimica et Biophysica Acta (BBA) - Molecular Basis of Disease* 2014; 1842: 1613–1621.

537. Kawasaki T, Chen W, Htwe YM, et al. DPP4 inhibition by sitagliptin attenuates LPS-induced lung injury in mice. *American Journal of Physiology-Lung Cellular and Molecular Physiology* 2018; 315: L834–L845.

538. Casrouge A, Sauer A V, Barreira da Silva R, et al. Lymphocytes are a major source of circulating soluble dipeptidyl peptidase 4. *Clin Exp Immunol* 2018; 194: 166–179.

539. Shiobara T, Chibana K, Watanabe T, et al. Dipeptidyl peptidase-4 is highly expressed in bronchial epithelial cells of untreated asthma and it increases cell proliferation along with fibronectin production in airway constitutive cells. *Respir Res* 2016; 17: 28.

540. Abbasi F, Adatorwovor R, Davarpanah MA, et al. A Randomized Trial of Sitagliptin and Spironolactone With Combination Therapy in Hospitalized Adults With COVID-19. *J Endocr Soc*; 2022. 6(4):bvac017

541. Solerte SB, D'Addio F, Trevisan R, et al. Sitagliptin Treatment at the Time of Hospitalization Was Associated With Reduced Mortality in Patients With Type 2 Diabetes and COVID-19: A Multicenter, Case-Control, Retrospective, Observational Study. *Diabetes Care* 2020; 43: 2999–3006.

542. Al-kuraishy HM, Al-Gareeb AI, Qusty N, et al. Impact of Sitagliptin on Non-diabetic Covid-19 Patients. *Curr Mol Pharmacol* 2022; 15: 683–692.

543. Singh SS, Chauhan SB, Kumar A, et al. Amphiregulin in cellular physiology, health, and disease: Potential use as a biomarker and therapeutic target. *J Cell Physiol* 2022; 237: 1143–1156.

544. Zhou Y, Lee J-Y, Lee C-M, et al. Amphiregulin, an Epidermal Growth Factor Receptor Ligand, Plays an Essential Role in the Pathogenesis of Transforming Growth Factor-β-induced Pulmonary Fibrosis. *Journal of Biological Chemistry* 2012; 287: 41991–42000.

545. Salimi M, Barlow JL, Saunders SP, et al. A role for IL-25 and IL-33–driven type-2 innate lymphoid cells in atopic dermatitis. *Journal of Experimental Medicine* 2013; 210: 2939–2950.

546. Schumacher MA, Danopoulos S, Al Alam D, et al. Growth Factors in the Intestinal Tract. In: *Physiology of the Gastrointestinal Tract*. Elsevier, 2018, pp. 71–101.

547. Jones JT, Akita RW, Sliwkowski MX. Binding specificities and affinities of *egf* domains for ErbB receptors. *FEBS Lett* 1999; 447: 227–231.

548. Ruysseveldt E, Martens K, Steelant B. Airway Basal Cells, Protectors of Epithelial Walls in Health and Respiratory Diseases. *Frontiers in Allergy*; 2021. 2:787128

549. Herman G, Stevens C, Vandyck K, et al. Pharmacokinetics and pharmacodynamics of sitagliptin, an inhibitor of dipeptidyl peptidase IV, in healthy subjects: Results from two randomized, double-blind, placebo-controlled studies with single oral doses. *Clin Pharmacol Ther* 2005; 78: 675–688.

550. Röhrborn D. DPP4 in diabetes. *Front Immunol*; 2015. 6:386.

551. Schneider WM, Chevillotte MD, Rice CM. Interferon-Stimulated Genes: A Complex Web of Host Defenses. *Annu Rev Immunol* 2014; 32: 513–545.

552. Mattes B, Scholpp S. Emerging role of contact-mediated cell communication in tissue development and diseases. *Histochem Cell Biol* 2018; 150: 431–442.

553. Nelson CM, Chen CS. Cell-cell signaling by direct contact increases cell proliferation via a PI3K-dependent signal. *FEBS Lett* 2002; 514: 238–242.

554. Hagihara M, Ohhashi M, Nagatsu T. Activities of dipeptidyl peptidase II and dipeptidyl peptidase IV in mice with lupus erythematosus-like syndrome and in patients with lupus erythematosus and rheumatoid arthritis. 1987; 33: 1463–5.

Chapter 12 - Appendix

Appendix 1: Study protocol for PHENOTYPE (V1.2 7th Feb 2021)

Study protocol can be accessed via the Clinical Trials.gov website:
https://clinicaltrials.gov/ct2/show/NCT04459351

Appendix 2: Patient information sheet and informed consent form for PHENOTYPE

PHenotyping pati**EN**ts admitted to hospital with c**O**vid-19 infection and iden**T**if**Y**ing **P**rognostic mark**E**rs

[PHENOTYPE]

Chief investigator: Professor Pallav Shah

Principal investigator: Professor Pallav Shah

Study Information Sheet

(Version 1.5 – 8th March 2021)

We would like to invite you to take part in this study.

SARS-CoV-2 (also known as COVID-19) has affected patients all over the globe. We now know that this virus can cause a spectrum of respiratory illness, ranging from mild, self-limiting symptoms (e.g. cough, nasal symptoms) to respiratory failure and death. It not only affects the lungs, but can also affect other organs, such as the heart, kidneys and gastro-intestinal system. We are keen to follow up patients like yourself, who have recovered from COVID-19 infection, to monitor your progress. We would also like to take blood samples and look through your medical notes prior to your infection to see if we can identify any risk factors or genetic predispositions that may have contributed to the severity of the symptoms you experienced and your rate of recovery.

What is the purpose of the study?

Currently we don't have any long-term data on how patients recover after having had COVID-19 infection. We are also uncertain as to whether COVID-19 has long-term health implications, both physically and mentally. Although some risk factors have been identified as contributing to a more severe disease presentation, more studies are required to fully understand these.

The aim of this study is to better understand the long-term outcomes of COVID-19 infection with a focus on the lung, heart, kidney and psychological complications and to identify potential risk factors that may be useful in predicting disease severity and disease course.

Why have I been approached?

You have been invited to take part as you have recently recovered from COVID-19 infection and have either been discharged from hospital or did not attend hospital but have ongoing symptoms. You have been offered follow up with the medical team in line with your local hospital and national guidelines.

What clinical care will I be provided if I don't take part in the research study?

You will receive the same clinical care whether or not you take part in the study. All patients who have been discharged after hospital admission for COVID-19 infection will invited for follow up with the clinical team. Additionally, any patients who have persistent symptoms (even if they did not need to attend hospital during the time of their COVID-19 infection), will be offered a follow up appointment. At these visits the team will assess your progress by discussing your symptoms with you and examining you. You will also be asked to complete a number of questionnaires, in particular to assess any residual respiratory symptoms you may have, such as breathlessness or cough, any psychological symptoms you may be experiencing as a result of your illness and how the illness has affected your quality of life. In addition to this, you will have a chest-xray (to look for any changes compared to when you were first admitted), an electrocardiogram (ECG) to assess your heart, a urine sample (to look for early signs of problems with your kidneys), and a routine set of blood tests (approximately 10mls, which equates to about 2 teaspoonfuls). You may also have a spirometry test (where you blow into a device, called a spirometer) to look at how your lungs work and to monitor progress between clinical visits. Depending on the results of the investigations and your symptoms, you may need additional tests such as a CT scan of your chest or scans to look more closely at your heart or kidneys.

In some cases, your doctor may decide that a bronchoscopy (camera test to look inside your lungs) would be helpful to get a better understanding of your lung condition. If this is the case, your doctor will carefully weigh up the pros and cons of this procedure and discuss this with you in detail, before booking the procedure.

As per local guidelines, patients will initially be seen at two time points: 6 weeks after discharge from hospital and then 3 months after discharge from hospital. These aren't precise time points, and it is possible that your appointment might be slightly earlier or later than anticipated. If your doctor feels that you would still benefit from being reviewed beyond 3 months, you will be invited to more

appointments based on your clinical need. This could range from 6 weeks after your last appointment, to 6 months after your last appointment, for instance.

Each appointment will last approximately 45 minutes during the initial stages to allow plenty of time to explore any issues or concerns you may be having and to complete the tests outlined above. As you start feeling better, the length of your appointment with be reduced to 15-30 mins, as you will probably need less medical input.

What additional samples will be taken as part of the research study?

At each clinical visit, we would like to take 20mls of additional blood samples to that described above. Therefore, in total we will take approximately 30mls of blood (10mls as part of your routine clinical care and 20mls for the research). This equates to approximately 6 teaspoonfuls of blood.

If the doctor who sees you in clinic recommends a bronchoscopy, then at this time we would ask you to take additional samples to understand the effect of COVID-19 on the lungs. The bronchoscopy would be performed with local anaesthetic and sedation. At the time of the bronchoscopy, the walls of your airways will be brushed using a tiny brush passed through the bronchoscope to collect cells from your lungs, followed by the introduction and removal of a small amount of salty water that will enable lung fluids (mucous) to be retrieved. Small pieces of tissue will then be collected from the airway using a small tool that is passed through the bronchoscope. These samples will then be assessed in a laboratory to help us better understand what is happening in the lungs.

What will the samples be analysed for?

We will look at inflammation, infection and immunity and try to see if there are any genetic signals that may be helpful to know about. We are trying to keep the analyses as broad as possible to allow as much information to be captured. We think this is the best way to approach this condition as there is a lot to learn about the infection and what factors influence disease severity.
If any incidental findings are found, we will ensure that your clinical team and GP are made aware of this to ensure you receive the best possible care going forward.

What will happen if I give consent to take part in the research study?

If you consent to the study, you will be asked to sign an informed consent form (ICF). The main things we'll ask your consent for are:

1. To access your future medical records after signing the consent form
2. To access your previous medical records (from before you signed the consent form)
3. For additional blood tests to be taken at every clinic visit (which will be initially stored in our laboratory and then analysed later)
4. If a bronchoscopy (a camera test to look into your airways) is deemed necessary by your medical team, for us to take samples to help us better understand how COVID-19 infection affects the lungs and airways.
5. To take part in a 30-45 minute interview with one of the researchers (which can be over the phone if you prefer) to help us better understand how COVID-19 infection has affected you and to see if we can establish relationships between yours and other patients' lifestyle and behaviours prior to their diagnosis of COVID-19 and the severity of the infection they experienced.

You can choose to give consent to only one (or more) of the above if you wish. You will also be asked if samples can be stored for future research, both COVID-19 related research and research not related to COVID-19.

What happens during the semi-structured interview?

The interview (if you agree) can be done over the telephone, or face-to-face after your clinic visit, whichever option is easier for you. We have a list of topics we'd like to cover such as how following the Public Health England (PHE) guidelines has affected you, any cultural or religious views that may have affected your approach to the condition, and your psychological wellbeing. The structure of the interview is not by any means rigid, so we will have time to explore these topics and any other topics you'd like to cover in as much or little detail as you'd like.

We envisage the interview will take approximately 30-45 minutes. We will record the interview on a password-protected device and then transcribe it as soon as possible. The recordings will be deleted once they have been transcribed.

Do I have to give consent?

We will trust and respect your judgement on whether you'd like to be part of the study. A member of the team will go through the information sheet with you and answer any questions you may have before you make a decision. Once you feel you've had enough time to understand what the study entails, if you decide to go ahead, we will ask you to sign a consent form. You can withdraw your consent at any time, without giving a reason and this will have no bearing on your clinical care going forward.

What are the possible disadvantages and risks of taking part?

We have tried our best to try and minimize any inconvenience to you. By timing research activity with your routine follow up clinic appointments, we have avoided the need to attend separate research visits.

The main potential disadvantages of this study are related to procedures. The main procedure we do will be blood tests, which are very straight forward and have minimal risks. These include pain at the site of the needle insertion, minor bleeding (usually self-limiting) and infection.

If your medical team feel that a camera test (bronchoscopy) is required as part of your medical care, we will take additional samples if you agree. The risks of bronchoscopy will be explained to you by your medical team, but the commonest problems experienced by patients after a bronchoscopy are sore throat, hoarse voice, fever (which should settle with paracetamol) and coughing up a tiny amount of blood (usually blood-stained sputum) if biopsies are taken.

What are the possible benefits of taking part?

As there is currently very little information on how patients who have had COVID-19 infection recover after infection, the results of this study will be very useful to help find a way to best manage the virus and its complications and determine which groups of patients are most at risk.

What happens when the research study stops?

Follow up visits with the medical team are as per local protocols and further visits/ additional tests will depend on your progress. The research study ends after 2 year of follow up after hospital discharge and so additional research samples beyond this time will not be requested. Although the follow up period is 2 years, if you choose to withdraw from the study, you can do so at any point, and this will not affect your medical care going forward.

What if there is a problem?

If you are unhappy with how you have been treated during the study, please let us know as soon as you can so that we can address this. If you would like to make a formal complaint or get advice without directly involving your researchers, you can do so via NHS PALS at cwpals@chelwest.nhs.uk or by calling the PALS Team on 020 3315 6727.

How will my information be kept confidential and secure?

We will need to use information about you from your medical records. Information that can identify you will include your NHS number, hospital number, name and contact details. We will use this information to ensure the research is being done properly. We will collect the minimum personally-identifiable information required for the study. Once enrolled in the study, you will be given a unique Study ID. Only members of the research team at your local site can use this study ID to link to your name or contact details. Any samples we collect, and interview transcripts will also be labelled with your unique study ID only. We will ensure all your information is kept safe and secure. If your samples are transferred to another laboratory or outside of the United Kingdom, we will ensure there are appropriate agreements to ensure the information is kept safe and confidential. In order to ensure the study is done in a reliable manner, we have to manage your records in a specific way and therefore you will not be able to see or change the data collected. The researchers, study sponsor and the regulatory bodies (who monitor the study and ensure that the study is being carried out correctly) will have access to your information. All computers used to store your information will have strict and specific security arrangements.

To find out more about how your information is used, you can ask one of the research team or access the following links:

- https://www.hra.nhs.uk/information-about-patients/
- www.hra.nhs.uk/patientdataandresearch

What if relevant new information becomes available?

If any new information becomes available, we will inform you straightaway so that you can decide whether you should continue with the study. If you decide to continue in the study, the research team may ask you to sign an agreement outlining the discussion.

What will happen if I want to withdraw consent?

You can choose to withdraw yourself from the study at any point. This will not in any way affect your future care. We will need to use the information and samples collected from you until the date you withdraw consent, but no further information about your health or progress will be collected.

Involvement of the General Practitioner/Family doctor (GP)

If you do decide to take part, we will liaise with your GP so that he/she has all the information about you to best look after you in the community.

What will happen to any samples?

Research blood samples (20mls, equating to 4 teaspoonfuls) will be collected at each clinic visit. Once collected, the samples will be labelled with a unique study number so that no identifiable information is recorded. These pseudo-anonymised samples will be stored at Chelsea & Westminster Hospital NHS Foundation Trust and analysed at a later date. Samples will be stored for as long as they are deemed valuable for future research and may need to be transported to other institutions, either within or outside of the UK, if such action enables us to learn more about fighting COVID-19 infection. We will ensure any institutions outside of the UK follow our rules on keeping information safe. We will also ensure there are clear agreements between us and any sites your samples are transferred to.

What will happen to the results of the research study?

We can make the study results available to you if you wish. All information will be presented in an anonymised way and your name will not be mentioned in any report or publication unless you have explicitly consented to this.
Some of the results from the study may be included in Dr Vijayakumar's PhD thesis, again, presented in an anonymised way.

Who is organising and funding the research?

The study is sponsored by Chelsea & Westminster Hospital NHS Trust. Funding is to be confirmed.

Who has reviewed the study?

All research in the NHS is looked at by an independent group of people, called a Research Ethics Committee, to protect your interests. This study has been reviewed and given favourable opinion by Yorkshire & The Humber - Sheffield Research Ethics Committee.

Contact for Further Information:

If you have any questions that haven't already been answered by the person consenting you, please feel free to contact us using the details below.

Bavithra Vijayakumar, Clinical Research Fellow
b.vijayakumar@rbht.nhs.uk

James Tonkin, Clinical Research Fellow
j.tonkin@rbht.nhs.uk

You will be given a copy of the information sheet and a signed consent form to keep.

Informed Consent Form

Version 1.5 – Date 8th March 2021

Study Title: **PH**enotyping pati**EN**ts admitted to hospital with c**O**vid-19 infection and identifying **P**rognostic mark**E**rs (PHENOTYPE)

Chief investigator: Professor Pallav Shah

Principal investigator: Professor Pallav Shah

IRAS number: 284497

Patient ID:

Please initial box

1. I confirm that I have read and understand the information sheet dated **8th March 2021** (version 1.5) for the above study. I have had the opportunity to consider the information, ask questions and have had these answered satisfactorily. ☐

2. I understand that my participation is voluntary and that I am free to withdraw at any time without giving any reason, without medical care or legal rights being affected. ☐

3. I agree for my medical notes prior to recruitment to the study to be used for research purposes to allow better understanding of my medical history ☐

4. I agree for my medical notes after recruitment to the study to be used for research purposes. ☐

5. I understand that relevant sections of my medical notes and data collected during the study, may be looked at by individuals from Chelsea & Westminster Hospital NHS Trust, from regulatory authorities or from my hospital, where it is relevant to my taking part in this research. I give permission for these individuals to have access to my records. ☐ ☐

6. I agree to my GP being informed of my participation in the study. ☐

7. I agree for blood samples to be collected and analysed for current COVID-19 research

8. I agree for my pseudo-anonymised endobronchial samples (washings/ brushings/ biopsies) to be taken and analysed for current COVID-19 research (if a bronchoscopy is deemed necessary for my clinical care) . ☐

9. I agree for pseudo-anonymised blood (and any endobronchial samples) to be stored for future COVID-19 research and research not related to COVID-19. ☐

10. I agree for my pseudo-anonymised research samples to be sent outside the UK for analysis ☐

11. OPTIONAL: I agree to take part in a semi-structured phone or face-to-face interview as part of the research study ☐

12. I agree for publication of anonymised direct quotations from the interviews (if performed) ☐

13. I would like to receive a copy of the study results. ☐

Name of Participant	Date	Signature
Name of Translator/ Interpreter (if appropriate)	Date	Signature
Name of Person taking consent	Date	Signature

When completed: 1 for participant; 1 (original) for researcher site file; 1 to be kept in medical notes.

Appendix 3 Topic guide for semi-structured interviews

Overview of experience

1. Could you tell me about how you were before you first got COVID-19?
2. Tell me about when you became ill
3. What do you remember about your time in hospital?
4. How have you been since then?

Quality of life

1. How do you perceive your current quality of life now?
2. Do you still have any symptoms due COVID-19?
3. How is your quality of life compared to before you were admitted to hospital with COVID-19?
4. Could you tell me about how it has changed over the last 2 years?
5. What factors have affected your quality of life (e.g. physical impairment, job loss, threat perception)?
6. Is there anything that has particularly helped?
    a. Physical
    b. Mental
    c. Social/community/work
7. Is there anything that's made it worse?
    a. Physical
    b. Mental
    c. Social/community/work
8. How has your mood been?
9. Do you have support (e.g. family, religious or community groups, work etc)?
10. What do you think could help improve your quality of life?
    a. Services – e.g. what type, access
    b. Social
    c. Broader pandemic impacts
11. Looking to the future, how do you see your health changing?